



The Proceedings
OF
THE INSTITUTION OF
ELECTRICAL ENGINEERS

FOUNDED 1871; INCORPORATED BY ROYAL CHARTER 1921

PART B

RADIO AND ELECTRONIC ENGINEERING
(INCLUDING COMMUNICATION ENGINEERING)

SAVOY PLACE · LONDON W.C.2

Price Ten Shillings and Sixpence

THE INSTITUTION OF ELECTRICAL ENGINEERS

FOUNDED 1871 INCORPORATED BY ROYAL CHARTER 1921

PATRON: HER MAJESTY THE QUEEN

COUNCIL 1958-1959

President

S. E. GOODALL, M.Sc.(Eng.).

Past-Presidents

W. H. ECCLES, D.Sc., F.R.S.
THE RT. HON. THE EARL OF MOUNT
EDGUMBE, T.D.
J. M. DONALDSON, M.C.
PROFESSOR E. W. MARCHANT, D.Sc.
H. T. YOUNG.
SIR GEORGE LEE, O.B.E., M.C.

SIR ARTHUR P. M. FLEMING, C.B.E.,
D.Eng., LL.D.
J. R. BEARD, C.B.E., M.Sc.
SIR NOEL ASHBIDGE, B.Sc.(Eng.).
COLONEL SIR A. STANLEY ANGWIN,
K.C.M.G., K.B.E., D.S.O., M.C.
T.D., D.Sc.(Eng.).

SIR HARRY RAILING, D.Eng.
P. DUNSHEATH, C.B.E., M.A., D.Sc.(Eng.).
SIR VINCENT Z. DE FERRANTI, M.C.
T. G. N. HALDANE, M.A.
PROFESSOR E. B. MOULLIN, M.A., Sc.D.,
LL.D.
SIR ARCHIBALD J. GILL, B.Sc.(Eng.).

SIR JOHN HACKING.
COLONEL B. H. LEESON, C.B.E., T.D.
SIR HAROLD BISHOP, C.B.E., B.Sc.(Eng.).
SIR JOSIAH ECCLES, C.B.E., D.Sc.
SIR GEORGE H. NELSON, Bart.
SIR GORDON RADLEY, K.C.B., C.B.
Ph.D.(Eng.).
T. E. GOLDFUP, C.B.E.

Vice-Presidents

SIR WILLIS JACKSON, D.Sc., D.Phil., Dr.Sc.Tech., F.R.S.

G. S. C. LUCAS, O.B.E.

SIR HAMISH D. MACLAREN, K.B.E., C.B., D.F.C., LL.D., B.Sc.

C. T. MELLING, C.B.E., M.Sc.Tech.

A. H. MUMFORD, O.B.E., B.Sc.(Eng.).

Honorary Treasurer

E. LEETE.

Ordinary Members of Council

J. A. BROUGHALL, B.Sc.(Eng.).
PROFESSOR M. W. HUMPHREY DAVIES, M.Sc.
SIR JOHN DEAN, B.Sc.
B. DONKIN, B.A.
J. M. FERGUSON, B.Sc.(Eng.).
D. C. FLACK, B.Sc.(Eng.), Ph.D.

J. S. FORREST, D.Sc., M.A.
R. J. HALSEY, C.M.G., B.Sc.(Eng.).
E. M. HICKIN.
J. B. HIGHAM, Ph.D., B.Sc.
F. C. MCLEAN, C.B.E., B.Sc.

B. L. METCALF, B.Sc.(Eng.).
J. R. MORTLOCK, Ph.D., B.Sc.(Eng.).
R. H. PHILLIPS, T.D.
H. V. PUGH.
J. R. RYLANDS, M.Sc., J.P.

D. P. SAYERS, B.Sc.
C. E. STRONG, O.B.E., B.A., B.A.I.
D. H. TOMPSETT, B.Sc.(Eng.).
H. WATSON-JONES, M.Eng.
H. WEST, M.Sc.

Chairmen and Past-Chairmen of Sections

Measurement and Control:

J. K. WEBB, M.Sc.(Eng.), B.Sc.Tech.
*H. S. PETCH, B.Sc.(Eng.).

Radio and Telecommunication:

G. MILLINGTON, M.A., B.Sc.
*J. S. MCPETRIE, Ph.D., D.Sc.

Supply:

D. P. SAYERS, B.Sc.
*PROFESSOR M. G. SAY, Ph.D., M.Sc.,
F.R.S.E.

Utilization:

R. A. MARRYAT, B.Sc.(Eng.).
*J. VAUGHAN HARRIES.

Chairmen and Past-Chairmen of Local Centres

East Midland Centre:

D. E. LAMBERT, B.Sc.(Eng.).
*J. D. PIERCE.

North Midland Centre:

J. D. NICHOLSON, B.Sc.
*A. J. COVENEY.

North-Western Centre:

PROFESSOR F. C. WILLIAMS, O.B.E.,
D.Sc., D.Phil., F.R.S.
*F. R. PERRY, M.Sc.Tech.

Scottish Centre:

R. J. RENNIE, B.Sc.
*E. O. TAYLOR, B.Sc.

Mersey and North Wales Centre:

J. COLLINS.
*T. MAKIN.

North-Eastern Centre:

A. T. CRAWFORD, B.Sc.
*T. W. WILCOX.

Northern Ireland Centre:

D. S. MCILLHAGGER, Ph.D., M.Sc.
*C. M. STOUFE, B.Sc.

South Midland Centre:

J. ASHMORE.
*L. L. TOLLEY, B.Sc.(Eng.).

Southern Centre:

G. BISHOP, B.Sc.
*L. G. A. SIMS, M.Sc., Ph.D., D.Sc.

Western Centre:

R. W. STEEL.
*J. F. WRIGHT.

* Past Chairman.

MEASUREMENT AND CONTROL SECTION COMMITTEE 1958-1959

Chairman

J. K. WEBB, M.Sc.(Eng.), B.Sc.Tech.

Vice-Chairmen

PROFESSOR A. TUSTIN, M.Sc.; C. G. GARTON.

Past-Chairmen

H. S. PETCH, B.Sc.(Eng.); DENIS TAYLOR, M.Sc., Ph.D.

Ordinary Members of Committee

E. W. CONNON, B.Sc.(Eng.), M.Eng.
W. S. ELLIOTT, M.A.
W. C. LISTER, B.Sc.

A. C. LYNCH, M.A., B.Sc.
A. J. MADDOCK, D.Sc.
R. E. MARTIN.

R. S. MEDLOCK, B.Sc.
A. NEMET, Dr.Sc.Tech.
G. A. W. SOWTER, Ph.D., B.Sc.(Eng.).

R. H. TIZARD, B.A.
F. C. WIDDIS, B.Sc.(Eng.).
M. V. WILKES, M.A., Ph.D., F.R.S.

And

The President (*ex officio*).

The Chairman of the Papers Committee.

J. B. HIGHAM, Ph.D., B.Sc. (representing the Council).

W. GRAY (representing the North-Eastern Radio and Measurement Group).

A Representative of the North-Western Measurement and Control Group.

G. H. RAYNER, B.A. (nominated by the National Physical Laboratory).

H. M. GALE, B.Sc.(Eng.) (representing the South Midland Radio and Measurement Group).

RADIO AND TELECOMMUNICATION SECTION COMMITTEE 1958-1959

Chairman

G. MILLINGTON, M.A., B.Sc.

Vice-Chairmen

M. J. L. PULLING, C.B.E., M.A.

R. J. HALSEY, C.M.G., B.Sc.(Eng.).

T. B. D. TERRONI, B.Sc.

Past-Chairmen

J. S. MCPETRIE, Ph.D., D.Sc.

R. C. G. WILLIAMS, Ph.D., B.Sc.(Eng.).

Ordinary Members of Committee

D. A. BARRON, M.Sc.
W. J. BRAY, M.Sc.(Eng.).
PROFESSOR A. L. CULLEN, Ph.D., B.Sc.
C. W. EARP, B.A.

L. I. FARREN, M.B.E.
V. J. FRANCIS, B.Sc.
G. G. GOURIET.
COMDR. C. G. MAYER, O.B.E., U.S.N.R.

J. MOIR.
B. G. PRESSEY, M.Sc.(Eng.), Ph.D.
W. E. WILLIS, M.B.E., M.Sc.Tech.
A. J. YOUNG, B.Sc.(Eng.).

The President (*ex officio*).

The Chairman of the Papers Committee.

C. E. STRONG, O.B.E., B.A., B.A.I. (representing the Council).

E. H. COOKE-YARBOROUGH, M.A. (Co-opted Member).

G. H. HICKLING, B.Sc. (representing the North-Eastern Radio and Measurement Group).

N. C. ROLFE, B.Sc.(Eng.) (representing the Cambridge Radio and Telecommunication Group)

J. MOIR (representing the South Midland Radio and Measurement Group).

K. J. BUTLER (representing the North-Western Radio and Telecommunication Group).

The following nominees of Government Departments:

Admiralty: CAPTAIN R. L. CLODE, R.N.

Air Ministry: GROUP CAPTAIN A. FODEN, B.Sc.Tech., R.A.F.

War Office: LIEUT.-COL. R. G. MILLER, M.A., R. Signals.

Secretary

W. K. BRASHER, C.B.E., M.A., M.I.E.E.

Assistant Secretary

F. C. HARRIS.

Deputy Secretary

F. JERVIS SMITH, M.I.E.E.

Editor-in-Chief

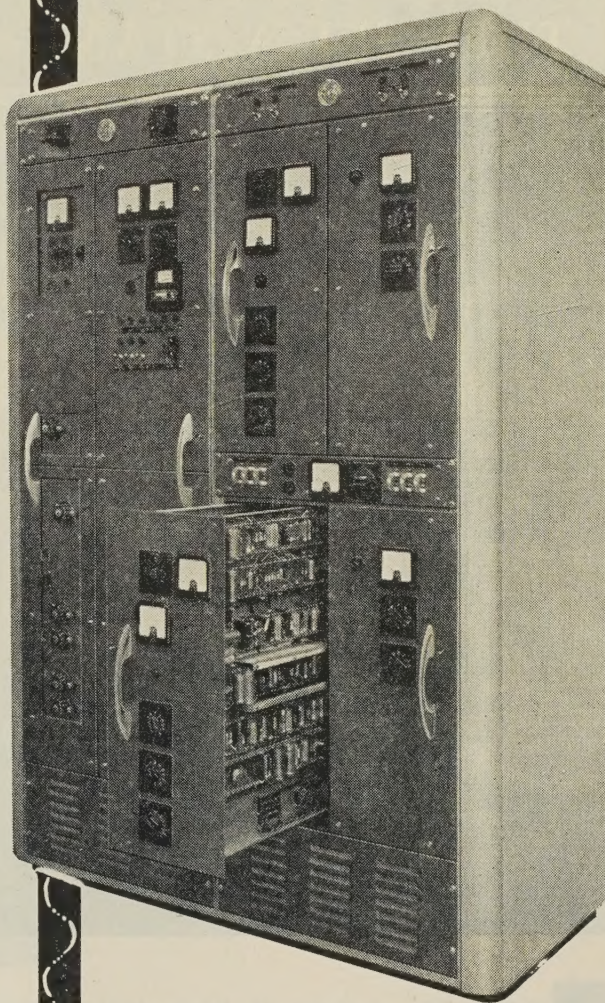
G. E. WILLIAMS, B.Sc.(Eng.), M.I.E.E.

NEW FM TRANSMITTERS

TYPE 505 SERIES

This new series of FM transmitters for Band II, with power output of 1 or 2 kW, is intended for remote-controlled, unattended operation. The design offers intrinsic flexibility, interchangeability of units, convenient duplication of the complete transmitter and easy accessibility for servicing. The basic units are: Drive unit, 1kW RF amplifier and associated power supplies. Various combinations of drive and amplifier units can be used so that several different programmes or powers can be radiated. A typical application could be the use of a pair of amplifiers in parallel with main and standby drive units. Automatic drive changeover facilities are provided. The drive unit embodies an entirely new technique of FM generation which greatly simplifies setting up and adjustment and provides good long term stability and low noise and distortion without the need for any special valve selection.

View of typical assembly showing 1kW RF Amplifier (left) and Drive Unit (withdrawn) on right



NEW FROM **E.M.I.**

NEW TELEVISION & FM TRANSMITTING AERIAL

TYPE 705 SERIES

For use on Television Bands I and III and FM Band II, this aerial is a new development based on the Mesny principle. The radiating system has been closely integrated with the design of the tower and the number of feed points has been reduced to a minimum. Several different versions are available with different power gains and polar diagrams.

For further details write or telephone to:—

E.M.I. ELECTRONICS LTD



BROADCAST EQUIPMENT DIVISION

HAYES · MIDDLESEX · TEL: SOUTHALL 2468

THEY SET A STANDARD



A Roman villa, A.D. 400

DURING their occupation of Britain (A.D. 50—A.D. 410), the Romans built themselves homes of great beauty. They brought from Egypt the art of brick-making—an art which disappeared when the Dark Ages came, and which was not recovered in England until the 13th Century. In architecture, as in many other fields, the Romans set a standard which few have equalled since. In cable making too, standards are of vital importance. For over 100 years members

of the Cable Makers Association have been concerned in all major advances in cable making. Together they spend over one million pounds a year on research and development. The knowledge gained is available to all members. This co-operation has contributed largely to the world-wide prestige that C.M.A. cables enjoy, and it has put Britain at the head of the world cable exporters. Technical information and advice is freely available from any C.M.A. member.

MEMBERS OF THE C.M.A.

British Insulated Callender's Cables Ltd. • Connollys (Blackley) Ltd.
Enfield Cables Ltd. • W. T. Glover & Co. Ltd. • Greengate &
Irwell Rubber Co. Ltd. • The Hackbridge Cable Co. Ltd.*
W. T. Henley's Telegraph Works Co. Ltd. • Johnson & Phillips Ltd.
The Liverpool Electric Cable Co. Ltd. • Metropolitan Electric Cable
& Construction Co. Ltd. • Pirelli-General Cable Works Ltd.
(The General Electric Co. Ltd.) • St. Helens Cable & Rubber Co. Ltd.
Siemens Edison Swan Ltd. • Standard Telephones & Cables Ltd.
The Telegraph Construction & Maintenance Co. Ltd.

* C.M.A. Trade Marks for Mains Cables only

*Insist on a
cable with the
C.M.A. label*



The Roman Warrior and the letters 'C.M.A.' are British Registered Certification Trade Marks.

CABLE MAKERS ASSOCIATION

CABLE MAKERS ASSOCIATION, 52-54 HIGH HOLBORN, LONDON, W.C.1. TELEPHONE: HOLBORN 7633

The best 75 volt stabilisers in the world



BRITISH SERVICES PREFERRED TYPE

M8225/CV4080

The high performance of the Mullard stabiliser 75C1 has led to the recent adoption of its Special Quality equivalent M8225/CV4080 by the British Services as their Preferred 75-volt stabiliser. The M8225/CV4080 is tested for specialised applications in which conditions of extreme shock and vibration are encountered.

Wide Current Range . . .

2 to 60 milliamps

Small Regulation Voltage . . .

Less than 9 volts

High Stability . . .

Typical variation in burning voltage less than $\pm 2\%$ in any 10,000 hours of operation.



GENERAL PURPOSE TYPE

75C1

The 75C1 is the best 75 volt stabiliser available in the world for general purpose use in industry and communications. It has the same electrical characteristics as the M8225/CV4080 and like this British Services Preferred valve provides an exceptional combination of long life, stability and good regulation.

*Full data is readily available
from the address below.*


MULLARD LIMITED
MULLARD HOUSE
TORRINGTON PLACE
LONDON · W.C.1
TEL: LANGHAM 6633

Mullard

GOVERNMENT AND
INDUSTRIAL VALVE DIVISION



See Mullard valves & tubes
on Stand 2 at the
**ELECTRONIC COMPUTER
EXHIBITION · Olympia**
November 28 to December 4



G.E.C.

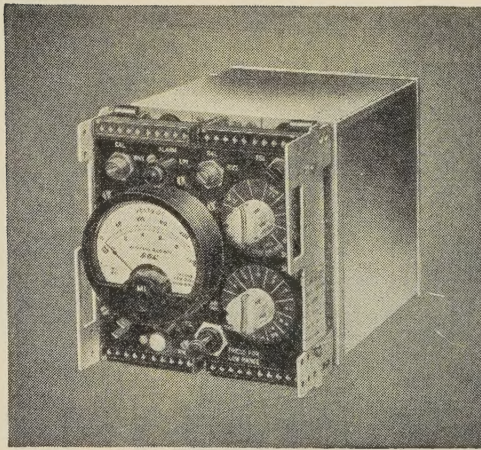
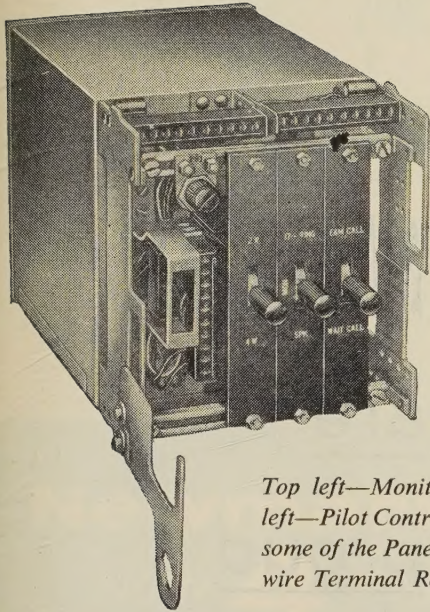
3 CIRCUIT AND 12 CIRCUIT

OPEN-WIRE CARRIER

Telephone Equipment

The equipment is suitable for operation under varied climatic conditions. For example, a G.E.C. 12-circuit system is operating successfully near the Arctic Circle where severe icing conditions are experienced during the winter months.

Everything for Telecommunications by open-wire line, cable and radio; single and multi-circuit



Top left—Monitor, top right—Alarm, bottom left—Pilot Control and bottom right—Amplifier, some of the Panels used in the 12-Circuit Open-wire Terminal Rack shown on the right.

G.E.C. 3-circuit and 12-circuit carrier telephone equipment provides for the transmission of three and twelve high-quality speech circuits, respectively, over an open-wire route. Each speech circuit effectively transmits the frequency band 300 c/s to 3400 c/s. Signalling is effected at the out-of-band frequency of 3825 c/s on each circuit.

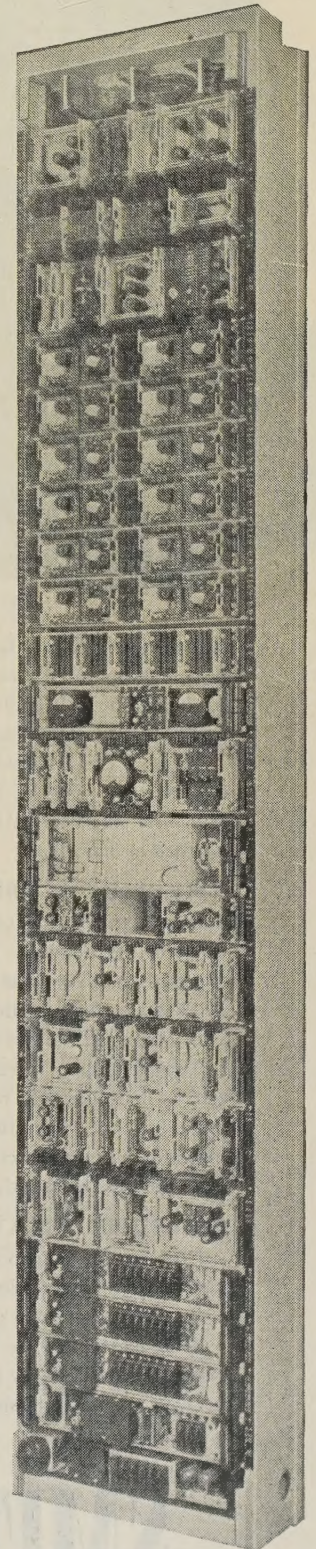
The signals transmitted to line in the 12-circuit system are within the frequency band 36 to 143 kc/s, and in the 3-circuit system within 3.16 to 31.1 kc/s in accordance with the recommendation of C.C.I.T.T.

Thus a 3-circuit and a 12-circuit system can operate over the same open-wire pair. Several systems can operate along the same route.

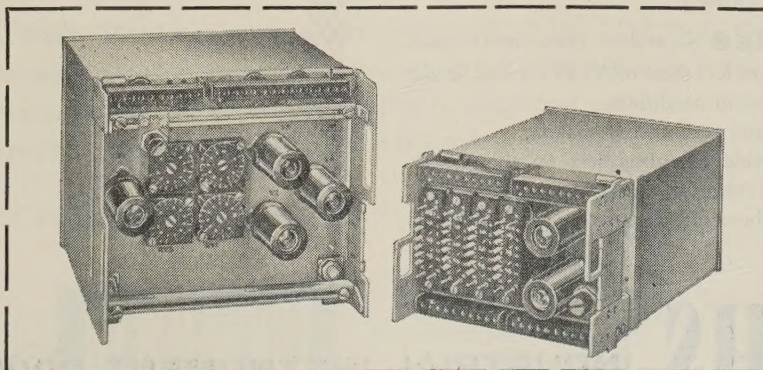
When required, a broadcast programme circuit of approximately 10 kc/s bandwidth can be inserted at the intermediate frequency of 84 to 96 kc/s, in place of three speech circuits in either system. In addition, twenty-four voice-frequency telegraph channels can be provided over any speech circuit.

By suitably spacing repeaters along the route, a system may be operated over distances of many hundreds of miles, the exact distance and spacing of repeaters depending on local conditions.

The equipment itself is the latest G.E.C. Type 56. A complete 3-circuit terminal or a complete 12-circuit terminal is accommodated on one single-sided rack.



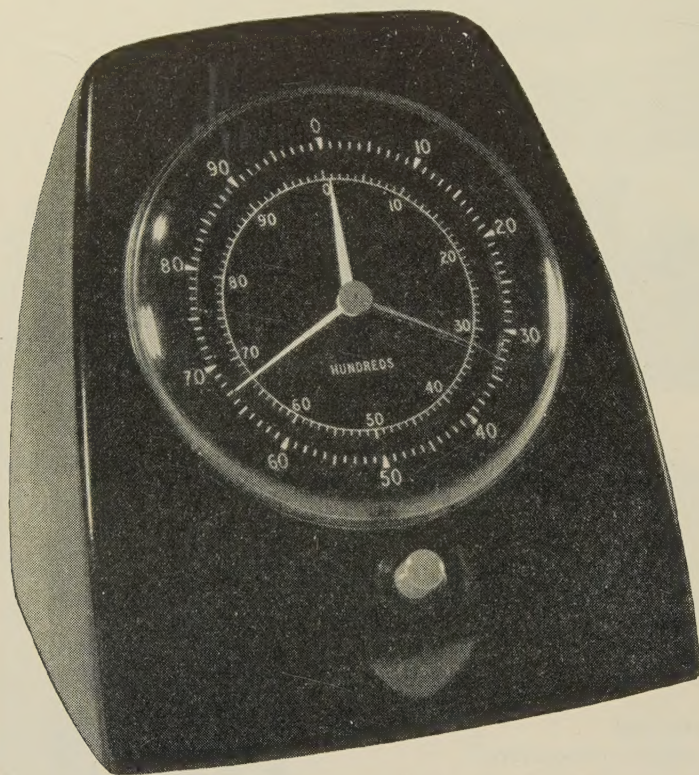
For further information please write for Standard Specifications
SPO1011
and
SPO1025



and TV link; short, medium and long haul. Automatic and Manual exchange.

TELEPHONE, RADIO & TELEVISION WORKS · COVENTRY · ENGLAND

G.E.C.



BACKGROUND On 1st December, 1958, the G.P.O.'s new Subscriber Trunk Dialling (S.T.D.) scheme comes into operation on the Bristol Central Exchange, by 1970 it will embrace three quarters of all trunk calls in the United Kingdom.

When S.T.D. is introduced, *all* telephone calls, whether trunk or local, can be dialled. The calls will be charged in twopenny units. *It is these units that SMITHS Subscriber's Private Meter has been designed to indicate.*

THE INSTRUMENT This consists essentially of a meter, designed to British G.P.O. specification, housed in a shock resisting plastic case. The meter dial has two scales marked 0-100 units. The outer scale in yellow registers units, the inner white scale registers hundreds. A yellow and white pointer are associated with the two scales.

A third pointer in red also registers units but can be reset to zero by depressing the red button in order to register the cost of an individual call. Operation of the reset button does not interrupt the function of the meter and the yellow and white pointers will continue to summate the call charges.

SALIENT FEATURES No audible noise interference.

Does not respond to voltages less than 100V. 25 c/s A.C. under normal ringing conditions or fault conditions.

Cannot be made to give false readings by shaking.

This meter will be available to subscribers on the S.T.D. system in the U.K. by rental from the G.P.O.

Overseas enquiries should be made direct to the address below.

SMITHS

are

proud

to be

associated

with

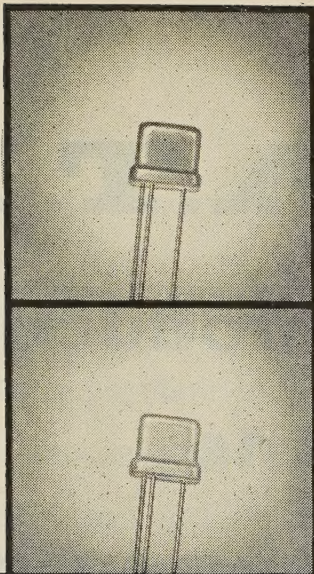
S.T.D.

SMITHS

INDUSTRIAL INSTRUMENT DIVISION

Chronos Works, North Circular Road, London, N.W.2.

Telephone: GLAdstone 1136

**RF** TYPES

6 Volts		Min. f_{α}
	V6/R8	8 Mcs.
	V6/R4	4 Mcs.
	V6/R2	2 Mcs.

Excellent general purpose R.F. transistors which are finding increasing uses in switching circuits. Have useful current gains at high pulse currents and can be selected for 15 and 30 Volt operation. Maximum dissipation now 75 mW; 125 mW on a heat sink. Clips supplied free.

AUDIO TYPES

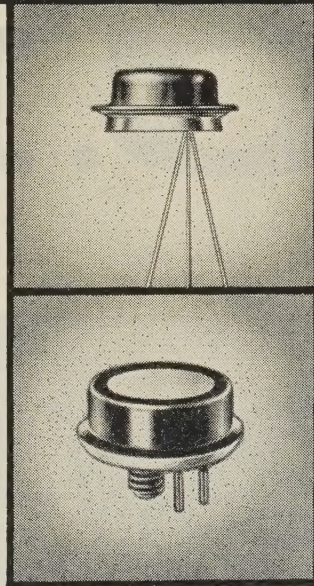
10 Volts		Min. Beta
	V10/50B	50
	V10/30A	30
	V10/15A	15

An ideal transistor for audio stages of portable receivers. Maximum dissipation now 125 mW; on a heat sink 200 mW. Clips supplied free. Selected types for 30 Volt operation can be supplied to order.

Newmarket ^{*}GOLTOP Transistors

NOW 4 RANGES IN PRODUCTION

ALL TRANSISTORS ACTUAL SIZE

**INTERMEDIATE POWER**

Volts		Min. Beta 20
15	V15/20IP	
30	V30/20IP	

With maximum power dissipation of 2 watts, this transistor fills the gap between the audio types and the 10 watt power types in both power output and frequency range. Excellent for low-power transmitters at frequencies up to 500 kc/s. Sealed by cold welding and supplied with special clip mounting, eliminating large fixing studs. 60-Volt types can be selected to order.

POWER

Volts	Minimum Beta		
	10	20	30
15	V15/10P	V15/20P	V15/30P
30	V30/10P	V30/20P	V30/30P
60	V60/10P	V60/20P	V60/30P

The widest range of power transistors available with the closest tolerances. Extremely robust, reliable and stable. High heat dissipation—up to 20 watts per pair used in Class B with suitable heat sink. Up to 80 watts per pair obtainable in Inverter applications. Matched pairs can be supplied.

Leading the way With four years manufacturing experience behind us we are still expanding our production, still increasing our efficiency by new techniques in mechanisation. This policy ensures that the latest developments in transistors will always be offered by Newmarket at extremely competitive prices. The special requirements of every customer receive individual attention.

** Identified by the gold top.*

NEWMARKET
TRANSISTORS

All enquiries to:

Newmarket
Transistor Co Ltd

Exning Road, Newmarket, Suffolk

Telephone: Newmarket 3381-4 Cables: Semicon Newmarket

A.T.E

introduces

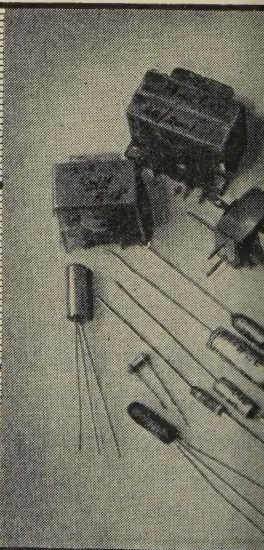
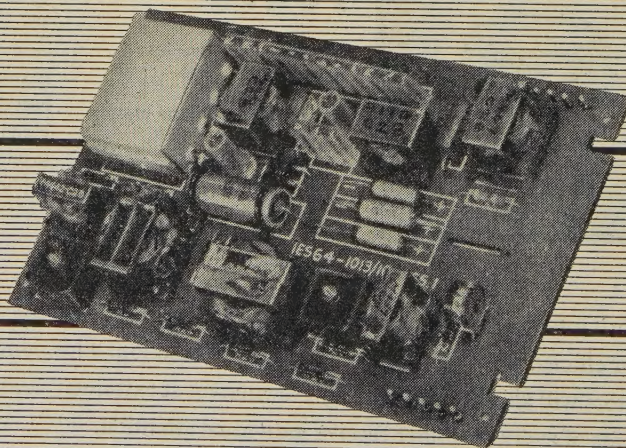
Line

Transmission

Equipment

TYPE

C.M



AUTOMATIC TELEPHONE

DESIGNED FOR CONTINUOUS SERVICE

The remarkable possibilities offered by modern components have been fully exploited by A.T.E. in the design of their latest range of transmission equipment. New mechanical design especially suited to printed circuitry has ensured compact assemblies with complete accessibility for maintenance. This card mounted equipment, which uses transistors throughout, has full C.C.I.T.T. performance. It is thus equally suitable for extending existing installations and for new projects.

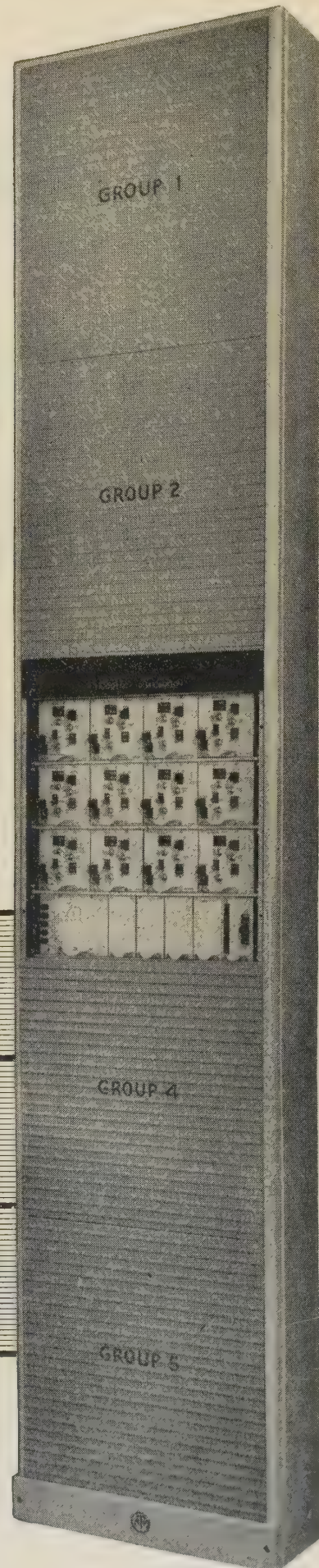
MODERN COMPONENTS

MODERN CIRCUITRY

MODERN MECHANICAL DESIGN

CTRIC COMPANY LIMITED

Strowger House, Arundel Street, London, W.C.2



A new **Plessey** range of Plugs and Sockets

COVERING THE ENTIRE 'AN' RANGE

The Plessey UK-AN series of electrical connectors is now available and, for the first time from a non-dollar source, manufacturers will be able to obtain a full range of plugs and sockets completely interchangeable with the existing AN range.*

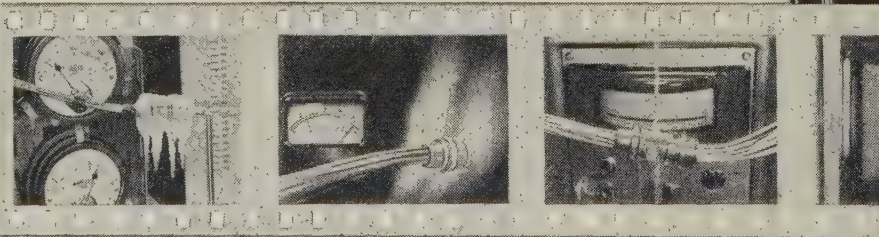
The Plessey UK-AN range has been designed and developed to M.O.S. Specification EL 1884 and RCS 321, and UK-AN connectors are fireproof, pressure sealed and environmental resisting. No separate wiring accessories are needed.

Write for test reports and full technical details.

Thawing out after low-temperature test at -60°C .

Fireproofness test (15 mins. at $1,100^{\circ}\text{C}$.)

Testing insulation resistance under direct water jet.



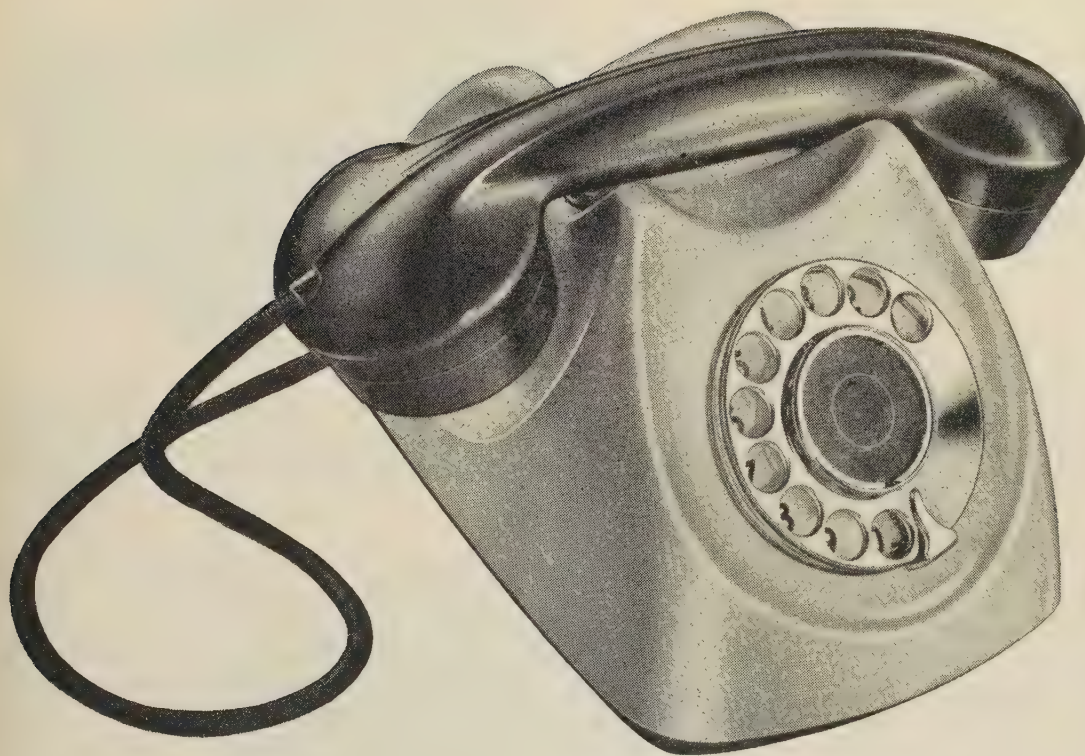
* There are many thousands of separate items in the AN range as it exists at present, whereas the ingenious Plessey UK-AN list comprises less than a thousand separate items, yet achieves the same service requirements.

ELECTRICAL CONNECTORS DIVISION

THE PLESSEY COMPANY LIMITED • CHENEY MANOR • SWINDON • WILTS

Overseas Sales Organisation: PLESSEY INTERNATIONAL LIMITED • ILFORD • ESSEX

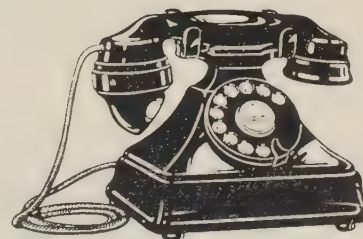




South Africa adopts the CENTENARY NEOPHONE

The telephone of today

The introduction of the Centenary Neophone aroused world-wide interest on account of its improved performance and appearance. Now the Department of Posts and Telegraphs of the Union of South Africa, after careful laboratory testing and comparison with other instruments, has selected the Centenary Neophone, with light grey case and maroon handset, as standard for all future requirements, and the first telephones will shortly be in service. This Administration, which installed the first automatic trunk switchboard in 1934, also standardised the original Siemens Neophone more than a quarter of a century ago, and its present action is a tribute to the service it has received.



The original Neophone

*The Centenary Neophone is also available in black
and nineteen other colour combinations.*



SIEMENS EDISON SWAN LTD *An A.E.I. Company*

Public Telephone Division, Woolwich, London, S.E.18. Telephone: Woolwich 2020

D1506



Pluggable Components

(Patents pending)

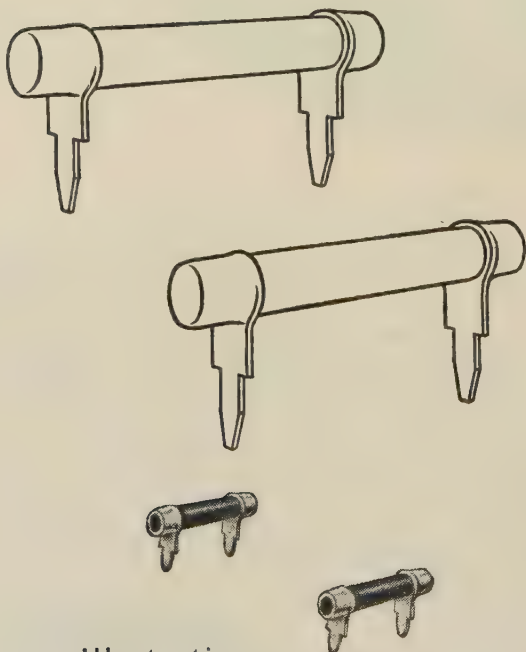


Illustration
actual size

THE most recent, the most outstanding, and the most revolutionary example which has emerged from the Erie principle of living together, and one which will be welcomed by all associated with the problems of adapting traditional components for printed circuits, is a component specially developed and specially tailored for the job.

This component, to which, for want of a better term, we ascribe the adjective "pluggable", is fitted with special strip terminations, shouldered and tapered at the end for easy insertion and positive location, thus avoiding crimping, looping, bending, cropping, and elaborate and expensive insertion machinery, as is necessary with the traditional wire ended component.

These terminations are spaced in integers of 0.1 in., and can be applied to any Erie tubular resistor or capacitor at present fitted with wire ends, and amongst their other advantages, they ensure that the component is mounted at a standard and safe distance above the printed circuit board, and that inductance and stray capacitance are both low and constant.

Pluggable components are firmly secured by the mere act of insertion, and, being raised from the board by means of the shoulder, can easily be clipped out in servicing, and replaced either by a component of the same type, or by the traditional wire ended component, whichever happens to be the more readily available.

ERIE



RESISTOR LIMITED

Carlisle Road, The Hyde, London, N.W.9. England, Tel: COL 8011

Factories: Great Yarmouth and Tunbridge Wells, England; Toronto, Canada; Erie, Pa. and Holly Springs, Miss., U.S.A.

NEW—from

Redifon

GR.310 1 watt H.F.

TRANSISTORISED

WALKIE - TALKIE

for telephony and CW

4 crystal-controlled spot frequencies
anywhere in the range 2.5 to 8 Mc/s

**LIGHT AND COMPACT
RUGGED AND TROPICALISED
NO TUNING
SIMPLE TO OPERATE**



Brief specification

Frequency Range: 2.5 to 8 Mc/s.
Power Output: 1 watt.
Receiver Sensitivity: 3—6 microvolts.

Batteries: Self-contained chargeable
lightweight silver-zinc cells.
Special charging board available
for plug-in block charging.

Consumption: 20 hours continuous
operation with 5 to 1 duty cycle
on one charge.

Full details on request

Radio Communications Division

**REDIFON LIMITED, BROOMHILL ROAD,
LONDON, S.W.18. VANDyke 7281**

A Manufacturing Company in The Rediffusion Group

and now ...

706, the new POST OFFICE



THE introduction of a new telephone by the POST OFFICE to their many millions of subscribers is an undertaking of great magnitude.

THE design and development of this new 706 type telephone has been completed by Ericsson Telephones Limited and Siemens Edison Swan Ltd. with the close co-operation of the Post Office Engineering Dept., and has resulted in an instrument having a very high standard of performance and elegance.

IN consultation with the Council of Industrial Design, a range of single and two tone colours has been selected suitable for harmonizing with a wide range of architectural colour schemes and furnishings with a maximum of tolerance.

TELEPHONE

in colour

AVAILABLE IN:—

TWO-TONE GREY

TWO-TONE GREEN

LACQUER RED

COLONIAL BLUE

TOPAZ YELLOW

IVORY

BLACK

The case and lightweight handset is moulded in Diakon, having a greatly improved functional shape and designed to completely eliminate the use of metal inserts.

The dial letters and numbers shown on an annular ring, surround the finger plate giving improved visibility of the characters, thus reducing the incidence of wrong numbers. "Grebe" grey cords and desk block are common to all colours.

The instrument can be fitted with a central press button for shared service, recall, etc.

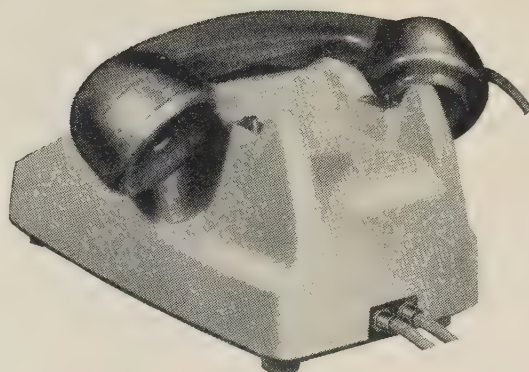
All components are mounted on the base, with operation completely independent of the case. Releasing two screws adjacent to the cradle plungers allows the case to be removed without inverting the telephone.

Conventional wiring is used with a one-piece moulded base of toughened polystyrene incorporating the terminal insulation, or alternatively with a PRINTED CIRCUIT using a pressed metal base.

The light action cradle switch with its enclosed springset is provided with a linesman's latch which holds the switch operated during maintenance.

Automatic regulation of the high performance is provided for short lines.

The rear aspect of the set is simple in form and the illustration below indicates the provision of an "off hook" rest position for the handset.



ERICSSON TELEPHONES LIMITED
ETELCO LIMITED

22 LINCOLNS INN FIELDS, LONDON, W.C.2
BEESTON, NOTTINGHAM & SUNDERLAND

SIEMENS EDISON SWAN LTD
WOOLWICH, LONDON, S.E.18 AN AEI COMPANY



There are many ways of keeping one's customers

...but the best way that we've found is quite simply to do the job exactly as it's wanted, and by the time it's wanted. If this is the service you're looking for, get in touch with:

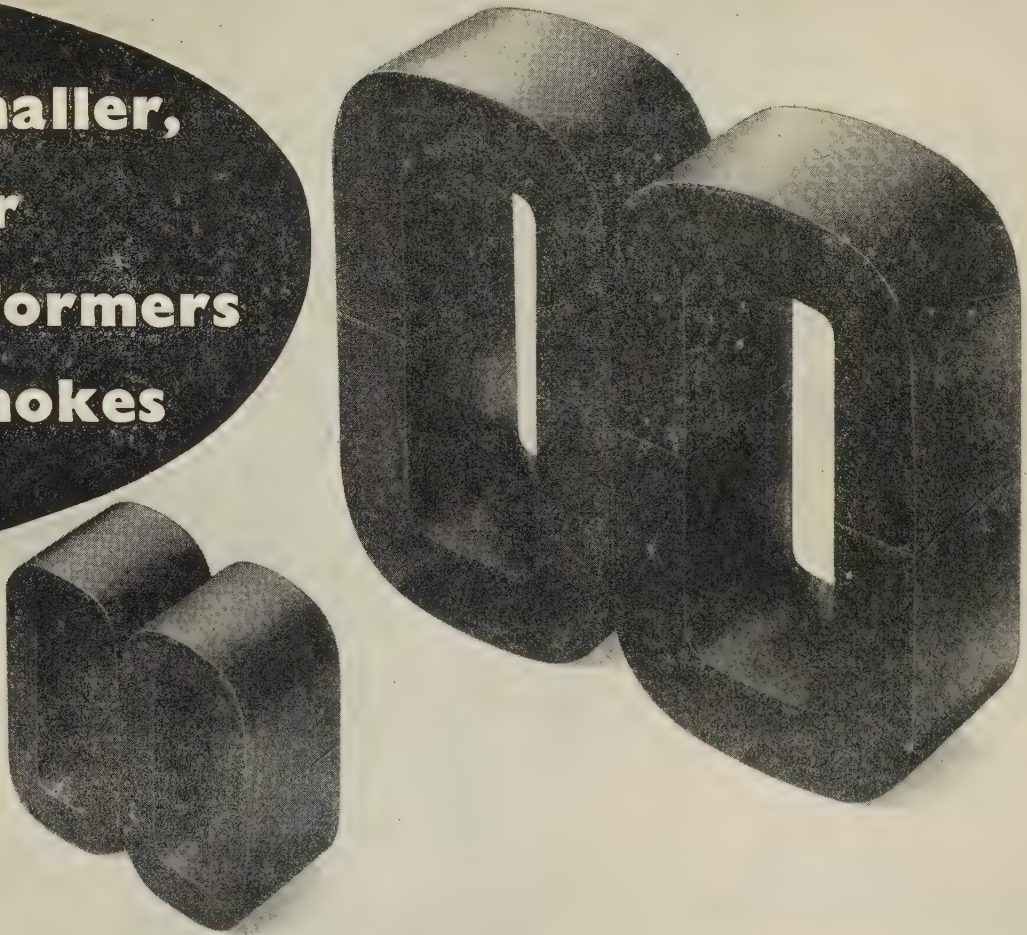
Metropolitan Plastics Ltd



Specialists in thermo-setting plastics

Glenville Grove, Deptford, London SE8
Telephone: TIDEway 1172

**for smaller,
lighter
transformers
and chokes**



Do your products embody transformers and chokes? 'ENGLISH ELECTRIC' 'C' cores satisfy the most exacting demands of the electronic industry. Leaders in the development of strip-wound cores, 'ENGLISH ELECTRIC' manufacture the full range of standard 'C' cores to RCL 193 and cores for special requirements. Detailed information is available on request.

Some of the advantages of using 'ENGLISH ELECTRIC' 'C' cores:

- ★ Easy to store and handle, their use results in reduced assembly time.
- ★ Transformers are up to 30% smaller and lighter.
- ★ Transformers have lower losses, lower magnetising VA and lower leakage flux.
- ★ Cores are suitable for oil-filled, open type or "resin cast" transformers.
- ★ Cores are stable up to 250°C.

'ENGLISH ELECTRIC'

'C' CORES

THE ENGLISH ELECTRIC COMPANY LIMITED, MARCONI HOUSE, STRAND, LONDON, W.C.2
Transformer Department, Liverpool

WORKS: STAFFORD • PRESTON • RUGBY • BRADFORD • LIVERPOOL • ACCRINGTON

*no rungs missing
of*

in the ladder of our range

QUARTZ CRYSTALS

G.E.C.

For long term stability and unfailing activity, G.E.C. Quartz Crystal Units provide the basis for reliable communications systems.

A complete range of units to meet D.E.F.5271 and R.C.L.271 Inter-Services styles can be supplied.

**From
200 cycles/sec
to
90 Mc/sec.**

SALFORD ELECTRICAL INSTRUMENTS LIMITED

(COMPONENTS GROUP)

TIMES MILL · HEYWOOD · LANCASHIRE Tel: Heywood 686

London Sales Office Tel: Temple Bar 4669

A SUBSIDIARY OF THE GENERAL ELECTRIC CO. LTD. OF ENGLAND



A.T.E. + MARCONI

Combined Operations

The complexity of modern radio-multichannel systems involving hundreds of telephone channels has brought about a collaboration between the two leading specialist organizations in the field—Marconi's in radio, and A.T.E. in carrier transmission.

This completely unified approach to development, systems planning, supply, installation, maintenance of equipment and training of personnel covers radio-multichannel systems in the V.H.F., U.H.F. and S.H.F. frequency bands all over the world.



Full information may be obtained from either:
MARCONI'S WIRELESS TELEGRAPH COMPANY
LIMITED, CHELMSFORD, ESSEX, ENGLAND.



or AUTOMATIC TELEPHONE & ELECTRIC
CO. LTD., STROWGER HOUSE, ARUNDEL
STREET, LONDON, W.C.2

SERIES**400****RECTIFIERS**

- New high voltage plates
- Fully comprehensive range of plate sizes
- Savings in space, weight and cost
- Available with or without cooling fins
- Supplied ready wired or bus-barred
- Simplified connection arrangements



SenTerCel SERIES 400 selenium rectifier stacks are available from stock and from production. The rectifiers are made from a new range of high voltage plates which, coupled with design changes, permit considerable savings in space, weight and cost. A new booklet No. MF/101 has just been published and is available free on request. Of interest to designers of conversion equipment, this publication gives full electrical and mechanical information concerning SERIES 400.



Standard Telephones and Cables Limited

Registered Office: Connaught House, Aldwych, London, W.C.2

RECTIFIER DIVISION: EDINBURGH WAY · HARLOW · ESSEX



Control at your fingertips

Remote Solenoid control by Push Button; easy, fast, with negative fatigue factor.

If you need to push, pull, press or punch fractions of an ounce to hundreds of pounds through thousandths of an inch to five inches by remote control, consult Oliver Pell Control Ltd., who manufacture the master range of Varley Solenoids. All normal voltages and ratings are "off-the-shelf". For any specific application, prototypes 7-10 days, quantity production 3-4 weeks.



Solenoids

FOR REMOTE CONTROL

For full details of Varley Solenoids mail this coupon:

OLIVER PELL CONTROL LIMITED

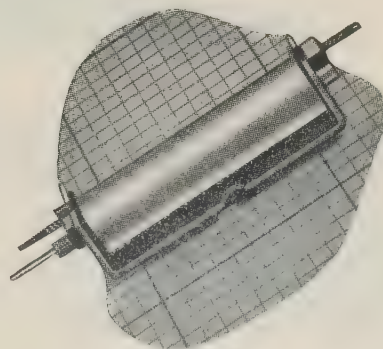
CAMBRIDGE ROW . WOOLWICH . LONDON S.E.18 . ENGLAND
CABLES: VARLYMAG, WOOLWICH . TELEPHONE: WOOLWICH 1422

NAME

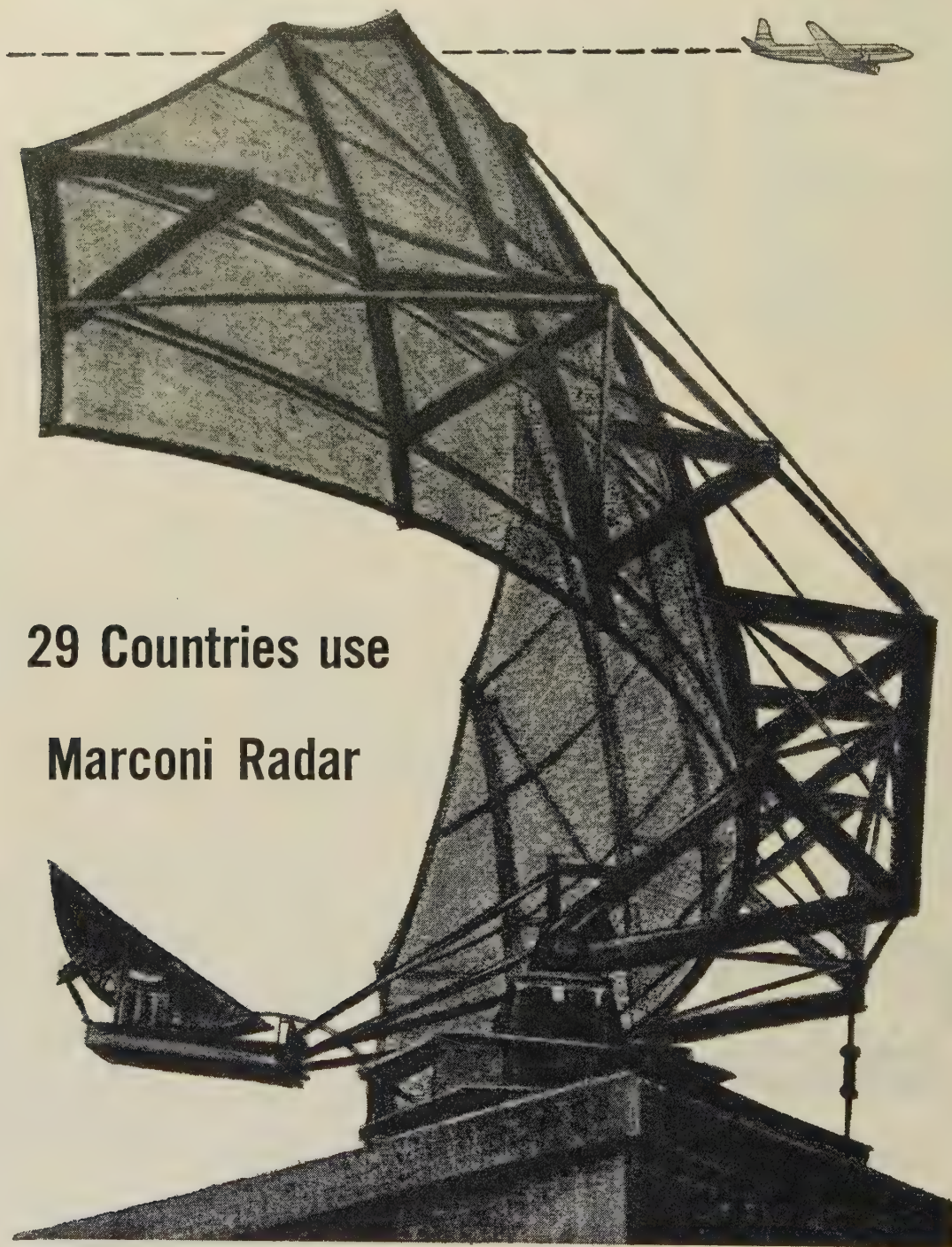
COMPANY

ADDRESS

.....



Marconi in Radar



**29 Countries use
Marconi Radar**

MARCONI

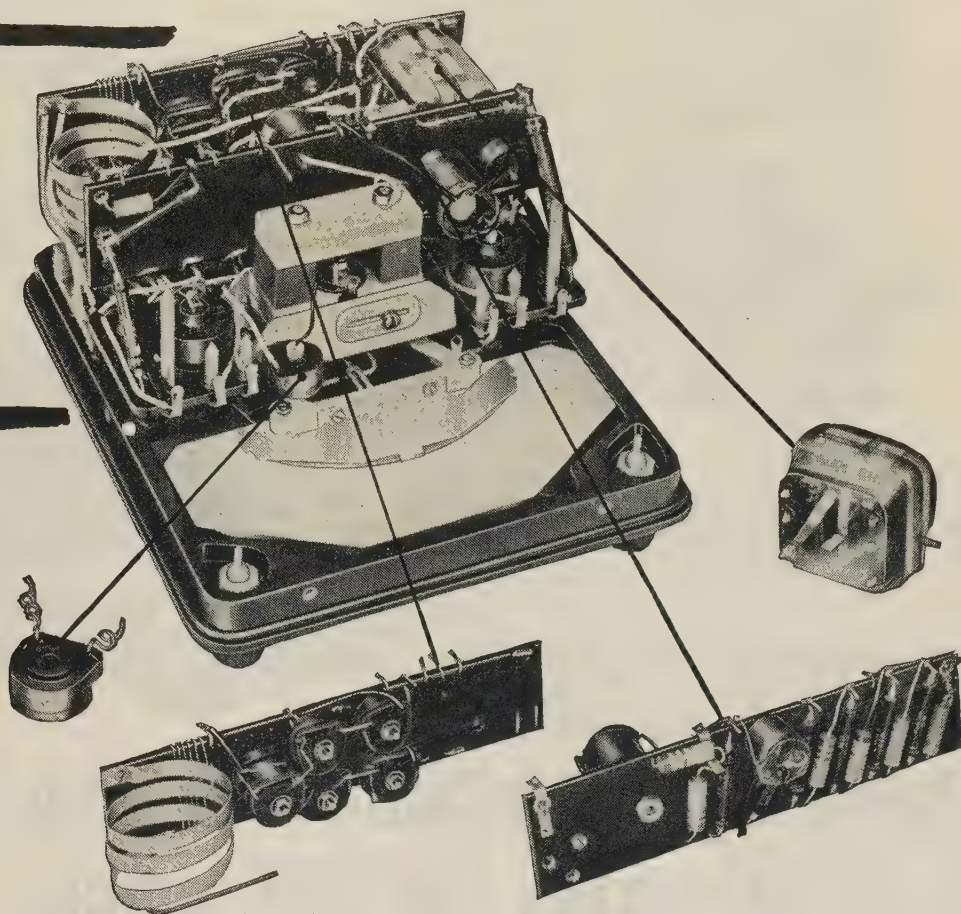
**COMPLETE CIVIL AND MILITARY
RADAR INSTALLATIONS**

MARCONI'S WIRELESS TELEGRAPH COMPANY LIMITED, CHELMSFORD, ESSEX, ENGLAND

M.6.

The famous Avometers are possibly the most widely used instruments of their type in the World and have an excellent record of service under all climatic conditions, even at arctic temperatures. In tropical climates, however, there is a constant risk of derangement due to humidity, heat, and the development of fungoid growths. To meet these conditions, the manufacturers of Avometers have produced special types known as Models 7X, 8X and 8(S)X, which are suitable for continuous use in any extremes of heat or cold. In these instruments, certain components are potted in Araldite epoxy resin, which has the advantages of remarkable adhesion to metals, ceramics, etc., good dielectric properties, low shrinkage, resistance to moisture and extremes of climate, and complete freedom from micro-biological attack.

Poles apart



Araldite epoxy resins have a remarkable range of characteristics and uses.

They are used

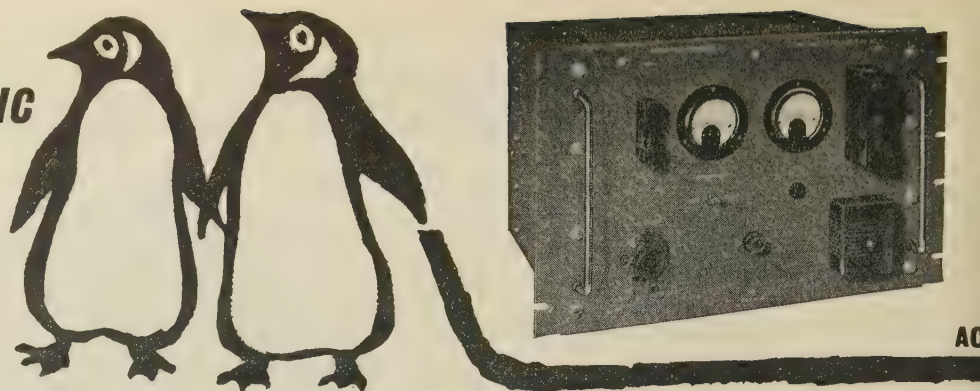
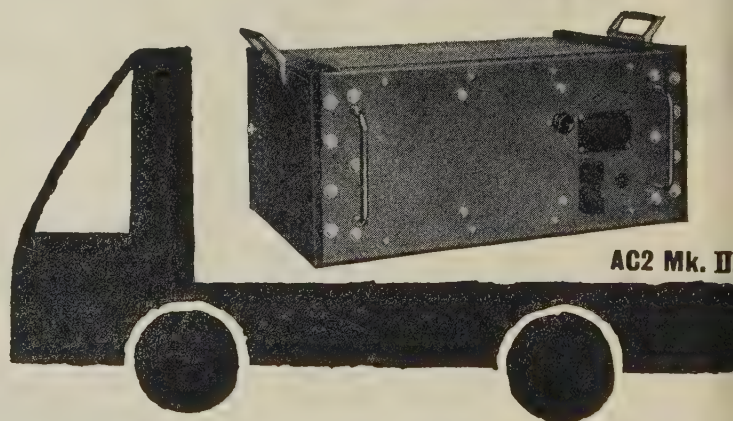
- ★ for bonding metals, porcelain, glass, etc.
- ★ for casting high grade solid insulation
- ★ for impregnating, potting or sealing electrical windings and components

- ★ for producing glass fibre laminates
- ★ for producing patterns, models, jigs, tools, etc.
- ★ as fillers for sheet metal work
- ★ as protective coatings for metal, wood and ceramic surfaces

Araldite epoxy resins

Araldite is a registered trade name

CIBA (A.R.L.) LIMITED Duxford, Cambridge. Telephone: Sawston 2121

TO THE ANTARCTIC**AC2 Mk. IIB****TO THE TROPICS****TO THE TEMPERATE ZONES****AC2 Mk. IIA****SERVOMEX**

standard A.C. stabilisers give A.1 service in all climates for ONE price

SERVOMEX a.c. voltage stabilisers are in use in the I.G.Y. programme in the Antarctic and in tropical Nigeria. These are in every way identical with the instruments in common use in this country. By extremely conservative design and by using components selected from the current inter-service approved list wherever possible, a very high degree of reliability is achieved. They will all withstand shock accelerations up to 40 g. These instruments introduce no distortion in the waveform whatever, and are not upset by changes of frequency, power factor, temperature, etc.

AC2 Mk. IIB and IIA

- 0 to 9 amps
- Range minus 17.5% to plus 8.75%
- 15 volts per second

AC7

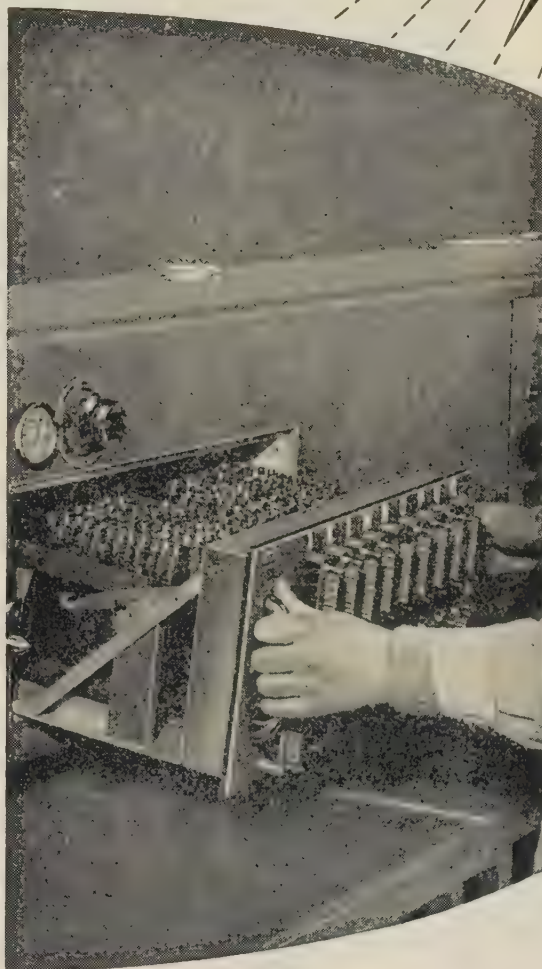
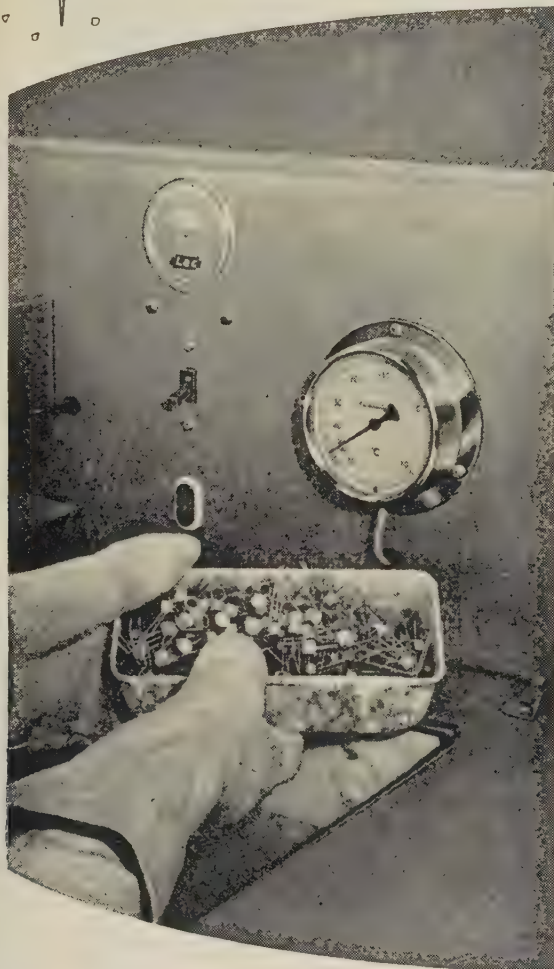
- 0 to 30 amps
- Range minus 20% to plus 10%
- 12 volts per second

Technical data sheets are available on request

**Servomex Controls Limited, Crowborough Hill,
Jarvis Brook, Sussex. Crowborough 1247**

-65°C**ENVIRONMENTAL TESTING**

Every Texas device is subjected to thorough environmental testing before despatch. This includes storage at -65°C. and +150°C. as well as continued operation at 150°C. After this, it is subjected to thorough drop and vibration testing.

+150°C

NEW 4 WATT POWER TRANSISTOR

THE NEW TEXAS medium power transistor with a collector dissipation of 4 watts makes possible a high degree of miniaturisation of servo amplifiers. For example a pair in Class 'B' push-pull operating from a 36 volt supply gives 4 watts output, sufficient to drive a size 10 servo motor at full torque.

Additional important features of these new devices are: a minimum alpha cut-off frequency of 4 Mc/s, collector voltages of 60 for the 2S017 and 100 for the 2S018, and a maximum storage temperature of 200°C.

Circuit design information on these and other Texas power transistors is provided in our Application Report on servo amplifier design.



TEXAS INSTRUMENTS LIMITED

Pioneers of Semiconductors

DALLAS ROAD, BEDFORD. TEL: BEDFORD 68051 CABLES: TEXINLIM BEDFORD

FERRANTI DUNDEE **offer a wide range of** **Microwave Components**

- 1** Ferrite Devices and Materials
- 2** Broad Band T.R. Cells
- 3** Tuneable T.R. Cells
- 4** Magnetrons
- 5** Noise Sources
- 6** Waveguide Windows

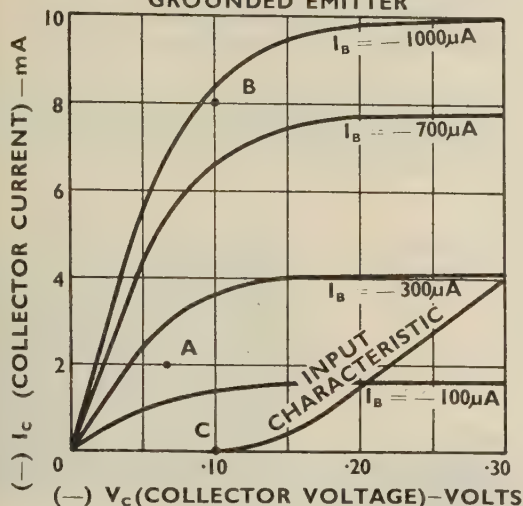
Please write for further details to:-



FERRANTI LTD · KINGS CROSS ROAD · DUNDEE

Telephone. DUNDEE 87141

**TYPICAL COLLECTOR CHARACTERISTIC
SATURATION REGION
SB 240 SURFACE BARRIER TRANSISTOR
GROUNDED EMITTER**



what does this mean?

CONTROLLED CHARACTERISTICS

"On" condition Point A $I_c = -2\text{mA}$ $V_{ce} < -70\text{mV}$
 Point B $I_c = -8\text{mA}$ $V_{ce} < -100\text{mV}$
 "Off" condition Point C $V_{be} = -100\text{mV}$ $I_c < -150\text{uA}$
 High Frequency current gain $h_{fe} > 5$ at 4 Mc/s
 Hole Storage factor $K's < 120$ millimicroseconds

These two superimposed curves of the Semiconductors SB 240 transistor mean that over 75% of computer components are no longer necessary.

The collector saturation voltage of the SB 240 is low enough to turn off the base current in the succeeding stage with direct connection—eliminating coupling capacitors, bias resistors and decoupling capacitors, and power supplies for bias purposes. These two bistable circuits indicate the possible simplification.

The unparalleled performance of the SB 240 in high speed switching circuits is due to the control of saturation voltage, input characteristic, high frequency current gain and hole storage factor. Experience in America indicates that these Surface Barrier Transistors are making possible a new order of Computer reliability, the direct result of the automatic equipment and ideal environmental conditions used by Philco—and also by Semiconductors Limited—in manufacture.

OTHER *Semiconductors* SWITCHING TRANSISTORS

SB 344
SB 345

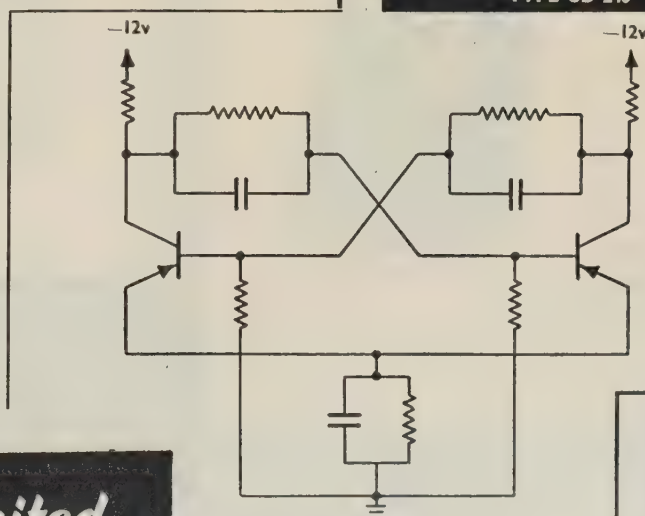
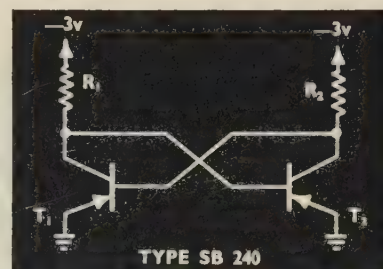
30 Mc/s Surface Barrier Transistors for use in less exacting applications than the SB 240.

2N393

40 Mc/s high gain Micro-Alloy Transistor particularly useful for driving a large number of parallel loads.

2N501

250 Mc/s Micro-Alloy Diffused Transistor for use when rise, fall and storage times of the order of 10 millimicroseconds are required.



CHENEY MANOR
SWINDON, WILTS
TELEPHONE: SWINDON 6421/2



SC 8

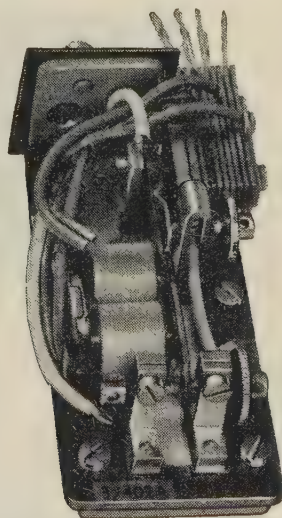
Semiconductors Limited

Full technical data on the application of the SB 240 to high speed computer circuits are available on request.

3

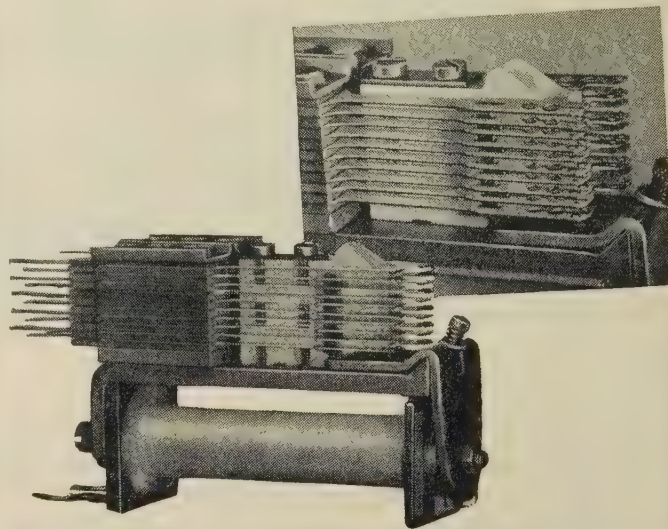
outstanding RELAYS

These relays are
available for early delivery;
your enquiries are welcomed.



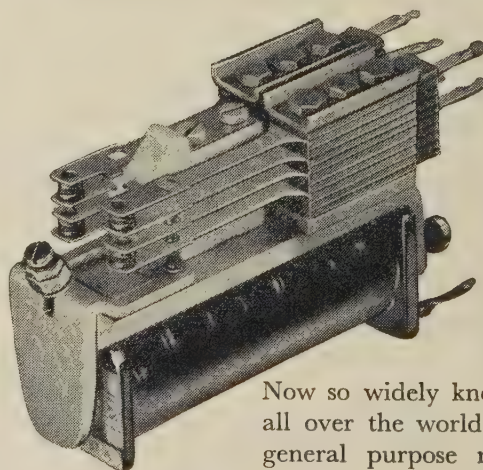
*High Speed
Relay.*

Originally developed for use in fast telephone switching circuits, this high speed relay is of great value in automation systems. It can effect a single changeover action in as little as 1.5 milliseconds. A high speed relay is also available with two changeover actions.



Comb Relay.

This is our latest development in relays and will give 100 million operations without the need for readjustment. Long life and reliability have led to its adoption by the British Post Office for use where continuous pulsing is required. A wide range of contact combinations is available with a maximum of 10 make or 10 break actions. It is suitable for switching light currents at 250 v.



*B.P.O.
3000 Type.*

Now so widely known and used all over the world, this versatile general purpose relay was designed by us in the early thirties for the British Post Office. Many millions are now in use in both telephone and industrial applications. It is available in an extremely wide range of coil resistances and spring set combinations for practically all normal voltages and frequencies.



SIEMENS EDISON SWAN LTD.

An A.E.I. Company

Woolwich, London, S.E.18

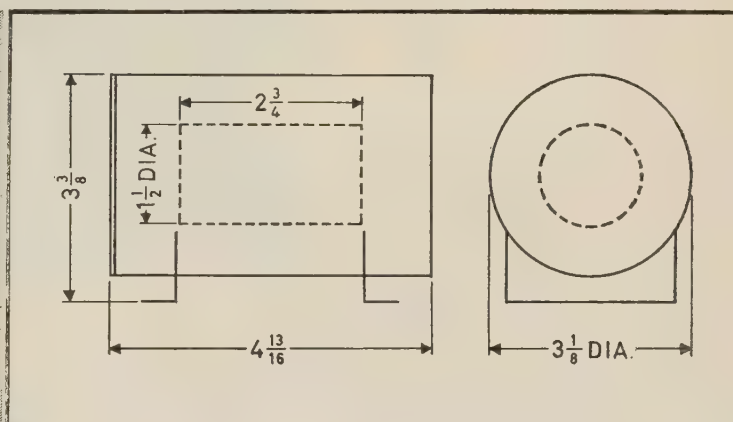
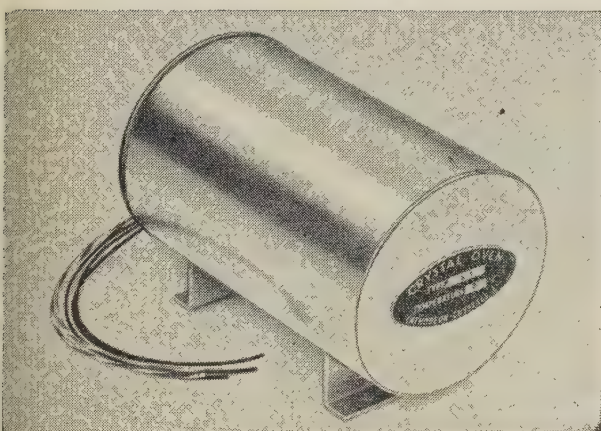
Telephone: Woolwich 2020 Extn. 621

CATHODEON

CRYSTALS LIMITED

Specialists in Frequency Control

... now introduce a range of **Thermostatically Controlled Ovens** specially designed to accommodate crystal units of all types. These ovens can also be used at lower temperature settings for electronic devices which are sensitive to ambient temperature changes such as transistors, diodes, etc.



"B" SERIES THERMOSTATICALLY CONTROLLED OVEN

B1. Bridge Controlled Circuit.	Temperature Stability	$\pm 0.01^{\circ}\text{C.}$
B2. Contact Thermometer Controlled	" "	$\pm 0.1^{\circ}\text{C.}$
B3. Bi-metal Thermostat Controlled	" "	$\pm 1^{\circ}\text{C.}$

All available in a wide range of temperature settings.

CATHODEON CRYSTALS LIMITED
LINTON CAMBRIDGESHIRE
TELEPHONE LINTON 501 (3 lines)



MUTUAL & SELF INDUCTANCE BRIDGE



Designed for the accurate measurement of either mutual or self inductance and resistance in the range $0.001\mu H$ to $30mH$ and $100\mu\Omega$ to 3000Ω respectively.

All measurements are made in the form of a four-terminal network and inductance and resistance of leads and clips are not included in the measurement.

Accuracy within $\pm 1\%$ frequency $1592c/s$ ($\omega = 10\,000$)

Full technical information on this and other 'Cintel' Bridges is available on request.

CINEMA TELEVISION LTD

A COMPANY WITHIN THE RANK ORGANISATION LIMITED

WORSLEY BRIDGE ROAD • LONDON • S.E.26
HITHER GREEN 4600

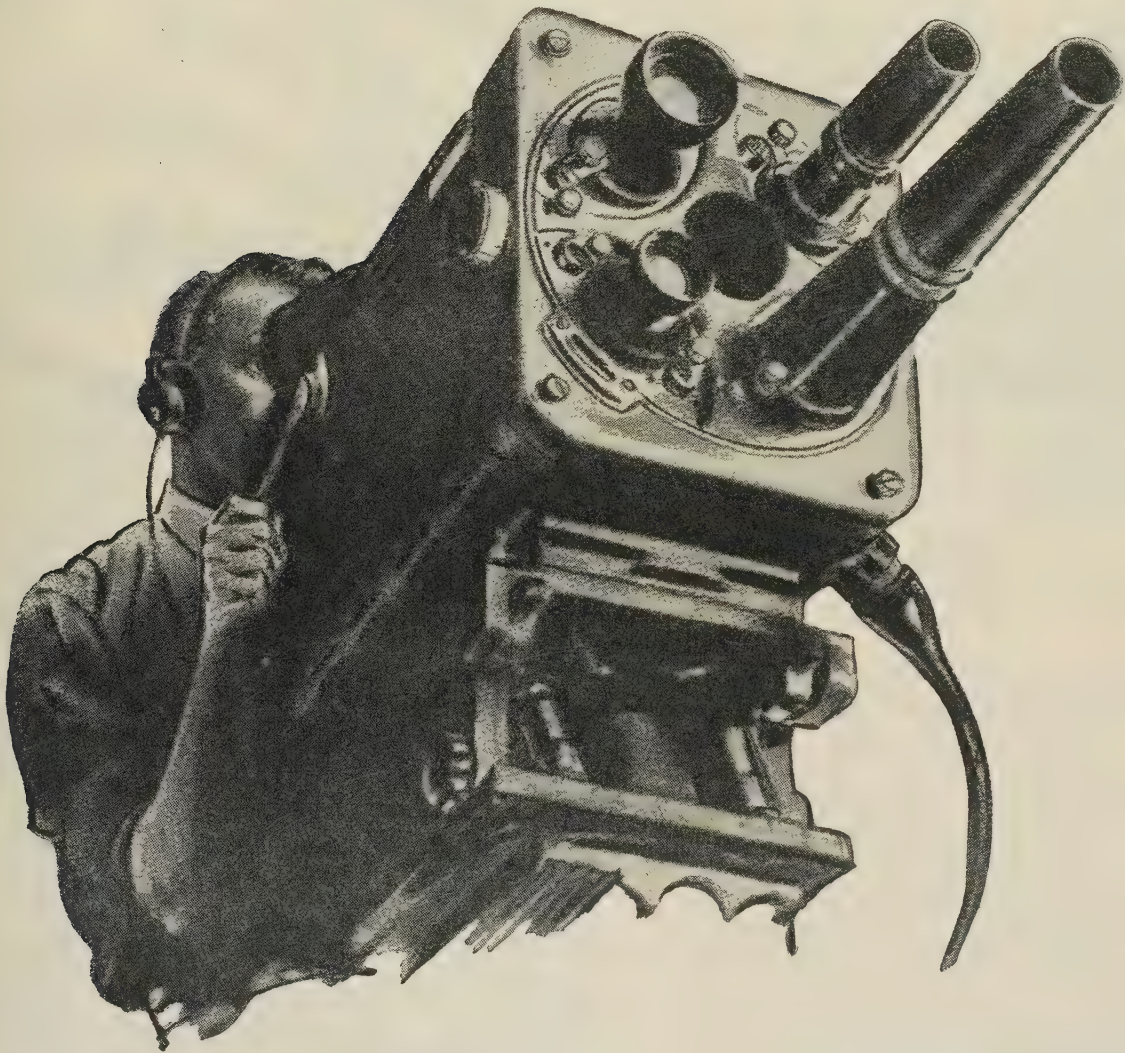
SALES AND SERVICING AGENTS

Hawnt & Co. Ltd., 59 Moor St. Birmingham 4

Atkins, Robertson & Whiteford Ltd., Industrial Estate, Thornliebank, Glasgow

McKellen Automation Ltd., 122 Seymour Grove, Old Trafford, Manchester 16

Marconi in Television

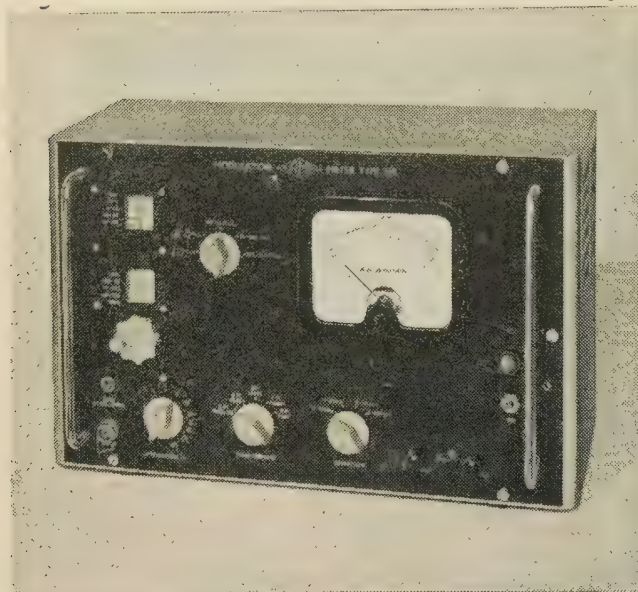


18 countries rely on Marconi Television
Transmitting or Studio Equipment

MARCONI

COMPLETE TELEVISION SYSTEMS

Measuring Modulation?



MODULATION METER

measures

- percentage modulation of amplitude modulated signals
- peak deviation of frequency modulated signals

THE MODULATION METER Type 210

may be used to measure the percentage modulation of amplitude modulated signals and the peak deviation of frequency modulated signals in the carrier frequency range 2.25 Mc/s to 300 Mc/s.

Outputs at the intermediate frequency of 750 kc/s and at low frequency are available from terminals on the front panel. These outputs enable the modulated envelope of the input signal and the demodulated signals to be observed on an oscilloscope.

The limiting action of the instrument is so effective that it can be used to measure spurious frequency modulation occurring on amplitude modulated signals. Furthermore, changes of mean carrier level when amplitude modulation is applied can be measured to an accuracy of better than $\pm 1\%$.

Simplicity of Operation

One of the most attractive features of the instrument is its simplicity of operation. The tuning control is adjusted until a meter reading is obtained, and the input attenuator adjusted for full scale deflection. It is then only necessary to switch to the A.M. or one of the F.M. positions to obtain a direct reading of modulation.

Statistics of Airmec Modulation Meter

- * Frequency range . . . 2.25 to 300 Mc/s in 7 bands (up to 600 Mc/s with reduced sensitivity)
- * Input level . . . A.M. 7-700 mV
F.M. 7 mV-10 V (3 kc/s-100 kc/s)
50 mV-10 V (0-3 kc/s)
- * Modulation Frequency range 30 c/s-15 kc/s
- * A.M. range . . . 0-100% $\pm 3\%$
- * F.M. range . . . 0-100 kc/s $\pm 5\%$

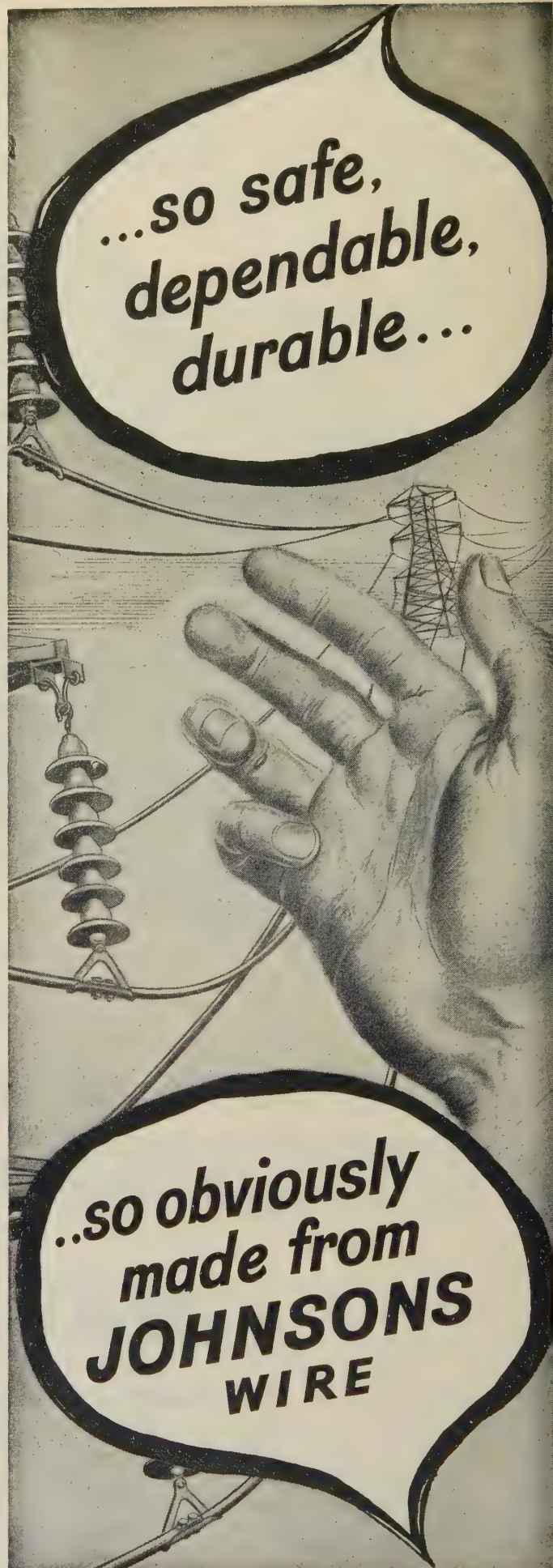
DELIVERY—EX STOCK

Airmec

**AM/FM Modulation
Meter Type 210**

AIRMEC LIMITED • HIGH WYCOMBE • BUCKS
Telephone: High Wycombe 2060

...so safe,
dependable,
durable...



..so obviously
made from
**JOHNSONS
WIRE**

No. 8



**Permanent
Magnets**

**Design
Advisory
Service**

Demagnetisation

Advertisements in this series deal with general design considerations. If you require more specific information on the use of permanent magnets, please send your enquiry to the address below, mentioning the Design Advisory Service.

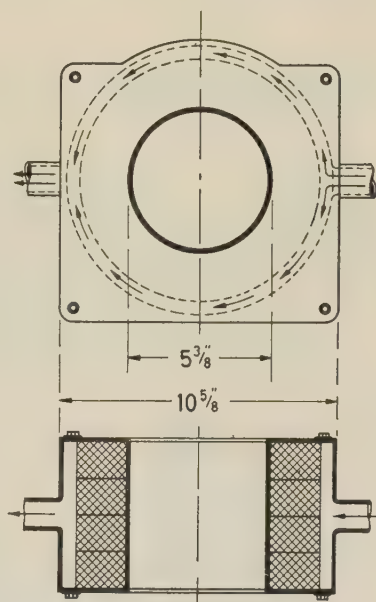
There are two types of demagnetisation normally associated with permanent magnets. The first can be considered the controlled or precision reduction of the field for adjustment or stabilisation purposes. The second is the complete demagnetisation of the magnet to facilitate handling and assembly, and the avoidance of collecting magnetic particles. Providing the magnets are relatively small—that is—not exceeding about 2 lb. in weight, both methods of demagnetisation can conveniently be used with normal 50 c.p.s. power supply.

The first type of demagnetisation can be achieved in an accurately controllable a.c. field, usually by putting the magnet assembly into an air cored coil and controlling the a.c. supply by means of a variable transformer. If a very fine control is required for precision adjustment, a series choke with a movable iron core can be used to give infinitely fine adjustment of the field.

The second type of demagnetisation can be carried out in a similar manner, except that considerably more power is used. Generally it is found most convenient to connect the power supply direct to the coil and to move the magnetised magnets fairly slowly through the coil. Although theoretically, a field of 1,200 oersteds is sufficient for 'Ticonal' magnets, due to the screening effect of associated iron circuits the effectiveness of the field is considerably reduced, and the exact field requirements for this process cannot easily be calculated. The quickest method of finding the actual field requirements and current necessary, is by experimentation.

For 'Magnadur' magnets a demagnetising field in the region of 6,000 oersteds is necessary. An alternative method is to raise the temperature of the whole magnet past the curie point which is approximately 450°C., care should be taken to keep the temperature gradient small to avoid fracture of the magnet due to thermal expansion.

The demagnetisation of large magnets sometimes necessitates the use of lower frequency than 50 c.p.s. but as large magnets constitute unusual or special cases for which general instructions cannot easily be given, we would recommend engineers request assistance from our Design Advisory Service if they meet any unexpected difficulty.



Typical Air Cooled Demagnetising Coil

Technical details of coil :

Four sections each consisting of 75 turns of 12 s.w.g. D.C.C. wire arranged as shown and connected in series.

Supply :

400 volts 50 c.p.s. at 25 amps approx.

Mullard



'TICONAL' PERMANENT MAGNETS
'MAGNADUR' CERAMIC MAGNETS
FERROXCUBE MAGNETIC CORES

**ELECTRONIC COMPUTER
EXHIBITION**

Nov. 28th—Dec. 4th
OLYMPIA · STAND 2

Wire for electrical progress

Lewmex or Lewkanex, Lewcosol or Lewco-glass—just a few of the 'LEWCOS' range of insulated wires designed to meet every need or application in the electrical industry, backed by intensive research and a first class technical service.



LEWCOS

*the largest manufacturers of
insulated wires and strips in Europe*

THE LONDON ELECTRIC WIRE COMPANY AND SMITHS LIMITED

LEYTON • LONDON • E10



ADCOLA
(Regd. Trade Mark)

Soldering Instruments

ILLUS- TRATED

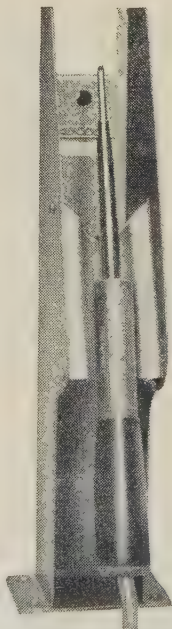
PROTECTIVE
SHIELD
(CAT. No. 68)

$\frac{1}{8}$ in. BIT
MODEL
(CAT. No. 70)

Primarily
developed for
the

TRANSISTOR &
ELECTRONIC
ERA.

Possessing the
sharp heat
essential for the
quick jointing
of Transistors,
Resistors, etc.,
thereby avoiding
damage to the
equipment from
heat transference



Cover all requirements
for thorough solder
jointing in all the fields
of

**TELECOM-
MUNICATIONS**

Fully Insulated
Elements

Suited to daily use for
bench line production

**MANUFACTURED
IN ALL VOLT
RANGES**

British and Foreign Pats.
Reg. designs, etc.

For further information
apply Head Office:

**ADCOLA
PRODUCTS LTD.
GAUDEN ROAD
CLAPHAM
HIGH STREET
LONDON, S.W.4**

Tel.: MACaulay 4272
& 3101

THE INSTITUTION OF ELECTRICAL ENGINEERS
presents

THE INQUIRING MIND

a film outlining the opportunities for a career
in the field of electrical engineering

Producer: Oswald Skilbeck Director: Seafeld Head

Commentator: Edward Chapman

Copies of the film may be obtained on loan by schools and other organisations for showing to audiences of boys and girls or others interested in a professional career in electrical engineering. The film is available in either 35mm or 16mm sound, and the running time is 30 min.

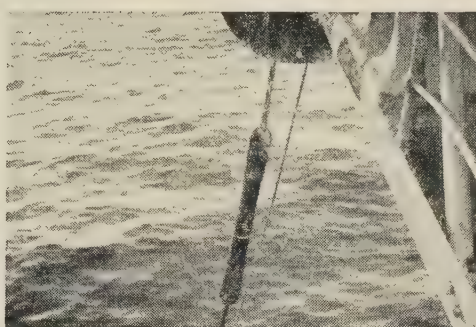
Application should be made to

THE SECRETARY

THE INSTITUTION OF ELECTRICAL ENGINEERS
SAVOY PLACE, LONDON, W.C.2



Communications by Submarine Cable



The laying of the trans-Atlantic telephone cable in 1956 ranks as one of the most important engineering feats in the history of telecommunications. Previously undersea communication had been limited to telegraph services and telephone facilities over relatively short distances. Amplification was the major obstacle—the problem of maintaining telephone signals at intelligible strength. This problem could only be solved by the use of repeaters spliced into the cable, and capable of working for many years unattended on the sea bed. On the important Nova Scotia—Newfoundland section of the trans-Atlantic cable, seventeen STC repeaters are used.

For over 30 years STC has taken the lead in the development of undersea communication equipment and techniques, and as the company celebrates its 75th. anniversary the latest important assignment has just been completed. This is the Anglo-Belgian Submarine Telephone Cable Scheme—a 55 nautical mile link that interconnects the national telephone networks of the two countries.

It is significant that this was the first time that one company had been entrusted with the manufacture of the undersea cable and submerged repeaters, as well as terminal equipment... a high tribute to the experience and unique resources of one of the Commonwealth's greatest telecommunications organisations.



Standard Telephones and Cables Limited

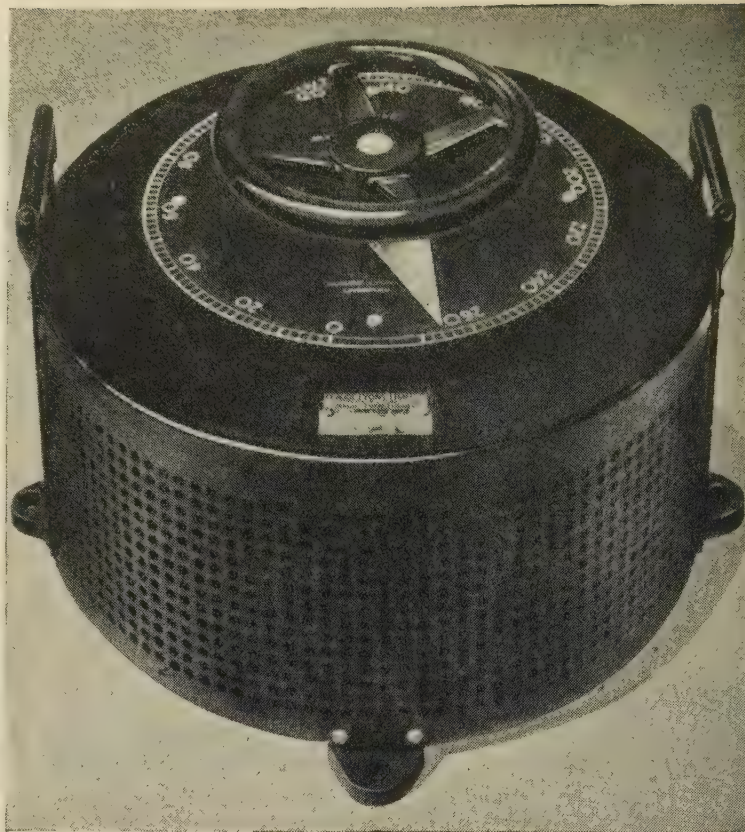
TELECOMMUNICATION ENGINEERS

CONNAUGHT HOUSE • ALDWYCH • LONDON • W.C.2
CAIRO • DUBLIN • JOHANNESBURG • KARACHI • NEW DELHI • SALISBURY

VARIACS for S-M-O-O-T-H Voltage Control

'VARIAC' is the *original*, continuously adjustable auto-transformer—and the only one having 'DURATRAK', a specially treated track surface. For varying the a-c voltage applied to any electrical, electronic, radar or communications equipment a 'VARIAC' offers considerable advantages over any other type of a-c control—it has longer life, absolute reliability, much increased overload capacity, resistance to accidental short-circuits and appreciably greater economy in maintenance. Voltages from zero to 17% above line are obtained by a 320° rotation of the shaft, which is equipped with an accurately calibrated direct-reading dial. Available in various sizes from 170 VA up to 25 kilowatts, including 3-gang assemblies for 3-phase working, 'VARIACS' are competitively priced, and, compared with the losses of resistive controls often save their initial cost within a year.

Most "VARIACS" are now MUCH REDUCED IN PRICE: send for our new, profusely illustrated Catalogue 424-UK/16, which gives complete information on the entire range. HUNDREDS of models—all available promptly—most EX STOCK.



Claude Lyons Ltd.

76 Oldhall Street, Liverpool, 3, Lancs. Telephone: Central 3641
Valley Works, Hoddesdon, Herts. Telephone: Hoddesdon 3007-8-9

CL31

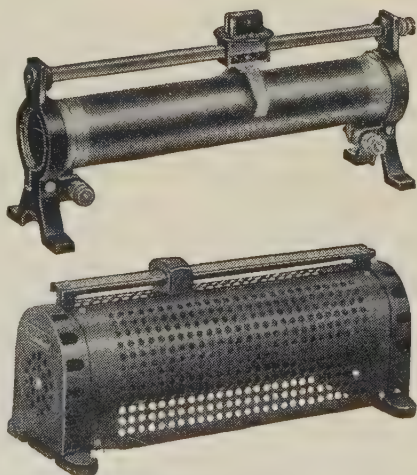
ZENITH

(REGD. TRADE-MARK)

TUBULAR SLIDING RESISTANCES

Zenith Resistances of proved durability are in constant satisfactory use in all parts of the world. They are available in a great variety of types and sizes, and are ideal for use in laboratories and test rooms.

Illustrated catalogue of all types free on request

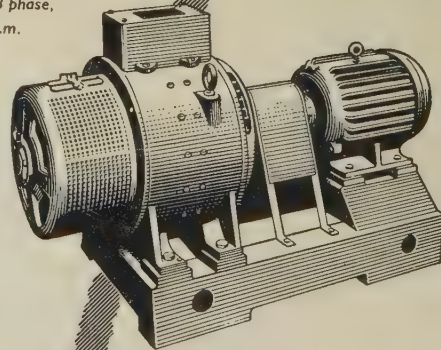


The ZENITH ELECTRIC CO. Ltd.
ZENITH WORKS, VILLIERS ROAD, WILLESDEN GREEN
LONDON, N.W.2

Telephone: WILlesden 6581-5 Telegrams: Voltaohm, Norphone, London
MANUFACTURERS OF ELECTRICAL EQUIPMENT
INCLUDING RADIO AND TELEVISION COMPONENTS

ELECTRICAL EQUIPMENT

High Frequency
Motor Alternator Set
5 kVA, 208 volts, 3 phase,
400 c.p.s. 3000 r.p.m.



A leaflet giving full particulars
will be sent on request.

NEWTON DERBY

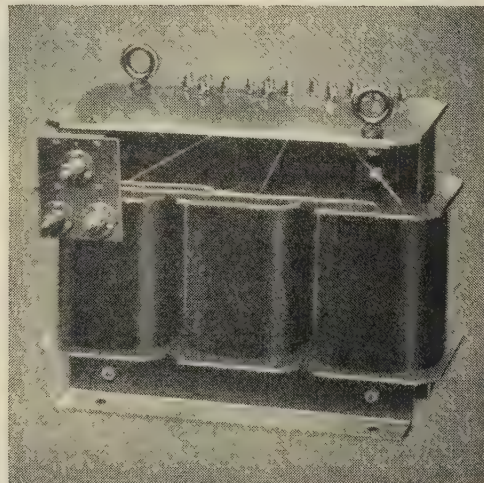
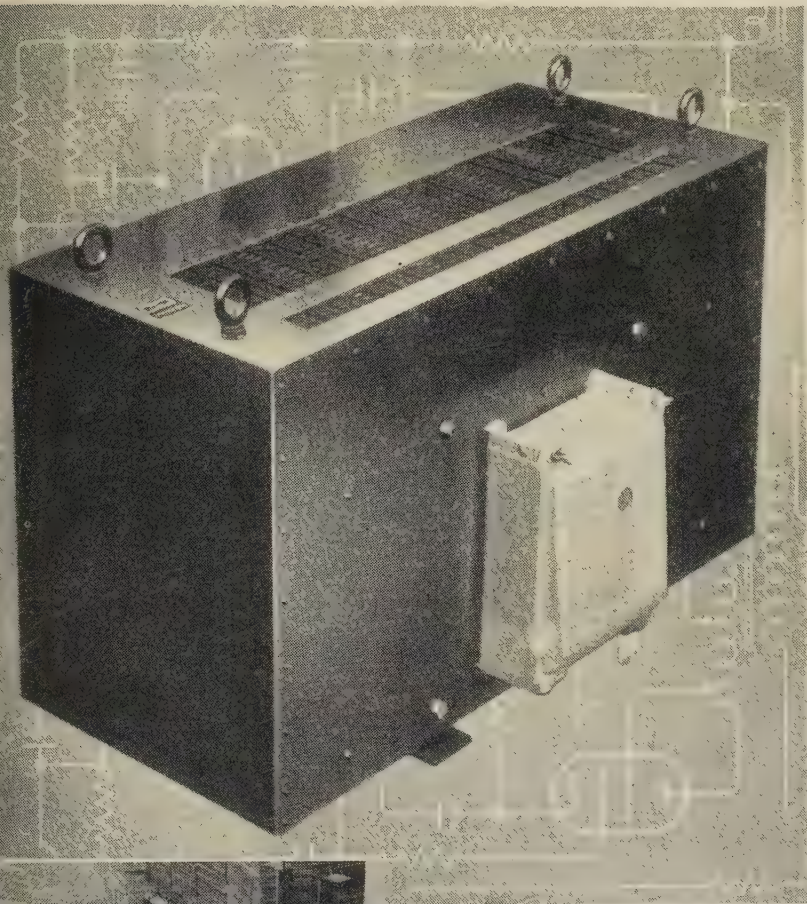
—NEWTON BROS. (DERBY) LTD

ALFRETON ROAD, DERBY

PHONE: DERBY 47676 (4 LINES) GRAMS: DYNAMO, DERBY
London Office: IMPERIAL BUILDINGS, 56 KINGSWAY W.C.

Complicated or simple

In all Massicore transformers, however complicated or simple, the essential ingredient is the same—conscientious craftsmanship. Massicore transformers are built to last a lifetime. Equally important is the individual attention given to all enquiries and orders regardless of size; and we make a point of keeping our delivery promises.



On the left (with an internal view shown beneath) is a three-phase power transformer with six channels per phase. Each channel has tapings to enable any voltage up to 180 to be selected in 5-volt steps. Maximum loading per channel—5 amps.

And above, less complicated but equally well made, is a three-phase H.T. transformer, delta-connected primary, star-connected secondary. Secondary 4300 v. 6 kVA. rating.

Your requirements may call for instruments very different from these examples. Please take advantage of our experience, knowledge and constructional skill in the production of all types of transformers.



Corner for Contented Customers

"I am writing to express my congratulations to you on the success of the Spark Gap Transformer which you made recently. The transformer, as I indicated over the 'phone, is functioning excellently and I do feel that your basis of design appears to be superior . . ."

C.E.T. BERKSHIRE



SAVAGE TRANSFORMERS LIMITED. Devizes, Wiltshire. Tel: Devizes 932

TP/57

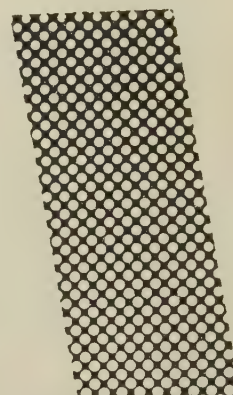


RIGHT Air-cooled Torch. For currents up to 100 amps.

LEFT Water-cooled Torch. Maximum current capacity 350 amps.

when heat is the problem

British Oxygen fit their Argon-arc welding torches with SINTOX Ceramic Shields, having proved that SINTOX successfully withstands the thermal stresses imposed by the process. SINTOX *is in the forefront of industrial development.*



...the unfailing answer is



Sintox Technical Advisory Service

This service is freely available without obligation to those requiring technical advice on the application of Sintox Industrial Ceramics. Please write for booklet or any information required enclosing blue print if available.

SINTOX
INDUSTRIAL CERAMIC

SINTOX IS MANUFACTURED BY LODGE PLUGS LTD., RUGBY

THE JOURNAL OF *The British* *Nuclear Energy Conference*

The Institution of Civil Engineers The Institution of Mechanical Engineers
The Institution of Electrical Engineers The Institute of Physics
The Institution of Chemical Engineers The Institute of Metals
The Iron and Steel Institute The Institute of Fuel
The Joint Panel on Nuclear Marine Propulsion



PUBLISHED JANUARY, APRIL, JULY, OCTOBER

The Journal contains Papers and discussions on the applications of nuclear energy and ancillary subjects

ANNUAL SUBSCRIPTIONS:

MEMBERS 30/- post free

NON-MEMBERS 60/- post free

Full particulars are available from

The Secretary • B.N.E.C. • 1-7 Great George Street • London • SW1

Marconi

V.H.F. SIGNAL GENERATOR TF 1064 and TRANSMITTER/RECEIVER OUTPUT TEST SET TF 1065

These two compact, portable units together provide full testing facilities for f.m. and a.m. mobile radio telephone sets. The range of tests which can be made is extremely comprehensive and for receivers includes sensitivity, bandwidth, signal-to-noise ratio, image rejection, discriminator symmetry, and a.f. power output. For transmitters, p.a. tuning, r.f. power output, and deviation can all be checked. If you would like further details of these versatile instruments, please write for Leaflets K138.



AM & FM SIGNAL GENERATORS • AUDIO & VIDEO OSCILLATORS
FREQUENCY METERS • VOLTMETERS • POWER METERS
DISTORTION METERS • FIELD STRENGTH METERS
TRANSMISSION MONITORS • DEVIATION METERS
OSCILLOSCOPES, SPECTRUM & RESPONSE ANALYSERS
Q METERS & BRIDGES

MARCONI INSTRUMENTS LTD • ST. ALBANS • HERTFORDSHIRE • TELEPHONE ST. ALBANS 56161
London and the South: Marconi House, Strand, London, W.C.2. Tel: COVent Garden 1234. Midlands: Marconi House, 24 The Parade, Leamington Spa. Tel: 1408
North: 23/25 Station Square, Harrogate. Tel: 67455.

TC 138

Publications of
THE INSTITUTION OF ELECTRICAL ENGINEERS

*Journal of The Institution—Monthly
Proceedings of The Institution*

PART A (Power Engineering)—Alternate Months
PART B (Radio and Electronic Engineering—including Communication Engineering)—
Alternate Months
PART C (Institution Monographs)—In collected form twice a year

Special Issues

VOL. 94 (1947) PART IIA (Convention on Automatic Regulators and Servomechanisms)
VOL. 94 (1947) PART IIIA (Convention on Radiocommunication)
VOL. 97 (1950) PART IA (Convention on Electric Railway Traction)
VOL. 99 (1952) PART IIIA (Convention on the British Contribution to Television)
VOL. 100 (1953) PART IIA (Symposium of Papers on Insulating Materials)
Heaviside Centenary Volume (1950)
Thermionic Valves: the First 50 years (1955)
VOL. 103 (1956) PART B SUPPLEMENTS 1-3 (Convention on Digital-Computer Techniques)
VOL. 103 (1956) PART A Supplement 1 (Convention on Electrical Equipment for Aircraft)
VOL. 104 (1957) PART B SUPPLEMENT 4 (Symposium on the Transatlantic Telephone Cable)
VOL. 104 (1957) PART B SUPPLEMENTS 5-7 (Convention on Ferrites)
VOL. 105 (1958) PART B Supplement 8 (Symposium on Long Distance Propagation above 30 Mc/s)
VOL. 105 (1958) PART B Supplement 9 (Convention on Radio Aids to Aeronautical and
Marine Navigation)



PROCEEDINGS - *Paper and Reprint Service*

PAPERS READ AT MEETINGS

Papers accepted for reading at Institution meetings and subsequent republication in the *Proceedings* are published individually without delay, free of charge. Titles are announced in the *Journal of The Institution*, and abstracts are published in *Science Abstracts*.

REPRINTS

After publication in the *Proceedings* all Papers are available as Reprints, price 2s. (post free). The Reprint contains the text of the Paper in its final form, together with the Discussion, if any. Those who obtain a copy of a Paper published individually—if they do not take the Part of the *Proceedings* in which it will be republished—are urged to apply in due course for a Reprint, as this is the final and correct version.

CONVENTION PAPERS

Papers accepted for presentation at a Convention or Symposium, and subsequent republication as a Supplement to the appropriate part of the *Proceedings*, are published shortly before the Convention, but are usually available only in sets. No Reprints are available.

MONOGRAPHS

Institution Monographs (on subjects of importance to a limited number of readers) are available separately, price 2s. (post free). Titles are announced in the *Journal* and abstracts are published in *Science Abstracts*. The Monographs are collected together and republished twice a year as Part C of the *Proceedings*.

An application for a Paper, Reprint or Monograph should quote the author's name and the serial number of the Paper or Monograph, and should be accompanied by a remittance where appropriate. For convenience in making payments, books of five vouchers, price 10s., can be supplied.

SCIENCE ABSTRACTS

Published monthly in two sections

SECTION A: Physics

SECTION B: Electrical Engineering

Prices of the above publications on application to the Secretary
of The Institution, Savoy Place, W.C.2.

EDISWAN Transistor news

MAZDA

Ediswan Mazda transistors are currently used in a wide range of electronic equipment. Get the facts about them at your finger tips—if you have not already applied for a complete set of Ediswan Mazda semiconductor Technical Data Sheets, we suggest that you do so now on your company's letter heading.

A SYMMETRICAL TRANSISTOR FOR SWITCHING CIRCUITS AND MODULATORS

The new Ediswan Mazda XS101 transistor has two identical 'P' type germanium electrodes; with appropriate bias conditions either will act as emitter with the other as collector. The average characteristics for the two conditions are identical.

**The new XS101 transistors can now be supplied, against order, for evaluation purposes.*

SYMMETRICAL TRANSISTOR TYPE XS 101

TENTATIVE RATINGS. Absolute values for 45°C. ambient

Maximum mean or peak collector/emitter voltage (with base maintained at least 1 v. positive with respect to the positive end of the emitter supply battery)	V	—20
Maximum mean or peak collector/emitter voltage (conducting)	V	—12
Maximum mean or peak collector to base voltage	V	—21
Maximum collector dissipation	mW	90
Maximum junction temperature	°C	75
Thermal resistance in free air	°C/mW	0.33

TENTATIVE CHARACTERISTICS at 25°C.

*Common base cut-off frequency (minimum)	Mc/s	2.5
*Average Current Amplification, Common Emitter (Degree of asymmetry, 1.5 to 1)	β	20
*Small signal values at $V_c = -5V$, $I_c = -1mA$.		

INCREASED RATINGS FOR EDISWAN MAZDA TRANSISTORS

The table on the right shows the increased ratings (absolute at 45°C.) which now apply.

TRANSISTOR TYPE XC 101

Maximum peak or mean collector/emitter voltage (common emitter circuit)	—16 v.
Maximum peak collector to emitter voltage with base driven to cut off (common emitter circuit) with external base/emitter circuit resistance less than 500 ohms	—35 v.
Maximum peak or mean collector/base voltage (common base circuit)	—35 v.
Maximum junction temperature	75°C.

TRANSISTOR TYPES XB 102 AND XB 103

Maximum peak or mean collector/emitter voltage (common emitter circuit)	—16 v.
Maximum peak collector to emitter voltage with base driven to cut off (common emitter circuit) with external base/emitter circuit resistance less than 500 ohms	—35 v.
Maximum peak or mean collector/base voltage (common base circuit)	—35 v.

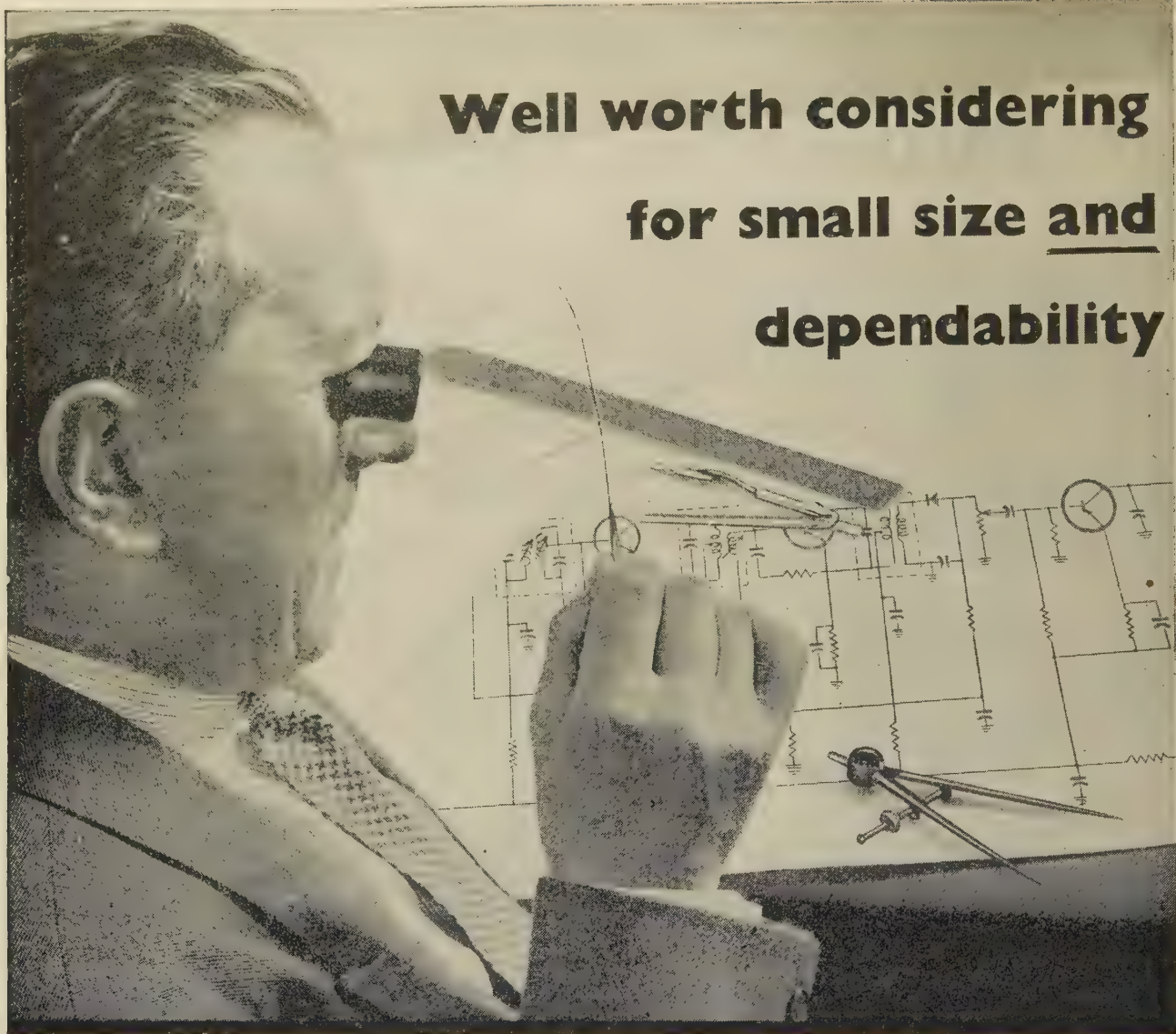
TRANSISTOR TYPES XA 101 AND XA 102

Maximum peak or mean collector/emitter voltage (common emitter circuit)	—16 v.
Maximum peak or mean collector/base voltage (common base circuit)	—20 v.

SIEMENS EDISON SWAN LIMITED, *An A.E.I. Company*

Valve and CRT Division, 155 Charing Cross Road, London W.C.1.

Well worth considering for small size and dependability



The new type BTH Germanium Point Contact Rectifiers —

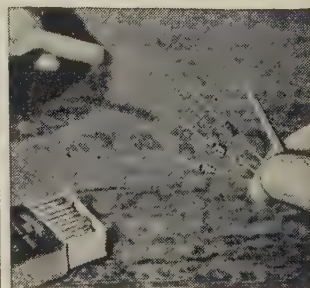
Only $\frac{1}{4}$ in. long, yet their miniature size is combined with high performance and complete dependability! They offer the following outstanding characteristics:

- HIGH TEMPERATURE STABILITY
- ABILITY TO WITHSTAND TROPICAL CONDITIONS
- SMALLER DIMENSIONS • VERY LONG LIFE

RATINGS · CONTINUOUS OPERATION AT 25°C. (77°F.)

TYPE	PEAK INVERSE VOLTAGE† V	MAX. INPUT CURRENT mA	MAX. RESISTANCE at + 1 volt ohms	MIN. RESISTANCE at - 50 volts kilohms
CV 448*	80	30	333	500
CG41-H	65	30	250	50
CG42-H	100	30	500	1,000
CG44-H	80	30	333	500
CG50-H	100	30	500	200

*Type CV 448 has been granted 'type approval'. †Corresponds to 1·2 mA inverse current.



BRITISH THOMSON-HOUSTON

THE BRITISH THOMSON-HOUSTON CO. LTD. · LINCOLN · ENGLAND

an A.E.I. Company

INDEX OF ADVERTISERS

<i>Firm</i>	<i>page</i>	<i>Firm</i>	<i>page</i>
Adcola Products Ltd.	xxxiv	Marconi Wireless Telegraph Ltd.	xxii & xxxi
Armec Ltd.	xxxii	Metropolitan Plastics Ltd.	xvi
Automatic Telephone & Electric Co. Ltd.	viii & ix	Metropolitan-Vickers Electric Co. Ltd.	
British Thomson-Houston Co. Ltd.	xlii	Mullard Ltd. (Magnetic)	xxxiii
Cable Makers Association	ii	Mullard Ltd. (Valves)	iii
Cathodeon Crystals Ltd.	xxix	Newmarket Transistors Co. Ltd.	vii
Ciba (A.R.L.) Ltd.	xxiii	Newton Bros. (Derby) Ltd.	xxxvi
Cinema Television Ltd.	xxx	Oliver Pell Control Ltd.	xxi
Clewthurst and Partner Ltd.		Philips Electrical Ltd.	xliii
Conovan Electrical Co. Ltd.		Plessey Co. (Swindon) Ltd.	x
English Electric Co. Ltd.	xvii	Redifon Ltd.	xiii
English Electric Valve Co. Ltd.	xliv	Salford Electrical Instruments Ltd.	xviii
E.M.I. Electronics Ltd.	i	Savage Transformers Ltd.	xxxvii
Electric Resistor Co. Ltd.	xii	Servomex Controls Ltd.	xxiv
Erranti Ltd.	xxvi	Semiconductors Ltd.	xxvii
F. Fox Ltd.		Smiths Industrial Instruments Ltd.	vi
General Electric Company (Telecommunications)	iv & v	Siemens Edison Swan Ltd. (Exchange Equipment)	xiv & xv, xxviii
Johnson & Nephew Ltd.	xxxii	Siemens Edison Swan Ltd. (Telecommunications)	xi
Page Plugs Ltd.	xxxviii	Siemens Edison Swan (Transistors)	xli
London Electric Wire Co. and Smiths Ltd.	xxxiv	Standard Telephones & Cables Ltd.	xx & xxxv
Maude Lyons Ltd.	xxxvi	Texas Instruments Ltd.	xxv
Marconi Instruments Ltd.	xxxix	R. Thomas and Baldwins Ltd.	
Marconi Wireless Telegraph Ltd./A.T.E.	xix	Zenith Electric Co. Ltd.	xxxvi

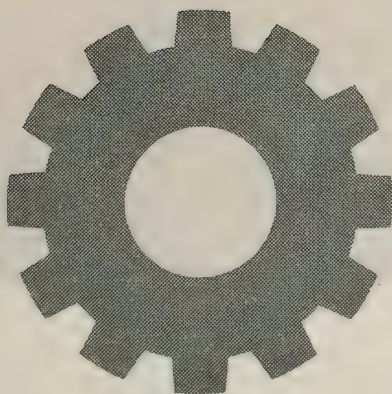


In Science and Industry alike . . .

among technicians, manufacturers and those engaged in the sale of electrical products — as well as among the public at large, the Philips emblem is accepted throughout the World as a symbol of quality and dependability.

PHILIPS ELECTRICAL LTD

Century House · Shaftesbury Avenue · London · WC2



Radio & Television Receivers · Radiograms & Record Players · Gramophone Records · Tungsten, Fluorescent, Blended and Discharge Lamps & Lighting Equipment · 'Philishave' Electric Dry Shavers · 'Photoflux' Flashbulbs · High Frequency Heating Generators · X-ray Equipment for all purposes · Electro-Medical Apparatus · Heat Therapy Apparatus · Resistance Welding Plant and Electrodes · Electronic Measuring Instruments · Magnetic Filters · Battery Chargers and Rectifiers · Sound Amplifying Installations · Cinema Projectors · Tape Recorders · Health Lamps · Hearing Aids · Electrically Heated Blankets

DAYLIGHT DIRECT-VIEWING STORAGE TUBE

E702

The E702 direct-viewing storage tube has electrostatic deflection and a useful screen diameter of 4 inches. The image on the screen persists without deterioration for one to two minutes, and is visible for periods up to ten minutes. It can be completely erased in 30 milliseconds by a small positive pulse applied to the backing electrode. Controlled persistence for longer periods can be obtained by varying the duration of shorter repetitive pulses.

Full technical details are available in our publication No. E.I., which can be obtained post free on request.



'ENGLISH ELECTRIC'

ENGLISH ELECTRIC VALVE CO. LTD.



Chelmsford, England
Telephone: Chelmsford 3491

The Institution is not, as a body, responsible for the opinions expressed by individual authors or speakers. An example of the preferred form of bibliographical references will be found beneath the list of contents.

THE PROCEEDINGS OF THE INSTITUTION OF ELECTRICAL ENGINEERS

EDITED UNDER THE SUPERINTENDENCE OF W. K. BRASHER, C.B.E., M.A., M.I.E.E., SECRETARY

VOL. 105. PART B. No. 24.

NOVEMBER 1958

21.317.33

The Institution of Electrical Engineers
Paper No. 2709 R
Nov. 1958

©

A NOVEL, HIGH-ACCURACY CIRCUIT FOR THE MEASUREMENT OF IMPEDANCE IN THE A.F., R.F. AND V.H.F. RANGES

By D. KARO, Dr.Eng., Ph.D., Dipl.Eng., Associate Member.

(The paper was first received 15th February, and in revised form 3rd April, 1958.)

SUMMARY

The paper describes a high-accuracy measuring circuit suitable for frequencies from 50 c/s to v.h.f.

There are two branches in the circuit, one of which contains the unknown impedance. The two branches are fed in phase opposition from the secondaries of two mutual inductors or two transformers.

Due to the feeding in opposition of the two branches, the transfer impedances are very simple, no negative real terms are present and no more than two variable standards are required for balance. The balance equations in the majority of cases do not contain the term ω (angular frequency), the frequency need not therefore be known very accurately and the calculations are simple.

Furthermore, at balance, the detector, source and all the circuit components except one have one terminal connected to earth. The potentials are therefore fixed and most of the capacitances to earth are eliminated; those that remain shunt one secondary and the standard in one branch of the circuit and can easily be determined or otherwise taken into account in the calculations.

Tests have been made over a wide range of resistance, inductance and capacitance between 100 c/s and 50 Mc/s. The error varied, according to the standards and the frequency used between $\pm 0.001\%$ and $\pm 0.01\%$.

(1) INTRODUCTION

The most serious disadvantages of the shunted-T circuits, whether simple or modified wide-range* are the presence of the term ω^2 (angular frequency) in the balance equations and the number of standards which have to be adjusted for balance. The presence of the term ω^2 requires that the frequency of the source be not only stable, but also known very accurately, whilst the large number of standards increases the possible error of measurement and also makes the manipulation more difficult.

The reason for the existence of these disadvantages is fairly obvious: as the currents from shunt and T flowing into the detector must be equal and in opposition, and as both shunt

and T are fed in phase from the source, a fairly complicated network, namely the T, is required.

The T must constitute an effective transfer impedance, equal and of opposite sign to that of the shunt (or the transfer impedance of shunting T)—hence the presence of the term ω^2 in the balance equations and the necessity for more than two variable standards.

A circuit could, however, be arranged consisting of two simple branches, one in lieu of the shunt and the other in lieu of the T, fed in opposition by means of transformers or mutual inductances. The two branches could then be composed of impedances of the same nature and could consist simply of a resistance and inductance or resistance and capacitance. The transfer impedances being very much simpler, the term ω^2 could be made to disappear from most balance equations, and at the most two variable standards would be required.

(2) BASIC CIRCUIT AND PRINCIPLE OF THE NOVEL METHOD OF MEASUREMENT

The measuring circuits described below, which could be named shunted-L circuits, are fed from the secondaries of two mutual inductors or two small Permalloy-core transformers (similar to those used in admittance bridges*), according to the frequency, the primaries or primary being connected to the source.

There are two branches containing standards: one is fed from one secondary, the other from the two secondaries, these being either in phase or in opposition.

One terminal of the detector is connected to the junction point of the two branches and the other to the return of one secondary; this return wire is earthed, together with one terminal of the source. At balance, therefore, the detector, source and all the circuit components except one have one terminal connected to earth.

The potentials are therefore fixed, and most of the capacitances to earth are eliminated; those earth capacitances that remain shunt one secondary and the standard in one branch of the circuit, and can be easily determined or otherwise taken into account in the calculations.

The earth capacitance that does remain in the other branch

* KARO, D.: 'A Modified Wide-Range Shunted-T Circuit for the Measurement of Impedance in the A.F., R.F., and V.H.F. Ranges', *Proceedings I.E.E.*, Paper No. 1958, M, January, 1953 (100, Part III, p. 25).

Written contributions on papers published without being read at meetings are accepted for consideration with a view to publication. D. Karo is in the Electrical Engineering Department, College of Technology, Birmingham.

* KIRKE, H. L.: Chairman's Address to Radio Section, *Journal I.E.E.* 1945, 92, Part III, p. 2.

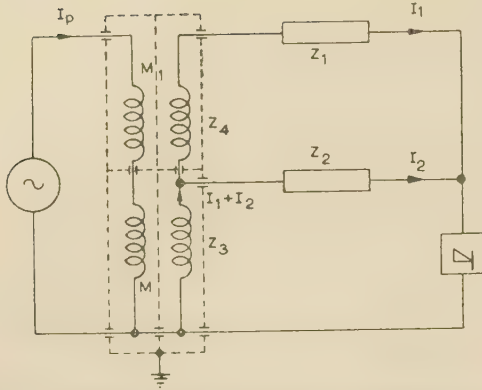


Fig. 1.—Basic circuit with two separate mutual inductors.

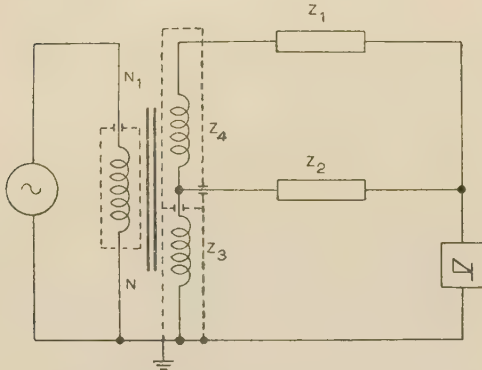


Fig. 2.—Basic circuit with two mutual inductors, or two transformers, having a common primary winding.

is of no consequence since it does not appear in the balance equation. The basic circuit is shown in Figs. 1 and 2.

Two mutual inductances or a mutual inductance with two secondaries, or a special transformer with two secondaries, are used. In the case of two separate mutual inductances the primaries are identical.

The primary or primaries are connected across the source, the secondaries feed the two branches containing Z_1 and Z_2 . The impedances of the secondaries are Z_3 and Z_4 , say.

At balance, $I_1 = -I_2$. Hence

$$\left. \begin{aligned} jM_1\omega I_p - Z_4 I_1 - Z_1 I_1 &= -Z_2 I_1 \\ jM\omega I_p - Z_3 I_1 + Z_3 I_1 &= -Z_2 I_1 \end{aligned} \right\} \quad \dots (1)$$

Therefore

$$\frac{M_1}{M} = \frac{Z_2 - Z_1 - Z_4}{Z_2}; \frac{M_1 - M}{M} Z_2 = -Z_4 - Z_1 \quad (2)$$

or in the case of Fig. 2,

$$\frac{N_1 - N}{N} Z_2 = -Z_4 - Z_1 \quad \dots (3)$$

N_1 and N are the effective or corrected numbers of turns in the secondaries.

As the source and the detector have one terminal connected to earth, so too do the impedances Z_1 and Z_2 at balance. The remaining earth capacitances are therefore as shown in Figs. 3 and 4.

The capacitances C_2 and C_3 alter the impedance Z_3 , and since Z_3 does not appear in the balance equations, they do not matter;

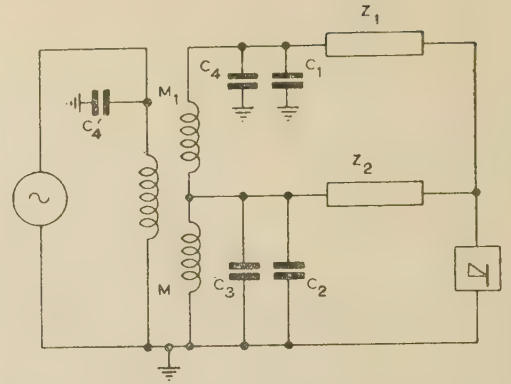


Fig. 3.—Earth capacitances in basic circuit with mutual inductors having a common primary winding.

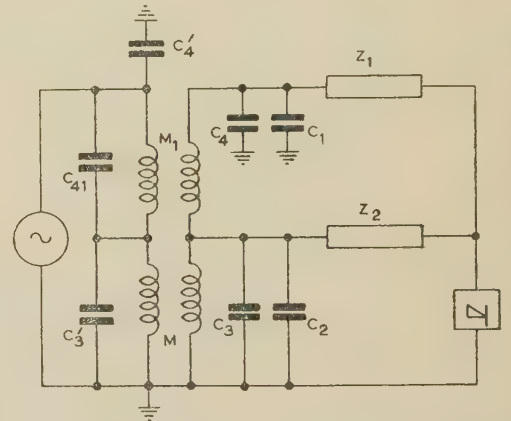


Fig. 4.—Earth capacitances in basic circuit with separate mutual inductors.

the impedance Z_2 will therefore be the measured balance impedance whenever possible.

The capacitances C_1 and C_4 shunt the impedance Z_1 . If C_1 is a capacitance standard it can be calibrated to include C_1 and C_4 , so that no error due to these earth capacitances would arise.

In Fig. 3 the capacitance C'_4 is simply a shunt across the source and therefore does not interfere with the measurement.

Fig. 4 the capacitance C'_3 shunts the primary of M whilst C'_4 shunts the source; in order to ensure, therefore, that the same current I_p flows through both primaries, a capacitance $C'_3 = C'_4$ should be connected across M .

The circuit can therefore finally be represented as in Fig. 5.

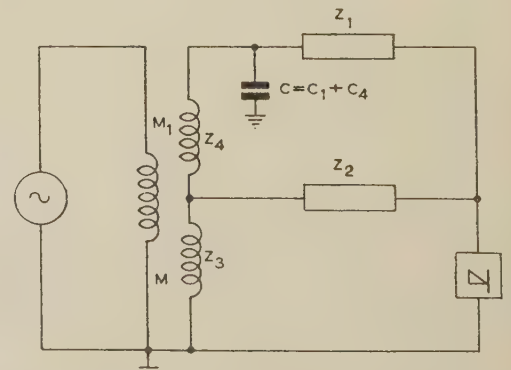


Fig. 5.—Basic circuit with sole relevant earth capacitance.

(3) ACTUAL MEASURING CIRCUITS

(3.1) Measurements where the Earth Capacitances are Neglected

(3.1.1) Measurement of an Inductive Impedance.

The circuit is shown in Fig. 6.

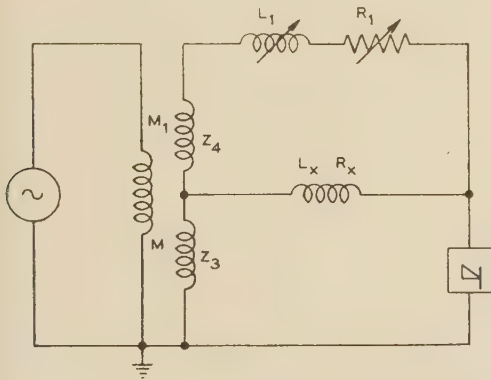


Fig. 6.—Circuit for the measurement of an inductive impedance.

L_x, R_x is the unknown; L_1, R_1 is a standard inductance. From eqn. (2),

$$\frac{M_1 - M}{M}(R_x + jL_x\omega) = -R_4 - jL_4\omega - R_1 - jL_1\omega$$

Hence, if $M > M_1$ (or $N > N_1$),

$$R_x = \frac{M}{M - M_1}(R_1 + R_4); L_x = \frac{M}{M - M_1}(L_1 + L_4)$$

The circuit can also be as in Fig. 7.

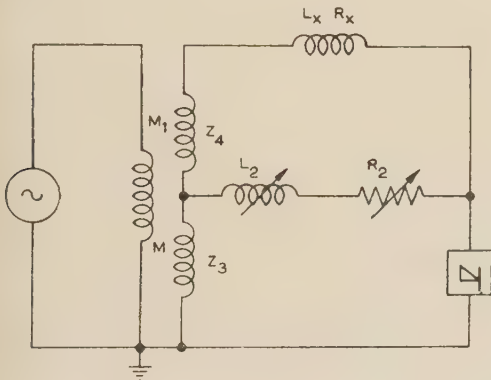


Fig. 7.—Circuit for the measurement of an inductive impedance.

$$\text{Here } \frac{M_1 - M}{M}(R_2 + jL_2\omega) = -R_4 - jL_4\omega - R_x - jL_x\omega$$

$$\text{so that } \frac{M - M_1}{M}R_2 - R_4 = R_x; \frac{M - M_1}{M}L_2 - L_4 = L_x$$

If M_1 is variable the circuit can be as shown in Fig. 8.

$$\text{Here } \frac{M_1 - M}{M}(R_x + jL_x\omega) = -R_4 - jL_4\omega - R_1$$

$$\text{so that } R_x = \frac{M}{M - M_1}(R_4 + R_1); L_x = \frac{M}{M - M_1}L_4$$

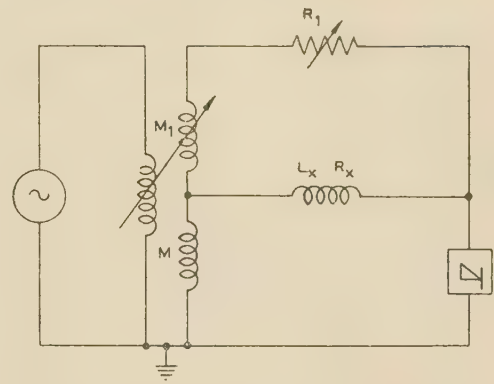


Fig. 8.—Circuit for the measurement of an inductive impedance with the aid of a variable mutual inductor.

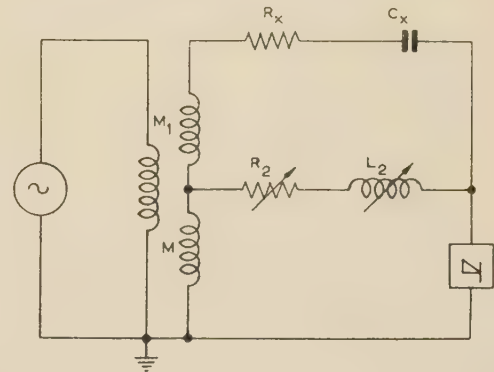


Fig. 9.—Circuit for the measurement of a capacitive impedance.

(3.1.2) Measurement of a Capacitive Impedance.

The circuit is shown in Fig. 9.

$$\text{Here } \frac{M_1 - M}{M}(R_2 + jL_2\omega) = -R_4 - jL_4\omega - R_x + \frac{j}{C_x\omega}$$

so that

$$\frac{M - M_1}{M}R_2 - R_4 = R_x; \frac{1}{C_x\omega} = \frac{M - M_1}{M}L_2\omega - L_4\omega$$

(3.2) Measurements where the Capacitances to Earth are not Neglected

(3.2.1) Measurement of a Capacitive Impedance.

The circuit is shown in Fig. 10. Two balances are made.

First balance.— C_1 is a loss-free capacitance standard calibrated to include the earth capacitance.

Z_x is not connected. The balance equation is

$$\frac{M - M_1}{M}R_2 = R_4; L_4\omega = \frac{1}{C_1\omega} \quad \dots \quad (4)$$

Second balance.— Z_x connected in parallel with C_1 is considered to be a loss-free capacitance C_x in parallel with an equivalent resistance R_x . C_1 is altered to C_{11} and R_2 to R_{22} .

The impedance of C_1 and Z_x is

$$Z_1 = \frac{1}{(C_x + C_{11})^2\omega^2 R_x} - \frac{j}{(C_x + C_{11})\omega} \quad [\text{if } (C_x + C_{11})^2\omega^2 R_x^2 \gg 1]$$

In consequence

$$\frac{M - M_1}{M}R_{22} = R_4 + jL_4\omega + \frac{1}{(C_x + C_{11})^2\omega^2 R_x} - \frac{j}{(C_x + C_{11})\omega}$$

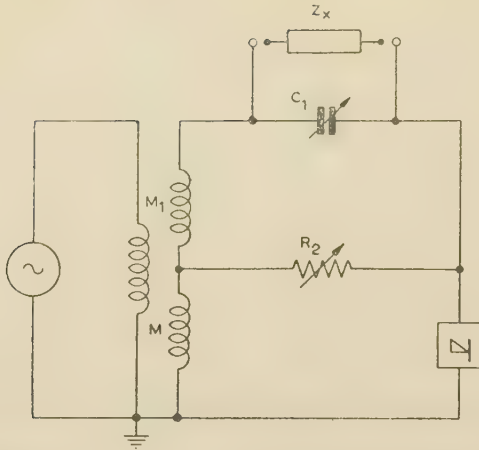


Fig. 10.—Circuit for the measurement of inductive or capacitive impedance.

Hence, combining with eqn. (4),

$$\frac{1}{R_x} = \frac{M - M_1}{M} (R_{22} - R_2) C_1^2 \omega^2; C_x = C_{11} - C_1$$

(3.2.2) Measurement of an Inductive Impedance.

The circuit is the same as shown in Fig. 10, Z_x is now an impedance $R_x + jL_x\omega$.

First balance.— Z_x is not connected. At balance,

$$\frac{M - M_1}{M} R_2 = R_4; L_4 \omega = \frac{1}{C_1 \omega} \quad (5)$$

Second balance.— Z_x is connected in parallel with C_1 , which for balance, is altered to C_{11} ; R_2 is altered to R_{22} .

As $L_x^2 \omega^2 \gg R_x^2$ the combined impedance of Z_x and C_{11} is

$$Z_1 \approx \frac{R_x - jL_x\omega(L_x C_{11}\omega^2 - 1)}{(1 - L_x C_{11}\omega^2)^2} \quad (5a)$$

Hence

$$\frac{M_1 - M}{M} R_{22} = -R_4 - jL_4\omega - \frac{R_x}{(1 - L_x C_{11}\omega^2)^2} - \frac{jL_x\omega}{(1 - L_x C_{11}\omega^2)}$$

and, combining with eqn. (5),

$$L_x = \frac{C_1}{C_{11} - C_1} L_4; R_x = \frac{M - M_1}{M} (R_{22} - R_2) \left(\frac{C_{11}}{C_{11} - C_1} + 1 \right)$$

The circuit for a second method of measuring an inductive impedance is shown in Fig. 11. M or M_1 is variable, and C

Table 1
RESULTS OBTAINED BY MEANS OF THE CIRCUITS OF FIGS. 7, 8 and 9

Method	Frequency	Certified values $L_x \pm 0.005\%$ $C_x \pm 0.001\%$ $R_x \pm 0.1\%$	Result of test	Standard deviation
Section 3.1.1, Fig. 7	c/s 100	$L_x = 49996.0 \mu\text{H}$ $R_x = 15.89 \Omega$	$49996.1 \mu\text{H}$ 15.89Ω	$1.1 \mu\text{H}$ 0.005Ω
	500	$L_x = 49996.2 \mu\text{H}$ $R_x = 15.89 \Omega$	$49996.3 \mu\text{H}$ 15.89Ω	$1.0 \mu\text{H}$ 0.006Ω
	1000	$L_x = 49998.0 \mu\text{H}$ $R_x = 15.90 \Omega$	$49998.2 \mu\text{H}$ 15.90Ω	$1.0 \mu\text{H}$ 0.009Ω
	2000	$L_x = 50004.0 \mu\text{H}$ $R_x = 15.90 \Omega$	$50004.2 \mu\text{H}$ 15.90Ω	$1.1 \mu\text{H}$ 0.01Ω
	5000	$L_x = 50058 \mu\text{H}$ $R_x = 15.92 \Omega$	$50058.2 \mu\text{H}$ 15.92Ω	$1.1 \mu\text{H}$ 0.01Ω
	1000	$L_x = 100000 \mu\text{H}$ $R_x = 42.10 \Omega$	$100000 \mu\text{H}$ 42.10Ω	$7.2 \mu\text{H}$ 0.01Ω
	1000	$L_x = 1000.1 \mu\text{H}$ $R_x = 1.67 \Omega$	$1000.1 \mu\text{H}$ 1.67Ω	$0.10 \mu\text{H}$ 0.01Ω
Section 3.1.1, Fig. 8	100	$L_x = 49996.0 \mu\text{H}$ $R_x = 15.89 \Omega$	$49996.0 \mu\text{H}$ 15.89Ω	$1.0 \mu\text{H}$ 0.005Ω
	500	$L_x = 49996.2 \mu\text{H}$ $R_x = 15.89 \Omega$	$49996.7 \mu\text{H}$ 15.89Ω	$1.0 \mu\text{H}$ 0.005Ω
	1000	$L_x = 49998.0 \mu\text{H}$ $R_x = 15.90 \Omega$	$49999.7 \mu\text{H}$ 15.90Ω	$1.1 \mu\text{H}$ 0.007Ω
Section 3.1.2, Fig. 9	100	$C_x = 0.100021 \mu\text{F}$ $R_x = 0.300 \Omega$	$0.100042 \mu\text{F}$ 0.300Ω	5.0 pF 0.009Ω
	500	$C_x = 0.100005 \mu\text{F}$ $R_x = 0.130 \Omega$	$0.100026 \mu\text{F}$ 0.125Ω	5.0 pF 0.005Ω
	1000	$C_x = 0.1000 \mu\text{F}$ $R_x = 0.063 \Omega$	$0.100021 \mu\text{F}$ 0.063Ω	5.2 pF 0.002Ω

The discrepancies between the measured and certified values for the circuits of Figs. 7 and 9 are due to c (Fig. 5) altering the effective values of L_x and C_x .

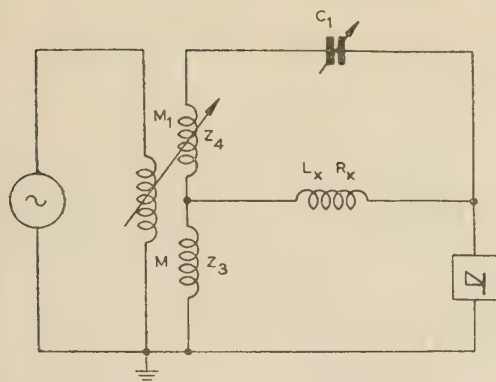


Fig. 11.—Circuit for the measurement of an inductive impedance with the aid of a variable mutual inductor.

is calibrated to include the relevant earth capacitances. At balance,

$$\frac{M_1 - M}{M}(R_x + jL_x\omega) = -R_4 - jL_4\omega + \frac{j}{C_1\omega}$$

Hence

$$R_x = \frac{M}{M - M_1}R_4; L_x = \frac{M}{M - M_1}\left(L_4 - \frac{1}{C_1\omega^2}\right)$$

(4) THE EFFECTS OF THE IMPURITIES IN THE MUTUAL INDUCTANCES AND OF THE PHASE DEFECT IN THE TRANSFORMERS

It is well known that, owing to imperfect insulation, eddy currents in wires and screens, inter-capacitances between primary and secondary and capacitances to earth, the e.m.f. induced in the secondary of a mutual inductance is not in exact quadrature with the primary current. Arising from these effects there appears

to be a component of the e.m.f. induced in the secondary of the mutual inductance which is in phase with the primary current, so that this e.m.f. is no longer $jM\omega I_p$ but $(jM\omega \pm \sigma)I_p$. The mutual inductance is then said to be impure, σ being the impurity.

The impurity σ , which is obviously a phase defect, can be positive or negative; it can be compensated so as to be small at the highest frequency used and negligible at lower frequencies since it diminishes somewhat faster than ω^2 .

Let the mutual inductances be compensated so as to have very small phase defects at the highest frequency used, and let them be nearly equal and of the same sign. The frequency defects will not matter provided that M and M_1 are known at the frequency used.

If the impurities in M and M_1 are σ and σ_1 , from eqn. (1),

$$(jM_1\omega \pm \sigma_1)I_p = -Z_2I_1 + Z_1I_1 + Z_4I_1$$

$$(jM\omega \pm \sigma)I_p = -Z_2I_1$$

Therefore,

$$\frac{jM_1\omega \pm \sigma_1}{jM\omega \pm \sigma} = \frac{-Z_2 + Z_1 + Z_4}{-Z_2}$$

hence,

$$Z_2\left(\frac{M_1 - M}{M \pm \sigma/j\omega}\right) + Z_2\left(\frac{\mp \sigma \pm \sigma_1}{jM\omega \pm \sigma}\right) = -Z_4 - Z_1$$

The first term contains σ/ω , which is negligibly small even if σ is only moderately small. The second term contains the difference between σ and σ_1 divided by approximately $M\omega$; hence it is negligibly small. It may therefore be accepted that, with compensated mutual inductances, the error due to the impurities will be zero.

Table 2

RESULTS OBTAINED BY MEANS OF THE CIRCUIT OF FIGS. 10 AND 11

Method	Frequency	Certified values	Result of test	Standard deviation
Section 3.2.1, Fig. 10	c/s 10^6	$C_x = 200.4 \text{ pF} \pm 0.01\%$ $R_x = 90 \times 10^6 \Omega \pm 1\%$	202.2 pF $90 \times 10^6 \Omega$	0.05 pF 252 Ω
		$C_x = 400 \text{ pF} \pm 0.01\%$ $R_x = 70 \times 10^6 \Omega \pm 1\%$	400 pF $70 \times 10^6 \Omega$	0.08 pF 120.2
	50×10^6	$C_x = 40 \text{ pF} \pm 0.05\%$ $R_x = 250 \times 10^3 \Omega \pm 1\%$	40 pF $250 + 10^3 \Omega$	0.05 pF 80 Ω
		$C_x = 80 \text{ pF} \pm 0.05\%$ $R_x = 200 \times 10^3 \Omega \pm 1\%$	80 pF $200 \times 10^3 \Omega$	0.1 pF 70 Ω
Section 3.2.2, Fig. 10	10^6	$L_x = 100 \mu\text{H} \pm 0.2\%$ $R_x = 1.56 \Omega \pm 0.2\%$	99.9 μH 1.56 Ω	0.10 μH 0.10 Ω
		$L_x = 200 \mu\text{H} \pm 0.2\%$ $R_x = 2.22 \Omega \pm 0.1\%$	200 μH 2.20 Ω	0.15 μH 0.01 Ω
	50×10^6	$L_x = 2 \mu\text{H} \pm 1\%$ $R_x = 2.10 \Omega \pm 0.2\%$	1.98 μH 2.10 Ω	0.007 μH 0.004 Ω
		$L_x = 3 \mu\text{H} \pm 1\%$ $R_x = 2.75 \Omega \pm 0.2\%$	3 μH 2.75 Ω	0.01 μH 0.005 Ω
Section 3.2.2, Fig. 11	1000 c/s	$L_x = 49998.0 \mu\text{H} \pm 2 \mu\text{H}$ $R_x = 15.90 \Omega \pm 0.01 \Omega$	49998.0 μH 15.90 Ω	0.5 μH 0.004 Ω
	100×10^3	$L_x = 500 \mu\text{H} \pm 0.05 \mu\text{H}$ $R_x = 1.03 \Omega \pm 0.005$	500 μH 1.03 Ω	0.020 μH 0.001 Ω

Writing $jmN\omega$ and $jmN_1\omega$ for the e.m.f.'s in the secondaries per unit current in the primary, and σ and σ_1 , which have the dimensions of resistance, for the phase defects, it is evident that by a similar calculation one obtains

$$Z_2 \left(\frac{N_1 - N}{N \pm \sigma/jm\omega} \right) + Z_2 \left(\frac{\mp \sigma \pm \sigma_1}{jmN\omega \pm \sigma} \right) = -Z_4 - Z_1$$

The same calculations apply, therefore, as for the mutual inductances.

(5) EXPERIMENTAL VERIFICATION

All the equipment used was certified by the N.P.L. for the manufacturers, and all necessary precautions were taken, the certification conditions and manufacturers' indications being adhered to. The systematic errors—those arising from the limited accuracy of the components in the circuit—the reading errors, etc., were very small and generally the same as the certification limits. The impurities in the mutual inductances and transformers were very small at the highest frequency used and their effect was therefore negligible. Each test was repeated 20 times and the standard deviation was calculated.

Table 1 shows some of the results obtained by means of the circuits of Figs. 7, 8 and 9. Table 2 shows some of those obtained by means of the circuits of Figs. 10 and 11.

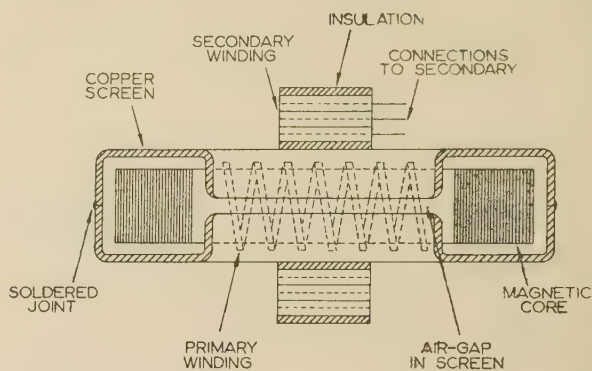


Fig. 12.—Cross-section of a transformer.

(6) APPENDIX

In construction, the transformers are similar to those used in admittance bridges.

The core is toroidal of spiral-wound Mumetal tape, of mean diameter 3 cm. The primary winding, consisting of insulated thin copper tape, is wound on the core; core and primary are surrounded by a thin copper shield as shown in Fig. 12. The secondary is wound on the copper screen and the whole transformer is placed in a copper screening box. Tappings from the secondary are taken as shown in the diagram.

A SIMPLE 3CM Q-METER

By A. E. BARRINGTON, Ph.D., B.Sc.(Eng.), Associate Member, and J. R. REES, Ph.D.

(The paper was first received 29th April, and in revised form 5th August, 1958.)

SUMMARY

Following a brief review of existing reflectometer methods for the measurement of Q-factors of microwave cavities, a simplified system is described in which the complexity and cost of components are reduced appreciably. Values of Q-factors, from 200 to 4000, measured in this way are in good agreement with those obtained with established techniques. Because the local oscillator is tuned manually, a frequency range wider than that obtainable with electronic tuning may be covered.

(1) INTRODUCTION

The advantages of reflectometer methods for the measurement of resonant-cavity Q-factors at wavelengths where the power output of local oscillators varies considerably over the required frequency range are well known. The necessary data are usually obtained from a cathode-ray-tube display. A horizontal frequency scale is obtained by using a signal proportional to the modulating voltage of a frequency-modulated local oscillator operating around the resonant frequency of the cavity resonator. Signals proportional to the power incident on and reflected from the resonator, obtained by means of a matched hybrid junction¹ or a pair of directional couplers,² are applied alternately to the vertical-deflection amplifier through a mechanical or electronic switch operating at the modulation frequency. Careful adjustment of the crystal detectors in the arms of the reflectometer is required for identical response over the frequency range. The reflection coefficient at resonance is measured with a calibrated attenuator in the incident power arm; the attenuation corresponding to the reflection coefficient at the half-power points can then be calculated (see Appendix), and the signal in the incident power arm is reduced accordingly. The frequencies at the points of intersection of incident and reflected power traces, measured with an absorption wavemeter in one of the arms, together with the frequency at resonance determine the Q-factor, Q_L .

The method gives quick and accurate results and is useful for the routine quality testing of microwave components. It is possible, however, to reduce both the complexity and cost of the apparatus appreciably by bearing in mind that the essential information can be obtained directly as power ratio. A simplified system, extending the scope of apparatus described previously for operation at 8.6 mm,³ has been developed accordingly.

(2) METHOD

If periodic signals proportional to the power incident on and reflected from a cavity are applied to the X- and Y-plates of a cathode-ray tube, a straight-line trace may be obtained. The tangent of the angle between trace and X-axis is then proportional to the power ratio. In commercial test equipment it is customary to apply square-wave modulation to the local oscillator. The required signal, after detection, is usually amplified with a selective amplifier tuned to the modulation frequency and only the fundamental component of the initial square waveform is preserved. With careful adjustment, two such amplifiers for X- and Y-amplification will give a satisfactory trace, but any phase difference will result in an elliptic rather than a straight-line display, making measurements somewhat uncertain. Greatly

improved performance can be obtained at little additional cost with untuned d.c.-coupled amplifiers. With these it is possible to obtain a display without phase errors and to establish an effective zero on the screen. Owing to preservation of the square waveform, the flat extremities of the modulating voltage are represented by two bright spots connected by faint lines, the contrast in brightness being controlled by the ratio of the pulse width to the pulse rise-time. Generally, owing to phase errors and reflector hysteresis, the faint lines do not coincide. It was found advantageous to increase the rise time of the modulation voltage to observe the transient operation of the klystron more readily, typical values being a rise time of 400 microsec for a pulse repetition frequency of 1000 pulses/sec. D.C. amplification also makes it possible, by adjusting both the reflector voltage and modulation amplitude, to ensure that the klystron is switched off between pulses rather than from one mode to another or between points on the same mode.

With the equipment, which is shown in Fig. 1, properly

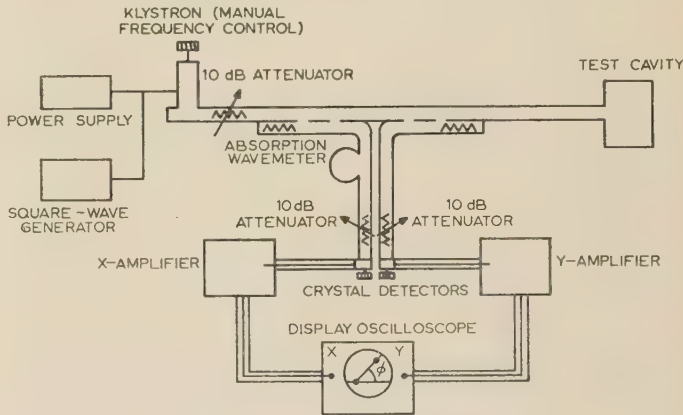


Fig. 1.—3 cm power-ratio display.

adjusted, the lower left-hand spot is the origin of the co-ordinate system, corresponding to zero incident and reflected power. The other spot has an abscissa proportional to incident power and an ordinate proportional to reflected power with the klystron operating at the peak of the modulating voltage.

The oscillograph is fitted with a recticle, as shown in Fig. 2, with lines radiating from the origin and labelled with the magnitude of the tangents of their respective angles with the X-axis. To calibrate the instrument, the cavity is replaced by a short-circuit and the X- and Y-channels are adjusted so that, with the left-hand spot at the origin, the right-hand spot lies on a convenient line, inclined to the X-axis at an angle, ϕ_1 , whose tangent is recorded. To simplify calculations, the 45° line, labelled 1.0, is normally chosen. It is necessary to ensure that the right-hand spot remains on the selected line while the klystron is tuned manually over the expected frequency range. If crystal diodes, selected for good square-law response, are used, identical response can be obtained by adjustments of the tunable crystal mounts.

The test cavity is then placed in position and the klystron is tuned manually to the resonant frequency of the cavity, which is

Written contributions on papers published without being read at meetings are invited for consideration with a view to publication.
Drs. Barrington and Rees are at Harvard University.

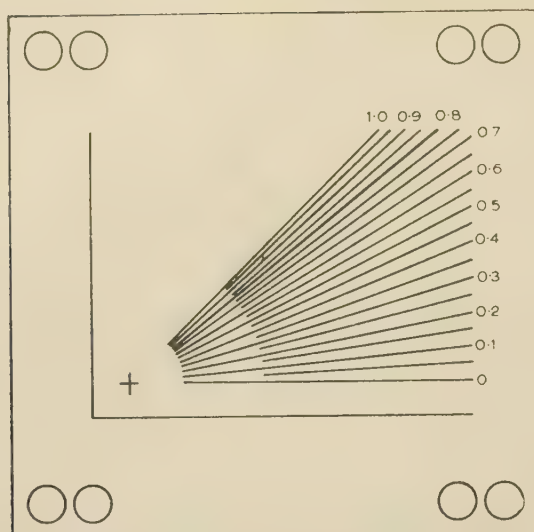


Fig. 2.—Oscilloscope tangent recticle.

indicated by the maximum dip of the right-hand spot on to a radial line inclined to the X-axis at a smaller angle, ϕ_0 . The resonant frequency, f_0 , is read off with the absorption wavemeter in the incident power arm, corresponding to a micrometer setting at which the right-hand spot suddenly moves to the left. It can be shown (see Appendix) that at the half-power-point frequencies, f_1 and f_2 , the right-hand spot lies on a radial line at an angle $\phi_{1,2}$ equal to $\arctan \frac{1}{2}(\tan \phi_1 + \tan \phi_0)$, which simplifies to $\arctan \frac{1}{2}(1 + \tan \phi_0)$ when ϕ_1 is 45° . The klystron is tuned manually to the two frequencies on either side of resonance where the spot lies on this line. These frequencies, f_1 and f_2 , are measured with the absorption wavemeter. The Q-factor, Q_L , is given by

$$Q_L = f_0 / (f_2 - f_1)$$

The internal Q-factor of the cavity, Q_0 , can then be obtained from the relation⁴

$$Q_0 = Q_L [2 / (1 - r_0)]$$

where r_0 is the reflection coefficient at resonance. But, from the Appendix,

$$r_0 = \pm (\tan \phi_0 / \tan \phi_1)^{1/2}, \text{ or } \pm (\tan \phi_0)^{1/2} \text{ when } \phi_1 \text{ is } 45^\circ$$

The sign of r_0 depends on the degree of coupling, being negative for undercoupled and positive for overcoupled cavities. It can be determined by a separate experimental observation of the position of the standing-wave pattern at resonance,¹ or more simply by varying the phase of a mismatch introduced between cavity and reflectometer and observing the cyclic variation of Q-factor and resonant frequency.² For routine production tests, a determination of Q_L will, in general, be sufficient.

(3) CONCLUSIONS

The useful range of the device is limited to Q-factors up to 4000; dynamic methods for higher Q-factors requiring more accurate frequency measurements have been described in the literature.⁵ However, unlike the sweep-frequency method, the range of measurement with manual tuning is not restricted to only 50 Mc/s, the extent of a klystron mode, and Q-factors of less than 200 may be measured. Because of the small variation of the power ratio near resonance, it is difficult to determine Q-factors of cavities whose coupling parameter Q_0/Q_x or Q_x/Q_0 exceeds 20.

Q-factors from 200 to 4000 determined by two independent

methods, namely the system described above and a frequency-modulated display using a calibrated attenuator in the incident power arm (see Appendix), showed excellent agreement. Since there is no requirement for a frequency time-base, a fast mechanical or electronic switch and a precision calibrated attenuator, the saving in cost is appreciable without affecting the simplicity of operation.

The accuracy of the method depends on the spot size on the oscilloscope screen, which in the equipment described above resulted in an uncertainty of the power ratio of about 5%. This is much larger than any inaccuracies to be expected from directional couplers with a directivity of 40 dB or better.⁶ Additional errors due to short-term frequency fluctuations of the local oscillator and non-linear response of crystal detectors and amplifiers are estimated to limit the accuracy of determining Q_L to about 10%.

(4) ACKNOWLEDGMENT

The work described was supported by the United States Atomic Energy Commission under contract No. AT(30-1)-1909.

(5) REFERENCES

- (1) REED, E. D.: 'A Sweep Frequency Method of Q Measurement for Single-Ended Resonators', *Proceedings of the National Electronics Conference*, 1951, 7, p. 162.
- (2) TWISLETON, J. R. G.: 'An X-Band Magnetron Q-Measuring Apparatus', *Proceedings I.E.E.*, Paper No. 2037 R, May, 1956 (103 B, p. 339).
- (3) BARRINGTON, A. E.: 'Cold Measurements of 8 mm Magnetron Frequency and Pulling Figure', *ibid.*, Paper No. 1792 R, March, 1955 (102 B, p. 247).
- (4) COLLINS, G. B.: 'Microwave Magnetrons' (McGraw-Hill, 1948), p. 715.
- (5) GINZTON, E. L.: 'Microwave Measurements' (McGraw-Hill, 1957), p. 431.
- (6) TWISLETON, J. R. G.: Discussion on 'An X-Band Magnetron Q-Measuring Apparatus', *Proceedings I.E.E.*, January, 1957 (104 B, p. 6).

(6) APPENDIX

If it is assumed that the power reflection coefficient, $|r_1|^2$, of a cavity at a frequency far from resonance is unity (this is the case for well-designed low-loss coupling circuits), the power reflection coefficient, $|r_{1,2}|^2$, at the half-power points of a cavity coupled to a matched waveguide is given by⁴

$$|r_{1,2}|^2 = \frac{1}{2}(1 + |r_0|^2) \quad (1)$$

where r_0 is the reflection coefficient at resonance.

If a calibrated attenuator in the incident power arm is used,

let $|r_0|^2 = A$ decibels and $|r_{1,2}|^2 = B$ decibels

From eqn. (1), $B = 10 \log \frac{1}{2}[1 + \text{antilog}(A/10)]$. . . (2)

B is the setting of the attenuator which at frequencies f_1 and f_2 , results in equal signals from the incident and reflected power arms when the detectors are calibrated for identical response.

Alternatively, let

$$|r_1|^2 = k \tan \phi_1 \text{ (equal to unity by definition)} \quad (3)$$

$$\text{and } |r_0|^2 = k \tan \phi_0 \quad (4)$$

where k is a constant.

From eqns. (1), (3) and (4), $|r_{1,2}|^2 = k \tan \phi_{1,2} = k \frac{1}{2}(\tan \phi_1 + \tan \phi_0)$, i.e.

$$\tan \phi_{1,2} = \frac{1}{2}(\tan \phi_1 + \tan \phi_0) \quad (5)$$

From eqns. (3) and (4),

$$r_0 = \pm (\tan \phi_0 / \tan \phi_1)^{1/2} \quad (6)$$

ULTRA-HIGH-FREQUENCY POWER AMPLIFIERS

By J. DAIN, M.A., Associate Member.

(The paper was first received 10th May, and in revised form 16th July, 1958.)

SUMMARY

The paper examines a few of the problems associated with the design and construction of power amplifiers operating in the frequency band 300–3 000 Mc/s.

Various types of amplifier are considered in turn, and the advantages and disadvantages of each particular class are examined in some detail.

LIST OF SYMBOLS

- A = Anode area, cm^2 .
 a = Ratio between r.f. and d.c. anode potentials.
 B_0 = Brillouin magnetic field, gauss.
 b = Ratio between instantaneous values of anode and grid potentials.
 C = Pierce's gain parameter.
 C' = Effective capacitance of external anode circuit, farads.
 d_1 = Grid-cathode spacing, cm.
 d_2 = Grid-anode spacing, cm.
 E = Axial component of electric field, volts/cm.
 f = Frequency.
 g = Ratio between r.f. and d.c. grid potentials.
 G = Gain factor.
 I_0 = Direct beam current, amp.
 J = Cathode current density, amp/cm^2 .
 \mathcal{P} = Beam perveance, pervs.
 P = Power flow, watts.
 P_0 = Output power, watts.
 P_1 = Grid dissipation, watts/cm^2 .
 P_2 = Anode dissipation, watts/cm^2 .
 Q = Space-charge parameter.
 r_0 = Beam radius, cm.
 T = Transit time, sec.
 u_0 = Beam velocity, cm/sec .
 u_p = Phase velocity, cm/sec .
 u_g = Group velocity, cm/sec .
 V_0 = Beam voltage, volts.
 v_1 = Instantaneous grid potential, volts.
 v_2 = Instantaneous anode potential, volts.
 V_a = Direct anode potential, volts.
 V_g = Direct grid potential, volts.
 W = Energy stored per unit length, joules/cm .
 β = Phase-change coefficient = ω/u_p , cm^{-1} .
 ϵ_0 = Permittivity of free space = $(1/36\pi)10^{-11}$ farads/cm.
 η = Overall efficiency.
 η_a = Anode efficiency.
 λ = Wavelength, cm.
 μ = Amplification factor.
 ω = Angular frequency, rad/sec .
 ω_q = Reduced plasma angular frequency, rad/sec .

(1) INTRODUCTION

Prior to 1940 the upper frequency limit on power-amplifier tubes was about 200 Mc/s. The wartime advances in pulsed tubes of the disc-seal, Resnatron¹ and klystron types opened up new avenues of approach to the problem. Still more recently the realization of the travelling-wave and backward-wave tubes has provided further scope for development. It should not be inferred, however, that progress has been made solely through the discovery of new principles of operation; technical improvements in methods and materials inevitably have played a crucial role in raising performance figures.

The present discussion will be concerned primarily with the ultra-high-frequency band extending from 300 to 3 000 Mc/s, because this is thought to be of particular interest. It will be shown, for example, that opinions differ on the type of tube which may be used to best advantage over the lower part of the range. This controversy has been undecided for a long time, and the present indications are that the issue will remain in the balance for some years to come. The band is of interest also for the reason that many applications extend their operating frequency range into it from either above or below. Broadcasting, tropospheric-scatter communication, navigational aids and radar systems have frequency allocations within it.

Various types of amplifier are used in the band. Triodes or tetrodes are often selected for the lower frequencies on the grounds of size and economy, but transit-time limitations render them less suitable for power operation at frequencies greater than about 1 Gc/s. Multi-cavity klystrons may be used anywhere in the band, although they become rather unwieldy when designed for the lower frequencies. This drawback is offset to a great extent by the very high stable gain which may be obtained. Travelling-wave tubes also have been built for frequencies throughout the band, and it is necessary to use them when the amplifier is required to have a bandwidth in excess of a few per cent. In general, these tubes have lower gains and lower efficiencies than klystrons. More recently, the principles of backward-wave interaction have been exploited to advantage in amplifier design. In various forms these have either high gain and relatively low efficiency or high efficiency with relatively low gain. The bandwidth also depends on the type, but voltage tuning may be applied to this class of tube more profitably than to any other.

(2) GRID-CONTROLLED VALVES

Triodes and tetrodes of conventional design have proved very successful and reliable in class-C amplifier circuits for output powers up to 10 kW mean at frequencies up to 150 Mc/s. In valves of larger size with a consequent limitation of the maximum operating frequency to about 50 Mc/s, powers of 100 kW or more per valve are readily obtained. The reliability of these designs has been demonstrated by lives in excess of 10 000 hours, which have become the rule rather than the exception.

The construction of most of these types is illustrated in Fig. 1 and follows a well-established pattern. The cathode is a cage of tungsten or thoriated-tungsten filaments surrounded by a

Written contributions on papers published without being read at meetings are invited for consideration with a view to publication.

This is an 'integrating' paper. Members are invited to submit papers in this category, giving the full perspective of the developments leading to the present practice in a particular part of one of the branches of electrical science.

Mr. Dain is with the English Electric Valve Co., Ltd.

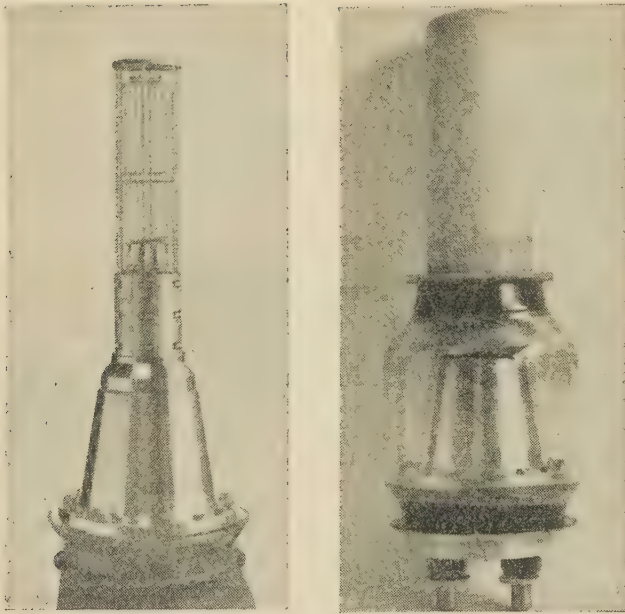


Fig. 1.—Construction of a high-power triode for frequencies up to 50 Mc/s.

grid or grids wound with molybdenum wire spot-welded to rigid support wires. The copper anode forms part of the vacuum envelope and is sealed with a glass insulator to the header on which the grid and cathode are already mounted. In this way the electrodes requiring accurate location with respect to one another may be adjusted before the final seal is made.

Various limitations of this design set in as the frequency of operation is increased. In many cases the transit time of the electrons becomes an appreciable fraction of the r.f. cycle, and this reduces both the gain and the efficiency. The power output is reduced by this fall in performance, but frequently it is reduced still further because the electrode structure has to be restricted in size. Neither the length nor the diameter of the active region of the tube may exceed some small fraction of the wavelength, to ensure that only minor variations in the amplitude of the r.f. field occur within it. The reduction in power output imposed by these considerations of size may be avoided if the specific loading of the electrode structure can be increased appropriately. Difficulties arise also in the design of the r.f. circuits associated with the valve. The impedance of the connections made through the vacuum envelope to the internal electrodes becomes appreciable and has the effect of decoupling the r.f. fields in the active region of the valve from the fields in the external circuits.

The first step to reduce the lead inductance is the adoption of a circular symmetry combined with the use of disc seals; the circuits are arranged for the valve to be plugged-in with contact made all round. This improvement is not necessarily adequate to give a satisfactory arrangement for the output tank circuit; this must include the anode insulator, which may be too long to permit the use of an efficient geometry. This remark applies especially to glass insulators, because the minimum safe length which can be used at ultra-high frequencies is determined by dielectric loss and not voltage flashover. The external connections to the anode may therefore be the source of high series inductance, which can be reduced only by decreasing the insulator length. This is done sometimes by modifying the overall design of the valve and its circuit so that the insulator is subjected to a lower r.f. voltage. Alternatively, shorter insulators of low-loss ceramic may be used, and this solution retains the advantage of keeping a significant part of the circuit, including the coupling

to the load, outside the vacuum envelope. The ultimate construction is to incorporate the r.f. circuits wholly within the envelope, with the d.c. connections taken in at nodes of the r.f. field.^{1,2} The disadvantages of this arrangement are that a more complex assembly must be made vacuum-tight, the tuning mechanism must be adapted to work *in vacuo* and the tuning range of a particular assembly is limited to about 10% of the mid-band frequency.

The problem of appreciable transit times is not solved so readily. Suppose the cathode/control-grid region of a tube is considered as a planar diode; under d.c. conditions with a space-charge-limited current the transit time, T , is given by

$$T = 6.7 \times 10^{-10} \left(\frac{d_1}{J} \right)^{1/3} \text{ second} \quad (1)$$

The power dissipated by the electron beam per unit area of the grid is given by

$$P_1 \propto J^{5/3} d_1^{4/3} \quad (2)$$

Thus, at constant current density the spacing must be scaled as the cube of the operating wavelength for the transit time to remain a given fraction of an r.f. cycle. The grid dissipation density then scales as the fourth power of the wavelength. At lower frequencies, cage filaments of thoriated tungsten give sufficient emission for operation to be restricted by the running temperature of the grid and not by the cathode loading. If, however, a design is scaled to shorter wavelengths, keeping both the current density and the electron transit-angle constant, the grid dissipation falls below the maximum safe value. It is therefore often desirable to increase the cathode loading to avoid decreasing the electrode spacings so rapidly.

An alternative scaling procedure recommends itself. It is suggested that the design should be varied with the operating wavelength in a way such that the grid dissipation density and the electron transit angle are unchanged. If the r.f. losses in the grid are ignored, this will be achieved if the electrode spacing and the cathode current density are scaled as

$$\left. \begin{aligned} d_1 &\propto \lambda^{5/3} \\ J &\propto \lambda^{-4/3} \end{aligned} \right\} \quad (3)$$

Fig. 2 shows the results of applying this system of scaling to a diode operating with a transit time of 0.2 cycle and with a cathode loading of 0.5 amp/cm² at 375 Mc/s. The Figure illustrates that designs for frequencies up to 1 Gc/s are prac-

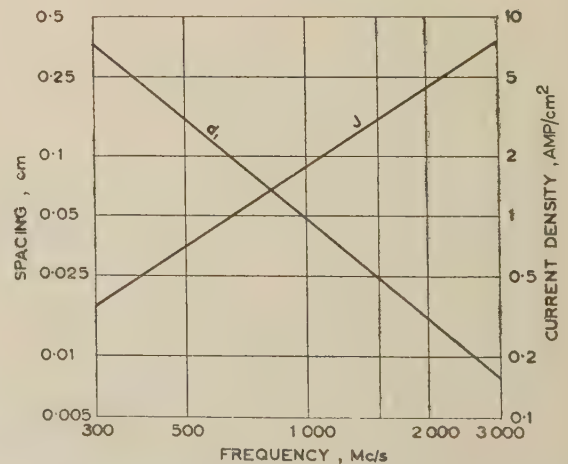


Fig. 2.—Typical electrode spacing and current density for a diode having an electron transit time 0.2 cycle.

ticable. It may prove possible to raise this limit to 1.5 Gc/s, but this will entail the use of high-current-density cathodes such as the impregnated type.³ Moreover, the mechanical design must be well engineered to obtain the structural rigidity required to control the grid-cathode spacing, which is typically 0.010 in, throughout the useful life of a tube.

The figure shows that continuous-wave working is not practicable at the high-frequency end of the band. However, it is well known that some thermionic emitters operate satisfactorily with very high loading, provided that the current is drawn from them only in pulses of short duration. It follows that the upper frequency limit is correspondingly higher for tubes designed specifically for this type of service.

The spacings between electrodes beyond the control grid are governed by considerations of space charge, conversion efficiency and bandwidth. The particular case of triode geometry will be discussed here, since this is sufficient to illustrate the argument. It will be assumed that transit times are negligible and that the cathode emission is space-charge-limited. The first effect to be considered is the depression of the potential in the electron stream caused by space charge. It is thought reasonable to apply the criterion that no potential minimum shall occur beyond the grid. For parallel flow this implies the condition

$$\left[\left(\frac{v_2}{v_1} \right)^{1/2} + 2 \right] \left[\left(\frac{v_2}{v_1} \right) - 1 \right]^{1/2} \geq \frac{d_2}{d_1} \quad (4)$$

The minimum value of v_2/v_1 so defined is plotted as a function of d_2/d_1 in Fig. 3. The grid-anode transit time is then somewhat less than $\frac{1}{3}(d_2/d_1)$ times the cathode-grid transit time.

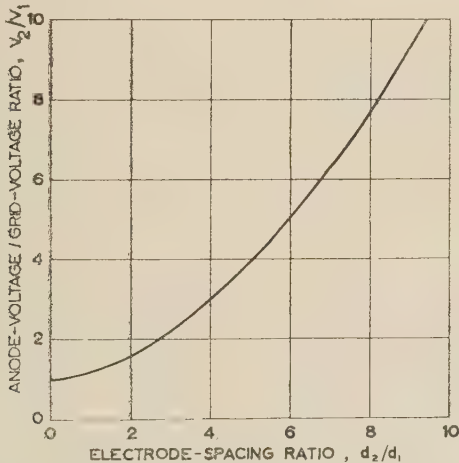


Fig. 3.—Minimum anode/grid voltage ratio required to avoid a potential minimum between these two electrodes.

This limitation on the minimum anode potential has a bearing on conversion efficiency. Suppose that the r.f. voltage on the anode is some fraction, a , of the direct anode voltage, V_a , and $-V_g$ is the standing bias on the grid which is driven by an r.f. voltage gV_g . Then the inequality (4) may be rewritten as

$$V_a(1 - a) \geq bV_g(g - 1) \quad (5)$$

As an approximation, V_a is of the order of μV_g , so that, from inequality (5),

$$a \leq 1 - \frac{b(g - 1)}{\mu} \quad (6)$$

The parameter a is also the maximum efficiency of the amplifier, and the relation shows that μ must be high to give good effi-

ciency. The power gain also depends on the amplification factor, and this is especially true for the earthed-grid circuit commonly used at these frequencies. In this case the gain, G , is approximately equal to the ratio between the r.f. voltages on the anode and cathode. The relation (5) may be recast to show that the limit imposed on the anode voltage by the potential depression of the space charge implies also an upper limit on the power gain. Simple substitution gives

$$G \leq \mu/g - b(1 - 1/g) \quad (7)$$

from which it is evident that the gain increases with μ . As an example, Fig. 4 shows the maximum values for both a and G plotted against μ for the values $b = 3$ and $g = 2$ which are considered typical.

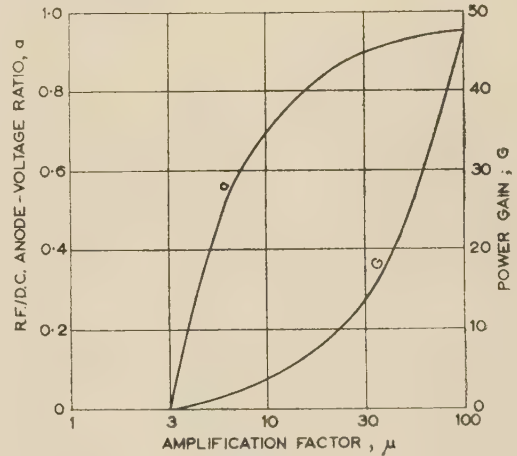


Fig. 4.—Maximum efficiency and the power gain of an earthed-grid triode circuit as functions of the amplification factor.

An increase in the grid-anode spacing of a triode necessitates an increase in b . The inequalities (6) and (7) show that this will result in lower efficiency and power gain. It must be remarked however, that a larger separation gives a wider bandwidth. By evaluating the Q-factor of the output circuit in its lumped effective form and with optimum loading, the bandwidth may be expressed in the form

$$\delta_f \propto \frac{JA}{aV_a \left(\epsilon_0 \frac{A}{d_2} + C' \right)} \quad (8)$$

The constant of proportionality depends on the form factor of the tube space current and on the utilization of the area available for electron emission. The expression (8) shows the functional dependence of the bandwidth on the efficiency parameter a and the grid-anode spacing d_2 . As d_2 is increased, a must be reduced and so the bandwidth is increased. Thus the choice of grid-anode spacing is necessarily a compromise between high gain and efficiency on the one hand and wide bandwidth on the other.

The expression (8) for bandwidth also shows that high-current low-voltage tubes have wider bandwidths. The low-voltage requirement is, of course, in conflict with a demand for high power.

It has been mentioned that the power output may be limited by the restriction on electrode size imposed by the need for uniformity of the electric field in the active region of the tube. In the coaxial form of construction the axial length of the active section should not exceed about $\lambda/8$ for a single-ended assembly or $\lambda/4$ for a double-ended one. It is preferable that the diameter

be kept less than $\lambda/3$ to avoid the occurrence of r.f. field distributions having circumferential variations. Unwanted modes should not be excited in a well-built tube, but constructional and other defects may give rise to non-uniformities in the electron current which will cause these modes to interfere with the correct operation of the amplifier. With these restrictions the power output, P_0 , is limited to the approximate value

$$P_0 = 0.2\lambda^2 P_2 \eta_a / (1 - \eta_a) \quad . \quad . \quad . \quad (9)$$

A water-cooled anode can be run with a dissipation of 500 watts/cm², so that, assuming $\eta_a = 50\%$,

$$P_0 = 100\lambda^2 \text{ watts} \quad . \quad . \quad . \quad (10)$$

when λ is measured in centimetres. For an operating frequency of 750 Mc/s ($\lambda = 40$ cm) the limiting power output would be 160 kW, so that it is reasonable to conclude that anode dissipation causes no limitation on power output.

In the u.h.f. range the choice between the triode and the tetrode remains rather undecided. The tetrode is at a disadvantage constructionally, and may suffer a deterioration in performance caused by unforeseen parasitic resonances in the cavity between the two grids. Such resonances are not necessarily easily suppressed when the valve is associated with a circuit tuning over a wide frequency band. On the other hand, the tetrode is capable of higher power gain and wider bandwidth; it provides greater isolation between input and output and is more economical in some applications. Current opinion seems to favour the tetrode for use at modest power levels where its advantages are best displayed. At higher power ratings the greater simplicity of the triode may make for more reliable operation.

The design of a u.h.f. triode or tetrode should comply as far as possible with the following conditions. The cathode must be capable of high emission and preferably in the form of a continuous surface rather than a filamentary structure. The grids must be spaced close to each other and to the cathode, and must be close-wound to obtain a high amplification factor. The electrodes must have low-inductance mountings, and all insulators placed in the r.f. fields should be as small as possible. The 1 kW tetrode shown in Fig. 5 embodies these features.⁴ It is of coaxial construction throughout, with the electrodes mounted directly off their respective terminals, which are brazed to high-alumina-content ceramic insulators. The cylindrical cathode surface is about 2 in in diameter and $\frac{1}{4}$ in high, and is made by impregnating a sintered-nickel mush with the emitting material. The two grids are cylinders of chrome copper which have been etched to provide the beam apertures,⁶ and the anode is a copper cylinder spaced about 5 mm from the second grid. The finned radiator attached to the anodes requires a flow of approximately 100 ft³/min of cooling air when the tube is run at its maximum rated dissipation. It should be noted that the use of ceramics not only allows short insulators to be used but also facilitates accurate positioning of the electrodes with respect to each other.

(3) KLYSTRONS

The basic principles of klystron operation are now firmly established and widely appreciated. Power is delivered to the output circuit by a density-modulated beam obtained by allowing electrons with an initial velocity modulation to drift until they become bunched.

In a grid-controlled tube the electrons interact with high-frequency fields directly they leave the cathode and before they have acquired a substantial velocity. In a klystron, however, the electrons are accelerated to the full velocity imparted by the direct voltage applied to the tube before they exchange energy

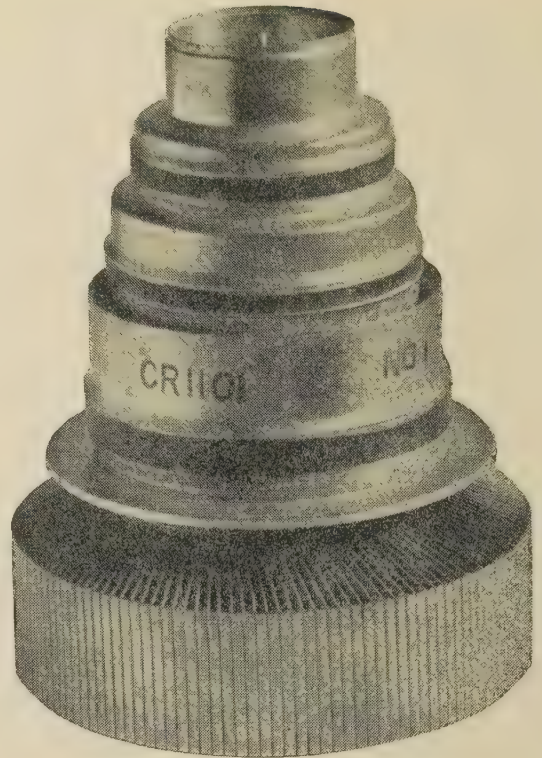


Fig. 5.—A 1 kW tetrode suitable for frequencies up to 1 Gc/s.

with the high-frequency fields. This process minimizes transit-time effects and is responsible for raising the highest practicable operating frequency by a factor of more than ten. Other outstanding features of this class of tube are the isolation between the r.f. input and output which is virtually complete and the high stable gain, which can exceed 70 dB in a modern multi-cavity klystron. The separation of the d.c. and r.f. fields also is considered to be advantageous.

On the other hand, klystrons suffer disadvantages in size, high operating voltage and a heavy concentration of the beam power. This, in particular, demands good focusing of the beam along the drift tubes, followed by defocusing before it impinges on the collector.

The efficiency of early designs was low, and the development of power klystrons was neglected for several years because of the superior efficiency of cavity magnetrons. The revival of interest in the klystron was due mainly to Hansen, whose foresight resulted in the successful development of a very-high-power pulsed amplifier.⁷ Since then, considerable advances have been made in the bunching of electron beams. These advances have been realized by studying systems using more than one bunching cavity⁸ and by considering in greater detail the effects of space charge in the bunched beam.^{9, 10} In both investigations the object has been to obtain a design in which the electrons arrive at the output cavity in the shortest possible bunch. The depressed-collector technique¹¹ is another step taken to increase the overall efficiency. In this arrangement the collector is no longer raised to the same potential as the main body of the klystron, but to a potential intermediate between the cathode and the body potentials. The spent electron beam therefore delivers less energy to the collector on arrival. Nowadays it is common for the efficiency of a klystron power amplifier to exceed 40%. This is comparable with the performance of other classes of tube at the frequencies under consideration.

Klystrons may be divided into those which require no externally applied constraints to focus the electron beam and those in which constraints are necessary to transmit a high proportion of the beam current through the drift tubes. It is usual to employ an axial magnetic field which is arranged to keep the beam diameter sensibly constant along the length of the tube. Klystrons with no external focusing require drift spaces of short length and large diameter with gridded interaction gaps to minimize stray coupling between the r.f. fields of the cavities and to give efficient interaction between these fields and the beam. The gain and bandwidth are restricted by the drift-tube geometry and the power output is limited by the presence of the grids which are heated by the small fraction of the beam current, which they intercept. Approximately 1 kW of mean power is practicable at 1 Gc/s and this limit is roughly proportional to the operating wavelength. If the beam is focused by a magnetic field, its diameter may be kept small in relation to the wavelength of operation and it is unnecessary to have grids in the interaction gaps. It follows that the power-handling capacity of this type of klystron is much greater, and mean powers of 10 kW have been obtained at frequencies of 2.5 Gc/s and higher. Moreover, the beam can be focused efficiently for an indefinite length, so that the number of cavities and the spacings between them can be optimized for each particular application. It must be appreciated, however, that the greater simplicity of the klystron with only space-charge focusing makes for a simpler installation and it is undoubtedly more suitable for certain equipments.

Klystrons are classified by the beam-focusing system and by the construction of the resonant cavities. These may be built wholly within the vacuum envelope of the tube so that, apart from the input and output windows, each cavity is of all-metal construction. Alternatively, the cavity may be partially external to the vacuum, in which case the interaction gap must be sealed from the external cavity by a suitable low-loss vacuum-tight insulator. This form of construction is to be preferred whenever the electrical specification for the tube will allow. The advantages are that the tube itself is simpler in form and may be used with a variety of external circuits. When used with a particular circuit the tuning range is at least twice that obtained with an integral cavity. Circuit design is easier and replacement costs are lower, because a new set of cavities is not required with each tube. The introduction of low-loss ceramics has greatly increased the power rating and operating frequency of external-cavity tubes, but it is not yet established whether dielectric loss or flashover is the limiting factor. In either case the maximum power obtainable will scale roughly as (frequency)^{-5/2}. On the other hand the power limit set by considering dissipation in the drift tubes and the collector scales as the inverse square of the frequency.

At the lower frequencies it follows that the power-handling

capacity of an external-cavity klystron will be limited by the dissipation in the collector or in the drift tube, and not by failure of the cavity ceramics. At higher frequencies the reverse will be true. Thus an integral-cavity tube must be used for any given power rating if the operating frequency exceeds some critical value. This critical frequency is dependent on the output power required; for example, on c.w. operation it is about 2 Gc/s at an output of 10 kW, but nearer 5 Gc/s at 1 kW.

The trend in modern klystron amplifiers is towards multi-cavity types with three or more resonators. In the u.h.f. band the efficiency of a 2-cavity amplifier is some 25–30% and it increases to about 40–45% for a 3-cavity design. The efficiency does not rise much above this figure however many cavities are used, and the advantage of klystrons with four or more cavities lies in the increased gain and bandwidth which can be obtained. It is usual to operate with the cavities stagger-tuned, because this gives a wider bandwidth and higher efficiency than can be achieved with all the cavities tuned to the same frequency. The theory of electron bunching in a multi-cavity klystron has been presented elsewhere.^{12, 13} From this the variation of the gain with frequency (Fig. 6) has been calculated for three tubes using numerical

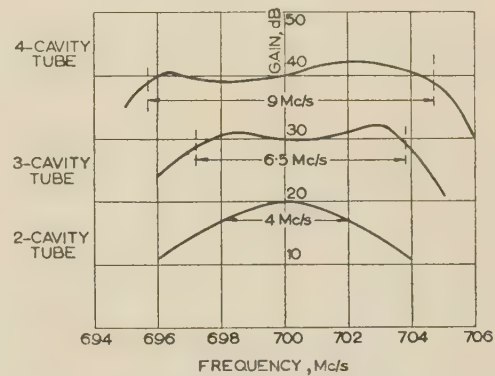


Fig. 6.—Typical gain/frequency characteristics of multi-cavity klystrons.

values which are considered typical of a klystron operating at 700 Mc/s. The data presented in Table 1 summarize the variation of the gain and bandwidth with the number of cavities used and with the tuning pattern of these cavities. In particular it will be noticed that the performance in terms of gain and bandwidth of the 4-cavity klystron is superior to that of two 2-cavity tubes in cascade. Its advantage is apparent.

The relatively high voltage required in a klystron constitutes the main drawback of this type of amplifier. It causes the long length of the drift tubes, because the electrons must drift for a given number of cycles of the r.f. field, and it is also inconvenient

Table 1

COMPARISON OF GAIN AND BANDWIDTH OF MULTI-CAVITY KLYSTRONS AT 700 Mc/s

Tube type	Gain		Bandwidth		Gain-bandwidth product	
	'In-line' tuning	Stagger tuning	'In-line' tuning	Stagger tuning	'In-line' tuning	Stagger tuning
	dB	dB	Mc/s	Mc/s		
2-cavity	20	—	4	—	4×10^2	—
3-cavity	45	30	2	6.5	6×10^4	6.5×10^3
4-cavity	70	40	1	9	10^7	9×10^4
Two 2-cavity tubes in cascade	40	—	2.5	—	2.5×10^4	—

in equipment design, because high-voltage supplies must be provided and adequate insulation is necessary on a number of components. An added complication arises in pulsed operation at very high peak powers when the electrons in the beam have sufficient energy to generate hard X-rays on being stopped by the walls of the tube. The X-radiation penetrates the vacuum envelope and an external shield, usually of lead, is required to protect the health of personnel working in the vicinity. It is well known that the beam current, I_0 , in a klystron is given in terms of the beam voltage, V_0 , by the simple relation

$$I_0 = \mathcal{P} V_0^{3/2} \text{ amperes} \quad (11)$$

where the constant \mathcal{P} , the perveance of the beam, is determined by the geometry of the electron gun. If V_0 is measured in volts, \mathcal{P} is usually about 1×10^{-6} pervs. Despite improvements in gun design¹⁴⁻¹⁶ it is unlikely that the perveance will be increased by an order of magnitude, except under circumstances which are of no immediate concern here. Using relation (11), the power output P_0 may be expressed in terms of the beam voltage and the efficiency η by

$$P_0 = \eta \mathcal{P} V_0^{5/2} \text{ watts} \quad (12)$$

In the v.h.f. band η is typically 40%.

The curves of power output and beam current as functions of the beam voltage are shown in Fig. 7 using the above numerical

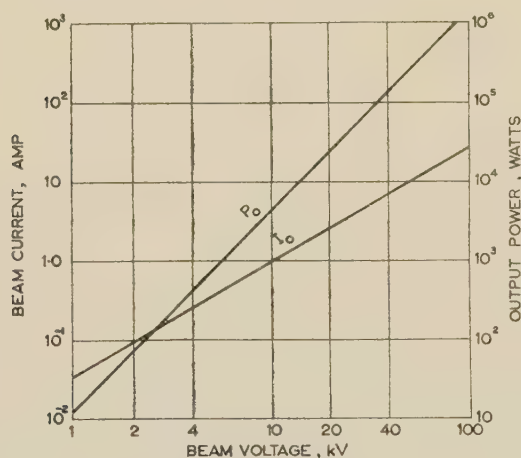


Fig. 7.—Beam current and power output of u.h.f. klystrons as functions of beam voltage.

values. Higher power output is obtained at a given beam voltage if the efficiency or the beam perveance is increased. Neither of these parameters can be increased indefinitely, and there is some limited experimental evidence which indicates that a high-perveance beam causes a reduction in efficiency.

High operating voltage is not the only factor contributing to the relatively long overall length of klystrons. The electron beam has to be restricted in diameter to ensure efficient interaction between the electrons and the gap voltages. The current density in the confined beam is therefore high; for example, in pulsed klystrons it may be as much as 50–100 amp/cm². This high current density is obtained by using a cathode with a large diameter and converging the beam profile in the first stages of its formation. The power density in the confined beam is also high; for example, the beam in a 10 kW c.w. klystron designed to operate at 700 Mc/s carries some 30 kW of power concentrated into an area of about 3 cm². It is therefore essential that the geometry of the electron collector and the trajectories of the electrons entering this collector are arranged to disperse the

electrons over an area sufficient to avoid overheating any part of the collector. Both the process of converging the beam when it is launched and that of dispersing it when it is collected add to the overall length of the tube.

The power output determines the beam voltage, and this in turn determines the drift-tube diameter and cavity gap-length. The choice of these dimensions is based on compromise; short gaps and narrow drift tubes give good coupling of the beam to the cavity fields and reduce the beam loading on the cavities.¹⁷ Short gaps give high r.f. fields across the gaps and increase the probability of voltage breakdown and loading by secondary emission effects.¹⁸ Narrow drift tubes require high focusing fields, because

$$B_0 = 8.3 \times 10^2 (\mathcal{P} V_0)^{1/2} / r_0 \text{ gauss} \quad (13)$$

where the Brillouin value, B_0 , of the magnetic field would maintain the beam radius constant at r_0 centimetres under ideal conditions. With small-diameter beams there are the added disadvantages that the space-charge debunching forces are increased and the beam power is unduly concentrated. As a rough guide the gap dimensions are chosen to be such that the transit angle is about 1 rad in the axial direction and about 2 rad across the drift-tube diameter.

The design of a tube is completed by determining the drift lengths between the cavities. The data required are the beam voltage and current, the gap factors for beam coupling and loading and the internal losses and effective capacitances of the cavities. The small-signal gain and frequency response are best evaluated by a space-charge-wave analysis,¹³ and experimental evidence suggests that these calculations are reasonably accurate up to relatively high signal levels; an alternative procedure⁸ is available for larger modulation depths. Even this theory is not strictly applicable when the velocity modulation is strong enough to cause overtaking of the electrons as they drift. The analysis of the bunching process in these circumstances has been solved only with such drastic assumptions that its validity is questionable.

The cavities associated with a klystron are of a size normal for a given wavelength, but an amplifier of this type usually requires more of them than a single-stage triode amplifier. The focusing solenoid and magnetic circuit also add to the bulk of the klystron amplifier. It must be remembered, however, that the high gain available from a single tube reduces the size and complexity of the r.f. driving circuits. There appears to be little to choose in size between a transmitter using a klystron in the power-output stage and one using triodes or tetrodes throughout all the stages.

The klystrons illustrated in Figs. 8 and 9 have been chosen as contrasting examples of modern klystron-amplifier design. The K347 shown in Fig. 8 is a 3-cavity amplifier for pulsed service in the band 575–625 Mc/s. It is air cooled and is used in conjunction with external cavities, each of which comprises a short length of rectangular-section waveguide split across the median plane to facilitate clamping into position around the tube. The tuning and coupling arrangements are all external to the vacuum envelope. Under typical conditions the tube is operated with pulsed beam voltage of 75 kV to give a peak power output of 500 kW at an efficiency of 35–40%. The mean output rating is 1.2 kW. The construction of this tube demonstrates a further advantage of the external-cavity amplifier. Furnace brazing is used only in the assembly of the separate drift-tube and ceramic sub-assemblies. Thus, although the complete klystron is 5 ft long, no dimension of the furnace-brazed part exceeds 16 in. Copper spinings are brazed on each end of the high-alumina-content ceramic cylinders which have previously been metallized, and the final assembly consists of stacking the

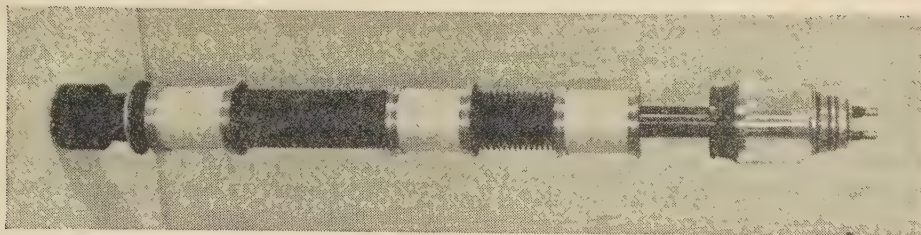


Fig. 8.—The K347: a 600 Mc/s klystron amplifier with a peak pulsed output of 500 kW.

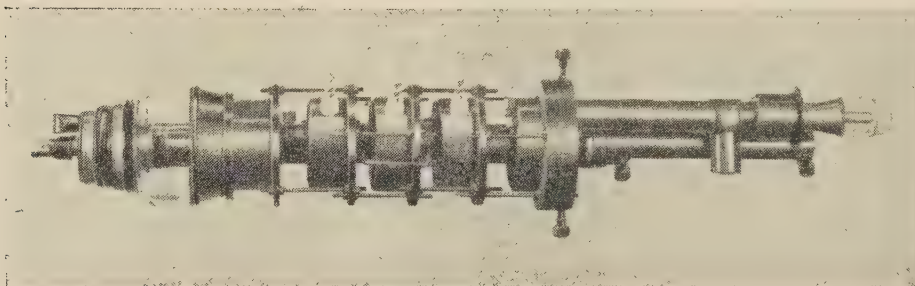


Fig. 9.—The K339: a 4-cavity klystron with a rated output of 10 kW, c.w., at 1.4 Gc/s.

ceramic sub-assemblies alternately with the individual drift-tube assemblies on to a vertical mandrel. Argon-arc welding is used to join together the various sub-assemblies. The collector is brazed by eddy-current-heating methods and the gun is sealed in on a glass lathe.

The K339 shown in Fig. 9 is a 4-cavity amplifier designed for c.w. operation in the band 1350–1450 Mc/s. The cavities are integral with the vacuum envelope and are tuned by varying the gap lengths through diaphragm-type mechanisms. The output coupling unit is a coaxial line with the inner supported by a quarter-wave stub. The coaxial line terminates in an aerial which couples the power output into a standard-size waveguide and the output window is a glass dome surrounding this antenna. Under normal operating conditions the power output is 10 kW for a beam voltage of 17 kV; the efficiency is 35%, the bandwidth 4 Mc/s, and the power gain approximately 40 dB. The drift tubes and the collector require water cooling, and air cooling is necessary for the gun insulating glass and the output window. This klystron has a gain of 55 dB if all four cavities are tuned to the same frequency; in these circumstances the saturated power output is 7 kW for the same beam voltage as before.

(4) TRAVELLING-WAVE TUBES

The helix-type travelling-wave tube, described originally by Kompfner¹⁹ and Pierce²⁰ and shown diagrammatically in Fig. 10, is capable of amplifying signals over a wide frequency range

without adjustment. Tubes are available with a 3 dB bandwidth of one octave. The essential feature of the construction which gives rise to the large bandwidth is the inclusion of an r.f. circuit which can propagate electromagnetic energy from the input to the output terminals in the absence of the electron beam. It follows that the group velocity of the system can be relatively high, so that the phase velocity will change slowly as the frequency is changed. In a klystron the resonator system may be considered as a filter circuit with zero group velocity, because there is virtually no transfer of electromagnetic energy from one cavity to the next without the electron beam; the finite bandwidth of the klystron is derived only from the coupling provided by the beam.

Two further important differences between the klystron and the travelling-wave tube arise from the change in the r.f. structure. The klystron is inherently stable, because the back coupling of r.f. energy is negligible; circuit feedback is possible in the travelling-wave tube and the tube is unstable without the addition of sufficient attenuation in the circuit. This attenuation is usually distributed over only a short length of the circuit, to minimize the reduction of efficiency and power output caused by it. It is situated between one-half and two-thirds of the distance along the tube and must be matched to the circuit at both ends with great care. The second different feature is the gain obtained in a given length. The resonant cavities of a klystron have low internal loss and large r.f. gap voltages are readily excited; this favours a high gain per unit length. In

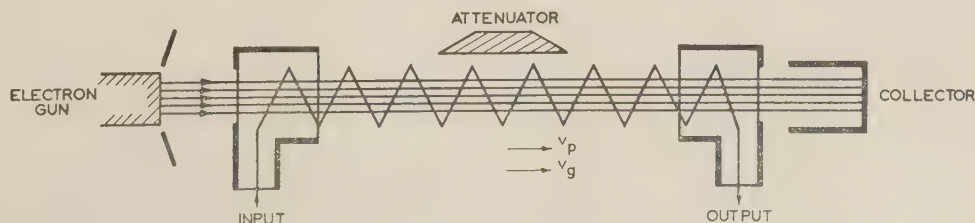


Fig. 10.—Diagrammatic representation of a travelling-wave tube.

the travelling-wave tube high fields in the circuit require a high flow of r.f. power along the tube, and this condition is unfavourable for a high gain per unit length.

The basic design of a power travelling-wave tube is concerned primarily with two parameters. Following the notation of Pierce,²¹ these are the gain parameter, C , and the space-charge parameter, Q , defined by the relations

$$\left. \begin{aligned} C^3 &= (E^2/2\beta^2 P)(I_0/4V_0) \\ 4QC^3 &= (\omega_p/\omega)^2 \end{aligned} \right\} \dots \dots (14)$$

The gain per unit length increases as C increases and Q decreases.

The electron optics of travelling-wave tubes are generally similar to those of klystrons and the beam perveance suffers the same restrictions in both cases. The expression (14) for C shows that a high-perveance beam is essential if the gain per unit length is to be as high as possible, and large-diameter hollow beams are finding increasing favour for this reason. A beam of this type, focused, for example, by Harris flow,²² may have a perveance as high as 15×10^{-6} perv without excessive velocity spread amongst the electrons. Hollow beams have not been used in the past for klystrons because the large diameter necessary for the drift tube increases the circuit feedback and impairs the stability. This type of feedback is inevitable in the travelling-wave tube, so that a large-diameter beam and circuit are not serious embarrassments.

At present the electron optics create only small restrictions on the capabilities of travelling-wave tubes; it is the circuit which requires improvement. The helix has proved admirable for low-power applications, but it limits the maximum mean power obtainable at 3 Gc/s to about 100 watts unless special precautions are taken to cool it. When designed to be used with a beam which has been accelerated by a potential of not more than a few kilovolts it has a high coupling impedance and low dispersion, but for pulsed tubes with high-voltage beams the coupling impedance is low. By contrast, the disc-loaded circular waveguide has a high impedance for all beam voltages; its dissipation properties are good, but it is a highly dispersive structure, owing to the large storage of energy in the individual cavities of the structure.

To appreciate the circuit problem it is helpful to state certain fundamentals of electromagnetic waves. The group velocity is a measure of the rate of change of phase velocity with frequency; thus

$$\left. \begin{aligned} u_p &= \omega/\beta \\ u_g &= \partial\omega/\partial\beta \end{aligned} \right\} \dots \dots (15)$$

from which it follows that

$$\partial u_p/\partial\omega = (1/\beta)(1 - u_p/u_g)$$

and it is clear that a high group velocity means a low rate of change of phase velocity with frequency, and hence a wide bandwidth. It has been shown that the group velocity is related to the power flow and the stored energy;²³ more specifically,

$$P = u_g W \dots \dots (16)$$

where P is the total power flow and W is the energy stored in the field per unit length of the transmission system. Now the requirement for high gain means minimum power flow for a given field strength, so that wide bandwidth can come only from a circuit with a low energy storage. In this connection it should be remembered that the electric and magnetic vectors of a travelling wave store equal amounts of energy.

The fundamental design of a circuit may now be formulated. In the region occupied by the beam there must be an E-wave propagating at the beam velocity; an H-wave in this region is

neither essential nor desirable. This wave carries power along the circuit and its field stores more electric energy than magnetic energy. The ideal slow-wave structure would make up the deficit of stored magnetic energy without adding either to the power flow or to the total stored electric energy. Such a circuit is not realizable, since it is impossible to create the necessary discontinuities in the components of the field.

The disadvantage of the single helix is that it couples the E-wave to an H-wave, which while restoring the energy balance doubles the power flow. The stored energy is not greatly increased above the minimum postulated above. The cross-wound helix²⁴ has a propagating mode in which the H-wave is absent, so that the power flow is reduced without much change in the stored energy. This circuit therefore has a higher coupling impedance obtained at the expense of bandwidth. Both structures are difficult to mount with good thermal conductance, although the cross-wound helix can be supported on a series of quarter-wave stubs with a small reduction in coupling impedance and bandwidth.²⁵

The disc-loaded structure has a power flow as close to the ideal minimum as the periodic nature of its construction will allow. On the other hand, much electric-field energy is stored between the discs, and this exceeds the energy stored in the beam region by a factor approximately equal to the delay ratio (c/u_p) of the structure. Thus the structure has a narrow bandwidth and is critical to dimensional tolerances. The stored energy may be decreased by reducing the area of the closely spaced metal walls of the discs, and Fig. 11 shows a structure

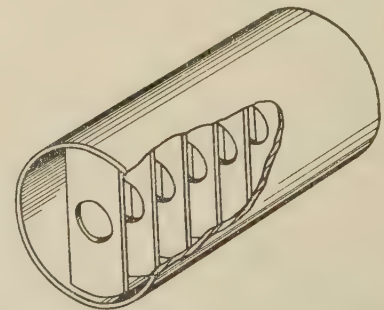


Fig. 11.—Modified disc-loaded circular waveguide.

with apertures incorporated for this purpose. Inductive coupling between the cavities occurs through the apertures, and such coupling is in the sense that increases the dispersion because it also reduces the net power flow. If the apertures are opened up sufficiently, the circuit becomes one having a reverse fundamental mode; this means that the fundamental mode has phase and group velocities of opposite sign. Even so, the circuit may still be used in a forward-wave amplifier, provided that the beam is arranged to interact with a forward-wave space harmonic and tubes²⁶ with pulsed outputs approaching 1 MW peak and bandwidths of almost 10% have been built to operate at 3 Gc/s.

The design of attenuators is closely linked with the form of the delay circuit. For power tubes the attenuator must be capable of dissipating appreciable energy, and it is desirable that it should be mounted outside the vacuum envelope. Usually this is impossible, because the coupling transformers between the internal circuit and the attenuator must match, not only over the normal frequency range of the tube, but also over a range of frequencies at which spurious oscillations could be generated. Internal attenuators must be of a material which will not impair the vacuum conditions and may need to be cooled by external means. They can be divided broadly into two classes, namely those working in a strong r.f. magnetic field and having the

characteristics of a lossy conductor, and those placed in a strong r.f. electric field which require the characteristics of a lossy dielectric. For the former, thin films of magnetic materials are used, deposited by such processes as the hot-spraying technique. Thin films of carbon are used at low powers to simulate lossy dielectric, but these are not very satisfactory at high power levels. Blocks of porous ceramic loaded throughout their volume with carbon have been used recently and this composite material promises to be capable of dissipating considerable energy.

Several analyses of the large-signal theory of travelling-wave tubes have been published²⁷⁻³¹ in which estimates of efficiency have been derived after considerable computation on a machine. The results indicate that efficiencies of the order of 30-40% will be obtained with well-designed tubes.

(5) BACKWARD-WAVE AMPLIFIERS

Any periodic waveguide structure will support a travelling-wave field built up from a set of component waves, usually referred to as 'space harmonics'.³² Certain of these have their

difference in the character of the mode: in the forward-wave tube an exponentially growing wave is excited to give the gain; in the backward-wave tube with high beam current the gain results from the interference between three non-growing waves.

The principles of backward wave amplification may be applied with advantage to tubes in which the electron beam interacts with the r.f. wave in a space spanned by crossed electric and magnetic fields. The magnetron oscillator has demonstrated the high efficiency of this type of interaction and has shown that the operating voltage for a given power output is considerably less than for a klystron or travelling-wave tube. Magnetron-type interaction has not proved very successful in forward-wave amplifiers, because the mechanism which leads to efficient operation causes the gain per unit length to be low. Backward-wave amplifiers have a higher rate of gain than forward-wave amplifiers under similar operating conditions, and it is therefore not surprising that crossed-field tubes of this type are proving successful. Tubes have been built with power gains of 10 dB over a voltage-tuned bandwidth of 10%. Operating at about 1.3 Gc/s, a pulsed power output of 1 MW has been obtained³⁶ at efficiencies up to 70%.

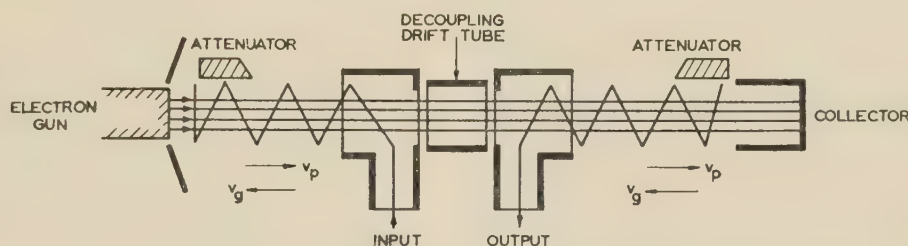


Fig. 12.—The cascade backward-wave amplifier (diagrammatic).

phase velocity directed in the opposite sense to the power flow of the total field. An electron beam travelling in synchronism with one such wave interacts with it, becomes bunched and is a source of r.f. power travelling one way. The field itself carries power in the opposite direction, so that feedback is present even though the waveguide may be matched at both ends. Such a system oscillates if the beam current exceeds some critical value, and the frequency of oscillation is tunable over a wide band simply by adjustment of the beam voltage.^{33, 34}

For currents below the critical value the system is stable and is capable of amplifying a signal injected at the collector end of the tube, the output being taken off at the gun end. The principal characteristics of the arrangement are high gain per unit length, narrow bandwidth, e.g. 10 Mc/s at 3 Gc/s, and a centre frequency tunable over a wide range by change of the beam voltage.

The prime disadvantage of a tube with a single circuit is that high gain is obtained only with currents close to the critical value for start of oscillation. The gain is then very dependent on the beam current. Recently it has been shown that a tube with two or more circuits arranged in tandem gives a substantial improvement in performance,³⁵ the arrangement being shown diagrammatically in Fig. 12. The two circuits are decoupled, and the result is that appreciable gain may be realized with a current well below the critical value for either section. This means that the performance is much less sensitive to changes in the beam current. Further advantages are that the input and output lines are decoupled and the bandwidth may be adjusted to some degree by operating the two circuits at different voltages. This is analogous to the stagger-tuning of multi-cavity klystrons. The problems of beam formation and circuit design are the same as for forward-wave amplifiers, but there is an essential

(6) CONCLUSIONS

Ten kilowatts is a conservative estimate of the mean power available from a single amplifier tube designed to operate in the range 300-3000 Mc/s. At the lower end of this band considerably more power should be obtained without difficulty.

Triodes and tetrodes compare favourably in size and efficiency with other types of amplifier at frequencies up to about 1 Gc/s. They are regarded as being unsuitable for use as power amplifiers at higher frequencies, because they would require an unduly high loading of the cathode and close spacing of the electrodes if designed to function satisfactorily. They have low gain and a bandwidth of not more than a few per cent of the operating frequency.

The klystron is currently the most highly developed power amplifier for the u.h.f. band. It can be designed to have high stable gain, good power-handling capacity and reasonable efficiency. It operates with a high beam voltage and has an instantaneous bandwidth which is about the same as that of a triode.

Travelling-wave tubes designed for a bandwidth of one octave are limited in their mean power output by overheating of the helix. Tubes built with other forms of slow-wave structure can handle much more power, but the bandwidth is only some 5-10% of the mid-band frequency. Most tubes operate with a high beam voltage and a moderate power gain.

Backward-wave amplifiers based on crossed-field interaction are the latest addition to the range of u.h.f. power amplifiers. Although they require the beam voltage to be varied to tune them over an appreciable frequency band, they have the merits of an inherently high efficiency and low operating voltage. Their gain is low, but their size is not unreasonable.

It is clear that significant improvements in the tube per-

formance are to be expected and development is proceeding now with the emphasis on tubes which, individually, will amplify efficiently and reliably over a wide bandwidth.

(7) ACKNOWLEDGMENTS

The paper is published by permission of the General Manager of the English Electric Valve Co., Ltd., and the author is indebted also to numerous friends for stimulating discussions on various topics discussed.

(8) REFERENCES

- (1) SALISBURY, W. W.: 'The Resnatron', *Electronics*, 1946, **19**, p. 92.
- (2) LEWIS, I. A. D., *et al.*: 'An Electron Gun for use in a Metre-Wave High-Power Triode', Atomic Energy Research Establishment, Report No. A.E.R.E., GP/M168, 1954.
- (3) LEVI, R.: 'Improved Impregnated Cathode', *Journal of Applied Physics*, 1955, **26**, p. 639.
- (4) BENNETT, W. P., and KAZANOWSKI, H. F.: 'One Kilowatt Tetrode for U.H.F. Transmitters', *Proceedings of the Institute of Radio Engineers*, 1953, **41**, p. 13.
- (5) BENNETT, W. P.: 'New Beam Power Tubes for U.H.F. Service', *Transactions of the Institute of Radio Engineers*, 1956, ED-3, No. 1, p. 57.
- (6) BENNETT, W. P., *et al.*: 'A New 100-Watt Triode for 1 000 Megacycles', *Proceedings of the Institute of Radio Engineers*, 1948, **36**, p. 1296.
- (7) CHODOROW, M., *et al.*: 'The Design and Performance of a High-Power Pulsed Klystron', *ibid.*, 1953, **41**, p. 1584.
- (8) WARNECKE, R., and GUÉNARD, P.: 'Les tubes électroniques à commande par modulation de vitesse' (Gauthier-Villars, 1951).
- (9) BECK, A. H. W.: 'High-Order Space-Charge Waves in Klystrons', *Journal of Electronics*, 1957, **2**, p. 489.
- (10) LABUS, J.: 'Space Charge Waves along Magnetically Focussed Electron Beams', *Proceedings of the Institute of Radio Engineers*, 1957, **45**, p. 854.
- (11) MORROW, W. E., *et al.*: 'Single-Sideband Techniques in U.H.F. Long Range Communication', *ibid.*, 1956, **44**, p. 1854.
- (12) SMULLIN, L. D., *et al.*: 'Multicavity Klystrons'. Paper presented at the 14th Annual Conference on Electron Tube Research, Boulder, Colorado, June, 1956.
- (13) KREUCHEN, K. H., *et al.*: 'A Study of the Broadband Frequency Response of the Multicavity Klystron Amplifier', *Journal of Electronics*, 1957, **2**, p. 529.
- (14) MÜLLER, M.: 'New Points of View in the Design of Electron Guns for Cylindrical Beams of High Space Charge', *Journal of the British Institution of Radio Engineers*, 1956, **16**, p. 83.
- (15) HEIL, O., and EBERS, J. J.: 'A New Wide-Range, High Frequency Oscillator', *Proceedings of the Institute of Radio Engineers*, 1953, **38**, p. 645.
- (16) SÜSSKIND, C.: 'Electron Guns and Focusing for High Density Electron Beams', *Advances in Electronics and Electron Physics* (Academic Press, 1956), Volume 8.
- (17) BECK, A. H. W.: 'Velocity-Modulated Thermionic Tubes' (Cambridge University Press, 1948).
- (18) MULLETT, L. B., *et al.*: 'Multipactor Effect in Linear Accelerators and Other Evacuated R.F. Systems, and a New Cold Cathode Valve', Atomic Energy Research Establishment, Report No. A.E.R. GP/R1076, 1953.
- (19) KOMPFFNER, R.: 'The Travelling Wave Valve', *Wireless World*, 1947, **52**, p. 369.
- (20) PIERCE, J. R.: 'Theory of the Beam-type Travelling-Wave Tube', *Proceedings of the Institute of Radio Engineers*, 1947, **35**, p. 111.
- (21) PIERCE, J. R.: 'Traveling Wave Tubes' (Van Nostrand, 1950).
- (22) HARRIS, L. A.: 'Axially Symmetric Electron Beams and Magnetic Field Systems', *Proceedings of the Institute of Radio Engineers*, 1953, **40**, p. 700.
- (23) SLATER, J. C.: 'Microwave Electronics' (Van Nostrand, 1950).
- (24) CHODOROW, M., and CHU, E. L.: 'Cross-Wound Twin Helices for Traveling-Wave Tubes', *Journal of Applied Physics*, 1955, **26**, p. 31.
- (25) BIRDSALL, C. K., and EVERHART, T. E.: 'Modified Contra-Wound Helix Circuits for High Power Traveling Wave Tubes', *Transactions of the Institute of Radio Engineers*, 1956, ED-3, No. 4, p. 190.
- (26) CHODOROW, M., and NALOS, E. J.: 'The Design of High-Power Traveling-Wave Tubes', *Proceedings of the Institute of Radio Engineers*, 1956, **44**, p. 649.
- (27) NORDSIECK, A.: 'Theory of the Large-Signal Behaviour of Traveling-Wave Amplifiers', *ibid.*, 1953, **41**, p. 630.
- (28) TIEN, P. K., *et al.*: 'A Large-Signal Theory of Traveling-Wave Amplifiers', *ibid.*, 1955, **43**, p. 260.
- (29) CALDWELL, J. J., and HOCH, O. L.: 'Large-Signal Theory of High-Power Traveling-Wave Amplifiers', *Transactions of the Institute of Radio Engineers*, 1956, ED-3, No. 1, p. 6.
- (30) ROWE, J. E.: 'A Large-Signal Analysis of the Traveling-Wave Amplifiers—Theory and General Results', *ibid.*, p. 36.
- (31) MOURIER, G.: 'Contribution à la théorie du grand signal des t.p.o.', *Annales de Radioélectricité*, 1956, **11**, p. 271.
- (32) MILLMAN, S.: 'A Spatial-Harmonic Traveling-Wave Amplifier for 6mm Wavelength', *Proceedings of the Institute of Radio Engineers*, 1951, **39**, p. 1035.
- (33) GUÉNARD, P., *et al.*: 'Nouveaux tubes oscillateurs à large bande d'accord électronique pour hyperfréquences', *Comptes Rendus*, 1952, **235**, p. 236.
- (34) KOMPFFNER, R., and WILLIAMS, N. T.: 'Backward-Wave Tubes', *Proceedings of the Institute of Radio Engineers*, 1953, **41**, p. 1602.
- (35) CURRIE, M. R., and WHINNERY, J. R.: 'The Cascade Backward-Wave Amplifier: a High-Gain Voltage-Tuned Filter for Microwaves', *ibid.*, 1955, **43**, p. 1617.
- (36) BROWN, W. C.: 'Description and Operating Characteristics of the Platinotron—a New Microwave Tube Device', *ibid.*, 1957, **4**, p. 1209.

AMPLITUDE-MODULATED TRANSMITTER CLASS-C OUTPUT STAGE

Operating Conditions when the Load Impedance Varies over the Working Frequency Band

By C. G. MAYO, M.A., B.Sc., and H. PAGE, M.Sc., Members.

(The paper was first received 18th February, and in revised form 21st June, 1958.)

SUMMARY

The mode of operation of the amplitude-modulated transmitter class-C output stage is discussed, with particular reference to the case where the load impedance varies over the working frequency band; a typical example is that of a long-wave broadcasting transmitter. The impedance presented to the anode must be symmetrical with respect to the carrier frequency if non-linear distortion of the radiated signal is to be avoided. The carrier can be modulated fully at high audio frequencies if the impedance rises symmetrically (but not if it falls symmetrically) on each side of the carrier frequency.

LIST OF PRINCIPAL SYMBOLS

- C = Capacitance of tank-circuit condenser.
 i_a = Anode current.
 i_{ad} = Direct component of anode current.
 i_{af} = Peak value of fundamental component of anode current.
 m_a = Depth of modulation of anode current.
 m_v = Depth of modulation of applied anode voltage.
 m_f = Depth of modulation of radiated field.
 R_{cd} = Source resistance of class-C valve in d.c. condition.
 R_{c0} = Source resistance of class-C stage in idealized case (angle of current flow vanishingly small).
 $R_{c\theta}$ = Source resistance of class-C stage in practical case (angle of current flow θ).
 V_0 = Direct voltage applied to anode of class-C valve.
 $Z_a = R_a + jX_a$ = Impedance presented to class-C stage.
 Z_m = Impedance presented to modulator.
 η = Efficiency of class-C output stage.
 θ = Angle of anode-current flow in class-C stage.
 ω_m = Angular frequency of modulation; the angular frequencies of the corresponding r.f. sidebands are $\omega \pm \omega_m$.
 ω = Angular frequency of carrier.

(1) INTRODUCTION

The working frequency band of a long-wave broadcasting transmitter is comparable with the carrier frequency. In addition, the aerial usually has a low radiation resistance and a reactance which varies rapidly with frequency. The output stage of the transmitter is therefore required to work into a load whose impedance varies appreciably over the working band. Consequently, unless special precautions are taken, the radiated signal will suffer distortion; throughout the paper the term 'distortion' is restricted to mean non-linear distortion of the modulation, since non-uniformity of the frequency characteristic can be corrected easily.

One solution is to make the impedance of the load presented to the output stage as uniform as possible over the working band, by means of reactance-correcting networks in the aerial circuit.¹ This method is described in the Appendix to Reference 1, and was adopted in one of the long-wave transmitters used at the

B.B.C.'s Droitwich station, which incorporated a series-modulated output stage. Since the load impedance could not be made sufficiently uniform, distortion was avoided by making the reactance-corrected impedance symmetrical with respect to the carrier frequency. Throughout the paper, for brevity, the term 'symmetrical' is applied to impedance characteristics in which the resistive component is symmetrical and the reactive component is skew-symmetrical with respect to the carrier frequency.

It is also permissible to present to the output stage a symmetrical impedance without any reactance correction,² and then to achieve a uniform frequency characteristic by equalization. Sandeman³ discussed the operation of a class-C output stage (a valve biased to pass short pulses of anode current) working into a symmetrical impedance; he concluded that it is impossible to modulate the output stage fully. It will be shown later that this conclusion is incorrect.

The class-C output stage is commonly used now in high-power installations, because of its high efficiency; it is therefore of great practical importance. The purpose of the paper is to discuss this case, and to compare the performance when different types of network are used for coupling the aerial to the transmitter. In practice, another important consideration is that of the current and voltage ratings of the components required, but such calculations present no difficulty and need not concern us here.

Section 2 deals with the form of impedance characteristic presented to the output stage, Section 3 with the idealized operating conditions of the a.m. stage and the associated modulator, and Section 4 with the difference between the idealized and practical cases. Section 5 gives the results of an experimental investigation.

(2) THE LOAD-IMPEDANCE CHARACTERISTIC

The impedance characteristic typical of a long-wave broadcasting aerial is shown in Fig. 1(a); here ω_m is the difference between the angular frequency under consideration in the r.f. band and the carrier angular frequency. By a combination of series and parallel reactances the aerial impedance may be transformed into the equivalent circuit shown in Fig. 1(b). The series resistance, R , is made the same at the extreme sideband frequencies, and is approximately constant over the intervening band; the series reactance is approximately equal to $jRk\omega_m$, where k is a constant depending on the dimensions of the aerial. The impedance rises symmetrically on each side of the carrier frequency to $R(1 + k^2\omega_m^2)^{1/2}$; we shall refer to this as the 'symmetrical rising impedance'.

If the aerial circuit shown in Fig. 1(b) is preceded by a matched quarter-wave network (i.e. a network introducing a phase change of $\pi/2$ rad), the resulting impedance falls symmetrically on each side of the carrier frequency to $R(1 + k^2\omega_m^2)^{-1/2}$; the equivalent circuit is shown in Fig. 1(c). We shall refer to this as the 'symmetrical falling impedance'.

Here we have tacitly assumed that the transfer parameters of

¹Written contributions on papers published without being read at meetings are considered for consideration with a view to publication.
 Mr. Mayo and Mr. Page are with the British Broadcasting Corporation.

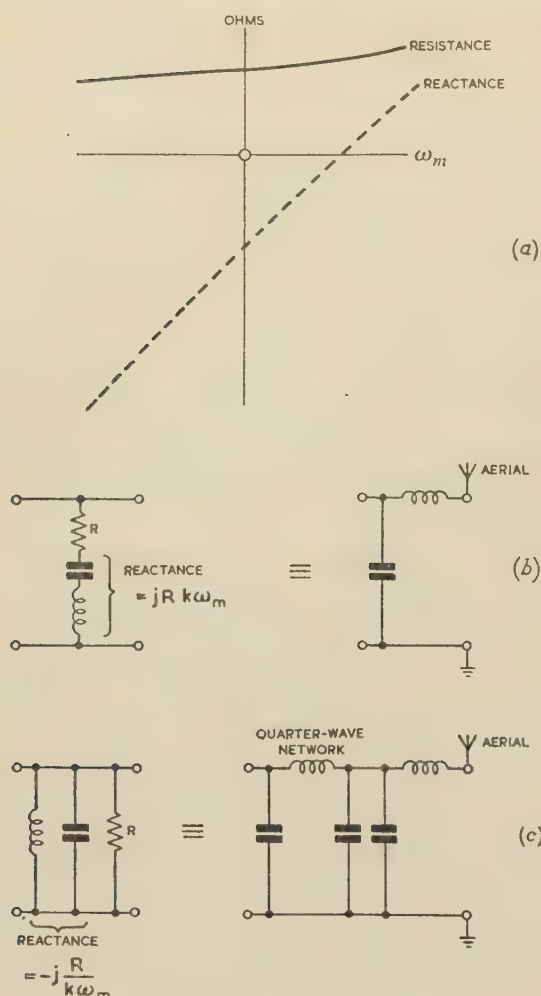


Fig. 1.—Load-impedance characteristic.

(a) Typical impedance characteristic of a long-wave aerial. ω_m is the difference between the angular frequency under consideration in the r.f. band and the carrier angular frequency.

(b) Aerial circuit having an impedance rising symmetrically at sideband frequencies.

(c) Aerial circuit having an impedance falling symmetrically at sideband frequencies.

the quarter-wave network are independent of frequency. A practical quarter-wave network increases the value of k , but generally to a negligible extent; it does not affect the symmetry of the impedance characteristic, provided that minor adjustments are made to the reactances in the aerial circuit. Similarly, the symmetry is unaffected by either the tuned anode circuit or the additional networks between the aerial and the transmitter output stage, provided that the total electrical length of these networks is an integral multiple of $\pi/2$ rad. If the integer is even, the symmetry is preserved without change of form, but if it is odd, the symmetrical rising impedance is transformed into the symmetrical falling impedance and vice versa.

For distortionless transmission the components of the radiated field at the complementary sidebands should be equal in amplitude and symmetrical in phase with respect to the carrier. The change in shape of the vertical radiation pattern of the aerial over the working band is negligible; the powers associated with the complementary sidebands must therefore be equal. Distortionless transmission is therefore achieved if an undistorted envelope of the modulation is obtained in an anode impedance which is symmetrical with respect to the carrier frequency, since in this case the phase/frequency transfer characteristic is sub-

stantially symmetrical. It is not necessary, for instance, for the resistance R in Fig. 1 to be constant over the working frequency band.

If the network connecting the symmetrical load impedance to the output stage has an electrical length other than an integral multiple of $\pi/2$ rad, the impedance presented to the output stage is asymmetrical with respect to the carrier frequency. It is shown in Section 3.1.4 that distortion of the radiated envelope results in this case.

(3) OPERATING CONDITIONS IN THE IDEALIZED CASE

(3.1) The Class-C Stage

(3.1.1) Carrier Unmodulated, Anode Circuit in Tune.

The circuit diagram of the idealized class-C stage is shown in Fig. 2. R is the load resistance, L the inductance of the coil and C the capacitance of the condenser in the anode tuned circuit, or tank circuit. The anode load is usually a virtual pure reactance at the harmonic frequencies, or it is made so by the inclusion of filters. The harmonic filter shown is taken from

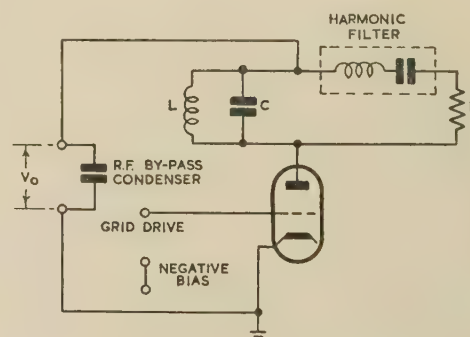


Fig. 2.—Circuit diagram of class-C stage.

have zero reactance at the fundamental frequency and a high reactance at the harmonic frequencies.

We will assume that the valve is heavily biased, passing infinitesimally short pulses of current, that its internal impedance is vanishingly small and that there is no limit to the current which the cathode can supply. At the start of the pulse a very large current flows; it decreases exponentially as the tank-circuit condenser becomes charged, and continues until the anode voltage is reduced to that of the cathode, which is taken as zero. The anode current therefore takes the form of impulses of large amplitude but short duration, repeated at time intervals of $2\pi/\omega$. If we write the fundamental component of anode current as $i_{af} \cos \omega t$, it follows from the Fourier expansion for a repeated impulse that the anode-current pulses occur at $\omega t = 0, 2\pi, \dots$ that the direct component of anode current, i_{ad} , is given by

$$i_{ad} = i_{af}/2 \quad \dots \quad (1)$$

and that the quantity of electricity flowing during each pulse is $\pi i_{af}/\omega$. This instantaneous change in charge can be accommodated only by the condenser C ; there is therefore a step of $\pi i_{af}/C\omega$ in the voltage across C , and a corresponding step of opposite sign in the anode voltage. The ratio between the step and peak value of the fundamental component is therefore $\pi/(RC\omega)$, or π/Q , where Q is the Q-factor of the load presented to the anode.

The fundamental and harmonic components of the anode current are in phase at $\omega t = 0, 2\pi, \dots$. Since the anode load

a pure reactance at harmonic frequencies, the total harmonic stage across the tank circuit is zero at the troughs and crests the fundamental component; it is also skew-symmetrical with respect to $\omega t = 0, 2\pi, \dots$. The value of V_0 minus the fundamental component of tank-circuit voltage at these instants is before one-half of the step. It follows that

$$V_0 - Ri_{af} = \pi i_{af} / (2C\omega)$$

$$V_0 = i_{af}(R + R_{c0}) \quad (2)$$

$$R_{c0} = \pi / (2C\omega) \quad (3)$$

other words, so far as the fundamental component is concerned, the valve behaves like a source having a peak e.m.f. of $i_{af}R$ and a source resistance of R_{c0} ; R_{c0} is usually small compared with R . The anode-voltage waveform for this idealized case is shown in Fig. 3(a).

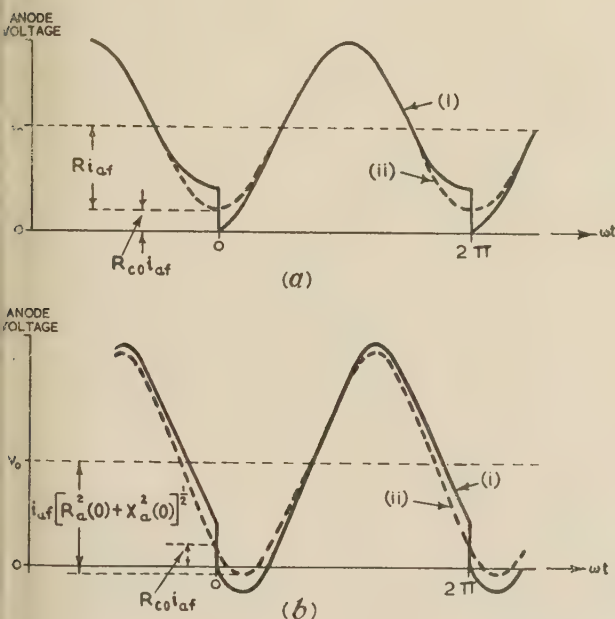


Fig. 3.—Anode-voltage waveforms (idealized case).

- (i) Anode voltage.
- (ii) V_0 plus fundamental component of anode voltage.
- { (a) Anode circuit in tune.
- { (b) Anode circuit mistuned.

We will designate the impedance presented to the modulator at zero frequency by $Z_m(0)$. From eqns. (1) and (2) it follows that

$$Z_m(0) = V_0 / i_{ad} = 2V_0 / i_{af} = 2(R + R_{c0}) \quad (4)$$

The efficiency of the stage, η , is defined as the ratio between the r.f. output power and the power supplied to the anode. It follows that

$$\eta = \frac{Ri_{af}^2}{2V_0i_{ad}} = \frac{1}{1 + \frac{R_{c0}}{R}} = \frac{1}{1 + \frac{\pi}{2Q}} \quad (5)$$

$Q = 10$, for instance, the efficiency is 87%. In view of the idealized conditions assumed, it might at first appear that the efficiency should be unity. However, power is lost if a condenser is charged directly from a battery, and the initial current tends to infinity. If, in our case, the internal resistance of the valve in the d.c. condition is R_{cd} , the

anode voltage immediately prior to the step is $\pi i_{af} / (C\omega)$; the anode current, i_a , is then given by

$$i_a = \frac{\pi i_{af}}{C\omega R_{cd}} \exp\left(-\frac{t}{CR_{cd}}\right)$$

The power loss in the valve is therefore

$$\frac{\omega}{2\pi} \int_0^{2\pi/\omega} R_{cd} i_a^2 dt = R_{c0} \frac{i_{af}^2}{2}$$

since we may take the contribution from the upper limit as zero. This result is independent of R_{cd} , and applies even if R_{cd} is a function of i_a , as will usually be the case. The calculated power loss in the valve is consistent with the expression for the efficiency in eqn. (5).

Throughout the remainder of the paper we shall be considering the effects either of mistuning, or of modulating, the class-C stage. For these cases it is convenient to work in terms of the r.f. impedance presented to the class-C stage, i.e. the impedance of the combined aerial load, tank circuit and any intervening networks. This impedance will be called the anode impedance and designated $Z_a = R_a + jX_a$; correspondingly we will write $Z_a(\omega_m) = R_a(\omega_m) + jX_a(\omega_m)$ as the anode impedance at an angular frequency $(\omega + \omega_m)$. In the modulated case ω_m is the angular frequency of the modulation. The harmonic filter ensures that R_a is zero at harmonics of any frequency.

(3.1.2) Carrier Unmodulated, Anode Circuit Mistuned.

The anode impedance in this case is $R_a(0) + jX_a(0)$, where $X_a(0)$ is a measure of the degree of mistuning. For anode current pulses at $\omega t = 0, 2\pi, \dots$ the fundamental component of anode current must be of the form $i_{af} \cos \omega t$; the corresponding tank-circuit voltage can be written

$$i_{af}[R_a(0) \cos \omega t - X_a(0) \sin \omega t]$$

The fundamental components of anode current and anode voltage are therefore not in phase. Since the $\sin \omega t$ term is zero at $\omega t = 0, 2\pi, \dots$, so far as the valve is concerned the value of $X_a(0)$ is immaterial; it follows that eqns. (2) and (3) apply in this case also, with $R_a(0)$ replacing R .

Compared with the case when $X_a(0) = 0$, the fundamental component of tank-circuit voltage is increased in the ratio $[R_a^2(0) + X_a^2(0)]^{1/2} / R_a(0)$, and is advanced in phase relative to the fundamental component of anode current by $\arctan [X_a(0) / R_a(0)]$; the anode voltage may therefore swing below zero if $X_a(0)$ is sufficiently large. Fig. 3(b) shows the anode-voltage waveform for a case in which the anode impedance is capacitive.

We therefore adopt the following procedure whether the anode circuit is in tune or not. An anode current with a fundamental component $i_{af} \cos \omega t$ is postulated, and the associated fundamental component of tank-circuit voltage is calculated. The applied voltage minus the tank-circuit voltage must then be equal to $R_{c0}i_{af}$ when $\omega t = 0, 2\pi, \dots$. R_{c0} has the value given in eqn. (3), but it is no longer equivalent to a source resistance when the anode circuit is mistuned.

(3.1.3) Carrier Amplitude Modulated, Symmetrical Anode Impedance.

The anode impedance corresponding to an angular frequency $(\omega + \omega_m)$ is $R_a(\omega_m) + jX_a(\omega_m)$; since it is symmetrical with respect to the carrier frequency, $R_a(\omega_m) = R_a(-\omega_m)$ and $X_a(\omega_m) = -X_a(-\omega_m)$.

Suppose that we have established a condition where the

fundamental component of the anode current is modulated to a depth m_c at an angular frequency ω_m . It may be written

$$i_{af}(1 + m_c \cos \omega_m t) \cos \omega t = \frac{1}{2} i_{af} [m_c \cos (\omega - \omega_m)t + 2 \cos \omega t + m_c \cos (\omega + \omega_m)t] \quad (6)$$

The corresponding fundamental component of tank-circuit voltage is

$$\frac{1}{2} i_{af} [m_c R_a(\omega_m) \cos (\omega - \omega_m)t + m_c X_a(\omega_m) \sin (\omega - \omega_m)t + 2 R_a(0) \cos \omega t + m_c R_a(\omega_m) \cos (\omega + \omega_m)t - m_c X_a(\omega_m) \sin (\omega + \omega_m)t] \quad (7)$$

When $\omega t = 0, 2\pi, \dots$ expression (7) becomes

$$i_{af} [m_c R_a(\omega_m) \cos \omega_m t - m_c X_a(\omega_m) \sin \omega_m t + R_a(0)] \quad (8)$$

It follows from the last paragraph of Section 3.1.2 that

Applied voltage

$$\begin{aligned} &= i_{af} [m_c R_a(\omega_m) \cos \omega_m t - m_c X_a(\omega_m) \sin \omega_m t \\ &\quad + R_a(0) + R_{c0}(1 + m_c \cos \omega_m t)] \\ &= i_{af} [R_a(0) + R_{c0}] \\ &\quad \left\{ 1 + m_c \frac{[R_a(\omega_m) + R_{c0}] \cos \omega_m t - X_a(\omega_m) \sin \omega_m t}{R_a(0) + R_{c0}} \right\} \quad (9) \end{aligned}$$

This can be written $V_0(1 + m_v \cos \omega_m t)$, where m_v is the depth of modulation of the applied voltage. We will express m_c/m_v as a complex number; the modulus is the ratio of the depths of anode-current and anode-voltage modulation, and the argument gives the relative phase.

Hence
$$i_{af} = \frac{V_0}{R_a(0) + R_{c0}} \quad (10)$$

and
$$\frac{m_c}{m_v} = \frac{R_a(0) + R_{c0}}{[R_a(\omega_m) + R_{c0}] + jX_a(\omega_m)} = \frac{R_a(0) + R_{c0}}{Z_a(\omega_m) + R_{c0}} \quad (11)$$

In other words, the anode-current modulation is a distortionless version of the applied modulated voltage, but differs in depth in the ratio $|R_a(0) + R_{c0}|/|Z_a(\omega_m) + R_{c0}|$ and is retarded in phase by $\arctan \{X_a(\omega_m)/[R_a(\omega_m) + R_{c0}]\}$.

For the reasons given in Section 2, the envelope of the radiated field will also be a distortionless version of the applied modulated voltage. The depth of modulation, m_f , is given by

$$\frac{m_f}{m_c} = \left[\frac{R_a(\omega_m)}{R_a(0)} \right]^{1/2} \quad (12)$$

The radiated signal is therefore distortionless, provided that the anode-impedance characteristic is symmetrical. A typical anode-voltage waveform is shown in Fig. 4(a). The peaks of the fundamental component of anode voltage nearly (but not quite) follow the applied modulated voltage, and the troughs follow the locus of the half-steps of anode current. Fig. 4(a) is drawn for the case when $m_v < m_c$, i.e. for the symmetrical falling impedance; the corresponding waveforms for the symmetrical rising impedance would be similar, except that m_c would then be less than m_v . However, the maximum achievable modulation depth for these two cases differs, and this point is discussed next.

(3.1.3.1) Symmetrical Falling Impedance.

For symmetrical falling impedance the ratio m_c/m_v given by eqn. (11) is greater than unity. When $m_c = 1$, the anode current, and simultaneously the anode voltage in the troughs, passes through zero at one point in the cycle. If the depth of voltage modulation is increased, the anode-voltage envelope can remain in step only if the valve passes a reverse current.

Since this is not possible, as the applied modulated voltage falls the anode voltage in the troughs falls with it, and becomes negative with respect to the cathode at the time when the pulses of anode current would normally flow. The after the anode voltage follows a damped oscillation, with steps, until the applied modulated voltage increases sufficiently to raise the anode voltage above zero. Consequently, the depth of modulation of the radiated field cannot exceed $[R_a(\omega_m)/R_a(0)]$ without introducing non-linear distortion of the modulation.

Fig. 4(b) shows the anode-voltage waveform when $m_v = 1$, i.e. $m_c > 1$. In that part of the modulation cycle requiring reverse anode current the r.f. envelope is 'flattened', as in a saturated amplifier.

(3.1.3.2) Symmetrical Rising Impedance.

For symmetrical rising impedance the ratio m_c/m_v given by eqn. (11) is less than unity. To modulate the anode current fully we must therefore modulate the applied voltage to a depth which is greater than unity. But there is a reason why the anode voltage should not be permitted to swing below zero; the steps now appear on the troughs of the waveform during part of the cycle, and on the crests the remainder of the cycle, as shown in Fig. 4(c). The anode current can therefore be fully modulated; the depth of modulation of the radiated field, m_f , is then given by eqn. (12).

If the tank-circuit reactance can be neglected, and if the equivalent circuit of the aerial is as shown in Fig. 1(b) with $R_a(\omega_m) = R_a(0)$, the radiated field can be fully modulated. For the symmetrical rising impedance the effect of the tank-circuit reactance is to make $R_a(\omega_m) > R_a(0)$. Not only is modulation, but genuine overmodulation, of the radiated field is therefore possible; an example is given in Section 5.4.

(3.1.4) Carrier Amplitude Modulated, Asymmetrical Anode Impedance.

Suppose next that

$$\begin{aligned} R_a(-\omega_m) &= R(\omega_m) - r(\omega_m), & R_a(\omega_m) &= R(\omega_m) + r(\omega_m) \\ X_a(-\omega_m) &= -X(\omega_m) + x(\omega_m), & X_a(\omega_m) &= X(\omega_m) + x(\omega_m) \end{aligned}$$

where $r(\omega_m)$ and $x(\omega_m)$ are the deviations of load resistance and reactance, respectively, from the symmetrical components $R(\omega_m)$ and $X(\omega_m)$.

Proceeding as in Section 3.1.3, we find that, in this case also, the anode-current modulation is a distortionless version of the applied modulated voltage, but differs in depth in the ratio given by eqn. (11) with $R(\omega_m)$ replacing $R_a(\omega_m)$ and $X(\omega_m)$ replacing $X_a(\omega_m)$; this ratio is independent of the values of $r(\omega_m)$ and $x(\omega_m)$. But since $R_a(-\omega_m) \neq R_a(\omega_m)$, the powers in complementary sidebands are unequal. It therefore follows from Section 2 that an asymmetrical load impedance results in non-linear distortion of the envelope of the radiated field.

(3.2) The Modulator

The audio-frequency current supplied by the modulator can be regarded as a slowly varying direct current supplied to the class-C stage. For voltage- and current-modulation depths m_v and m_c respectively, it follows from eqns. (4), (10) and (11) that the impedance $Z_m(\omega_m)$ presented to the modulator at angular frequency ω_m is given by

$$Z_m(\omega_m) = \frac{2V_0 m_v}{i_{af} m_c} = 2[Z_a(\omega_m) + R_{c0}]$$

In the case of an asymmetrical anode impedance the same result applies with $Z_a(\omega_m)$ replaced by the symmetrical component defined in Section 3.1.4.

As the modulation frequency increases, the symmetrical falling

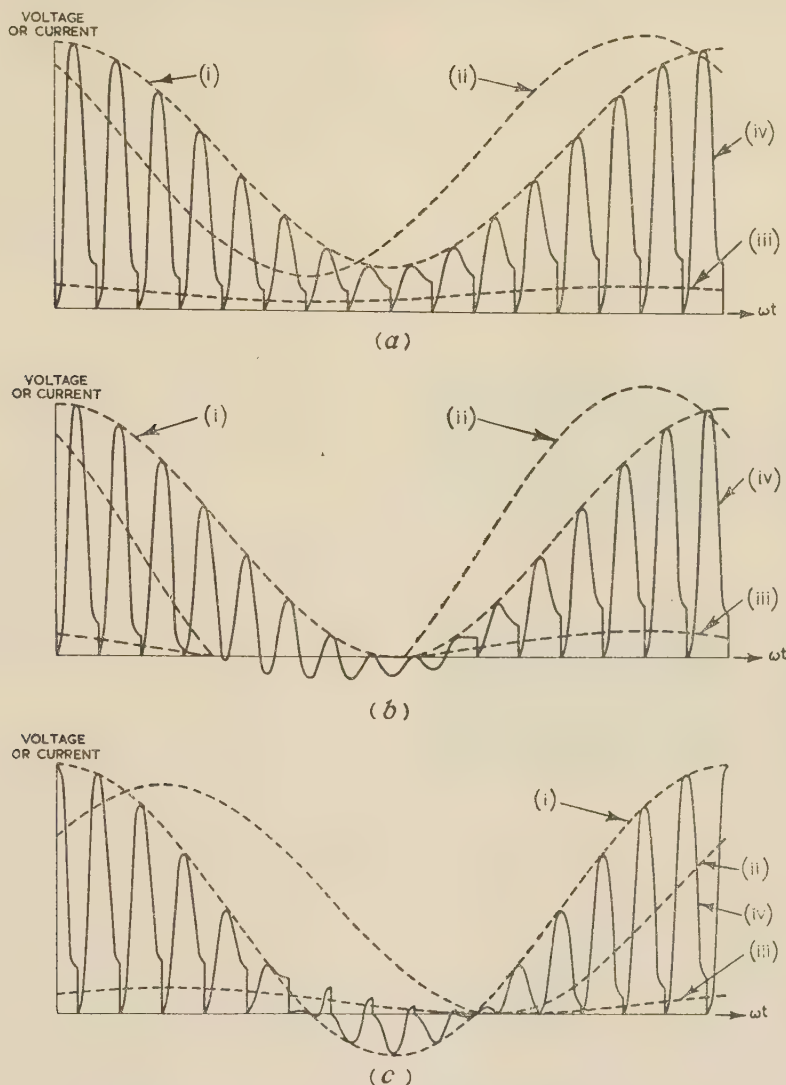


Fig. 4.—Anode-voltage waveforms (idealized case).

- (i) Envelope of anode voltage.
 - (ii) Envelope of anode current.
 - (iii) Envelope of half step.
 - (iv) Anode-voltage waveform.
- $\begin{cases} (a) m_v < 1, m_e < 1; \\ (b) m_v = 1, m_e > 1; \\ (c) m_v > 1, m_e = 1; \end{cases}$
- $\begin{cases} (a) \text{symmetrical falling impedance.} \\ (b) \text{symmetrical rising impedance.} \\ (c) \text{symmetrical rising impedance.} \end{cases}$

characteristic consequently presents a falling impedance to the modulator, and the symmetrical rising characteristic presents a rising impedance. Unless special precautions are taken, therefore, the frequency characteristic of the modulator will be affected by the non-uniform load impedance presented to it. This can be corrected in a low-power a.f. stage, but the maximum modulation depth achieved may then be limited by the power-handling capacity of the modulator. Alternatively, the impedance presented to the modulator may be equalized by means of reactance elements; but the cost of such high-power components may be large, and it may be just as convenient and cheap to equalize the impedance of the anode load presented to the class-C output stage.

In a practical case the r.f. by-pass condenser from the tank circuit to earth may also have an important effect on the impedance presented to the modulator; it may, however, be possible to incorporate it in the equalizing network mentioned above.

(4) OPERATING CONDITIONS IN THE PRACTICAL CASE

So far we have idealized conditions by assuming that the class-C valve has a vanishingly small d.c. source resistance, and that the anode current takes the form of infinitesimally short pulses. In practice, the valve has a finite internal resistance of R_{cd} . Provided that the grid drive is sufficient, the valve may be regarded as a switch which is closed when the grid voltage is sufficiently high to permit the valve to conduct. The equivalent circuit is shown in Fig. 5*; it is assumed that the tank circuit is in tune. The anode current can be determined in specific cases, but to obtain a general result it is necessary to make approximations. We will assume that the duration of the current pulse is small, but not vanishingly small as heretofore. It will be defined by the angle of current flow, θ , where θ/ω is the pulse duration;

* If the grid voltage is allowed to exceed the anode voltage at any instant there are subsidiary effects and our equivalent circuit is no longer valid; this case is excluded. In other respects, too, our equivalent circuit is greatly simplified, in order to facilitate the analysis.

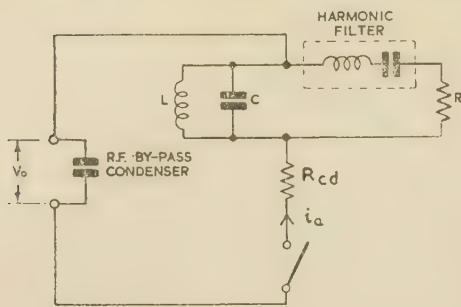


Fig. 5.—Equivalent circuit of class-C stage.

θ is assumed to be sufficiently small to make $1 - \cos \frac{1}{2}\theta \ll 1$. The fundamental component of anode voltage [curve (a) in Fig. 6] is then virtually constant throughout the pulse. The anode voltage at the beginning of the pulse may therefore be taken as $V_0 - R_a(0)i_{af} + R_{c0}i_{af}$, since, from Section 3.1.1, the tank-circuit voltage decays over one half-cycle in the ratio $1 - [R_{c0}/R_a(0)]$.

During the current pulse it is permissible to neglect the current in L and R in Fig. 5 compared with that in C ; we obtain

$$i_a = \frac{V_0 - R_a(0)i_{af} + R_{c0}i_{af}}{R_{cd}} e^{-t/CR_{cd}}$$

where t is the time from the start of the pulse. The anode-current waveform is shown in Fig. 6; it rises initially to a value

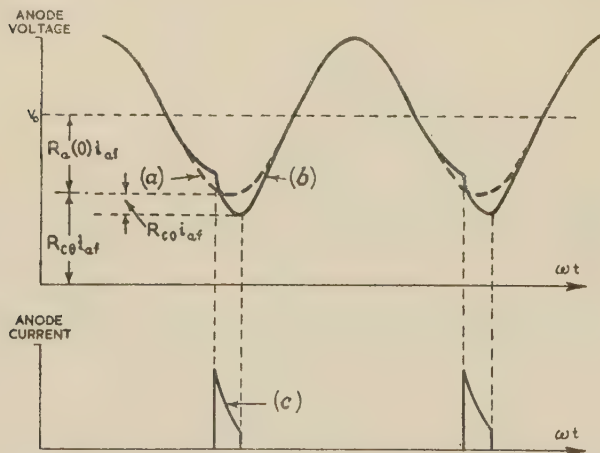


Fig. 6.—Anode-voltage and anode-current waveforms for circuit shown in Fig. 5.

- (a) V_0 plus fundamental component of anode voltage.
(b) Anode voltage.
(c) Anode current.

determined by R_{cd} ; decreases exponentially, and terminates abruptly when $t = \theta/\omega$. Since θ is assumed to be small, the peak value of the fundamental component is given by

$$i_{af} = \frac{\omega}{\pi} \int_0^{\theta/\omega} i_a dt = \frac{C\omega}{\pi} [V_0 - R_a(0)i_{af} + R_{c0}i_{af}] (1 - e^{-\theta/C\omega R_{cd}})$$

Let $V_0 = i_{af} [R_a(0) + R_{c0}]$

where R_{c0} is the effective source resistance of the stage for an angle of current flow θ . Using the value for R_{c0} given in eqn. (3), we have

$$R_{c0} = R_{c0} \left(\frac{1 + e^{-\theta/C\omega R_{cd}}}{1 - e^{-\theta/C\omega R_{cd}}} \right) = R_{c0} \coth \left(\frac{\theta}{2C\omega R_{cd}} \right) \quad (14)$$

To give the performance of the practical class-C stage, therefore, we must replace R_{c0} in the formulae in Section 3 by $R_{c\theta}$. For instance, eqn. (5) can be used to give the efficiency in practical case for any load resistance.

We see from eqns. (3) and (14) that, when θ is very small,

$$R_{c\theta} \approx \pi R_{cd} \theta \quad (15)$$

whereas R_{c0} is $\pi/(2C\omega)$; unlike R_{c0} , therefore, $R_{c\theta}$ is independent of C when θ is very small. Moreover, even when θ is not very small, $R_{c\theta}$ does not depend greatly on C , provided that $\theta/C\omega R_{cd} < 1$.

A further effect of the finite resistance of the valve is that since the minimum anode voltage is proportional to the anode current at the end of the pulse, the voltage minima in curve (b) of Fig. 6 will follow the anode-current modulation; in the ideal case shown in Fig. 4, on the other hand, the voltage minima are on the zero-voltage axis.

(5) EXPERIMENTAL RESULTS

(5.1) The Experimental Arrangement

The circuit diagram is shown in Fig. 7. For convenience a receiving-type valve (type EL84) was used, working on a carrier frequency of 180 kc/s; the output power was about 2 watts. The modulation frequency was made a submultiple of the carrier

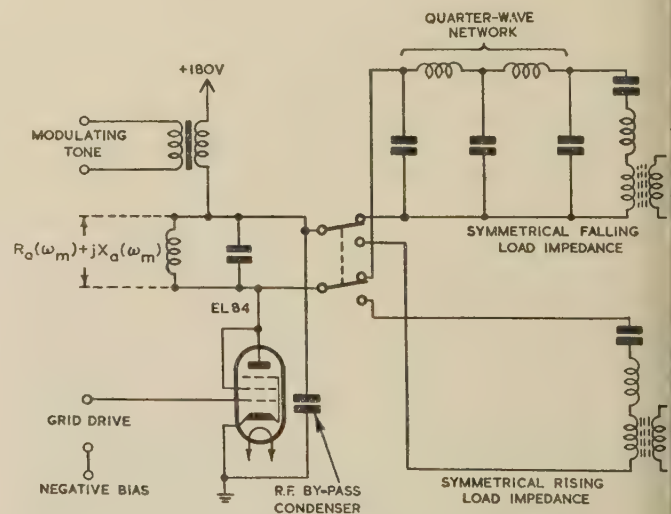


Fig. 7.—Circuit diagram of experimental arrangement.

frequency, in order to obtain a stationary display of the waveforms on the screen of the cathode-ray tube. A high modulation frequency was chosen (11.25 kc/s), in order to exaggerate the effects under investigation. A low-impedance drive source was used in order to minimize feedback from the anode circuit.

The symmetrical rising impedance was simulated by a series-tuned circuit; it included a transformer to simplify connection of the oscillograph. A symmetrical falling impedance was obtained by adding a quarter-wave network in cascade.

(5.2) Internal Resistance of the Class-C Stage

The effective source resistance was found by measuring the fundamental component of output voltage with various load resistances and for two values of θ , namely 50° and 100° . The series-tuned circuit was connected in series with the load resistance to act as a harmonic filter. The results are shown in Fig. 8; the reciprocal of the output voltage and the load c

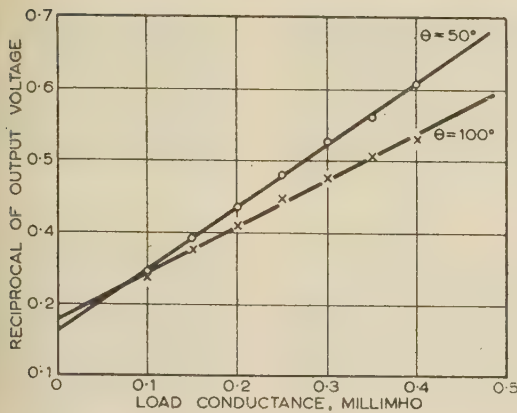


Fig. 8.—Reciprocal of output voltage as a function of load conductance.

istance are linearly related, demonstrating that the stage plays a linear source resistance. The experimental values derived from Fig. 8 are shown in Table 1. For comparison, the theoretical values given in eqn. (14) are also tabulated.

Table 1

INTERNAL RESISTANCE OF THE CLASS-C STAGE

Angle of current flow	Effective source resistance	
	Measured	Theoretical
deg	ohms	ohms
50	3 300	4 600
100	2 100	2 600

The theoretical and measured values are in reasonable agreement, bearing in mind the approximations made in deriving eqn. (14). The theoretical method used therefore gives a useful guide to the value of $R_{c\theta}$, but if an accurate value is required, it must be determined experimentally.

The measured values of $R_{c\theta}$ in Table 1 were determined for a supply voltage of 180 volts, the value used in the experiment. Tests were also carried out with reduced supply voltages; for each value the direct grid current was observed for the normal drive and load resistance, and then maintained at this value the load resistance was changed, by controlling the grid drive.

The value of $R_{c\theta}$ was found to be the same for supply voltages down to 25 volts; in other words, the stage was linear up to high levels of modulation.

In passing, it should be mentioned that the values of $R_{c\theta}$ given here apply to a receiving-type valve. They are not necessarily typical of those applying to high-power transmitting valves.

(5.3) Anode Voltage and Current Waveforms

Fig. 9 shows the anode-voltage and anode-current waveforms for two values of θ (50° and 100°) and two values of Q (4 and 8); the horizontal lines correspond to voltages of 0, V_0 and $2V_0$.

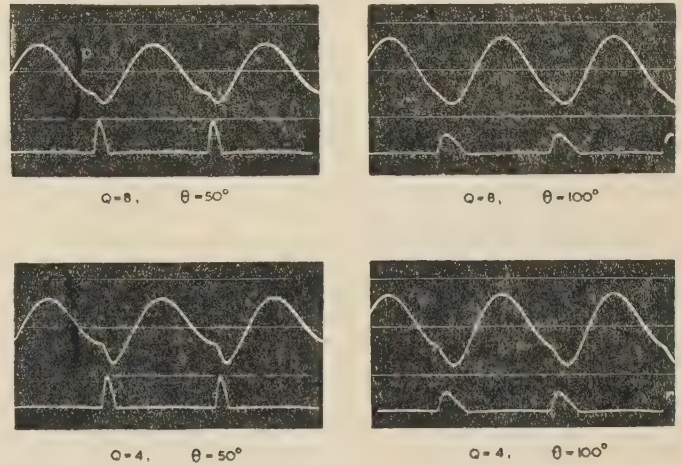


Fig. 9.—Anode-voltage and anode-current waveforms.

The general shape of the current pulses is in accordance with expectations; the leading and trailing edges are much more gradual than predicted, but this is not surprising, in view of the somewhat crude assumptions made in Section 4. The difference is probably due to the controlling effect of the grid; this cannot be avoided if there is a large capacitance across the anode circuit, as in the conventional class-C stage. The ratio between the voltage step and the peak value of the fundamental component is in good agreement with the theoretical value for short pulses, namely π/Q .

(5.4) Modulation Characteristics

The load circuits used are shown in Fig. 7, and their characteristics are summarized in Table 2. The load impedance was

Table 2

Parameter	Symmetrical falling impedance			Symmetrical rising impedance		
	Angular frequency			Angular frequency		
	$\omega - \omega_m$	ω	$\omega + \omega_m$	$\omega - \omega_m$	ω	$\omega + \omega_m$
	kilohms	kilohms	kilohms	kilohms	kilohms	kilohms
Load	$1.7 + j2.1$	$5.7 + j0$	$1.8 - j2.0$	$4.7 - j6.8$	$5.0 + j0$	$5.2 + j6.8$
Tank circuit	$+j9.2$	∞	$-j10.4$	$+j9.2$	∞	$-j10.4$
Load + tank circuit	$1.2 + j1.9$	$5.3 + j0$	$1.2 - j1.8$	$11.9 + j3.3$	$4.8 + j0$	$12.0 - j1.0$
$Z_{a(\omega_m)}$ (measured)		3.3			3.3	
Anode impedance = $Z_{a(\omega_m)} + R_{c\theta}$	$4.5 + j1.9$	$8.6 + j0$	$4.5 - j1.8$	$15.2 + j3.3$	$8.1 + j0$	$15.3 - j1.0$
m_v		1.75			0.53	
m_c		0.48			1.58	
m_0		0.84			0.83	

measured after adjustment for symmetry, and the tank circuit after tuning at the carrier frequency. The load impedance was then readjusted to make the impedance of the combination as symmetrical as possible; this impedance is therefore only approximately equal to the parallel combination of the previously measured load and tank-circuit impedances.

The waveform of the modulated signal across the load resistor was photographed for different depths of modulation of the applied voltage. The radiated field would have a similar waveform in this case, since the resistance is independent of frequency. The anode-voltage waveform (without the d.c. component) was also photographed, in order to study some of the features previously discussed. Only the portion near the voltage minimum is shown, since this is the region of greatest interest.

The angle of current flow was maintained at 50° and the Q-factor was approximately 4.4 throughout this series of tests, in order to make the anode-voltage step more obvious in the photographs. The depth of modulation of the applied voltage was deduced by measuring the direct voltage and the a.f. voltage supplied by the modulator.

(5.4.1) Symmetrical Falling Impedance.

The results for the symmetrical falling impedance are shown in Fig. 10(a). For curve (i) $m_f = 37\%$ and $m_v = 47\%$; hence $m_f/m_v = 0.79$ —a value in good agreement with the ratio predicted in Table 2. The anode-current modulation, as indicated by the height of the steps in curve (ii), is advanced in phase with respect to the voltage modulation. For curve (iii), m_v was increased until the steps at the centre of curve (iv) just disappeared; m_v was then 63% . The measured value of m_f was 49% ; from Table 2 the predicted value is 48% . For curve (v) m_v was increased to 108% ; the output envelope is distorted, being flattened in the negative part of the modulation cycle. The steps are absent from the corresponding part of the trace in curve (vi).

(5.4.2) Symmetrical Rising Impedance.

Fig. 10(b) is similar to Fig. 10(a), but applies to the symmetrical rising impedance; the measured ratio m_f/m_v is in good agreement with the predicted ratio. The chief feature of interest is that, as shown in curve (iii), it is possible to modulate the radiated field fully; the steps on the anode voltage in curve (iv) then appear on the crests during that part of the cycle corresponding to overmodulation. It should, however, be mentioned that, in order to achieve full modulation without distortion, exact symmetry of the anode-impedance characteristic is very important. The tuning of the tank circuit therefore requires great care, and should preferably be carried out in conjunction with a waveform display. It is also of interest to see from curve (v) that genuine overmodulation of the output signal is possible. This is because the compensating effect of the tank-circuit reactance results in the series resistance of the anode impedance rising at the side-band frequencies.

Table 3

Frequency	Impedance presented to modulator ($\theta = 50^\circ$)			
	Symmetrical falling impedance		Symmetrical rising impedance	
	Theoretical	Measured	Theoretical	Measured
kc/s	kilohms	kilohms	kilohms	kilohms
0	17.2	17.1	16.2	17.1
0.5	$17.2 \angle 0^\circ$	$18.1 \angle 0^\circ$	$16.2 \angle 0^\circ$	$18.1 \angle 0^\circ$
11.25	$9.8 \angle -22^\circ$	$11.1 \angle -15^\circ$	$31.0 \angle -8^\circ$	$31.5 \angle -9^\circ$

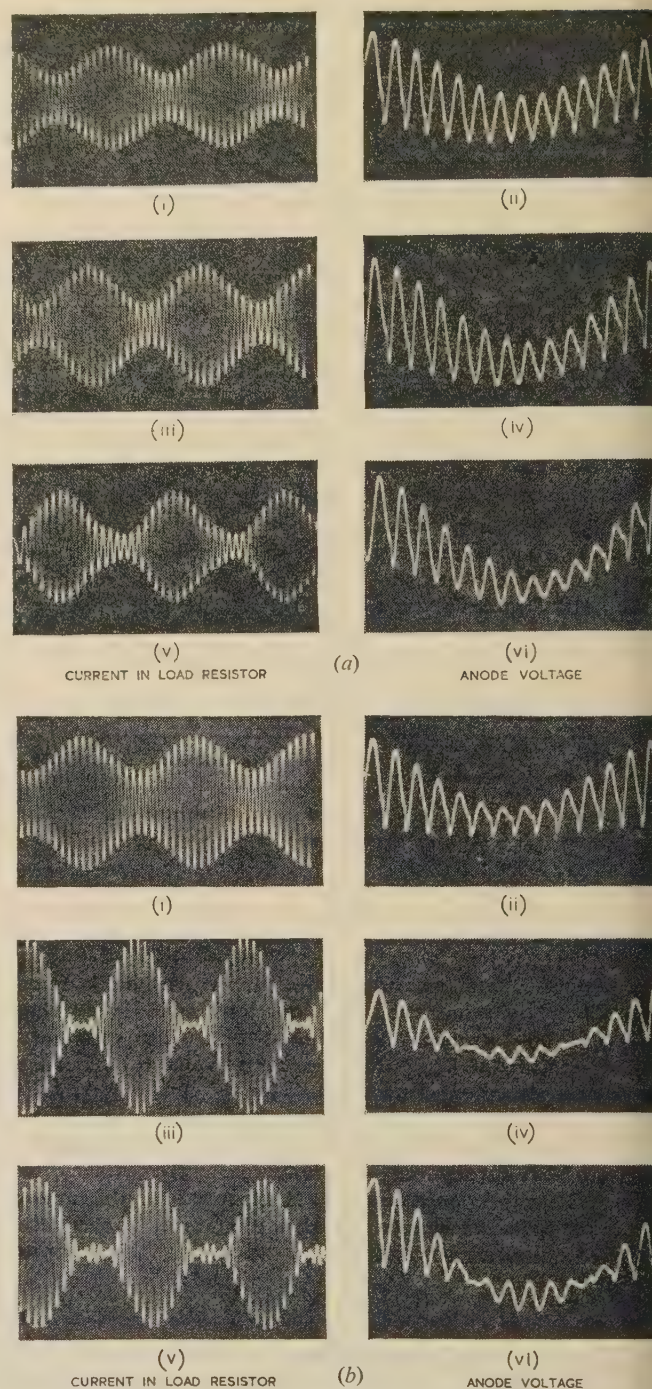


Fig. 10.—Load-current and anode-voltage waveforms.

(a) Symmetrical falling impedance.
(b) Symmetrical rising impedance.

(5.5) The Modulator

The impedance presented to the modulator was measured means of a bridge. In order to avoid dilution of the required impedance by the r.f. by-pass condenser, the bridge was designed both to incorporate this condenser and also to provide the supplies to the class-C stage. In a practical case, of course, reactance of the r.f. by-pass condenser is an additional parallel load on the modulator. The results are shown in Table 3; there is reasonable agreement between theoretical and measured values.

(6) CONCLUSIONS

A symmetrical anode impedance permits the radiation of an undistorted output envelope, whereas an asymmetrical impedance does not; only symmetrical anode impedances are therefore considered in the following conclusions.

The symmetrical falling impedance imposes a limit on the depth of modulation equal to the square root of the ratio between the resistive component of the anode impedance at the extreme sideband frequencies and that at the carrier frequency. In practice, the depth of modulation at the upper audio frequencies is not usually high, and it is a matter of opinion whether this limitation is important. On the other hand, in the case of the asymmetrical rising impedance the radiated signal can be fully modulated, but the degree of symmetry must then be high to achieve this condition.

The impedance presented to the modulator is twice the sum of the anode impedance at the upper sideband frequency and the average resistance of the class-C stage. The frequency characteristic will therefore be affected to an extent depending on the average impedance of the modulator. If only low depths of modulation at the upper audio frequencies are catered for, the equalization can be included in an earlier part of the a.f. chain. Higher depths of modulation can be achieved, apart from the limitation referred to above, by equalizing the a.f. impedance presented to the modulator, using reactance elements. In

practice it may be easier and cheaper to equalize the r.f. load impedance. The r.f. by-pass condenser from the tank circuit to earth will also affect the impedance presented to the modulator.

The anode circuit having a symmetrical falling impedance has the advantage that the peak voltage at the modulator output will be less than for the circuit having a symmetrical rising impedance.

(7) ACKNOWLEDGEMENTS

The authors wish to thank the Chief Engineer of the British Broadcasting Corporation for permission to publish the paper. They also wish to acknowledge the assistance given by their colleague Mr. D. W. Osborne, who carried out the experimental investigation.

(8) REFERENCES

- (1) ASHBRIDGE, SIR NOEL, BISHOP, H., and MACLARTY, B. N.: 'The Droitwich Broadcasting Station', *Journal I.E.E.*, 1935, **77**, p. 437.
- (2) MACNAMARA, T. C., HOWE, A. B., and BEVAN, P. A. T.: 'The Design and Operation of High-Power Broadcast Transmitter Units with their Outputs combined in Parallel', *ibid.*, 1948, **95**, Part III, p. 183.
- (3) SANDEMAN, E. K.: 'Radio Engineering' (Chapman and Hall, 1949), Vol. II, p. 421.

THE REDUCTION OF LOW-FREQUENCY NOISE IN FEEDBACK INTEGRATORS

By E. M. DUNSTAN, M.Sc., and M. J. SOMERVILLE, B.Sc., Graduate.

(The paper was first received 19th December, 1957, and in revised form 30th May, 1958.)

SUMMARY

Two methods of designing a feedback integrator for use with repetitive inputs are described. Each results in a considerable improvement in signal/noise ratio compared with that of a conventional direct-coupled integrator.

The first method uses an error amplifier containing a single CR coupling. In the second, phase correction is applied to the output from a low-accuracy direct-coupled integrator, increasing the accuracy but retaining the relatively high signal/noise ratio of the low-accuracy integrator.

LIST OF SYMBOLS

- $f_s = \omega_s/2\pi = 1/2T_s$ = Repetition frequency of the input signal.
 M, M_1, M_2, M_3 = Integrator closed-loop gains.
 A, A_1, A_2, A_3 = Error amplifier gains.
 T, T_1, T_2, T_3 = Integrator time-constants.
 $v_p, v_{p1}, v_{p2}, v_{p3}$ = Amplitudes of in-phase error components.
 $v_q, v_{q1}, v_{q2}, v_{q3}$ = Amplitudes of quadrature error components.
 v_{ni}, v_{na} = Amplitudes of low-frequency sinusoidal noise voltages.
 V_n = Amplitude of total low-frequency output noise.
 $\overline{\sigma_i^2}, \overline{\sigma_a^2}$ = Mean-square amplitudes per unit bandwidth of random noise.
 $\overline{V_n^2}$ = Mean-square amplitude of total random output noise.
 $V_s, V_{s1}, V_{s2}, V_{s3}$ = Peak value of output signal from integrators.
 $\delta_1, \delta_2, \delta_3$ = Fractional errors.
 $f_c = \omega_c/2\pi$ = Corner frequency of direct-coupled integrator.
 $T_0 = R_0C_0$ = Time-constant of coupling in CR -coupled integrator.
 $T_a = R_aC_a$ = Time-constant of stabilizing network in CR -coupled integrator.
 $f_0 = \omega_0/2\pi$ = Unity open-loop gain frequency for CR -coupled integrator.
 $f_1 = \omega_1/2\pi$ = Cross-over frequency of low- and high-frequency asymptotes in CR -coupled integrator.
 ϕ_m = Phase margin of CR -coupled integrator.
 $\alpha = (1 + C_a/C_0)$ = Constant relating to stability of CR -coupled integrator.
 $\left. \begin{matrix} T_4 = R_4C_4 \\ k = R_4/(R_4 + R_5) \end{matrix} \right\}$ = Constants of the compensating network used with the phase-corrected integrator.
 $f_3 = \omega_3/2\pi$ = Corner frequency of phase-corrected integrator.
 T_c = High-frequency time-constant of the error amplifier.

(1) INTRODUCTION

The perfect electronic integrator is characterized by transfer function

$$\frac{v_o}{v_i} = \frac{1}{pT}$$

where T is the time-constant of integration, and determines sensitivity $v_o/\int v_i dt = 1/T$ (output voltage per volt-second input). With a sinusoidal input ($p = j\omega$) the integrator gain/frequency response therefore falls at 6 dB/octave and has a constant phase shift of 90° . Thus at low frequencies the gain becomes very large, and an extremely small low-frequency noise can produce an appreciable disturbance at the integrator output. This inherent characteristic thus imposes a severe limitation on practical use of the electronic integrator.

One general application in which excessive low-frequency output noise is often encountered occurs when a flux waveform is to be obtained and measured (Section 10.4 of Reference 1). This may be accomplished by integrating the e.m.f. induced in a small coil linking the flux. When this e.m.f. is very small, for example when the B/H loop of a small ferromagnetic sample is required, pick-up and amplifier noise can easily result in intolerable output signal/noise ratio.

In this and similar applications the integrator input is a repetitive signal with a mean level of zero. The repetition frequency f_s is then the lowest signal frequency present in the input. Accurate integration is therefore only required above the frequency f_s , and it is possible to modify the perfect integrator characteristics so as to reduce the gain and hence the noise output at low frequencies.

Fig. 1 shows the modification to the low-frequency response

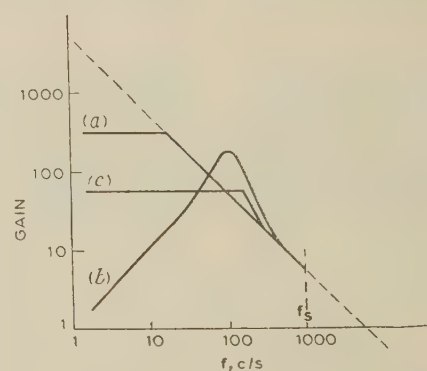


Fig. 1.—Low-frequency integrator characteristics.

- Perfect integrator.
 (a) Direct-coupled integrator.
 (b) CR -coupled integrator.
 (c) Phase-corrected integrator.

of the three different feedback integrators to be considered. Fig. 1(a) shows the frequency characteristic of a conventional direct-coupled integrator, Fig. 1(b) shows the result of including a single CR coupling in the feedback loop, whilst Fig. 1(c) shows the effect of phase correcting a direct-coupled integrator which has a low-gain error amplifier.

Corresponding to the low-frequency open-loop gain requirements, it is necessary to maintain the perfect integrator characteristic up to a sufficiently high frequency to obtain adequate speed of response (i.e. to give proper integration of the highest put harmonics). An amplifier having effectively a single h.f. time-constant is assumed (this characteristic being compatible with the high-frequency stability requirement of the feedback loop), and a relation is obtained between the amplifier h.f. time-constant and the required speed of response.

(2) GENERAL CONSIDERATIONS

(2.1) Input Waveform

Calculation of the accuracy of an integrator must, in general, be performed for the specific input waveform encountered. A repetitive waveform consisting of impulses of alternating sign (e.g. a differentiated unity mark/space ratio square wave) has been selected for analysis, since it approximates to the input waveform in a number of practical cases, e.g. in flux measurements on magnetic cores. Thus, for the differentiated square-wave input, the analysis yields the deviation from the square-wave output which would result from perfect integration.

(2.2) Representation of Errors

In considering errors resulting from modification of the low-frequency response of an integrator, it is assumed that the amplifier gain remains constant at high frequencies.

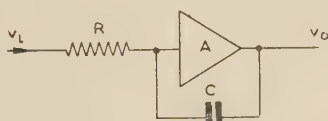


Fig. 2.—Feedback integrator.

Analysis of the feedback integrator circuit, shown in Fig. 2, yields the following closed-loop gain at angular frequency ω :

$$M = \frac{-A}{1 + T(1 + A)j\omega} \quad (1)$$

where $T = CR$

At high frequencies this reduces to

$$M_{HF} \approx \frac{-A}{T(1 + A)j\omega}$$

which represents a perfect integrator with a time-constant $1/(1 + A)/A$.

Accurate measurement of integrator gain is normally obtained by a bridge method (see Fig. 3), and the integrator time-constant derived from such a measurement performed with a high-frequency sinusoidal input has the value $T(1 + A)/A$. The error

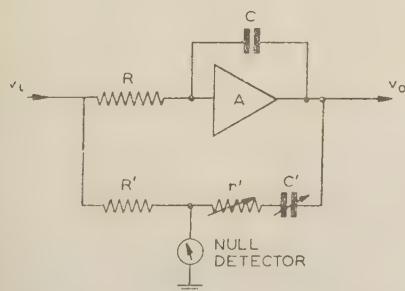


Fig. 3.—Measurement of integrator gain.

in integration is therefore best taken as the difference between the actual output and that of an ideal integrator of closed-loop gain

$$v_o'/v_i = -A/[T(1 + A)j\omega] \quad (2)$$

At any frequency, the integrator error is represented by error vectors v_p in phase and v_q in quadrature with the ideal output v_o' (Fig. 4). For small errors, v_p then represents the amplitude error and v_q the phase deviation in the output.

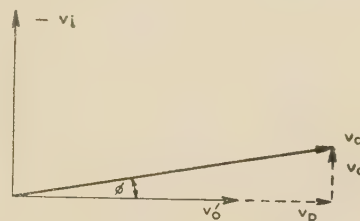


Fig. 4.—Representation of errors.

If the differentiated square wave is expressed as a Fourier series, the integrator output is the summation of the series obtained by applying the sine-wave analysis to each frequency component in turn. This method may be applied, in general, to other input waveforms for which the Fourier series is known or can be obtained.

(2.3) Output Noise

The main sources contributing to the output noise of a feedback integrator are as follows:

- (a) Noise already contaminating the input signal.
- (b) Valve noise such as microphonics, flicker noise, pick-up from heaters, etc.
- (c) Noise from the power supplies and from thermal drift of resistors in the amplifier.

Contributions (b) and (c) constitute amplifier noise and may be lumped together to give an equivalent noise referred to the amplifier grid, since, at this point, its value is little influenced by the magnitude of the amplifier gain. Fig. 5 shows two noise

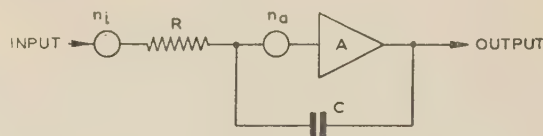


Fig. 5.—Equivalent circuit for noise signals.

generators representing the input noise, n_i , and the equivalent amplifier noise, n_a .

Comparison of the relative noise outputs of the three integrators is considered for very-low-frequency noise, and also for random noise having a flat frequency spectrum.

(2.3.1) Low-Frequency Noise.

It is assumed that n_i and n_a are sinusoidal noise voltage generators having amplitudes v_{ni} and v_{na} , respectively, and the comparison is restricted to frequencies low relative to f_g , since it is here that a reduction in output noise is mainly required.

At the output, n_i results in a noise Mv_{ni} , where M is the integrator closed-loop gain; n_a produces an output noise $M(1 + Tj\omega)v_{na}$ which, at frequencies below $\omega = 1/T$, has the value Mv_{na} . The total noise output is then

$$V_n = Mv_n \quad (3)$$

where $v_n = v_{na} + v_{ni}$

The corresponding output signal/noise ratio is represented by V_s/V_n , where V_s is the peak value of the signal at the output.

(2.3.2) White Noise.

For the case of white noise, n_i and n_a are random noise voltage generators having mean-square amplitudes per unit bandwidth of σ_i^2 and σ_a^2 , respectively. It is assumed, for simplicity, that the gain to both noise generators over the whole frequency spectrum is the closed-loop gain M . This has the effect that the noise contributed by n_a over the shaded region of Fig. 6

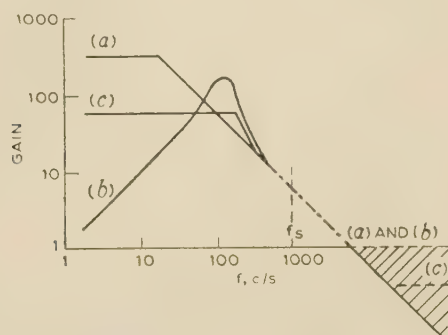


Fig. 6.—Gain to noise signals for different integrators.

— Gain to n_i .
 - - - Gain to n_i and n_a .
 . . . Gain to n_a .

is neglected. Since the gain to n_a is low over this region, the contribution is, in practice, negligible compared with the total low-frequency output noise. Thus the total mean-square output noise voltage \bar{V}_n^2 can be calculated as that due to a single noise-voltage generator of mean-square amplitude per unit bandwidth σ^2 , in series with the input signal ($\sigma^2 = \sigma_i^2 + \sigma_a^2$).

Comparison of \bar{V}_n^2 for the different integrators then provides an estimate of the average reduction in output noise.

In this case the corresponding output signal/noise ratio is represented by $\sqrt{(V_s^2/\bar{V}_n^2)}$.

(3) DIRECT-COUPLED INTEGRATOR

To provide a basis for comparison, expressions for the accuracy and noise output of a conventional direct-coupled integrator are derived. In particular, it is shown that the output signal/noise ratio is a function only of the integrator accuracy.

(3.1) Accuracy

For the direct-coupled integrator, the amplifier gain A_1 is assumed to be independent of frequency. Thus, from eqn. (1),

$$v_o = M_1 v_i = \frac{-A_1 v_i}{1 + (1 + A_1)T_1 j\omega} \quad (4)$$

and the ideal integrator output defined by eqn. (2) is given by

$$v_o' = \frac{-A_1 v_i}{(1 + A_1)j\omega T_1} \quad (5)$$

At any angular frequency ω , the difference between the actual and ideal outputs is shown in Section 11.3 to be composed mainly of the quadrature error component v_{q1} of magnitude

$$v_{q1} \approx \frac{v_i}{\omega^2 T_1^2 A_1} \quad (6)$$

For the differentiated square-wave input of Fig. 7(a) (derived from a square wave of peak amplitude V and repetition angular

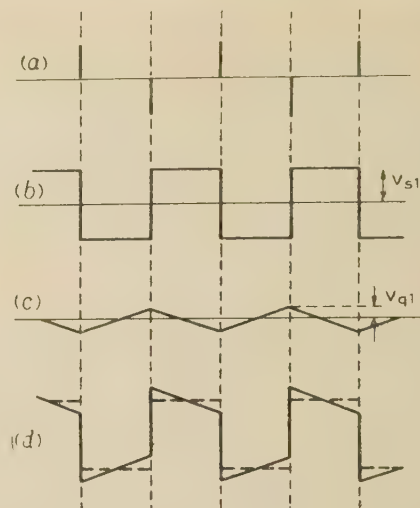


Fig. 7.—Direct-coupled integrator waveforms.

(a) Impulse input.
 (b) Ideal output.
 (c) Quadrature error.
 (d) Output.

frequency ω_s), the input waveform is represented by the Fourier series

$$v_i = \frac{4V_s}{\pi} [\cos \omega_s t + \cos 3\omega_s t + \cos 5\omega_s t + \dots] \quad (7)$$

Combining eqns. (5) and (7) gives, for the ideal output,

$$\frac{-A_1}{(1 + A_1)} \frac{4V}{\pi T_1} [\sin \omega_s t + 1/3 \sin 3\omega_s t + 1/5 \sin 5\omega_s t + \dots]$$

which represents a square wave of peak amplitude

$$V_{s1} = \frac{V}{T_1} \frac{A_1}{1 + A_1} \quad (8)$$

as shown in Fig. 7(b).

Similarly, combining eqns. (6) and (7), and remembering that v_{q1} is in phase with the input, gives a resultant error

$$\frac{4V}{\pi \omega_s T_1^2 A_1} [\cos \omega_s t + 1/3^2 \cos 3\omega_s t + 1/5^2 \cos 5\omega_s t + \dots]$$

which represents a triangular wave [Fig. 7(c)] of amplitude

$$V_{q1} = \frac{V\pi}{2T_1} \frac{1}{\omega_s T_1 A_1}$$

Adding the waveforms of Figs. 7(b) and 7(c) together gives the integrator output shown in Fig. 7(d), namely a square wave with a droop $2V_{q1}$. The fractional error δ_1 is

$$\delta_1 = \frac{\pm V_{q1}}{V_{s1}} \approx \frac{T_s}{2T_1 A_1} \quad (9)$$

($T_s = \pi/\omega_s$ = Half-period of the input waveform.)

(3.2) Output Noise

Fig. 8 shows the closed-loop gain characteristic $|M_1|$ where the 'corner' frequency ω_c is approximately equal to $1/T_1 A_1$.

(3.2.1) Low-Frequency Noise.

In the frequency range $0 < \omega < \omega_c$, the integrator gain is so that, applying eqn. (3), the noise output has the value

$$V_{n1} = A_1 v_n \quad (10)$$

2.2) White Noise.

The mean-square output noise $\overline{V_{n1}^2}$ is given by

$$\overline{V_{n1}^2} = \sigma^2 A_1^2 \omega_c \pi / 2 \quad (11)$$

$\pi/2$ being the noise bandwidth of the gain characteristic $|M_1|$.

(3.3) Signal/Noise Ratio

3.1) Low-Frequency Noise.

The combination of eqns. (8), (9) and (10) gives the signal/noise ratio in the angular-frequency region $0 < \omega < \omega_c$:

$$\frac{V_{s1}}{V_{n1}} \approx \frac{V}{v_n} \frac{2}{T_s} \delta_1$$

3.2) White Noise.

From eqns. (8), (9) and (11),

$$\sqrt{\frac{V_{s1}^2}{V_{n1}^2}} = \left(\frac{V^2}{\sigma^2} \frac{4}{\pi T_s} \delta_1 \right)^{1/2}$$

Thus, for a given repetition period, the signal/noise ratio of a direct-coupled integrator depends only on the integrator accuracy δ_1 depending in turn on the product $T_1 A_1$. Fig. 8 shows

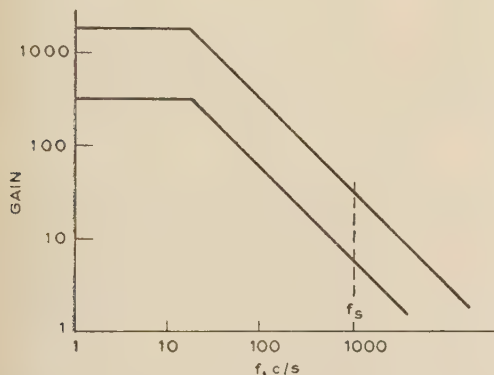


Fig. 8.—Direct-coupled integrator frequency characteristics.

closed-loop gain characteristics for two integrators having different values of T_1 , but the same value of the product $T_1 A_1$, and therefore giving equal accuracies.

(4) THE CR-COUPLED INTEGRATOR

Whereas there is no optimum design for a direct-coupled integrator of given accuracy, it is found that, to obtain the best output signal/noise ratio for a CR-coupled integrator, the necessary circuit values are uniquely determined for a given accuracy and repetition frequency.

Fig. 9(a) shows the circuit of a CR-coupled integrator. Since the CR couplings ($C_0 R_0$ and $C_2 R_2$) are in cascade within the feedback loop, it is necessary to include the stabilizing network R_a to maintain stability at low frequencies [see Fig. 9(b)]. Figs. 10(a) and 10(b) show the integrator characteristic with and without the stabilizing network, respectively.

(4.1) Design of the Stabilizing Network

The low-frequency stabilizing network $C_a R_a$ provides a stabilizing lag only over a limited frequency range. The values C_a and R_a are therefore adjusted so that this lag has a maximum value ϕ_m at the angular frequency ω_0 , where the open-loop gain is unity. Assuming that the integrating components C_2 and R_2 contribute 90° lead at this frequency, and that these components give negligible loading of the CR-coupling network,

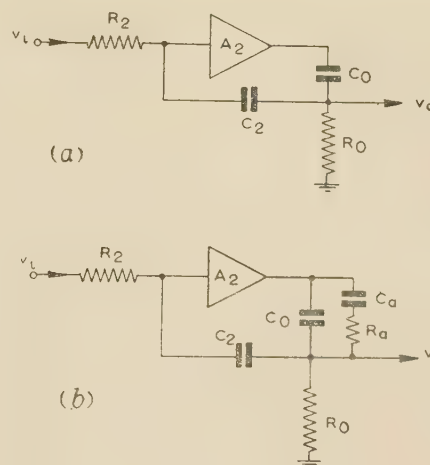


Fig. 9.—CR-coupled integrator.

(a) Without stabilizing network.
(b) With stabilizing network.

the maximum phase lag ϕ_m is the phase margin of stability and has the value (see Section 11.1)

$$\phi_m = \arctan \frac{(\alpha - 1)}{2\sqrt{\alpha}} \quad (12)$$

where

$$\alpha = \left(1 + \frac{C_a}{C_0} \right)$$

Also the angular frequency ω_0 , the time-constant $T_a = C_a R_a$

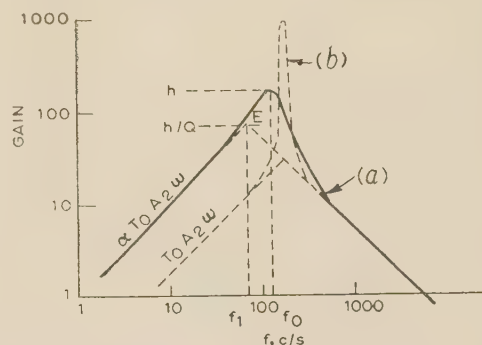


Fig. 10.—CR-coupled integrator frequency characteristics.

(a) With stabilizing network.
(b) Without stabilizing network.

and the values of h and Q (Fig. 10) are given by the equations (see Section 11.2)

$$\omega_0 = \frac{1}{\alpha^{1/4} \sqrt{T_0 T_2 A_2}} \quad (13)$$

$$T_a = \frac{\sqrt{\alpha}}{\omega_0} \quad (14)$$

$$h = Q \alpha^{1/2} \sqrt{\frac{T_0 A_2}{T_2}} \quad (15)$$

$$Q = \frac{\sqrt{(\alpha + 1)}}{\alpha^{1/4} \sqrt{2[(\sqrt{\alpha}) - 1]}} \quad (16)$$

where $T_0 = R_0 C_0$

$T_2 = R_2 C_2$

$A_2 =$ Amplifier gain

Eqns. (12), (13) and (14) enable the optimum value for the time-constant of the stabilizing network to be determined, for given values of T_0 , T_2 , A_2 and the phase margin. [A 30° phase margin (for which $\alpha = 3$) normally provides adequate stability.]

(4.2) Accuracy

For angular frequencies $\omega \gg \omega_0$ the reactance $1/\omega C_a$ is very much less than R_a , and the equivalent circuit of the coupling network is as shown in Fig. 11(c). Since, in practice, $R_a \gg R_0$

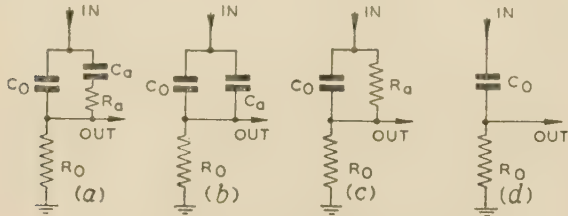


Fig. 11.—Equivalent circuits of coupling network.

- (a) Coupling network.
- (b) Equivalent circuit for $\omega \leq \omega_0$, where $XC_a \geq R_a$.
- (c) Equivalent circuit for $\omega \geq \omega_0$, where $XC_a \leq R_a$.
- (d) As for (c) but for $\omega \approx 1/C_0 R_0$ ($R_a \geq R_0$).

and $1/\omega_s C_0 \approx R_0$,* $R_a \geq 1/\omega_s C_0$ and the equivalent circuit shown in Fig. 7(d) is applicable at angular frequencies greater than or equal to ω_s . Thus in the calculation of accuracy, where only the angular frequency range $\omega > \omega_s$ is relevant, the effective amplifier gain A has the approximate value

$$A = \frac{A_2 T_0 j\omega}{1 + T_0 j\omega}$$

A_2 being assumed independent of frequency.

Combination of this with eqn. (1) gives the closed-loop gain M_2 :

$$\frac{v_o}{v_i} = M_2 = \frac{-A_2 T_0 j\omega}{\{[1 - T_2 T_0 \omega^2 (1 + A_2)] + j\omega(T_2 + T_0)\}}$$

and the ideal integrator output defined by eqn. (2) has the value

$$v_o' = \frac{-A_2 v_i}{(1 + A_2) T_2 j\omega}$$

The difference between the actual and the ideal outputs can be represented by the components v_{p2} in phase and v_{q2} in quadrature with the ideal output, and of magnitudes (Section 11.3)

$$v_{p2} \approx \frac{v_i}{\omega T_2} \frac{1}{\omega^2 T_2 T_0 A_2} \quad \text{and} \quad v_{q2} \approx \frac{v_i}{\omega^2 T_2 A_2} \left(\frac{1}{T_2} + \frac{1}{T_0} \right)$$

If these equations are used in an error analysis similar to that in Section 3.1, the output (for a differentiated square-wave input) is the sum of

(a) The ideal output [Fig. 12(b)], a square wave of amplitude

$$V_{s2} = \frac{VA_2}{T_2(1 + A_2)} \quad (17)$$

(b) The total in-phase error component, giving a waveform composed of half-cycles which are sections of parabolas [Fig. 12(c)] having a peak amplitude

$$V_{p2} = \frac{4V}{\pi T_2} \frac{1}{\omega_s^2 T_2 T_0 A_2} \frac{\pi^3}{32}$$

* Of the values of $T_0 (= C_0 R_0)$ derived in Section 4.5, the optimum design gives the smallest, namely $T_s/4$. Putting $T_s = \pi/\omega_s$, the maximum value of $1/\omega_s C_0$ is $4R_0/\pi$.

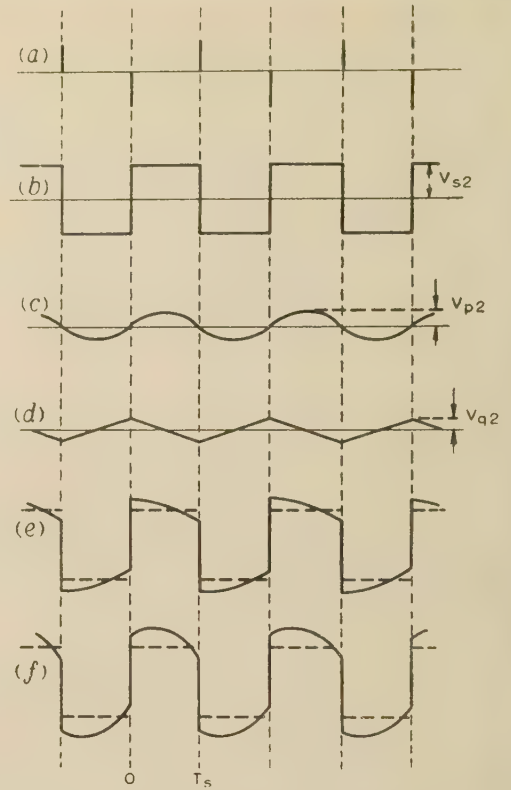


Fig. 12.—CR-coupled integrator waveforms.

- (a) Impulse input.
- (b) Ideal output.
- (c) In-phase error.
- (d) Quadrature error.
- (e) Output.
- (f) Output.

(c) The total quadrature error component, giving a triangular wave [Fig. 12(d)] of peak amplitude

$$V_{q2} = \frac{\pi V}{2T_2} \frac{1}{A_2} \left(\frac{1}{\omega_s T_2} + \frac{1}{\omega_s T_0} \right)$$

The integrator output waveform is obtained by adding the waveforms (b), (c) and (d) of Fig. 12. The relative values V_{p2} and V_{q2} can be set by choice of A_2 , T_2 and T_0 . Figs. 12(e) and 12(f) show the output for integrators having different relative values of V_{p2} and V_{q2} .

At the beginning and end of a half-period the contribution from V_{p2} is zero, so that the error at these instants depends on V_{q2} , i.e. the phase error in the integrator transfer characteristic. If the total error at intermediate times is not to exceed $\pm V_{q2}$, the relative values of V_{p2} and V_{q2} must be such that the initial slope of the output waveform is less than or equal to zero. The necessary condition is shown in Section 11.4 to be

$$T_0 + T_2 \geq \frac{T_s}{2} \quad (1)$$

The fractional error is then*

$$\delta_2 = \pm \frac{V_{q2}}{V_{s2}} \approx \frac{T_s}{2A_2} \left(\frac{1}{T_2} + \frac{1}{T_0} \right) \quad (1)$$

Criteria which impose various other limits on the relative

* Comparison of this with eqn. (9), giving the droop for a direct-coupled integrator shows that the effect of a CR coupling on the droop is the replacement of the integrator time-constant T_2 by T_2 and T_0 in series. This is also true for more time constants provided that the additional phase error introduced is small at the repetition frequency.

values of V_{p2} and V_{a2} could be taken. These would give rise to conditions similar to that of eqn. (18).

(4.3) Output Noise

4.3.1) Low-Frequency Noise.

At frequencies $\omega \ll \omega_0$ where the reactance $1/\omega C_a$ is very much greater than R_a , the coupling network [see Fig. 11(b)] is equivalent to a simple CR circuit of time-constant $(C_0 + C_a)R_0 = T_0$. Thus the low-frequency asymptote to the closed-loop response is given by

$$\left| \frac{v_o}{v_i} \right| = \alpha \omega T_0 A_2$$

Combination of this with eqn. (3) gives the output noise

$$V_{n2} = \omega \alpha T_0 A_2 v_n \quad (20)$$

4.3.2) White Noise.

The mean-square output noise $\overline{V_{n2}^2}$ is determined by assuming the integrator closed-loop response [Fig. 10(a)] to be approximately that of a single tuned circuit of Q -factor equal to Q , resonant angular frequency ω_0 and peak magnitude h . (This assumption is found to fit the practical curves reasonably.) The noise bandwidth is then $\omega_0 \pi / 2Q$, so that, subject to the assumptions outlined in Section 2.3.2,

$$\overline{V_{n2}^2} = h^2 \frac{\omega_0}{Q} \frac{\pi}{2} \sigma^2$$

Substitution for ω_0 and h from eqns. (13) and (15) gives

$$\overline{V_{n2}^2} = \alpha^{3/4} \frac{\pi Q}{2} \frac{1}{T_2} \sqrt{\frac{T_0 A_2}{T_2}} \sigma^2 \quad (21)$$

(4.4) Signal/Noise Ratio

4.4.1) Low-Frequency Noise.

The combination of eqns. (17), (19) and (20) gives the signal/noise ratio in the angular-frequency region $0 < \omega \ll \omega_0$:

$$\frac{V_{s2}}{V_{n2}} = \frac{V}{v_n} \frac{2}{T_s} \frac{1}{\alpha \omega} \frac{\delta_2}{T_2 + T_0}$$

4.4.2) White Noise.

From eqns. (17), (19) and (21),

$$\sqrt{\frac{V_{s2}^2}{V_{n2}^2}} = \left[\frac{V^2}{\sigma^2} \frac{\alpha^{3/4} Q (\pi/2)}{T_s^{1/2}} \frac{2\delta_2}{T_2 + T_0} \right]^{1/2}$$

These equations show that, for a given accuracy and repetition period, the best signal/noise ratio is obtained when $(T_0 + T_2)$ is minimized. The ultimate limit to reduction of $(T_0 + T_2)$ set by eqn. (18) determines the maximum signal/noise ratio.

Inserting the value of Q [eqn. (16)] in the above expression for signal/noise ratio, and then differentiating with respect to α , gives the result that, for maximum signal/noise ratio, $\alpha = 4.88$. For the case of low-frequency noise, however, the signal/noise ratio is seen in Section 4.4.1 to be proportional to $1/\alpha$, and a small value of α then gives best signal/noise ratio. A value $\alpha = 3$ has been taken (Section 7.1) as a reasonable compromise, and results in a reduction of the signal/white-noise ratio by only a factor of 1.37 from its optimum value.

(4.5) Optimum Design of the CR -Coupled Integrator

The condition for maximum signal/noise ratio is

$$T_0 + T_2 = T_s/2 \quad (22)$$

Optimization of the design involves choosing T_2 and T_0 (subject to this condition) so as to minimize the fractional error.

Combination of eqns. (19) and (22) gives the fractional error

$$\delta_2 = \frac{T_s^2}{4A_2} \frac{1}{T_2 \left(\frac{T_s}{2} - T_2 \right)}$$

This is minimized when $T_2 = T_s/4$, giving

$$T_2 = T_0 = T_s/4 \quad (23)$$

and

$$A_2 = 4/\delta_2 \quad (24)$$

Eqn. (23) gives the optimum values of T_2 and T_0 , whilst eqn. (24) gives the amplifier gain necessary to secure the optimum design.

In practice, the optimum gain may not be readily obtainable. The problem is then to obtain the best signal/noise ratio with a given amplifier gain A_2' and with a specified accuracy. Two cases may be considered:

- (a) A_2' less than optimum.
- (b) A_2' greater than optimum.

(a) A_2' Less than Optimum.

Rewriting eqn. (19):

$$\frac{1}{T_2} + \frac{1}{T_0} = \frac{2A_2'\delta_2}{T_s}$$

For given values of error and amplifier gain, it is required to choose T_2 and T_0 so as to minimize $(T_2 + T_0)$ for the best signal/noise ratio. This again occurs when $T_2 = T_0$, so that

$$T_2 = T_0 = T_s/A_2'\delta_2 \quad (25)$$

is the required criterion when A_2' is less than the optimum value $4/\delta_2$ [eqn. (24)]. [Substitution of $A_2' < 4/\delta_2$ in eqn. (25) gives $T_2 = T_0 > T_s/4$, so that $(T_0 + T_2) > T_s/2$, satisfying the criterion of eqn. (18)].

(b) A_2' Greater than Optimum.

With $A_2' > 4/\delta_2$ the condition $T_2 + T_0 = T_s/2$ can now be readily satisfied, and T_2 and T_0 are chosen so that the accuracy equation

$$\delta_2 = \frac{T_s}{2A_2} \left(\frac{1}{T_2} + \frac{1}{T_0} \right)$$

is satisfied subject to this condition.

Thus

$$T_2 + T_0 = T_s/2$$

and

$$T_2 T_0 = T_s^2 / 4A_2' \delta_2$$

Solution of these simultaneous equations then gives the values of T_2 and T_0 . Two possible values of T_2 (and therefore of T_0) are obtained. The lower of these is normally taken, since this yields a greater integrator sensitivity.

It should be noticed that the increased integrator sensitivity is the only result of having an amplifier gain greater than optimum, no further improvement in signal/noise ratio being obtained.

(5) PHASE-CORRECTED INTEGRATOR

In order to obtain some idea of the relative importance of phase and amplitude errors, a direct-coupled integrator having a low-gain error amplifier, and designed to give a fractional error of 10% is considered. An analysis similar to that of Section 3.1 shows that, for the differentiated square-wave input, the output is the sum of three waveforms. These are as follows:

- (a) The ideal output, a square wave of amplitude V/T .
- (b) A triangular wave of amplitude $V/10T$ due to phase errors. (T is the integrator time-constant.)

(c) A waveform, due to amplitude errors, consisting of half-cycles which are sections of a parabola, and having a peak amplitude $V/200T$.

This shows that phase errors have a much greater magnitude than amplitude errors. (The ratio between these errors increases as the accuracy of the integrator is raised.) If phase correction could be applied without introducing any additional amplitude errors, the accuracy of the integrator would be considerably increased, and a high-accuracy integrator obtained having the relatively low output noise of a low-accuracy integrator. All-pass networks are capable of providing a large degree of phase equalization, but, in general, are fairly complex. However, good results can be obtained using the simple 'minimum phase' network of Fig. 13(a). This provides a phase lag which, in the

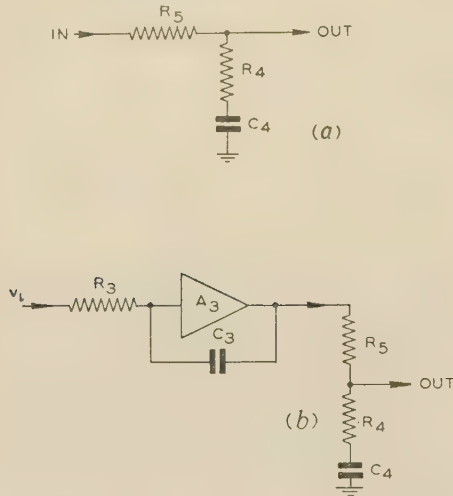


Fig. 13.—Phase correction of direct-coupled integrator.

(a) Phase-retard network.
(b) Phase-corrected integrator.

appropriate frequency range, is approximately inversely proportional to frequency. In this case a certain amount of excess amplitude error is introduced, and it is found that the residual error is due mainly to amplitude deviations.

This procedure cannot be applied to correction of a CR -coupled integrator, since the amplitude error is of the same order of magnitude as the phase error. Complete removal of the phase error therefore results in only a slight improvement.

(5.1) Phase Correction of a Direct-Coupled Integrator by a Phase-Retard Network

Fig. 13(b) shows a direct-coupled integrator followed by the phase-retard network R_4 , R_5 and C_4 .

The gain of the feedback integrator is given by

$$\frac{v_o}{v_i} = \frac{-A_3}{1 + T_3(1 + A_3)j\omega} \quad (26)$$

and the associated phase lag ϕ has a value given by

$$\tan \phi = -\omega T_3(1 + A_3)$$

At angular frequency ω , the phase deviation β from 90° is then

$$\beta = \arctan \frac{1}{\omega T_3(1 + A_3)}$$

or for small angles (for the 10% integrator $\beta = 3.8^\circ$ at $\omega = \omega_s$)

$$\beta \approx 1/\omega T_3(1 + A_3) \quad (27)$$

For the phase-retard network,

$$\frac{v_o}{v_i} = \frac{1 + j\omega T_4}{1 + j\omega T_4/k} \quad (28)$$

where

$$T_4 = R_4 C_4$$

$$k = \frac{R_4}{R_4 + R_5} = \text{H.F. attenuation of network}$$

and the associated phase lag θ has the value

$$\theta = \arctan \frac{(1 - k)\omega T_4}{k + \omega^2 T_4^2}$$

or for small angles

$$\theta \approx \frac{(1 - k)\omega T_4}{1 + k/\omega^2 T_4^2} \quad (29)$$

Reference to eqns. (27) and (29) shows that substitution of*

$$\frac{1 - k}{T_4} = \frac{1}{T_3(1 + A_3)} \quad (30)$$

provides a first-order phase correction, the degree of approximation depending on the value of k ; the smaller the value of k , the better is the correction. However, small values of k imply large attenuations at high frequencies, so that k must be chosen to give a compromise between good correction and small attenuation.

This compromise is achieved by giving k the value which provides a maximum signal/noise ratio.

(5.2) Accuracy

Combination of eqns. (26) and (28) gives the overall gain

$$M_3 = \frac{-A_3}{1 + T_3(1 + A_3)j\omega} \frac{1 + j\omega T_4}{1 + j\omega T_4/k}$$

The ideal output is given by the value of M_3 at high frequency.

$$\frac{v'_o}{v_i} = \frac{-A_3 k}{T_3(1 + A_3)j\omega}$$

This differs from the ideal output represented by eqn. (2) by the factor k due to the high-frequency attenuation introduced by the external phase-correction network.

Application of the condition of eqn. (30) shows that the difference between the actual and ideal outputs is composed mainly of the in-phase error component v_{p3} (Section 11.5) having the magnitude

$$v_{p3} \approx k^2 A_3 v_i / \omega^3 T_3^3 (1 + A_3)^3 (1 - k) \quad (\omega > \omega_s)$$

An analysis similar to that of Section 3.1 shows that, for the differentiated square-wave input, the output is the sum of the two waveforms shown in Fig. 14. These are as follows:

(a) The ideal output [Fig. 14(b)], a square wave of amplitude

$$V_{s3} = V k A_3 / T_3 (1 + A_3) \quad (31)$$

(b) The sum of amplitude error components, giving a waveform composed of half-cycles which are sections of parabola [Fig. 14(c)], and have a peak amplitude

$$V_{p3} = \frac{4V A_3}{32\omega_s^2} \frac{\pi^2}{[T_3(1 + A_3)]^3} \frac{k^2}{1 - k}$$

* It should be noticed that eqn. (30) involves the amplifier gain of the direct-coupled integrator. If the condition is to be maintained with sufficient accuracy, it is necessary to stabilize the gain. This can be achieved by the use of local feedback in the amplifier stage.

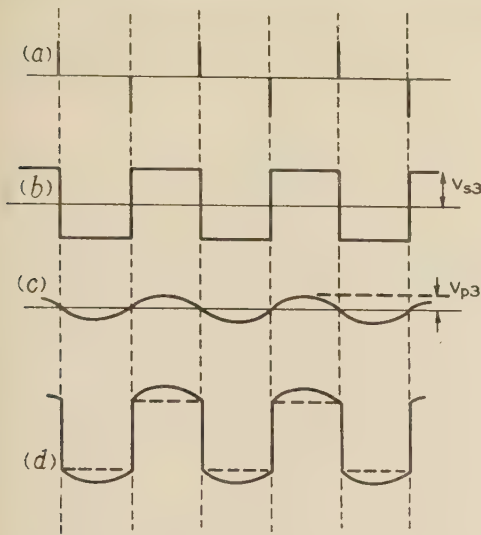


Fig. 14.—Phase-corrected integrator waveforms.

- (a) Impulse input.
(b) Ideal output.
(c) In-phase error.
(d) Output.

The resultant output is shown in Fig. 14(d), and the fractional error has the value

$$\delta_3 = \frac{V_{p3}}{V_{s3}} = \frac{1}{8} \frac{k}{1-k} \left[\frac{T_s}{T_3(1+A_3)} \right]^2 \quad (32)$$

(5.3) Output Noise

Fig. 15 shows the input/output segmented gain characteristic $|M_3|$, where

$$\begin{aligned} \omega_3 &= 1/T_3(1+A_3) \\ \omega_4 &= 1/T_4 \\ \omega_5 &= k/T_4 \end{aligned}$$

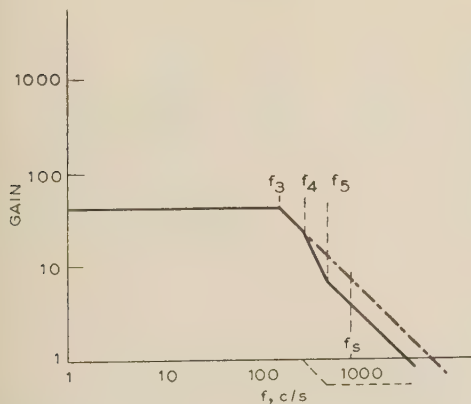


Fig. 15.—Phase-corrected integrator frequency characteristics.

- Gain of integrator $[A_3/(1+A_3) \times 1/T_3\omega]$.
--- Gain of correction network.
—— Gain overall.

(5.4.1) Low-Frequency Noise.

In the frequency range $0 < \omega < \omega_3$, the integrator gain varies as A_3 , and application of eqn. (3) gives the noise output

$$V_{n3} = A_3 v_n \quad (33)$$

(5.3.2) White Noise.

It can be shown that the noise bandwidth of the gain characteristic $|M_3|$ is given by

$$\omega_3 k(1+k-k^2)\pi/2$$

whence the mean-square output noise $\overline{V_{n3}^2}$ has the value

$$\overline{V_{n3}^2} = A_3^2 \omega_3 k(1+k-k^2) \frac{\pi}{2} \sigma^2 \quad (34)$$

(5.4) Signal/Noise Ratio

(5.4.1) Low-Frequency Noise.

Combination of eqns. (31) and (33) gives the signal/noise ratio

$$\frac{V_{s3}}{V_{n3}} = \frac{V}{v_n} \frac{k}{(A_3+1)T_3} \quad (\text{for } \omega < \omega_3)$$

(5.4.2) White Noise.

From eqns. (31) and (34),

$$\sqrt{\frac{V_{s3}^2}{V_{n3}^2}} = \left[\frac{V^2}{\sigma^2} \frac{k}{1+k-k^2} \frac{1}{T_3(1+A_3)} \frac{2}{\pi} \right]^{1/2}$$

(5.5) Optimum Design of the Phase-Corrected Direct-Coupled Integrator

Optimization of the design consists in choosing k so as to yield the best signal/noise ratio for a given accuracy.

For low-frequency noise it is required to maximize $k/T_3(1+A_3)$. Putting

$$X = k/T_3(1+A_3)$$

and combining this with eqn. (32),

$$X^2 = Kk(1-k)\delta_3$$

where K is a constant for a given repetition period.

Setting $\partial(X^2)/\partial k = 0$ for a maximum signal/noise ratio,

$$k = 0.5$$

It can be shown that $k = 0.5$ also satisfies the condition for maximum signal/noise ratio for white noise.

Substituting $k = 0.5$ in eqns. (30) and (32),

$$T_4 = \frac{T_3(1+A_3)}{2}$$

$$\delta_3 = \frac{1}{8} \left[\frac{T_s}{T_3(1+A_3)} \right]^2$$

When T_s and δ_3 are specified, these equations enable the component values in the integrator and compensating network to be calculated.

(6) COMPARISON OF INTEGRATORS

In order to compare the noise output from a direct-coupled integrator with the noise outputs of the CR -coupled and phase-corrected integrators, the accuracy and the sensitivity of each (for a differentiated square-wave input) are made equal

$$\text{i.e.} \quad \delta_1 = \delta_2 = \delta_3 = \delta$$

and

$$V_{s1} = V_{s2} = V_{s3} \quad (35)$$

Under these conditions, the ratios

$$F_2 = V_{n1}/V_{n2} \text{ and } F_3 = V_{n1}/V_{n3}$$

give the improvement in low-frequency signal/noise ratio of the CR -coupled and phase-corrected integrators, respectively. The corresponding improvements for white noise are given by

$$N_2 = [\bar{V}_{n1}^2 / \bar{V}_{n2}^2]^{1/2} \text{ and } N_3 = [\bar{V}_{n1}^2 / \bar{V}_{n3}^2]^{1/2}$$

Combining eqn. (35) with eqns. (8), (17) and (31):

$$T_1 = T_2 = T_3/k \text{ (assuming } A_1, A_2 \text{ and } A_3 \gg 1)$$

For optimum design, the CR -coupled integrator has $T_2 = T_0 = T_s/4$ [eqn. (23)] and for the phase-corrected integrator, $k = \frac{1}{2}$, whence

$$\left. \begin{aligned} T_1 &= T_s/4 \\ T_2 &= T_s/4 \\ T_3 &= T_s/8 \end{aligned} \right\} \dots \dots \dots (36)$$

By combining eqn. (9) with eqns. (10) and (11), eqn. (19) with eqns. (20) and (21), and eqn. (32) with eqns. (33) and (34) so as to eliminate the amplifier gains, and then substituting for T_1 , T_2 and T_3 from eqn. (36), the noise outputs V_{n1} , \bar{V}_{n1}^2 , etc., are obtained as a function of the accuracy δ and the repetition period $2T_s$. Hence

$$F_2 = \frac{2}{\pi\alpha} \frac{\omega_s}{\omega}, \quad N_2 = \left(\frac{1}{\alpha^{3/4} Q} \frac{1}{\sqrt{\delta}} \right)^{1/2}$$

$$F_3 = \sqrt{\frac{1}{2\delta}} \text{ and } N_3 = \left[\frac{1}{5} \sqrt{\frac{8}{\delta}} \right]^{1/2}$$

These ratios are shown in Table 1 for integrators of various accuracies. The frequencies f_c , f_0 and f_3 below which the low-frequency noise ratios apply are also included.

Table 2 gives the corresponding results obtained when the

input is a pure sine wave of frequency $\omega_s/2\pi$. The design procedure in this case, and in general, is the same as that employed for an impulse input. For the CR -coupled integrator the fractional error is taken as the ratio of quadrature error to output magnitude, giving

$$\delta'_2 = \frac{T_s}{\pi A_2} \left(\frac{1}{T_2} + \frac{1}{T_0} \right)$$

Also, the in-phase error is restricted to be less than the quadrature error, thereby imposing the condition $T_0 + T_2 > T_s/4$. These equations differ only by a constant from eqns. (19) and (18). This will, in fact, be the case for any repetitive input signal, if the given design procedure is followed. The conditions to obtain optimum design of the CR -coupled integrator will therefore always be $T_0 = T_2$ and $T_0 + T_2 > \text{constant} \times T_s$.

For the phase-corrected integrator with sine-wave input the error is taken as the ratio of in-phase error to output magnitude giving

$$\delta'_3 = \frac{k}{\pi^2(1-k)} \left[\frac{T_s}{T_3(1+A_3)} \right]^2$$

which differs from eqn. (32) by only a constant. This will again be the case for any repetitive input, with the result that for optimum design of the phase-corrected integrator k must always equal 0.5. The results of Table 2 show that the gains A_1 and A_3 happen to be the same as the corresponding values in Table 1. This will not generally be the case.

(7) PRACTICAL INTEGRATING CIRCUITS

The procedure for designing the CR -coupled and phase-corrected integrators is given below for the particular case of

Table 1
IMPULSE INPUT

Accuracy	Direct-coupled		CR coupled					Phase corrected				
	A_1	f_c	A_2	T_a	f_0	F_2 at f_c	N_2	A_3	T_4	f_3	F_3 below f_c	N_3
%		c/s		millisec	c/s				millisec	c/s		
3.33	60	21	120	3.1	88.3	10	1.28	14.5	0.485	164	3.9	1.76
1.00	200	6.4	400	5.7	48.3	33	1.73	27.3	0.885	90	7.1	2.39
0.333	600	2.1	1200	9.9	27.8	100	2.28	48	1.53	52	12.3	3.14
0.100	2000	0.64	4000	18	15.3	330	3.07	88.5	2.8	28.5	22.4	4.25
0.0333	6000	0.21	12000	31	8.83	1000	4.05	154	4.85	16.4	39	5.58
0.0100	20000	0.064	40000	57	4.83	3300	5.49	282	8.85	9.0	71	7.54

Characteristics of optimum designed integrators of various accuracies based on $f_s = 1 \text{ kc/s}$. $T_1 = T_2 = 2T_3 = T_s/4$ = optimum value for CR -coupled integrator, $\alpha = 3$, $k = 0.5$.

Table 2
SINE-WAVE INPUT

Accuracy	Direct-coupled		CR coupled					Phase corrected				
	A_1	f_c	A_2	T_a	f_0	F_2 at f_c	N_2	A_3	T_4	f_3	F_3 below f_c	N_3
%		c/s		millisec	c/s				millisec	c/s		
3.33	60	33.3	120	1.97	139	10	1.28	20.9	0.435	183	2.74	1.48
1.00	200	10.0	400	3.63	75.9	33	1.73	39.00	0.795	100	5.00	2.0
0.333	600	3.33	1200	6.3	43.7	100	2.28	68.3	1.38	57.5	8.68	2.63
0.100	2000	1.0	4000	11.5	24	330	3.07	125.5	2.52	31.5	15.8	3.56
0.0333	6000	0.333	12000	19.7	13.9	1000	4.05	218	4.35	18.3	27.4	4.67
0.0100	20000	0.100	40000	36.3	7.59	3300	5.49	399	7.95	10.0	50.0	6.31

Characteristics of optimum designed integrators of various accuracies based on $f_s = 1 \text{ kc/s}$. $T_1 = T_2 = 2T_3 = T_s/2\pi$ = optimum value of CR -coupled integrator, $\alpha = 3$, $k = 0.5$.

integrators required to give an accuracy of 1% with a differentiated square-wave input of repetition frequency 1000 c/s. ($T_s = 500$ microsec.)

(7.1) CR-Coupled Integrator

For optimum design, $A_2 = 4/\delta_2 = 400$ [eqn. (24)] and $T_0 = T_2 = T_s/4 = 125$ microsec [eqn. (23)].

Stabilizing Network.

$\alpha = 1 + C_a/C_0 = 3$ gives a phase margin of 30° , and results in adequate stability ($Q = 1.47$).

Thus $C_a/C_0 = 2$
and $T_a = R_a C_a = \alpha^{3/4} \sqrt{(T_0 T_2 A_2)}$ [eqns. (13) and (14)]

Putting $T_0 = R_0 C_0 = T_2$, $\alpha = 3$ and $C_a = 2C_0$ in the above equation:

$$R_a = 22.8 R_0$$

A single-stage amplifier [Fig. 16(a)] is suitable for relatively low-accuracy integrators ($\delta \geq 1\%$). Component values for the integrating and coupling networks are chosen so that there is

negligible loading of the coupling network by the integrating network.

$$\text{Making } R_0 = 22 \text{ k}\Omega, C_0 = \frac{125 \times 10^{-6}}{22000} = 0.0057 \mu\text{F}.$$

$$\text{Thus } R_a = 22.8 R_0 = 500 \text{ k}\Omega \text{ and } C_a = 2C_0 = 0.0114 \mu\text{F}.$$

$$\text{Making } R_2 = 100 \text{ k}\Omega, C_2 = \frac{125 \times 10^{-6}}{100000} = 0.00125 \mu\text{F}.$$

The nearest preferred values have been incorporated in the circuit of Fig. 16(a), for which the theoretical and practical frequency-response curves are shown in Fig. 16(b). When it is necessary to decouple the d.c. component from the input, the network $C_b R_b$ [Fig. 16(a)] is included within the feedback loop. Any phase shift produced by this network and by the screen and cathode by-pass time-constants must be small at the frequency ω_0 so as to have negligible effect on stability. Also, when a high-accuracy integrator is required, a multi-stage error amplifier is needed to secure the necessary open-loop gain. If the operating frequency is sufficiently high, CR interstage couplings may be used. Otherwise, a drift-corrected² direct-coupled amplifier is required to prevent overloading due to d.c. drift at the output.

(7.2) Phase-Corrected Integrator

For optimum design, $k = 0.5$, giving (see Section 5.5)

$$T_4 = \frac{T_3(1 + A_3)}{2} \text{ and } \delta_3 = \frac{1}{8} \left[\frac{T_s}{T_3(1 + A_3)} \right]^2$$

Combining these equations,

$$T_4 = \frac{T_s}{4\sqrt{(2\delta_3)}} = 0.88 \text{ millisecc}$$

and

$$1 + A_3 = \frac{2T_s}{4T_3\sqrt{(2\delta_3)}}$$

Putting $T_3 = \frac{T_2}{2} = \frac{T_s}{8}$, the overall gain at high frequencies will be the same as that of the CR-coupled integrator above [see eqn. (36)] and

$$1 + A_3 = 28.3$$

or

$$A_3 = 27.3$$

Thus $T_3 = 125/2 = 62.5$ microsec ($R_3 = 100 \text{ k}\Omega$, $C_3 = 0.000625 \mu\text{F}$) and making $R_4 = R_5 = 10 \text{ k}\Omega$, $C_4 = T_4/R_4 = 0.088 \mu\text{F}$.

Although the gain required in the phase-corrected integrator is small, its value must be maintained within narrow limits over a wide range of frequency and for all required values of output signal magnitude. Fig. 17 shows a circuit for the phase-corrected integrator with the nearest preferred values of components incorporated. The gain, A_3 , of the error amplifier is stabilized

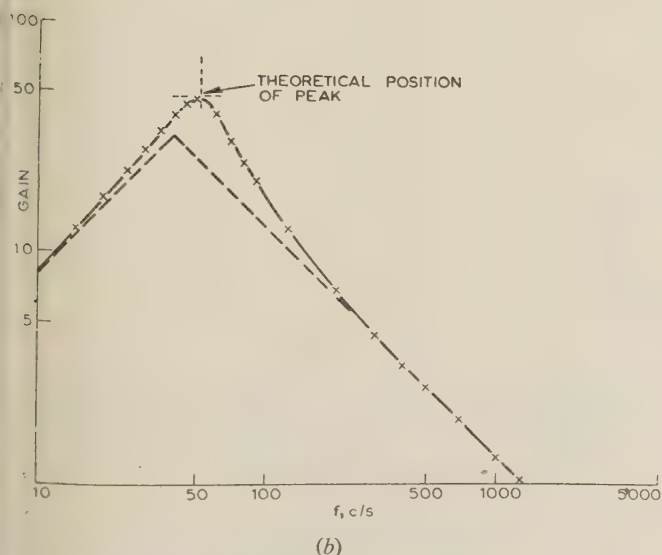
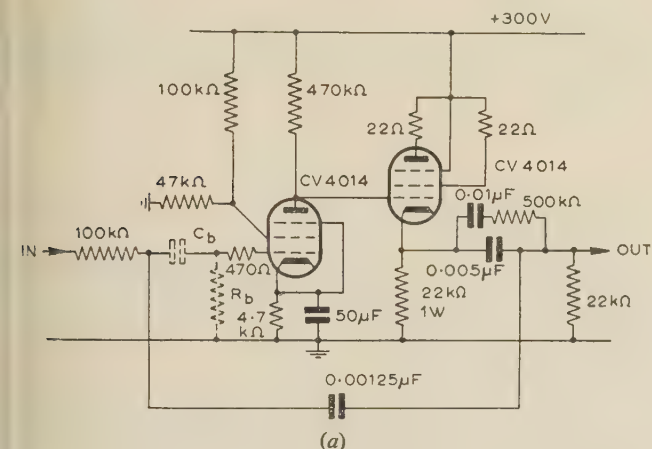


Fig. 16.—Practical 1% CR-coupled integrator.

(a) Circuit.
All resistors are $\frac{1}{2}$ watt rating unless otherwise stated.
(b) Closed-loop gain.
x Indicates experimental point.

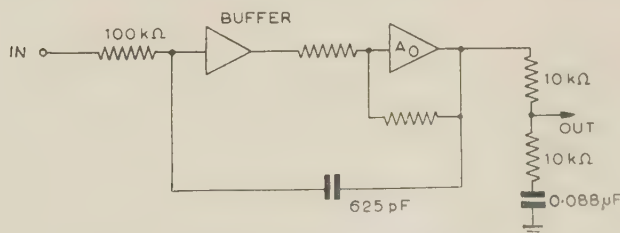


Fig. 17.—Practical 1% phase-corrected integrator.

by local feedback, and the buffer stage is necessary to prevent loading of the integrating network. If the error amplifier itself incorporates an amplifier gain $A_0 > A_3$, a large variation in A_0 causes a relatively small change in the closed-loop gain, A_3 , of the error amplifier.

For a $\pm 50\%$ variation in A_0 the value of A_0 required to maintain A_3 with sufficient accuracy so that the quadrature error remains smaller than the in-phase error can be shown to be approximately equal to the gain A_2 required in the corresponding CR -coupled integrator.

(8) EFFECT OF AMPLIFIER HIGH-FREQUENCY RESPONSE

An assessment of the bandwidth necessary in the error amplifier of a feedback integrator may be obtained by consideration of the effect of amplifier high-frequency fall-off on the integrator impulse response. Let the gain of the amplifier be given by

$$\frac{A}{1 + T_c p}$$

(It is assumed that the gain A is maintained down to zero frequency.) Then, for the feedback integrator of Fig. 2,

$$\frac{v_o}{v_i} = \frac{-\frac{A}{1 + pT_c}}{1 + \left[1 + \frac{A}{1 + pT_c}\right]Tp}$$

whence the impulse response is

$$\frac{v_o}{v_i} = \frac{-\frac{A}{T_c}P}{p^2 + p\left[\frac{1}{T} + \frac{1+A}{T_c}\right] + \frac{1}{TT_c}} \quad (37)$$

The solution of this equation is approximately

$$\frac{-A}{T_c + T(1+A)} \left\{ 1 - e^{-t\left[\frac{1}{T} + \frac{1+A}{T_c}\right]} \right\} \quad (\text{Section 11.6.})$$

In practice, $T_c \ll T(1+A)$, so that the impulse response is approximately

$$\frac{-A}{(1+A)T} \left[1 - e^{-\frac{t(1+A)}{T_c}} \right]$$

Thus, provided that $T_c \ll T(1+A)$, the integration of an impulse yields a step, subject to an exponential delay of time-constant $T_c/(1+A)$ and of magnitude $A/T(1+A)$ independent of the value of T_c . For example, an integrator having an amplifier with a high-frequency bandwidth of 40 kc/s and $A = 400$ would have a rise time (for impulse input) of 0.01 microsec.

High-frequency fall-off in the error amplifier also results in direct feed-through of input components with frequencies $\omega > (1+A)/T_c$. If the output impedance is r_0 and the integrating resistance is R , then, at very high frequencies, no feedback signal occurs and a voltage $v_i r_0/(R + r_0)$ is fed through direct to the output. Such a feed-through signal occurs even at frequencies $\omega \ll (1+A)/T_c$, but, in this case, it is reduced by a factor $1/(1+A)$ (see Section 10.2 of Reference 1). A cathode-follower is normally used in the output circuit to minimize r_0 .

The effects of h.f. fall-off are illustrated by the following example. Consider an integrator used in obtaining a display of the B/H loop of a magnetic material having an ideal square-loop characteristic (see Fig. 18). With a sinusoidal magnetizing current $\hat{I} \sin \omega t$, the input to the integrator will be a series of

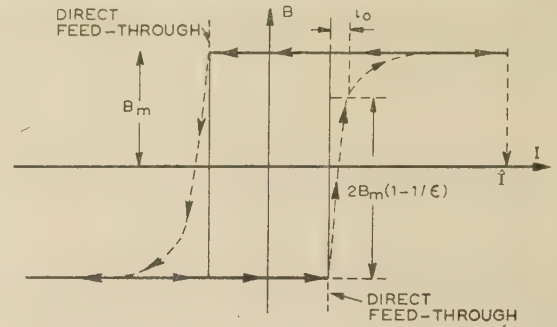


Fig. 18.—Illustration of the effect of h.f. fall-off in error amplifier.

impulses of alternating sign. A c.r.t. display of the integrator output against $\hat{I} \sin \omega t$ will then give the dotted curve in Fig. 18.

For the practical integrator amplifier considered, the rise time of the output is 0.01 microsec, and if the frequency of the magnetizing current is 10 kc/s, the value of i_0 (see Fig. 18) is

$$i_0 = \frac{1}{100} \times 10^{-6} \times \hat{I} \times 10^4 \times 2\pi = 6 \times 10^{-4} \hat{I}$$

i.e. 0.06% of the peak current \hat{I} . Such a discrepancy will not result in any distinguishable difference on the surface of a cathode-ray tube between the actual display and the theoretical square loop.

(9) CONCLUSIONS

Two particular approaches to the low-frequency noise problem have been discussed.

The introduction of a CR -coupling in the feedback loop of a feedback integrator leads to a considerable reduction in low-frequency output noise, but the frequency below which an improvement can be realized is, of necessity, somewhat removed from the signal frequency.

In Section 5, the principle of phase equalization as applied to an integrator has been introduced, and it is shown that phase correction of a direct-coupled integrator with a low-gain error amplifier gives a lower output noise than a direct-coupled integrator of the same accuracy. This method results in a relatively high output impedance necessitating a buffer stage to avoid loading. An extension of equalization procedures centres on the synthesis of an approximation to an ideal integrator characteristic by application of, first, amplitude and then phase correction to existing circuits, e.g. a direct-coupled integrator in conjunction with a high-pass filter. Such methods could be considered in an exacting situation.

It has also been shown that the ultimate limit to the speed of integrator response is set by $(1+A)/T_c$, i.e. by the frequency at which the error-amplifier gain reaches unity.

(10) REFERENCES

- (1) THOMASON, J. G.: 'Linear Feedback Analysis' (Pergamon Press).
- (2) LANDSBERG, S.: 'A General-Purpose Drift-Free D.C. Amplifier', *Philips Research Reports*, 1956, 11, p. 161.

(11) APPENDICES

(11.1) Design of the CR -Coupled Integrator Stabilizing Network

In the angular frequency region $\omega \sim \omega_0$, the parallel impedance of C_0 and the stabilizing network $R_a C_a$ (Fig. 11a) is much

greater than R_0 so that the transfer function of the coupling network is approximately

$$\frac{v_o}{v_i} = \frac{R_0}{\frac{1}{j\omega C_0} \left(R_a + \frac{1}{j\omega C_a} \right) + R_a + \frac{1}{j\omega C_a} + \frac{1}{j\omega C_0}}$$

Putting $T_0 = R_0 C_0$, $\alpha = \left(1 + \frac{C_a}{C_0} \right)$, and $T_a = R_a C_a$:

$$\frac{v_o}{v_i} = \frac{j\omega T_0}{(1 + \omega^2 T_a^2)(\alpha + T_a^2 \omega^2) - j\omega T_a(\alpha - 1)} \quad (38)$$

The phase shift of the coupling network is thus 90° lead minus the angle $\phi = \arctan [\omega T_a(\alpha - 1)/(\alpha + \omega^2 T_a^2)]$. Assuming that the integrating components C_2 and R_2 contribute a further 90° lead at low frequencies ($\omega \sim \omega_0$), ϕ is the phase margin of the feedback loop. The maximum value (ϕ_{max}) is obtained by putting $d(\tan \phi)/d(\omega T_a) = 0$, whence $\alpha = T_a^2 \omega^2$.

$$\text{Thus} \quad \phi_{max} = \arctan \frac{\alpha - 1}{2\sqrt{\alpha}} \quad (39)$$

This phase margin produces greatest stability if it is made to occur at $\omega = \omega_0$, where the open-loop gain is unity. Substituting $\alpha = T_a^2 \omega_0^2$ in eqn. (38), the transfer function of the coupling network is

$$\left(\frac{v_o}{v_i} \right)_{\omega_0} = \frac{j\omega_0 T_0}{1 + \alpha} [2\alpha + j(\sqrt{\alpha})(\alpha - 1)]$$

$$\text{Therefore} \quad \left| \frac{v_o}{v_i} \right|_{\omega_0} = \omega_0 T_0 \sqrt{\alpha}$$

The gain of the integrating network $R_2 C_2$ at $\omega = \omega_0$ is approximately $\omega_0 T_2$. Thus, at the unity-gain frequency ω_0 ,

$$\omega_0 T_2 \omega_0 T_0 (\sqrt{\alpha}) A_2 = 1$$

$$\text{whence} \quad \omega_0 = \frac{\alpha^{-1/4}}{\sqrt{(T_0 T_2 A_2)}} \quad (40)$$

$$\text{and} \quad T_a = \alpha^{3/4} \sqrt{(T_0 T_2 A_2)}$$

The low-frequency asymptote to the closed-loop gain characteristic (Fig. 10) has the equation $\alpha T_0 \omega A_2$, and meets the high-frequency asymptote

$$\frac{1}{\omega T_2} \frac{A_2}{1 + A_2}$$

at an angular frequency ω_1 , such that

$$\frac{A_2}{1 + A_2} \frac{1}{\omega_1 T_2} = \alpha T_0 \omega_1 A_2$$

$$\text{whence} \quad \omega_1 \simeq \frac{1}{\alpha^{1/2} \sqrt{(T_0 T_2 A_2)}} \quad (A_2 \gg 1)$$

(11.2) Derivation of the Values of Q and h (see Fig. 10)

The closed-loop gain of the CR -coupled integrator is given by

$$\frac{A}{1 + j\omega T_2(1 + A)} \quad [\text{see eqn. (1)}]$$

where A is complex and has the value $\frac{j\omega T_0 A_2}{1 + j\omega T_0}$

$$\text{At} \quad \omega = \omega_0, \quad \left| \frac{v_o}{v_i} \right| = \frac{|A|}{|1 + j\omega_0 T_2(1 + A)|} = h \quad (41)$$

Also the magnitude of the point E is approximately

$$\frac{1}{\omega_1 T_2} = \frac{\alpha^{1/4}}{\omega_0 T_2} = \frac{h}{Q} \quad (42)$$

Thus, combining eqns. (41) and (42),

$$Q \simeq \frac{\alpha^{-1/4} |j\omega_0 T_2 A|}{|1 + j\omega_0 T_2 A|}$$

$j\omega_0 T_2 A$ is the open-loop gain G_0 at the angular frequency ω_0 , so that

$$Q \simeq \alpha^{-1/4} \frac{|G_0|}{|1 + G_0|}$$

Fig. 19 shows the values of G and $1 + G$ on the Nyquist diagram, G_0 being the open-loop gain where the phase margin

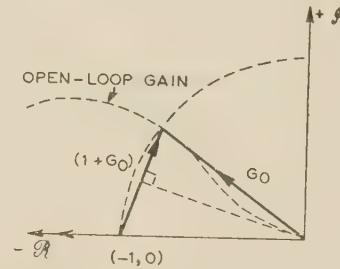


Fig. 19.—Nyquist diagram showing relation between phase margin and Q-factor.

is ϕ_{max} . Thus, from the Figure (assuming that the peak in the closed-loop response occurs at ω_0),

$$Q = \alpha^{-1/4} \frac{1}{2 \sin \frac{\phi_{max}}{2}}$$

Combining this with eqn. (39),

$$Q \simeq \frac{\sqrt{(\alpha + 1)}}{\alpha^{1/4} (\sqrt{2}) [(\sqrt{\alpha}) - 1]}$$

Substitution for ω_0 in eqn. (42) gives

$$h = Q \alpha^{1/2} \sqrt{\frac{T_0 A_2}{T_2}}$$

(11.3) Derivation of Errors in the CR - and Direct-Coupled Integrators

From Section 4.2, the actual output v_o and the ideal output v'_o from the CR -coupled integrator are given by

$$v_o = \frac{-A_2 T_0 v_i j\omega}{\{ [1 - T_2 T_0 \omega^2 (1 + A_2)] + j\omega (T_2 + T_0) \}}$$

and

$$v'_o = \frac{-A_2 v_i}{(1 + A_2) T_2 j\omega}$$

Therefore

$$v_o - v'_o =$$

$$v'_o \left[\frac{-A_2 T_0 j\omega}{\{ [1 - T_2 T_0 \omega^2 (1 + A_2)] + j\omega (T_2 + T_0) \}} \frac{(1 + A_2) T_2 j\omega}{-A_2} - 1 \right] \\ = v'_o \left\{ \frac{1}{\left[1 - \frac{1}{T_2 T_0 \omega^2 (1 + A_2)} - \frac{j\omega (T_2 + T_0)}{T_2 T_0 (1 + A_2) \omega^2} \right]} - 1 \right\}$$

Since $\omega^2 \gg \frac{1}{T_2 T_0 (1 + A_2)}$, $\omega^2 \gg \frac{1}{(T_2 + T_0)^2}$ and $A_2 \gg 1$

$$v_o - v'_o \simeq \frac{+v'_o}{\omega^2 T_2 T_0 A_2} + \frac{jv'_o(T_2 + T_0)}{T_0 T_2 A_2 \omega}$$

Thus the error consists of two components v_{p2} , in phase, and v_{q2} in quadrature with the ideal output. These have magnitudes (expressed in terms of v_i) as follows:

$$v_{p2} \simeq \frac{v_i}{T_2^2 T_0 A_2 \omega^3} \text{ and } v_{q2} \simeq \frac{v_i}{\omega^2 T_2 A_2} \left(\frac{1}{T_2} + \frac{1}{T_0} \right)$$

For the direct-coupled integrator, A_2 is replaced by A_1 , T_2 by T_1 and $T_0 = \infty$, giving

$$v_{p1} \simeq 0 \text{ and } v_{q1} \simeq \frac{v_i}{\omega^2 T_1^2 A_1}$$

(11.4) Criterion for Relative Values of In-Phase and Quadrature Errors in the CR-Coupled Integrator

In the time interval $0 < t < T_s$ (see Fig. 12), the total error expressed as a function of time is given by

$$V_{p2} \left[1 - \left(\frac{t - T_s/2}{T_s/2} \right)^2 \right] + V_{q2} \left(1 - \frac{2t}{T_s} \right) \quad (43)$$

Since the slope of the in-phase error has its maximum value at $t = 0$, and the slope of the quadrature error is constant in the specified interval, it follows that, if the initial slope of the combined error waveforms is less than, or equal to, zero, the error can never exceed $+V_{q2}$ (at $t = 0$) or $-V_{q2}$ (at $t = T_s$).

Differentiation of eqn. (43) with respect to time and substitution of $t = 0$ yields the initial slope of the total error waveform, whence the required criterion is given by

$$\frac{V_{p2}}{V_{q2}} \leq \frac{1}{2}$$

From Section 4.2,

$$\frac{V_{p2}}{V_{q2}} = \frac{T_s}{4(T_2 + T_0)}$$

whence

$$T_2 + T_0 \geq \frac{T_s}{2}$$

(11.5) Derivation of Errors in the Phase-Corrected Integrator

From Section 5.2, the actual output v_o and the ideal output v'_o are given by

$$v_o = \frac{-A_3 v_i}{1 + T_3(1 + A_3)j\omega} \frac{1 + j\omega T_4}{1 + \frac{j\omega T_4}{k}}$$

and

$$v'_o = \frac{A_3 k v_i}{T_3(1 + A_3)j\omega}$$

Combining the equations:

$$v_o = v'_o \left[\left(1 + \frac{1}{T_3(1 + A_3)j\omega} \right)^{-1} \left(1 + \frac{1}{j\omega T_4} \right) \left(1 + \frac{k}{j\omega T_4} \right)^{-1} \right]$$

Putting $\frac{1}{T_3(1 + A_3)\omega} = x$ and $\frac{1}{\omega T_4} = y$ ($x \ll 1$ and $y \ll 1$)

$$v_o = v'_o [(1 - jy)(1 - jx)^{-1}(1 - jkx)^{-1}]$$

Expanding this equation (ignoring anything higher than cubic

terms) and substituting the condition for first-order phase correction [eqn. (30)], namely $x = y(1 - k)$:

$$v_o = v'_o \left[1 + \frac{kx^2}{(1 - k)} + \frac{j k x^3}{(1 - k)^2} \right]$$

Therefore

$$v_o - v'_o = \frac{v'_o k x^2}{1 - k} + \frac{j v'_o k x^3}{(1 - k)^2}$$

Thus the residual quadrature error has a magnitude $x/(1 - k)$ times that of the in-phase error.

$$\text{Now } \frac{x}{(1 - k)} = \frac{1}{(1 - k)(1 + A_3)T_3\omega}$$

which is much less than unity for $\omega \gg \omega_3$, and the error is therefore composed mainly of the in-phase component, of magnitude (expressed in terms of v_i)

$$v_{p3} \simeq \frac{k^2 A_3 v_i}{(1 - k)[\omega T_3(1 + A_3)]^3}$$

(11.6) Relation of Impulse Response to Amplifier High-Frequency Cut-Off

From eqn. (37),

$$v_o = \frac{\frac{-A}{TT_c}}{p^2 + p \left(\frac{1}{T} + \frac{1 + A}{T_c} \right) + \frac{1}{TT_c}}$$

The solution of this equation is of the form

$$v_o = \frac{-A}{TT_c} \left[\frac{\varepsilon^{(\gamma + \beta)t} - \varepsilon^{(\beta - \gamma)t}}{2\gamma} \right]$$

where $\beta \pm \gamma$ are the roots of the equation $p^2 + p \left[\frac{1}{T} + \frac{(1 + A)}{T_c} \right] + \frac{1}{TT_c} = 0$,

$$\text{i.e. } \beta = \frac{-1}{2TT_c} [T_c + T(1 + A)]$$

$$\text{and } \gamma = \frac{1}{2TT_c} [T_c + T(1 + A)] \sqrt{1 - \frac{4TT_c}{[T_c + T(1 + A)]^2}}$$

Expanding to a first order only $\left\{ \frac{4TT_c}{[T_c + T(1 + A)]^2} \ll 1 \right\}$:

$$\gamma = \frac{1}{2TT_c} [T_c + T(1 + A)] \left\{ 1 - \frac{2TT_c}{[T_c + T(1 + A)]^2} \right\}$$

$$\text{Therefore } \gamma + \beta = -\frac{1}{T_c + T(1 + A)}$$

$$\text{and } \beta - \gamma = -\frac{1}{TT_c} [T_c + T(1 + A)]$$

Therefore

$$v_o \simeq \frac{-A}{[T_c + T(1 + A)]}$$

$$\left\{ \exp \frac{-t}{T_c + T(1 + A)} - \exp \frac{T_c + T(1 + A)t}{TT_c} \right\}$$

and for

$$t \ll [T_c + T(1 + A)]$$

$$v_o \simeq \frac{-A}{[T_c + T(1 + A)]} \left[1 - \varepsilon^{-t \left(\frac{1}{T} + \frac{1 + A}{T_c} \right)} \right]$$

MEASUREMENTS ON GAS-DISCHARGE NOISE SOURCES AT CENTIMETRE WAVELENGTHS

By A. C. GORDON-SMITH and J. A. LANE, M.Sc., Associate Member.

(The paper was first received 18th March, and in revised form 5th June, 1958.)

SUMMARY

Measurements are described in which the effective noise temperature of the type CV1881 argon discharge tube is determined by comparison with both a thermal noise source and a continuous-wave signal, at a wavelength of 3.2 cm (frequency, 9.4 Gc/s). The results obtained were $10590 \pm 500^\circ\text{K}$ and $11050 \pm 1350^\circ\text{K}$, respectively. The results are compared with data previously given for argon noise sources.

(1) INTRODUCTION

The technique in which centimetre-wave receivers are calibrated by gas-discharge noise sources is now well known,^{1,2} and is generally preferred to the alternative method which requires a continuous-wave source of known intensity. Measurements of the output power of such noise sources are consequently of general interest. In the helium and neon discharges, the output depends to a marked extent on the discharge current. This effect, however, is relatively small with argon sources. These, when calibrated, are therefore used extensively as convenient substandards. It is the purpose of the paper to summarize results obtained by the authors and others in calibration measurements on argon sources, with particular reference to the type CV1881. This discharge tube, which contains argon at a pressure of 0.001 mm Hg, is widely used in the United Kingdom.

At the commencement of the work described below, no published information was available on the properties of the type CV1881 source. Calibrations by both noise and c.w. signals were therefore undertaken with a view to comparing the results obtained by the two quite different methods. Such a comparison is of additional interest, since it relates c.w. power standards operating at levels of several watts with low-level thermal sources. Further independent investigations of the power output of the type CV1881 source have been described by Hughes³ and Sutcliffe,⁴ and their results are compared with those of the authors later in the paper.

(2) EXPERIMENTAL PROCEDURE

The argon source was compared with (a) a thermal noise source at a known temperature, and (b) a c.w. signal of known level, using a superheterodyne receiver of known bandwidth. Both experiments were carried out at a wavelength of 3.2 cm. In the former experiment, the technique followed was essentially the same as that described by Hughes³ in his measurements at 3.0 cm. In the following description experimental details are therefore included only where they serve to illustrate additional features of interest in procedure or equipment.

The thermal-noise source comprised a tapered mica vane sputtered with platinum which could be heated to a known, uniform temperature of approximately 300°C . The discharge tube, in a 10° or 15° E-plane mount, was connected to the main waveguide assembly between the noise source and a radiometer receiver by means of a directional coupler of coupling factor

15.5 dB. This arrangement facilitated the rapid comparison of two noise powers of approximately equal intensity. The radiometer was of the type described by Dicke,⁵ the noise input being compared with thermal noise at room temperature by a modulation technique using a rotating disc of attenuating material in the input waveguide. In order to achieve a constant conversion loss in the radiometer it was necessary to ensure that the source impedance presented to the crystal mixer at signal and image frequencies was the same for each observation. The final comparisons between the argon discharge tube and the thermal noise source were made by adjusting the temperature of the latter so that identical outputs were indicated by the radiometer in the two measurements. If the effective noise temperature of the discharge tube is T_e , and the temperatures of the thermal load and the ambient surroundings at T_1 and T_0 , respectively (all temperatures being in degrees Kelvin), we have

$$(T_e - T_0)/T_0 = \alpha(T_1 - T_0)/T_0 = \text{antilog } \frac{N}{10} \quad (1)$$

where α is the coupling factor of the directional coupler (expressed as a power ratio), and N is the excess noise/temperature ratio. T_e is thus found from measurements of T_1 , T_0 and α .

The procedure in the continuous-wave technique was similar to that usually followed in measurements of receiver sensitivity by means of a standard signal generator. The experimental difficulties encountered in such measurements are considerable, owing to the large attenuation which is necessary between the c.w. source and the receiver. The errors in the determination of this attenuation, the effect of stray leakage signals, etc., combine to give a total inaccuracy which may be as much as $\pm 2\text{dB}$. It is for these reasons, of course, that the method of receiver calibration by noise sources is frequently preferred to the c.w. technique. Nevertheless, comparison measurements with a c.w. source were felt to be worth while in the present investigation, especially since the necessary equipment was already available and its accuracy known.

The experimental equipment for comparing the gas-discharge tube with a c.w. source of known intensity is shown in Fig. 1.

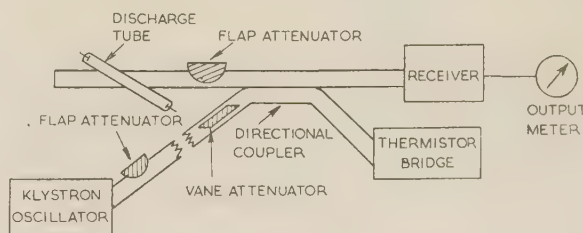


Fig. 1.—Calibration of discharge tube by c.w. method.

The output from the oscillator was first measured by the thermistor bridge, which had been calibrated in subsidiary experiments by reference to a water calorimeter⁶ and a differential air thermometer.⁷ The vane attenuator was then adjusted so

Written contributions on papers published without being read at meetings are not considered for publication.
This paper is an official communication from the Radio Research Station, Department of Scientific and Industrial Research.

as to produce an output at the receiver equal to that due to the discharge tube. The output indicator was a galvanometer connected to a thermo-junction in the final intermediate-frequency stage of a superheterodyne receiver. The total attenuation between source and receiver was approximately 90 dB, and careful screening of the source was therefore necessary to ensure that the effect of stray leakage signals was reduced to a minimum. Measurements of the i.f. bandwidth were made by means of a standard signal generator, each measurement requiring a large number of observations and an integration of the resulting response curve. The bandwidth B is defined by

$$B = \int_0^{\infty} \frac{Gdf}{G_m} \quad \dots \quad (2)$$

where G is the receiver gain, with a maximum value of G_m . The receiver response was identical at signal and image frequencies, so that the total output, P , when using the noise source is given by

$$P = 2kT_0BFG_m + 2kBG_m(T_e - T_0) = 2kBG_m[T_0(F - 1) + T_e] \quad \dots \quad (3)$$

where k is Boltzmann's constant, and F is the effective noise factor of the receiver. Similarly, in the c.w. measurement, we have

$$P = 2kT_0BFG_m + P'G_m$$

where P' is the c.w. input power to the receiver.

Therefore

$$P' = 2kB(T_e - T_0) \quad \dots \quad (4)$$

T_e is thus readily obtained from the measured quantities B and T_0 .

(3) EXPERIMENTAL RESULTS AND DISCUSSION

The results obtained for the effective temperature, T_e , of the type CV1881 source, both in the investigation described above and elsewhere, are summarized in Table 1, together with the estimated maximum error.

Table 1

EFFECTIVE NOISE TEMPERATURE OF THE TYPE CV1881 GAS DISCHARGE TUBE (DISCHARGE CURRENT 180 mA)

Authors	Method	Frequency	T_e	N
Hughes ..	Noise source and radiometer	Gc/s 2.86	°K 11 140	dB 15.73 ± 0.1
Sutcliffe ..	Noise source and superheterodyne receiver	9.4	11 190	15.75 ± 0.3
Gordon-Smith and Lane	Noise source and radiometer	9.4	10 590	15.5 ± 0.2
Gordon-Smith and Lane	Calibrated c.w. signal	9.4	11 050	15.7 ± 0.5

Although a relatively large cumulative error is difficult to avoid in the continuous-wave technique, which requires many subsidiary measurements, the results obtained by the methods outlined above are in good agreement. Together with the data previously published,^{3,4} they confirm the merits of the type CV1881 discharge tube as a substandard noise source. The results of some subsidiary measurements with discharge currents

between 160 and 200 mA were consistent with a mean temperature coefficient in the value of N of -0.004 dB/mA, as quoted by Hughes.³

Further experimental results on argon discharge sources have been given recently by other workers. Although the precise operating conditions are not always specified, so that a direct comparison with the results in the Table is of limited value, the results quoted illustrate the range of values obtained for the noise temperature of argon sources of various types. Bridges⁸ obtained a value for T_e of $11\,500^\circ\text{K}$ ($N = 15.9$ dB) at a wavelength of 0.8 cm for an argon source operated at a pressure of 30 mm Hg and a current of 45 mA. Using both a Dicke-type radiometer and a conventional superheterodyne receiver, Davies⁹ and Cowcher⁹ measured T_e to be $10\,300^\circ\text{K}$ ($N = 15.4$ dB) at a wavelength of 10 cm. A somewhat higher value, $T_e = 15\,100^\circ\text{K}$ ($N = 17.1$ dB), has been quoted by Knol,¹⁰ who used a thermal noise source at a temperature of $1\,300^\circ\text{K}$ at 3 cm wavelength. The standard deviation in 28 measurements of T_e is given as 600°K . The discharge current was 60 mA, but since the pressure is not stated the significance of the result in the present comparison is uncertain. The precise nature of the physical processes responsible for the production of noise in gas discharges is still in some doubt, so that no reliable theoretical analysis of the effect of varying the pressure or the discharge current is possible. It has been known for some time, however, that the argon discharge becomes unstable at low pressures; striations exist in the positive column and an audio-frequency oscillation can be detected across the tube. For a given pressure, these effects can be reduced by increasing the discharge current or reducing the diameter of the tube. The critical current, above which the audio-frequency oscillations are relatively small and have no effect on the measured conductance of the discharge, is approximately 150 mA for the type CV1881 source. It is possible, therefore, that the relatively high noise temperature measured by Knol is due, in part at least, to an instability of the type described above.

(4) CONCLUSIONS

The effective noise temperature of the type CV1881 argon-discharge noise source has been determined for an E-plane mount at a discharge current of 180 mA by comparisons against a thermal noise source and a c.w. oscillator at 3.2 cm. The results obtained were $10\,590 \pm 500^\circ\text{K}$ and $11\,050 \pm 1\,350^\circ\text{K}$, respectively (i.e. excess noise/temperature ratios of 15.5 ± 0.2 dB and 15.7 ± 0.5 dB). These results indicate agreement, within the accuracy of the comparison, between high-power c.w. standards and the thermal noise source.

(5) ACKNOWLEDGMENTS

The work described in the paper was carried out as part of the programme of the Radio Research Board and is published by permission of the Director of Radio Research of the Department of Scientific and Industrial Research.

(6) REFERENCES

- (1) MUMFORD, W. W.: 'A Broad-Band Microwave Noise Source', *Bell System Technical Journal*, 1949, **28**, p. 608.
- (2) JOHNSON, H., and DEREMER, K. R.: 'Gaseous Discharge Super-High-Frequency Noise Sources', *Proceedings of the Institute of Radio Engineers*, 1951, **39**, p. 908.
- (3) HUGHES, V.: 'Absolute Calibration of a Standard Temperature Noise Source for Use with S-Band Radiometers', *Proceedings I.E.E.*, Paper No. 2125 R, September 1956 (103 B, p. 669).

- (4) SUTCLIFFE, H.: 'Noise Measurements in the 3-cm Waveband using a Hot Source', *ibid.*, Paper No. 2130 R, September, 1956 (103 B, p. 673).
 - (5) DICKE, R. H.: 'The Measurement of Thermal Radiation at Microwave Frequencies', *Review of Scientific Instruments*, 1946, 17, p. 268.
 - (6) LANE, J. A.: 'The Measurement of Power at a Wavelength of 3 cm by Thermistors and Bolometers', *Proceedings I.E.E.*, Paper No. 1918 R, November, 1955 (102 B, p. 819).
 - (7) GORDON-SMITH, A. C.: 'A Milliwattmeter for Centimetre Wavelengths', *ibid.*, Paper No. 1888 R, September, 1955, (102 B, p. 685).
 - (8) BRIDGES, T. J.: 'A Gas-Discharge Noise Source for Eight-Millimetre Waves', *Proceedings of the Institute of Radio Engineers*, 1954, 42, p. 818.
 - (9) DAVIES, L. W., and COWCHER, E.: 'Microwave and Metre Wave Radiation from the Positive Column of a Gas Discharge', *Australian Journal of Physics*, 1955, 8, p. 108.
 - (10) KNOL, K. S.: 'A Thermal Noise Standard for Microwaves', *Philips Research Reports*, 1957, 12, p. 123.
-

METHODS OF CALCULATING THE HORIZONTAL RADIATION PATTERNS OF DIPOLE ARRAYS AROUND A SUPPORT MAST

By P. KNIGHT, B.A., Associate Member.

(The paper was first received 21st May, and in revised form 29th July, 1958.)

SUMMARY

Many v.h.f. broadcast transmitting aerials consist of an array of dipoles mounted on a supporting mast. Some theoretical methods which may be used to determine their horizontal radiation patterns are described and their limitations discussed. Patterns calculated by these methods are compared with those measured using small-scale models.

(1) INTRODUCTION

V.H.F. broadcasting aerials often consist of arrangements of dipoles mounted on a supporting structure. The support is usually of metallic construction and currents are induced on it. The field associated with these currents may modify the radiation pattern to such an extent that the supporting mast must be considered as an integral part of the aerial system.

The supporting mast is usually of lattice construction, and in the absence of screening, its effect would be difficult to predict, as it depends on the arrangement of the structural members. The mast is, however, often covered by a screen of wires parallel to the plane of polarization of the radiated wave in order to reduce the fields within the structure. Its outer surface then behaves as a continuous sheet and may be treated as such theoretically.

The cross-section of the mast usually takes the form of a circle, a square or an equilateral triangle. The horizontal radiation patterns of arrays of vertical dipoles on masts of circular cross-section may be calculated exactly (see Section 2), but no such solution exists for masts of any other shape, or for horizontal dipoles. Approximate methods of treating these cases are described.

(2) CARTER'S METHOD FOR CYLINDRICAL MASTS

If a cylinder is placed near a Hertzian doublet, currents will be induced on its surface and the radiation pattern of the doublet will be modified. The polarization of the resultant wave will depend on the relative orientation of the doublet and the cylinder and will in general be elliptical. The electric field can always be resolved into two orthogonal components normal to the direction of propagation; it is convenient to resolve the field into vectors perpendicular to, and lying in, the plane containing the axis of the cylinder.

Carter¹ has derived exact solutions for these two components by treating the doublet as a receiving aerial. The voltage induced in the doublet is calculated in turn for incident waves polarized in the directions of the two components; these voltages are, by the principle of reciprocity, proportional to the two components of the field which would be radiated if the doublet were driven.

Each of the incident waves is assumed to be plane and is resolved into a set of standing cylindrical waves whose axes are coincident with the axis of the cylinder. The field re-radiated by the currents induced on the surface of the cylinder can also be

resolved into a similar set of cylindrical waves, and their amplitudes and phases may be determined by equating the sum of the two sets of waves to zero at the surface of the cylinder, since no tangential electric field can exist there. Both sets of waves are then completely specified and the voltage induced in a doublet having any position and orientation may now be calculated.

Carter's results are stated for doublets having the three orthogonal orientations shown in Fig. 1; the field due to a

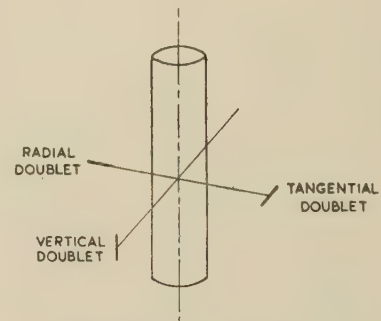


Fig. 1.—Types of doublet.

doublet having any other orientation can, of course, be obtained by resolving it into three component doublets. In this paper, attention has been confined to the fields set up by each of these arrangements of doublets in the plane perpendicular to the cylinder, which is assumed to be vertical. Carter's formulae for these horizontal radiation patterns (h.r.p.'s) take the form of Fourier series with complex coefficients and are closely related to the corresponding formulae for the doublets in free space.

The formulae for the h.r.p.'s of arrangements of vertical doublets apply exactly to similar arrangements of vertical dipoles, since the radiation patterns of all the elementary doublets which form a dipole are identical in shape. The h.r.p.'s of horizontal dipoles mounted on a cylinder could be calculated by applying the formulae for tangential and radial doublets to the elementary doublets forming the dipoles, but the necessary integration can only be performed numerically; this method is therefore impracticable. The pattern may, however, be calculated fairly accurately if each dipole is replaced by a doublet situated at its mid-point. A more accurate result is obtained if this substitution is used to calculate only the field radiated by the currents induced in the cylinder, the direct contributions from the dipoles themselves being determined exactly by the usual geometrical method (this method was used for the patterns described in Section 5). Alternatively, tangential dipoles may be assumed to behave as dipoles bent into arcs of circles concentric with the cylinder. Although an exact solution exists for this arrangement, the use of this approximation for linear dipoles gives a less accurate result because the contributions from the dipoles themselves are calculated only approximately.

Carter's method may be used to obtain an approximate solu-

Written contributions on papers published without being read at meetings are invited for consideration with a view to publication.

Mr. Knight is with the British Broadcasting Corporation.

ion for a mast of polygonal cross-section provided that the width of each face is sufficiently small compared with the wavelength. If the radiating elements are vertical, the mast may be replaced by an equivalent cylinder having the same inductance per unit length; the radius of this equivalent cylinder may be calculated exactly if the mast is a regular polygonal prism.² Thus triangular and square masts having faces of width s may be replaced by cylinders of radii $0.42s$ and $0.59s$ respectively. But when the radiating elements are horizontal, the diameter of the equivalent cylinder depends not only on the shape of the mast but also on its orientation relative to the elements. For example, if the supporting mast were a thin strip it would have no effect on the h.r.p. of a dipole at A (Fig. 2), but a maximum



Fig. 2.—Horizontal dipoles near a support of 'strip' cross-section.

effect for a dipole at B. For masts whose cross-sections are regular polygons, however, experience has shown that for horizontal radiating elements a good approximation is a cylinder of the same perimeter.

Comparison of measured and calculated patterns has shown that these approximations give reasonably accurate results for triangular masts whose sides are less than 0.3λ wide and for square masts less than 0.5λ wide.

(3) THE INFINITE-PLANE METHOD FOR LARGE POLYGONAL MASTS

If the faces of square, triangular or other polygonal masts are so wide that the radiating elements may be mounted more than a wavelength from the corners, each face may be treated as an infinite plane and its effect calculated by the method of images. The total field in any direction may then be obtained by adding the contributions from those faces which are visible, with due regard to phase.

This method can be used only for masts whose faces are at least 2λ wide. It fails to give accurate results for smaller masts, because diffraction effects at edges cannot be neglected in such cases.

(4) METHODS FOR POLYGONAL MASTS OF INTERMEDIATE SIZE

Square or triangular masts whose sides are less than 0.5λ or 0.3λ wide respectively may be replaced by equivalent cylinders and the patterns of dipoles mounted upon them calculated by Carter's method, described in Section 2. Alternatively, if the faces are at least 2λ wide the infinite-plane method described in Section 3 may be used. Both these methods fail if the width of the faces lies between these limits. Two methods which give more accurate results when the mast is of intermediate size are described in this Section.

(4.1) The Induced-Current Method

Moullin has shown³ that the radiation pattern of a current filament F (Fig. 3) parallel to a ribbon AB can be calculated with little error by assuming that the current density at any point on the ribbon is the same as that at the corresponding point of a strip AB of an infinite plane EC. No minimum width for the ribbon was stated, but it was shown that radiation patterns calculated by this method are in good agreement with measured patterns, provided that the ribbon is more than a wavelength wide.

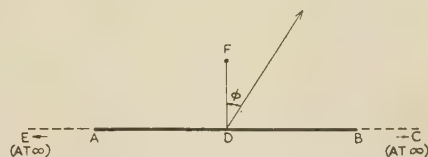


Fig. 3.—A filament parallel to a conducting ribbon.

The radiation pattern in a plane perpendicular to the axis of the ribbon is unchanged if the infinite filament is replaced by one of finite length or by a dipole. In applying it to arrays of dipoles mounted on polygonal masts, each face which has a dipole associated with it is assumed to carry the current which would be induced on it if it were part of an infinite plane. The currents induced on the face by dipoles mounted on other faces are disregarded; these currents will be very small for square and triangular masts, since the face always lies in the shadow of the adjacent dipoles.* The radiation pattern of each face and the dipole upon which it is mounted is then calculated over the complete range of angles, and the fields produced by all the dipoles are added, with due regard to phase, to give the resultant h.r.p. The method of calculation is described in greater detail in Section 9.1.

If the filament is replaced by a line doublet (Fig. 4), the currents



Fig. 4.—Ribbon and line doublet.

Arrows show direction of current flow.

induced on an infinite plane will change their direction through a right angle, but their amplitudes and phases will remain the same. It is reasonable to suppose that no great change in the distribution will occur if the plane is replaced by a ribbon more than one wavelength wide. This assumption has therefore been used as a basis for calculating the radiation patterns of horizontal dipoles mounted on polygonal masts, each dipole being treated as a line doublet.

It is shown in Section 9.1 that the radiation pattern of a line doublet parallel to a ribbon may be derived from the corresponding pattern for a filament parallel to a ribbon simply by multiplying by $\cos \phi$ (Fig. 3). If the radiating element is a horizontal dipole the filament pattern may instead be multiplied by the dipole radiation pattern. This alternative is thought to be slightly more accurate, since the pattern of the dipole itself is not distorted. This method was therefore used for the calculations described in Section 5.

(4.2) The Diffraction Method

A disadvantage of the method described in Section 4.1 is that the currents induced on the faces adjacent to those upon which

* If the mast has more than four faces, each face may be illuminated by dipoles on adjacent faces and the resulting induced currents may not be small. Since, however, the cross-section will more nearly resemble a circle, Carter's method should be applicable to masts of greater cross-sectional area.

the radiating elements are mounted are assumed to be zero and are therefore neglected. These currents, although small, nevertheless contribute to the distant field. Their presence can be demonstrated by the fact that the h.r.p. of a single horizontal dipole mounted on a large mast does not, in general, exhibit zeros. Had the current been confined to the face parallel to the dipole, two diametrically opposite zeros would have been present.

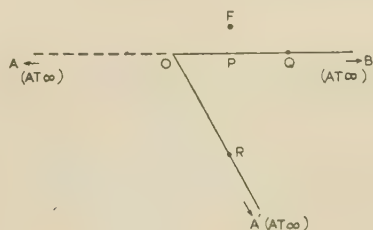


Fig. 5.—A current filament near a conducting wedge.

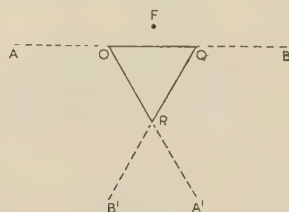
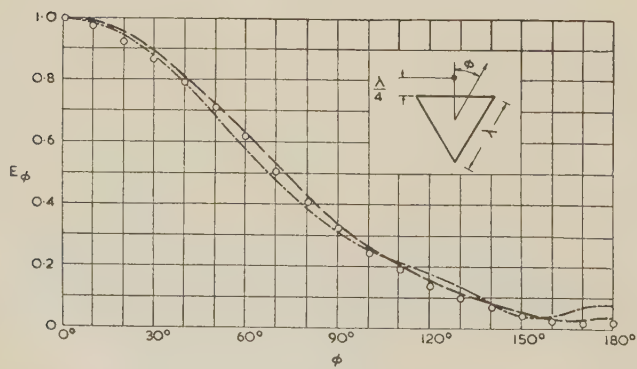
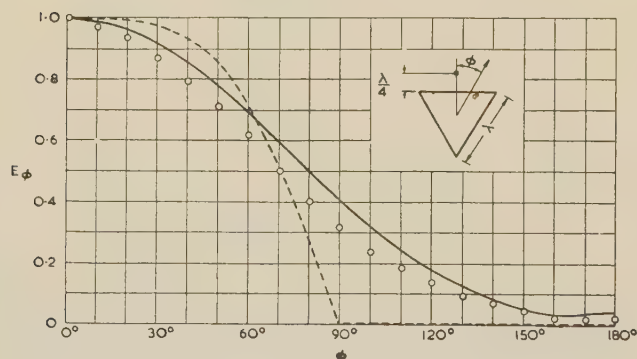


Fig. 6.—A current filament near a conductor of triangular cross-section.



(a)

(b)

Fig. 8.—Theoretical and measured h.r.p.'s of a dipole spaced 0.25λ from a triangular mast 1.0λ wide.

- (a) Vertical dipole. (b) Horizontal dipole.
 — H.R.P. calculated by Carter's method.
 - - - H.R.P. calculated by the infinite-plane method.
 - · - H.R.P. calculated by the induced-current method.
 - - - H.R.P. calculated by the diffraction method.
 ○ ○ Measured points (averaged over 360°).

To overcome this difficulty, Schelkunoff's formulae⁴ for the diffraction of a cylindrical wave by a wedge have been applied to the corners of polygonal masts. Schelkunoff gives an expression for the radiation pattern of a filament F in the presence of a whole plane bent into a wedge A'OB (Fig. 5); it can be shown that a similar expression may be derived when the filament is

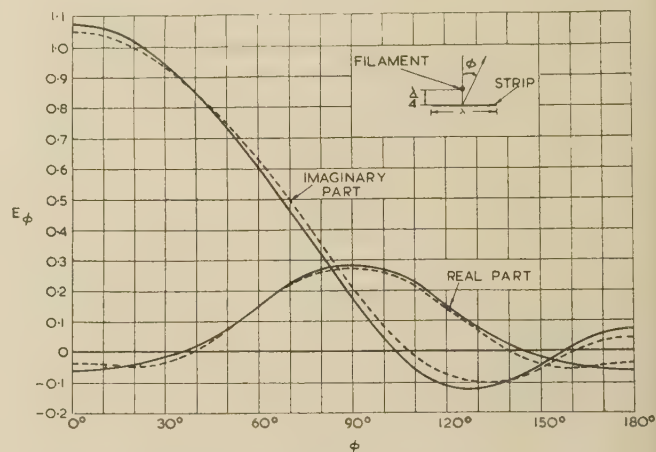


Fig. 7.—The radiation pattern (in complex form) of a current filament parallel to a strip one wavelength wide.

- Radiation pattern calculated by the induced-current method.
 - - - Radiation pattern calculated by the diffraction method.

The phase of the field is referred to the mid-point of the strip. In the absence of the strip its amplitude would be 0.5.

replaced by a line doublet (see Section 9.2). If the field of the filament in the presence of the whole plane AOB is subtracted from that of the filament in the presence of the wedge, the difference is equal to the diffracted field which is set up when the plane is bent.

In applying this result to a mast we will assume that the field diffracted at O* will be changed very little if the plane is bent again at Q and R, although these bends will, of course, set up additional diffracted fields. This assumption is reasonable provided that Q and R are a wavelength or more from O; it is similar to Moullin's assumption that no change takes place in the current distribution near the edge of a half-plane when most of the half-plane is removed. Thus in calculating the pattern of an element at F, the fields diffracted by the corners at O and Q are calculated separately by assuming that these are corners of infinite wedges. The two diffracted fields are then added to the field which the element would set up over an infinite plane AB. The fields diffracted at all other corners are neglected.

When the radiating element is a vertical dipole the solution for a filament is used. When it is a horizontal dipole the diffracted fields appropriate to a line doublet are added to the infinite-plane solution for a dipole, as the diffracted fields for a dipole cannot easily be calculated. The error resulting from the use of this approximation is very small.

* For simplicity the expression 'the field diffracted at O' is used to denote the change in field caused by bending an infinite plane at O to form a wedge.

Horizontal radiation patterns calculated by the method described exhibit small discontinuities resulting from the approximation made. For example, referring to Fig. 6, the field diffracted at O is necessarily assumed to be zero in the sector A'OB, and the field diffracted at Q is assumed to be zero in the sector B'QA. It follows that the total field calculated will, in general, be discontinuous along the lines OA, QB, RA' and RB'. With horizontal polarization the value of the field will be discontinuous; for example, the field diffracted at O will be finite up to the boundary (A'OB) of the sector in which it is zero. With vertical polarization the field diffracted at O will fall to zero at the boundary A'OB, so that the discontinuity will be one of gradient only. In all h.r.p.'s computed for vertical polarization the discontinuity in gradient has proved imperceptible. The discontinuities of both types would vanish if account could be taken of multiple diffraction.

It is of interest to compare the patterns calculated by the two methods described in this Section for the special case where the 'mast' is a thin strip. The pattern of this arrangement is calculated directly by the induced-current method and may be calculated by the diffraction method by bending the plane through 180° at O and Q. The patterns for a filament distant $\lambda/4$ from a strip one wavelength wide calculated by these two methods are compared in Fig. 7, and it will be seen that the agreement is quite good. Equally good agreement was obtained when the calculations were repeated for a line doublet.

(5) COMPARISON OF CALCULATED WITH MEASURED PATTERNS

Radiation patterns have been calculated by all the methods described in the paper for horizontal and vertical dipoles mounted centrally on the faces of square and triangular masts. For both mast shapes the width of each face was one wavelength, this value being chosen because it lies within the range in which both of the approximate methods described in Sections 2 and 3 fail. The object was to determine whether the methods described in Section 4 gave more accurate results. Horizontal radiation pattern measurements were therefore made with small-scale models. All the h.r.p.'s have been normalized so that their maximum values are unity.

The h.r.p.'s for a triangular mast associated with a single dipole are compared in Fig. 8. Considering first vertical polarization [Fig. 8(a)], it will be seen that the h.r.p.'s calculated by Carter's method show fairly good agreement with the measured results, but the infinite-plane method gives poor results because backward radiation is entirely neglected. The methods described in Section 4 both show better agreement.

With a horizontal dipole [Fig. 8(b)] the infinite-plane method is a better approximation than Carter's method, the latter giving too large a field in the backward directions. Both the methods described in Section 4 give reasonably good agreement. The discontinuities in the curve calculated by the diffraction method should be noted; the reason for them was explained in Section 4.

Fig. 9 shows the corresponding patterns for co-phased dipoles mounted on all three faces. These patterns were calculated by combining the single dipole patterns with due regard to phase. The methods which gave the closest agreement with the measured patterns for single dipoles would also be expected to give the best agreement in this case. It will be seen that this is, in fact, true, the two methods of Section 4 showing quite good agreement throughout.

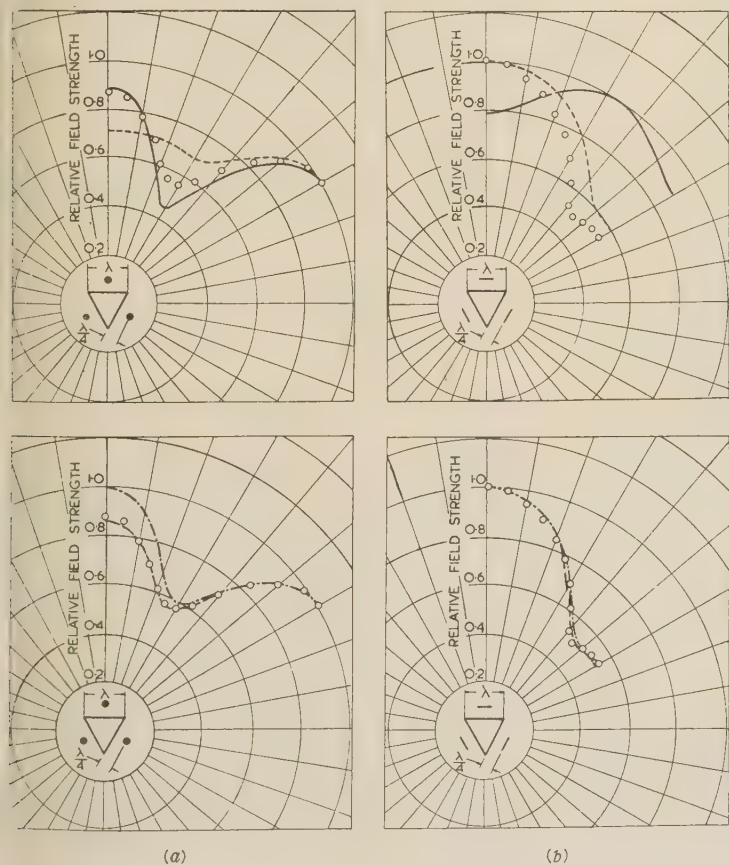


Fig. 9.—Theoretical and measured h.r.p.'s of co-phased dipoles spaced 0.25λ from a triangular mast 1.0λ wide.

- (a) Vertical dipoles. (b) Horizontal dipoles.
 — H.R.P. calculated by Carter's method.
 - - - H.R.P. calculated by the infinite-plane method.
 . . . H.R.P. calculated by the induced-current method.
 — H.R.P. calculated by the diffraction method.
 ○ ○ Measured points (averaged over 360°).

With a square mast, the h.r.p.'s calculated by the methods described in Section 4 again showed good agreement with measured values. Carter's method and the infinite-plane method were also fairly accurate when the dipoles were vertical.

(6) CONCLUSIONS

By using the more accurate methods described in Section 4, the h.r.p. of a dipole mounted on a mast of polygonal cross-section may be calculated when the size of the mast is such that neither Carter's method nor the infinite-plane method can be used. But, in practice, the calculation involved is long and tedious, and the solution to the problem can usually be obtained more easily by making measurements with a model.

The fact that it is possible to calculate an accurate pattern when the mast is of intermediate size shows that the initial assumptions made about the current distribution were justified. A better understanding of the way in which the combination of mast and dipole radiates has therefore been obtained. Thus when a dipole is mounted at the centre of a face one wavelength or more wide, the currents induced on other faces are small and contribute little to the radiated field. With masts of this size a practical implication is that screening rods may be required only on those faces which have dipoles mounted upon them.

If measurement is not possible and calculation becomes necessary, the most suitable method must be chosen. If the size of the mast is such that neither Carter's method nor the infinite-plane method is suitable, one of the methods described in Section 4 must be used. These lead to results of similar accuracy, so that preference may be given to the method requiring the simplest calculation.

Radiation patterns may be calculated directly from tabulated functions by the diffraction method, but the calculation is long and tedious. With the induced-current method a number of numerical integrations must be performed (unless the mast is large enough for the integrals to be replaced by asymptotic approximations) and the calculation of a single radiation pattern is no shorter. However, the functions which require to be integrated depend only on the spacing of the element from the mast face, and once these have been plotted the patterns for a variety of mast widths and element positions may be rapidly obtained by integrating between different limits. Moreover, when the field of an element, and the face from which it is supported, has been calculated, it may be used for square, triangular or other polygonal masts without modification. A further advantage is that the patterns for horizontal dipoles may be derived from the corresponding patterns for vertical dipoles by a simple multiplication. Thus, although the work involved in calculating an isolated pattern by either method is considerable, the induced-current method is much more flexible in its application and is therefore to be preferred.

(7) ACKNOWLEDGMENTS

The author would like to record his thanks to Mr. A. Brown, for performing the measurements, and to Mr. K. Hughes, for drawing attention to the paper by Professor Moullin and suggesting that the methods described therein could be applied to the problem discussed here. He would also like to thank Mr. G. D. Monteath for valuable advice and encouragement, and he is indebted to the Chief Engineer of the British Broadcasting Corporation for permission to publish the paper.

(8) REFERENCES

- (1) CARTER, P. S.: 'Antenna Arrays around Cylinders', *Proceedings of the Institute of Radio Engineers*, 1943, **31**, p. 671.
- (2) OTAKE, T.: 'Calculation of Electrostatic Capacities of Long, Straight Cylinders with some Geometrical Cross-Sections', *Kyushu University College of Engineering Memoirs*, 1913, **1**, p. 31.
- (3) MOULLIN, E. B.: 'On the Current Induced in a Conducting Ribbon by a Current Filament Parallel to it', *Proceedings I.E.E.*, Monograph No. 71, August, 1953 (**101**, Part IV, p. 7).
- (4) SCHELKUNOFF, S. A.: 'Advanced Antenna Theory' (John Wiley and Sons, New York, 1952), p. 181.

(9) APPENDICES

(9.1) Formulae for Calculating Radiation Patterns by the Induced-Current Method

In the method described in Section 4.1 the current distribution induced on a mast face by a filament or a line doublet is assumed to be the same as that which would have been induced had the face formed part of an infinite plane. The field due to the current on the face is then obtained by integrating over the width of the face and is added to the field due to the radiating element itself.

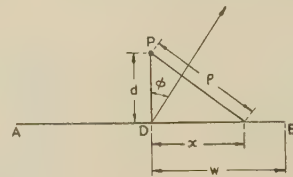


Fig. 10.—A current filament parallel to a conducting strip.

The field at a distant point radiated by the current induced on a strip AB (Fig. 10) by a current filament at P carrying a current I is

$$E_z = K \int_A^B J_z e^{j\beta x \sin \phi} dx \quad (1)$$

where K is a constant and J_z is the surface current density, given by

$$J_z = j \frac{\pi I}{\lambda} \frac{d}{\rho} H_1^{(2)}(\beta \rho)$$

The phase of the field is referred to the point D. This integral cannot be solved analytically. A numerical integration must be performed for each value of ϕ , but the actual process of integration need only be performed within a range of 90° because the function is symmetrical. If the integration is carried out graphically the same curves may be used if the width of the strip or the position of the filament changes, provided that the spacing d remains unaltered; only the limits are changed.

The field due to the filament itself referred to the point D is $K I e^{j\beta d \cos \phi}$; the total field is the sum of the two fields. In the region $90^\circ < \phi < 270^\circ$ the two fields tend to cancel, giving a small residual field in the backward direction.

This method will now be extended to the case in which the radiating element is a line doublet. If the moment of the doublet is M per unit length the surface current density is

$$J_x = j \frac{\pi M}{\lambda} \frac{d}{\rho} H_1^{(2)}(\beta \rho) \quad (2)$$

and the field radiated by the current induced in the strip is

$$E_\phi = K \cos \phi \int_A^B J_x e^{j\beta x \sin \phi} dx \quad (3)$$

This integral is identical with the previous result for a filament, since $J_x/M = J_z/I$. The field due to the doublet itself is $M \cos \phi e^{j\beta d \cos \phi}$. It will therefore be seen that the radiation pattern of a doublet and a strip may be derived from the corresponding pattern for a filament and a strip simply by multiplying by $\cos \phi$.

If AD and DB (Fig. 10) are greater than $3\lambda/4$, and if PD is less than $\lambda/4$, the radiation pattern may be calculated by an approximate method. When these conditions are satisfied, x and ρ are approximately equal in all parts of the plane outside AB and the asymptotic form of the Hankel function may also be used. The integral can then be solved between any limits which do not include the strip AB. Thus, if the radiating element is near a whole-plane, the contribution to the total field which is due to the currents induced on those parts of the plane outside AB may be calculated separately. If this contribution is subtracted from the total field the remainder is equal to the field which would be set up by the element in the presence of the strip AB; when the radiating element is a filament this is therefore equal to

$$j2KI \sin(\beta d \cos \phi) - E_{z1} - E_{z2} \quad (4)$$

where

$$E_{z1} = K \int_{-\infty}^A J_z e^{j\beta x \sin \phi} dx$$

and

$$E_{z2} = K \int_B^{\infty} J_z e^{j\beta x \sin \phi} dx$$

since the current distribution is given approximately by

$$J_z \simeq -\epsilon^{j\pi/4} \frac{d}{\lambda} I \beta \sqrt{(2\pi)} \frac{e^{-j\beta x}}{(\beta x)^{3/2}} \quad (5)$$

the field radiated by the currents on the part of the plane beyond B is

$$E_{z2} \simeq -K \epsilon^{j\pi/4} \frac{d}{\lambda} I \beta \sqrt{(2\pi)} \int_w^{\infty} \frac{e^{-j\beta x(1-\sin \phi)}}{(\beta x)^{3/2}} dx \quad (6)$$

where DB = w

Making the substitution $t = \beta x(1 - \sin \phi)$ gives

$$E_{z2} \simeq -K \epsilon^{j\pi/4} \frac{d}{\lambda} I \sqrt{[2\pi(1 - \sin \phi)]} \int_v^{\infty} \frac{e^{-jt}}{t\sqrt{t}} dt \quad (7)$$

where $v = \beta w(1 - \sin \phi)$

$$\int \frac{e^{-jt}}{t\sqrt{t}} dt = -2 \left[\frac{e^{-jt}}{\sqrt{t}} + j\sqrt{(2\pi)} \int \frac{e^{-jt}}{\sqrt{(2\pi t)}} dt \right] \quad (8)$$

$$\begin{aligned} \int_v^{\infty} \frac{e^{-jt}}{t\sqrt{t}} dt &= 2 \left[\frac{e^{-jv}}{\sqrt{v}} - j\sqrt{(2\pi)} \int_v^{\infty} \frac{e^{-jt}}{\sqrt{(2\pi t)}} dt \right] \\ &= 2 \left\{ \frac{e^{-jv}}{\sqrt{v}} - j\sqrt{(2\pi)} \left[\frac{1}{2} - j\frac{1}{2} - C(v) + jS(v) \right] \right\} \quad (9) \end{aligned}$$

where $C(v)$ and $S(v)$ are Fresnel's integrals, defined in the form*

$$C(v) - jS(v) = \int_0^v \frac{e^{-jt}}{\sqrt{(2\pi t)}} dt \quad (10)$$

* or a Table of Fresnel's integrals in this form see 'Tables of Functions' by Jahnke and Emde, p. 35.

The field due to the currents in the part of the plane beyond B is therefore

$$E_{z2} \simeq K \epsilon^{j\pi/4} \frac{2d}{\lambda} I \left\{ -\sqrt{\frac{\lambda}{w}} e^{-jv} + j2\pi\sqrt{(1 - \sin \phi)} \left[\frac{1}{2} - j\frac{1}{2} - C(v) + jS(v) \right] \right\} \quad (11)$$

E_{z1} may be evaluated in a similar way.

(9.2) Schelkunoff's Formulae for Diffraction at a Wedge

Schelkunoff gives two formulae⁴ in the form of infinite series for the field at a point P [Fig. 11(a)] due to a current filament F

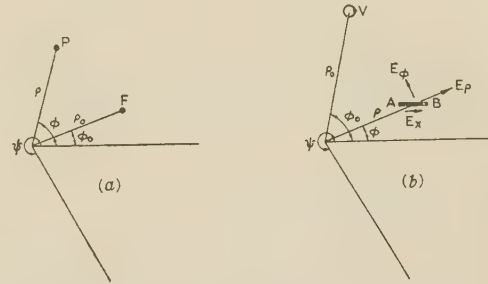


Fig. 11.—Radiating elements parallel to a conducting wedge.

(a) An electric current filament.
(b) A magnetic current filament.

near a wedge of external angle ψ . These two formulae are identical if ρ is equal to ρ_0 . When ρ is not equal to ρ_0 one series diverges and cannot be used, but the other converges. If P is a distant point, ρ is greater than ρ_0 and the convergent series is then the expression for $E_z^+(\rho, \phi)$, which is

$$E_z^+(\rho, \phi) = -\frac{\pi\beta\eta I}{\psi} \sum_{m=1}^{\infty} J_v(\beta\rho_0) H_v^{(2)}(\beta\rho) \sin v\phi_0 \sin v\phi \quad (12)$$

where $v = m\pi/\psi$, η is the intrinsic impedance of the medium surrounding the wedge and I is the filament current.

In the present case we are only concerned with the field at a distant point, and for this the asymptotic form of the Hankel function may be used. Thus as $\rho \rightarrow \infty$

$$H_v^{(2)}(\beta\rho) \rightarrow \sqrt{\frac{2}{\pi\beta\rho}} e^{-j(\beta\rho - \pi/4 - v\pi/2)} \quad (13)$$

The factor $-\frac{\beta\eta I}{2} \sqrt{\frac{2}{\pi\beta\rho}} e^{-j(\beta\rho - \pi/4)}$, which does not involve ϕ , may be neglected. The field at a large constant radius from the apex of the wedge is therefore proportional to

$$\frac{2\pi}{\psi} \sum_{m=1}^{\infty} J_v(\beta\rho_0) e^{jv\pi/2} \sin v\phi_0 \sin v\phi \quad (14)$$

The amplitude of the field given by this expression is such that, if the wedge were removed, the field radiated by the filament would be of magnitude one-half in all directions. The phase term indicates the variation in the phase of the field at a large constant radius from the apex of the wedge.

The corresponding formula for a line doublet and a wedge is not given by Schelkunoff, but it may be derived from his expression for the field produced by a magnetic current filament (a source of cylindrical waves with the magnetic vector parallel to its length).

Fig. 11(b) shows a wedge, a magnetic current filament V and a non-radiating doublet AB. The electric field at the doublet

may be defined by E_ρ and E_ϕ ; the field in the direction AB is then $E_x = E_\rho \cos \phi - E_\phi \sin \phi$. This will vary as V moves round the wedge, and the current induced in the doublet will vary accordingly.

If the principle of reciprocity is applied, this variation of E_x will also describe the variation in the current induced in a receiving loop aerial placed at the position of V if the doublet is driven. If ρ_0 is then made sufficiently large the electric intensity at the loop will be perpendicular to the line joining it to the apex of the wedge and the variation of E_x will describe the far-field radiation pattern.

By expressing Maxwell's equation $E = (1/j\omega\epsilon) \text{curl } H$ in polar form we obtain

$$E_\rho = \frac{1}{j\omega\epsilon\rho} \frac{\partial H_z}{\partial \phi}, \quad E_\phi = \frac{j}{\omega\epsilon} \frac{\partial H_z}{\partial \rho} \quad (15)$$

where H_z is the magnetic field parallel to the length of the magnetic current filament. Since $\rho_0 > \rho$, Schelkunoff's expression for $H_z^-(\rho, \phi)$ must be used; this is

$$H_z^-(\rho, \phi) = -\frac{\pi\beta V}{2j\eta} \left[H_0^{(2)}(\beta\rho_0) J_0(\beta\rho) + 2 \sum_{m=1}^{\infty} H_v^{(2)}(\beta\rho_0) J_v(\beta\rho) \cos v\phi_0 \cos v\phi \right] \quad (16)$$

where $v = m\pi/\psi$ and V is the magnetic displacement current.

Now when $\rho_0 \rightarrow \infty$

$$H_0^{(2)}(\beta\rho_0) \rightarrow \sqrt{\frac{2}{\pi\beta\rho_0}} \epsilon^{-j(\beta\rho_0 - \pi/4)}$$

$$H_v^{(2)}(\beta\rho_0) \rightarrow \sqrt{\frac{2}{\pi\beta\rho_0}} \epsilon^{-j(\beta\rho_0 - \pi/4 - v\pi/2)}$$

Neglecting the common phase term $\epsilon^{-j(\beta\rho_0 - \pi/4)}$ and denoting the constants outside the brackets by κ we have

$$H_z = \kappa \left[J_0(\beta\rho) + 2 \sum_{m=1}^{\infty} \epsilon^{jv\pi/2} J_v(\beta\rho) \cos v\phi_0 \cos v\phi \right] \quad (17)$$

Then

$$E_\rho = \frac{1}{j\omega\epsilon\rho} \frac{\partial H_z}{\partial \phi} = \frac{-2\kappa}{j\omega\epsilon\rho} \sum_{m=1}^{\infty} \epsilon^{jv\pi/2} v J_v(\beta\rho) \cos v\phi_0 \sin v\phi$$

$$= \frac{-\kappa\beta}{j\omega\epsilon} \sum_{m=1}^{\infty} \epsilon^{jv\pi/2} \frac{2v}{\beta\rho} J_v(\beta\rho) \cos v\phi_0 \sin v\phi$$

$$= \frac{j\kappa\beta}{\omega\epsilon} \sum_{m=1}^{\infty} \epsilon^{jv\pi/2} [J_{v-1}(\beta\rho) + J_{v+1}(\beta\rho)] \cos v\phi_0 \sin v\phi \quad (18)$$

Also

$$E_\phi = \frac{j}{\omega\epsilon} \frac{\partial H_z}{\partial \rho} = \frac{j\kappa\beta}{\omega\epsilon} \left[J_0'(\beta\rho) + 2 \sum_{m=1}^{\infty} \epsilon^{jv\pi/2} J_v'(\beta\rho) \cos v\phi_0 \cos v\phi \right]$$

$$= \frac{j\kappa\beta}{\omega\epsilon} \left\{ -J_1(\beta\rho) + \sum_{m=1}^{\infty} \epsilon^{jv\pi/2} [J_{v-1}(\beta\rho) - J_{v+1}(\beta\rho)] \cos v\phi_0 \cos v\phi \right\} \quad (19)$$

Substituting these values in the expression

$$E_x = E_\rho \cos \phi - E_\phi \sin \phi$$

we obtain the electric field in the direction AB at the doublet rearranging it may be shown that

$$E_x = \frac{j\kappa\beta}{\omega\epsilon} \left\{ J_1(\beta\rho) \sin \phi + \sum_{m=1}^{\infty} \epsilon^{jv\pi/2} [J_{v-1}(\beta\rho) \sin(v-1)\phi + J_{v+1}(\beta\rho) \sin(v+1)\phi] \cos v\phi_0 \right\} \quad (20)$$

Thus, when the doublet radiates, the electric field E_ϕ at a large constant radius from the apex of the wedge is proportional to

$$\frac{2\pi}{\psi} \left\{ J_1(\beta\rho) \sin \phi + \sum_{m=1}^{\infty} \epsilon^{jv\pi/2} [J_{v-1}(\beta\rho) \sin(v-1)\phi + J_{v+1}(\beta\rho) \sin(v+1)\phi] \cos v\phi_0 \right\} \quad (21)$$

The amplitude of the field given by this expression is such that if the wedge were removed, the maximum field radiated by the doublet would be of magnitude one-half. The phase term indicates the variation in the phase of the field at a large constant radius from the apex of the wedge.

SIMULTANEOUS VARIATION OF AMPLITUDE AND PHASE OF GAUSSIAN NOISE, WITH APPLICATIONS TO IONOSPHERIC FORWARD-SCATTER SIGNALS

By T. HAGFORS, Siv.Ing., and B. LANDMARK, Dr.Phil.

(The paper was first received 25th April, and in revised form 5th August, 1958.)

SUMMARY

The conditional probability density $p(\phi/A)$ is obtained for Gaussian noise, where $\phi = \Psi_2 - \Psi_1$ is the difference in phase as observed at the two times t and $t + \tau$ and A the envelope at either t or $t + \tau$. The mean of $|\phi|$ subject to the condition of a particular value of A is evaluated using numerical methods, and the variation of $|\phi|_A$ with A is discussed. A simple relation is obtained for the limiting case when $\tau \rightarrow 0$.

The noise character of the signal in an ionospheric scatter circuit has been tested. It is concluded that the simultaneous variations of signal amplitude and phase are in good agreement with those to be expected for Gaussian noise, and also that the assumption of a randomly phased angular spectrum appears to be justified.

LIST OF SYMBOLS

- ϕ = Phase difference.
- Ψ = Phase angle.
- A = Signal amplitude.
- ρ = Correlation function.
- τ = Time difference.
- ξ = Aerial separation measured, wavelengths.
- v = Mean phase angle.
- f = Frequency.
- $\Delta\omega$ = R.M.S. angular frequency deviation.
- α = Off-path angle.
- S = $\sin \alpha$.
- $w(f)$ = Power (frequency) spectrum.
- $|F(S)|^2$ = Angular power spectrum.
- P_0 = Total noise power.
- μ_{13} = Cosine-Fourier transform of $w(f)$.
- μ_{14} = Sine-Fourier transform of $w(f)$.
- $R = \sqrt{(\mu_{13}^2 + \mu_{14}^2)/P_0}$.
- $p(x)$ = Probability density of x .
- $p(x/z)$ = Probability density of x for given values of z .
- $p(x, z)$ = Probability density of x and z .

(1) INTRODUCTION

The weak signals which are received at very high frequencies over distances of 1000–2000 km by ionospheric forward scattering have been extensively studied during the last few years. It is now well known that the signal consists of a discontinuous first component due to specular reflections from meteor trails, and a continuous Rayleigh fading component, the origin of which is still under debate. The noise properties of the signal are usually tested by examining whether the envelope of the signal conforms to a Rayleigh distribution. Generally it is thought, however, that this test is not very satisfactory in that signals other than those of a Gaussian noise type might well have Rayleigh envelope distribution.

It is the purpose of the paper to deduce some properties of Gaussian noise in which both the phase and amplitude of the signal are involved, and to apply these results to test the noise character of an ionospheric scatter signal.

Rice in his papers on random noise¹ has shown how a large class of properties of the noise can be derived from a knowledge of the power spectrum. In particular, it is stressed that a Fourier relationship exists between the power spectrum $w(f)$ and the correlation function $\rho(\tau)$.

A number of workers have applied noise theory to diffraction problems associated with ionospheric propagation, and a summary of this work has been given by Ratcliffe.² Plane waves which are incident on a one-dimensional screen imposing random variation in phase and amplitude are shown to be spread out in a cone of waves. The diffracted waves may be described in terms of an angular (complex) spectrum $F(S)$. A Fourier relationship connects $|F(S)|^2$ and the autocorrelation function $\rho(\xi)$, where ξ is the spacing (measured in wavelengths parallel to the screen) between the points at which the signal is observed. If, in particular, the diffracted waves can be considered as originating in a large number of independent scattering elements, the angular spectrum must become 'randomly phased', since it is composed of elementary waves of different directions and with random phases. In an analogous way the power spectrum $w(f)$ can be considered as being composed of sinusoidal element waves of different frequencies and with random phases. Under the conditions stated it can therefore be expected that results of the classical noise theory may be applied directly to diffraction phenomena provided that $w(f)$ is replaced by $|F(S)|^2$, and $\rho(\tau)$ by $\rho(\xi)$.

(2) THEORETICAL CONSIDERATIONS

In the calculations given below, all results are derived in the time/frequency domains. The theoretical results are, however, applied to test both the noise characteristics and the assumption of a randomly-phased angular spectrum of an ionospheric forward scatter signal.

In Section 2.1 an expression is derived for the conditional probability density $p(\phi/A)$, where $\phi = \Psi_2 - \Psi_1$, Ψ_2 being the phase at the time $t + \tau$ and Ψ_1 that at t , and where A is the instantaneous signal amplitude either at $t + \tau$ or at t . This result is used in Section 2.2 to calculate $|\phi|$ as a function of amplitude A , and finally in Section 2.3 a limiting operation is performed on $|\phi|_A$ to derive a relation between the mean of the modulus of the rate of change of phase, $|\dot{\Psi}|$, and amplitude A .

(2.1) Derivation of Conditional Probability Density $p(\phi/A)$

Starting with the joint probability density of $A_1 A_2 \Psi_1 \Psi_2$ it can be shown³ that (see also Reference 1):

$$P(A_1, A_2, \phi) = \frac{A_1 A_2}{2\pi B} e^{-\frac{1}{2B}[(A_1^2 + A_2^2)P_0 - 2A_1 A_2 P_0 C]} \quad (1)$$

Written contributions on papers published without being read at meetings are held for consideration with a view to publication.
Hagfors and Mr. Landmark are at the Norwegian Defence Research Establish-

where

$$B = P_0^2 - \mu_{13}^2 - \mu_{14}^2 = P_0^2(1 - R^2)$$

$$C = \mu_{13} \cos \phi + \mu_{14} \sin \phi = R \cos(\phi - \nu)$$

$$\tan \nu = \mu_{14}/\mu_{13}$$

$$P_0 = \int_0^\infty w(f) df$$

$$\mu_{13} = \int_0^\infty w(f) \cos 2\pi(f - f_0)\tau df$$

$$\mu_{14} = \int_0^\infty w(f) \sin 2\pi(f - f_0)\tau df$$

f_0 = Centre frequency of noise spectrum.

The joint probability density of the phase difference ϕ and A_1 is found by integration over A_2 . It should be observed that expression (1) is symmetrical in A_1 and A_2 . Hence $p(A_1, \phi)$ and $p(A_2, \phi)$ must be identical. The subscripts of the A 's are therefore omitted, and in what follows it is understood that A means the amplitude either at the beginning or at the end of the interval τ .

The integration can be carried out in a straightforward manner, giving

$$p(\phi, A) = \frac{A}{2\pi P_0} e^{-\frac{P_0 A^2}{2B}} \left\{ 1 + \sqrt{(2\pi)U} e^{U^2/2} [0.5 \pm \operatorname{erf}(U)] \right\} \begin{matrix} U > 0 \\ U < 0 \end{matrix} \quad (2)$$

$$\text{where } U = T \cos(\phi - \nu) = \frac{A}{\sqrt{P_0}} \frac{R}{\sqrt{(1 - R^2)}} \cos(\phi - \nu)$$

$$\operatorname{erf}(U) = \frac{1}{\sqrt{(2\pi)}} \int_0^U e^{-x^2/2} dx$$

It is well known that the amplitude A is Rayleigh distributed, and hence

$$p(\phi/A) = \frac{p(\phi, A)}{p(A)} = \frac{1}{2\pi} e^{-T^2/2} \left\{ 1 + \frac{U[0.5 \pm \operatorname{erf}(U)]}{\frac{1}{\sqrt{(2\pi)}} e^{-U^2/2}} \right\} \begin{matrix} U > 0 \\ U < 0 \end{matrix} \quad (3)$$

with the notations as above. This density function is plotted in Fig. 1 for $\nu = 0$ with $T = (A/\sqrt{R_0})[R/\sqrt{(1 - R^2)}]$ as para-

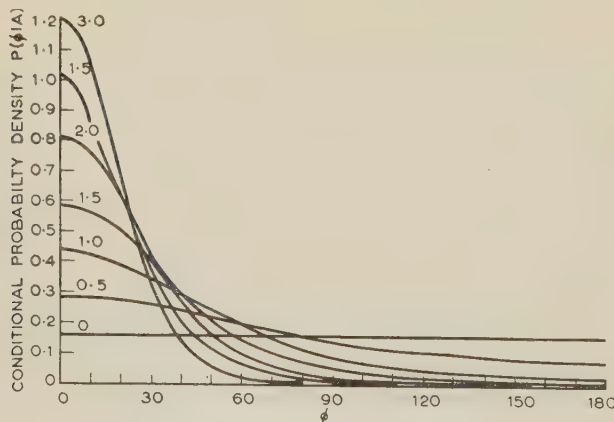


Fig. 1.—Conditional probability density of the phase difference ϕ for prescribed values of amplitude A .

$$\text{Parameter } T = \frac{A}{\sqrt{P_0}} \frac{R}{\sqrt{(1 - R^2)}}$$

meter. Other values of ν only shift the position of the maximum of the function, but this does not change the form of the distribution.

(2.2) Evaluation of $|\phi|_A$

The mean of $|\phi|$ subject to the condition of a particular value of A , again assuming $\nu = 0$, is given by

$$|\phi|_A = 2 \int_0^\pi \phi p(\phi/A) d\phi \quad (4)$$

It appears difficult to give the results by an analytical expression and numerical methods were resorted to. $|\phi|$ was first found for a set of values of T , which is actually the only parameter. The result is shown in Fig. 2, which is a plot of $|\phi|$ versus T .

The information obtained in Fig. 2 can be employed to

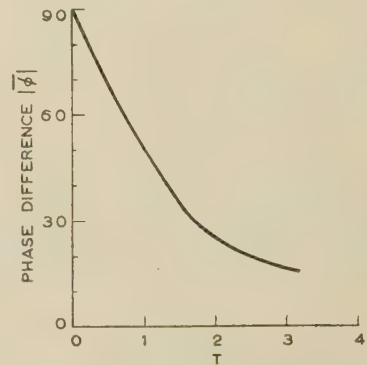


Fig. 2.—Mean of the modulus of phase difference ϕ plotted against T

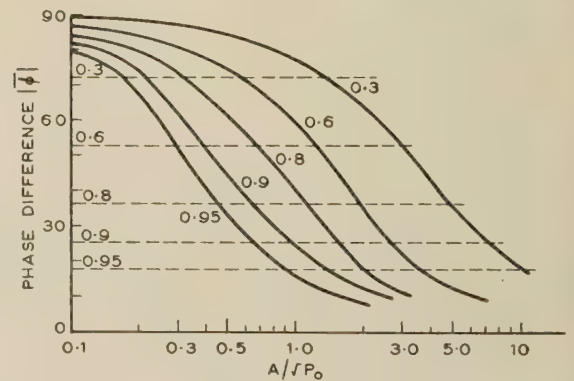


Fig. 3.—Mean of the modulus of phase difference ϕ plotted against $A/\sqrt{P_0}$ with R as parameter.

determine $|\phi|_A$ as a function of $A/\sqrt{P_0}$ with R as parameter. The interrelation between $|\phi|_A$ and $A/\sqrt{P_0}$ is shown in Fig. 3 for a set of values of the correlation R . It is observed that small phase differences can be expected at high amplitude levels and vice versa. The dotted horizontal lines in Fig. 3 give the value of $|\phi|$ disregarding the value of A (i.e. $|\phi| = \arccos R$).

(2.3) Derivation of a Relation Between $|\Psi|$ and A

When the time separation τ between the points at which the phase and amplitude are observed becomes very small, it is evident that

$$\frac{\phi}{\tau} \rightarrow \frac{d\Psi}{dt} = \dot{\Psi}$$

and that $A_1 \simeq A_2 = A$. As τ tends to zero, the quantity $|\phi|$ tends to unity, and eqn. (3) reduces to

$$p(\phi/A) \rightarrow \frac{U}{\sqrt{(2\pi)}} e^{-\frac{1}{2}(T^2 - U^2)} \quad (5)$$

furthermore

$$T \rightarrow \frac{A}{\sqrt{P_0}} \frac{1}{\Delta\omega\tau}$$

where

$$(\Delta\omega)^2 = \frac{1}{P_0} \int_0^\infty (\omega - \omega_0)^2 w(f) df$$

$$p(\phi/A) \rightarrow \frac{1}{\sqrt{(2\pi)}} \frac{A}{\sqrt{P_0}} \frac{\cos \phi}{\Delta\omega\tau} e^{-\frac{1}{2} \frac{A^2}{P_0} \frac{1}{(\Delta\omega\tau)^2} \sin^2 \phi} \quad (6)$$

now $|\overline{\phi}|_A$ is evaluated with this form of $p(\phi/A)$, one obtains

$$\frac{|\overline{\phi}|_A}{\tau} = \Delta\omega \sqrt{\frac{2}{\pi}} \frac{\sqrt{P_0}}{A}$$

and accordingly in the limit as $\tau \rightarrow 0$

$$\frac{A}{\sqrt{P_0}} |\overline{\Psi}| = \Delta\omega \sqrt{\frac{2}{\pi}}$$

this result can also be found directly from a knowledge of (A, Ψ) .

(3) OBSERVATIONAL RESULTS

This result of Section 2 will now be applied to test both the noise characteristics of the signal in an ionospheric scatter circuit and the assumption of a randomly-phased angular spectrum. The transmitter for the scatter circuit is located at Tromsø (70°N, 19°E) and the receiver station is at Kjeller (60°N, 11°E), the path being 1180 km. The transmitted power was 4 kW and a frequency of 46.8 Mc/s was used. A rhombic aerial of 15° between half-power points was used at the transmitter, and Yagi aerials of 66° between half-power points at the receiver station. The maximum sensitivity of all polar diagrams was at an elevation of 6°.

(3.1) The Relation Between A and $|\overline{\Psi}|$

In order to observe variations of amplitude and phase with time, the two quadrature components of the scatter signal were obtained in the following way: The signal was mixed with two local-oscillator signals having a phase difference of 90°, and the resulting signals were recorded by a twin-channel pen recorder. A typical record sample showing the two signal components is given in Fig. 4.

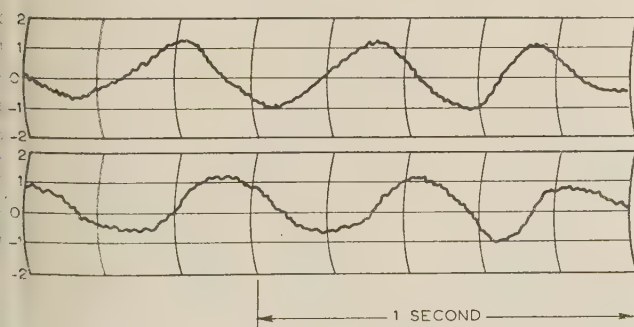


Fig. 4.—Sample from the record of the two quadrature components of the scatter signal obtained on 10th January, 1958, at 1210 hours M.E.T.

It was observed that during short time intervals (of the order 10–20 sec) the rate of change of phase, Ψ , varied round a mean value. In interpreting the observed variations of phase, it is assumed that this mean phase drift is due to imperfection of the equipment, and that the irregular variations round the mean are due to actual variations of signal phase. This assumption has been checked using a local test transmitter.

In Section 2.3 it was shown that the relation between A and $|\overline{\Psi}|$ for a Gaussian noise signal is

$$\frac{A}{\sqrt{P_0}} |\overline{\Psi}| = \Delta\omega \sqrt{\frac{2}{\pi}}$$

This relationship was applied to test the noise character of the observed signal. Five record samples obtained at different times were analysed. For each of the samples, $|\overline{\Psi}|$ was obtained for different amplitude levels, and $\Delta\omega$ was deduced from the readings at all levels. The observed values of $|\overline{\Psi}|$ divided by $\Delta\omega\sqrt{2/\pi}$ were then plotted against $A/\sqrt{P_0}$ on log-log paper. The results are given and compared with the theoretical line in

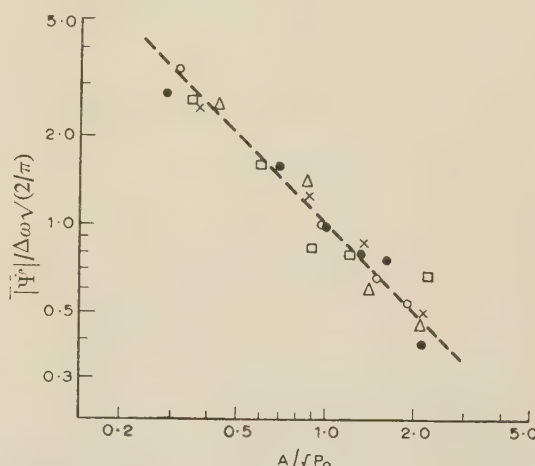


Fig. 5.— $|\overline{\Psi}|/\Delta\omega\sqrt{2/\pi}$ plotted against $A/\sqrt{P_0}$ for five different record samples.

- × 21st January, 1957 1625 hours M.E.T.
- 3rd January, 1958. 1410 hours M.E.T.
- △ 9th January, 1958. 1110 hours M.E.T.
- 10th January, 1958. 1210 hours M.E.T.
- 21st January, 1958. 1450 hours M.E.T.

Fig. 5. We see that there is a reasonable agreement between the observed values and the theoretical line.

The values deduced for $\Delta\omega$ for the five different samples are listed in Table 1.

Table 1
WIDTH OF THE SPECTRUM OF THE SCATTER SIGNAL

Date	Time of day	Duration	$\Delta f = \Delta\omega/2\pi$
	hours M.E.T.	sec.	c/s
21.1.57	1625	20	1.6
3.1.58	1415	25	0.8
9.1.58	1110	15	1.1
10.1.58	1210	15	1.0
21.1.58	1450	20	1.5

(3.2) Observation of Differential Phase on Spaced Aerials

The scatter signal was received on two aerials at a spacing of two wavelengths perpendicular to the great-circle path between Kjeller and Tromsø. Equipment⁴ was available for the measurement of the instantaneous phase difference between the two signals. The instantaneous phase difference and the signal envelope at one of the aerials were recorded on a twin-channel pen recorder. A sample from one of the records is shown in Fig. 6.

The theoretical results derived in Section 2 can now be

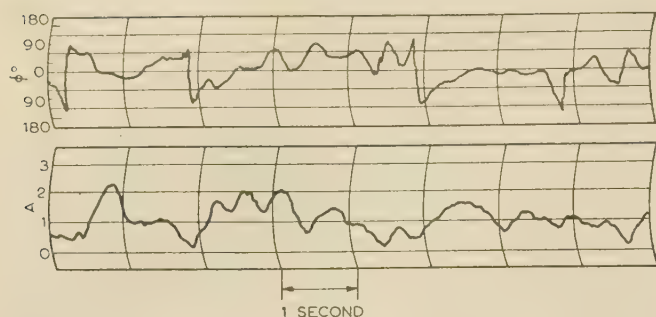


Fig. 6.—Sample from record of amplitude and differential phase on spaced aerials obtained 6th December, 1957, at 2310 hours, M.E.T.

applied to the analysis of this type of record, provided, as described in Section 1, the following reinterpretations are made:

$$\mu_{13} = \int_{-\infty}^{+\infty} |F(S)|^2 \cos 2\pi\xi S dS$$

$$\mu_{14} = \int_{-\infty}^{+\infty} |F(S)|^2 \sin 2\pi\xi S dS$$

where

$S = \sin \alpha$

α = Angle between direction of great-circle path and direction of elementary wave

ξ = Aerial separation, wavelengths.

Four samples were selected from records showing a steady, fading background signal. From the envelope channel the value of P_0 was determined, and a set of values of $A/\sqrt{P_0}$ was selected. $|\phi|$ was then determined for each level, and a plot of $|\phi|_A$ versus $A/\sqrt{P_0}$ could be made. In Fig. 7 an example of

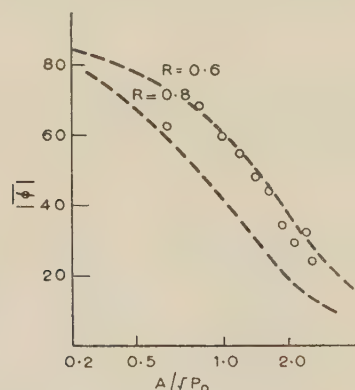


Fig. 7.—Determination of R for sample 2 of Fig. 8.

Plot of $|\phi|_A$ against $A/\sqrt{P_0}$.

such a plot is shown and compared with the theoretical curves of Fig. 2. In each of the four samples analysed there was a close agreement between the observed values and the theoretical results. From plots of the type of Fig. 7 the value of R could be determined by interpolation, and hence $|\phi|_A$ plotted against $T = (A/\sqrt{P_0})[R/\sqrt{1-R^2}]$. The observed values of $|\phi|_A$ for all four samples were plotted against T in Fig. 8, where the theoretical relation between $|\phi|_A$ and T is shown as a dotted curve. Again the agreement between theory and observations is good. The slight discrepancy at low values of $A/\sqrt{P_0}$ is of instrumental origin, since at low signal levels the signal/noise

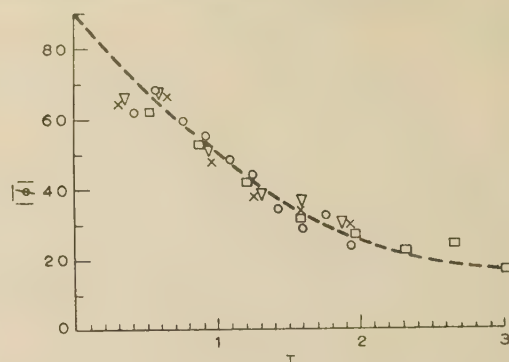


Fig. 8.—Graph of $|\phi|$ plotted against T for four different samples.

× 28th November, 1957. 0823 hours M.E.T.
○ 28th November, 1957. 0952 hours M.E.T.
□ 5th December, 1957. 1214 hours M.E.T.
▽ 6th December, 1957. 2310 hours M.E.T.

ratio was not sufficient for satisfactory operation of the phase meter.

The values of R derived from the four samples are given in Table 2.

Table 2

VALUES OF R OBSERVED WITH AERIAL SPACING OF TWO WAVE LENGTHS ACROSS THE PATH

Date	Time of day	Duration	R
	hours M.E.T.	sec	
28.11.57	0823	66	0.70
28.11.57	0952	32	0.62
5.12.57	1214	38	0.81
6.12.57	2310	85	0.80

(4) SUMMARY OF RESULTS

It has been shown how, for Gaussian noise, a relationship can be found between $|\Psi(t+\tau) - \Psi(t)|$, i.e. the mean of the modulus of the phase difference over a time interval τ , and the amplitude $A(t+\tau)$ or $A(t)$. From this result a relation between $|\Psi|$, i.e. the mean of the modulus of the rate of change of phase $\Psi'(t)$ and the amplitude $A(t)$ was derived.

A signal received over an ionospheric forward scatter circuit was analysed. It was found that the scatter signal possessed characteristics similar to those of Gaussian noise, and the width of the power spectrum Δf was reduced for five different samples.

The theory was also applied to test some spatial properties of the scatter signal from observations of differential phase or spaced aerials. It was found that the angular spectrum of received elementary waves appeared to be randomly phased, as one would expect of a signal originating in a large number of independent scattering elements. It was also shown for four samples how the correlation between the two signals could be evaluated from the combined amplitude and differential phase records.

(5) ACKNOWLEDGMENTS

The work reported in the paper is part of a research project sponsored by the Mutual Weapons Development Programme. The authors are indebted to their colleagues at the Norwegian National Defence Research Establishment for helpful co-operation, and, in particular, to Mr. K. Endresen, who designed the equipment used in the observations.

(6) REFERENCES

- (1) RICE, S. O.: 'Mathematical Analysis of Random Noise', *Bell System Technical Journal*, 1944, **23**, p. 282, and 1945, **24**, p. 46.
- (2) RATCLIFFE, J. A.: 'Some Aspects of Diffraction Theory and their Application to the Ionosphere', *Reports on Progress in Physics*, 1956, **19**, p. 188.
- (3) BRAMLEY, E. N.: 'Diversity Effects in Spaced-Aerial Reception of Ionospheric Waves', *Proceedings I.E.E.*, Paper No. 1062 R, January, 1951 (**98**, Part III, p. 19).
- (4) ENDRESEN, K., HAGFORS, T., LANDMARK, B., and RÖDSRUD, J.: 'Observations of Angle of Arrival of Meteor Echoes in V.H.F. Forward Scatter Propagation', *Journal of Atmospheric and Terrestrial Physics*, 1958, **12**, p. 329.

DISCUSSION ON

'A TRANSISTOR HIGH-GAIN CHOPPER-TYPE D.C. AMPLIFIER'*

NORTH-EASTERN RADIO AND MEASUREMENT GROUP AT NEWCASTLE UPON TYNE, 17TH MARCH, 1958

Mr. P. J. Price: The chopper amplifier described uses a blocking oscillator to supply the switching waveform by means of a transformer. It is possible, however, to generate these waveforms in a multivibrator, and to dispense with the transformer. Since the extra drift introduced by slight changes of frequency and mark/space ratio appears to be only a second-order effect, it would appear to be economical to make this change. Had the authors some particular reason for using their system?

The delay circuit shown in Fig. 12(c) is so interesting that I should like the authors to explain its mode of action in more detail, especially the apparent regenerative flick back to -15 volts.

The system suggested in Section 8.2 of correcting a wide-band amplifier for drift by means of a chopper amplifier is at present under investigation for use in a proposed transistor analogue computer at King's College, Newcastle. It has been found that, if the d.c. stabilizing loop is removed from the wide-band amplifier as suggested, the output still drifts considerably when the system is used for integration. Owing to the low input impedance of the transistor amplifier, the drift of the output voltage is approximately $i_d Z_f$, where i_d is the drift current of the chopper amplifier referred back to the input; when Z_f is capacitive, this is unfortunately large. However, the rate of drift appears to be a function of the overall gain of the two amplifiers, which may be several million. Good correction may thus be obtained if the d.c. stabilization is left on the wide-band amplifier, and the overall d.c. gain is reduced to, say, 10000. With the rate of drift reduced the system virtually becomes an open-loop drift-free amplifier and not an integrator to very low frequencies. The above remarks are, of course, true only if the system is also arranged so that there is no positive feedback round the drift-free amplifier.

Dr. G. B. B. Chaplin and Mr. A. R. Owens (in reply): The use

of a blocking oscillator for waveform generation is mainly a matter of convenience, since waveforms of any required amplitude, polarity and d.c. level may be obtained using suitable secondary windings on the transformer. This is not always easily done with multivibrator circuits. In addition, the use of a transformer replaces a transistor which is rather more expensive.

The delay circuit shown in Fig. 12(c) is bottomed during the 'off' period of the blocking oscillator, hold-on bias to the base of J_{10} being applied from the $+10$ -volt line through R_{25} and D_6 . Approximately 5 mA flows in this path, since the emitter is returned to $+15$ volts. When the blocking oscillator is switched on, D_6 is cut off by the 5-volt positive pulse applied to its cathode through R_{25} , removing the hold-on bias from the base, and effectively substituting a turn-off current of 0.3 mA from the $+18$ -volt line through R_{24} . This causes the collector potential of J_{10} to fall from $+15$ volts, its rate being defined by C_6 , which acts as a Miller capacitance. However, when the collector potential has fallen to $+10$ volts, diode D_7 conducts and prevents any further negative movement of the lower plate potential of C_6 , and the Miller feedback removed the collector potential falls rapidly to a level where the output chopper, J_8 , becomes actuated. The effect of the slow Miller rundown for the first 5 volts of the fall of collector potential is to delay the actuation of J_8 by 30 microsec.

At the end of the clamped period the blocking-oscillator pulse collapses and 5 mA again flows out of the base of J_{10} through D_6 . The effect of this is to cause the collector potential of J_{10} to rise towards $+15$ volts. The last 5 volts of this rise is retarded slightly by the action of C_6 , which provides Miller feedback when the collector potential is above $+10$ volts. However, the base is now 5 mA, compared to 0.3 mA which flows during the first delay period, and so the retardation of the rise is only $0.3/5 \times 30 = 2$ microsec.

The results quoted by Mr. Price for the chopper-corrected amplifier are very encouraging.

* CHAPLIN, G. B. B., and OWENS, A. R.: Paper No. 2442 M, November, 1957 (*ibid.* **105 B**, p. 258).

A TRAIN PERFORMANCE COMPUTER

By Prof. E. BRADSHAW, M.B.E., Ph.D., M.Sc.Tech., Member, M. WAGSTAFF, M.Sc.Tech., Graduate and F. COOKE.

(The paper was first received 19th March, and in revised form 7th August, 1957. It was published in November, 1957, and was read before a joint meeting of the MEASUREMENT AND CONTROL SECTION and the UTILIZATION SECTION 15th April, 1958.)

SUMMARY

The computer employs a 50 c/s computing circuit, with induction-type energy meters as integrators, and gives automatic prediction of speeds, running times, energy consumption and r.m.s. motor current.

Typical studies of train performance are illustrated.

(1) INTRODUCTION

A train is subject, at a given speed and position on the route, to forces which, individually, tend to accelerate or decelerate it. If the accelerating and decelerating forces are regarded as positive and negative, respectively, they include:

Tractive effort, F_T (positive).

Tractive resistance, F_R (negative).

Gradient force, F_G (positive or negative).

Braking force, F_B (negative).

Net tractive force, $F = F_T - F_R \pm F_G - F_B$.

F_T and F_R are primarily functions of speed, F_G is primarily a function of distance and F_B is, to a first approximation, capable of being maintained constant.

Basically, the determination of the dynamic performance of the train consists of finding, continuously, the net accelerating force F acting on a train of effective mass m_e , and thence the acceleration $f = F/m_e$. The speed change from time t_1 to t_2 is

$$v_2 = \int_{t_1}^{t_2} f dt \quad (1)$$

and the corresponding distance travelled in this time is

$$s_2 = \int_{t_1}^{t_2} v dt \quad (2)$$

The problem is essentially the solution of a differential equation of the form

$$\frac{d^2s}{dt^2} + P\left(\frac{ds}{dt}\right) + Q(s) + K = 0 \quad . . . (3)$$

where $P\left(\frac{ds}{dt}\right)$ and $Q(s)$ are functions of speed and position, respectively.

In the absence of any mechanical or electrical computing aids, the solution of eqns. (1) and (2) is normally performed by one of several step-by-step processes. For example, starting from rest, the net tractive effort may be evaluated from known data and position of the train and the time calculated at the end of a speed increment Δv . The new forces are then evaluated for this velocity and position, and increments of time and distance are found for a further speed increment Δv , and so on. These processes are, by their nature, approximations, but, by taking

suitably small increments and recognizing that many of the data are known only to a limited degree of accuracy, the methods give acceptable solutions. Even though the time taken to make such calculations is reduced by various 'short-cut' and graphical artifices, the work is lengthy and tedious.

The problem can clearly be solved by computing devices which provide continuous solutions for eqns. (1) and (2). Several such computers have been constructed,¹⁻⁶ most of which employ mechanical integrators of the ball and disc or wheel and disc types. Varying provision is made in these computers for the automatic insertion of the continuously-changing working forces but, in general, much more manual control is necessary than with the computer described in the paper.

A device to provide a fully automatic solution of train operation under all conditions would be complicated and possibly uneconomic; there are, of necessity, alternatives in the manner in which a given journey can be performed which must be left to judgment, and this calls for some manual control of the computer. It is considered that the need for, and the ability to exercise, such judgment during a run is a factor in favour of a computer of the analogue type (operating at or about real time), rather than one of a digital type, for much of the work to be done in this field. The programming of a digital computer for train-performance problems has been described by Gilmour.⁷ Such a computer can predict the mechanical and electrical performance of a train many times more rapidly than the analogue computer described in this paper.

In addition to train-motion calculations, it is often desirable to evaluate such quantities as energy or fuel consumed, and motor current and heating when an electric drive is employed. This information is derived by additional calculations in the step-by-step method, but provision is made for such quantities to be determined automatically by the present computer.

(2) THE COMPUTER

(2.1) Principle

The computing circuit (Fig. 1) operates at 50 c/s and employs two induction energy meters, M_1 and M_2 , to perform the integrations.

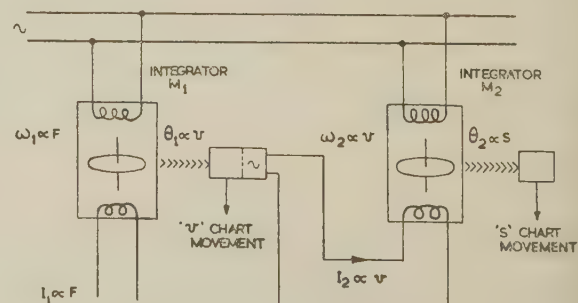


Fig. 1.—Principle of computer.

Prof. Bradshaw is Professor of Electrical Engineering, Manchester College of Science and Technology.

Mr. Cooke is, and Mr. Wagstaff was formerly, at the Manchester College of Science and Technology.

Mr. Wagstaff is now with Ferranti, Ltd.

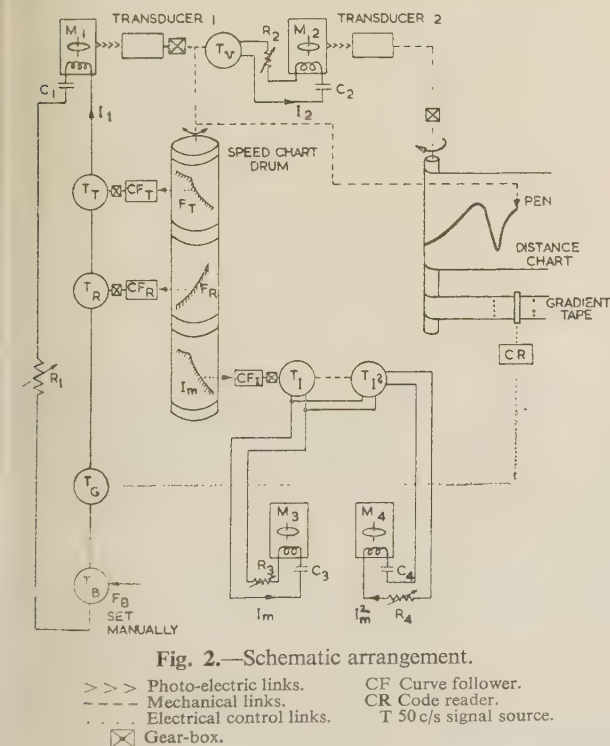
ns $\int f dt$ and $\int v dt$, respectively. They are operated with constant potential difference applied to their voltage coils; their current coils are supplied with currents I_1 and I_2 , such that I_1 is proportional to the net accelerating force F , and I_2 is proportional to the speed of the train v .

Since the angular velocity ω_1 of the disc of M_1 is proportional to the net accelerating force, and therefore to the train acceleration, the angular displacement θ_1 of this disc will be proportional to train speed (or change in speed if the computation is made from a non-zero initial speed). By means of a transducer which does not impose any restraint on the disc of M_1 , the motion of the disc is arranged to control a signal source so that a current proportional to θ_1 is supplied to the integrator M_2 . It also serves to drive a 'speed'-chart table, in the form of a drum, which carries curves of speed-dependent functions used in the computing processes, an angular displacement being proportional to speed. The angular velocity ω_2 of the disc of the integrator M_2 is proportional to speed, and the angular displacement θ_2 of this disc is proportional to the distance travelled by the train.

A transducer similar to that used with M_1 produces a mechanical motion proportional to θ_2 which imparts a displacement, proportional to distance travelled, to 'distance' charts on which distance-dependent information is stored and on which the output speed/distance curves are automatically plotted.

The 50 c/s signals proportional to the various quantities in the equation of motion of the train are produced from sources controlled by function readers, which extract information from curves or punched tape carried on the 'speed'- and 'distance'-chart carriers. The number of speed- and distance-dependent functions which are involved in the dynamic study of the train and in other computations such as motor current and energy losses, determines the number of 'reading' elements in the whole computer.

Fig. 2 shows the schematic arrangement of the computer as



usually employed, including a circuit for the determination of $\int I_m dt$ and $\int I_m^2 dt$, where I_m is the motor current. The net accelerating-force signal at a given speed and position

of the train on the track is produced by four 50 c/s sources in series. Two are variable auto-transformers, T_T and T_R , operated by curve-following units CF_T and CF_R , which rotate the transformer moving contacts through angles proportional to the ordinates of the tractive-effort/velocity and tractive-resistance/velocity curves carried on the cylindrical 'speed'-chart drum; the third is a variable auto-transformer, T_B , set manually to represent a given braking force, and the fourth is a tapped transformer, T_G , with output windings selected by relays controlled via a code reader CR , from coded punched holes in the gradient record carried on the 'distance'-chart table.

The rotation of the disc of M_1 is followed by a photo-electrically operated transducer which performs the following functions:

- It rotates the 'speed'-chart drum.
- It rotates the moving contact of a variable auto-transformer T_V to give $I_2 \propto v$.
- It controls a pen to record velocity on the 'distance' chart and/or on a 'time' chart (the latter is not shown in Fig. 2).

The rotation of the disc of M_2 similarly controls the movement of the 'distance'-chart mechanism.

In addition to the curve followers and signal generators for the mechanical quantities, another curve follower CF_1 operates on a motor current/speed curve on the 'speed'-chart drum. This curve follower controls two mechanically-coupled variable auto-transformers, T_1 and T_2 , so that the first gives a signal proportional to I_m and the second, fed from the first, gives a signal proportional to I_m^2 . Two integrating meters, M_3 and M_4 , with constant potential difference applied to their voltage coils record $\int I_m dt$ and $\int I_m^2 dt$, respectively, for the purpose of computing energy consumption and motor heating when an electric drive is employed.

It is a feature of the computer that most quantities are available both as an electrical equivalent (current or voltage) and a mechanical displacement (shaft rotation, etc.). The computer is also particularly flexible in respect of the number of points at which different ranges and scales may be introduced for operational convenience, by gear ratios and electrical circuit changes.

So far as the authors are aware, no previous use has been made of induction energy meters as integrators in train-performance computers. Their use in other forms of computer has, however, been described by several workers.^{8,9}

(2.2) Circuit and Constructional Details

(2.2.1) Computing Circuits.

The integrators M_1 , M_2 , M_3 and M_4 , are induction energy meters having a disc speed of 1 r.p.s. with an m.m.f. 400 AT in the current coils. These coils, normally wound for a current of 5 amp (= 400 AT), are rewound for a current of 100 mA (= 400 AT), and are made substantially non-reactive by neutralizing the current-coil inductance by series capacitances C_1 – C_4 in order to produce the maximum torque per unit current.

Fig. 3 shows the arrangement of the computing circuits of the four integrators.

In the circuit of M_1 , those signal sources which consist of variable auto-transformers, T_T , T_R and T_B , are provided with 1 : 1 isolating transformers, T_1 , T_2 and T_3 . T_T , T_R and T_G are additionally provided with variable auto-transformers, T'_1 , T'_2 and T'_3 , for scaling. T_G is a transformer with seven isolated secondary sections with voltage outputs in the ratio of 1 : 2 : 4 : 8 : 16 : 32 : 64, which are connected in any desired series combination by sets of relay contacts A_2 , A_3 – G_2 , G_3 . The sign of the resulting combination is controlled by relay contacts P_2 and P_3 . Relays A–G and P are controlled by punched tape carrying the gradient information in a binary-coded form.

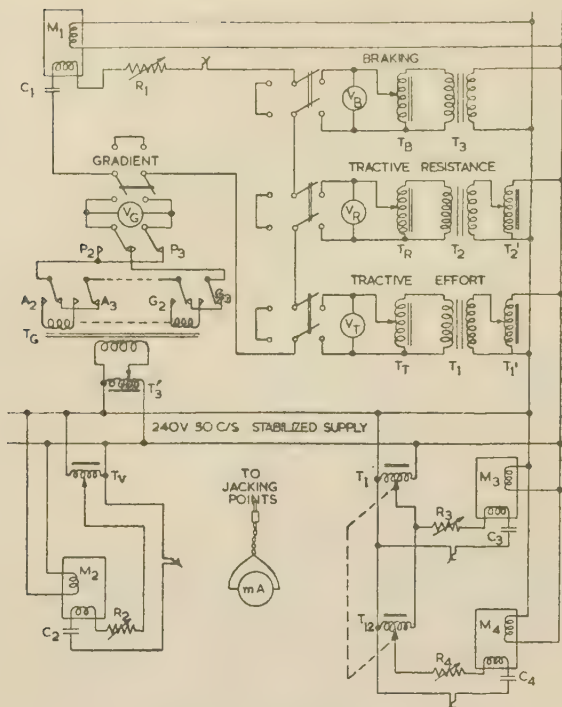


Fig. 3.—Signal circuits.

The signal sources of M_2 , M_3 and M_4 consist simply of variable auto-transformers, T_v , T_1 and T_{12} , respectively.

A precision millimeter can be inserted in a jack into each of the computing circuits for setting-up purposes.

(2.2.2) Curve Followers.

Signals proportional to F_T , F_R and I_m at all speeds are 'read' automatically from curves of these quantities plotted to a base of speed, carried on the 'speed'-chart drum.

A curve-following circuit is shown in Fig. 4A. As the 'speed'-

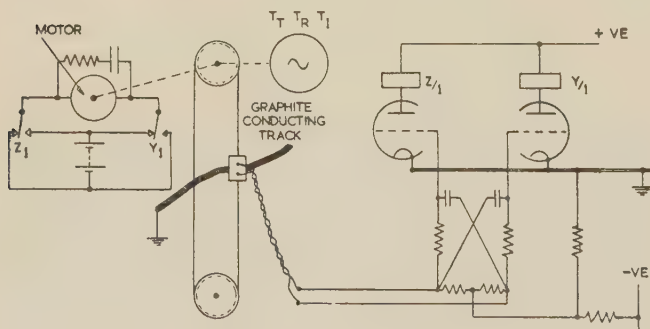


Fig. 4A.—Curve follower.

chart drum rotates the motor is controlled by the relays Y and Z , so that the probe carriage is driven until one probe is just off and one just on the upper edge of the conducting graphite track.

Manual control of the motor is also available for the initial positioning of the probes on one of several curves when alternative operating conditions, such as field-weakening steps, are available.

(2.2.3) Gradient-Record Reader.

The gradient force is a function of distance, and is discontinuous in value and sign. The gradient information is recorded by combinations of holes in eight positions across a 3 in-wide

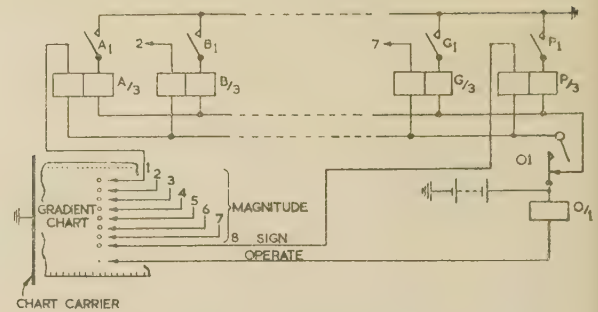


Fig. 4B.—Gradient reader.

tape, which is carried on the 'distance'-chart carrier (Fig. 4B). Holes 1-7 control 'magnitude' relays A-G (see Section 2.2.1) and hole 8 controls the 'sign' relay P. An additional small hole controls the 'operate' relay O after the correct conditions have been established by a combination of holes 1-8. When a particular gradient combination is set up, the operated relay self-holds through the contacts $A_1 \dots P_1$, so that the gradient information is held until the new gradient change occurs.

(2.2.4) Disc-Rotation Transducers.

Two forms of transducer have been used. In the original form of computer, pulses are derived via a photo-electric cell from successive reflecting and non-reflecting sectors on the edge of the integrator disc. These pulses, after shaping, control a uniselector switch via a high-speed relay. In the case of M which is required to operate in both directions, the pulses are routed by a change-over switch, controlled by a phase-sensitive circuit, to one of two uniselectors, the outputs of which are combined by a differential gear [Fig. 5(a)].

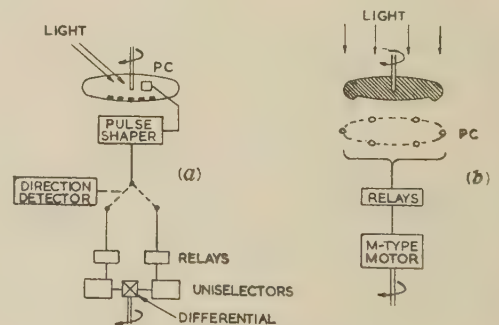


Fig. 5.—Transducer arrangements.

In a later form of computer, a simpler transducer, shown in Fig. 5(b) is used. Here an M -type motor is controlled by relay energized by photocells which are successively illuminated as shown. This form of transducer does not require a separate directional element.

(2.2.5) Physical Arrangement.

The computer is housed in two Post Office racks, between which is a control panel and an output table.

(3) SCALE FACTORS

(3.1) Mechanical Quantities

(3.1.1) Basic Relations.

F, F_T, F_R, F_B and F_G = Operating forces, lb wt.

m = Actual mass of locomotive and train tons.

- m_e = Effective mass of locomotive and train
 = $m \times k$, where k is a rotational inertia factor, commonly about 1.07.
 n_1 = R.P.S. per ampere of M_1 (=10).
 n_2 = R.P.S. per ampere of M_2 (=10).
 i_1 = Current in M_1 per unit F/m_e .
 p_1 = Number of revolutions of M_1 per 1 m.p.h. movement of 'speed' chart.
 p_2 = Number of revolutions of M_2 per 1 in movement of 'distance' chart.
 i_2 = Current in M_2 per 1 m.p.h. movement of 'speed' chart.

The acceleration imparted to a mass m_e by a force F is $0.0098F/m_e$ m.p.h./sec. The scale factors for the computers are given by

Train quantities	Computer equivalents
1 m.p.h./sec	$i_1/0.0098$ amperes
1 m.p.h.	i_2 amperes
1 sec	$0.0098p_1/i_1n_1$ sec
1 mile	$3600r i_2n_2/p_2$ inches on 'distance' chart

where r = ratio of machine time to train time = $0.0098p_1/i_1n_1$.

Although experience has shown that it is convenient to use the machine with $r = 1$ and with 1 in on the chart equivalent to 1 mile on the track, variations of time and distance equivalents over a wide range can be effected for the following reasons:

- (a) i_1 and i_2 can be selected to have any value between an upper limit imposed by the self-heating of the integrator current coils and a lower limit imposed by a loss of integrator accuracy.
 (b) p_1 can be varied by change of gear ratio between M_1 and the 'speed'-chart table and by the choice of the abscissae scale of the 'speed' charts.
 (c) p_2 can be varied by change of gear ratio between M_2 and the 'distance'-chart carrier.

1.2.) Setting-up Procedure.

Let us take, as an example, a 1000-ton train, hauled by a locomotive with a maximum tractive effort of 48000 lb on a route having a maximum gradient of 1 in 70. The tractive resistance is 12 lb/ton at 50 m.p.h. and the maximum braking effort is 0.75 m.p.h./sec. With a rotary inertia factor of 1.08, the values of F/m_e for the various forces are as follows:

Tractive effort	$\frac{48000}{1.08 \times 1000} = 44.4$
Tractive resistance 12/1 = 12	
Braking	$\frac{0.75}{0.0098} = 76.5$

i_1 is therefore determined by the maximum value of F/m_e , i.e. by the braking conditions.

If 76.5 F/m_e units is equivalent to 70 mA, then i_1 equals $0.915 \times 10^{-3}/76.5$, which is 0.915 mA per F/m_e unit.

If the computation is required to be performed in half train time, $r = 0.5 = 0.0098p_1/i_1n_1$, which gives $p_1 = 0.466$. If 'speed'-chart scale of 100 m.p.h. equivalent to 20 in is chosen and if the available gear ratios between M_1 and the 'speed'-chart drum allow a value of $p_1 = 0.4$ to be used, i_1 becomes 0.784 mA per unit F/m_e . This modified value is used to set i_2 , in turn, the current produced by the several components of the signal circuit.

Thus

- Braking = $76.5 \times 0.784 \times 10^{-3} = 60$ mA.
 Tractive effort = $44.4 \times 0.784 \times 10^{-3} = 34.7$ mA.
 (setting point, 48000 lb).
 Motional resistance = $12 \times 0.784 \times 10^{-3} = 9.4$ mA.
 (setting point, 12 lb/ton).

In order to achieve the maximum signal-circuit resistance, the braking signal is set up first, using the maximum output voltage from T_B and adjusting R_1 to give $I_1 = 60$ mA.

Since the gradient signal can be represented on the binary-coded tape by numbers from 1 to 127, a gradient of 1 in x is given by $8890/x$ if 1 in 70 is represented by 127. The gradient signal is adjusted, with all relays energized, to represent a gradient of 1 in 70, to give $0.784 \times 10^{-3} \times 2240/70 = 25$ mA.

The distance scale on the output chart may be controlled within wide limits by the choice of p_1 , p_2 , i_1 and i_2 . It has been found that 1 in = 1 mile on the output chart and 4 in = 1 mile on the gradient tape (which is driven by a 4 : 1 gear from the output chart) is generally convenient. The values previously selected for i_1 and p_1 give $i_2 = p_2/18000$. A value of $p_2 = 15$ gives $i_2 = 0.834$ mA, and $I_2 = 0.834 \times 10^{-3} \times 50 = 41.6$ mA at 50 m.p.h.

(3.2) Electrical

T = Actual journey time, sec.

r = Ratio of computer time to train time.

k_3 = Ratio of current in M_3 to motor current.

k_3 = Ratio of voltage of M_3 to motor voltage.

k_4 = Ratio of current in M_4 to (motor current)².

V_4 = Potential difference applied to voltage coil of M_4 , volts.

d_3 = Dial reading of M_3 , watt-sec.

d_4 = Dial reading of M_4 , watt-sec.

Energy consumed per motor = $10^9 d_3 k_3 k'_3 r$, watt-sec.

R.M.S. motor current = $\sqrt{\frac{d_4}{V_4 k_4 r T}}$, amp.

k_3 and k_4 are adjusted by variation of R_3 and R_4 to give currents in M_3 and M_4 of about 75 mA at maximum motor current.

(4) ACCURACY

(4.1) Sources of Error

The chief factors that affect the accuracy of the computer are briefly considered as follows:

(a) *Supply voltage of computing circuits.*—This is maintained within $\pm 1\%$ by a stabilized supply.

(b) *Integrators.*—At normal voltages, these were found to have an error not exceeding $\pm 1\%$.

(c) *Computing-circuit impedance.*—The effect of the varying ratios of the signal-source auto-transformers is negligible. The variation, due to self-heating, of the resistance of the modified current coils of the integrators at maximum ampere-turns made it desirable to avoid operating with currents in excess of 75 mA for other than short periods. Since, for most of the time, M_1 operates at very small currents (small acceleration or deceleration) and M_2 at normal currents (normal train speed), it is reasonable to operate M_1 at a somewhat higher maximum current than M_2 .

(d) *Signal sources.*—The significance of errors in the individual signal sources depends on the relative magnitude of these signals. Considering a typical locomotive-hauled passenger train and assuming an initial tractive effort of about 70 lb/ton (=100), the starting tractive resistance is about 8. At a balancing speed of 70 m.p.h. on an up-gradient of 1 in 100, the tractive effort is about 46, the gradient is about 29, and the tractive resistance is about 17.

(e) *Miscellaneous components.*—The first model of the computer used readily available gears and other mechanical parts. No serious errors were introduced by backlash, etc., but the greater mechanical precision in a new model since constructed has been found beneficial.

(4.2) Tests for Accuracy

It is not easy to predict the effects of the various sources of error mentioned in Section 4.1 under the widely varying conditions of operation of the computer. Tests of accuracy were made by comparing the performance of the computer with cases which could be easily checked by calculation, e.g. straight-line functions of tractive-effort/speed and motional-resistance/speed. The results indicated overall limits of error of $\pm 1.5\%$. This is also borne out by the results from several computations of actual train runs for which point-by-point calculations were made as a check.

(5) USE OF COMPUTER

(5.1) Preparation of Data

Curves of the speed-dependent functions are first plotted, the speed range covered being made to utilize as much as possible of the available chart width, namely 22 in. Tractive effort, tractive resistance and current are drawn on charts having maximum heights of 24, 12 and 12 in, respectively. Any convenient scales may be used, since scaling facilities are provided in the computer circuits. A graphite band is then drawn downwards for about $\frac{1}{4}$ in from each curve to form a conducting track.

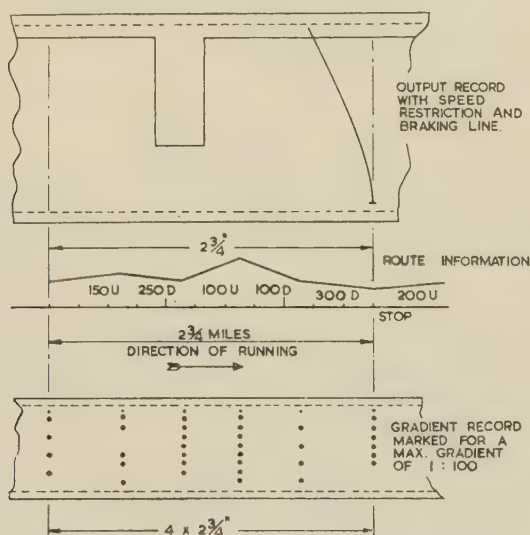


Fig. 6.—Preparation of gradient and output records.

The gradient record (Fig. 6) is punched to the scale selected, say 1 mile = 4 in, as described in Section 3.1.2.

These four records may be used repeatedly for runs with the same or different train weights or may be used individually with other records available from the 'library' of information which is accumulated after some use of the computer.

No preparation of the output chart is required beyond marking the extent and value of any speed restrictions imposed by the route or the train, and any stopping places. It is convenient to draw, with the aid of a template, braking curves down to each stopping place, on the assumption of either a constant deceleration rate or a constant braking force and level track.

(5.2) Operation

After setting up the signal sources, as described in Section 4, the computer is set to zero velocity, time and distance and the unselector operating circuits energized. No manual control of the computer is thereafter needed unless

- (a) The speed tends to exceed a restricted value.
- (b) It is desired to coast or brake.
- (c) It is desired to change the operating conditions of the tractor.

During speed restrictions, the 'speed' unselector is de-energized and M_3 and M_4 are switched out. The energy consumed at the average value of I_m^2 are calculated for each speed-restricted section, allowing for the gradients of the sections. This is a simple matter, since, for a constant speed on a constant gradient the operating forces, and therefore the motor current, are constant. If the train is near its balancing speed during a speed restriction, the direction of rotation of M_1 is observed. Should M_1 reverse, indicating that the train would decelerate as a result of a gradient change, the computer is restored to normal operation; the speed of train will then fall below the restricted value.

For coasting, the tractive-effort signal is switched out. For braking, two cases may be distinguished; it may be desired to represent a constant braking force or to produce a constant deceleration. In the former case, the tractive-effort signal is switched out and the braking-force signal is switched in; in the latter case, the tractive effort, tractive resistance and gradient signals are switched out and a braking signal representing constant deceleration is switched in.

Braking is begun when the output recorder pen crosses the previously-drawn braking line, after either normal running or coasting (see Fig. 7). Under conditions of constant braking force

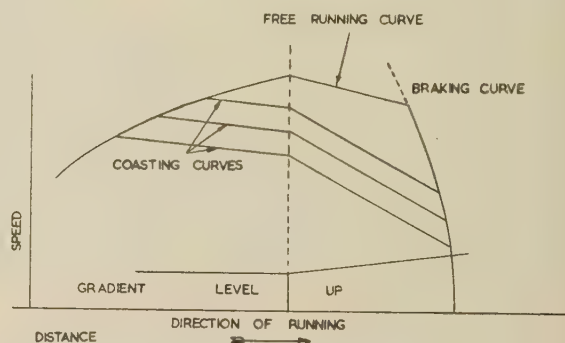


Fig. 7.—Coasting and braking conditions.

it is possible to judge satisfactorily, after some experience with the computer, how much before or after this intersection braking should be begun, if the track between this point and the desired stopping point is on a down- or an up-grade, respectively.

The performance of the train with different combinations of coasting and braking can be examined by setting back the computer to successive points on the output speed curve.

When it is desired to change the operating conditions, e.g. field weakening, tap changing, etc., it can be done by 'freezing' the machine (by de-energizing both unselector circuits) and transferring the probes on the tractive-effort/speed and cur

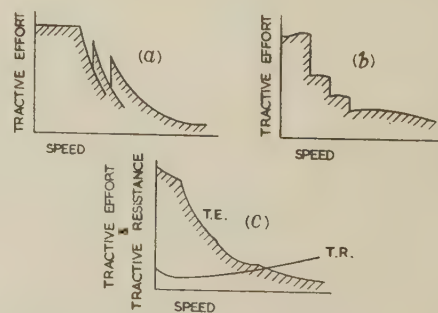


Fig. 8.—Tractive-effort characteristics.

- (a) D.C. locomotive with field weakening.
- (b) Diesel-mechanical rail car.
- (c) Diesel-electric multiple unit set.

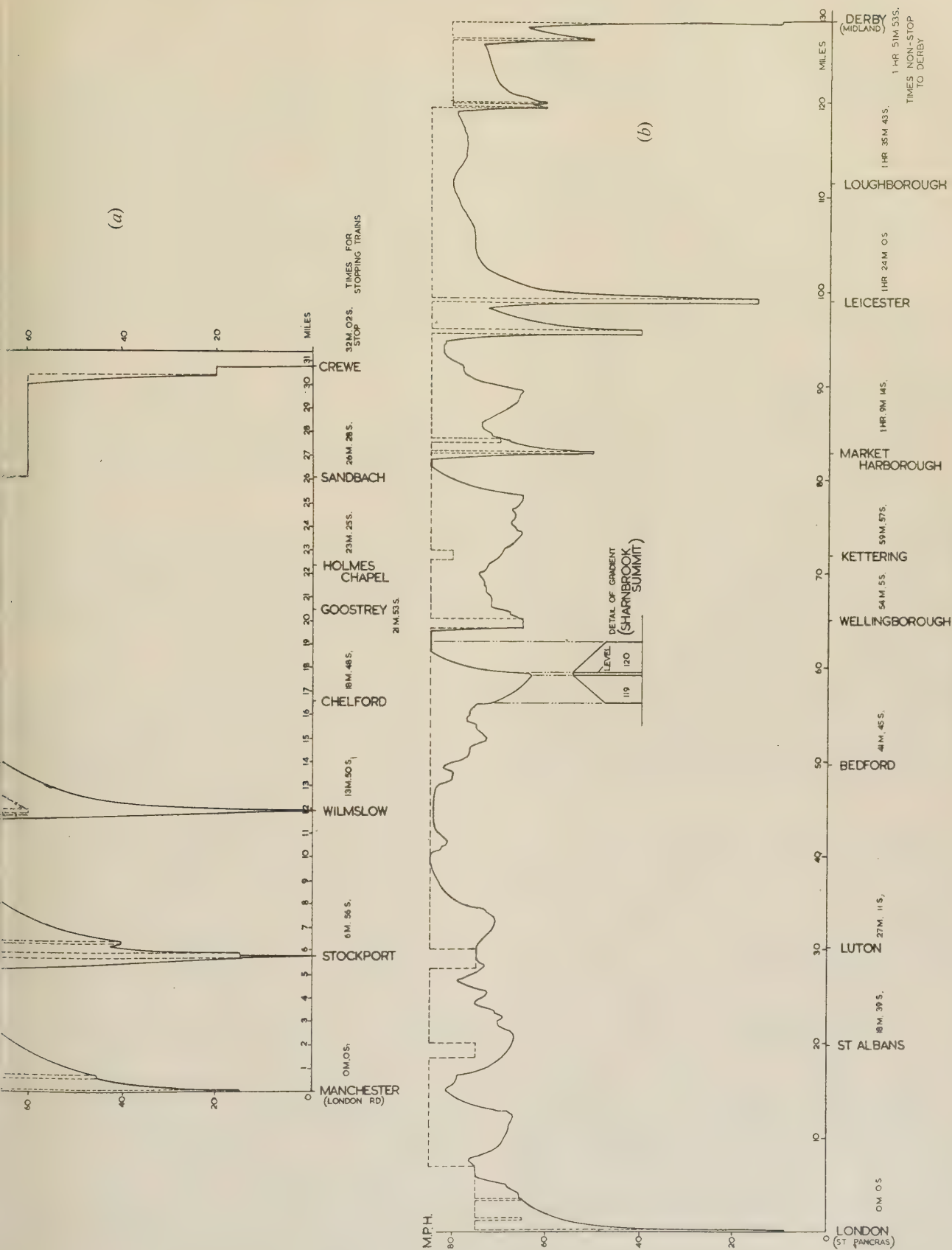


Fig. 9.—Performance studies.

(a) Diesel-electric multiple unit.
Maximum $F/m_e = 105 \text{ lb/ton}$.
52 gradient changes.

(b) Diesel-electric railcars.
Maximum $F/m_e = 156 \text{ lb/ton}$.
317 gradient changes.

— Stopping at Stockport and Wilmslow.
- - - Non-stop Manchester-Crewe.

rent/speed graphs to the appropriate curves, by manual control of the curve-follower motors. If the operating regime of the train is such that these changes are required at given speeds, a composite curve may be drawn, as in Fig. 8(a), thereby eliminating manual control. Other typical tractive-effort/speed curves are shown in Figs. 8(b) and 8(c).

(5.3) Examples

Fig. 9 shows two speed/distance curves on which are marked the times at selected points. In example (a) the maximum speed is limited for a considerable portion of the run by speed restrictions; in example (b) it is only on one or two occasions, on down-grades, that the limiting speed is reached.

(6) POSSIBLE MODIFICATIONS

Although several modifications have been investigated or considered, only those changes which appear to offer reasonable improvements of accuracy or convenience are considered in the paper.

It is thought that the only source of error which would be worth reducing is that due to the change of computing-circuit resistance resulting from self-heating of the rewound integrator coils. A temperature compensation could be envisaged for this purpose. In the early stages of development of the computer an energy meter with standard (5 amp equivalent to 400 AT) current coil was used in association with a 0.1/5 amp current transformer. This was perfectly satisfactory, but the modified meters were adapted to save the expense of current transformers of special construction. It is possible, however, that normal meters and current transformers would be less prone to self-heating errors.

Experience has shown that no changes in the arrangement or method of operation of the computer are necessary if the main interest of the user is the prediction of speed/distance or speed/time curves. It may be noted that the speed of computation is unaffected by the frequency at which the gradient changes occur. However, when energy consumed or r.m.s. motor current is the main object of the study, experience suggests that it might be worth while providing the computer with auxiliary equipment to deal automatically with speed restrictions. One method is shown in Fig. 10. During speed restrictions,

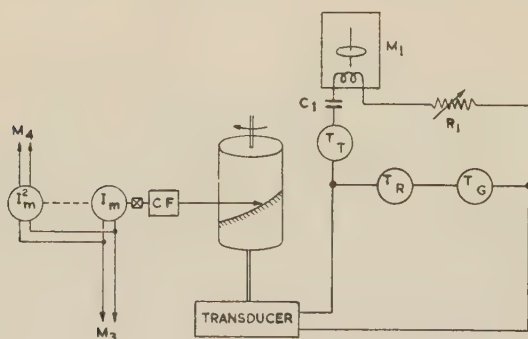


Fig. 10.—Auxiliary circuits for speed-restriction computation.

current and (current)² are derived, not as in normal operation from the current/speed chart, but from a current/tractive-effort chart on an auxiliary drum. The angular rotation of this drum is controlled from a transducer fed by the sum of the outputs of T_G and T_R which, at constant speed, is proportional to the tractive effort that must be produced by the tractor. It has, however, been found quite convenient to 'drive' the train through a speed restriction by manual operation on the several tractive-

effort/speed characteristics so as to keep the train speed at or about the required value.

(7) CONCLUSION

The saving of time resulting from the use of the computer instead of normal computation is variable. Since, for any new problem, train and track data must be prepared for the computer, the greatest saving in time occurs for long runs, particularly if it is desired to make several runs with certain changes in the operating conditions. Changes of train mass do not require any new data to be prepared; a change in tractive resistance may not do so either, if it is considered satisfactory that the ordinates of the tractive-resistance/speed curve be scaled, by the use of T_R . The saving of time is also affected by the number of speed restrictions and changes in the operating conditions of the tractor which have to be considered. Operators who have had experience of the normal methods of calculation suggest that many problems can be solved about ten times more rapidly by the use of the computer.

(8) ACKNOWLEDGMENTS

The authors are indebted to Messrs. J. Prince and M. Whitehead, of Ferranti, Ltd., for their valuable advice and help in the provision and modification of the integrators. They also acknowledge gratefully the help of their colleagues, particularly that of Messrs. A. Glynne, V. H. Attree, P. L. Taylor and B. A. Tomlinson.

The investigation was undertaken at the request of Mr. S. F. Warder, Chief Electrical Engineer, British Transport Commission with the aid of a grant from the Technical Development and Research Committee of the Commission. The authors are grateful for the encouragement and help of Mr. J. A. Broughal, British Transport Commission.

(9) REFERENCES

- (1) HARTREE, D. R., and INGHAM, J.: 'Note on Application of Differential Analyser to Calculation of Train Running Times', *Memoirs and Proceedings of the Manchester Literary and Philosophical Society*, 1938-39, **83**, p. 1.
- (2) PERKINSON, T. F.: 'A Machine for the Calculation of Train Performance Data', *General Electric Review*, 1937, **40**, p. 574.
- (3) DUBOIS, F.: 'Automatic Computation of Railway Train Schedules', *Engineering*, 1952, **174**, p. 717.
- (4) SMITH, S. V.: 'Electric Train Calculator', *Transactions of the American I.E.E.*, 1951, **70**, p. 657.
- (5) HARVEY, A. F.: 'A Train Run-Curve Grapher', *B.T.E. Activities*, 1957, **28**, p. 87.
- (6) KOTHE, H.: 'Schwungrad-Messtände zur Fahrzeit- und Verbrauchswertmittlung sowie zur Fahrer ausbildung für Triebfahrzeuge aller Art', *Glaser's Annalen*, 1957, **2**, p. 50.
- (7) GILMOUR, A.: 'The Application of Digital Computers to Electric Traction Problems', *Proceedings I.E.E.*, Paper No. 2113 M, September, 1956 (**103 B**, Supplement No. 1, p. 59).
- (8) GILMOUR, A.: 'Fuel Consumption and the Speed of Railway Transport', *Proceedings of the Institution of Mechanical Engineers*, 1955, **169**, p. 811.
- (9) VARNEY, R. N.: 'An All-Electric Integrator for solving Differential Equations', *Review of Scientific Instruments*, 1942, **13**, p. 10.
- (10) KUSKO, A., and HELLER, P. N.: 'Computer for Automating Network Analyser Operation', *Transactions of the American I.E.E.*, 1955, Part I, **74**, p. 208.

DISCUSSION BEFORE A JOINT MEETING OF THE MEASUREMENT AND CONTROL SECTION AND THE UTILIZATION SECTION, 15TH APRIL, 1958

Mr. J. A. Broughall: Since the railway modernization plan involves many electrification schemes, British Railways knew at some kind of computer would be necessary for calculating train times. They had to choose between a digital computer, which would be very expensive, and the more modern kinds of analogue computers, which would be far less expensive. It was decided that the latter would do the job very well, and would have some advantages.

The authors are very fair about this matter. There are certain purposes for which the time of setting up is not worth while and the ordinary longhand method is the right answer. There are other jobs where a digital computer, which takes a long time to set up and does the whole calculation in a few seconds, is the right answer. But I think that there is a wide field for an analogue computer running at about train speed, although, in using the first model, we have found it quite convenient to run it even as fast as twice the train speed.

I would like to know more about the Mark III model. The British Transport Commission have a Mark I model, and there have been times when we wished that we had the Mark III, but for fairness to the authors I should say that, although we have had a few difficulties, they have all been solved, and no doubt all the necessary improvements are contained in the later models.

The accuracy of $\pm 1\frac{1}{2}\%$ mentioned in the paper is not good enough, because $1\frac{1}{2}\%$ on a run from King's Cross to Newcastle means about 6 min, which is quite important with modern train speeds. For example, it is of the same order as the result of a permanent-way slack for maintenance.

It is important to follow up further modifications on the lines indicated in the paper. I do not think that it is very important to insert speed checks automatically, because one of the attractive things about this kind of computer is that one can see what is happening and have the feeling that one is driving a train. It is important to retain that picture, which is one of the reasons why any development which makes it more like a train is to be commended. At present we simply follow one characteristic curve, i.e. running in top notch, which is quite satisfactory if you want to see how quickly you can get to some spot, but it means that you do not necessarily take much account of the cost of current of getting there. The question of coasting, using lower notches, etc., is important, and you want to find out what the train performance is when rail conditions do not permit you to be in top notch right up.

I think that more work should be done on this side of the problem, and the authors should try to allow for a variable current. We would then have not only a very useful computer but also possibly a very useful tool for training drivers. In view of the importance of training drivers to drive trains as fast as they can with safety and efficiency—the two are not necessarily the same—this might provide a very useful tool for the training schools.

Mr. G. R. Higgs: My remarks relate to experience with the original prototype of the train performance computer and the first production model in the project design office of a manufacturer of electrical equipment.

For the majority of this work the computer can effect savings over the manual graphical method. In the general case the saving referred to in the paper is conservative, and in many cases it can be much greater.

The housing of the machine is important. Where office space is at a premium, the working load factor of the computer is too low to justify its occupying an engineer's living space. A

separate room is therefore essential, which has the merit of making it easier to provide a dust-free atmosphere.

The staffing of the machine is another important consideration. We like each project engineer to work the machine for his own problems, but we think that one particular engineer should have specialized knowledge of its capabilities and maintenance requirements.

Not all problems susceptible of computer solution are worked out in that way, because the manual graphical method is the only way in which junior engineers can be given a true appreciation of the important relationships between motor characteristics, acceleration rates, timings and economic equipment design.

A point to be noted is that during coasting not only is the tractive effort cut off but negative tractive effort is imposed, owing to the friction and windage of the traction motor. Allowance for this must be made in operating the computer.

It would be very convenient if a means could be devised to use the gradient chart in both directions so as to avoid making a chart for each direction. There are, however, certain disadvantages, particularly relating to compensated gradients, which would introduce complications.

Mr. S. D. Van Dorp: My remarks concern train-performance computation. I have been associated with the design and construction of a mechanical analogue computer built for the solution of the same problem, and I am therefore interested in making comparisons between these two fundamentally similar machines.

In the electrical analogue computer described in the paper, 'time' is represented by a constant potential applied to the voltage coils of the induction energy meters used to perform the required integrations; i.e. the speed of computation is fixed for a particular run and is a function of real time.

In the mechanical analogue computer, 'time' is represented by the angular displacement of a motor-driven shaft, and by varying the angular velocity of this shaft, the rate of change of 'time' and hence the speed of computation can be controlled.

In practice, this has been found to be an invaluable asset. It enables the operator to adjust the speed of computation in relation to the frequency at which changes occur in the track associated data.

I believe that, with the introduction of the simpler type of transducer shown in Fig. 5(b), it will be possible to vary the speed of computation during a run, and I should like to have details of how this will be done and whether it will affect the accuracy of calculation.

My other question concerns the type of automatic curve followers used. I am surprised that a graphite conducting track was considered to be the best solution. In the latest type of mechanical analogue computer, photo-electric curve followers are used in conjunction with electronic amplifiers. These avoid the use of graphite paint, thus enabling curves to be drawn normally with indian ink, and greatly reducing the size of graph paper and of the speed-related functions drum required, without loss of accuracy.

I should be interested to know the advantages of the type of curve followers used in the electrical analogue computer.

Mr. M. Whitehead: The train performance computer is largely based on the watt-hour meter, and it is gratifying to see another successful extension of its use, which already includes several other analogue computers.

The meters have a designed measuring range of 100 : 1 with corresponding speed and standstill torque ranges of 60–0·6 r.p.m. and 23–0·23 g-cm, respectively. Although substantially standard, they differ in two respects; first in adjustment and secondly

in the current coil. Some are required to perform equally well in either direction of rotation, which means that the error/current curve must be sufficiently good at low loads to allow operation on the natural curve without bias, i.e. without the small constant driving torque known as low load compensation.

The second difference from standard, namely the current coil, sets up a second-order effect of self-heating, which is the only error considered to be worth reducing [see Sections 4.1(c) and 6]. This is not surprising, since the adoption of a 100 mA rating instead of 5 amp or more reduces the copper space factor from 60% to 30%, with a corresponding increase in current density. The commercial watt-hour meter is a complex device serially produced in very large quantities, and if a design is really economic it cannot be extended. It is suggested in Section 6 that the error is mainly due to the change in computer circuit resistance arising from the change in meter current-circuit resistance, thus giving low registration against computer circuit voltage. With higher temperature, however, the meter itself will register high against current, and there is thus already some measure of compensation.

Temperature compensation, however, is unnecessary, as the error can be reduced to a negligible value by operating within

the designed range, say 5 amp. This is obtained in one of three ways, first by increased computer circuit current, secondly, by the use of a current transformer, or thirdly, with a degenerative amplifier.

Dr. J. H. Westcott: I was very encouraged by Mr. Broughall who said that ordinary analogue computers can have their advantages. One advantage ought to be cheapness. Unfortunately, one of the sad things about the development of this art is that it is perpetually dogged by the lack of suitable components, and this has a reflection in the fact that analogue computers are not as cheap as they might be.

Perhaps I could quote an example from my own experience. If you have to test servo-mechanisms you need a multiplier but you cannot use servo-multipliers. The alternative is to use an electronic multiplier, in which case you have rows of valves drift problems and many troubles. There is one other possibility, however, and that is the use of a wattmeter movement. This is light, it can give a rapid response and is very convenient but unfortunately it is not cheap.

I think that, in this matter of analogue-computing components an opportunity has been missed to apply familiar principles in a new role.

THE AUTHORS' REPLY TO THE ABOVE DISCUSSION

Prof. E. Bradshaw and Messrs. M. Wagstaff and F. Cooke (in reply): In reply to Mr. Broughall, Mark I is the laboratory-made prototype now in use by British Railways, while Mark II and Mark III are subsequent commercial models with certain refinements and increased facilities, but with no difference in the principle of operation, except that Mark III uses the M-type motor form of rotation transducer shown in Fig. 5(b).

We were anxious not to make unjustified claims for the computer, and are therefore gratified to learn from Mr. Higgs that the claim for a 10:1 saving of time is conservative. We now believe that the estimate of the possible errors was also conservative; the consistency has been found to be very good (often of the order of $\frac{1}{4}\%$), and it is likely that the error limits are much less than the $\pm 1\frac{1}{2}\%$ referred to by Mr. Broughall. In considering the accuracy of this or any similar computer, it should not be forgotten that much of the input data is subject to some uncertainty.

The suggestions, for operation on other notches by Mr. Broughall, and for allowance for negative tractive effort when coasting and the use of reversible gradient records by Mr. Higgs, are among the improvements embodied in the Mark III computer. The detailed improvements made in later models owe much to the helpful advice of engineers of the British Transport Commission and of the manufacturers of traction equipment who have used the computer.

Mr. Broughall's belief that an analogue computer has the advantage that one has a 'feel' of the problem is noted with interest, as is his suggestion that the device might be used for the training of drivers. For the latter purpose, it would probably have to be associated with ancillary equipment which would give the trainee some sense of motion, such as a ciné film of the route and a 'cab' subject to vibration and sound related to 'speed'.

Although Dr. Westcott states that, owing to the lack of suitable components, analogue computers are not as cheap as they might

be, the analogue computer is, as Mr. Broughall points out, far less expensive than a digital computer. The ratio in cost is perhaps 30:1, but this is not altogether a meaningful comparison as it would be unreasonable to contemplate the use of a digital computer unless it were to be employed for work other than this special problem.

We are in full agreement with Mr. Higgs concerning the housing and maintenance of the computer.

We appreciate Mr. Whitehead's comments about the advantages of using normal 5 amp integrators. Of his suggested modifications, that of using a larger current in the computing circuit is not acceptable because of the power dissipated and the influence of variable impedances in the signal sources. Of the other two suggestions, that of current transformers seems to be the more desirable.

The use of photo-electric curve followers, suggested by Mr. Van Dorp, would be equally suitable, but we have found the graphite track system to be reliable and to involve a minimum of associated equipment. It has also been found that curves drawn with a soft pencil give sufficient conductivity for reliable operation.

We agree with Mr. Dorp about the advantage of a variable time scale, implicit in the mechanical analogue computer to which he refers, and think it would be desirable to consider this in future models of our computer. This can be done quite easily, by the introduction of simultaneous changes of gear ratios at four points: in the output drives of transducer 1 and transducer 2 and in the dial mechanisms of integrators M_3 and M_4 (see Fig. 2). The use of the M-type motor form of integrator disc-rotation transducer makes this modification much easier since all that is required is to arrange that each integrator controls an M-type motor, which, in turn, drives a commutator with several output rates, which can be selected at will to control a second M-type motor. Such a modification would not affect the accuracy of computation.

THE SIMULATION OF DISTRIBUTED-PARAMETER SYSTEMS, WITH PARTICULAR REFERENCE TO PROCESS CONTROL PROBLEMS

By J. F. MEREDITH, B.Sc., Ph.D., Graduate, and E. A. FREEMAN, B.Sc., Graduate.

The paper was first received 27th December, 1956, and in revised form 1st April, 1957. It was published in July, 1957, and was read before a joint meeting of the MEASUREMENT AND CONTROL SECTION and the UTILIZATION SECTION 15th April, 1958.)

SUMMARY

Simulator techniques for solving certain partial differential equations, generally occurring in process-control engineering (e.g. heat exchangers), are investigated. Limitations associated with the method of dividing a distributed-parameter system into a series of elements which may be represented by lumped-constant electrical networks are discussed, and an alternative method of simulation is suggested which overcomes these limitations.

To illustrate the advantages of this alternative technique two practical distributed-parameter systems are simulated. In the first, which is a heat exchanger, the technique suggested affords a great saving in apparatus for a given accuracy. The second example considered is a non-linear distributed-parameter system for which previous methods of simulation are impracticable because of the amount of apparatus involved.

LIST OF SYMBOLS

- $Q(x, t)$ = Quantity of substance on unit length of conveyor belt.
 $R(x, t)$ = Substance removed from unit length of conveyor belt, situated a distance x from the origin, in unit time.
 l = Length of conveyor belt or total immersed length of the inner tube of the heat exchanger.
 $v(x, t)$ = Velocity of conveyor belt, or volume of water passing a section at x in unit time.
 $\tau = n\delta t$ = Distance/velocity lag or time delay of the system.
 θ, θ_0 = Temperature of fluid in inner tube of heat exchanger and inlet, respectively.
 u = Mean circumference of the tube, cm.
 v_1 = Velocity of fluid flow in the inner tube, cm/sec.
 α_0 = Overall heat-transfer coefficient for tube.
 c_1 = Thermal capacity of the tube fluid per unit length, cal/cm-deg C.
 c_2 = Thermal capacity of the tube per unit length, cal/cm-deg C.
 T, T_i = Temperature of the outer fluid and inlet, respectively.
 v_2 = Effective velocity of outer fluid flow, cm/sec.
 $\sigma(x, t)$ = Quantity of solute A passing a section x in unit time.
 C_w, C_s, a = Constants.

INTRODUCTION

The rapid increase in the application of automatic process control in industry has led to the need for a method of designing a controller to obtain optimum plant performance. The advantages of analogue-computing techniques in this design procedure have been pointed out by Ford,¹ who has presented a method of simulating commonly encountered distributed-parameter elements in the form of, for example, heat exchangers.² This method requires that the system be split up into a finite number

of sections each of which may be represented in the computer by a lumped-constant electrical network. Such a technique is satisfactory when the partial differential equation defining the distributed-parameter system is linear. The accuracy with which the computer represents the practical system may be improved by increasing the number of lumped-constant sections employed in the simulator.

If the defining equation of the practical system is non-linear, as would occur, for example, in a heat exchanger in which the supply of fluid to be cooled varied as a function of time, the complexity of the analogue rapidly becomes prohibitive. The authors have considered an alternative method of simulating distributed-parameter systems, which, for a given accuracy, employs fewer pieces of apparatus than the above method, and in which the complexity encountered by the introduction of non-linearities is considerably reduced.

To illustrate the advantages of this technique two practical distributed-parameter systems are simulated. The first of these is a heat exchanger simulated by Ford² using the lumped-constant network technique. The second problem arose out of the work of one of the authors where the system could not practicably be simulated by use of previous methods.

(1) DISTRIBUTED-PARAMETER SYSTEMS

In a distributed-parameter system the dependent variable, e.g. the temperature of the liquid to be cooled in a heat exchanger, is a function of two independent variables, position and time. Thus an exact analogue of such a system must have two independent variables.

However, in electronic computers time is the only independent variable. The effect of the second independent variable, position, may be introduced in two ways. In order that the physical significance of these two methods may be more readily appreciated, they will be introduced in terms of a particularly simple system, their application to two more complicated practical systems being considered later.

Let substance be removed from a unit length of belt at a distance x from the origin at a rate $R(x, t)$, and consider a unit length of the belt (Fig. 1) situated a distance x from the origin at time t . The quantity of substance in the element is $Q(x, t)$. At a time δt later, the element having moved forward a distance δx , the quantity of substance in the element is $Q(x + \delta x, t + \delta t)$.

The quantity of substance removed from the unit length of belt in the time δt is

$$R(x + \frac{1}{2}\delta x, t + \frac{1}{2}\delta t)\delta t = Q(x, t) - Q(x + \delta x, t + \delta t) \quad (1)$$

$$\text{Now } f(x + \delta x, t + \delta t) = f(x, t) + \frac{\partial f}{\partial x}\delta x + \frac{\partial f}{\partial t}\delta t \quad (2)$$

Hence, from eqn. (1) we have, neglecting second-order small quantities,

$$-R(x, t) = v \frac{\partial Q}{\partial x} + \frac{\partial Q}{\partial t} \quad (3)$$

The authors are in the Electrical Engineering Department, King's College, Newcastle upon Tyne.

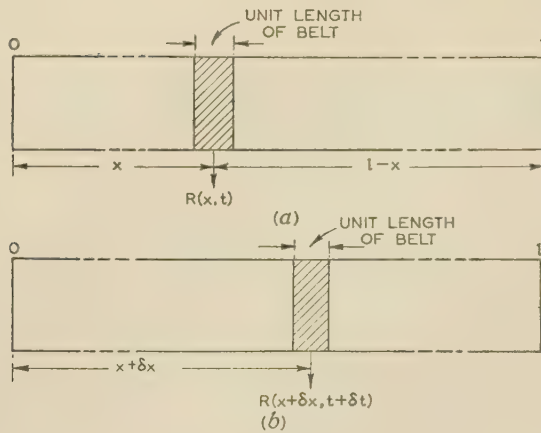


Fig. 1.—Conveyor belt.

(a) At time t .
(b) At time $t + \delta t$.

We will now consider methods of solving eqn. (3) using analogue-computing techniques.

(2) SIMULATION BY A SERIES OF LUMPED-CONSTANT ELEMENTS

Each element of the distributed-parameter system can be represented by a lumped-constant electrical network. Eqn. (1) defines the quantity Q of substance in an element of belt at time $t + \delta t$ in terms of the quantity on the same element at time t . Eqn. (1) may therefore be rewritten

$$Q(x + \delta x, t + \delta t) = Q(x, t) - \frac{1}{v} R(x, t) \delta x \quad (4)$$

Thus, if the conveyor belt of length l be divided into n elements such that $l/n = \delta x$, then an analogue of each element is required to solve eqn. (4) (see Fig. 2). An analogue of the complete system consists, therefore, of n such elements connected in series.

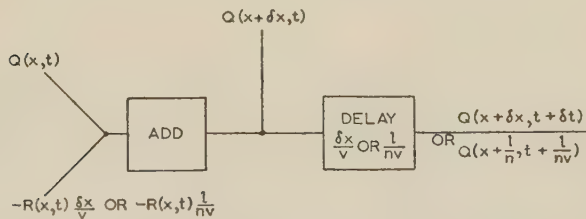
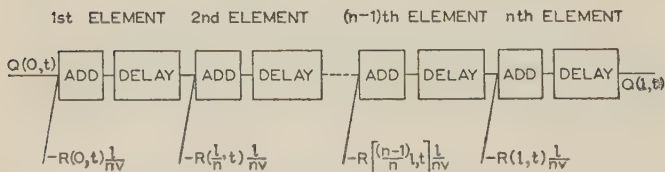
Fig. 2.—Analogue of an element ($\delta x = l/n$) of conveyor belt.

Fig. 3.—Analogue of complete system.

Let us now consider the equation which is solved by the element analogue shown in Fig. 3.

For the first element we have

$$Q(\delta x, t + \delta t) = Q(0, t) - \frac{1}{v} R(0, t) \delta x \quad (5)$$

For the second element,

$$Q(2\delta x, t + 2\delta t) = Q(\delta x, t + \delta t) - \frac{1}{v} R(\delta x, t + \delta t) \delta x \quad (6)$$

Substituting in eqn. (6) for $Q(\delta x, t + \delta t)$, we obtain

$$Q(2\delta x, t + 2\delta t) = Q(0, t) - \frac{\delta x}{v} [R(0, t) + R(\delta x, t + \delta t)] \quad (7)$$

Hence, for the k th element we obtain

$$Q(k\delta x, t + k\delta t) = Q(0, t) - \frac{\delta x}{v} \sum_{\phi=0}^{k-1} R(\phi\delta x, t + \phi\delta t) \quad (8)$$

The output of the system is found by putting $k = n$, the number of elements in the analogue. Thus

$$Q(l, t + n\delta t) = Q(0, t) - \frac{l}{nv} \sum_{\phi=0}^{n-1} R\left(\phi \frac{l}{n}, t + \phi\delta t\right) \quad (9)$$

Substituting $n\delta t = \tau$, the distance/velocity lag or time delay of the system, and $t + \tau = t'$ in eqn. (9), we obtain

$$Q(l, t') = Q(0, t' - \tau) - \frac{l}{nv} \sum_{\phi=0}^{n-1} R\left[\phi \frac{l}{n}, t' - \tau \left(1 - \frac{\phi}{n}\right)\right] \quad (10)$$

As $n \rightarrow \infty$ and $\delta x \rightarrow 0$ such that $n\delta x = l$, then

$$\frac{l}{nv} \sum_{\phi=0}^{n-1} R\left[\phi \frac{l}{n}, t' - \tau \left(1 - \frac{\phi}{n}\right)\right] \rightarrow \frac{1}{v} \int_0^l R\left(x, t' - \tau + \frac{x}{v}\right) dx$$

Hence, in the limit, the analogue gives an exact solution of eqn. (3).

(2.1) Geometrical Interpretation

Eqn. (3) defines a surface in the Q, x, t space (Fig. 4), the form of this surface depending upon the functions $R(x, t)$, $Q(0, t)$. The

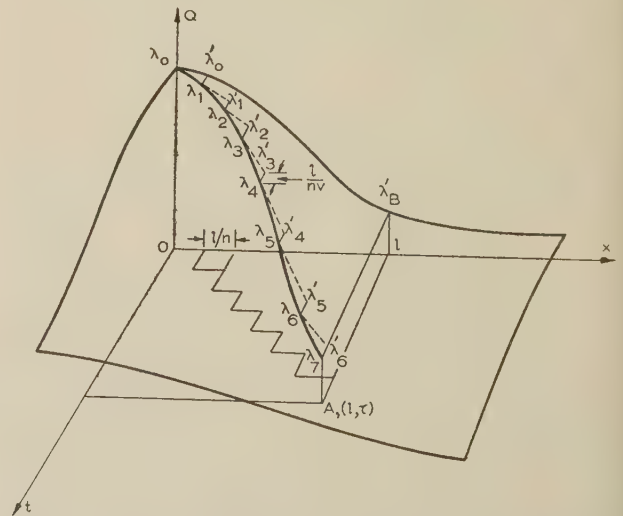


Fig. 4.—Geometrical interpretation of the solution of eqn. (3).

analogue is required to determine $Q(l, t')$ as a function of $Q(0, t' - \tau)$; this means that, taking a particular example, given the ordinate $Q(0, 0)$ the ordinate A , i.e. (l, τ) , is required. The analogue determines $Q(l, \tau)$ in a step-by-step manner. $Q(\delta x, 0)$ is calculated (λ_0, λ'_0) and the result delayed by a time δt (λ'_0, λ_1), to give $Q(\delta x, \delta t)$. Similarly $Q(2\delta x, 2\delta t)$ is determined ($\lambda_1, \lambda'_1, \lambda_2$), and hence $Q(l, \tau)$ is obtained (Fig. 4). It may be seen that the

accuracy of this method depends upon the validity of the approximation that $Q(\lambda'_k) = Q(\lambda_{k+1})$, i.e. it requires that $Q(x)$ does not vary appreciably over a time interval δt . It follows, therefore, that if $Q(x)$ is a sufficiently slowly varying function of time $Q(\lambda'_k) = Q(\lambda_\tau) = A, (l, \tau)$. Hence the delays $l/(nv)$ after each element of the analogue may be lumped together to form a single delay $\tau = l/v$, and in this case the analogue determines $Q(\lambda'_k)$ which is then delayed to give $Q(\lambda_\tau) = Q(l, \tau)$.

(3) ALTERNATIVE SIMULATOR TECHNIQUE

An alternative method focuses attention on an element of Q entering the system at time t , and follows its progress down the conveyor belt. We assume initially that the time τ taken for the element to travel the length of the conveyor belt is short compared with the period of expected variation of $Q(0, t)$. On this assumption it follows that an element selected at time t is typical of all elements entering the system in the time interval $t - \frac{1}{2}\tau \leq t \leq t + \frac{1}{2}\tau$. For such an element distance down the conveyor belt is related to time by the equation

$$x = \int_0^t v dt$$

where v is the velocity of the element.

Hence Q is defined in terms of only one independent variable, time. The problem is therefore amenable to simulation using the conventional techniques for ordinary differential equations.

Output information is obtained from the simulator at a time t such that $\int_0^t v dt = l$, the length of the conveyor belt. Hence, in following one element of Q one 'bit' of output information is obtained. The simulator is operated repetitively, so that after an element has travelled the length of the conveyor belt output information is selected and the simulator reset to initial conditions in order to follow another element.

(3.1) Geometrical Interpretation

The analogue determines $Q(l, \tau)$ in terms of $Q(0, 0)$ by solving eqn. (3) along a path in the x, t plane defined by the equation $x = \int_0^t v dt$. Output information is obtained at $A, A', A'' \dots$ corresponding to times $\tau, 2\tau, 3\tau \dots$

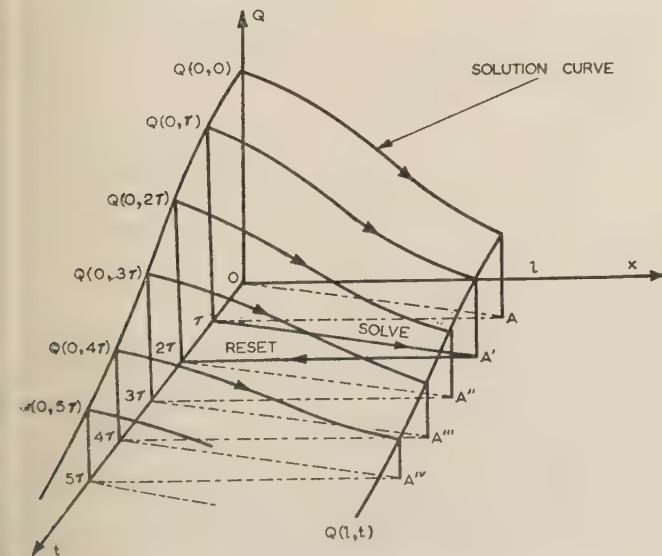


Fig. 5.—Geometrical interpretation of repetitive solution technique.

Fig. 5 corresponds to the case where v is a constant. In general, when the velocity is not constant the paths $OA, \tau A', 2\tau A'' \dots$ are no longer straight lines.

(4) ANALYSIS OF THE TECHNIQUE

Considering again eqn. (1), we have

$$Q(x, t) - Q(x + \delta x, t + \delta t) = R(x, t)\delta t \quad (11)$$

For an element of the belt,

$$x = g(t) = \int_0^t v dt$$

Substituting this in eqn. (1), we obtain

$$Q[g(t), t] - Q[g(t + \delta t), t + \delta t] = R[g(t), t]\delta t$$

or

$$Q[F(t)] - Q[F(t + \delta t)] = R[\beta(t)]\delta t \quad (12)$$

where

$$Q[F(t)] = Q[g(t), t]$$

and

$$R[\beta(t)] = R[g(t), t]$$

Now, writing $Z(t) = Q[F(t)]$ in eqn. (12), we obtain

$$Z(t) - Z(t + \delta t) = R[\beta(t)]\delta t$$

Hence,

$$-\frac{dZ}{dt} = R[\beta(t)] \quad (13)$$

The distributed-parameter system has thus been expressed as a function of one independent variable, time.

(5) THE 'ONE-SIDE-MIXED' HEAT EXCHANGER

In order to illustrate the above technique we will consider the simulation of the 'one-side-mixed' heat exchanger as discussed by Ford² (Fig. 6).

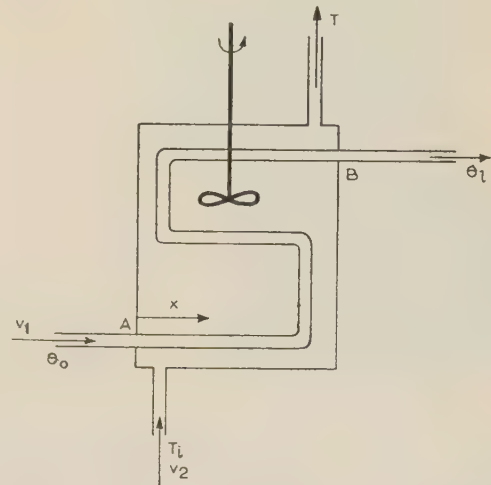


Fig. 6.—Schematic of 'one-side-mixed' heat exchanger.

It may be shown³ that the equations defining the system are

$$\frac{\partial \theta}{\partial t} + v_1 \frac{\partial \theta}{\partial x} = \frac{u\alpha_0}{c_1} (T - \theta) \quad (14)$$

$$l \frac{dT}{dt} + v_2 (T - T_i) = \frac{u\alpha_0}{c_2} \int_0^l (\theta - T) dx \quad (15)$$

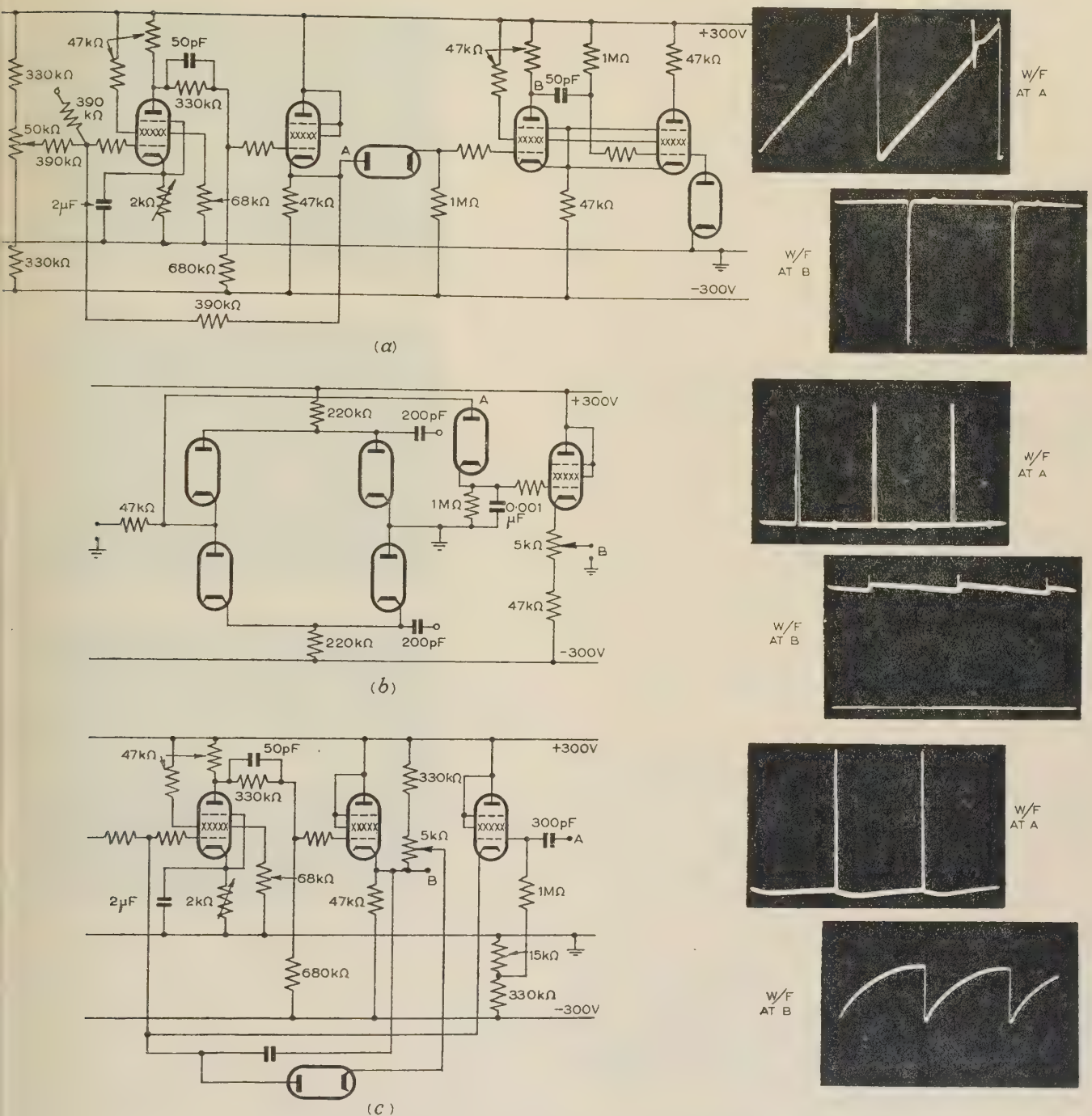


Fig. 9.—Circuits and waveforms illustrating operation of simulator.

(a) Amplitude comparator.

Waveform at A, $\int v dt$.
Waveform at B, pulse defining the instant τ when $\int v dt = I$.

(b) Selector circuit.

Waveform at A, selected information at instant $t = \tau$.
Waveform at B, information after peak-rectification.

(c) Integrator resetter.

Waveform at A, integrator resetting pulse.
Waveform at B, periodic resetting of an integrator.

through a hollow tube,⁵ the reabsorption occurring through the walls of the tube.

The following equations define the system:

$$\frac{\partial v}{\partial x} + \frac{a}{v} \frac{\partial v}{\partial t} = -(P - P_b)C_w \quad . \quad . \quad . \quad (19)$$

$$\frac{\partial \sigma}{\partial x} + \frac{a}{v} \frac{\partial \sigma}{\partial t} = -(E - E_b)C_\sigma \quad . \quad . \quad . \quad (20)$$

where $P_b = K \left(\log_{\frac{\sigma}{\sigma_0}} - \log_{\frac{v}{v_0}} \right) \quad . \quad . \quad . \quad (21)$

$$P_b = -E_b \quad . \quad . \quad . \quad . \quad . \quad . \quad (22)$$

$$P = f(t) \quad . \quad . \quad . \quad . \quad . \quad . \quad (23)$$

$$E = g(t) \quad . \quad . \quad . \quad . \quad . \quad . \quad (24)$$

$v(x, t)$ = Volume of water passing a section at x in unit time.
 $\sigma(x, t)$ = Quantity of solute A passing a section at x in unit time.
 Since $v(0, t)$ and $\sigma(0, t)$ do not vary appreciably over a time interval τ , where τ is given by eqn. (25),

$$l = \int_0^\tau \frac{v}{a} dt \quad . \quad . \quad . \quad . \quad . \quad (25)$$

Eqns. (19) and (20) may be rewritten

$$\frac{dv}{dt} = -(P - P_b)C_w \frac{v}{a} \quad . \quad . \quad . \quad . \quad (26)$$

$$\frac{d\sigma}{dt} = -(E - E_b)C_\sigma \frac{v}{a} \quad . \quad . \quad . \quad . \quad (27)$$

where

$$\frac{dv}{dt} = \frac{dv}{dx} \frac{v}{a}$$

Eqns. (26) and (27) define v and σ at a position x along the tube given by

$$x = \int_0^t \frac{v}{a} dt$$

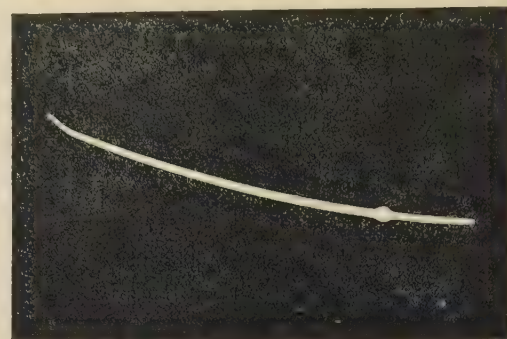
(7) SIMULATOR

The operation of the simulator is similar to that of the one-side-mixed heat exchanger. It may be seen that the simulator requires four non-linear elements. Multiplication of two variables is effected by the method of quarter-squares, the parabolic characteristics of the squarers being obtained using a network of biased diodes.⁶ The logarithmic characteristics are obtained using the same technique.

(7.1) Selecting and Resetting Circuits

As mentioned earlier in the paper, the output from this type of simulator is obtained by selecting the value of the dependent variables (σ and v in this case) at the instant τ defined by

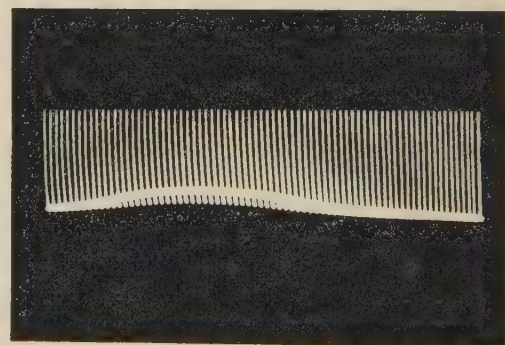
$l = \int_0^\tau (v/a) dt$, and then peak-rectifying the instantaneous values so obtained. The simulator is reset to initial conditions after each selection. The circuits employed for generating the selecting pulse, selecting and peak-rectifying the outputs and resetting the integrators are shown in Figs. 9 and 10, together with waveforms illustrating their operation.



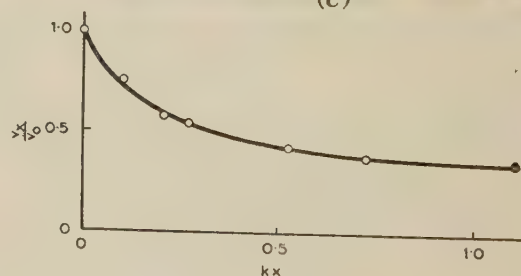
(a)



(b)



(c)



(d)

Fig. 10.—Simulator solution curves and comparison with calculated curve.

(a), (b), (c) Simulator solution curves. Brightness modulation of the traces occur at the instants when $\int v dt = l$.

In (c) the curves are shown for the case where $E = A + B \sin 450t$. (This frequency is five times greater than the variation of E in the practical application, and was employed solely in order that both the individual solution curves and the low-frequency envelope could be seen clearly.)

(d) Simulator solution curve and calculated curve for a case where E and P are constant.

— Calculated.
 ○ Measured.

8) A LUMPED-CONSTANT ELEMENT ANALOGUE FOR THE NON-LINEAR DISTRIBUTED-PARAMETER SYSTEM

In order to compare the method discussed above with the conventional lumped-constant element technique we will derive the block diagram of one element of the conventional computer (Fig. 11).

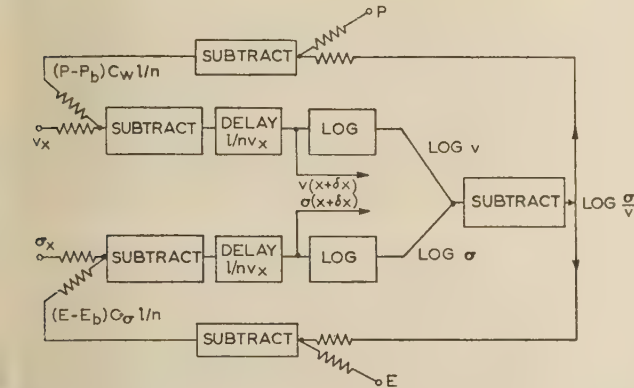


Fig. 11.—Block diagram of one element of conventional computer for non-linear distributed-parameter system.

It may be seen from Fig. 11 that each element of the computer contains two logarithmic non-linearities and two delays of value $l/(nv_x)$, which are variable since v is a variable. It has been shown by Ford⁴ that in order to obtain reasonable accuracy at least 10 elements must be used. Clearly, therefore, this computer uses many more pieces of apparatus, and is inherently less reliable than the computer suggested by the authors.

In the work in which eqns. (19)–(24) arose, the quantity C_w was also a function of time. Using the computer suggested by the authors, this requires one additional multiplier, whereas using the lumped-constant element computer it requires one additional multiplier per element.

(9) DISCUSSION AND CONCLUSIONS

In this Section the two methods of simulating distributed-parameter systems which have been presented in the paper will be compared.

Using the lumped-constant element analogue the amount of apparatus required to include a delay $l/(nv)$ after each section is in general prohibitive. To overcome this practical difficulty a single delay may be included at the end of the analogue. This, however, imposes a limitation upon the accuracy of the analogue and requires, as discussed in Section 2.1, that the dependent variable at any x is a slowly varying function of time, i.e. it requires that the period of variation of $Q(x)$ is much greater than the delay time τ . Also, it has been shown that the only factor affecting the accuracy of the alternative technique is the variation in $Q(x)$ during the delay time τ . Consequently this alternative technique imposes no additional limitations upon the function $Q(x, t)$. If the limitation on $Q(x, t)$ is satisfied the alternative technique of simulation produces an exact solution of the differential equation of the system. With the lumped-constant element analogue this is not so, the accuracy of simulation depending in addition upon the number n of elements employed. It should, however, be pointed out that whereas the lumped-constant element analogue produces a continuous output, the alternative technique produces output information in 'bits'. Thus, because of the limitation placed upon $Q(x, t)$, a bit of information obtained at time t represents accurately the output in the time interval $t - \frac{1}{2}\tau \leq t \leq t + \frac{1}{2}\tau$.

It is clear from the two examples considered in the paper that

the alternative technique employs much less equipment than the lumped-constant element method. This is particularly so when the system being simulated is non-linear. Such a saving in pieces of apparatus must make the computer inherently more reliable.

(10) ACKNOWLEDGMENTS

The authors are indebted to Professor J. C. Prescott of King's College, Newcastle upon Tyne, for the facilities placed at their disposal during the course of the work described, and to Mr. F. J. U. Ritson of the Electrical Engineering Department, King's College, Newcastle upon Tyne, for his advice and encouragement.

(11) REFERENCES

- (1) FORD, R. L.: 'The Determination of Optimum Process-Controller Settings and their Confirmation by means of an Electronic Simulator', *Proceedings I.E.E.*, Paper No. 1533 M, July, 1953 (**101**, Part II, p. 141).
- (2) FORD, R. L.: 'Electrical Analogues for Heat Exchangers', *ibid.*, Paper No. 1934 M, January, 1956 (**103 B**, p. 65).
- (3) TAKAHASHI, Y.: 'Transfer Function Analysis of Heat Exchange Processes' from 'Automatic and Manual Control' (Butterworth, London, 1952).
- (4) FORD, R. L.: 'The Determination of Optimum Process-Controller Settings and their Confirmation by Means of an Electronic Simulator', Ph.D. Thesis, King's College, University of Durham, July, 1953.
- (5) COLE, D. F., and MEREDITH, J. F.: 'Target Organ Interaction', *Bulletin of Mathematical Biophysics*, 1957, **19**, p. 23.
- (6) BURT, E. G. C., and LANGE, O. H.: 'Function Generators based on Linear Interpolation with Applications to Analogue Computing', *Proceedings I.E.E.*, Monograph No. 137 M, June, 1955 (**103 C**, p. 51).

(12) APPENDIX: SIMULATOR ERROR FOR ONE-SIDE-MIXED HEAT EXCHANGER

When simulating the 'one-side-mixed' heat exchanger using the authors' technique it was assumed that $\partial\theta/\partial t = 0$ over a time interval τ . The error introduced by this assumption will now be investigated.

The equations defining the system are

$$\frac{\partial\theta}{\partial t} + v_1 \frac{\partial\theta}{\partial x} = \frac{u\alpha_0}{c_1} (T - \theta) \quad \dots \quad (28)$$

$$l \frac{dT}{dt} + v_2 (T - T_i) = \frac{u\alpha_0}{c_2} \int_0^l (\theta - T) dx \quad \dots \quad (29)$$

Since $\theta_0(t)$ is a slowly varying function we may put $\partial\theta/\partial t = \psi$ over an interval of time $\tau = l/v_1$. Thus eqn. (28) becomes

$$\frac{\partial\theta}{\partial x} = -\frac{\psi}{v_1} + \frac{u\alpha_0}{v_1 c_1} (T - \theta) \quad \dots \quad (30)$$

Integrating eqn. (30) with respect to x , we have

$$\log_e \left[\frac{\left(T - \frac{\psi c_1}{u\alpha_0} \right) - \theta_0}{\left(T - \frac{\psi c_1}{u\alpha_0} \right) - \theta_l} \right] = \frac{u\alpha_0 l}{v_1 c_1}$$

Therefore,

$$\theta_l = \theta_0 \exp \left(-\frac{u\alpha_0 l}{v_1 c_1} \right) + \left(T - \frac{\psi c_1}{u\alpha_0} \right) \left[1 - \exp \left(-\frac{u\alpha_0 l}{v_1 c_1} \right) \right] \quad (31)$$

Had we assumed that $\psi = 0$, i.e. that θ_0 did not vary over the time interval τ , then eqn. (31) would be

$$\theta_l = \theta_0 \exp\left(-\frac{u\alpha_0}{v_1 c_1} l\right) + T \left[1 - \exp\left(\frac{u\alpha_0}{v_1 c_1} l\right)\right] \quad (32)$$

The error introduced by assuming $\psi = 0$ is therefore

$$-\frac{\psi c_1}{u\alpha_0} \left[1 - \exp\left(\frac{u\alpha_0}{v_1 c_1} l\right)\right]$$

If the error is small then the percentage error in θ_l is given by

$$\text{Percentage error} = \frac{-\frac{\psi c_1}{u\alpha_0} \left[1 - \exp\left(\frac{u\alpha_0}{v_1 c_1} l\right)\right] \times 100}{\theta_0 \exp\left(\frac{u\alpha_0}{v_1 c_1} l\right) + T \left[1 - \exp\left(\frac{u\alpha_0}{v_1 c_1} l\right)\right]} \quad (33)$$

Then writing

$$k\tau = \frac{u\alpha_0}{c_1} \frac{l}{v_1}$$

and

$$\Delta\theta_0 = \psi \frac{l}{v_1}$$

eqn. (33) becomes

$$\text{Percentage error} = \frac{(\Delta\theta_0/\theta_0) \times 100}{k\tau \left[\frac{T}{\theta_0} + \frac{\exp(-k\tau)}{1 - \exp(-k\tau)} \right]} \quad (34)$$

A criterion for the accuracy of the simulator is the percentage error arising from a given percentage change in the input conditions over the time interval τ .

Therefore,

$$\Gamma = \frac{\text{Percentage error}}{\frac{\Delta\theta_0}{\theta_0} \times 100} = \frac{1}{k\tau \left[\frac{T}{\theta_0} + \frac{\exp(-k\tau)}{1 - \exp(-k\tau)} \right]} \quad (35)$$

The maximum value of Γ is the greatest error that the simulator can produce for a given change in input conditions. This maximum error occurs when $1/\Gamma$ is a minimum.

$$\frac{d(1/\Gamma)}{d\alpha} = \beta + \frac{\exp(-\alpha)}{1 - \exp(-\alpha)} - \alpha \frac{\exp(-\alpha)}{[1 - \exp(-\alpha)]^2} \quad (36)$$

where $\beta = T/\theta_0$ and $\alpha = k\tau$.

For a stationary value of Γ ,

$$\frac{d(1/\Gamma)}{d\alpha} = 0$$

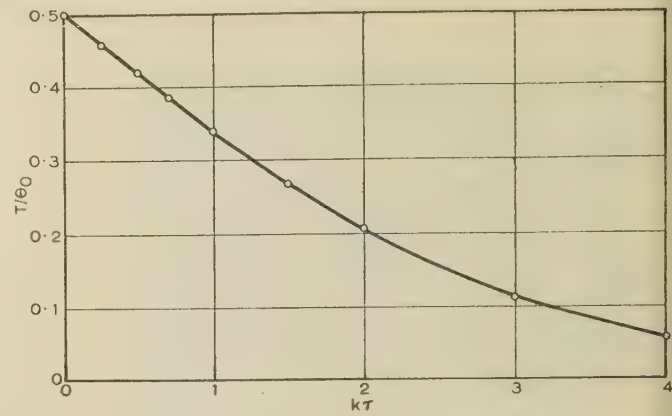


Fig. 12.—Value of T/θ_0 which for a particular value of $k\tau$ gives the maximum of the error function Γ .

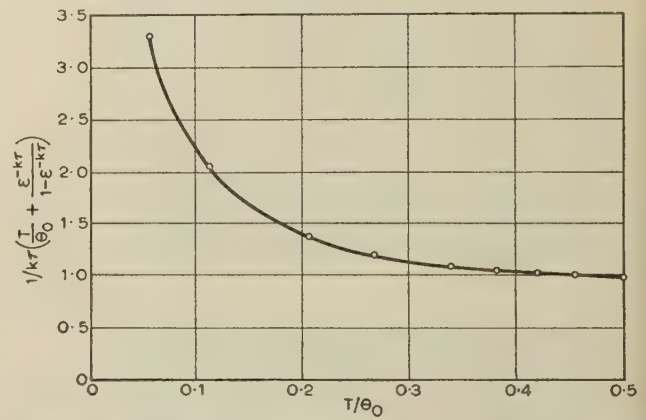


Fig. 13.—Maximum value of error function Γ as a function of T/θ_0 .

Fig. 12 shows the values of β which for any α gives this condition. Substituting the values so obtained in eqn. (35), we obtain the maximum possible value of the error function Γ as a function of T/θ_0 (Fig. 13). For $T/\theta_0 > 0.5$ the function Γ has no maximum for real α . However, Γ for $T/\theta_0 > 0.5$ is always less than the maximum error for $T/\theta_0 = 0.5$. Since T and θ_0 are absolute temperatures, the practical range of T/θ_0 is most unlikely to exceed $0.5 \leq T/\theta_0 \leq 1$. Therefore, the percentage error in θ_l is less than $(\Delta\theta_0/\theta_0) \times 100$.

A MAGNETIC-DRUM STORE FOR ANALOGUE COMPUTING

By J. L. DOUCE, M.Sc., Ph.D., Graduate, and J. C. WEST, Ph.D., D.Sc., Associate Member.

(The paper was first received 7th March, and in revised form 18th May, 1957. It was published in July, 1957, and was read before a joint meeting of the MEASUREMENT AND CONTROL SECTION and the UTILIZATION SECTION 15th April, 1958.)

SUMMARY

The paper describes how a conventional magnetic drum may be used in an analogue computer. The magnetic drum becomes a versatile element in this computer, giving a large storage capacity combined with a relatively short access time. Several of the important facilities obtainable by this technique are discussed.

INTRODUCTION

The use of a rotating magnetic drum is well known in the field of digital computing.¹ The periphery of the drum is nickel-coated, and combined 'read-write' heads are situated near to the drum surface. A large current is passed through the 'write' head so as to saturate a portion of the nickel coating. As the drum rotates the remanent magnetism of the drum surface induces a voltage into the 'read' head, enabling the recorded data to be reconstructed. Each head is made as narrow as possible so that many heads can be used with one drum. That portion of the drum associated with one head is termed a 'track'. About 250 tracks can be accommodated on a typical magnetic drum.

The disadvantage of the magnetic drum for digital-computer application is the access time required to deliver the stored information. However, this access time is short compared with the speed of operation of some analogue computers, and where the drum is used to record analogue information the device gives a short-access-time permanent store of large capacity.

A small analogue computer has been constructed to exploit the advantages of the analogue store. Following a description of the basic units, some applications of this machine are given.

(1) THE BASIC TECHNIQUE

In recording a signal on the drum, it is not legitimate to assume that there is a linear relationship between magnetization of the drum surface and head current. In the first case, the magnetization characteristic of the nickel surface will be non-linear, although this may be partially overcome by the use of a suitable high-frequency bias current.² More serious disadvantages are that the nickel surface is of non-uniform thickness, giving different characteristics along a track, and there exists a non-uniform air-gap as the drum rotates, owing to drum eccentricity. In the worst cases, eccentricity causes the output signal to vary in amplitude by a factor approaching 2 : 1.

For these reasons, a form of pulse modulation is employed, whereby the drum is saturated all the time, and the information is stored by varying the time spent in alternate states of saturation. This mode of operation ensures that any recording erases previous information on the drum.

Two forms of modulation may be considered: frequency modulation and pulse-width modulation. A disadvantage of frequency modulation in this particular application is that any variation in drum rotational frequency produces a corresponding variation in the output of the device.

Pulse-width modulation does not suffer from this disadvantage, and renders unnecessary the accurate control of drum speed. A

further advantage is that the variable-width pulses can be used directly in a pulse-height-pulse-width multiplier.¹⁰

The system chosen employs pulse-width modulation of a 10 kc/s carrier signal. Automatic gain control in the read circuits enables the position of the pulses to be detected accurately as the pulse amplitude varies. The carrier-signal frequency should be as high as possible, since the amount of data stored per track is proportional to this frequency. The upper limit is imposed by the mechanical details of the drum and head construction and the properties of the magnetic material employed.

Thus the basic system comprises a modulator, magnetic drum and demodulator. The incoming analogue voltage varies the mark/space ratio of a 10 kc/s pulse train, and these pulses then magnetize the drum surface to saturation point. The read-head signal is proportional to rate of change of flux, and hence is composed of alternate positive and negative pulses. The demodulator employs these pulses to trigger a bistable flip-flop, reconstructing the original pulse train. After smoothing out the carrier frequency, the original information is recovered.

The following Section gives a more detailed description of the basic equipment. The application considered first is important since it shows how all information is fed on to the drum. The recording of long-period phenomena was also the first suggested use for the device; only later were its versatile properties appreciated.

(2) THE RECORDING OF LONG-PERIOD PHENOMENA

In the testing of automatic control devices, it is frequently required to observe the transient behaviour of the system. The period of observation usually lies in the range from one second up to several hours. For the faster systems, the response may be displayed on a cathode-ray tube having a long afterglow. This is a convenient technique, but it is often difficult to obtain an accurate visual picture of the overall response, owing to the decay of the cathode-ray-tube image.

It was decided to construct a device which enabled the system response to be displayed repetitively on a cathode-ray tube, producing the effect of infinite afterglow.

This involved storing the transient over a long period of time, and displaying repetitively the instantaneous content of the store.

One magnetic track is used for each variable being recorded. The input information is sampled once per drum revolution and the sample recorded on successive sections of the magnetic track. The recorded information is read off continuously and applied to the Y-plates of a cathode-ray tube. X-deflection is provided by a linear sawtooth voltage synchronized to the drum rotation, so that the whole of the long recorded function is displayed repeatedly at drum repetition rate. By suitable gating of the output of the store, the recorded data can be obtained with any desired expansion or compression of the time scale.

(3) EXPERIMENTAL DETAILS

The operation of the equipment must be synchronized to the drum rotation, and to obviate accurate control of drum speed¹ the clock pulses required are recorded on the drum.³ Two sets of pulses are required. First we need a pulse occurring once

Dr. Douce and Dr. West were formerly in the Electrical Engineering Laboratories, University of Manchester, and are now at the Queen's University, Belfast.

per revolution, defining the datum point along each track. This pulse controls a Miller integrator, producing a linear sawtooth voltage synchronized to the rotation of the drum.

The other clock pulse needed is a high-frequency pulse train (nominally 10 kc/s) used for driving the input modulator. Both sets of pulses are recorded on a single track. This is conveniently achieved by writing a continuous line of 10 kc/s pulses on the clock track, and then erasing these for a short distance. The absence of 10 kc/s pulses is then used to synchronize the sawtooth waveform.

Since the period of the linear sawtooth waveform is identical to the time for one drum revolution, each voltage level of this waveform corresponds to one particular point along each track. This enables any point on a track to be specified by means of a voltage.

To record a long-period transient, an additional linear sawtooth voltage is generated, whose period is equal to the time of observation of the transient. This slow sawtooth is compared with the synchronized time-base, so that coincidence occurs at a varying point along the fast time-base run-down, corresponding to a varying point on each track opposite to the head. The instant of coincidence hence defines the instant at which writing must commence and the position of storage along the track. As the slow time-base voltage varies, the point at which writing starts will move along the track, gradually filling it with the encoded information.

A block schematic of the recording system is shown in Fig. 1(a).

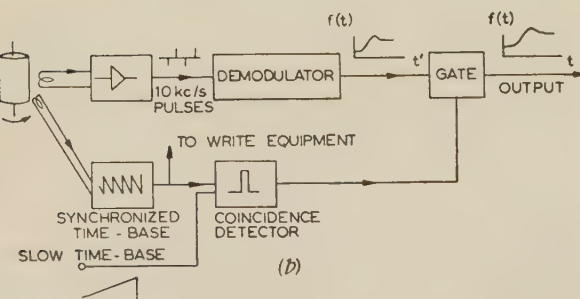
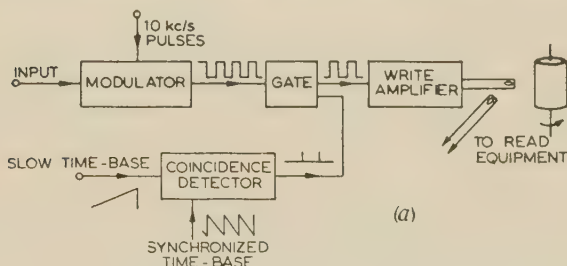


Fig. 1.—Apparatus for the recording of long-period phenomena.

(a) 'Write' equipment.
(b) 'Read' equipment.

The recorded information is obtained repetitively as the output of the track. The demodulator incorporates a circuit compensating for the variation in pulse amplitude due to drum eccentricity.

To obtain the recorded function for a particular value of time, the output of the track is gated at the corresponding distance along the track. If the gating pulse slowly moves along the track, the gated signal slowly reproduces the recorded information. In particular, if the gating pulse moves at the same rate as the writing pulse, the recorded information is delivered on a 1:1 time scale.

Fig. 1(b) illustrates how the recorded information is delivered as a slowly-varying function of time. Gating pulses are pro-

duced at the instant of coincidence of the synchronized time-base waveform and a slowly varying linear time-base. These pulses gate the repetitive output of the demodulator, the particular values of the data being stored from one gating pulse to the next. When the slow time-base is identical to that used when recording the transient, the final output reproduces the original signal.

As an example of this device, the response of a Velodyne incorporating integral control has been recorded. Fig. 2(a)

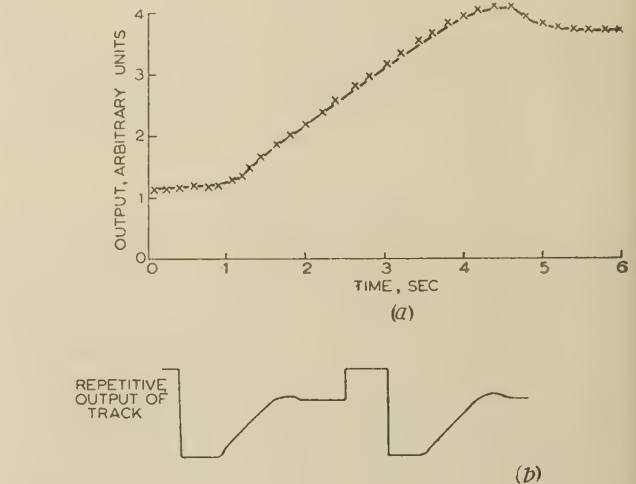


Fig. 2.—The recording of long-period phenomena.

(a) Output velocity as a function of time.

— Direct. × After recording on drum.

(b) Repetitive output of track, together with synchronizing signal.

shows the output velocity as a function of time, in response to a step demand of velocity. For comparison, the transient is shown after being recorded and subsequently played back on a unity time scale.

Fig. 2(b) shows the repetitive output of the track used, together with the synchronizing signal.

The magnetic drum may be compared with other methods of recording long transients, such as photographic recording, magnetic tape, or conventional recording on a roll of paper.⁴ One advantage of the device discussed is that the whole of recorded information is immediately available for inspection, whilst recording is taking place. Further, the recorded information is available as a voltage, as opposed to the position of a mark on a piece of paper or film, so that it is in a form suitable for feeding into a computer.

The disadvantages of the system are that only a relatively small amount of information can be stored on one track, and the maximum frequency which can be recorded is limited, owing to the sampling technique employed.

Using a 10 kc/s carrier frequency, together with a drum rotating at 50 c/s, it follows that 200 cycles of the modulated carrier may be recorded on one track. Thus the information is stored as a series of 200 spot values. This is normally sufficient to record the transient response of a servo system.

Since the incoming information is recorded once per drum revolution, no significant variation must occur in $\frac{1}{50}$ sec. This imposes a basic limitation to the high-frequency response of the system. Appreciable phase-shift occurs when recording a sinusoidal signal if its frequency is higher than 4 c/s.

(4) THE GENERATION OF NON-LINEAR FUNCTIONS

The simulation of non-linear characteristics is desirable in any versatile analogue computer. The simplest and most widely used technique employs a series of biased diodes.⁵ This is particularly convenient where the required characteristic is a smooth curve. Even so, many diodes may be necessary if reasonable accuracy, together with a large change of slope, is required. For example, a cubic characteristic was constructed for the investigation of sub-harmonic resonance.⁶ Twenty-four diodes were found necessary to give a suitable characteristic.

Cathode-ray-tube curve-follower function generators have been employed in analogue computing⁵ and non-linear servo-mechanisms.⁷ They offer the combined advantages of ease of modification of the function and high operational speed. Any single-valued function can be obtained by inserting a suitable mask.

One track on the magnetic drum may readily be used as a non-linear function generator, capable of storing any single-valued function which may be represented by 200 spot values.

To store the function $y = f(x)$ the distance along a track is taken as corresponding to the voltage x . In a manner similar to the recording of a long-period transient, a slowly varying voltage is derived, passing through the range of values of x . This voltage can be any function of time, and is most simply obtained from a potentiometer set manually. As the voltage x is varied, the corresponding value of $f(x)$ is set up on a further potentiometer. This value of $f(x)$ is then automatically recorded at the correct point along the track, since the position is defined by coincidence of voltage x with the linear-time-base voltage.

In this way, the function can be recorded step by step, from tabulated values. Any reasonable number of discontinuities in the desired characteristic can be faithfully recorded.

To find $f(x)$ corresponding to a given voltage x , it is necessary to gate the output from the drum track at the appropriate time. The correct instant is given by coincidence of the position-defining sawtooth voltage and the input voltage x . At this instant, the demodulated signal from the track is delivered to the output circuit. This circuit consists of a condenser large enough to store the voltage $f(x)$ from one gating period to the next. Thus, if x were held constant a signal from the read head corresponding to the appropriate $f(x)$ would be read once per revolution of the drum. The output from the smoothing circuit would be a constant voltage proportional to $f(x)$.

Fig. 3 shows two non-linear functions recorded on the drum, together with the response to a sinusoidal signal of 1.5 c/s.

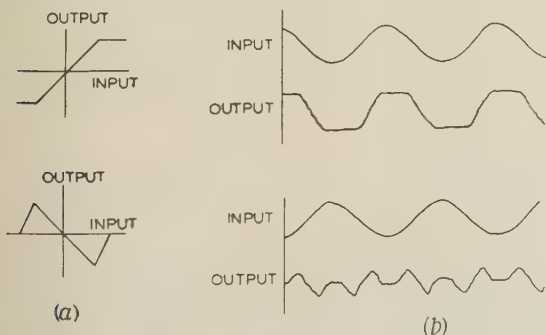


Fig. 3.—Response of non-linear function generator.

(a) Non-linear function.
(b) Sinusoidal response.

The limitations imposed on the use of the drum as a function generator are that the function shall be accurately represented by 200 spot values, and that the input x to the non-linear unit shall not change appreciably in $\frac{1}{50}$ sec, or one drum revolution.

A special feature of the function generator described is that the form of the function is determined by recording the variation of one voltage with another. This feature has important potential advantages. For example, the function generator could be used to provide a non-linear device for optimizing the transient response of a remote-position-control servo-mechanism.

In its present form, the drum function generator has proved reliable and simple in operation.

(5) THE MAGNETIC DRUM AS A DELAY NETWORK

A pure time delay is frequently encountered in the analysis of automatic control systems. Process controllers and nuclear reactors involving heat exchangers are some of the most important practical examples.

A multiple delay network can also be used as a complete analogue of any linear system.⁸

The simulation of a pure time delay is not simple using conventional feedback amplifiers, especially where a large time delay is required. As more phase-lag is required in the delay network, more stages of computing amplifiers are required, and the more rapidly does the behaviour of the simulator deviate from the desired characteristic as the input frequency is increased.

Thus, simple delay networks suffer from two disadvantages. First, the complexity of the equipment increases as the desired delay increases, which normally implies that the characteristic deviates more from the ideal as the delay is increased. Secondly, the delay is simulated by discrete separate networks so that the output time delay is variable only in finite steps.

The magnetic drum offers several advantages over conventional delay networks. Given the basic equipment as used for the previous applications, little additional complexity is involved. The time delay available is unlimited, is smoothly variable, and can be controlled by a voltage signal. The departure from the ideal characteristic is independent of the delay. At any instant the input signal can be obtained with any delay up to the maximum demanded. Limitations on the range of operation are imposed by the drum rotational frequency, and by the limited capacity of one track of the drum store. These limitations will be discussed later.

The method adopted involves sampling the input signal once per drum revolution, and recording the samples on successive portions of a track. The process is made continuous, so that when the track is completely filled writing carries on, overwriting the first sample recorded. In this way, the track always contains the present value of the input signal and all past values up to a time τ seconds previously, where τ is the time taken for the track to be completely filled by the incoming signal.

The point along a track at which recording takes place moves once around the track every τ seconds. Similarly, the point containing the data recorded at some time τ' seconds previously will move around the track in τ seconds, with a constant positional displacement from the point at which writing is taking place. Thus, the recorded signal may be read off at a time τ' after being recorded by gating the repetitive output of the track at a fixed time interval $\delta\tau'$ ($\delta\tau' < \frac{1}{50}$ sec) after a write pulse. For example, suppose the write circuit is arranged so that the track is completely over-written in a period of 10 sec. Then, at any instant, the information recorded 5 sec previously will be stored at a point along the track diametrically opposite to the point at which writing occurs. With the drum rotating at 50 c/s, if the repetitive output of the track is gated at $\frac{1}{100}$ sec after writing, the resultant output is the input signal, delayed by 5 sec. Increasing the delay of the gating pulse decreases the time delay of the output waveform, and vice versa.

The method employed for producing the variable delay uses a linear sawtooth voltage initiated by the write waveform. Each

voltage level of this sawtooth corresponds to a given delay, so that when the voltage passes through some predetermined value the output of the track is gated and fed to the smoothing network. The delay is variable, since this only implies varying the mean level of the sawtooth waveform. If the mean value of the sawtooth voltage is allowed to vary periodically, e.g. by adding a low-frequency signal to it, a periodically-varying time delay is obtained. The mechanism here is similar to the technique for the generation of non-linear functions.

Before considering the experimental behaviour of the system, the limitations imposed on the delay unit will be discussed. As in all applications of the magnetic drum, the access time limits the maximum input frequency, and the phase shift will deviate from its desired value when the input frequency is above about 4 c/s.

The limited capacity of one track (200 elements) limits the information which can be stored at any time and the maximum phase delay obtainable. For example, if it is sufficient to represent one cycle of a sine wave by 16 spot values, at the highest frequency of interest, no more than 12 cycles can be stored on any track. Thus, the maximum phase change of the delay system is of the order of 4000° . In practice, it is not possible to read off a track immediately writing stops, because the write signal saturates the read amplifiers. This cuts down the maximum phase delay by about 10%.

The advantages of the system are as follows. Although the maximum phase delay is limited, no upper limit is imposed on the time delay of the system. The time delay is easily adjustable, and may be controlled by an input voltage. A delay of 10 cycles is available.

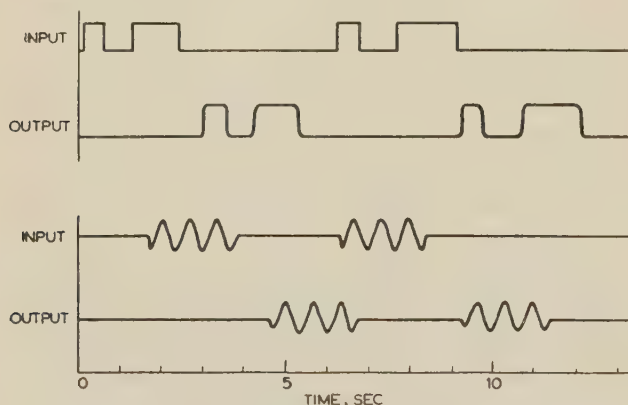


Fig. 4.—Response of delay network.

Experimental behaviour of the system is shown in Fig. 4. This shows the input and output of the delay network for a rectangular pulse and for a discontinuous sine-wave.

DISCUSSION BEFORE A JOINT MEETING OF THE MEASUREMENT AND CONTROL SECTION AND THE UTILIZATION SECTION, 15TH APRIL, 1958

Mr. J. K. Webb: Have the authors considered the use of pulse-code modulation as an alternative to the scheme which they propose? From a rough calculation it would appear to offer the possibility of appreciably increasing the capacity of the store from the 200 spot values mentioned. As a matter of more general interest, a method has been developed which overcomes the non-uniformity of the air-gap as the drum rotates owing to its eccentricity. The drum heads are assembled in specially shaped blocks which are kept off the drum by a pulley system. When the drum has reached speed, the pulleys lower the blocks slowly on to the drum and then the blocks seat themselves on an air

(6) CONCLUSIONS

It has been shown how a magnetic drum can be used as a storage element for analogue data. Advantages are the large total storage capacity and short access time. The short access time enables the storage system to be incorporated in an analogue computer. In this application, besides presenting a convenient source of input functions, the device can be used as a flexible non-linear function generator. The storage of information by pulse-width modulation enables analogue multiplication to be performed in a simple manner.

The magnetic drum can also be used to simulate a pure time delay. This time delay is unlimited, provided that the waveform can be represented by 200 spot values over the delay period.

It is considered that the magnetic drum has sufficient advantages as a versatile element of an analogue computer to compensate fully for the complexity of the basic equipment.

(7) REFERENCES

- (1) WILLIAMS, F. C., and WEST, J. C.: 'The Position Synchronization of a Rotating Drum', *Proceedings I.E.E.*, Paper No. 1073 M, February, 1951 (98, Part II, p. 29).
- (2) AXON, P. E.: 'An Investigation into the Mechanism of Magnetic Tape Recording', *ibid.*, Paper No. 1149 R, June, 1951 (99, Part III, p. 109).
- (3) KILBURN, T., GRIMSDALE, R. L., and WEBB, D. C.: 'A Transistor Digital Computer with a Magnetic Drum Store', *ibid.*, Paper No. 2043 M, March, 1956 (103 B, Suppl. 3, p. 390).
- (4) MADDOCK, A. J.: 'Servo-Operated Recording Instruments', *ibid.*, Paper No. 2131, September, 1956 (103 B, p. 617).
- (5) WASS, C. A. A.: 'An Introduction to Electronic Analogue Computers' (Pergamon Press, London, 1955).
- (6) WEST, J. C., and DOUCE, J. L.: 'The Mechanism of Sub-Harmonic Generation in a Feedback System', *Proceedings I.E.E.*, Paper No. 1693 M, July, 1954 (102 B, p. 569).
- (7) HOPKIN, A. M.: 'A Phase-Plane Approach to the Compensation of Saturating Servomechanisms', *Transactions of the American I.E.E.*, 1951, 70, p. 631.
- (8) WESTCOTT, J. H.: 'The Continuous Delay-Line Synthesizer as a System Analogue', *Proceedings I.E.E.*, Monograph No. 176 M, May, 1956 (103 C, p. 357).
- (9) DOUCE, J. L., and WEST, J. C.: 'The Application of Analogue Techniques to a Continuously Rotating Magnetic Drum', *Transactions of the Institute of Radio Engineers*, PGI-5, June, 1956, p. 107.
- (10) CZAJKOWSKI, Z.: 'Electronic Methods of Analogue Multiplication', *Electronic Engineering*, July, 1956, 28, p. 283.
- (11) WILLIAMS, F. C., KILBURN, T., and THOMAS, G. E.: 'Universal High-Speed Digital Computers: A Magnetic Store', *Proceedings I.E.E.*, Paper No. 1191 M, October, 1951 (99, Part II, p. 94).

cushion which maintains a constant gap width of about 0.0003 in, despite eccentricity. Should the drive power to the drum fail, the pulley motor actuates and withdraws the blocks.

Drs. J. L. Douce and J. C. West (in reply): Mr. Webb is correct in suggesting that a digital recording technique would increase the storage capacity. For a 100 kc/s repetition frequency 2000 digits will fill one track, so that approximately 300 spot values could be stored with an accuracy of 1%. It was considered, however, that the advantages of a simple analogue recording system outweighed the additional complexity involved in the digital coding and decoding.

A NEW CATHODE-RAY TUBE FOR MONOCHROME AND COLOUR TELEVISION

By Prof. D. GABOR, Dr. Ing., F.R.S., Member, P. R. STUART, Ph.D., and P. G. KALMAN, Ph.D.

(The paper was first received 4th November, 1957, and in revised form 17th March, 1958. It was published in May, 1958, and was read before the RADIO AND TELECOMMUNICATION SECTION 14th May, 1958.)

SUMMARY

A flat, thin television cathode-ray tube for monochrome or colour, whose thickness is only about one-quarter of its screen diagonal, has been developed by the authors to the point at which the feasibility of its essentially novel features could be tested singly, and partly in combination. In the flat tube the electron beam—and in the case of a colour tube, three beams—issuing from the same gun is launched vertically downwards. A line-deflection system imparts to it a pendulating motion in a vertical plane, and a reversing lens turns this plane by 180° , increasing the deflection angle by a factor of about 4. Just before reaching the screen region the beams are turned into the vertical direction by a magnetic collimator. The beams now enter a narrow space between the phosphor screen and a 'scanning array', consisting of parallel, horizontal conductors, arranged in a plane parallel to the screen. At a certain level the beam is thrown against the phosphor screen by an electric field, which travels downwards with the speed of the frame scan. This travelling field is produced by the beam itself, which, in the intervals between line scans, falls on the conductors of the array in a narrow zone, discharges them, and thereby pushes the field to a lower level. Recharging of the array after the frame scan is also effected by the electron beam, making use of the secondary emission of the array conductors. This is the principle of self-scanning. Colour is produced by shooting three beams on parallel lines and close together into the screen region. The deflecting field between screen and array acts as an efficient short-focus lens, and unites the three beams in one small spot at the screen, which they approach at different angles. Colour discrimination is produced by a line shadow mask about 0.5 mm only from the screen, and fixed to it by means of small, invisible bridges. This also serves as a mask in producing the colour-phosphor strips by a powder-settling process in air. The extensive electron-optical development work is described in detail, and mention is also made of special technological problems raised by the new c.r.t. design, and of their solution.

INTRODUCTION

The television set of the future, which will hang on the wall like a picture, has been for years a standing feature of imaginative American advertisements.* They started at the time when electroluminescence had its first successes, and what the copy-writers or their scientific inspirers had in mind was some electroluminescent plate, backed by the future marvels of solid electronics. Whether these glimpses of the future were truly prophetic or not, they acted as a challenge to old-fashioned vacuum electronics. We want to show that the 'telescreen on the wall', in monochrome or in colour, can be realized by a tube using electron beams, although it is a tube which has completely lost its 'tubularity'.

After a short time of development in the 1930's, the modern television tube has settled down to its present well-known funnel-shape, and has become an object of mass production. It was evident from the start that the rather revolutionary new flat tube would be more expensive in itself than the conventional mono-

chrome tube, and although this may be partly offset by savings in circuit design and cabinet costs, it appears questionable whether the public would be willing to pay the extra price just to be able to hang the television picture on the wall. What encouraged us to start the development, and the National Research Development Corporation to sponsor it, was the expectation that television was due for a revolution anyway, by the advent of colour. As will be shown in detail later, the flat monochrome tube can be changed into a colour tube with only a few modifications, very simple in comparison with the step from conventional to colour tubes, and we believe that the resulting tube will well bear comparison commercially with other colour tubes. Though colour television may not have gained as much ground as was generally expected five years ago, there can be no doubt of its ultimate overriding popularity once the public can be offered colour sets at a reasonable price, and with the same standards of safe operation as monochrome television. It is therefore fair to expect that television may be able to take two steps at once—from monochrome to colour, and from the bulging cod's eye to the flat screen on the wall.

The novelty of the flat tube resides chiefly in its unconventional electron optics and scanning mechanism, and the major part of the paper will be devoted to these. Comparatively little space can be spared for the technological problems raised by its manufacture, and its circuit design will be reserved for later publications.

At the time of writing the development has just about reached the limit to which it can be taken in an academic laboratory by postgraduate students. This is restricted not so much by the material means available as by the requirement that workers for higher degrees must keep clear of routine jobs, and be employed only on problems of scientific interest, which give them experience in original work. Development to the commercial stage must, of necessity, be left to industry.

(1) GENERAL DESCRIPTION OF THE TUBE

In conventional cathode-ray tubes, ever since the days of Ferdinand Braun, the beam approaches the screen in a straight line, like a pencil pivoted by its end. In the new flat tube, the beam is folded over on itself, and runs for most of its length parallel to the picture screen, bending towards it only on the last short section of its trajectory.*

The tube, shown schematically in Fig. 1, is an all-glass version of a colour television tube, but it will be convenient to leave the explanation of the colour production for later. The tube is essentially a flat glass box, with a depth of about $3\frac{1}{2}$ in outside, 2 in inside for a screen with 12 in diagonal. It is divided in depth by a base-plate, on which are mounted all the electrode structures, and which, in turn, is carried by four elastic metal

* It was, in fact, such an advertisement of a great American company in the *Saturday Evening Post* in 1952 which started one of the authors (D. G.) thinking about a flat tube. The first Patent Application was filed in 1952. Experimental work, under the auspices of the N.R.D.C. was started in 1953, with the assistance of Dr. Stuart, whose responsibility was the electron-optical development, while P. G. Kalman, who joined the work in 1956, was engaged in technological developments.

The authors are in the Department of Electrical Engineering, Imperial College of Science and Technology, University of London, where Prof. Gabor is Professor of Applied Electron Physics.

* Launching the beam parallel to a phosphor screen and deflecting it by an electrostatic travelling field towards the screen was independently proposed by one of the authors¹ and by the American inventor W. Ross Aiken. Apart from this basic common feature the flat tubes developed by Aiken and by the authors are different in every respect. In the Aiken-Kaiser tube, both the line and the frame scan are effected by waves travelling along a relatively small number of electrodes (10 and 7, respectively), which are driven by outside circuits. Colour is produced by two beams scanning a thin transparent double-sided phosphor screen. Particularly interesting is a completely transparent tube, fixed on the windshield of an aeroplane, which was successfully tested in flight² in August, 1957.

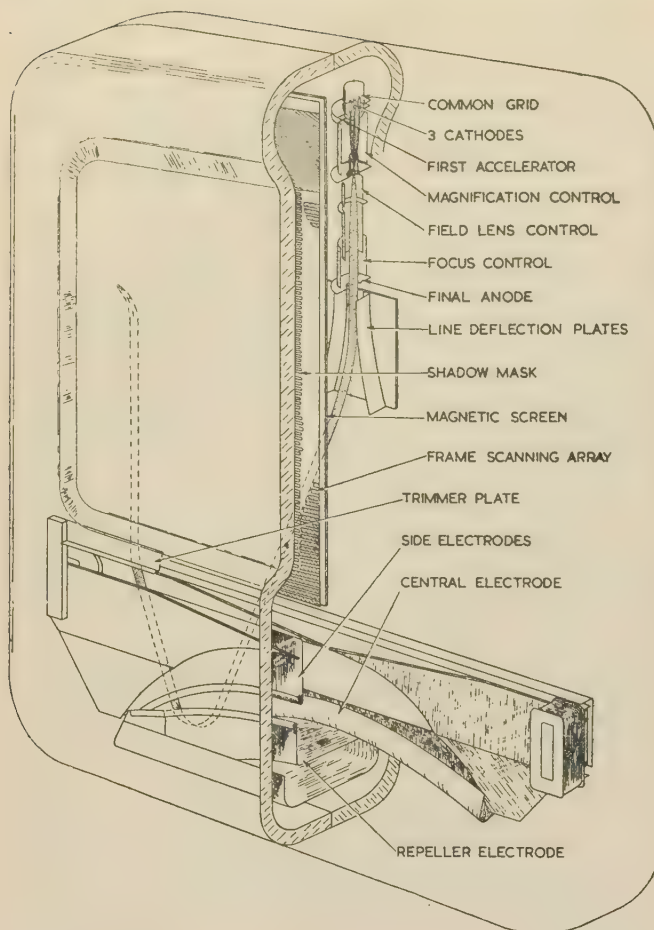


Fig. 1.—Gabor-N.R.D.C. colour television tube, all-glass version.

rods let into the joint of the two glass shells. It is preferable to make this plate of a material with high magnetic permeability, such as Permalloy, so that it may act at the same time as a very efficient magnetic screen.

The electron gun can be a conventional type in the monochrome version; the special gun for colour tubes will be described later. It is mounted behind the partition, near the top, and

launches the electron beam vertically downwards. The beam passes through the line- or X-deflection plates, so that it swings parallel to the plane of the base-plate, in the rhythm of the line scan, with an angular excursion of about $\pm 15^\circ$.

The gun and X-deflectors are more or less conventional, but the beam next passes into a new type of electron-optical element, called the reversing lens. This is a somewhat complicated electrode structure, the discussion of which will take up a good part of the paper, but for the present it will be sufficient to mention two of its many functions. The reversing lens rotates the plane formed by the fan of rays issuing from the deflector by 180° into another plane, parallel to the picture screen, while increasing the divergence angle of the fan by a factor of about 4. This means that, on leaving the reversing lens, the deflected rays sweep through an angle of about 120° . Owing to this large divergence, the beam sweeps out the whole horizontal width of the picture only a few inches above its lowest point. At this level the beam passes through another novel structure called the collimator, which is the only magnetic element in the otherwise purely electrostatic electron-optical system. This can be considered as a very powerful flat lens, which collimates the rays, i.e. it sends the beam exactly vertically upwards, into the space between the base-plate and the luminescent screen.

The base-plate carries, near its front face and spaced from it by a few millimetres, an electrode structure called the scanning array, visible in Fig. 1 and in more detail in Fig. 2. The purpose of this device is to bend the beam towards the screen at a certain level, at the same time focusing it, and to sweep this level downwards at the speed of the vertical scan.

As seen in Fig. 2, the scanning array consists of a large number (about 100) of thin linear conductors, which can be realized for instance by metal strips printed on an insulating base, and which are not connected to anything. They are charged and discharged by the writing beam itself, as will be explained later. For the present, let us assume that up to a certain level (the lowest of the group of four lines explicitly shown in the middle of Fig. 2) the conductors are charged up to the maximum positive potential V_m , which is also the potential of the luminescent screen. Up to this level, therefore, the electron beam proceeds vertically. Above a certain level (the top line of the group of four) the potential may be, say, $\frac{1}{2}V_m$, i.e. strongly negative with respect to the screen, while the four lines themselves represent a transition region. The trajectories will then curve towards the screen in this region, in a way which is shown in full detail in Fig. 3, obtained by field mapping in the electrolytic tank, and by

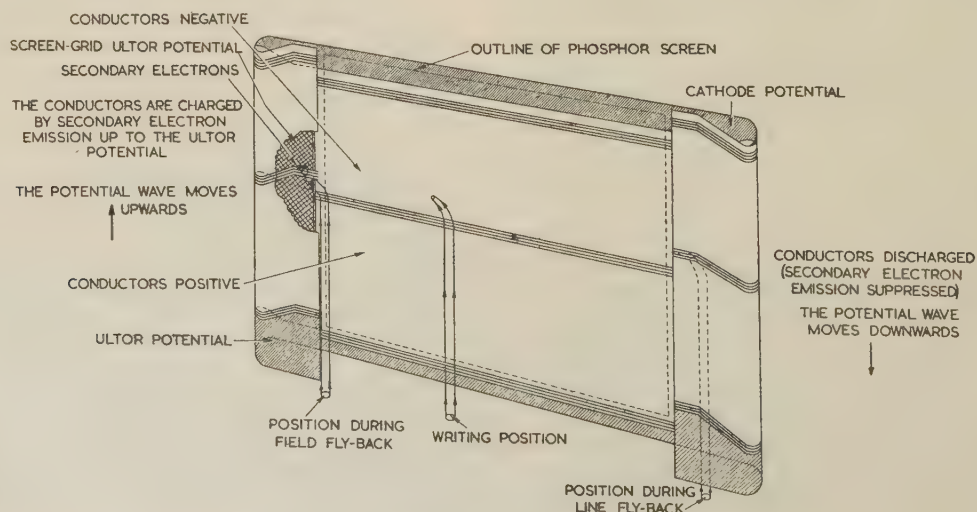


Fig. 2.—The principle of self-scanning by writing beam.

graphical trajectory plotting. It is seen that the beam is not only bent but focused; this is the effect of 'deflection focusing', which is well known in television tubes as a serious disadvantage of electrostatic deflection, and is here made to serve a useful purpose. We will deal with it later in more detail, since it is the basis of colour production in the flat tube.

(2) THE SELF-SCANNING PRINCIPLE

Fig. 2 illustrates also the second function of the array—the vertical or frame scan which is effected by the writing beam itself. The scanning array forms U-shaped loops at both sides of the picture area, and in this region the conductors are slanting upwards, terminating in horizontal sections, which are staggered upwards by a certain amount relative to their long, horizontal central sections. As long as the beam remains inside the picture area, the charge of the conductors remains unaltered, and hence the spot describes an exactly straight horizontal line. But when a line scan is finished, the beam moves into the loop at the right-hand side, and here, if the stagger is properly dimensioned, the beam will spray one or several conductors in the transition region. The area opposite this is at a lower potential and acts as a suppressor of secondary electrons. In consequence, the sprayed conductors are discharged by the full amount of negative electron charge which they collect from the beam. This causes the transition region to move downwards, and hence the next line sweep of the spot will be at a somewhat lower level. If the beam current during the time between two line sweeps, while the beam rests in the loop at the right, is properly dimensioned, the spot will move down just by a step of the desired length.

It remains to be shown that conditions can be found such that the discharge wave moves downwards not only at the right speed, but without distortion, i.e. the process described is stable, and moreover that, by suitable choice of the stagger, the stable discharge wave can be made to have the right sort of profile required for effective focusing of the writing beam. This was verified experimentally, and a mathematical discussion is given in Appendix 12.4.

When the beam has run down and the array is discharged, it is recharged again by the writing beam. This is done by stopping the line scan and moving the beam into the loop at the left-hand side. This differs from the other loop by a somewhat larger stagger and by the presence of a screen grid between the beam and the terminal portion of the array. This screen grid is maintained at the maximum positive potential V_m , called the 'ultor' potential, and therefore acts as a collector of secondary electrons. If the secondary yield, δ , of the array conductors exceeds unity, the effect is as if $\delta - 1$ positive electrons had landed on it instead of one negative electron, and the conductors charge themselves up gradually to the screen-grid potential V_m , while the beam moves upwards, to the top.

A metal strip called the 'C-plate' is arranged at the top, and maintained permanently at a level near cathode potential. When the new frame starts, the line scan is switched on again, and the beam moves from the region of the screen grid into the region of the C-plate, which throws it against the luminescent screen. The C-plate is at such a distance from the top conductor that the scanning wave is, as it were, 'preformed', so that the run-down can start automatically, with the right waveshape and at the right speed. Interlacing is effected by giving the C-plate somewhat different potentials in alternate frames, so that the scan starts at levels differing by a line spacing.

An essential element in this self-scanning process is the good secondary emission of the array conductors in the section facing the screen grid in the left-hand loop. As television tubes are operated with voltages of 12–25 kV, and the best known secondary emitters have 'sticking potentials' of 12–15 kV, this

might appear a very serious difficulty. In fact, it appeared so serious that rather complicated schemes were evolved for spraying the conductors with slower electrons, and also for recharging them by photoconductivity or by bombardment-induced conductivity. Fortunately these fears were unfounded. The data for secondary emission usually given in literature relate to normal incidence. The angle of incidence makes little difference with rough surfaces, such as fluorescent powders or magnesium-oxide smoke, but a very great deal for polished surfaces. Roughly speaking an electron of energy W incident at an angle θ to the normal releases a comparable number of secondary electrons to an electron with perpendicular incidence and an energy $W \cos^2 \theta$. Hence an electron of 20 keV energy incident at 60° is roughly equivalent to a 5 keV electron. There exist a fair number of suitable materials which have secondary yields well above unity at 5 keV 'perpendicular energy', and the incidence can be easily made very oblique. We will return to this question later in connection with the technological problems of the flat tube.

(3) COLOUR CONTROL

It may be seen in Fig. 3 that a vertical collimated beam filling one-third of the spacing, Y , between the array and the screen is concentrated by deflection focusing into a narrow region of about $0.12Y$ vertical width, in which the marginal rays arrive with a convergence angle of 30° . If the beam, instead of being collimated, is made slightly convergent (prefocused), the vertical spot width can be reduced to $0.05Y$, with only an insignificant decrease of the convergence angle, as has been verified experimentally.

A convergence angle of the order of 30° or 0.5 rad is quite unusual in cathode-ray electron optics; even projection tubes

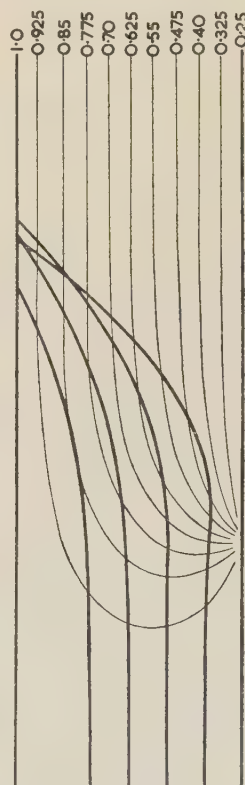


Fig. 3.—Focusing of parallel electron trajectories between an equipotential phosphor screen and a scanning array at distance Y by a wave of base length $Y/12$, which discharges the array from the screen potential V to $0.25V$.

Focusing satisfactory in the zone between the 2nd and 4th ray from the left.

have convergence angles of, at the most, 0.05 rad. The reason is that, in the flat tube, the spot is carried along, as it were, by a short-focus cylindrical lens, close to the screen, while, in conventional tubes, the focusing is effected by the electron gun, at a large distance from it.

This is the basic advantage of the flat tube in colour television, and Fig. 4 illustrates schematically how this advantage may be

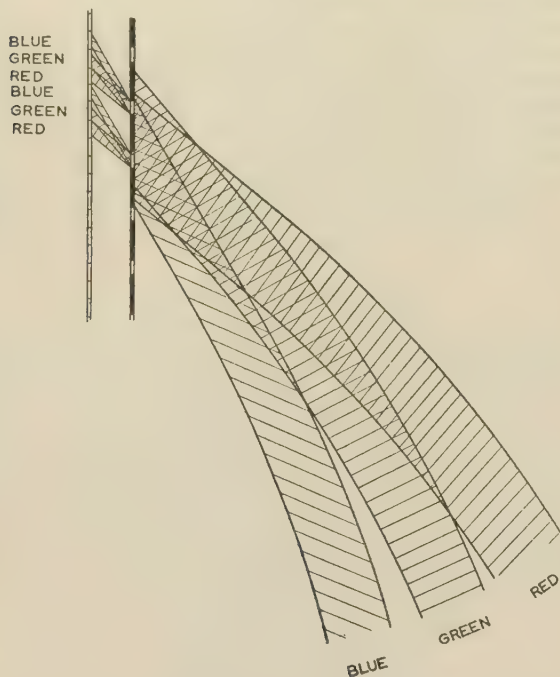


Fig. 4.—Colour production by means of a shadow mask in the flat tube.

The spacing between the phosphor screen and mask is somewhat less than the spacing of the slits in the mask.

utilized. A shadow mask, which is essentially a plane metallic structure with evenly spaced horizontal (or nearly horizontal) slits, is placed before the screen, which carries a system of phosphor strips in the three fundamental colours, red, green and blue, with one colour cycle per slit. The phosphor strips are so arranged that, at a certain angle of incidence, or near it, the electrons excite only one colour.

This principle is well known, and has been widely utilized in existing colour tubes. The advantage of the flat tube is in the dimensions. In the conventional colour tubes, in which three beams produced by three separate guns converge at an angle of about 6° to one another, the distance of the shadow mask from the screen must be made about $\frac{1}{2}$ in. In the flat tube, with incidence angles between 30° and 60° the distance is $\frac{1}{40}$ in or even $\frac{1}{50}$ in. Therefore, while in the existing shadow-mask systems, the shadow mask has to be fixed, with elaborate precautions, independently of the screen but in accurate register with its line or dot pattern, in the flat tube it becomes possible to fix it on the screen surface itself, thus eliminating all possible distortions of the mask. Moreover, it now becomes possible, for the first time, to stick the shadow mask on the screen first and produce the phosphor lines behind it in automatic register with the slits, by a simple method which will be explained later.

There also exists a second possibility for exploiting the advantages of the flat-tube electron optics for colour production. It has been often proposed to use composite screens, formed by the superposition of three layers of colour phosphors, utilizing the different penetration of electrons of different energies for

differential excitation of the three colours. These suggestions failed for two reasons. First, it is practically impossible to focus three beams with energies of, say, 5, 10 and 15 keV simultaneously on all points of a television picture. The electron-optical problem is not so difficult in a sequential system, but frame-sequential systems are ruled out by their bandwidth requirement, and a point-sequential system in which the gun, or a fine grid near the screen, is modulated with a swing of ± 5 keV in point sequence requires a high-frequency power supply of prohibitive size. Secondly, the effect itself is so impure as to be practically non-existent so long as powder screens are used, with the usual grain sizes of at least a few microns, i.e. about the total penetration depth of 15–30 keV electrons.

The first difficulty does not arise in the flat tube. To a reasonable approximation the penetration depth of a fast electron is determined by its velocity normal to the surface. If the angle of incidence is θ the equivalent energy is $W \cos^2 \theta$. If we assume that $W = 20$ keV and the incidence angles of the three colour-beams are 30° , 45° and 60° , respectively, this gives equivalent (normal) energies of 15, 10 and 5 keV, and the coincidence of the three beams at the screen is, of course, ensured.

There now exists at least a possibility that the second difficulty may also be overcome, since Feldman and his collaborators³ have succeeded in producing grainless luminescent films by evaporation with very even thicknesses of the order of 1 micron, and have successfully demonstrated a two-colour screen, in which both colours could be fully saturated by a voltage swing of 4–8 keV. These almost fully transparent screens have also remarkable contrast; the picture can be viewed in a room illuminated so brightly that a picture on a powder screen becomes completely invisible. However, there are some serious disadvantages. The present method is slow, since it requires lengthy baking after evaporation at temperatures which require the use of quartz or Vycor glass. Moreover the luminous efficiency of the transparent layers is about one-fifth of that of a powder screen of the same material, because the major part of the emitted light remains imprisoned in the thin layer, owing to its high refractive index. Nevertheless, a method of producing colour-television pictures without any shadow mask or other structure before the screen, and which at the same time allows pictures to be viewed in bright rooms, is too attractive to be dismissed out of hand, even if it gives an efficiency somewhat lower than that of the shadow-mask method.

(4) THE ELECTRON-OPTICAL REALIZATION OF COLOUR CONTROL

The electron optics of colour control in the flat tube is illustrated in Fig. 5, which is a section of the tube in the symmetry plane $X = 0$. It is best to look first at the left-hand side, in order to realize the conditions imposed on the system. The central rays of the three colour beams, which will be called principal rays, are shown to run vertically upwards, equally spaced from one another. They are then brought together by the deflecting field of the array in a rather small spot. As was mentioned before, this is not the ideal system, since slightly convergent principal rays give a smaller spot, but this is of little importance, for two reasons. First, as is well known, only the definition in the basic colour green need be high; the red and blue pictures need not be equally sharp. This fact is taken into account by giving them narrower wavebands in the simultaneous system. One should therefore make the central ray green. But over-sharp focusing might give moiré effects with a shadow mask, if the spot were so narrow that it could be completely obscured by the mask. It is therefore better not to focus either of the beams too sharply, but to give them a final width at least equal to a period of the mask. On the other hand, in order to

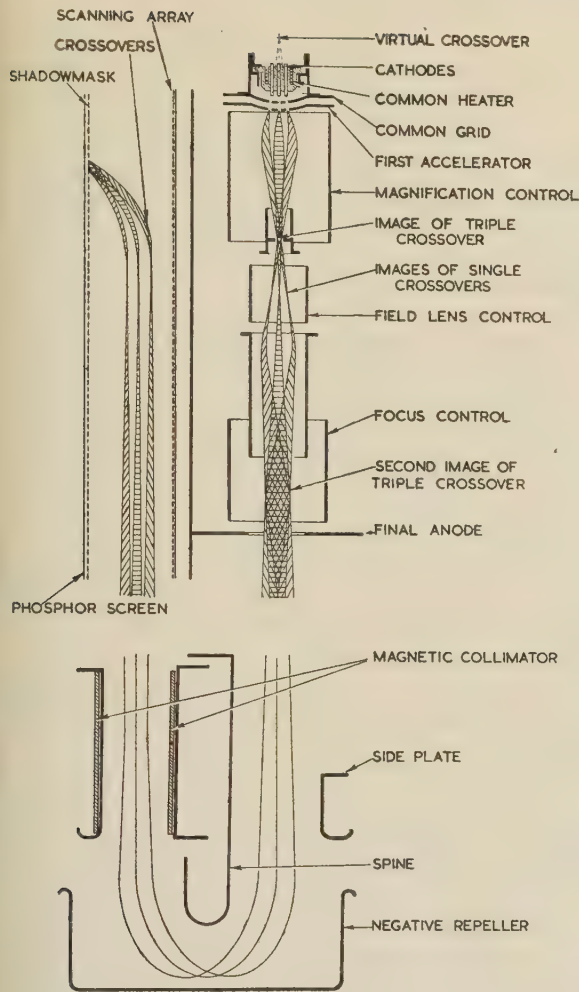


Fig. 5.—Electron optics and colour control.

ensure colour purity, it is advantageous to let each colour beam be collimated in itself where it strikes the shadow mask, so that each has a definite incidence angle. This is achieved, as shown in the Figure, by focusing the three beams not on the screen but a little before it, and near the rear focus of the deflection lens.

Defocusing for the avoidance of moiré effects does not mean a sacrifice of definition, because, as will be shown later, the shadow mask and the phosphor screen can be made with a much finer period than in other colour tubes. We have realized shadow masks with 50 lines/in (150 colour strips per inch) which gives nearly 400 lines in a tube with a 12 in diagonal and about 550 lines in a 20 in tube. This would be sufficient for 625 transmitted lines for the first, and about 1000 lines for the second size, because, in interlaced pictures, the effective definition is not more than about 60% of the nominal.

We can now formulate the conditions to be fulfilled by the electron-optical system consisting of gun, X-deflectors, reversing lenses and collimator as follows. This system must launch the principal rays of the three colour beams vertically into the space between the screen and the array, in three predetermined equidistant planes. These remain stationary during the scanning process (apart from minor corrections for achieving optimum convergence, which may be left out of consideration), while the focal points of the three colour beams slide down in them with the speed of the frame scan.

While the problem of colour convergence, which presents such

great difficulties in the known three-gun shadow-mask tubes, is solved almost automatically in the flat tube, the achievement of colour purity imposes stringent conditions on the perfection of the optics. We have made these conditions even more stringent by postulating from the start that the correction of electron-optical errors must not be left to the circuit engineer, as it is in conventional shadow-mask tubes ('dynamic convergence'), and that the number of trimming devices corresponding to the numerous small correcting magnets now attached to the neck of colour tubes must be reduced to a minimum. Moreover we have set ourselves the task of making the magnetic screening good enough to avoid adjustments *in situ*, so as to reduce the servicing problem, which has proved such a hindrance to the spreading of colour television, and to avoid the necessity of using highly-stabilized power supplies.

Fig. 5 shows how these conditions are met in the central, $X = 0$, plane. The three-colour gun has three cathodes side by side, located in an insulating body, with a common heater. This feature makes it easier to use impregnated high-density cathodes in place of the common coated ones, and it also makes it possible to arrange another couple of cathodes spaced at right angles to the plane of the drawing. These may be used for the flyback, which requires a stronger current than the picture, and, apart from the saving in life time, such separate flyback cathodes have advantages from the point of view of the circuit engineer.

The three cathodes face a common grid and a common accelerator. Modulation is achieved by applying the signals to the cathodes, not to the grid. The grid and the accelerator are both spherically curved, so that the axes of the three beams diverge from an intersection point, called the virtual cross-over. The grid apertures are preferably oblong-shaped or elliptical, with the major axis in the plane of the drawing. This is because the magnification of the cathode on the screen is smaller in the vertical than the horizontal direction, and hence, in order to achieve a round spot, the effective area should be elliptical.

For the convenience of the circuit designer, all potentials used in the gun are either equal to the maximum or ultor potential V_m , or within 5% of V_m from the cathode potential. The first accelerator has a potential of $0.03-0.05V_m$, and emits three beams with axes divergent by a total of about 0.25 rad. From this point onwards the gun is rotationally symmetrical. The beams enter an accelerating lens, consisting of a large-diameter tube which is called the 'magnification control' because the angular spacing of the three beams issuing from the gun can be controlled to a certain extent by varying its potential in the limits $0-0.05V_m$. The other electrode of the accelerating lens is a small-diameter tube, containing a stop, which trims off the outer 'halo', and transmits only the inner portions of the three beams, not too wide to be handled without appreciable aberrations by the final lens.

For the convenience of the circuit designer we are using a final lens of the usual single-lens type although it is well known that its spherical aberration is appreciably larger than what can be achieved in the same space by a lens of the accelerating type. Such a lens, if it is not made larger than usual, can handle one beam with fairly small spherical aberration, but not three divergent beams. We therefore found it necessary to insert between the stop and the final lens a 'field lens', also of the single-lens type, whose purpose is to produce an image of the stop in the middle of the central electrode of the final single lens, called 'focus control' in the Figure. Thus the cross-section filled by the three beams in the last lens is not appreciably larger than that required for a single beam, and the aberrations become correspondingly small. There is, however, another important advantage achieved by this arrangement. As the second image of

the triple cross-over is in the centre of the final lens, variation of the potential of the control electrode of this lens will not affect the principal rays at all, but will only make the foci glide up and down on these rays which themselves remain fixed. This is just what is required by the optics of the flat tube in the screen region, as we have explained above. Once the principal rays are properly adjusted by the magnification control, they remain fixed, and only one potential, the voltage of the focus-control electrode, need be varied in accordance with the height of the writing spot, in the rhythm of the frame scan.

One could derive this focusing voltage (in the limits $0.02-0.05V_m$) from a multivibrator synchronized to the frame signals. But as the self-scanning principle of the flat tube makes a field-scan multivibrator unnecessary, it would be wasteful to introduce it just for the focusing. Fortunately there is no need for it, as one can derive a suitable signal very readily from the scanning array itself, by coupling it capacitively with a vertical metal strip earthed through a suitable resistance. This will take on a charge opposite in sign and proportional to that of the array, so that its potential will follow a sawtooth curve of the right frequency, which can be directly used for focusing.

The three colour beams leave the gun in slightly diverging directions and after passing the X-deflectors, not shown in Fig. 5, they enter the reversing lens, shown in a central cross-section. The reversing lens consists of three positive electrodes called the 'spine' and the front and rear side-plates, all three at V_m , and a negative, trough-shaped electrode called the 'repeller' at cathode potential. A detailed discussion of it will be given in the next Section. For the present, it is sufficient to note the task set for the reversing lens. It must turn round the central ray by 180° , and must produce such a divergence or convergence between the two side rays that, after passing through the collimator, all three rays emerge parallel and vertical. The collimator is a positive, converging lens in the plane at right-angles to Fig. 5. In the plane $X = 0$ it acts as a diverging lens, and hence the principal rays must leave the reversing lens with a certain small convergence in order to be ultimately collimated. It will be shown later that, off the central plane, the divergent effect of the collimator decreases and changes sign, so that the reversing lens must, in fact, satisfy different conditions in different zones.

(5) THE REVERSING LENS

It can be understood from the foregoing explanations that the reversing lens is the most crucial device in the flat tube. Not only must it produce a family of principal rays to very exacting specifications, but almost the whole burden of correcting the focusing errors arising in the other electron-optical elements is thrown on it. We have refused to contemplate correcting electron-optical errors by suitable modulation of potentials ('dynamic focusing') in the belief that the simplification of circuit design will ultimately compensate for the time of development, which took over three years.

This is the list of conditions imposed on the reversing lens:

- It must rotate every principal ray issuing from the line deflector by 180° around a horizontal axis.
- It must increase the deflection angle of every principal ray by a factor of about 4. This was dictated by considerations of the saving in line-scanning circuits, and also by the consideration that electrostatic deflection by more than about $\pm 20^\circ$ would produce focusing errors which are almost unmanageable.
- After these two rotations the principal rays must again be contained in a plane.
- The final X co-ordinate must be a linear or very nearly linear function of the line deflection voltage.

These four conditions relate to the principal rays (in the case of three-colour tubes to the *central* principal rays). The others concern the focusing properties of the system, relative to these

principal rays considered as curved optic axes. It is convenient to separate these into X and Y conditions, i.e. to focusing in the plane of the principal rays and at right-angles to it. At the screen these turn into horizontal and vertical focusing conditions respectively. It is proved in Appendix 12.2 that a ray which originally in the plane of the principal rays remains in it permanently, and that a ray which departs from a principal ray in the direction at right-angles from this plane remains permanent in a strip at right-angles to it. In other words, there is no skewing of axes in the first-order approximation, which is a great advantage of electrostatic systems as compared with magnetic ones.

(e) At a set focus of the electron gun, the X-focus must remain permanently on a horizontal line, so that no 'dynamic' adjustment of the gun potentials is required during a line scan.

(f) In the Y-direction the second-order aberration of narrow pencils centring on a principal ray must be zero. This condition must be imposed not so much in order to improve the vertical focus of the beams, which is almost automatically of good quality, but in order to ensure that the red and blue colour axes are equidistant at the two sides of the green axes.

(g) The third-order Y-aberration must be as small as possible. This condition is important chiefly because, since space is restricted, it is desirable to make the dimensions of the reversing lens in the direction at right-angles to the picture as small as possible, and hence it is necessary to fill a considerable part of its aperture with electrons.

(h) In the Y-direction the reversing lens, in tandem with the collimator must (i) focus the cross-over of the three colour axes at the gun at infinity, i.e. turn these axes into parallel lines which (ii) must have the same spacing independently of the X-deflection.

This double condition is the most exacting, and it was the most difficult to meet. Once realized, it has several important advantages. If condition (h)(i) is met the field lens in the gun can be set once and for all, i.e. the cross-over can be fixed without a 'dynamic' adjustments. If (h)(ii) is met, the same applies to the magnification control, which regulates the spacing of the colour axes. The complex of the three colour beams will have exactly the same configuration at every point of the picture, so that the colour strips have the same relation to the slits in the shadow mask all over the picture and no complicated 'grouping' of the phosphor areas is necessary to compensate for varying angles of incidence as in other colour tubes.

Moreover, once a reversing lens satisfies conditions (h)(i) and (ii) it meets also, with sufficient accuracy, the equally important condition that no dynamic correction need be applied to the focusing electrode of the electron gun during a line scan.

We could list as a tenth and last condition the requirement that the reversing lens must operate irrespective of fluctuations of the voltage supply. This condition is exactly satisfied with grid-modulated guns, since the reversing lens is a unipotential system with electrodes which are either connected with the cathode, or at ultor potential. It is not exactly met in the case of cathode modulation, which has considerable advantages for the gun design, but we have found that, with a grid base of not more than 0.5% of V_m , it is sufficient to keep the repeller at the mean cathode potential.

Instead of discussing conditions (a)-(h) in the order in which they are listed, it will be more convenient to follow the line which we took in the development. We started from the central plane $X = 0$, and after having obtained suitable electrode profiles in this plane, we proceeded outwards.

Fig. 6 is a cross-section in the central plane of a reversing lens showing the equipotentials and a set of electron trajectories. We started, as first approximation, with cylindrical fields (independent of the co-ordinate at right-angles to the drawing) which were obtained from electrolytic tank plots, and after having obtained a satisfactory cross-section, applied the rather small correction to the field which arise from the curvature of the lens. In the

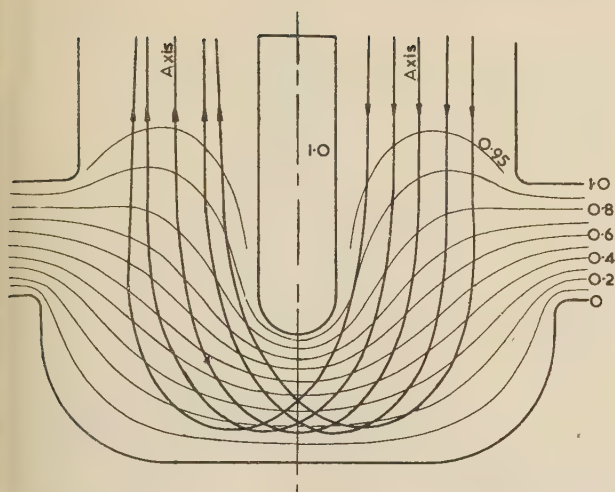


Fig. 6.—Electron trajectories in the central cross-section of the reversing lens at telescopic adjustment, showing positive third-order aberration.

field maps we plotted the electron trajectories with a tracing device of the kind described by Gabor⁴ and Hollway⁵ but not an automatic one.

A reversing lens, consisting of the central positive electrode called the 'spine', the two positive side-plates and the negative repeller can be made convergent or divergent by varying the distance of the repeller from the positive electrodes. It is divergent if the distance is small, and convergent if it is large. Fig. 6 illustrates the position in which the lens is telescopic, i.e. in which it converts a parallel incident pencil of rays into a parallel outgoing pencil.

Making the cross-section symmetrical to a vertical ($Y = 0$) axis brings with it an automatic advantage. There must exist it (within certain limits of design) a trajectory such that it cuts the vertical-symmetry axis at right-angles and runs asymptotically parallel to it, at equal distance from it at both sides. It was one of the first objectives of design to bring this special trajectory, which can be considered as a curved optic axis, into a convenient position near the centre of the clearance between the spine and the positive electrodes.

When the lens is telescopic it is easy to see that this curved axis has a property similar to that of the straight optic axes in cylindrical electron lenses; narrow pencils close to it have no resulting second-order error, i.e. they are symmetrical at the exit if they were symmetrical at the entrance [condition (f)]. This can be easily understood from the fact that the optic axis intersects the vertical-symmetry axis at the lowest point; all other trajectories intersect it higher up. There is therefore a strong second-order error at and near the focus. This is an advantage from the point of view of space-charge effects, because at this point the electron beam passes through its lowest potential, and high concentration might lead to defocusing. It is also an advantage that the focus is a line focus, and not a point one. Ultimately, however, the second-order error cancels out. In a sufficiently narrow bundle, two trajectories parallel and equidistant to the optic axis at the entrance, at both sides of it, will intersect the vertical-symmetry axis in the same point, and at equal and opposite angles to the horizontal. Since the lens is, by assumption, telescopic, the rays will leave the lens parallel to the optic axis and at equal distances from it, because the outer trajectory at the right-hand side continues at the left as the inner trajectory at the right-hand side and vice versa. There exists an optic axis in this sense also for reversing lenses

which are convergent or divergent, but the property is not so easy to understand, because there is then no left-right symmetry in the trajectories, and the optic axis will not necessarily turn round by exactly 180° . One can then meet the two conditions (a) and (f) together by giving the incident beam a small deflection, e.g. by applying a small voltage difference between the rear positive electrode and the central spine, or by skewing the repeller a little. By using both means, one can then place the outgoing beam both in the right position and in the right (vertical) direction.

Not only must the curved optic axis with zero second-order error be in the right position, but the third-order error must be small. The third-order error is of the type of the common 'cylindrical aberration'. One can analyse these errors in the way illustrated in Fig. 7, in which the emergence angles dy/dz

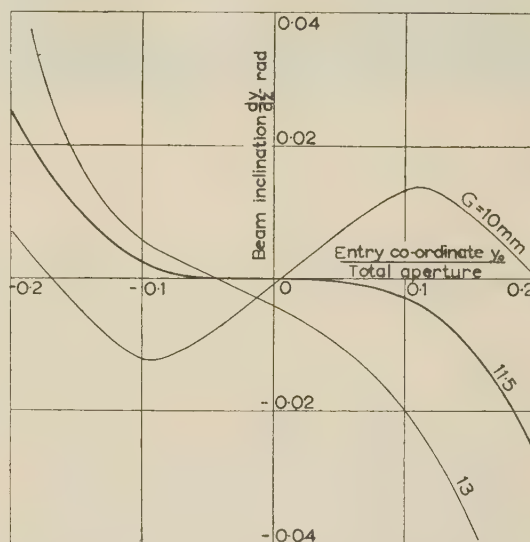


Fig. 7.—Inclination of the rays at the exit plotted against the position at the entry, at parallel incidence, for several gaps in the central cross-section of a reversing lens.

are plotted against the distance y_0 from the vertical symmetry axis at the entrance, for a family of lenses differing in the gap widths G . A point of inflection indicates the position of the optic axis, an upward slope at this point meaning a divergent lens, and a downward slope a convergent lens. The departure of a plot from a straight line, so far as it is expressible by a cubic parabola, represents the third-order error or cylindrical aberration. This has been found remarkably independent of the gap width g , and hence it is essentially given by the electrode shapes, independently of their adjustment. We have carried out graphical tests on a great variety of shapes until we adopted the profiles shown in Fig. 6. These remained unchanged throughout two further years of development until we found, quite recently, that the third-order aberration can be appreciably reduced by using a T-shaped instead of a U-shaped central positive electrode.*

Meeting the conditions outside the central plane $X = 0$ required considerably more work. We were faced here with 3-dimensional electron-optical problems, and 3-dimensional ray tracing in electrostatic fields, although feasible, is very time-wasting. Mathematical analysis was used to some extent for exploration in advance, but only in broad outlines; all quantitative material was collected from experiments on models in demountable tanks, one of which is shown in Fig. 8. This was equipped with movable luminescent screens, allowing the accurate

* This was obtained in co-operation with M. C. S. Upadhyay on leave from the Indian Institute of Science, Bangalore.

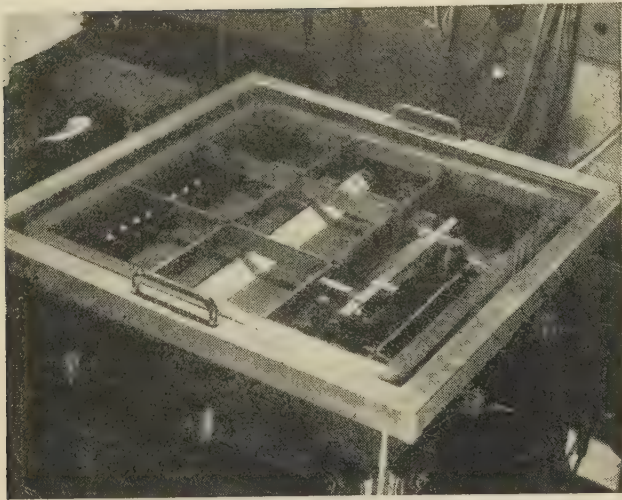


Fig. 8.—View of one of the demountable vacuum tanks in which the electron optics of the flat tube was developed, showing a movable phosphor screen and a repeller suspended in a frame with four degrees of freedom.

location of the electron rays before entering the reversing lens, and after leaving it. Guns with pepperpot apertures were used in many of these experiments, so that a principal ray and its accompanying pencil of rays could be tracked simultaneously. The tanks were fitted with means for moving the electrodes about without breaking the vacuum, and in some cases also for deforming them. Up to eight independent movements were used in some experiments. Even with these powerful aids almost 100 electron-optical arrangements of deflectors, reversing lenses and collimators had to be measured out, singly and in combination, before all the requirements were satisfied.

Condition (b), which relates to the magnification of deflections by the reversing lens, is illustrated in Fig. 9, which shows the projection of the family of principal rays on the picture plane (XZ-plane) traced from the line deflectors, with deflection centre C, through the reversing lens and collimator. The straight tangents of all rays have been measured and the curved portions are interpolated.

We specify the optical properties of the reversing lens for the family of principal rays by means of two curves. One is the intersection line I-I, in which the initial and the final rays intersect. Experience has shown this to be a very nearly straight line in almost all reversing lenses. The second curve is the envelope of the final rays, mMm , which is a curve with a cusp. In order to construct the final ray corresponding to any initial rays passing through the deflection centre C one has only to extend this to I-I and draw a tangent to mMm from the intersection point. There is also a second curve which one can use for the specification, i.e. the envelope $o-O-o$ of the bisectors of the original and final rays. This again is a curve with a cusp O. The interest of this curve lies in the fact that, in all reversing lenses with otherwise rather widely differing properties in which the spine and the bottom of the repeller trough were concentric, the experimentally found bisector centre O coincides very accurately with their centre. This, of course, would have to be exactly the case if all the electrodes were coaxial with an axis passing through O at right-angles to the plane of the drawing, because, in that case, there would exist an exact angular-momentum integral relative to this axis, and hence the bisector would have to pass through it. The experiments have shown that this remains true to a good degree of approximation in reversing lenses in which only the two profiles shown in the drawing are

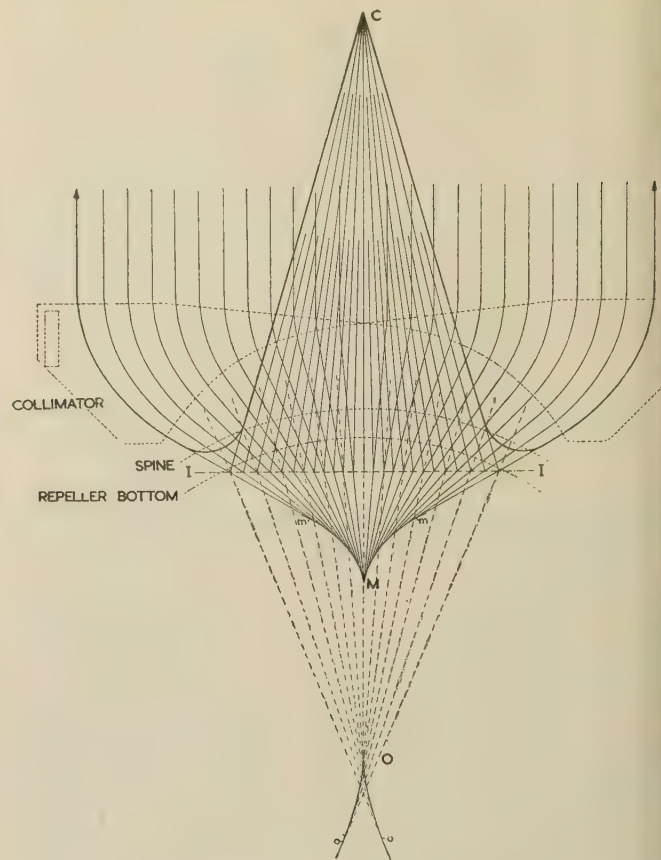


Fig. 9.—Projection of the principal rays on the picture plane. C is the centre of the X-deflection system.

concentric, while the profiles of the positive plates, for instance, are far from coaxial. This property will now be used in the practical theory of X-focusing, illustrated in Fig. 10.

In this theory it is assumed that a narrow pencil of rays intersecting I-I near a point P will be ultimately reflected, as it were, from an equivalent cylindrical mirror passing through P with its axis passing through O on the envelope of bisectors. This means that we assume that an angular-momentum integral exists relative to the axis O', not only for the principal rays, but also for all other rays sufficiently close to them. This is certainly a reasonable approximation, and appears to be well supported by experiment.

Using the well-known laws of reflection on a cylindrical mirror, we can now work out the locus of the points F in which the pencils coming from the deflector must be focused if they are to be collimated after reflection. It is seen that this locus, the line FF, is a little inside the circle drawn concentric with the deflector with means that one can allow a certain small amount of deflection over-focusing. We will return to this question later.

It is shown at the right-hand side what happens to the collimated pencils after emerging from the reversing lens. The collimator is, by definition, so dimensioned that it turns every principal ray into a vertical line. This is equivalent to the statement that every narrow sector of the collimator has its focus at C', the line in which the principal ray is tangential to the M-line. One can consider C as the image of the deflection centre C formed by the reversing lens, but by principal rays only.

It is therefore legitimate to replace the collimator in every narrow sector by a small prism, which accounts for the rotation

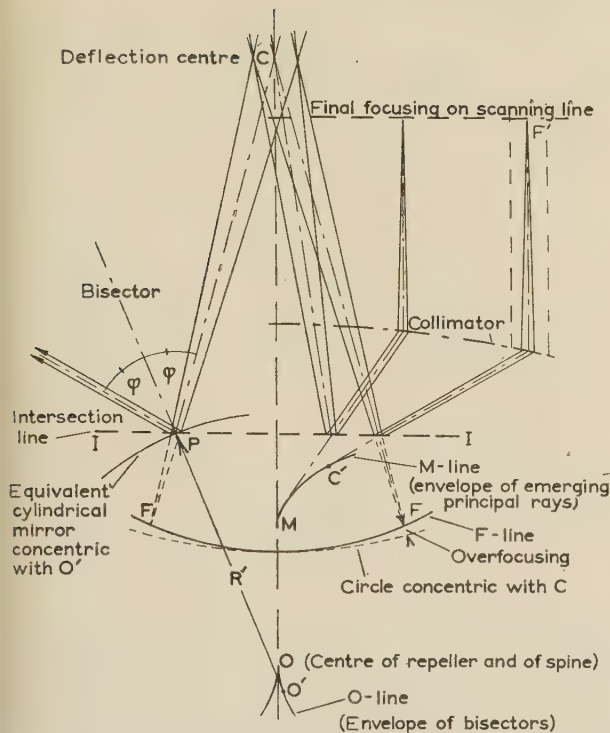


Fig. 10.—Illustrating the theory of the correction of the X-errors produced by the X-deflection system by the reversing lens and collimator.

of the principal ray, plus a small condensing lens with its rear focus in C' , both prism and lens being located in the somewhat curved line in which the initial and the final principal rays intersect. It follows that, if a collimated narrow pencil falls in the collimator, it will be focused on a vertical line, in a point F' which is at the same distance from the collimator curve as this is from C' . It so happens that the combination of the M-line and the collimator line results in a practically straight and horizontal locus for the final X-foci F' . This is a rather fortunate circumstance, because the collimator curvature was originally arrived at from different considerations.

This Figure only shows that the locus of the X-foci can be straightened out for a certain scanning line, near the middle height of the picture. Other loci will not be perfectly straight, but no excessive accuracy is required, as the convergence angle of the beams in the XY-plane is rather small. This is a consequence of a general theorem of optics, which states that, at a given refractive index (given electron energy), magnification of an image in a ratio M has to be paid for by a reduction of the convergence in the ratio $1/M$ (see Appendix 12.2). By means of the reversing lens we have magnified the X-dimensions in such a way that, with a primary deflection of about $\pm 15^\circ$, we can cover an image, say 12 in wide, with a longitudinally strongly shortened system. Because of this optical theorem, the convergence angle will be the same as if we had obtained the image directly, i.e. by placing the deflection centre about 24 in from the image. The somewhat surprising fact should be noted that, from the same theorem, the convergence angle will not change at all while the scanning sweeps from the top of the picture to the bottom. The same applies, perhaps more obviously, to the convergence angles in the YZ-planes. Therefore, in principle, all image points in the flat tube can have the same quality and the same spot size. Inaccuracies in the realizations and aberrations will, of course, in general favour the areas near the bottom of the picture.

It is now opportune to explain that the term 'lens' can be legitimately applied to such an unusual structure as the reversing lens. It is indeed a lens, but with a one-dimensional field; it images the line FF with a stop at C at infinity. The term would have been less legitimate if this imaging had been obtained by 'dynamic focusing', since the line FF could not then have been simultaneously imaged.

It is clear from Fig. 10 that an exactly straight locus of X-foci can be produced only if the deflection over-focusing has a certain positive, but very small, value. We must now explain how we have achieved this by suitable shaping of the line deflectors and the consequences this has for the remaining design problems of the reversing lens.

It is well known that the cylindrical electrode pairs used in cathode-ray tubes have considerable deflection over-focusing. If θ is the deflection angle, the effect is as if, in addition to a prism which achieves the deflection, the deflector contained a positive lens with a focal power

$$1/f_x = A_x \theta^2$$

where A_x is the coefficient of deflection astigmatism in the x-direction. Its value in not too long deflectors is approximately $2/L$, where L is the length of the deflector plates. For $\theta = 15^\circ$, f_x is about $8L$, but for $\theta = 30^\circ$ it drops to $2L$. Moreover, the deflecting voltage required increases approximately as θ^2 , because the plates must be spaced apart, about proportionally to θ . This is the reason why television tubes with electrostatic deflection dropped out of the race 20 years ago when the shortening of television tubes started.

For economy in the deflecting voltage we have limited the maximum deflection of $\theta = \pm 15^\circ$ which can be achieved with about $\pm 0.1 V_m$, or $0.2 V_m$ (peak to peak). But even at this rather small angle, the deflection over-focusing is almost ten times larger than that required by optimum X-focusing, as illustrated in Fig. 10. However, in the flat tube the deflectors are used for one direction only (for the line scan), and they need not therefore be cylindrical. As was first shown by Recknagel,⁶ for a deflecting system of given length which is non-cylindrical, we have the relationship

$$(A_x + A_y) \geq 2/L$$

and the minimum can be very closely approached. We can therefore exchange focusing in the direction of deflection, x , for focusing in the direction, y , at right-angles to it. In particular, we can eliminate the deflection over-focusing altogether, at the cost of additional focusing in the y -direction.

Fig. 11 illustrates a series of deflecting systems which have been investigated, and from which we have made our final choice. The cylindrical system (a) is useless, because of its strong deflection astigmatism, and also because, in the restricted space available in the flat tube, it does not provide sufficiently safe screening from external fields. System (b) provides good screening, but its effect has the wrong sign, the X-focal power is enhanced, and negative Y-power is produced. We experimented with this design at a time when we had difficulties in meeting conditions (h)(i) and (ii). The negative Y-power of the deflector had the right sign for compensating the errors of the early reversing lenses, but the X-errors were inadmissible. Finally we chose (c), which has shallow channel-shaped deflectors, covered top and bottom with plates at mid-potential. This could be dimensioned so as to reduce A_x to a small fraction of the value $2/L$, or even to zero. At the same time A_y becomes rather large, but this is an aberration small enough to be compensated by the reversing lens.

We have explained how the reversing lens must be designed to compensate for the X-errors all over the field. This is mainly

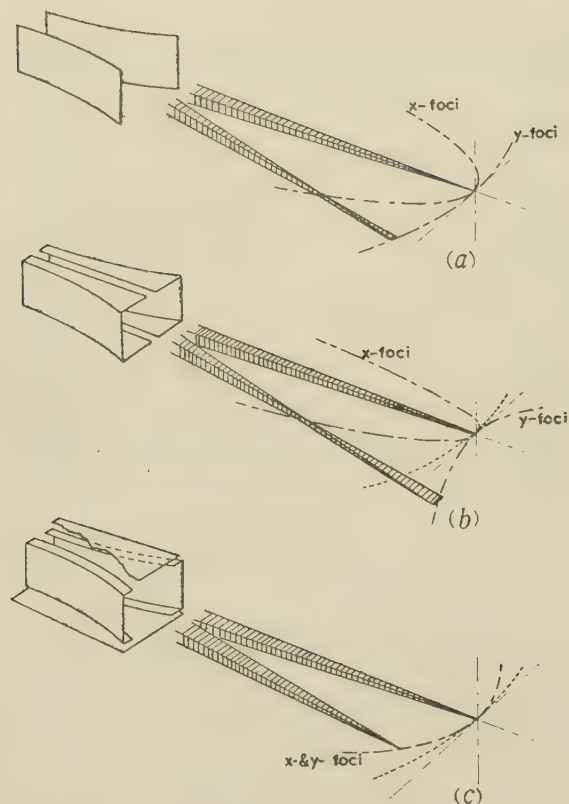


Fig. 11.—Three varieties of X-deflection system.

- (a) Parallel field. Focusing in x direction only.
 (b) Channel-shaped deflectors, overfocused x -wise.
 (c) Almost open channel with plates at top and bottom at middle potential.

a matter of the two profiles (spine and repeller bottom), shown in Fig. 9. As these were fixed by the condition of magnification of deflection angles, the burden of compensation had to be thrown on the line deflecting system. We have also explained how the central cross-section of the reversing lens had to be designed to satisfy all conditions in the symmetry plane $X = 0$. It remains now to design the cross-sections off this plane in such a way as to satisfy condition (c) and conditions (h)(i) and (ii), to which we will refer briefly as the Y -conditions. They state that at every deflection angle, θ , the three principal colour rays must be ultimately vertical, and moreover keep equal distances from one another, independently of θ .

These were the most difficult problems, because they are 3-dimensional. In order to make them amenable to analysis we experimented for some time with reversing lenses which were at least approximately rotationally symmetrical with respect to the axis O of the repeller bottom. In such systems we could adopt a modified method of ray tracing, with an equivalent potential taking account of the momentum integral, i.e. including the centrifugal force. In order to simplify the problem, symmetry around the $Y = 0$ plane was also retained, at least in shaping the repeller. We soon found that it was necessary to make at least the rear and front positive plates different in order to meet condition (c), i.e. achieving a plane central ray surface. However, all models failed to satisfy the condition (h). Without exception they acted as convergent lenses at the sides when the central ($X = 0$) cross-section was made telescopic.

We could make headway only after abandoning rear-front symmetry altogether. The successful reversing lenses have only one symmetry plane, $X = 0$. The essential step was the recogni-

tion that the optical symmetry, which in the $X = 0$ plane is achieved by geometrical symmetry, could be achieved off this plane only by abandoning geometrical symmetry. The successful semi-empirical design method which was adopted is explained in Appendix 12.2, which also contains the detailed design data of reversing lenses. Briefly the method consists in dividing up the trajectory into sections, and, taking into account the difference between the electrostatic potential and the effective potential due to the inclination of the trajectory to the normal plane of the cross-section, imitating for every trajectory as exactly as possible the dynamical conditions in the central cross-section $X = 0$. This method proved so successful that the first repeller design pre-calculated by this method could be used in all subsequent experiments. Only relatively minor modifications were required, which could be met by varying the radii of curvature of the front and rear positive plates.

The first successful model of the reversing lens was designed to operate with an ideal collimator, and its data are given in Appendix 12.1.* An ideal collimator is one which rotates all principal rays into the vertical, but which has either no Y -focusing effect, or one which is constant over its whole extension. A real collimators are far from ideal in this respect, the design can be used only for monochrome television tubes, but it also has considerable interest should the flat design be adopted for oscillograph tubes, without a collimator. An oscillograph with 120° electrostatic deflection angle, in the form of a shallow box has now become possible as a by-product of our development.

In the flat tube with a 'unipotential' reversing lens the negative trough has the largest depth of all elements, and thereby determines the thickness of the tube. Recently we have achieved further reduction of the overall thickness, by introducing an electrode at an intermediate potential, as shown in Fig. 12. I

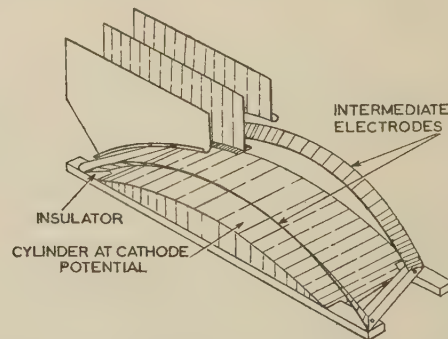


Fig. 12.—Space-saving realization of the reversing lens.

The intermediate electrodes are frustro-conical strips with 45° semi-angle.

this 'space-saving' design the positive electrodes (at a potential V_m) are the same as before, while the repeller is replaced by a two-electrode structure. This consists of the cylindrical repeller bottom, at cathode potential, and of the intermediate electrode which consists of two frustro-conical metal strips, connected by two bridges at the ends. These are shaped, on the basis of experiments in the electrolytic tank, in such a way that, when the intermediate electrode is at a potential $0.1-0.05V_m$, the field in the space utilized by the electrons is the same as with one of our well-tried repeller troughs. The screening effect provided by the conical strips is sufficient to make the field inside very insensitive to potentials outside this structure. Fig. 12 also shows the new T-shaped spine, which represents a great improvement in third-order aberrations over the previous U-shape.

We have not so far mentioned condition (d), which is the

* The development is described in full detail in Reference 7.

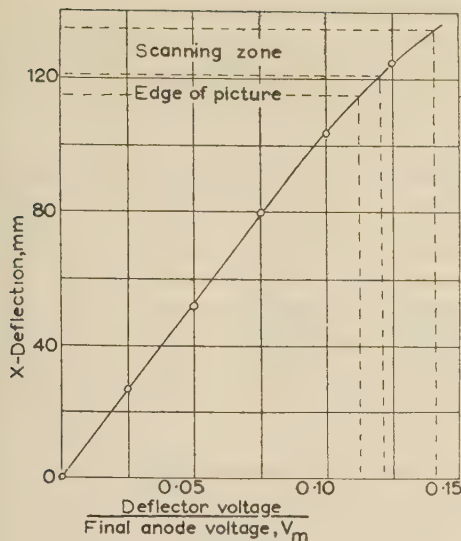


Fig. 13.—Line-scan deflector characteristics.

postulate that the final horizontal excursion X shall be as nearly as possible proportional to the deflecting voltage, because almost all our models happened to meet this very satisfactorily. Fig. 13 shows the deflection/deflecting-voltage characteristic of our latest system. It is slightly less than proportional at the marginal deflections. It could be made exactly linear by several methods, for instance by giving the spine profile a fourth-order correction, so that outside it bends a little stronger than a circle. We have produced a machine for this purpose, and made some experiments, but we believe that although an exactly linearized scale might be of interest for instance in a precision oscillograph, in television tubes where only one deflecting frequency is used the small correction for linearity can be left to the circuit designer.

(6) MAGNETIC COLLIMATOR

The collimator was not foreseen in the original conception of the flat tube in 1952, but it became a necessity when the self-scanning principle was introduced. It has also the advantages that it makes complicated 'grouping' of the colour areas unnecessary, it evens out the spot size over the whole picture area, and makes it unnecessary to use trapezium correcting circuits. These advantages are worth the complication of using a magnetic device in an otherwise purely electrostatic electron-optical system.

The collimator is a 'strong' lens, i.e. it uses a first-order effect (linear in B), instead of a second-order effect (quadratic in B). It fully deserves to be called strong, because its aperture is about $f0.5$.

The purpose of the collimator is to rotate any ray with deflection angle θ into the vertical. It must therefore have a transverse field B_y such that

$$\int \frac{ds}{R} = \frac{e}{mv} \int B_y ds = \theta$$

for any trajectory, where R is the radius of curvature. This therefore requires a field such that the integral of the transverse field along the trajectory (or the flux across a strip of unit width following the trajectory) is proportional to the angle of entry. Such a field can be produced in various ways. The first collimator was a magnetic frame with a long, narrow window, one end of which carried an even winding. This was abandoned, because it gave appreciable aberrations, and hardly any possibilities for correcting them. The type finally adopted is shown in Fig. 14 and the trajectories are shown in Fig. 9.

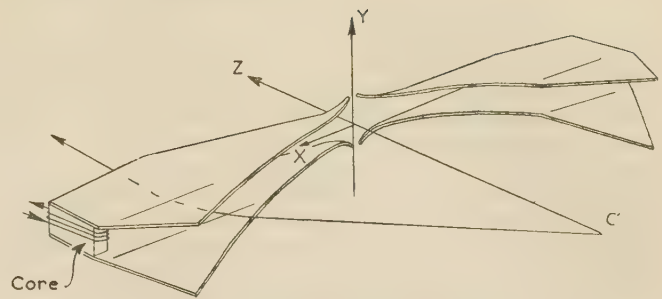


Fig. 14.—Magnetic collimator.

The collimator consists of four magnetic pole-pieces, joined by two cores carrying windings. The shape of the pole-pieces is the result of many experiments. Starting from a simple triangular shape they were gradually trimmed down, until the collimation was perfect. It was found necessary to bend out the finely tapering ends in the way shown, approximately in the shape of equilateral hyperbolae. In this central region the field passes through zero and changes sign. To avoid hysteresis the pole-pieces are preferably made of a highly permeable material with low remanence, such as Permalloy C. There is no need to avoid saturation; on the contrary, 50% saturation has great advantages. The focal power of such a strong lens varies as $I/V^{1/2}$ where I is the magnetizing current and V is the potential to which the electrons are raised, whereas the focal power of an ordinary weak lens varies as I^2/V . In both cases it is therefore necessary to increase the current by $\frac{1}{2}\%$ if the accelerating voltage varies by 1%. This is easily achieved if the magnetic circuit has 50% saturation at the operating point. We can then derive I proportionally from the tube voltage.

The condition of collimation can be met for a given reversing lens by a variety of collimators, but not all are equally suitable. It is shown in Appendix 12.3 that a magnetic field which collimates the rays in the XZ-plane has unavoidably a focusing effect at right-angles to this plane. In the symmetry line, $X = 0$, the Y-focusing effect will be exactly as strongly negative as the X-focusing effect is positive. Moreover it is shown that the negative Y-focusing effect necessarily decreases with increasing distance from the symmetry line, changes sign, and then becomes increasingly positive. There is no possibility of avoiding this effect; we can only reduce it by making the collimator pole-pieces broad, i.e. making the deflection very gradual. There are, however, limits to this broadening, as there is only a restricted space available for the collimator, and moreover the deflection sensitivity decreases if the collimator extends too near the deflection centre C' .

Therefore, a compromise had to be struck, which, of course, threw a further burden of compensation on the reversing lens, of the type which for a long time we found so difficult to produce, i.e. the reversing lens had now to be convergent in the Y-sense in the $X = 0$ plane, and become gradually more and more divergent outside it.

Fortunately this could be met, after considerable further experiments, by three simple modifications. The radius of curvature of the front positive plate was reduced from 250 to 150 mm, and the rear radius from infinity to 110 mm. Finally the cross-piece of the new T-shaped spine, instead of being a straight rectangular strip, is now bounded by two nearly parallel curves, in such a way that, while the central cross-section is symmetrical, at the two ends the cross-piece is closer to the exit than the entrance side by about 5 mm. This proved an effective method for evening out the 'axis spacing' and for producing three plane ray surfaces, as required in the colour tube.

(7) TOLERANCES AND TRIMMERS

It is natural to ask whether a complicated structure like the reversing lens, which is specified by not less than 13 essential data can be realized with reasonable manufacturing tolerances. But it must first be made clear that the difficulty of developing satisfactory models had little to do with accuracy. It was difficult enough to find the right point in universes with 4-6 dimensions, but the steps which led to it were, by no means, small. For example, it takes a change of about 2% in the curvature of the profiles of the front or rear positive plate to produce a noticeable departure from straightness in the principal ray surface, i.e. one which dips or raises the sides by 1 mm against the middle in a picture width of 250 mm. It happens that just those dimensions which were the most difficult to ascertain allow the widest limits in tolerances.

Starting with the gun, and using jigs and mandrels similar to those used in manufacture, we did not experience any difficulty in making guns which produced three coplanar and equidistant colour beams with a cross-over in the centre of the stop. We gave considerable attention to the alignment of the deflector system, so that it produced plane ray fans instead of conical ones, and regularly succeeded in obtaining planes with unmeasurably small curvature.

In order to be certain that the experiments are not marred by inaccuracies, we used, for some time, spines and repeller troughs made by electroforming from accurately machined models, but later we succeeded in obtaining completely satisfactory results with all parts of the reversing lens made from sheet metal, 0.008-0.015 in thick. All electrodes were made of non-magnetic (44-56) nickel-copper alloy, with the exception of the spine, which is made of Permalloy C to screen off the stray field of the magnetic collimator. There were, however, occasional difficulties owing to the imperfect shape of the repeller bottom, and there may be an advantage in having this part made by electroforming or by chemical deposition.

On the other hand, considerable accuracy is required in aligning the positive electrodes of the reversing lens with the repeller. It was found experimentally that a 1° tilt in the repeller causes an angular change of 4.5° in the emerging ray. In a colour tube it is desirable to keep the ray within ± 0.5 mm of the best position, and hence with a distance of 10 in from the I-line to the top of the picture the permissible angular error is only about $\pm 1/8^\circ$, which makes the tolerance in repeller tilt about $\pm 1/40^\circ$. If the repeller trough is imperfectly centred with respect to the positive electrodes, the outgoing angle changes by about 3.5° for 0.040 in shift, and thus little more than ± 0.001 in tolerance can be allowed in centring.

Such accuracies cannot, of course, be achieved in sheet-metal work, and we have therefore, from the start, foreseen the necessity of small electrical corrections by 'trimmer' electrodes. There are altogether five parameters which may require small corrections. Three of these relate to the position of the principal-ray plane (the central principal-ray plane, in the case of colour tubes). They are, in turn, the position of this plane (a parallel shift), a tilt around a horizontal axis and a tilt around a vertical axis. The first two can arise by misalignment of the repeller relative to the positive electrodes, and have already been referred to. The third can easily arise by a twist of the repeller around its longitudinal X-axis. The first two require for correction two Y-deflecting electrodes, deflecting in the Y-direction, both with d.c. bias. The third correction can be easily achieved, without using a further electrode, by applying to one of these 'trimmer' electrodes a voltage proportional to the line-scanning voltage.

An error in the spacing of the repeller from the positive electrodes will not only change the angular position of the central

ray plane, but will also produce a slight divergence of the red and blue ray planes from the central (green) plane, which ought to be parallel. In the previous models with 'unipotential' reversing lenses this was corrected by a small voltage applied to the repeller. In the new model it is more convenient to apply the correcting voltage to the intermediate electrode.

The fifth and last correction, which may not be necessary if the sheet-metal work is of sufficiently high quality, is the correction of a small conical curvature of the principal-ray surface. This too, can be achieved without a 'dynamic' correcting voltage (i.e. one proportional to the square of the X-scan voltage) simply by using a third trimmer electrode, with a parabolic instead of a straight edge, to which a suitable d.c. bias is applied. It may be mentioned that even a cubic error, i.e. a departure from a plane proportional to the cube of the X-deflection, could be corrected by applying to such a quadratically-shaped trimmer electrode a voltage proportional to the X-scan, but it is not expected that this will be necessary. For the last-mentioned corrections we use the rear positive plate, which has, for other reasons, a parabolically-shaped edge, so that only two trimmer electrodes need be specially provided, one near the gun and the other immediately below the phosphor screen.

(8) TECHNOLOGICAL FEATURES OF THE TELEVISION TUBE

A development carried out in a University laboratory cannot be expected to give complete solution of all the problems which may arise in the manufacture of such a typical complicated mass product as a colour-television tube. Nevertheless we had to pay considerable attention to these, because, once the electron-optical problems are solved, the commercial chances of the tube depend entirely on its ease of manufacture and reliability of service.

The flat tube raises manufacturing problems mainly by reason of two of its new elements; the scanning array and the shadow mask fixed on the phosphor screen, but also by its flat screen and box-shaped envelope. These will now be discussed in turn.

(8.1) The Scanning Array

In the course of the development we tested a number of different designs for the array. These became gradually simpler rather than more complicated, because, in the original design the array conductors were continued into the shadow mask, and hence they had to be very fine and very closely spaced. Our design consisted of metal tapes stretched between glass rods to which they were superficially fused. Another was a fabric in which the warp consisted of metal tapes, while the weft was a mixture of glass fibres and fibres of sodium-ammonium alginate. The alginate fibres made it possible to handle the fabric until it was fixed between supports, but these were ultimately dissolved in hot water, leaving enough glass fibres to hold the conductors in position. A third design was essentially the same as this, described in the next Section, but with the difference that the metal tapes were crimped around glass fibres.

Considerable simplification became possible when the scanning array was separated from the shadow mask, and the present self-scanning principle was introduced. It now became possible to operate with 60 to 120 conductors in the scanning array, instead of 400 or more. At that time, in 1954, we became aware of the excellent insulating qualities of silicone-coated glass fabrics, and found that fabric coated with the silicone resin MS994 could be completely outgassed *in vacuo* at 400°C with only moderate disintegration. On the other hand, it is a disadvantage of silicones that they cannot be easily cemented to metal, and hence we could not follow the obvious course of producing

arrays by sticking printed circuits to silicone-glass cloth. A few such arrays which we have produced were useful for our experiments in demountable vacuum, but they could not be trusted to resist the baking process in sealed-off tubes. At that time an ingenious process for producing printed circuits by evaporation had just been invented, and we obtained a number of scanning arrays, which consisted of a base of silicone-coated glass fabric, on which the whole pattern was deposited in the form of evaporated silver, backed by nichrome. With these we achieved our first successful self-scanning experiments.

It is questionable whether it would be wise to introduce such a novel device as the flat tube with silicones as insulators, which are, as yet, almost entirely untried as high-vacuum materials. In fact, they require long outgassing, in the course of which they are likely to form insulating deposits on the walls and electrodes, unless they have been pre-baked in vacuum or in an inert gas. Therefore, although we still consider the silicone-based printed circuit made by this method to be a very interesting proposition, we have also recently considered less revolutionary array designs. One is the self-supporting array shown in Fig. 15. If fairly thin

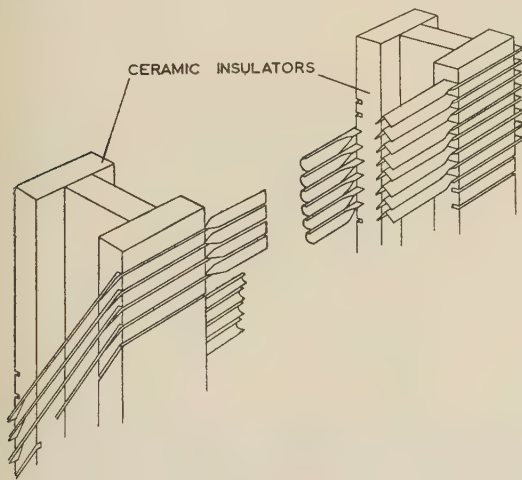


Fig. 15.—Self-supporting scanning array, of metal tape.

The beam scans down in the right-hand loop, and runs up in the left-hand loop, which contains a screen grid at ulior potential (not shown).

apes, 0.125 in \times 0.005 in, of nickel-copper alloy or Nichrome are drawn to a semi-circular cross-section they become stiff enough to support themselves between two insulators placed 0.01 in apart, with 12 conductors to the inch, i.e. about 80 for a 12 in-diagonal tube. At the right-hand side, at which the beam has to discharge the array, the tape is bent into a roof-shape. This was adopted because, in previous experiments, considerable difficulty was experienced with secondary electrons, which cascaded down the array and spread out the wavefront. With the shape now adopted the secondary electrons will get only as far as the next conductor. At the left-hand side, where the electrons have to recharge the array with the aid of a screen grid at ulior potential, not shown in the Figure, the conductors are plane vertical strips.

It was mentioned, in connection with the self-scanning principle, that the good secondary yield at 10 keV electron energy or more, which is required for the frame flyback, appeared to present a serious difficulty, until it was recognized that polished surfaces had far higher sticking potentials (second cross-overs) for electrons incident at small glancing angles than for normal incidence. Fortunately the arrays produced for us had a silver surface (on Nichrome backing), because silver is a metal very suitable for evaporation. Like all pure metals, it is

a poor secondary emitter, and we intended to replace it later by an oxidized silver-magnesium alloy which is known to have a sticking potential at 12–15 keV. But, to our great surprise, the flyback mechanism was still operating satisfactorily at 8 kV (the highest voltage which we then tested). We realized that this was much more than the obliquity effect, and was due to the fact that, after a few days exposure to the London atmosphere, silver is coated with a uniform layer of silver sulphide, which is an excellent secondary emitter. Thus, so far, we have found no need for any of the special surface treatments which we intended to apply.

(8.2) The Shadow Mask and the Phosphor Screen⁸

The most important special advantage of the flat tube is that it allows the shadow mask to be fixed on the screen, owing to the very small spacing (about a colour-cycle) required for colour separation. Suggestions for exploiting this advantage by making the shadow mask of one piece with the screen, and applying the phosphors by blowing the powder through the slits of the mask, were contained in the first Patent Application of 1952. Here, again, the development proceeded from more complicated towards simpler schemes, because, in the original project, the shadow-mask conductors were connected, line by line, with the array conductors, to improve the colour convergence. It was a great simplification when this could be replaced by an equipotential shadow mask, which could be produced in one piece.

Fig. 16 illustrates the shadow mask now adopted, and its manufacture. The starting point is a thin sheet, 0.0015 in thick, made of copper or some suitable alloy. This is printed, photographically or by means of rollers, with 40 to 50 parallel strips per inch of an acid-insoluble resist, leaving 20–25% of the metal area bare. This sheet is now crimped by a process to be explained below, i.e. it is folded sharply, so as to form thin parallel ribs, about as high as the strip spacing is wide. The spacing between the ribs can be made wider, even several times wider than the spacing between the strips, without the ribs becoming visible at the distances at which the picture is viewed. In the design of the first crimping machine we have taken, for safety, 0.036 in as the rib spacing, while the strip spacing is 0.025 in–0.020 in (40 to 50 strips per inch).

The crimped sheet is also completely coated with resist on the underside, and immersed in an etching solution for a limited time, until the result shown in the third illustration is produced, i.e. the blank spaces between the resist are etched through, but not the ribs. Alternatively one can produce this result without coating the back, by placing the crimped mat on an insulator, and etching it from above electrolytically, with an electrolyte of small throwing power. Finally the resist is removed with a suitable solvent.

The manufacture of the shadow mask, by means of a specially constructed machine, is illustrated schematically in the bottom half of Fig. 16. The resist-coated metal sheet first runs over a deeply slotted roller. A steel blade, 0.004 in thick, dives into a notch, and produces the required deep and narrow folds. In order to prevent the material from flowing backwards, and thus partly destroying the previously made fold, a retaining tooth, also 0.004 in thick, moves into the next slot, a little ahead of the blade. This operation is called 'crinkling'.

The crinkled mat is now picked up by a roller fitted with fine radial teeth, and inserted into the notches of a rubber coating, only a little thicker than the ribs are high, which covers a steel roller. It next passes under a pressure roller. This compresses the rubber, which flows almost like a liquid, filling in the space between the two steel rollers, and in the process compresses the folds as sharply as if they had been squeezed between steel jaws. The number of notches simultaneously under the pressure roller

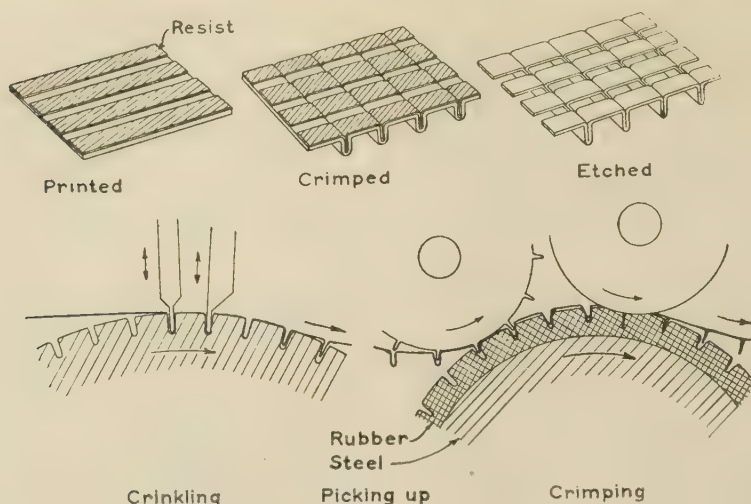


Fig. 16.—Manufacture of the shadow mask.

must, of course, be much larger than shown in the Figure. The sharp folds are easily released by the rubber, which expands again after moving past the pressure roller. The experimental machine is made for a strip width of 4 in. On the basis of the experience collected with this machine it appears perfectly feasible to produce shadow masks with 12 in width (for 20 in colour screens) in one operation.

The crimped, etched and washed shadow mask is now stuck on the glass plate serving as envelope, preferably with a cement such as a silicone resin, which remains a little tacky until it is cured, and has sufficient adhesion to hold the mask in position. The coating operation can now follow immediately. Originally it was planned to blow in the powder through the slits, at the same angles as would later be taken by the electrons, but the very simple process illustrated in Fig. 17 has a great advantage. The screen is placed in an inclined position in a vertical pipe filled with stagnant air. Above this there is another similar pipe, separated from the first by a horizontal shutter. A measured quantity of phosphor powder of the right colour is injected into the top pipe, and after the air currents caused by the injection have ceased, the shutter is removed. The column of powder now descends almost exactly vertically, with speeds of only a few centimetres per second. As it has only about 0.020–0.030 in to fall between the slits and the tacky screen surface, the outlines will be very precise, as seen in Fig. 18. If the dose is right, there will be no bouncing of the grains, although this is not very critical, since it was found that, at these low speeds, even those grains which fall on other grains instead of the tacky base do not bounce. The process is now repeated for the other colours. It has been found quite easy to remove the loose powder from the shadow mask by means of a powder puff or an electrified conductor. The tacky base solidifies during the baking of the tube.

This process, which is extremely simple compared with those used for conventional shadow-mask tubes, can be applied, of course, only to flat tubes, owing to its two distinctive properties:

- (a) The distance between shadow-mask and phosphor screen is very small.
- (b) For a certain colour the angle of incidence is the same all over the screen.

(8.3) The Envelope⁸

In order to exploit fully the advantages of the flat tube, it is highly desirable to give it a plane screen, instead of the usual dished envelopes. It used to be, and perhaps still is, generally

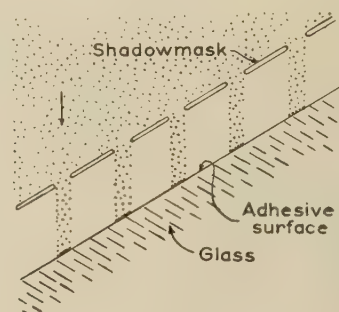


Fig. 17.—Coating colour screens by dropping phosphor powder in stagnant air through the slits of the shadow mask.

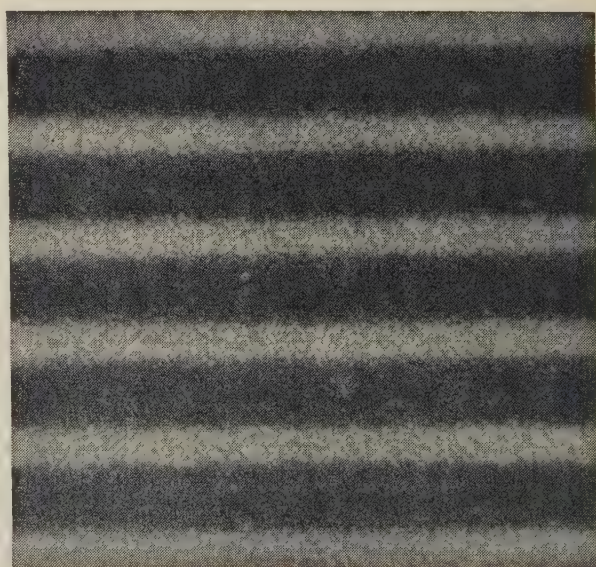


Fig. 18.—Microphotograph of a screen with 50 lines per inch, coated with one colour only.

believed that it is unprofitable to make the glass so thick that it shall withstand atmospheric pressure without dishing. This is, of course, perfectly true for ordinary glass, but not for toughened plates, which have been suddenly quenched from near the yield point to a temperature well below it. The outer crust solidifies first, and when the inner layer follows suit, this will be strongly stretched, while the outer layers are correspondingly compressed. These plates owe their great breaking strength, which may be six to eight times that of ordinary plates of the same thickness, to two characteristic properties of glass. The first is that its compression strength exceeds its tensile strength several times, and the second is that surface cracks, which gradually form by weathering and which reduce the tensile strength to about one-third of its initial value, cannot propagate in a compressed layer.

For example, if a plate has been toughened in such a way that its surface layer is under compression by six times the tensile strength, and its central layer is stretched correspondingly to three times this amount, it will not experience any tension on the surface under a load six times its normal breaking strength, and will crack only under a load of seven times the normal. There is a further advantage in the fact that strongly pre-stressed glass, once it cracks, disintegrates into small fragments, and not into large jagged pieces like ordinary glass. Implosion in a flat tube is rather a harmless affair anyway, compared with that in ordinary tubes, since the glass fragments can travel only about $\frac{3}{4}$ in before they hit the base-plate, as against 10–20 in in conventional television tubes. The particularly dangerous, though fortunately rare, type of implosion in which the gun hits the screen from the inside cannot happen at all. We believe that flat tubes made of toughened glass could be so safe that one could dispense even with the safety screen, replacing it perhaps by a dip into a transparent plastic substance to prevent the splinters from scattering.

For these reasons we have devoted considerable attention to the development of a suitable toughening process for the all-glass type of envelope shown in Fig. 1. The ordinary process used for plate glass, in which the whole article is uniformly quenched, is not very suitable. The flat tube, which is made of two pressed-glass shells, lends itself very well to a manufacturing process in which all glass-blowing work is avoided, sealing together the two shells with the leads, mostly tapes, between them by means of the excellent enamel glasses now available. But this makes it necessary to grind the two rims flat, with notches for the thicker leads and the exhaust tube, and if in this process one grinds through the compressed skin, the pre-stressed envelope will shatter. We have therefore developed a process in which the flat screen, together with its thickened surround, is fully toughened, while the pre-stressing gradually fades out and reaches a zero value at the rim. Our best result obtained so far is a fourfold increase in strength. If this could be obtained regularly, $\frac{5}{16}$ in plate thickness would be sufficient for a 12 in-diagonal tube, $\frac{1}{2}$ in thickness for a 20 in-diagonal tube, to pass the test at a pressure of 3 atm outside with vacuum inside.

However, especially at the larger screen sizes, which are now the most popular in television, it appears that the flat tube with a metal envelope and an evenly toughened glass window not larger than the screen has decisive advantages over the all-glass tube. Fig. 19 is a cross-section of a metal envelope. The whole electrode system is mounted on the lid, which has the shape of a tray with a network of stiffening ribs outside. This tray fits into the casing, and is argon-arc welded to it along the rim. The tube can be reconditioned by cutting away, say, $\frac{1}{8}$ in of this rim, withdrawing the mount, repairing the faulty parts, and rewelding the rim. Thus the envelope and the electrode system can be used four times until the thickness has been reduced to $4\frac{1}{8}$ in. All leads are arranged at the back, and they project into the set,

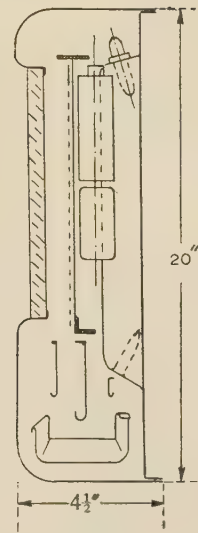


Fig. 19.—Cross-section of flat television-tube with metal casing.

The bottom, welded to the casing along the edge of the rim, carries two deep pockets at either side of the gun, which protect the insulators and the exhaust tube and can also accommodate part of the circuit. The dimensions shown apply with the 20 in screen-diagonal tube. The overall dimensions of the 12 in tube are 12 in \times 3 $\frac{1}{2}$ in.

which is arranged behind the tube, to a depth of about 2 in. All controls are arranged at the sides. The cabinet is reduced to a minimum, i.e. to four plates forming a frame which snugly surrounds the tube. A front cover is unnecessary, and if the tube is given a pleasant finish it looks like a television set. The question of whether the sound will be satisfactory with elongated, narrow loudspeakers opening towards the sides or towards the top will not be discussed. Otherwise the preliminary work done so far on the circuit design for the flat tube gives us confidence that there will be no difficulty in accommodating the complete circuits in a depth of 2 in, which is about 0.5 ft³.

It is too early to discuss the vacuum-holding qualities of the flat tube, and particularly the metal tube, but at the back plate it offers a gettering area of more than 2 $\frac{1}{2}$ ft², which cannot be seen by the phosphor screen.

(9) CONCLUSIONS

The development of the flat television tube for monochrome and colour has reached a stage at which the feasibility of every one of its novel features has been tested singly, and partly in combination. The major part of the work consisted in the development of the electron-optical system consisting of a 3-beam electron gun, a line-deflector system, an electrostatic reversing lens and a magnetic collimator, which launches the three colour beams into the space between the phosphor screen and the scanning array, on three accurately parallel and equidistant planes, and ensures focusing along any scanning line without 'dynamic' corrections. The second part was the development of a scanning array which enables the beam to effect the frame scan by itself. The third part was a simple method for producing the pattern of colour-phosphor strips, in automatic register with the shadow mask which is fixed immediately on the glass screen. The first two developments were tested in combination, and the third, for the time being, only on small samples of colour screens. Work was also done on the use of pre-stressed (toughened) glass plates, to enable the construction of large tubes of at least 20 in diagonal with plane screens, without excessive glass thickness. All experiments were carried out in continuously-pumped, demountable vacuum tanks. No sealed-off complete tube has been produced so far, and this stage of the development would

be more appropriately carried out in industrial establishments than in an academic laboratory.

(10) ACKNOWLEDGMENTS

It is a pleasure to acknowledge the aid given by the National Research Development Corporation, the sole supporters and financiers of the development, so far as it has been described in the paper, without whom the whole invention would have remained almost certainly just a patent. To the Imperial College we owe the liberal use of their general resources. More recently we enjoyed also the assistance of the Siemens Edison Swan Company, in particular in the development of suitable circuits. The Mullard Radio Valve Co. assisted us obligingly with special materials. We wish to thank Fothergill and Harvey, Ltd., for supplying us with the woven arrays mentioned in Section 8.1, and also Dr. F. Ashworth and Mr. R. H. Alderson of the Metropolitan-Vickers Electrical Co., Ltd., for supplying us with arrays of silver evaporated on to silicone-coated glass fabric specially prepared for us by Ioco Ltd. The shadow-mask crimping machine described in Section 8.2 was supplied by the Epsilon Research and Development Co., with the co-operation of its Managing Director, Mr. L. Nemenyi-Katz. Our thanks are due also to Mr. W. P. Goss for assistance in much of the work and in the preparation of this paper, and also to Mr. G. McDermott, senior technician, whose skill in producing most of our experimental devices was invaluable to us.

(11) REFERENCES

- (1) GABOR, D.: U.S. Patent Application No. 309677. 15th September, 1952.
'A New Flat Picture Tube', *Journal of the Television Society*, 1956, **8**, p. 142.
- (2) AIKEN, W. R.: U.S. Patent Application No. 355965. 19th May, 1953.
'A Thin Cathode Ray Tube', *Proceedings of the Institute of Radio Engineers*, 1957, **45**, p. 1599.
- (3) FELDMAN, C., and O'HARA, M.: 'Formation of Luminescent Screen by Evaporation', *Journal of the Optical Society of America*, 1957, **47**, p. 300.
- (4) GABOR, D.: 'Mechanical Tracing of Electron Trajectories', *Nature*, 1937, **139**, p. 373.
- (5) HOLLWAY, D. L.: 'An Electrolytic-Tank Equipment for the Determination of Electron Trajectories, Potential and Gradient', *Proceedings I.E.E.*, Paper No. 1837 M, May, 1955 (**103** B, p. 155).
- (6) RECKNAGEL, A.: *Zeitschrift für Physik*, 1938, **111**, p. 61.
- (7) STUART, P. R.: 'The Electron Optics of a Novel Form of Cathode Ray Tube' (Ph.D. Thesis, University of London, 1957).
- (8) KALMAN, P. G.: 'Investigation of Physical and Design Problems relating to a Novel T.V. Tube' (Ph.D. Thesis, University of London, 1958).

(12) APPENDICES

(12.1) A Semi-Empirical Method used in Designing Reversing Lenses

Trajectory tracing through the fields of the central cross section ($X = 0$), as determined in the electrolytic tank, have shown that, if the depth H of the repeller trough is increased by 1 mm, the optic axis is moved out on each side by 0.7 mm. Similarly, if the gap widths G between the trough rims and the positive side-plates are increased by 1 mm, the axis moves out on each side by approximately 0.28 mm. These effects are approximately linear over quite a wide range. So far as the effect on the axis is concerned, we may define a quantity D ,

which we shall call the 'effective trough depth', given by the equation

$$D = H + \frac{0.28}{0.7} G = H + 0.4G$$

Strictly this holds only for the central cross-section $X = 0$, but the assumption that the factor 0.4 holds for all cross-section seems justified by the results of experiments in demountable vacuum chambers.

Using the data from an accurately-made rotationally-symmetrical reversing lens having the cross-section shown in Fig. 21 it was possible to find the dependence of the Y-focal power on the ratio D/w (where w is the trough half-width) for various values of ϕ (Figs. 10 and 20) and also to calculate the varia-

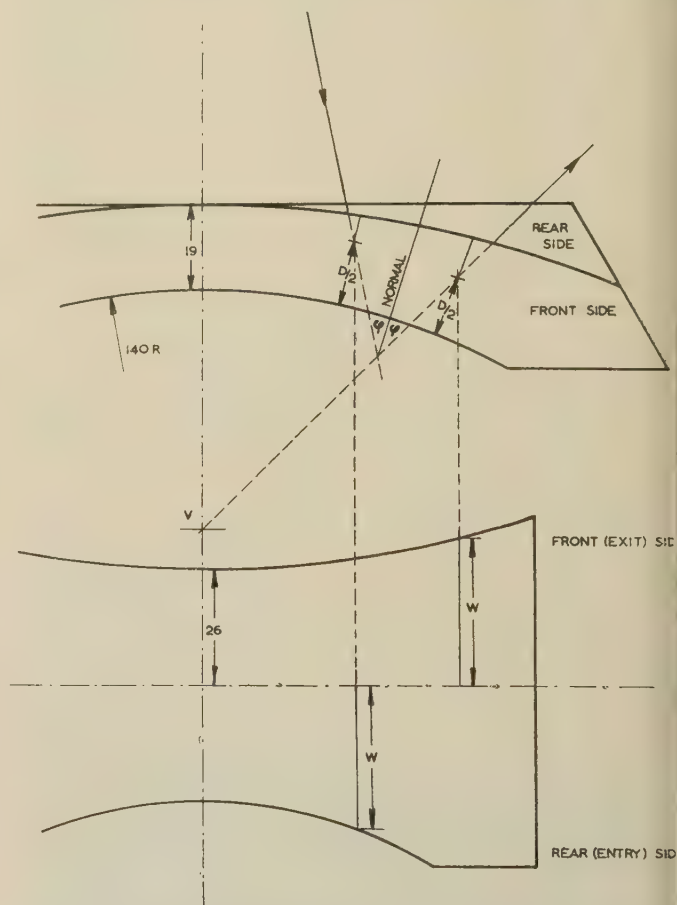


Fig. 20.—Illustrating the design procedure for an asymmetrical repeller which is effectively symmetrical.

tion of axis spacing A (Fig. 21) with ϕ . The design of a successful lens now involves scaling up D and w , so that the axis distance A is constant for all values of ϕ , and that for each value of ϕ the ratio of D/w on both the entry and exit sides is such as to give the required Y-focal power. From the calculated values of D new actual trough depths H can now be determined, such that the gap width G remains constant for all values of ϕ .

As an example we shall calculate the increases in w and D (26 and 19 mm, respectively, in the central cross-section) so that the reversing lens of a 12 in tube shall be telescopic.

In the telescopic case the gap width G_0 of the rotationally-symmetrical lens was 10.7 mm in the central cross-section. Measured values of axis distance A_0 , and scaled-up values of trough half-width w and trough depth H are given in Table 1.

Table 1

θ , primary X-deflection angle, deg	0	5.7	8.0	9.8	11.3
ϕ , angle of incidence to trough bottom, deg ..	0	13	18.5	22.5	26
G_0 for telescopicity with $H = 19$ mm	10.7	9.9	9.1	8.3	7.5
Axis spacing A_0 for $H = 19$ mm, and $w = 26$ mm	27.0	25.7	24.4	23.05	21.75
D_0 (rotationally symmetrical lens), mm	23.3	22.95	22.65	22.3	22.0
D for $A = 27$ mm $\left(= \frac{27D_0}{A_0} \right)$, mm	23.3	24.2	25.0	26.2	27.3
w for $A = 27$ mm $\left(= \frac{27 \times 26}{A_0} \right)$, mm	26.0	27.3	28.8	30.4	32.2
H for $G = 10.7$ mm	19.0	19.9	20.7	21.9	23.0

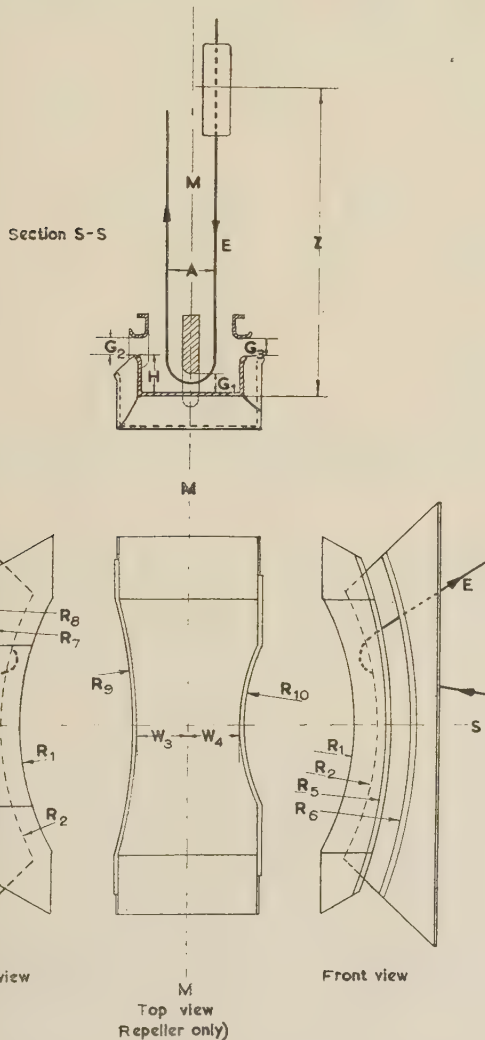


Fig. 21.—Design data of a reversing lens for operation without collimator.

It is clear from the last two rows that the trough must be widened and deepened towards the ends, the increase in width being very nearly proportional to $\sec^2 \phi$. However, the trough must not be made symmetrical to the $Y = 0$ plane, or the branches of the trajectory at the two sides of this plane would, in fact, 'see' different fields. In practice, it has been found satisfactory to consider the half-widths w given in Table 1 as belonging to the cross-sections intersected by the asymptotes of the two branches at a distance $D/2$ from the trough bottom.

Table 2

R_1	R_2	R_5	R_6	R_7	R_8	R_9	R_{10}	Z	$w_3 + w_4$	H	G
5.2	5.55	9.25	9.6	∞	∞	9.25	3.7	6.2	1.9	0.71	0.37

This is illustrated in Fig. 20, which shows the ray for which $\theta = 11.3^\circ$. The front and rear halves of the trough are made 23.0 mm deep and 32.2 mm in width in those cross-sections through which the projections of the incoming and outgoing beams pass at a distance $D/2 = 13.65$ mm from the bottom of the repeller. In practice, it has not been found necessary to alter the distance between the positive side-plates and the spine.

When several points on the trough lips have been determined, it is found that they lie fairly closely upon circular arcs, and it is thus possible to describe the repeller by a number of radii, as shown in Fig. 21. Table 2 gives the dimensions of a successful telescopic lens, in units of the axis distance A , which was taken as 27 mm for a 12 in tube.

Although the two halves of the central cross-section are geometrically symmetrical, the electric fields in each will be slightly different, since they are influenced by the shapes of the dissimilar neighbouring portions of the trough walls. The result of this is that the beam direction will be turned by slightly more than 180° . This effect may be compensated by slightly offsetting the repeller relative to the positive plate assembly, so that w_3 is slightly larger than w_4 , i.e. ($w_3 - w_4 = 0.06A$).

(12.2) Mathematical Theory of the Reversing Lens

The problem of designing an electrostatic reversing lens to given optical specifications is considered. The chief purpose of the theory is to reveal the degrees of freedom of the problem, i.e. those parameters which can be freely disposed of, and which may be used for further improvements.

The problem is illustrated in Fig. 22. The principal rays start in a plane fan from the deflection centre C . After passing through the lens they appear to diverge, approximately from a centre C' , with larger angles to the Z -axis. It is stipulated that the principal ray surface (p.r.s.) shall asymptotically approach a plane, parallel to the original. These are the conditions for the principal rays.

We introduce a suitable co-ordinate system, in the form of the orthogonal curvilinear system (u, v) in the p.r.s. and the rectilinear co-ordinate w at right angles to it. The lines $v = \text{constant}$ (u -lines) are the principal rays, and the equation of the p.r.s. is $w = 0$. The metric is

$$ds^2 = dx^2 + dy^2 + dz^2 = h_1 du^2 + h_2 dv^2 + h_3 dw^2 \quad (1)$$

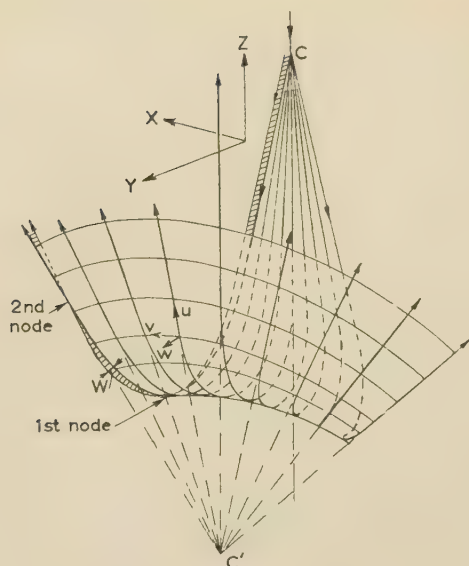


Fig. 22.—Theory of the reversing lens.
The principal-ray surface.

We put $h_3 = 1$, but it will be convenient to leave it standing in some formulae for the sake of symmetry.

We can now formulate the focusing properties of narrow pencils centring on the principal rays. We specify first the focusing of rays which depart from a principal ray only in the w -direction, at right angles to the p.r.s., by stipulating that these shall follow certain paths $w = W(u, v)$, $v = \text{constant}$. Previously these were called 'Y-conditions'. It will be shown later that this stipulation is consistent, because a trajectory starting as a W-ray always keeps to the condition $v = \text{constant}$.

In order to specify the condition for lateral focusing (previously called 'X-focusing') for rays which depart from principal rays but remain in the p.r.s. it is convenient to imagine the p.r.s. conformally represented on a plane, as shown in Fig. 23.

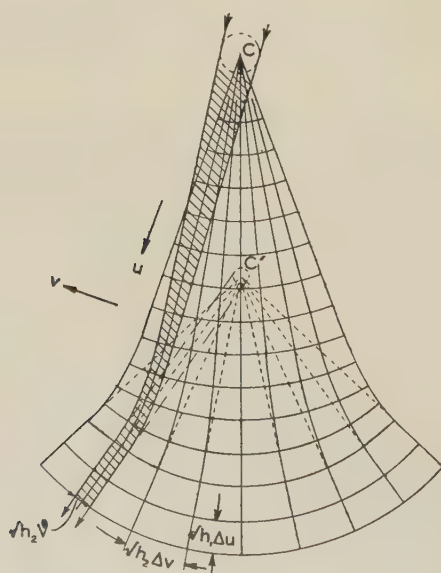


Fig. 23.—Theory of the reversing lens.
Conformal representation of the principal-ray surface on a plane.

The p.r.s. is not applicable to a plane, except in its initial region near C, and its asymptotic emerging region, because in the regions its total curvature is zero. It is applicable there without deformation, even if the p.r.s. does not approach a plane because in the regions of constant potential, $\phi = \phi_0$, the trajectories become straight rays, and hence the surface is developable.

The lateral trajectories, $w = 0$, $v = V(u, v)$ cannot be freely prescribed once the network of co-ordinates, h_1, h_2 is laid down. This is anticipated in Fig. 23, which shows a certain relation between the initial and final divergences of a V-beam, to be derived and explained later.

The general method to be followed is this. First we establish the dynamical equations for trajectories in narrow pencils around principal rays, in the co-ordinate system (u, v, w) , a Laplace's equation for the electrostatic potential $\phi(u, v, w)$ without any reference to the position of the p.r.s. in space. Combining the conditions, we obtain sufficient equations specifying $\phi(u, v, 0)$ in the p.r.s. and its gradient at right-angles to it, $\partial\phi/\partial w$. Once the p.r.s. is given, this is sufficient to determine $\phi(u, v, w)$. Finally we make use of Gauss's equation for the total curvature of a surface which can accommodate a network (u, v) with given metric coefficients $h_1(u, v)$, $h_2(u, v)$. This still leaves a certain amount of freedom, which we will then discuss.

Dynamical Equations.—We start from Lagrange's equation for an electron (e, m) in a potential field ϕ

$$\frac{d}{dt} \frac{\partial L}{\partial \dot{q}_i} - \frac{\partial L}{\partial q_i} = 0 \quad \dots \quad (1)$$

where the co-ordinate q_i represents either u, v or w and $L = T(q_i, \dot{q}_i) - e\phi$ is the kinetic potential. T is the kinetic energy, expressed in terms of the co-ordinates q_i and their rate of change \dot{q}_i . In our curvilinear co-ordinate system

$$T = \frac{1}{2} m (h_1 \dot{u}^2 + h_2 \dot{v}^2 + h_3 \dot{w}^2) \quad \dots \quad (2)$$

We now distinguish the co-ordinate u , which we introduce instead of the time t as an independent variable. Using $d/dt = \dot{u} du$, and the energy integral

$$T = \frac{1}{2} m h_1 \dot{u}^2 \left(1 + \frac{h_2}{h_1} v'^2 + \frac{h_3}{h_1} w'^2 + \dots \right) = -e\phi \quad \dots \quad (3)$$

Here, as later, primes stand for differentiation with respect to u . The terms written out in eqn. (4) are sufficient for the discussion of trajectories to the second order, but we will now restrict ourselves to first-order (Gaussian) optics relative to the principal rays, and use the first term only, i.e.

$$\dot{u} = (-2e\phi/mh_1)^{1/2} \quad \dots \quad (4)$$

With this approximation, substituting in turn v and w for q_i in Lagrange's equation, and replacing differentiations with respect to time by $\dot{u} du$, we obtain the two trajectory equations

$$\begin{aligned} \frac{h_2}{h_1} \left[v'' + \left(\frac{h_2'}{h_2} - \frac{1}{2} \frac{h_1'}{h_1} + \frac{1}{2} \frac{\phi'}{\phi} \right) v' \right] &= \frac{1}{2} \left(\frac{1}{h_1} \frac{\partial h_1}{\partial v} + \frac{1}{\phi} \frac{\partial \phi}{\partial v} \right) \\ \frac{h_3}{h_1} \left[w'' + \left(-\frac{1}{2} \frac{h_1'}{h_1} + \frac{1}{2} \frac{\phi'}{\phi} \right) w' \right] &= \frac{1}{2} \left(\frac{1}{h_1} \frac{\partial h_1}{\partial w} + \frac{1}{\phi} \frac{\partial \phi}{\partial w} \right) \end{aligned} \quad \dots \quad (5)$$

We have left h_3 standing, for symmetry, but we have taken $h_3' = 0$ into account.

On the right-hand side of these equations we have $(1/2h_1\phi)\partial/\partial v(h_1\phi)$ and $(1/2h_1\phi)\partial/\partial w(h_1\phi)$, and as these equations relate to narrow beams, the derivatives are understood to be taken at $w = 0$, at any principal ray $v = \text{constant}$. As t

right-hand sides are of the first order in v , w , no zero-order terms can appear at the right, and we have

$$\frac{\partial}{\partial v}(h_1\phi) = 0 \quad \frac{\partial}{\partial w}(h_1\phi) = 0 \text{ for } w = 0$$

This gives the important integral

$$h_1\phi = f(u) \quad (w = 0) \quad . \quad . \quad . \quad . \quad . \quad (8)$$

everywhere in the p.r.s. The arbitrary function $f(u)$ is of no importance; it corresponds only to a renumbering of the v -lines (v -lines). This integral can be interpreted as expressing Huyghens's principle of wavefront propagation in a medium with refractive index proportional to $\sqrt{\phi}$. In fact the spacing of two v -lines is $h_1^{1/2}du$, and from eqn. (8) this is inversely proportional to the refractive index along this wavefront. For simplicity we will now make $f(u) = \text{constant}$.

As the right-hand side of eqn. (6) vanishes everywhere in the p.r.s. and as from eqn. (8), with $f(u) = \text{constant}$,

$$h_1'/h_1 = -\phi'/\phi \quad . \quad . \quad . \quad . \quad . \quad (9)$$

we obtain for the equation of the V-rays

$$V'' + \left(\frac{h_2'}{h_2} + \frac{\phi'}{\phi} \right) V' = 0 \quad . \quad . \quad . \quad . \quad (10)$$

the right-hand side must vanish, because for any principal ray, $\phi = \text{constant}$ is a possible trajectory. This equation can be immediately integrated and it gives the second important integral

$$h_2\phi V' = g(v) \quad (w = 0) \quad . \quad . \quad . \quad . \quad (11)$$

again the arbitrary function $g(v)$ is of no importance; it corresponds only to a renumbering of the u -lines, and we will make it constant.

Eqn. (11) can be interpreted dynamically as a momentum integral or optically as an expression of the Smith-Lagrange-Helmholtz theorem. This can be seen as follows: The distance between two neighbouring principal rays is $h_2^{1/2}dv$, and hence $h_2^{1/2}$ is a measure of the transverse magnification. The angle between a ray and its $v = \text{constant}$ axis is $(h_2/h_1)^{1/2}V'$. Substituting from eqn. (8) $h_1 = \text{constant}/\phi$, we can therefore express eqn. (11) in the form

Transverse magnification \times Angular convergence
 \times Refractive index = invariant

which is the Smith-Lagrange-Helmholtz theorem of optics.

The two results $h_1\phi = \text{constant}$ and $h_2\phi V' = \text{constant}$ allow us to obtain an intuitive insight into the problem of the reversing lens. Let us first lay down in a plane a conformal representation of the (u, v) network, with the initial and final regions undistorted, as shown in Fig. 23. In this map we can also draw the family of V-lines, since these are geometrically connected with the u, v network, but let us do it so that in the asymptotic regions

$$h_2V' = \text{constant}$$

that the Smith-Lagrange-Helmholtz theorem is not violated. This is what we have done in Fig. 23 by making the initial and final rays tangential to two circles, one centring on C, and the other on C', with radii in the inverse ratio of magnification. It is clear that, if the locus of convergence of the final V-pencils is preserved, this imposes certain conditions either on the initial locus of convergence, or on the magnification, which will then, in general, not remain a constant. This question has been previously discussed in detail in connection with Fig. 10.

By making

$$(h_2V')_{\text{initial}} = (h_2V')_{\text{final}}$$

we have made the complex of the V-pencils optically realizable in the two asymptotic regions in which $\phi \rightarrow \phi_0$ and the rays become straight lines. We can now easily complete the picture in the regions between, by first calculating a plane potential field $\phi_p(u, v)$ in which the principal rays, as drawn, become actual trajectories. We do this by using eqn. (8) in the form

$$\phi_p(u, v) = \phi_p(u, 0) \frac{h_1(u, 0)}{h_1(u, v)} \quad . \quad . \quad . \quad . \quad (12)$$

We can do this graphically by proceeding from the symmetry axis $v = 0$ outwards. The spacing between two neighbouring v -lines is $h_1^{1/2}du$, and hence the potential ϕ_p increases inversely as the square of this spacing. It is seen that the potential on the symmetry axis, $\phi_p(u, 0)$ remains undetermined in this process. (It becomes determined if one wants to realize ϕ_p with a cylindrical electrostatic field.) We can now also draw the V-rays in the intermediate region, using eqn. (11) (after having made some assumption about $\phi_p(u, 0)$, but this is not of great interest, as only the final rays are important.

From this plane map of the trajectories, which represents a plane diverging lens, we can now pass over to a 3-dimensional reversing lens, as follows. Let us assume that we know the potential $\phi(u, v)$. From eqns. (8) and (11) we have only to enlarge the meshes of the network *conformally* by the factor

$$[\phi_p(u, v)/\phi(u, v)]^{1/2}$$

in order to get another realization of the same optical problem, but the p.r.s. will now be no longer plane. For simplicity let us make $\phi_p(u, 0) = \phi(u, 0)$ so that there is no deformation at the symmetry axis. But outside this, where the meshes are crowding together in Fig. 22 these will now be enlarged, and here the p.r.s. will bulge out of the plane. One could realize this surface with fair accuracy by making up the (u, v) network out of steel wire, welded at right angles at the nodes, with meshes of the precalculated size. (One could also make it up 'paillette' fashion, out of small rectangles, welded together at the corners with flexible wire.) These models are useful, since they give an intuitive idea of the equations of differential geometry, to be introduced later. It is, at once, clear that such a surface is not a unique realization. In whatever way we distort the steel network or the paillette-mail, we obtain another valid realization, so long as the wires or the joints are not stretched, because all these are *applicable* surfaces, with the same total curvature. In particular, it is clear that we can bend the surface in such a way that the two asymptotic regions become parallel planes, thereby satisfying all conditions imposed in a reversing lens on the principal rays and on the V-pencils. These lenses will not, in general, have the desired properties for the W-rays, and this is what we must now consider.

On the right-hand side of eqn. (7) for W-rays, we have the term

$$\frac{1}{2} \left(\frac{1}{h_1} \frac{\partial h_1}{\partial w} + \frac{1}{\phi} \frac{\partial \phi}{\partial w} \right) = \frac{1}{2h_1\phi} \frac{\partial}{\partial w}(h_1\phi) \quad . \quad . \quad (13)$$

which we have already used to derive eqn. (8) for h_1 in the p.r.s. We now interpret it, by using the geometrical equation

$$\frac{1}{R_u} = \frac{1}{2} \frac{1}{h_1} \frac{\partial h_1}{\partial w} \quad . \quad . \quad . \quad . \quad (14)$$

where R_u is the radius of curvature of the u -lines in the plane (u, w) , i.e. the normal curvature of the p.r.s. associated with the direction of the principal rays. The vanishing of the term in eqn. (13), for $w = 0$, which is a consequence of the fact that the principal rays must be trajectories, therefore means that

$$\frac{1}{R_u} = -\frac{1}{2} \frac{1}{\phi} \frac{\partial \phi}{\partial w} \quad . \quad . \quad . \quad . \quad (15)$$

This equation is well known. It gives directly the potential gradient normal to the principal-ray surface, which is one of the data we require for specifying the potential field, the other being of course the potential $\phi(u, v, 0)$ in the p.r.s.

Eqn. (13) vanishes at $w = 0$ but not at $w = W$, where it is, in our first-order approximation,

$$W \frac{\partial}{\partial w} \frac{1}{2} \left(\frac{1}{h_1} \frac{\partial h_1}{\partial w} + \frac{1}{\phi} \frac{\partial \phi}{\partial w} \right) = \frac{1}{2} W \left[\frac{1}{h_1} \frac{\partial^2 h_1}{\partial w^2} - \left(\frac{1}{h_1} \frac{\partial h_1}{\partial w} \right)^2 + \frac{1}{\phi} \frac{\partial^2 \phi}{\partial w^2} - \left(\frac{1}{\phi} \frac{\partial \phi}{\partial w} \right)^2 \right] \quad (16)$$

By eqns. (14) and (15) the second and the fourth term can be expressed by $1/R_u$. The first term, which contains the second derivative of h_1 can be also reduced to it, because the w -axis is rectilinear, and hence we have exactly

$$h_1^{1/2}(u, v, w) = h_1^{1/2}(u, v, 0) \left(1 + \frac{w}{R_u} \right)$$

which expresses the fact that the arc length is proportional to the distance from the curvature centre.

$$\text{Hence} \quad (1/h_1) \partial^2 h_1 / \partial w^2 = 2/R_u^2 \quad \dots \quad (17)$$

Substituting these results into eqn. (7) we obtain the equation of the W-rays

$$\frac{h_3}{h_1} \left(W'' + \frac{\phi'}{\phi} W' \right) = \left(-\frac{3}{R_u^2} + \frac{1}{2} \frac{1}{\phi} \frac{\partial^2 \phi}{\partial w^2} \right) W \quad (18)$$

This, and its counterpart eqn. (10), incidentally verify the theorem, already anticipated, that V-rays and W-rays remain V-rays and W-rays during their passage through the reversing lens; there is no skewing of axes in the first-order approximation.

Laplace's Equation.—The second derivative of ϕ with respect to the normal is determined by Laplace's equation in terms of the distribution of ϕ in the p.r.s. and its first derivative. This equation is, in orthogonal curvilinear co-ordinates,

$$\frac{\partial}{\partial u} \left[\left(\frac{h_2 h_3}{h_1} \right)^{1/2} \frac{\partial \phi}{\partial u} \right] + \frac{\partial}{\partial v} \left[\left(\frac{h_3 h_1}{h_2} \right)^{1/2} \frac{\partial \phi}{\partial v} \right] + \frac{\partial}{\partial w} \left[\left(\frac{h_1 h_2}{h_3} \right)^{1/2} \frac{\partial \phi}{\partial w} \right] = 0 \quad \dots \quad (19)$$

The last term is, putting $h_3 = 1$ and writing $(h_1 h_2)^{1/2} = h$,

$$\begin{aligned} \frac{\partial}{\partial w} \left[(h_1 h_2)^{1/2} \frac{\partial \phi}{\partial w} \right] &= (h_1 h_2)^{1/2} \left(\frac{1}{2} \frac{1}{h_1} \frac{\partial h_1}{\partial w} \frac{\partial \phi}{\partial w} \right. \\ &\quad \left. + \frac{1}{2} \frac{1}{h_2} \frac{\partial h_2}{\partial w} \frac{\partial \phi}{\partial w} + \frac{\partial^2 \phi}{\partial w^2} \right) = -h \left[2 \left(\frac{1}{R_u} + \frac{1}{R_v} \right) \frac{\phi}{R_u} - \frac{\partial^2 \phi}{\partial w^2} \right] \quad \dots \quad (20) \end{aligned}$$

Here we have used eqns. (14) and (15), and we have introduced

$$\frac{1}{R_v} = \frac{1}{2} \frac{1}{h_2} \frac{\partial h_2}{\partial w} \quad \dots \quad (21)$$

for the normal curvature of the v -lines.

We now introduce the second normal derivative of ϕ from eqns. (19)–(20) into eqn. (18) at the same time making use of eqn. (8) in the form $h_1 \phi = \phi_0$. This gives us the equation of the W-rays in the final form

$$\frac{1}{\phi_0} \frac{d}{du} (\phi W') = \left\{ -\frac{2}{R_u^2} + \frac{1}{R_u R_v} - \frac{1}{2\phi h} \left[\frac{\partial}{\partial u} \left(\frac{h_2}{h_1} \right)^{1/2} \frac{\partial \phi}{\partial u} + \frac{\partial}{\partial v} \left(\frac{h_1}{h_2} \right)^{1/2} \frac{\partial \phi}{\partial v} \right] \right\} W \quad (22)$$

This equation gives the W-focusing properties of the reversing lens as a function of the potential in the p.r.s. of the metric h_1, h_2 defined by the principal rays, and of the two curvatures $1/R_u, 1/R_v$ at right angles to one another. Conversely, if we prescribe the function $W(u, v)$ in the p.r.s., eqn. (22) is a linear second-order partial differential equation for ϕ in the p.r.s. [The apparent non-linearity vanishes after substituting h_1, h_2 from eqns. (14) and (15).]

Equations of Differential Geometry.—The quantities R_u, R_v and h_1, h_2 , which figure in eqn. (22), are not independent of one another, because, by Gauss's theorem, the total curvature of a surface, i.e. the product of its two principal curvatures, is determined by the metric h_1, h_2 in the surface, by the relation

$$\frac{1}{R_1 R_2} = \frac{1}{R_u R_v} - \left(\frac{1}{R_{uv}} \right)^2 = -\frac{1}{2h} \left[\frac{\partial}{\partial u} \left(\frac{1}{h} \frac{\partial h_2}{\partial u} \right) + \frac{\partial}{\partial v} \left(\frac{1}{h} \frac{\partial h_1}{\partial v} \right) \right] \quad (2)$$

Here R_1 and R_2 are the two principal curvature radii, and $1/R_{uv}$ is a parameter which determines the angles of the principal sections with the axes u, v .

From the theorems of the differential geometry of surfaces it is only the total curvature which is determined by the metric h_1, h_2 . All surfaces with the same total curvature in corresponding points are applicable. The mean curvature, $\frac{1}{2}(1/R_u + 1/R_v)$, on the other hand, remains quite undetermined. We are therefore free to choose, for instance, R_u as an arbitrary function of u, v , as clearly suggested by the model of a steel-wire network.

A purely analytical procedure for designing reversing lenses would be rather complicated, owing to the circumstance that the W-ray equation (22) contains the product $1/R_u R_v$ instead of the total curvature $1/R_1 R_2$, so that a knowledge of the quantity $1/R_{uv}$ is required. This is given, in terms of R_u and R_v , by the two Mainardi-Codazzi equations of differential geometry. Manipulating these two equations together with eqns. (22) and (23) is too complicated to be practical.

Solution by a Model Method.—A more practical procedure is as follows:

Produce a model of the principal-ray surface, for instance in wood or in plaster of Paris, which has two plane and parallel asymptotic regions and approximately the right shape in the curved region. How to produce approximately the right surface may be explained in a special case which is of considerable interest by its simplicity, in which the principal rays are geodesics.

Lay down first the 'crest' of the p.r.s., i.e. the approximate circular profile in the $X = 0$ plane where the trajectories reach their lowest point, midway between the asymptotic planes, around off the transition region in some convenient way. Fix a string to a peg at the point C and draw it tight on the surface at various initial angles. We will assume these shortest paths or geodesics to be the principal rays. Differential geometry gives the result that the u -lines are geodesics if and only if

$$\partial h_1 / \partial v = 0 \quad \dots \quad (2)$$

i.e. if the metric coefficient h_1 is a function of u alone. In eqn. (8) these lines will be dynamically possible trajectories if the v -lines are equipotentials.

We now modify the $X = 0$ profile until the desired angular magnification properties are obtained. By departing from the circular shape we can also obtain any desired deflection/voltage characteristics, for instance an exactly linear one.

Next we trace the v -lines at right-angles to the u -geodesics and copy these in a network of welded-steel wires. We now remove the p.r.s. model, retaining only a board between the

two asymptotic regions. We can, with the given network and unchanged asymptotes, distort the principal-ray surface in an infinity of ways, without stretching the wires or distorting their rectangular joints. This family of reversing lenses which we obtain with one wire model has, in common, the asymptotic behaviour, and also the property that the u -lines remain geodesics and the v -lines equipotentials. Apart from being free to vary the p.r.s. there is a further important degree of freedom; the potential $\phi(u)$ can still be freely determined. This is easily understood, because the u -lines are not refracted at the equipotentials which they traverse at right angles, whatever the potential gradient.

Substitute now in the W-ray eqn. (22) the geodetic condition $\phi = \phi(u)$ and use eqns. (8) and (11) in the form

$$h_1\phi(u) = \phi_0 \quad h_2\phi(u)V'(u, v) = \phi_0 G(v)$$

We then obtain the W-ray equation in the greatly simplified form

$$\frac{1}{\phi_0} \frac{d}{du}(\phi W') = \left[-\frac{2}{R_u^2} + \frac{1}{R_u R_v} - \frac{1}{2\phi_0} \left(\phi'' - \frac{1}{2} \frac{V''}{V'} \phi' \right) \right] W \quad (25)$$

This equation makes it easy to deal with the most important of the postulated properties of the reversing lens—the independence of its W-focusing properties on v . Only the asymptotic behaviour is important, but for the present it may be simpler to postulate

$$W = W(u) \quad (26)$$

and investigate the requirements. In eqn. (25) the whole left-hand side and the third term at the right-hand side are independent of v . Eqn. (25) therefore becomes consistent with the assumption [eqn. (26)] if, and only if

$$\begin{aligned} -\frac{2}{R_u^2} + \frac{1}{R_u R_v} + \frac{1}{4\phi_0} \frac{V''}{V'} \phi' \\ = -\frac{2}{R_u^2} + \frac{1}{R_u R_v} - \frac{1}{4\phi_0} \left(\frac{h_2'}{h_2} + \frac{\phi'}{\phi} \right) \phi' = F(u) \end{aligned} \quad (27)$$

where F is an arbitrary function. In the second form we have used eqn. (10) for V''/V' , in order to make it clear that this quantity is defined by the (u, v) -network and by the potential, independently of the distortions of the network. It is clear that (within limits, which we do not investigate) the condition of independent W-focusing can be realized by suitable distortions of the p.r.s.

In reality the conditions in eqn. (26) are too stringent, as we are interested only in the asymptotic behaviour. Let us instead postulate that the lens must be *telescopic*, independently of v . This means that if $W' = 0$ at the start, it must be zero also at the end. Integration of eqn. (25) gives immediately the condition

$$\int_{-\infty}^{\infty} \left[-\frac{2}{R_u^2} + \frac{1}{R_u R_v} - \frac{1}{2\phi_0} \left(\phi'' - \frac{1}{2} \frac{V''}{V'} \phi' \right) \right] W du = 0 \quad (28)$$

independently of v . This is a much less stringent condition than eqn. (27), because the variations of W with v can now be used to compensate those of the bracket expression.

Without going into more detail it can now be seen that all conditions can be satisfied with a reversing lens of the geodetic type. This is rather different from the one which we have experimentally realized, and we have chosen it here only for the simplicity of explanation.

The last step in the design of any such mathematically con-

structed reversing lens is the calculation of the potential $\phi(u, v, w)$ in space, from its values in the p.r.s. and its normal gradient, given by $1/R_u$. This can best be carried out by series expansion in powers of w , using eqn. (19) and its derivatives. This need not be unduly laborious if the series is broken off at a point at which it gives the approximate shape of the electrodes, and if the final corrections are carried out in an electrolytic tank model.

(12.3) Theory of the Magnetic Collimator

The magnetic collimator, as a 'strong lens', is unavoidably astigmatic. It is the purpose of the present theory to show up certain connections between its focusing properties in the principal XZ-plane and at right angles to it, as a function of the design data. In particular, we want to show that, while in the symmetry plane $X = 0$ the Y-power is necessarily negative, it becomes increasingly positive off this plane, and that this undesirable property can be minimized.

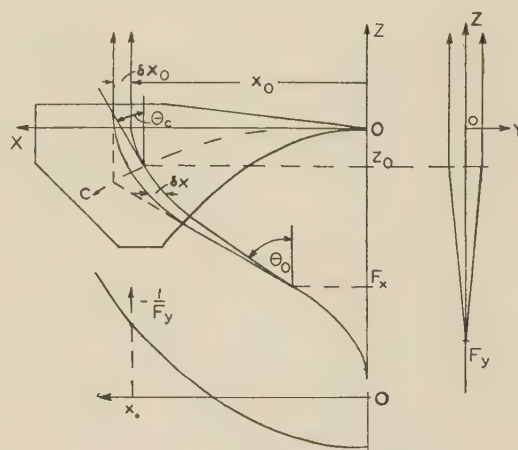


Fig. 24.—Illustrating the theory of the magnetic collimator.

The notations are shown in Fig. 24. Using a right-handed system X, Y, Z , the equations of electron motion are

$$\dot{v}_x = \frac{e}{m}(v_y H_z - v_z H_y) \quad \dot{v}_y = \frac{e}{m}(v_z H_x - v_x H_z) \quad (29)$$

We will eliminate time and introduce z as the independent variable. As the total velocity v is a constant, we obtain

$$\frac{d}{dz}(v_x/v) = \frac{d}{dz} \sin \theta = \frac{dt}{dz}(\dot{v}_x/v) = \frac{e}{mv v_z}(v_y H_z - v_z H_y)$$

and as, for the principal rays in the symmetry plane $Y = 0$, the component v_y is zero, this is

$$\frac{d}{dz} \sin \theta = \frac{e}{mv} H_y \quad (30)$$

The collimator must be so designed that the total deflection angle is equal to the initial angle ϕ_0 , which gives the design condition

$$\sin \theta_0 = \frac{e}{mv} \int_{-\infty}^{\infty} H_y dz \quad (y = 0) \quad (31)$$

It will now be assumed that this design condition is satisfied for every principal ray, and we will discuss the consequences for narrow pencils of rays centring on the principal rays. It will be convenient to introduce a simplifying approximation for the distances $\delta x, \delta y$ of a ray from a principal ray, which is illustrated

Here θ_c is the angle of the principal ray at the intersection with the line c . Both terms inside the last square brackets are positive, but the effect is, in fact, beneficial, because for large angles, F_y , is negative. Substituting this into eqn. (37) we obtain the first 'thick'-lens approximation

$$-\frac{1}{F_y} = \frac{\frac{1}{F_x} + \int_{-\infty}^{\infty} \frac{ds}{(R \cos \theta)^2}}{1 + (\cos \theta_c - \cos \theta_0) + \int_{-\infty}^{z_0} \frac{(z_0 - z) ds}{(R \cos \theta)^2}} \quad (43)$$

This formula contains only such data as can be obtained directly from a plan of the principal rays, as shown in Fig. 9 (F_x , θ_0 and θ_c) or integrals which can be easily computed graphically from the same plan, and gives a plot of the Y-power versus θ_0 or x_0 , as shown in Fig. 25.

The most important term is the second in the numerator. As there is only a limited arc length s available in the collimator, this is minimized by making

$$R \cos \theta = R_0 = \text{constant} \quad (44)$$

which means that the curvature must be made small at the entry, where $\cos \theta$ is small. It can be shown that this is satisfied by a curve

$$x = -R_0 \log \cos (z/R_0) \quad (45)$$

or by any part of such a curve. It is therefore possible to build up the collimator in such a way that all principal rays inside it follow segments of different lengths of the same curve. It can also be shown that, if we neglect H_x , the magnetic field H_y , H_z , which produces these trajectories, can be represented by the formula

$$H_y + jH_z = \cosh (y/R_0) e^{jz/R_0} \quad (46)$$

This can be derived from a magnetic potential

$$\Psi = \sinh (y/R_0) \cos (z/R_0) \quad (47)$$

which is realized by shaping the pole pieces so that their $x = \text{constant}$ sections conform to $\Psi = \text{constant}$. This gives approximately parabolical sections, which we have approached by two planes, joined together at an angle. For the very reason that there is an optimum, the shape is not very critical, and the approximation was found to be practically satisfactory.

(12.4) Theory of Self-Scan Stability

Consider a staggered array, as shown in Fig. 25, with the x co-ordinate running downwards. Connected conductors are considered as having the same value of x . Let c be the capacitance per unit length (to earth), $V(x, t)$ the voltage (also to earth) and $J(x, t)$ the current density per unit length of x . The equation connecting V and J is

$$c \frac{\partial V}{\partial t} = -J \quad (48)$$

where the electron current is considered to be positive. If this is to have a solution corresponding to an undistorted wave running down the array with a velocity u , so that $V(x - ut) = V(x, t)$, we must have

$$\frac{\partial V}{\partial t} + u \frac{\partial V}{\partial x} = 0$$

and consequently the current density must satisfy the equations

$$J(x, t) = J(x - ut) = cu \frac{\partial V}{\partial x} \quad (49)$$

Such a wave, once launched, would maintain itself, because the electrical and electron-dynamical conditions are uniform along the array, but the question is whether it will be stable, and, in particular, should it initially have a slightly wrong shape, whether it will asymptotically approach the shape which will run down undistorted.

Let us write $(V + v)$ for the voltage and $(J + j)$ for the current density, of a slightly distorted wave. We introduce a running co-ordinate system, travelling downwards with the speed

$$u = \left(\int_{-\infty}^{\infty} J dx \right) / c(V_{\max} - V_{\min}) \quad (50)$$

$$\text{by} \quad x' = x - ut \quad (51)$$

and denote differentiation with respect to time in this running system by D/Dt

$$\frac{D}{Dt} = \frac{\partial}{\partial t} + u \frac{\partial}{\partial x}$$

Substituting $(V + v)$ instead of V and $(J + j)$ instead of J in eqn. (48) gives

$$c \frac{Dv}{Dt} = -j(x', t) \quad (52)$$

This gives the *distortion speed* of the voltage wave, which will be zero only if $j = 0$.

Eqn. (49) presumes that the electric field V , ($v = 0$) produces a current distribution $J(x - ut)$ which satisfies this equation. The effect of small perturbations v will be, to a first approximation, expressible by an equation of the form

$$j(x', t) = \int_{-\infty}^{\infty} K(x', x'') v(x'', t) dx'' \quad (53)$$

i.e. a disturbance $v \cdot dx''$ at the (running) co-ordinate x'' produces at an arrival point x' the current disturbance $Kv dx''$. If the beam were very thin (i.e. a single ray) the kernel K would be, because of the uniformity of the array, of the form $K(x'' - x')$, but if the beam has appreciable thickness it will not be of this Laplacian type. The kernel is restricted by the condition

$$\int K(x', x'') dx' = 0 \quad (\text{for any } x'') \quad (54)$$

because, so long as the voltage disturbances are not very large, the total current collected by the array is unchanged.

A sufficient (but not necessary) condition of stability can be derived by substituting eqn. (53) into eqn. (54), multiplying both sides by $v(x')$ and integrating over all values of x'

$$\frac{1}{2} c \frac{D}{Dt} \int_{-\infty}^{\infty} v^2(x', t) dx' = - \iint_{-\infty}^{\infty} K(x', x'') v(x', t) v(x'', t) dx' dx'' \quad (55)$$

At the left-hand side we have the rate of increase of an essentially positive quantity, which represents the electrostatic energy of the disturbance. The right-hand side represents the total power of the beam which goes into decreasing or increasing this energy. If the kernel K is such that the integral at the right-hand side is a definite positive form of the variables $v(x') dx'$, $v(x'') dx''$, the energy of the disturbance will steadily decrease until $v = 0$ everywhere. Examples of such kernels are

$$K = p(x') \delta(x'' - x')$$

where p is a non-negative function, δ is a Dirac function, and

$$K = \sum_i F_i(x') F_i(x'')$$

where F is an arbitrary function.

For further investigations it is convenient to represent the kernel in the form

$$K(x', x'') = -\frac{\partial}{\partial x'} [J(x') S(x', x'')] \quad (56)$$

where $J(x')$ is, as before, the density of the electron current at the level of arrival, and $S(x', x'')$ is the shift of the arrival level at the point x' , caused by a delta-function disturbance in v at the point x'' . Eqn. (56) is more easily understood by substituting it into eqn. (53), giving the disturbance current density

$$j = -\frac{\partial}{\partial x'} \int_{-\infty}^{\infty} J(x') S(x', x'') v(x'') dx'' \quad (57)$$

This satisfies the condition that the total disturbance current is zero. The shift function S can be obtained from graphical ray tracing. S is always negative, because an excess positive potential anywhere in the array will always shift the arrival point upwards, i.e. towards negative x' . S will monotonically increase with x'' . It is also evident that it will fall to very small values for x'' corresponding to levels near to and above the point of arrival. A third, and the most important, property of S is that it is a *slow* function of x' relative to the current-density function $J(x')$ in sharply focused spots. We can therefore approximately write $S(0, x'')$ instead of $S(x', x'')$ where $x'' = 0$ may correspond to the centre of the spot. This enables us to write the stability-determining equation (55) in the simplified form

$$\frac{1}{2} \frac{e D}{D t} \int_{-\infty}^{\infty} v^2(x') dx' = \int_{-\infty}^{\infty} S(0, x'') v(x'') dx'' \int_{-\infty}^{\infty} \frac{dJ(x')}{dx'} v(x') dx' \quad (58)$$

i.e. as the product of two integrals.

It would take us too far to discuss the general question of stability, i.e. the question of whether, and how fast, the beam will eliminate disturbances of uniformity along the whole array, such as may have been caused by imperfections in the recharging of the array after the previous scan. We can, however, easily show that only 'short-wave', abrupt, disturbances will affect the beam, and will be affected by it. In the integral

$$\int_{-\infty}^{\infty} \frac{dJ(x')}{dx'} v(x', t) dx'$$

the first factor goes through a maximum and a minimum with a change of sign between, inside the spot width. If the second factor $v(x', t)$ is a relatively slow function, the integral will not depart appreciably from zero. Only if at some instant the spot passes through a zone in which the disturbance changes its sign with the first factor can the right-hand side of eqn. (58) become appreciable, positive or negative. This means that the spot, so long as it is sharply focused, will not appreciably affect the field $v(x)$ of disturbances, nor will it be permanently affected by them, because it will leave them behind. This answers the second question raised at the beginning, of whether a slight distortion in the launching field (near the C-plate) will permanently affect the beam. The answer is in the negative. There will be no growing instability, at any rate not within the limits of the linearized small-perturbation theory.

DISCUSSION BEFORE THE RADIO AND TELECOMMUNICATION SECTION, 14TH MAY, 1958

Dr. J. D. Stephenson: The authors have presented a paper in which they describe the theoretical and practical problems involved in a task which industry would regard as very formidable, but which the authors have attempted with the resources of a university post-graduate department.

The solutions of the many and difficult electron-optical problems inherent in the authors' proposals constitute an important contribution to our knowledge of this highly specialized branch of science.

I agree with the authors that their proposals would be completely uneconomic for black-and-white television presentation. In the case of colour, I am still very doubtful whether the proposed simplification of shadow mask and screen assembly compensates adequately for the intricate electron-optical system required.

Indeed, I find some difficulty in commenting upon certain aspects of the paper because the authors propose the use of techniques which have been discarded long ago by industry as impracticable and unsatisfactory.

In my opinion, the saving of space by the introduction of the reversing lens could well be sacrificed and use made of a conventional 110° or 130° magnetic deflection system. The variable deflection energy as the line traverses the screen would not be difficult of solution.

The number of variables which influence the spot size and shape is eight if we include the magnetic collimator. If we add the numerous trimmers referred to but not described or shown, we get some idea of the possible difficulties in reproducing such tubes. I am reminded of a story from America of the colour-television set with 33 knobs, the adjustment of any one of which only made the picture worse.

The self-scanning device is one of the principal features of the authors' work, and it is certainly the most original. More clarification of the principles involved and much experimental verification would be required before I could be convinced of the reproducibility of such a scanning system. The manufacture of this scanning system is formidable in itself and the authors' proposals in Section 9 appear to be far from practicable in this respect.

The second part of the paper describes the work done by the authors in solving the technological problems associated with the manufacture of the tube, and I would like to comment on certain of their proposals as follows:

(i) The all-glass version shown in Fig. 1 could not, in my opinion, be made without the risk of implosions, particularly when one considers that a 21 in picture would require a tube about 24 in square.

(ii) The actual manufacture of the tube, with its intricate gun system, magnetic collimator and associated coils, reversing lens and scanning system, would be an impossible task with regard to thermionic emission, life, and shelf life. In my opinion, the device could work only as a continually evacuated system, or with some replenishable gettering device.

(iii) The authors' methods for phosphor-layer preparation and the rather liberal use they make of silicon varnishes have been tried and discarded long ago as impracticable and unsatisfactory.

In conclusion, I would add that the television-tube manufacturing industry would require much discussion upon each of the numerous problems which present themselves, before being able to give anything in the nature of a positive 'yes' to the

possibilities of producing such tubes. I am nevertheless full of admiration for the ingenuity, abilities and zeal of the authors; I am doubtful of any practicable propositions in the near future resulting from their efforts.

Mr. G. G. Gouriet: The tube described in the paper bears the mark of many revolutionary inventions of the past, inventions which may not at the time have fulfilled a pressing need, but which nevertheless blazed the trail for future progress. This tube is as different from the conventional picture tube as is the turbo-jet engine from the conventional petrol engine, and indeed the difficulties encountered would seem to have been of a similar magnitude.

I do not think that such research requires justification at all, and I was rather surprised to hear colour television mentioned in this connection. It is probably true that the one thing above all retarding the progress of colour television is the cost and complexity of the colour tube and its ancillaries. We still require a cheap and simple display device, and I do not think that the advantages of the authors' tube lie in this direction.

Would the fact that the scanning beam itself is used to produce the field scan introduce a difficulty with regard to control of brightness? Perhaps some additional circuit would be required to provide brightness control without affecting the scan amplitude.

Do the authors think that this tube will be able to provide the size of picture which can be obtained with large conventional tubes? Would it be feasible, for example, to have a screen of 24 in diagonal?

Finally, taking into account the long path over which the electron beams must travel and the complexity of the electron optics, is it not likely that a small amount of distortion of the elements owing to change of temperature will have a pronounced effect on colour registration?

Dr. M. E. Haine: Apart from the basic invention, which represents the height of ingenuity, one of the most outstanding features of this development is the remarkable perseverance and ingenuity which has gone into solving the very difficult three-dimensional electron-optical problems. It should be emphasized that the solution of these problems has not just involved first-order trajectory plotting. It has been necessary to calculate or determine and compensate some higher-order aberrations. It would be useful to know more about the actual methods used and the order of accuracies determined.

I should like to know what the authors think about the possibility of eliminating the reversing lens and putting the electron gun on the top or bottom of the tube, using conventional magnetic deflection for the line scan. This was suggested in the early days of the development. The difficulties were pointed out, and they were fairly obvious, but that was before the collimator lens was introduced. The presence of the collimator would appear to make the suggestion more practicable, thus offering a considerable mechanical simplification without detracting seriously from the flat-tube conception.

Perhaps the authors would indicate in more detail the limitations imposed by the use of fewer bars in the scanning array. American workers seem to have produced a very useful raster of high definition, using a very limited number of bars, and I am not quite clear why the authors wish to use such a large number.

Mr. T. Kilvington: I was rather disappointed to learn that this flat tube would be more expensive than conventional tubes. The various parts of the tube do not appear to be too difficult to manufacture and should be amenable to mass production; and we have been assured that extremely close tolerances are not required. Could the authors say what are the particular features that will increase the cost?

I do not agree with the statement in Section 4 that a colour

tube with 400 lines is sufficient for the reproduction of a 625-line signal. It is well known, of course, that with any system only about 60 or 70% of the theoretical definition in the vertical direction can be obtained. This is inherent in the scanning method and the information is lacking in the electrical signal that represents the picture. If the picture is now reproduced on a device that is only capable of reproducing 400 lines there must be a further degradation of vertical definition.

The greatest disappointment is the fact that we have not seen a television picture reproduced upon the tube. Could the authors say whether the American flat tube to which they have referred has, in fact, been used to display a standard television picture?

Certainly if this tube can be developed and brought to fruition it will alter the shape of television sets to come. About a year ago in a discussion in this Lecture Theatre a speaker said that the size of the television screen was limited by the width of the door in the viewer's home. If this tube goes into production it will no longer be limited by the width of the door but by the height!

Mr. P. S. Carnt: There are two observations I should like to make on this tube. The first is that the colour version has apparently only one modulation electrode per gun. In a colour receiver of the N.T.S.C. type this means that the number of different circuits which can be used is quite severely restricted, and those which can be used are liable to be rather unsatisfactory from the point of view of the picture quality.

If two modulating electrodes per gun are available, such as in the shadow-mask tube, the tube itself can be used as a convenient matrix to add the wide-band luminance signal to the narrow-band colour-difference signals.

On the other hand, if only one modulating electrode per gun is available, the signals required are inevitably red, green and blue, each of which must have a wide-band frequency response to preserve the definition of the total luminance. This requires a wide band and therefore a low-impedance matrix, which would call for considerable power in the case of high-level demodulation. High-level demodulation, which is a convenient and stable decoding technique, would therefore be uneconomical.

The alternative is low-level demodulation followed by three separate video-frequency amplifiers, one for each colour. Such an arrangement inherently provides a poor grey scale which is likely to drift.

Another rather more elementary point is that, from the demonstration given, the frequency of the frame scan was of the order of 0.1 c/s. This is about three orders down on what is required in practice, and to say that this is a small step is rather like saying that to ride a bicycle at 18 m.p.h. is very nearly the same thing as orbiting the earth at 18 000 m.p.h.

Mr. C. L. Hirshman: With regard to the question of charging and discharging their array, if we take a practical requirement—that we would, say, require a picture size of not less than 16 in \times 12 in with, say, 16 kV—the scanning array might have a total capacitance of not much less than 300–350 pF. In the proposed tube the beam moves across the screen to produce a line and has to carry out a discharge during part of the flyback time. Even if we allow about one-third of the line flyback time for the discharge, which would increase the line-scanning power considerably, I estimate that it would need a peak current of about 4 mA, which would be very difficult to obtain.

About the same current is required for a rectangular-frame charging pulse, but matters could be even worse if we used a square waveform of 50% duty cycle for charging. A peak current of about 8 mA could then be required.

It seems that the authors' proposal for five cathodes in a common gun structure does allow two of the cathodes to have a higher current density, but it still restricts the time available

during which they can be used. It might be better to provide three separate guns (the beam of only one of the guns being deflected) so that there was one gun for providing the picture information, one for providing the line discharge and another for providing the array charge.

THE AUTHORS' REPLY TO THE ABOVE DISCUSSION

Prof. D. Gabor, and Drs. P. R. Stuart and P. G. Kalman (in reply): Dr. Stephenson, as well as Dr. Haine, favours a design, in which the reversing lens is abandoned. It would be roughly of the shape of a hand mirror, with 110° or even 130° magnetic deflection followed by a collimator. This is certainly a feasible design: it would empty the tube of all non-conventional elements except the scanning array, because the magnetic collimator, as well as the magnetic deflector, could be arranged outside the envelope; and it would make outgassing of the gun easier and the tube would become even thinner. The height, on the other hand, would be almost doubled. It would be of interest to make comparative price estimates and to probe the reactions of the public.

We are not in a position to give estimates of the baking time, cathode life and shelf life. The 'built-in' gettering device mentioned by Dr. Stephenson may well become of practical interest. An X-ray tube has just appeared on the American market which has not been baked in the exhaust at all but contains a built-in 'ionic pump'. This may be the answer also to his doubts raised about the use of silicone varnishes in a vacuum device. It may be mentioned though that, in our experience, the silicone known by the trade name of MS994 can be completely outgassed at 400°C , and that a valve containing a silicone-varnished glass fabric has recently come into practical use in the United States.

According to our information, the method of settling phosphors on the screen through the holes of the shadow mask has been discarded, not because it fails to produce sharply delineated and uniform patterns, but because in conventional shadow-mask tubes the dot-pattern on the screen is not identical with the hole-pattern in the shadow mask, and must be derived from it by a rather complicated projection method.

We quite agree with Mr. Gouriet that it may be advantageous to provide one or two separate cathodes for producing the scanning beam, so that the scanning circuits can be completely separated from the brightness-modulation circuits.

A question raised by Mr. Gouriet, as well as by Dr. Stephenson, is the realizability of large screens, such as 24 in square. A toughened-glass plate of $\frac{1}{2}$ in thickness of this size will withstand a pressure of 3 atm, and its cost is less than that of a moulded cathode-ray-tube cap of the same size. If one wanted to make even larger screens, they ought to have cylindrical curvature. The reversing lens and the collimator can be modified without difficulty for producing a cylindrical instead of a plane principal-ray surface. With regard to distortions by temperature, local temperature differences which could produce such distortions can arise only in the shadow mask, and this is securely anchored to the glass screen.

The electron-optically interesting problem of third-order aberrations, raised by Dr. Haine, is under revision, because recently we have succeeded in reducing them to a small fraction of their previous value. The theory is rather complicated, and not yet complete.

It is quite correct that W. Ross Aiken has succeeded in producing a frame scan with only slight periodic errors with only 7 bars in the scanning array instead of the 80 in our tube, and it is estimated that 16 bars would be sufficient to make the moiré pattern invisible. Our preference for the larger number has

I should like to query the use of the metal container which involves the cathodes being at not less than, say, -16 kV . It seems that the cost and the circuit complications of such an arrangement are prohibitive, and one should really consider an all-glass envelope.

two reasons. One is that, in the colour tube, we must operate with a wide beam, and the periodic changes in incidence angle arising from the change-over from one bar to the next would produce a periodic colour change which would be very disturbing. The other is that the self-scanning principle does not operate well with a small number of bars, owing to the secondary electrons which jump from one bar to the one below it, and tend to wash out the wavefront. On the other hand, we are not restricted in the number of bars, as we do not take them outside the vacuum envelope.

In reply to Mr. Kilvington, it is quite likely that a television set with a flat monochrome tube will ultimately be cheaper than present-day sets, by the savings in the circuits, the cabinet and transport costs. The tube itself, however, is at a disadvantage because the conventional tube contains almost nothing—just a screen, a gun and vacuum.

We agree that a colour raster of 400 lines falls short of the ideal with regard to vertical definition; in considering this as acceptable we were only quoting present-day colour-tube practice. There is some loss, but it was preferable to accept it rather than increase further the number of raster holes or grid wires, which would mean, of course, even more restricted tolerances in the manufacture. With our shadow-mask technique there is no such limit, and we could produce 80, and perhaps even 100, lines per inch.

We regret that we were not in a position to show a television picture, while W. Ross Aiken produced them several years ago. Our progress was slower, not only because of the natural limitations of an academic laboratory, but because we believe in solving certain problems by electron-optical improvements which, in the Aiken tube, are solved by circuit techniques, and electron-optical development is slower than circuit work.

In principle, it is possible to use the N.T.S.C. system with pure cathode modulation, but we agree with Mr. Carnt that it may be of advantage for the circuit engineer to add two extra grids for gamma correction of the red and blue beams. This can be done without difficulty.

The last point raised by Mr. Carnt was answered in a demonstration after the discussion. In the demonstration before the discussion we showed a slow run-down, to prove that the line was not 'washed out' during the scan and that the scanning speed could be modulated by the beam current. In the second demonstration the current was raised to about 1 mA, and the frame scanning speed was of the order required in practical operation.

We agree with Mr. Hirshman that, with array capacitances of the order of 300–350 pF, the scanning currents required become rather large. One way of reducing these is to increase the spacing between the array and the base-plate. This does not mean increasing the tube depth, because it is sufficient to withdraw the base-plate at the two sides of the gun. But the suggestion of two extra guns for scanning also deserves serious consideration, because their advantages for the circuit engineer might outweigh their extra cost.

We also agree with Mr. Hirshman that operation with an earthed screen has great disadvantages, and we intend to change this in our next model. However, this does not necessarily mean an all-glass envelope, but merely a front glass plate somewhat larger than the screen.

A SURVEY OF PERFORMANCE CRITERIA AND DESIGN CONSIDERATIONS FOR HIGH-QUALITY MONITORING LOUDSPEAKERS

By D. E. L. SHORTER, B.Sc.(Eng.), Associate Member.

(The paper was first received 12th November, 1957, and in revised form 10th February, 1958. It was published in April, 1958, and was read before the RADIO AND TELECOMMUNICATION SECTION 23rd April, 1958.)

SUMMARY

Loudspeakers used for monitoring purposes in broadcasting and recording studios are designed to give the nearest practicable approach to realistic reproduction. The paper discusses the various criteria which can be applied to the performance of such loudspeakers; together with the relationship between the measured free-field characteristics and the response as subjectively assessed in the working environment.

While the degree of realism achieved in sound reproduction can only be judged aurally, even subjective assessments can be misleading unless carried out under controlled conditions and with clearly defined terms of reference; the precautions necessary in such tests are discussed.

Some of the less obvious design considerations are reviewed and illustrated by examples.

with that of the high-quality radio-receiving and record-reproducing equipment required to do justice to it.

(1.2) Scope of Paper

Although considerable literature on various aspects of loudspeaker design exists, the fundamental question of the requirements to be met by the finished article is less fully documented. A large part of this survey is therefore devoted to the various performance criteria, subjective as well as objective, which have from time to time been proposed. Various means of meeting present-day requirements are also discussed. It should be emphasized, however, that at present no clear-cut solution is possible. It is not the function of the paper to add to the already long list of publications advocating particular methods of achieving the desired result; the examples cited are intended solely to illustrate some modern trends of development and to show the limitations, as well as the possibilities, of particular lines of approach.

(1) INTRODUCTION

(1.1) Functions of a Monitoring Loudspeaker

Broadcasting and recording organizations use high-quality loudspeakers to assess the aesthetic and technical merits of the programme material which they originate and to guide them in the control of such variables as the placing of artistes and microphones in the studio. It is sometimes suggested that monitoring of this kind should be carried out with loudspeakers of mediocre quality, such as are used by the majority of the public, the implication being that the programme material ought to be modified as necessary to offset the shortcomings of these instruments. In fact, the various types of low-grade sound-reproducer, while having certain features in common, differ so much in many respects that attempts to compensate for the characteristics of one lead to unnecessarily poor reproduction with another. Moreover, the occasional presence of fault conditions, to which every system is liable, is most noticeable with high-grade reproducing equipment, and it is clearly undesirable that the existence of technical faults should become apparent to even a minority of listeners while remaining unobserved by the operating staff. Finally, if progress in the science of sound transmission is to continue, the technical equipment concerned in originating the programme should have a higher standard of performance than that employed in reproducing it, since the former can be replaced only at long intervals while the latter is more frequently renewed and can more easily be kept up to date. It is therefore customary for loudspeaker systems employed for monitoring purposes to be made as free as possible from technical defects. There must be, however, a limit to the degree of elaboration to which it is proper to go; for example, the use of two or more separate loudspeakers to give a pseudo-stereophonic effect would be completely unrealistic at the present time. Moreover, even a broadcasting or recording organization must limit the size and cost of its listening equipment. In practice, a monitoring loudspeaker is intended to represent the best product of its kind which could be used by a member of the listening public, assuming an outlay comparable

(2) CRITERIA OF LOUDSPEAKER PERFORMANCE

(2.1) Terms of Reference

It is assumed that the ideal to be aimed at in sound reproduction is realism, i.e. that the sound pressures produced at the observer's ears should at any moment be equal to those which would obtain if either the original source of sound were brought into the listening room, or the observer were transported to some designated spot in the vicinity of the sound source. It should, however, be appreciated that, while the first condition might conceivably be produced if the geometry of the reproducing system bore some relation to that of the original sound source, the second, which is the one required for the majority of programme items, is fundamentally impossible to achieve—at all events, by a single loudspeaker.* It would require that the sound reaching the listener's ears from every direction should be related to the acoustic properties of the studio or concert hall but not to those of the room in which the loudspeaker is placed. The characteristics of a loudspeaker required to give the nearest approach, from an observer's point of view, to this impossible ideal depend upon subjective factors and cannot yet be prescribed from first principles. Fortunately, every broadcasting or recording organization employs a number of operating staff, whose daily activities involve listening alternately in studios and monitoring rooms and making critical comparisons between the sounds heard in the two places. Such observers are probably the best available judges of realism, and since their function constitutes them a species of consumers' representative, it seems reasonable to regard them as the final arbiters.

(2.2) Difficulties of Objective Assessment

Since the product of loudspeaker reproduction cannot be objectively defined, all that can be done is to specify those

Mr. Shorter is with the British Broadcasting Corporation.

* Stereophonic or pseudo-stereophonic systems are excluded from this discussion.

characteristics of the vibrating and radiating system which are thought to be relevant to the final result. Few of these characteristics can be varied independently of the others, while some of them cannot be accurately reproduced in nominally identical specimens. As a result, deductions regarding the influence of the various factors on the subjective end-product are often very uncertain, and any advance in making meaningful measurements is a slow process of trial and error. The position could be improved by more frequent publication of experimental results by those able to produce significant data, so that a body of experience could be built up. A greater degree of standardization in methods of measuring and expressing the performance of loudspeakers is, however, desirable; in this connection, attention may be drawn to the British Standard¹ of 1954 dealing with this subject.

The significance of the various measurable characteristics will now be discussed.

(2.3) Effects of Environment and Directional Characteristics

For the purpose of this discussion the term 'loudspeaker' includes the complete radiating system, comprising one or more vibrating diaphragms and some form of baffle or enclosure. It is a 3-dimensional device which is invariably small compared with the longest wavelength of sound to be radiated and large compared with the smallest. Its directional properties therefore vary widely with frequency; i.e. its frequency response varies widely with the direction of radiation. In general, loudspeakers are used indoors, so that much of the sound reaching the listener arrives indirectly, after having been radiated in various directions and reflected from the boundaries of the room, being further modified in the process through the variation of reflection coefficient with frequency. By some process not fully understood, the listener is able without conscious effort to integrate all the resulting stimuli into a single impression. It is clear, therefore, that any attempt to predict from the free-field characteristics of a loudspeaker the frequency response as it appears to the listener must take into account the radiation in various directions. For simple cases, where the relationship between the frequency characteristics for various angles of radiation is fixed, empirical rules, based on subjective assessment, have been formulated. Thus, McMillan and West² adopted the mean spherical response as a criterion; they described a loudspeaker, having a 7 in diameter cone, in which the mean spherical response* was held constant with frequency by making the axial frequency characteristic rise by about $2\frac{1}{2}$ dB per octave. This principle is not, however, universally applicable, and experience with loudspeakers covering frequencies up to 10 kc/s or above suggests that, if a single quantity representing 'effective' response is to be found at all, it will lie somewhere between the axial and mean spherical response. Such a quantity could be obtained by carrying out a modified spherical integration at each of a number of frequencies, taking zones concentric with the loudspeaker axis, and applying some weighting function which would give the front response more prominence. The measurement could be economically undertaken by using the normal equipment for tracing directivity patterns with the addition of a suitable signal-integrating device.³

Deduction of the effective frequency response of a loudspeaker from its free-space characteristics usually involves the tacit assumptions that complete diffusion of sound energy exists, and that the reaction of the reflected sound upon the loudspeaker, as manifested by changes in the acoustic impedance presented to the latter, may be neglected. These assumptions become invalid

at wavelengths comparable with the dimensions of the room; where these dimensions are small, the sound level below 100 c/s is difficult to predict, and it may be desirable to adjust the low-frequency characteristics of the loudspeaker to suit local conditions. It should also be pointed out that most monitoring loudspeakers are required to operate in a variety of positions, so that devices such as corner horns, which can only function at particular places in the room, are unsuitable for general use.

So far, the question of directional characteristics has been considered only in relation to the apparent frequency response of the loudspeaker/room combination. However, the final result as assessed by the listener also includes the apparent size and position of the sound source; this attribute of a loudspeaker cannot be directly specified, but is likewise a function of the directivity pattern. Single-cone loudspeakers of conventional construction become increasingly directional with increasing frequency, and in rooms of average reverberation time give the impression of a clearly localized small source of sound. Less directional loudspeakers produce more reverberant sound in the listening room and give a more spacious effect; and with a nearly omnidirectional system the source appears to be distributed over a wide area. It by no means follows, however, that omnidirectional radiation at all frequencies represents the ideal condition. From subjective experiments with loudspeakers of widely differing directional characteristics, Kaufmann⁴ recently concluded that the preferred form of polar distribution was that of the original source of sound. Further subjective studies are now required to decide on the best compromise for all purposes.

(2.4) Significance of Broad Trends in Response

(2.4.1) General.

Because of the irregular nature of loudspeaker frequency characteristics, which commonly exhibit local fluctuations of ± 5 dB or more about the mean, the effects of smaller deviations in the broad trend of the response, such as would be considered significant in other parts of the transmission chain, are often underrated. Changes of ± 2 dB or less in the general trend or in the relative level of certain critical frequency bands can be detected in whatever part of the transmission chain they occur; for example, two frequency characteristics, each within ± 2 dB of uniformity but one increasing slowly and the other decreasing slowly throughout the range, give distinctly different subjective effects. It is therefore convenient to consider the broad trends in the response of the system, averaged over a series of frequency bands by the use of wide-range warble tones or bands of noise; in dealing with derived quantities such as the mid-band sensitivity or the mean spherical response, such an approach may in any case be necessary on practical grounds. For instrumental reasons, the accuracy with which the details of a frequency response curve can be delineated is often little better than ± 2 dB. However, many of the errors to which this type of measurement is subject are absent for a noise-band test, in which results can usually be repeated to better than $\frac{1}{2}$ dB; such tests are of practical value for routine maintenance, since valid comparisons between loudspeakers of the same type can be made in a 'live' room.

(2.4.2) Significance of Specific Frequency Bands.

Experience with loudspeakers of known characteristics, supplemented by experiments on raising or lowering the response in specific regions by means of band-pass or band-stop circuits, enables the subjective effect of an excess or deficiency to be predicted. Many of the conclusions to be drawn from such experience are too well known to require recapitulation; two, however, are worth mentioning because of their bearing on design.

If a progressive decline in response with increasing frequency

* The term 'mean spherical response' in acoustics relates to the total acoustic power output from a sound source and is analogous to the term 'mean spherical candle power' used in optics.

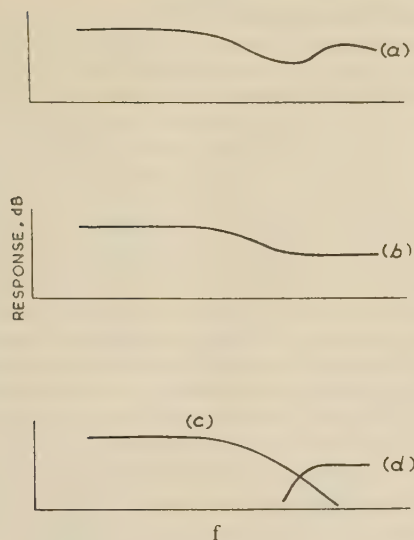


Fig. 1.—Typical defects in upper-frequency response.

is followed by an increase, giving the type of characteristic illustrated in curve (a) of Fig. 1, the upper frequency range will be heard to stand out in unnatural relief, even though the response nowhere rises above the mid-band level. It should be noted that this form of frequency characteristic modifies the spectrum of the reproduced sound in a way not experienced when listening to natural sounds. Progressive attenuation with increasing frequency is an everyday occurrence—it is experienced, for example, when listening to sound which has travelled round a corner—but, apart from isolated cases of specular reflection, selective reinforcement of the upper frequency range does not appear in nature. Even a shelving characteristic, such as that shown in curve (b) of Fig. 1, can give the effect of a 'disembodied' high-frequency output, a result which could be explained on the assumption that the energy spectrum is subjectively analysed into a continuously falling curve (c) of Fig. 1, with the addition of a secondary curve, (d). The above remarks naturally apply to some extent to the sound radiated in all directions and it seems to be a safe rule that the ear, in integrating the characteristics for the various angles of radiation, will take in the most well-defined—which in practice means the worst—features of each. Unfortunately, the off-axis frequency characteristics of wide-range multi-radiator loudspeakers are particularly likely to be of the humped or shelving type shown in curves (a) and (b), even though the axial characteristic may be flat.

The second observation concerns the critical nature of the frequency band in the region 2–4 kc/s, the level of which, relative to the remainder of the spectrum, has a pronounced effect upon the apparent auditory perspective. Deficiency in this band gives a distant impression; slight excess gives a forward quality, sometimes referred to as 'presence'. The tonal quality associated with extreme deficiency or excess in this region ranges from hollow, or distant, to hard or metallic.* This complete gamut of effects can often be passed through with a change in level of plus or minus a few decibels in the band concerned. With most cone radiators designed to cover the lower-frequency range the response in the 2–4 kc/s region is difficult to control and often varies widely in manufacture. To obtain consistent performance in production, therefore, it is

desirable in multi-unit loudspeaker systems, first, that the first cross-over frequency should not be higher than 2 kc/s, and secondly, that means should be provided for adjusting, in steps not greater than 2 dB, the relative levels of the signals applied to the high- and low-frequency units to compensate for production variations in sensitivity.

(2.4.3) Overall Slope of Response Characteristics.

It is often tacitly assumed that, for the highest degree of realism in sound reproduction by a single loudspeaker, the axial response, the mean spherical response or some intermediate quantity ought to be held constant with frequency. This assumption is not always supported by subjective judgment. Observers who with one type of loudspeaker prefer an axial response rising slightly with increasing frequency may demand with another type that the axial characteristic, and hence all other characteristics, should fall. The desire for a reduced high-frequency output is often expressed when the frequency response curve in the upper part of the range is not smooth; in other cases, the varying preferences may be connected with the directional characteristics. Again, with loudspeakers of conventional directional properties, a uniform axial frequency response is necessarily accompanied by a considerable increase in total sound output at the lower frequencies; this increase is seldom regarded as excessive and is sometimes felt to be insufficient. The demand for an overemphasized low-frequency response may be partly accounted for by the apparent weakening of the lower-frequency components which is observed when a sound is reproduced at a level below that of the original. However, in view of the complexity of the factors on which the illusion of reality depends, varying preferences such as those referred to need occasion no surprise and it seems unprofitable to be dogmatic on the subject. The only firm conclusion which can safely be drawn is that with wide-range loudspeakers of conventional directional characteristics a flat axial response may be acceptable but a flat mean-spherical response is intolerable.

(2.5) Frequency-Response Irregularity and Related Criteria

(2.5.1) General.

So far, attention has been concentrated on broad trends in the frequency characteristics such as would remain after averaging the response over bands of, say, $\frac{1}{2}$ –1 octave. Performance criteria based on such a smoothing process represent a minimum requirement. Clearly, the response within each band should vary as smoothly as possible with frequency; the permissible degree of fluctuation has, however, always been open to doubt. Much of the published work on this subject is concerned with the relationship between the frequency response of the system and the time response as shown by the reproduction of transient signals; it will therefore be convenient to survey these two subjects together, along with the closely connected subject of phase distortion.

Most of the detailed studies of frequency characteristics have treated the loudspeaker as a minimum-phase-shift device; in such a case, supplementary measurements of phase shift or transient response could be undertaken for convenience but would in principle be unnecessary. The practical limitations imposed by the minimum-phase-shift assumption will be discussed later.

(2.5.2) Transient Response.

The direct observation of transient phenomena in loudspeakers has been the subject of a number of publications. Early investigations were carried out by McLachlan and Sowter, using a unit-step signal, and in 1937 Helmbold,⁵ using an interrupted tone, was able to demonstrate the relationship between build-up time and steady-state frequency response.

* Such expressions as these may seem out of place in a technical context. They are, however, typical of the terms in which the end product of a sound-reproduction system is described by the observer, and when employed by individuals known to be capable of consistent judgment must be treated with respect.

Some years ago the author suggested⁶ that, since correlation between subjective quality and frequency-response irregularity was still unsatisfactory, the interrupted-tone testing method should be extended to the later stages of the transient, the form of which can in simple cases be related to the smaller fluctuations in the frequency characteristic. Attention was concentrated on the decay transient, the envelope of which had been found at particular frequencies to take the form approximately represented in Fig. 2(a). The slowly decaying tail presumably represents the sound output from some resonant element having relatively

little damping; this sound can thus be regarded as having been diluted by the main sound output in the ratio $A'_0 : A_0$, which, in conjunction with the two decay factors Δ_1 and Δ_2 , serves as a useful quantitative index to the transient behaviour of the system. At the cost of some instrumental complication, the data obtained from oscillograms can be presented as a function of the frequency of the interrupted tone. To this end the cycle of interruption is repeated at short intervals while the frequency is slowly varied and the envelope amplitude A_1 , appearing a time t_1 after the start of the decay, is plotted; the same process repeated for times t_2, t_3 , etc., gives a family of curves, of the form shown in Fig. 2(b), which exhibit peaks at the various frequencies of resonance. This presentation can be used even where the decays are not exponential. The information shown in Fig. 2(b) can also be presented as a 3-dimensional model representing amplitude, frequency and time; Fig. 2(c) shows such a model constructed from experimental data.

Following the same approach, Corrington,⁷ in the United States, showed experimentally the connection between various modes of cone resonance, the associated transient phenomena observed with an interrupted tone signal and the corresponding fluctuations in the frequency characteristic, many of which, in the examples given, were less than 1 dB in extent. As a sequel to this work, an ingenious electronic device was designed⁸ to interrupt the test tone at intervals corresponding to a prescribed number of cycles and to record, as a function of frequency, the mean sound output registered during the nominally silent periods. From the results, it was suggested^{8,9} as a criterion that the mean sound pressure during the first 16 cycles of the decay transient should not exceed some 12% of the steady-state pressure at the same frequency.

In contrast to the methods just described is the work of Hentsch¹⁰ and Seemann,¹¹ in Switzerland, on the influence of irregularities in the frequency characteristic. Seemann proposed some empirical rules, based on subjective experiments with interrupted tone passed through various resonant circuits and filters and presented to the observers by high-quality earphones; he concluded that, *inter alia*, irregularities in frequency response up to ± 2 dB are imperceptible.

The various lines of approach outlined above have more in common than may at first appear. Consider a case in which irregularities of ± 2 dB, i.e. approximately $\pm 25\%$ about the mean response curve, are caused by the presence in the loudspeaker system of a series of subsidiary resonant elements, the maximum output from each element being 25% of the mean output and either in phase or in antiphase with it.⁶ The tail of the transient will then start its decay with an amplitude A' which is 0.25 of the mean steady-state sound pressure in the frequency region concerned. Let it now be assumed, for example, that the final rate of decay is 1 dB/millisecond ($\Delta_2 = 115$), a figure which lies roughly in the middle of the range encountered in practice and within one order of the extreme values—and the $\Delta_1 \gg \Delta_2$; it is then readily shown that at 1 kc/s the average level of the transient tail taken over the first 16 cycles is 0.48 A' , or 0.12 of the mean steady-state pressure. In the example given, therefore, the frequency response which just satisfies Seemann's criterion of ± 2 dB is associated with a form of transient which just meets the 12% requirement laid down by Corrington.

(2.5.3) Effect of Non-Minimum-Phase-Shift Condition.

In all the work described in the last Section, frequency response irregularity and transient distortion existed simultaneously and no attempt was made in the experiments to introduce the one without the other. In any system to which the minimum-phase-shift condition does not apply, the two

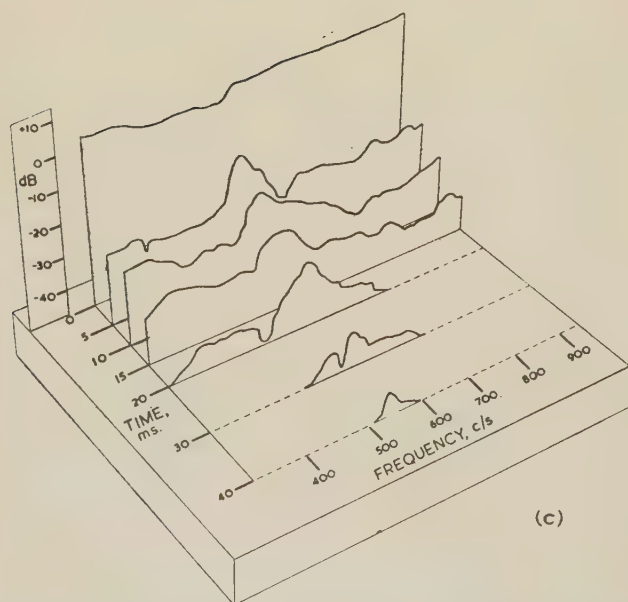
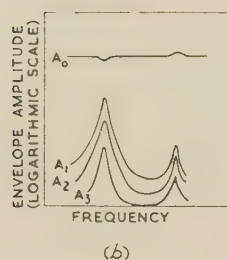
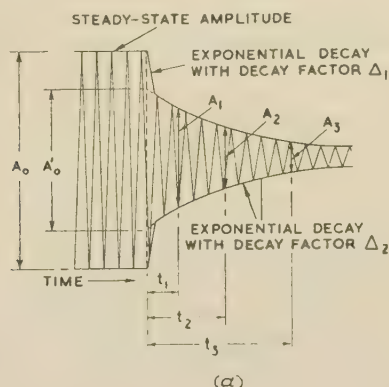


Fig. 2.—Methods of representing response of multiple resonant system to interrupted tone.

- (a) As a function of time.
- (b) As a function of time and frequency.
- (c) As a 3-dimensional model in time and frequency.

tributes can, of course, be independent of each other, but little information is available on the subjective effect of varying them separately. Hentsch,¹⁰ however, described some tests carried out with a series of all-pass networks, which allowed phase shifts to be introduced into the transmission chain without alteration of the frequency characteristic; the networks gave a maximum group delay, i.e. rate of change of phase with frequency, up to 35 msec at 524 c/s but very little delay at other frequencies. Interrupted tone at 524 c/s was passed through the delay networks and presented to the observers through high-quality headphones; the smallest perceptible group delay time was found to be of the order of 10 msec. Tests were also carried out with a simple resonant circuit tuned to a frequency of 524 c/s; a circuit of this kind, having a time-constant of about 2 msec, was found to have the same—just perceptible—subjective effect as the all-pass system with a group delay of 10 msec. These results illustrate the limitations of transient-response measurement when minimum-phase-shift conditions cannot be assumed. In such circumstances, however, the steady-state response/frequency characteristic is equally inadequate as an index of performance unless supplemented by the corresponding phase/frequency characteristic.

(2.5.4) Phase Distortion.

Many cases occur in practice in which a loudspeaker imposes on the reproduced sound a strong characteristic coloration, although the frequency response curve in the region concerned is smooth and level or has been made so by electrical equalization. These loudspeakers presumably cannot be regarded as minimum-phase-shift devices, and consideration of their phase distortion is indicated. Measurement of phase distortion in loudspeakers has hitherto received little attention, probably because of the instrumental difficulties involved, though Ewaskio and Mawardi¹² have published some group-delay/frequency characteristics for single- and double-unit loudspeakers, together with the corresponding amplitude-response/frequency characteristics. Measurements of this kind may ultimately provide the solution in otherwise intractable cases, but much further work will be necessary before the practical value of this approach can be properly assessed.

(2.5.5) Effect of Interference.

In the foregoing discussion it is tacitly assumed that sound from the various parts of the radiating surface reaches the measuring point by paths of nearly equal length so that interference effects are negligible. To achieve such a condition, even on the axis of a small diaphragm, is less simple than might be expected. Even though the radiation from the rear of the diaphragm is completely suppressed, interference can be caused by reflection at the discontinuity formed by the edges of the enclosure. This effect, first demonstrated by Nichols¹³ and Olson,¹⁴ may extend throughout the audio-frequency range; it can be minimized by mounting the radiating unit asymmetrically and by rounding or chamfering the front edges of the enclosure.

A difficult situation arises when the loudspeaker consists of several units. Where each unit covers a different band of frequencies, interference is confined to the cross-over region. If, however, two or more units are used to cover the same band—a growing practice in loudspeakers intended to give wide-angle radiation at high frequencies—the effect will extend over a wider band and it may be impossible to find any point equidistant from all the radiating surfaces at which to measure the response.

As long as interference effects in free space vary with the position at which the pressure measurement is taken and do not affect the average response of the loudspeaker over a wide band, they fall into the same category as interference effects produced

by reflections in a live listening room and may be relatively harmless. Some method of measurement which would automatically discount irregularities in the frequency characteristics arising from interference, while retaining enough information about irregularities arising from other causes, is therefore desirable. Meanwhile, it may be necessary, in investigating the performance of a multi-unit loudspeaker, to test each unit separately, if necessary in another enclosure.

(2.6) Non-Linearity

(2.6.1) General.

The effects of non-linearity in loudspeakers differ from those occurring in most other parts of a sound transmission system in the manner in which they vary with the frequency of the signal. Apart from a gradual increase in distortion towards the lower end of the working frequency range, pronounced non-linearity often appears in a series of very narrow bands,¹⁵ so that measurements are laborious and the results are particularly difficult to interpret for a complex signal waveform. It is therefore not surprising that the literature on the subject is concerned more with the description of methods of distortion measurement, illustrated by results for particular cases, than with systematic investigations to discover the maximum permissible values. With some forms of distortion it would probably be easier, as well as more profitable, to remove the cause by appropriate design than to discover rules for assessing the effect. More information on the mechanism of the various forms of distortion in loudspeakers is therefore required; to obtain this information various refinements of measuring techniques may be necessary.

Measurements of non-linearity in loudspeakers at discrete frequencies are of limited value unless these frequencies are chosen by ear, using a gliding-tone signal. Ideally, distortion should be measured as a continuous function of frequency, and this can be done by heterodyne methods or by switching filters.

(2.6.2) Application of Harmonic and Intermodulation-Distortion Tests.

In single-tone distortion testing, it is advisable to measure the individual harmonics, since loudspeakers are prone to a type of non-linearity¹⁶ which is more offensive to the ear than the total harmonic content would suggest. Such distortion can arise when some vibrating element, e.g. the cone surround, is in resonance and reaches the limit of its excursion while the rest of the moving system is still operating linearly.

Fig. 3 shows an example of a harmonic-distortion measurement on a loudspeaker made by means of a gliding-tone heterodyne analyser. The signal at the input of the associated amplifier was held constant with frequency at such a value as to produce at 400 c/s and at 4 ft 6 in distance an axial sound pressure of 10 dyn/cm² r.m.s. (94 dB above the reference level, 2×10^{-4} dyn/cm²). Fig. 3 shows the fundamental and harmonics up to the sixth in their correct relative positions on a decibel scale. The degree of distortion shown at the highest and lowest frequencies is not reached in practice, since the spectrum of normal programme material falls at the extremes of the frequency band.^{17,18} To cover all conditions it would be possible to repeat the distortion measurements at a series of different input levels. A less laborious alternative would have been deliberately to reduce the applied signal at high and low frequencies according to some law based on the spectrum of the programme; to this end it would be helpful if agreement on a standard law of attenuation could be reached.

Harmonic-distortion tests cannot be extended to the upper end of the audio-frequency range, since many of the distortion products then fall outside the pass-band of the loudspeaker or measuring equipment; this limitation is not serious unless the

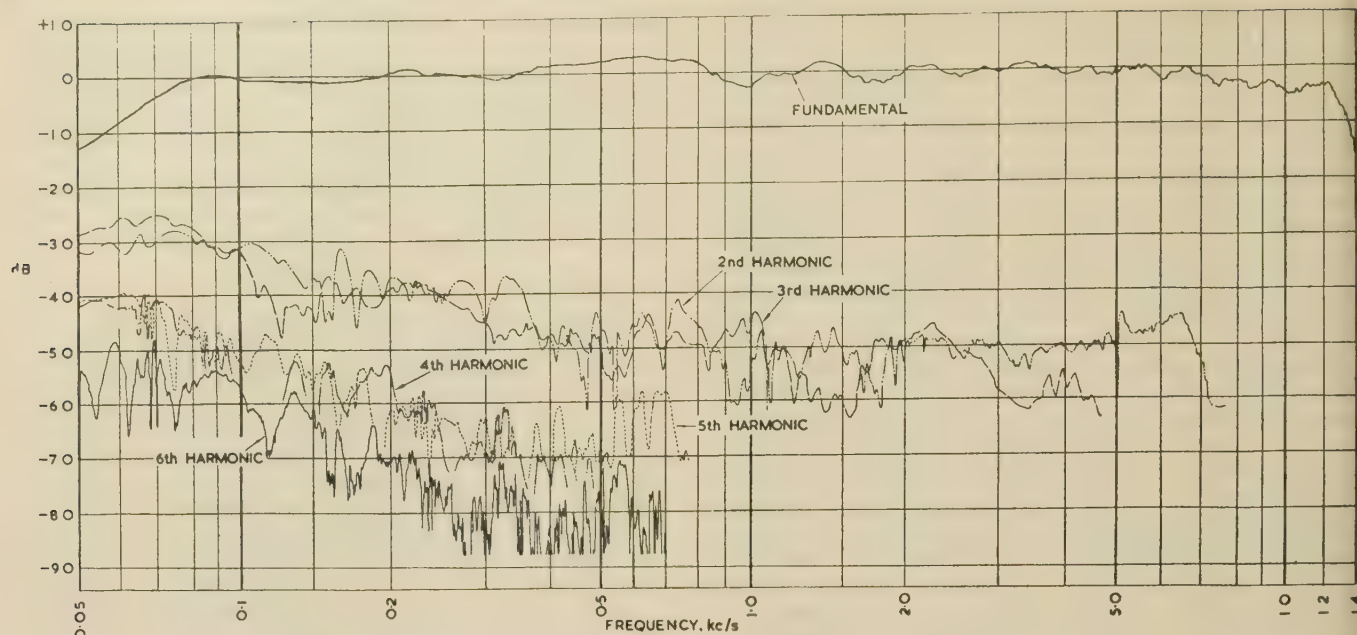


Fig. 3.—Fundamental and harmonics in output of loudspeaker excited with gliding tone.

distortion produced by the loudspeaker or its associated amplifier increases at higher frequencies. Where it is important to test the linearity of the system up to the limit of the audio-frequency band, an intermodulation test with two gliding tones, of frequencies f_1 and f_2 ($f_2 > f_1$) and a constant difference $f_2 - f_1$, may be applied. Fig. 4 shows the results of such a test on the loudspeaker of the last example. The amplitude of each tone was $1/\sqrt{2}$ of the amplitude of the single tone in the harmonic measurement and $f_2 - f_1$ was 120 c/s. The curves show the relative levels of the fundamental signals and the intermodulation products having frequencies $f_2 - f_1$, $2f_1 - f_2$, $3f_1 - 2f_2$ and $4f_1 - 3f_2$. It will be seen that in tests of this kind it is insufficient to take the difference frequency alone; on the other hand, the measurement of one or two of the higher-order products will probably give all the information that is required.

In a more common form of intermodulation test, two tones widely separated in frequency are applied; the amplitude of the higher-frequency tone is generally made about one-quarter that of the lower-frequency signal¹ and the distortion is assessed in terms of the degree of modulation of the former by the latter. This type of measurement is primarily intended to indicate non-linearity at frequency f_1 , the signal of frequency f_2 being regarded as a pilot tone, the precise frequency and amplitude of which are unimportant, and which in itself creates no distortion products. The method has the great advantage that the acoustic measurement can be confined to a small range of frequencies in the middle of the audio-frequency band. In an alternative scheme proposed by Ingerslev¹⁹ the two applied signals are of equal amplitude and the level of the intermodulation products is plotted as a function of f_2/f_1 remaining fixed. The results of such a measurement must, however, depend on the degree of non-linearity existing at both f_1 and f_2 , and a number of tests would be necessary to identify the various sources of distortion.

(2.7) Methods of Subjective Assessment

(2.7.1) General.

The subjective assessment of loudspeaker performance might appear to be a simple and straightforward operation and was once so regarded. It was common practice to judge loudspeakers by their reproduction of a variety of transmitted

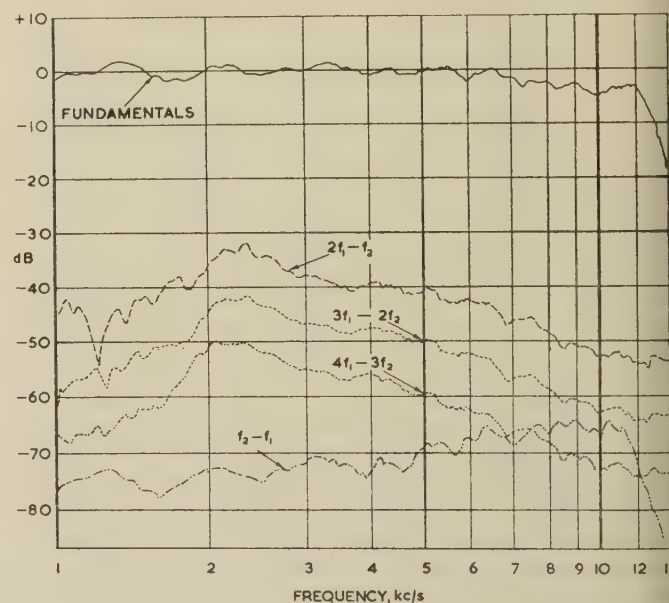


Fig. 4.—Fundamental and intermodulation products in output of loudspeaker excited with two gliding tones of equal amplitude having a constant frequency difference.

programme material without reference to the original sound. Sometimes the criterion of the 'most pleasing sound' was adopted. However, when the standard of reproduction advanced to the point where some slight semblance of realism was possible, this somewhat naïve approach had to be abandoned, for the order of merit was found to vary with the type of programme material, the studio acoustics, the microphone placing, and with other factors such as the position of the different loudspeakers in the listening room. Further experience showed that, by systematic listening tests carried out under more carefully controlled conditions, the effects of irrelevant factors could be largely eliminated and the risk of a wrong judgment, i.e. one which would later have to be revised after a period of service, much reduced.

2.7.2) Noise Tests.

Many of the salient features of loudspeaker response can be very quickly appreciated subjectively by applying to the input a continuous-spectrum random-noise voltage. To avoid aural fatigue and to render the test more sensitive, it is advantageous for this and other subjective assessments to place a second loudspeaker beside the one under consideration and to switch back and forth between the two; by contrast, the individual peculiarities of both loudspeakers will then become evident. This test will usually disclose differences even between nominally identical loudspeakers.

2.7.3) Speech Tests.

The realistic, as distinct from the merely intelligible, reproduction of speech is particularly difficult to achieve; the transmission of a voice which is familiar to the observers is a stringent test for a loudspeaker. Male voices are the most suitable, as they reveal various defects common in the 250–2000 c/s band. The speech should be transmitted from a non-reverberant room or from the open air, for it is not the function of a loudspeaker to compensate for peculiarities in the acoustics of studios. It is not permissible to reduce the amount of transmitted reverberation by bringing the microphone close to the speaker's mouth; speech picked up at distances less than 12 in has an unnatural character, particularly at high frequencies, which cannot be compensated by electrical equalization.

For these and the remaining subjective tests, the loudspeakers to be compared should be concealed from the observers to prevent identification.

2.7.4) Music Tests.

The final test consists of a comparison between live and reproduced music, the listening point being established as near as possible to the studio or concert hall so that the observers may pass freely between the two. Such freedom of movement is possible only during rehearsals, and observers must note the final quality being produced in the studio *at the time*, since musicians often reserve their fullest efforts for the final performance. Good sound insulation between studio and listening room is important, especially at the extremely low frequencies, at which an attenuation of at least 35 dB is essential.

The quality of reproduction obtained will naturally depend on the disposition of the performers and of the microphones in the studio—technically known as the ‘balance’ of the transmission. It is important, however, that defects in the loudspeaker should not be unwittingly compensated by an alteration in balance; for the purpose of the test, therefore, the instruments of the orchestra should be arranged to give an acceptable result as heard in the studio, and a single microphone, so placed as to avoid over-emphasis of any one instrument, should be used. It is true that in certain types of programme more than one microphone is frequently employed; with dance bands, to take an extreme example, a separate microphone may be provided for each group of instruments, and by this means effects can be produced which are not audible to a listener in the studio. Programme material of this type is, however, inadmissible when an unambiguous comparison between original and reproduced sound has to be made.

In studios and concert halls having good sound diffusion—a condition which can be verified by direct listening—the microphone placing is not highly critical.²⁰ For a particular orchestral layout, however, there is usually a preferred position, and this position in itself gives an additional check on loudspeaker performance. The better types of loudspeaker, while each departing in a different way from the ideal and so giving an appreciably different version of the transmitted sound, have in

practice so much in common that the best microphone position for any one of them is nearly the same. On the other hand, a loudspeaker having some peculiarity in response, which, for example, throws into prominence one type of orchestral instrument, may require for best results a different microphone position or even a different orchestral layout.

All that has been said on the subject of optimum microphone placing applies equally to the directional characteristics of the microphone required to give the best overall effect. Differences in performance between high-quality microphones having the same nominal directional characteristics are too small to affect the order of preference between different loudspeakers.

(3) DESIGN CONSIDERATIONS

(3.1) Electrical Equalization

The loudspeaker designer's task could frequently be eased by modifying the frequency characteristics of the preceding amplifier chain. This expedient, often employed in one form or another in the design of radio receivers, introduces some obvious instrumental complications when applied to an independent loudspeaker, but has important advantages where an exceptionally high and consistent standard of performance is required. It may even be practicable to introduce corrective circuits between the final amplifier and the loudspeaker proper, due regard being paid to the power-handling capacity of the system.

A notable example of electrical equalization of loudspeaker characteristics is furnished by the ‘omnidirectional’ radiating system produced by Harz and Kösters²¹ in Germany for broadcast monitoring purposes; in this type of loudspeaker, the associated power amplifier is preceded by a separate low-power equalization amplifier, incorporating both low- and high-frequency pre-emphasis circuits, together with as many as six other networks designed to correct specific features in the frequency characteristics.

Electrical compensation for low-damped resonances in a loudspeaker is impracticable, if only because of the difficulty in maintaining long-term stability of the mechanical system. Electrical control of general trends in the frequency characteristics or of the response within a broad band is, however, perfectly feasible; it allows adjustments to be made to offset production variations in the electro-acoustic transducers or to compensate for differences between the acoustic conditions in individual listening rooms.

(3.2) Division of Frequency Range

In the design of wide-range loudspeakers it is usual either to provide a separate unit for the higher end of the audio-frequency band or to employ a single unit, equipped with an auxiliary diaphragm in the form of a concentric dome or cone driven from the common speech coil, to give the same effect. The change-over from the low-frequency to the high-frequency radiating system should preferably take place at a frequency at which the former is not appreciably directional. If this requirement is not met, a state of affairs arises which is represented, in simplified form, in Fig. 5. Assume that a low- and a high-frequency unit, each having uniform axial response, are mounted on a common axis and fed through a cross-over network in such a way that the combined axial response ($\theta = 0$) is likewise uniform. If, at the cross-over frequency f_{co} , the low-frequency radiator is appreciably directional, the frequency characteristics at angles θ_1, θ_2 , etc., will exhibit a depression in the region just below f_{co} . This effect could be largely avoided if the frequency range were divided into three bands, using diaphragms of progressively smaller diameters; for most purposes, however, this solution is uneconomic, not only because of the extra

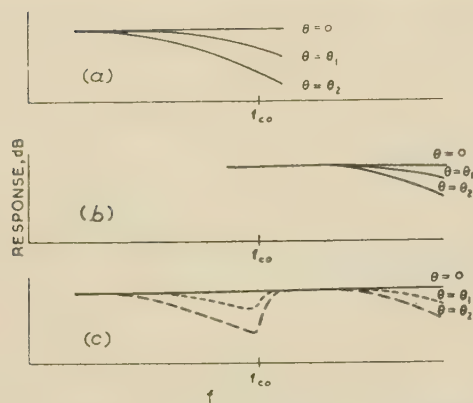


Fig. 5.—Two-unit loudspeaker: effect on overall frequency characteristics of change in directional properties at cross-over.

- (a) Frequency response of low-frequency unit.
 (b) Frequency response of high-frequency unit.
 (c) Combined frequency response.

radiating system, but also because of the additional cross-over networks and the extra setting-up adjustments required in production.

(3.3) General Properties of Cone Radiators

Although cone loudspeakers have been in common use for more than 30 years, the amount of systematic research carried out on their performance is surprisingly small and their design is still, to a large extent, a matter of trial and error. The behaviour of the diaphragm is not readily amenable to mathematical treatment, the difficulty of analysis being aggravated by the various departures from the simple conical form which in course of time have been empirically introduced. Experimental studies are hampered by the high price of the tools required to form the diaphragm; it may cost several hundred pounds to discover the effect of a minor change in profile.

The diaphragm of a cone loudspeaker is a complex vibratory system capable of motion in various regimes. The quality of sound produced by it is not always predictable from the frequency/response characteristics, even in the region below 1 kc/s where these may be relatively smooth. In particular, an objectionable type of coloration in the lower-middle-frequency range seems to be characteristic of a large number of units of less than 10 in cone diameter. The effect is usually associated with the presence of low-damped radial modes; however, attempts to simulate the subjective result electrically by the introduction of single tuned circuits having a comparable decrement have not been successful, and it may be that, as in the study of reverberation phenomena, a combination of modes is involved. Until this difficulty is overcome, it may be necessary in high-quality loudspeakers to employ diaphragms having areas much greater than those dictated by considerations of power-handling capacity.

(3.4) Alternative Radiating Systems for High Frequencies

The most economical form of direct radiator for the upper frequency band is undoubtedly a smaller version of the cone unit used for the low-frequency range, employing a pulp or plastic diaphragm. However, with the relatively small radiating area required, other forms of construction become possible. Small horn-type units, having coil-driven or ribbon-type diaphragms, have been extensively used; while horn radiators have been demonstrated²² in which the diaphragm was replaced by a modulated high-frequency glow discharge taking place in a quartz tube. In recent years, there has been a revival of the electrostatic radiator for high frequencies, though not all of

these units have been in the high-quality class. Finally, a form of direct radiator has been developed which is similar in structure to the moving-coil elements commonly used in conjunction with horns. Fig. 6 shows the construction of a commercial unit of

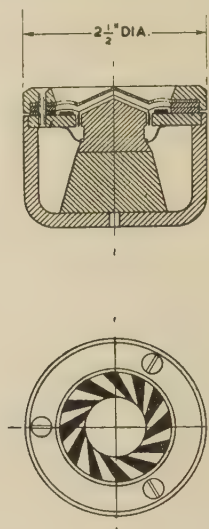


Fig. 6.—Example of modern direct-radiator high-frequency unit.

this type; the diaphragm, of plastic-impregnated fabric, moves as a whole at frequencies up to at least 10 kc/s. Because of its small dimensions the unit is less directional at high frequencies than a conventional cone or single horn radiator.

Other things being equal, the usefulness of a high-frequency radiator is limited by the acoustic power which it can produce without distortion or damage, and this usually diminishes rapidly with decreasing frequency. Direct radiating units which are small enough not to be unduly directional are generally suitable only for frequencies above 1.5 kc/s, while some are unusable below 3 kc/s. Moving-coil-driven horn systems offer some improvement in this respect and allow a nominal cross-over frequency which usually lies between 1 and 2 kc/s.

Attempts have been made to produce a radiating system substantially omnidirectional even at high audio frequencies. The best-known example of such a design is the loudspeaker of Harz and Kösters previously referred to.²¹ Here the frequency range above 400 c/s is radiated by 12 small cone units mounted on the faces of a dodecahedral structure, thus giving an approximation to a spherical radiator. Fig. 7 shows an external view of the omnidirectional assembly placed a short distance away from the associated low-frequency unit, which is mounted, with axis vertical, in the top of its enclosure. In a later version²³ of the loudspeaker the number of high-frequency units has been increased to 32.

The design of such omnidirectional assemblies is hampered by the lack of suitable cone units. Few commercial units small enough for the purpose have the wide frequency range, smooth frequency response and freedom from non-linear distortion which experience shows to be necessary in high-quality loudspeakers of the conventional type, and there is no evidence that the special directional characteristics allow the normal requirements to be relaxed.

The effect of an omnidirectional loudspeaker can be partly simulated by directing the radiation from a conventional unit towards a corner of the listening room and relying on the scattering of the sound by multiple reflection; the results, however, depend so much on local conditions that the method is not universally applicable.

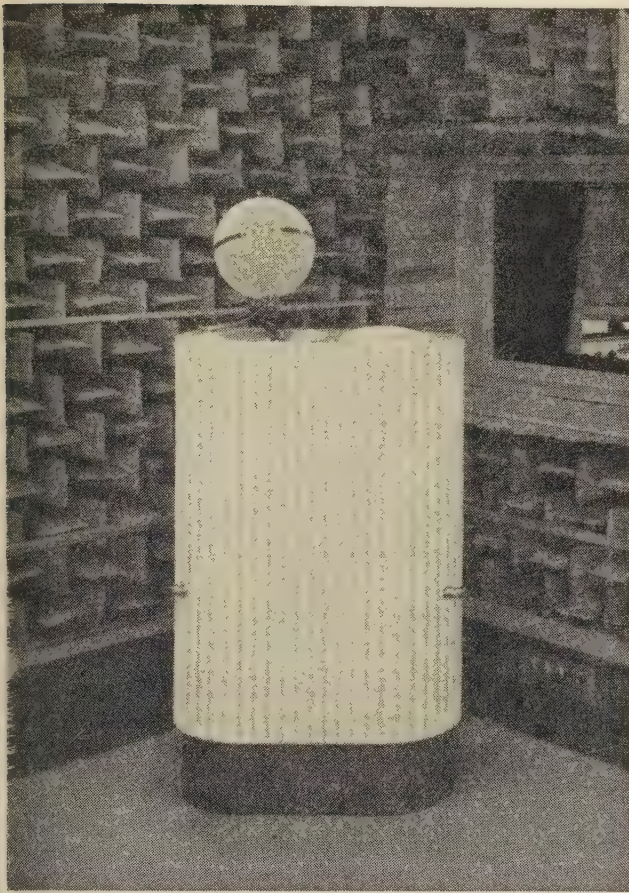


Fig. 7.—Omnidirectional loudspeaker using 12 high-frequency units.

(3.5) Factors influencing Low-Frequency Response

(3.5.1) Enclosure.

With the exception of the large-area electrostatic loudspeaker referred to in Section 5, every direct-radiator loudspeaker designed to operate to the lower limit of the audio-frequency range includes some kind of baffle or enclosure designed to prevent destructive interference by sound radiated from the rear of the diaphragm.

During the past decade, a considerable amount of literature on the design of such enclosures has appeared and many ingenious devices for reducing the volume required for a given performance have been described. Unfortunately, most of the publications concerned are largely theoretical or descriptive in character and seldom include any results of acoustic response measurements to support the claims made. The basic form of enclosure employed with wide-range loudspeakers has remained unchanged for some 20 years. In some arrangements the space at the rear of the diaphragm is completely closed; most designs, however, employ the well-known phase-inverting device due to Thuras,²⁴ whereby sound escapes at low frequencies through an auxiliary aperture or vent in aiding phase and thus increases the low-frequency range of the loudspeaker by half an octave or more. The effectiveness of this arrangement depends, however, on the relationship between the mechanical impedance presented by the cone and the acoustic load imposed on it by the enclosure. With enclosures of small volume the requirements can best be met when the area of the cone is likewise small; where it is not, for the reasons indicated in Section 3.3, to employ large cones in conjunction with small enclosures, the introduction of a vent may be useless or even detrimental to performance.

Except in very large enclosures, there is no difficulty in making the walls stiff enough to prevent any appreciable transmission of sound at frequencies below 100 c/s. At higher frequencies, a certain minimum mass of material per unit wall area is required to give adequate attenuation; further increasing the mass by increasing wall thickness, however, does not give a proportionate advantage unless the material exhibits sufficient internal damping at the various resonance frequencies.

A useful comparative test of materials can be carried out by constructing experimental enclosures without the normal sound outlets, setting up sound pressures by an internal sound source—a heavy-duty 'pressure' unit of the kind employed to operate cinema-type horn loudspeakers is suitable—and measuring, as a function of frequency, the pressures produced at some external point. Fig. 8 shows curves obtained by this method, the current in the speech coil of the pressure unit being the same in each case. Curve (a) relates to a bare enclosure constructed of $\frac{3}{8}$ in plywood, and curve (b) to the same enclosure after the addition of an internal layer of $\frac{3}{8}$ in soft building board firmly bonded to the wood. The increase in mass produced by the addition of the building board is only about 11% and the principal reason for the reduced sound transmission is the increased damping of the flexural modes. Measurements of this kind, while purely empirical in character, can lead not only to improved performance of the loudspeaker as a whole, but to appreciable saving in weight, an important factor in transportable equipment.

(3.5.2) Electro-Mechanical Efficiency.

The electro-mechanical efficiency of most early moving-coil loudspeakers was relatively low and the motional impedance was often negligible. This position has been greatly changed in recent years, largely by the introduction of improved magnetic materials. The high electro-mechanical efficiency obtained with many modern units presents, however, another design problem, for the motional impedance at low frequencies rises to high values and may reduce the current entering the speech coil below the value required for uniform frequency response; the effect is most marked when the loudspeaker is fed from an amplifier of low output impedance. At frequencies for which the motional impedance is high, any increase in flux density beyond a certain point will actually *reduce* the motion of the speech coil and hence the acoustic response of the system, the increase in electro-mechanical efficiency being more than offset by the reduction in power transfer from amplifier to loudspeaker. The situation can be eased by the use of a vented enclosure designed to present an appropriate acoustic impedance to the diaphragm. However, if the volume of the enclosure is restricted, the loading may be effective only over a narrow band.

One solution to this problem is to apply to the signal entering the associated amplifier such low-frequency pre-emphasis as will produce the desired overall frequency response. To obtain the maximum undistorted power output from the amplifier/loudspeaker combination, the amplifier must then be designed for a load intermediate between the low-frequency and mid-band impedance of the loudspeaker. Alternatively, it may be possible to obtain a better overall result at comparable total cost by reducing the flux density of the loudspeaker field and increasing the amplifier power.

The use of loudspeaker units having high electro-mechanical efficiency has been advocated on account of the heavy damping of the mechanical system at low frequencies which results when the electrical terminals are connected to a circuit of low resistance; to increase the damping even further, amplifiers with a negative output resistance have been employed to nullify part of the speech-coil resistance. It is often suggested that the damping of the fundamental resonance ought to be as high as possible

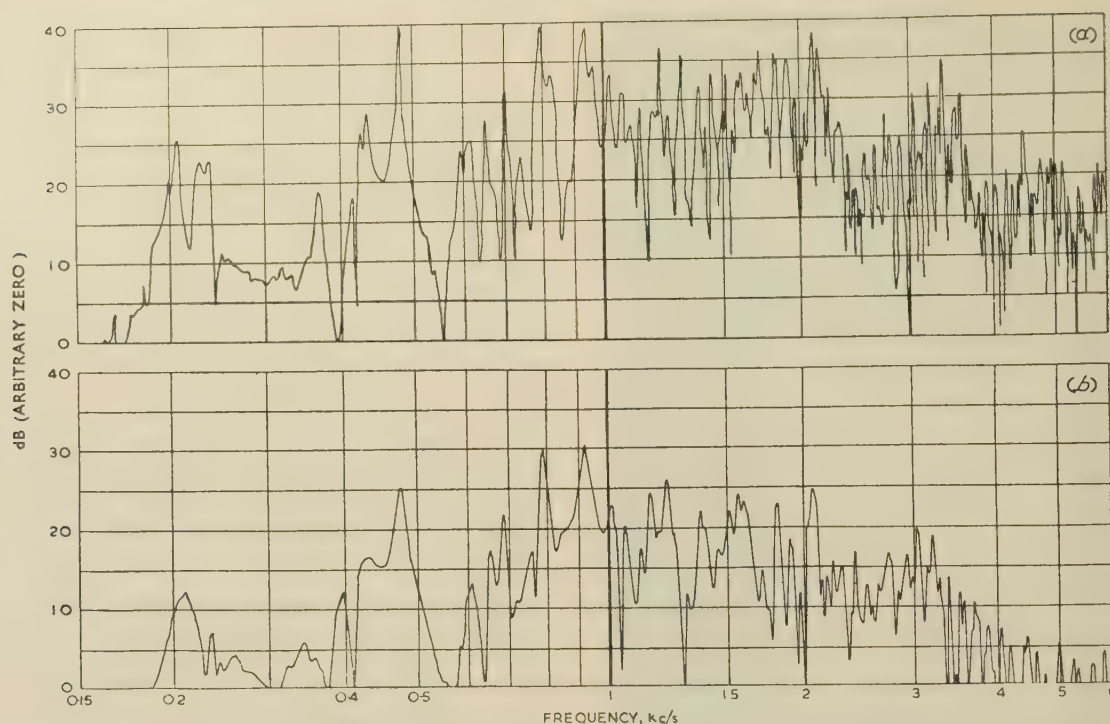


Fig. 8.—Level of sound transmitted through walls of plywood loudspeaker enclosure.
(a) Bare. (b) With damping introduced by lining of building board.

and certainly above the critical value, which corresponds to a Q-factor of 0.5. The necessity for such a high degree of damping does not appear to have been demonstrated by subjective investigation, and is all the more difficult to appreciate when it is considered that the associated enclosure, if vented, will have a low-frequency resonance of its own with a Q-factor of 3 or more.

(4) EXAMPLES OF CURRENT DESIGN

(4.1) General

To illustrate some of the points discussed in Sections 2 and 3, two types of monitoring loudspeaker recently developed by the B.B.C. will now be briefly described. One of these, referred to as loudspeaker A, is designed to meet the requirements for studio monitoring; the other loudspeaker, B, forms part of the portable equipment designed for use on outside broadcasts. Both employ similar high- and low-frequency units, so that a comparison of their performance enables the influence of other factors to be studied.

(4.2) Construction of Loudspeaker A

Fig. 9 shows the construction of loudspeaker A; the enclosure is of $\frac{3}{4}$ in veneered chipboard, reinforced by metal struts to restrict the vibration of the rear panel. The internal volume of the enclosure is 4.7 ft³; a small vent resonating with the volume at about 50 c/s gives a slight increase in low-frequency output.

The low-frequency unit used is a 15 in commercial type which has an axial frequency range extending to about 4 kc/s, and which has been found to be relatively free from the coloration effect referred to in Section 3.3. Fig. 10 shows the constant-voltage frequency characteristics of the l.f. unit alone taken on the axis and at 45° to the axis in the horizontal plane. The curves of Fig. 10(a) relate to an enclosure similar to that of Fig. 9 but having a circular opening 12½ in in diameter; above 500 c/s the system is appreciably directional. By restricting the sound

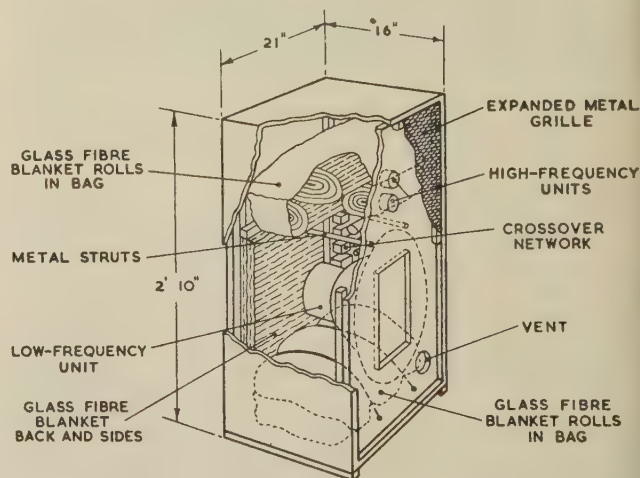


Fig. 9.—Loudspeaker A: structural details.

outlet to a vertical slot—a device due to Chapman and Trier²⁵—the axial response at the upper end of the range is slightly lowered and the response at oblique angles in the horizontal plane is raised, as shown in Fig. 10(b), thus helping to redress the balance. The optimum slot width—in this case 7½ in—depends upon the geometry of the cone but is not critical.

Commercial high-frequency units of the type shown in Fig. 9 are used, two of them to increase the power-handling capacity of the system. Low- and high-frequency units are mounted in a vertical line as shown in Fig. 9; under normal listening conditions the separation between sound sources is not noticeable to observers listening at distances over 4 ft.

Both high- and low-frequency units have been tested with interrupted-tone input in the manner described in Section 2.5.1 and found to be free from any prominent low-damped resonances

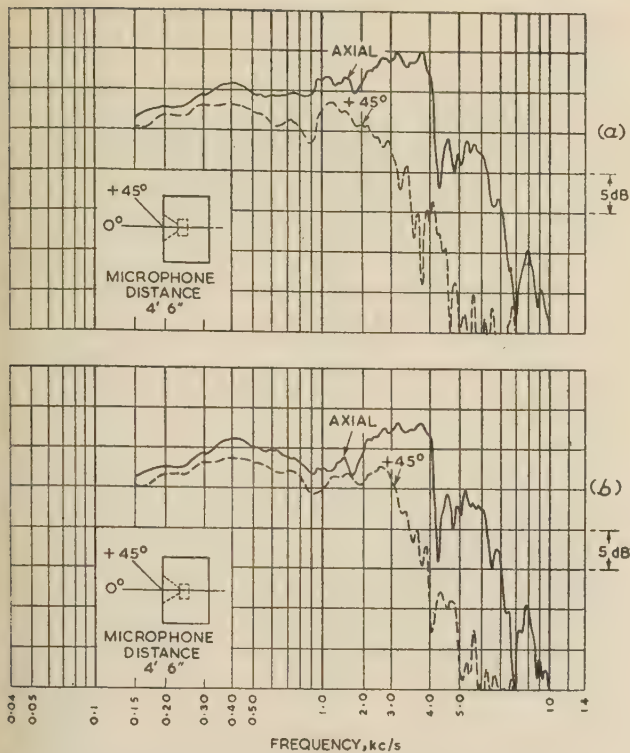


Fig. 10.—Constant-voltage response of 15 in low-frequency unit, measured on axis and at 45° in horizontal plane.

(a) With 12½ in diameter baffle aperture.
(b) With 7½ in wide vertical slot aperture.

The sound pressures produced on the axis by these units are made equal at 1.45 kc/s, though this is not the frequency at which equal power inputs are supplied to the two. In designing the cross-over network, the form of which is shown in Fig. 11, account had to be taken of the motional impedance of the h.f. unit at the lower end of its range. It was found that the requirements could most easily be met by parallel-connected high- and low-pass filters working independently of one another; with modern low-output-impedance amplifiers, interaction between the two filters is negligible and a constant-resistance cross-over network is unnecessary. On grounds of economy, inductors wound on laminated gapped nickel-iron cores are used instead of the usual air-cored coils; by designing for low flux density, intermodulation effects arising in the iron core are made smaller than those produced by the loudspeaker units themselves. The combined choke and auto-transformer T_1 is tapped to allow initial adjustment of the signal level applied to the h.f. units; to avoid any change of frequency characteristic with tap adjustment, alternative capacitors C_1 , C_2 and C_3 are provided.

The resistor R_1 , shunted by the inductor L_2 , is introduced in series with the speech coil of the l.f. unit to correct, at the cost of a certain amount of mid-band loss, for the positive slope in the axial frequency response which would otherwise occur between 100 c/s and 1 kc/s; this feature of the characteristic represents the combined effects of loss at low frequencies due to motional impedance and gain at high frequencies due to increased directivity. The rejector circuit L_3C_6 is employed to reduce the output of the low-frequency unit in the 2.2 kc/s region, thereby avoiding some interference effects which would otherwise appear

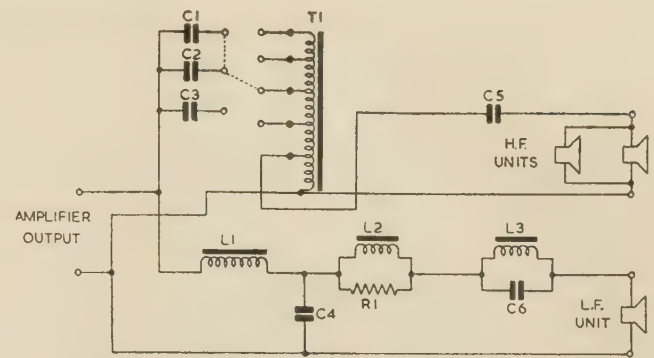


Fig. 11.—Loudspeaker A: circuit of cross-over network.

in the cross-over region. Provision for adjusting the shape of the frequency characteristics above 3 kc/s and below 150 c/s is made in an electrical network introduced into the circuit ahead of the associated power amplifier.

(4.3) Construction of Loudspeaker B

Loudspeaker B, shown in Fig. 12, is an adaptation of the basic design of loudspeaker A and employs similar low- and high-frequency units; it illustrates some of the compromises which may be necessary in special cases.

Because of the restrictions placed on the size and weight of portable equipment, the internal volume of the enclosure used for loudspeaker B is only 2.8 ft³; with a 15 in cone unit the performance of the loudspeaker at low frequencies is better without a vent. Because of the reduced dimensions of the enclosure, a slightly lighter wall construction than with loudspeaker A is permissible, and the combination of 3/8 in plywood lined with an equal thickness of soft building board (see Section 3.5.1) is used. Electrical equalization is again employed to control the axial frequency characteristics, but in this instance all the networks involved are introduced after the associated amplifier and form part of the loudspeaker. In spite of the loss of

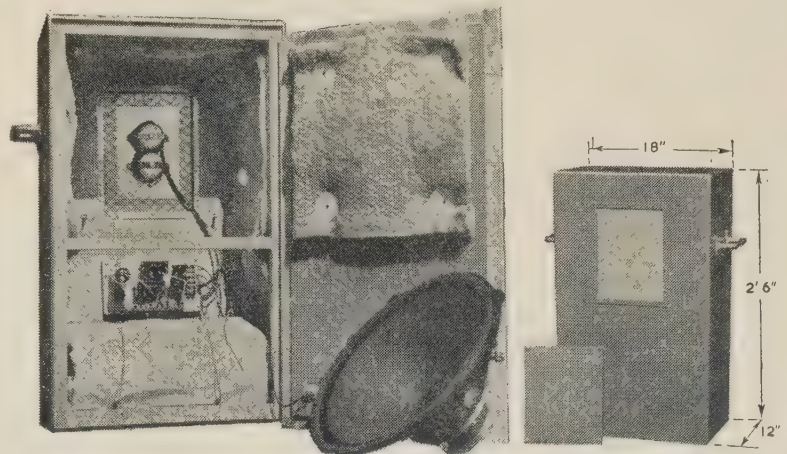


Fig. 12.—Loudspeaker B: internal and external views.

efficiency thus occasioned, adequate sound level can be produced by the use of a power amplifier rated at 15 watts output.

At outside broadcasts the space available for technical equipment is often very limited and the listener may be very close to the loudspeaker; it is therefore essential that the low- and high-frequency radiating systems should be as nearly as possible coaxial. The two h.f. units of loudspeaker B are accordingly

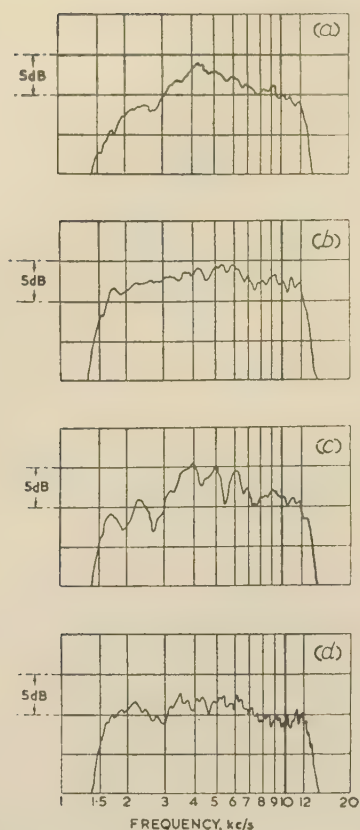


Fig. 13.—Effect of mounting on axial response of a pair of high-frequency units.

- (a) Free space.
- (b) Large baffle.
- (c) Baffle with slot $7\frac{1}{2}$ in \times 10 in.
- (d) As (c) but with perforated baffle plate.

mounted within the cone of the l.f. unit, on a partially perforated metal plate. This plate (see Fig. 12) acts as a baffle in the upper part of the range while offering little obstruction to sound from the l.f. unit. The advantage of providing some form of baffle for the h.f. units is evident from Fig. 13; the curves show the frequency response obtained on the axis mid-way between the two units mounted (a) in free space, (b) in a large baffle, (c) in the $7\frac{1}{2}$ in \times 10 in opening in front of the cone, and (d) as in (c) but with the perforated plate. It should be noted that these curves include the effect of the internal cross-over and corrective networks.

(4.4) Frequency Characteristics of Loudspeakers A and B

Fig. 14 shows the overall frequency response of loudspeaker A with its associated amplifier, measured at various angles in the horizontal and vertical planes and for two different settings of the l.f. response adjustment. At frequencies above 150 c/s measurements were made with the loudspeaker in a non-reverberant room having a working space 15 ft \times 10 ft 8 in \times 7 ft 4 in high; the response at lower frequencies was obtained in the open air with the loudspeaker mounted on a tower 55 ft high. The mean spherical response and the directivity index, both measured in half-octave bands, are also given. As an illustration of the observations made in Section 2.4.3, it may be noted that, at the listening levels usual in studio monitoring practice,²⁶ the l.f. response of curve (i) is sometimes regarded as insufficient, while in certain rooms that of curve (ii) is not found excessive.

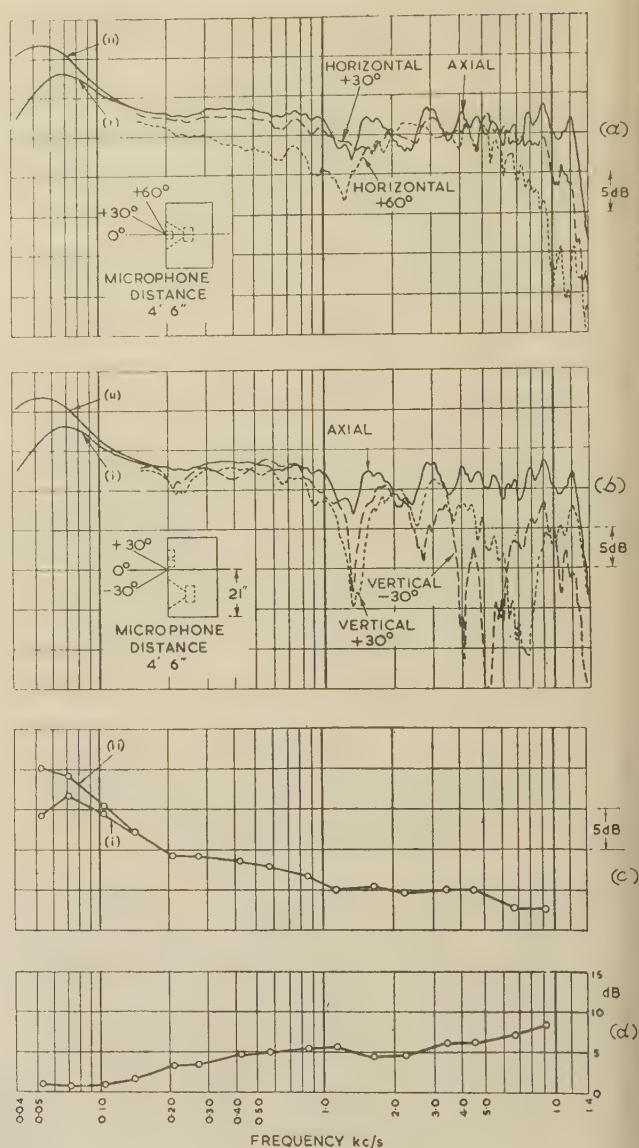


Fig. 14.—Loudspeaker A characteristics.

- (a) and (b) Frequency characteristics in horizontal and vertical planes.
- (c) Mean spherical frequency response.
- (d) Directivity index.

Fig. 15 shows the frequency/response curves of loudspeaker B together with the mean spherical response and directivity, again averaged over half-octave bands.

The differences between the directional properties shown in Figs. 14 and 15 are mainly attributable to the difference in geometry of the two systems and in particular to the form of the sound outlet for the l.f. unit of loudspeaker B. It should be noted in comparing the curves that for measurement purposes loudspeaker A has been assigned an arbitrary axis passing between the low- and high-frequency systems.

Figs. 14 and 15 illustrate the difficulty of describing the various attributes of a loudspeaker without either emphasizing irrelevant detail or losing important information through over-simplification. For example, the disposition of the h.f. units in loudspeaker B allows the observer to listen at close range without becoming aware of more than one sound source; there is, however, little in the curves to suggest that loudspeaker A is different in this respect. Again, the difference in directional properties

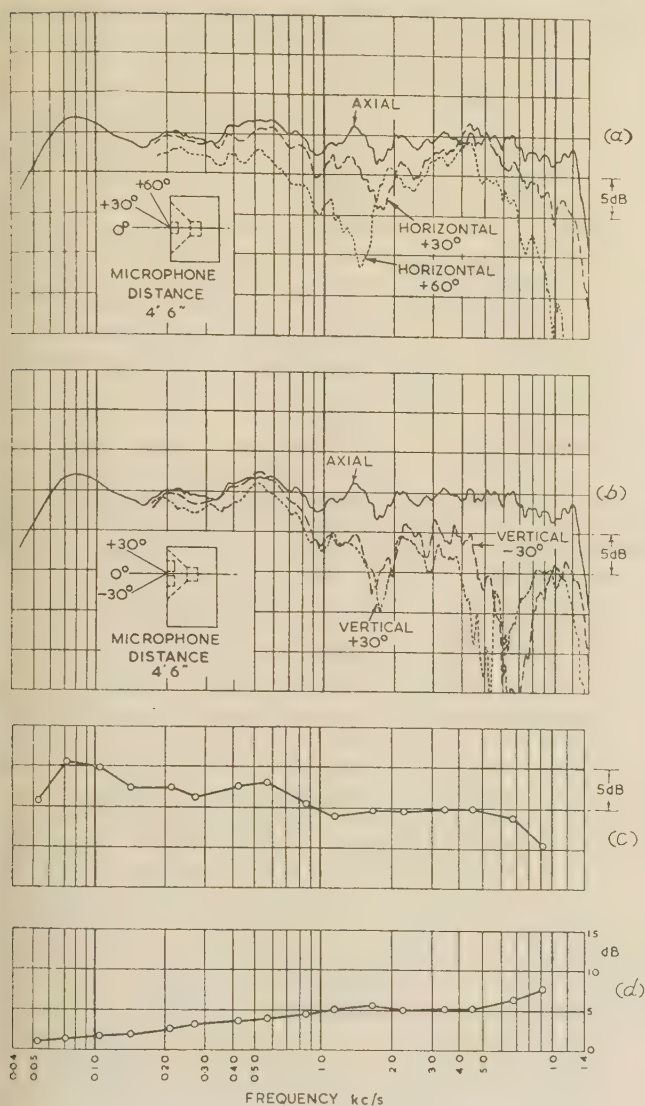


Fig. 15.—Loudspeaker B characteristics.

- (a) and (b) Frequency characteristics in horizontal and vertical planes.
 (c) Mean spherical frequency response.
 (d) Directivity index.

of the two loudspeakers, as shown by the spacing of the response curves taken at various angles, is not apparent in the directivity or mean spherical response characteristics, and it would clearly have been misleading to take the latter as the sole criterion of frequency response.

Although the results of the change in directional properties of the loudspeaker at cross-over are not in either case serious, the effects referred to in Section 3.2 are present to some extent in both A and B. The change of régime at cross-over is accompanied by a change in the slope of curves (d) of Figs. 14 and 15; for reasons partly connected with the action of the perforated baffle plate, the effective cross-over frequency in loudspeaker B is somewhat higher than in loudspeaker A, the axial sound pressures produced by the high- and low-frequency units being equal at 1.6 kc/s.

The data on harmonics and intermodulation distortion, given as examples in Section 2.6.2, Figs. 4 and 5, relate to loudspeaker B. The difference at low frequencies between the shape of the frequency-response curve for the fundamental and that shown in Fig. 15 arises mainly from residual reflections from the walls of

the non-reverberant room in which the distortion measurements were carried out; the separation between fundamental and harmonics below 100 c/s is, in fact, somewhat greater than that indicated.

(5) FUTURE TRENDS IN DESIGN

Apart from any radical change in the operating principles of loudspeakers, many of the refinements introduced during the next few years are likely to be concerned with directional properties.

Because of the pleasantly 'spacious' subjective effects to be obtained by wide-angle distribution of sound, commercial receivers incorporating two or more supplementary loudspeaker units mounted in different faces of the enclosure²⁷ have recently been produced. This practice, were it to become widespread, might lead the users of monitoring loudspeakers to call for a corresponding refinement, though it is not suggested that an omnidirectional system such as that referred to in Section 3.4 should necessarily be adopted.

While the potential applications of stereophonic transmission to broadcasting are limited, the development of stereophonic recording is proceeding rapidly and will probably create a demand for monitoring loudspeakers having special polar characteristics. Some workers²⁸ in this field have advocated the use of directional loudspeakers to reduce the variation in the position of the apparent sound source with the position of the observers. However, since the required directional characteristics cannot be maintained throughout the audio-frequency range, other designers²⁹ prefer to aim at a uniform response over the widest possible angle in the horizontal plane.

Perhaps the most notable development in recent years is the design of electrostatic loudspeakers covering the complete audio-frequency range,³⁰ instead of being confined, as hitherto, to the region above 1 kc/s. Loudspeakers of this type have been produced during the last few years but have only recently become generally available in this country; little detailed information has so far been published on their construction and performance. The two principal factors which have stimulated their development are the production of plastics suitable for the manufacture of diaphragms having a sufficiently low mass and stiffness, and the realization of the fact, demonstrated by Hunt³¹ in America, that the non-linear distortion can be greatly reduced by keeping the polarizing charge, as distinct from the polarizing voltage, constant.

To produce the required sound level without exceeding the linear limits of the electrostatic system, diaphragms of large area have to be employed. In order to avoid unwanted directional effects, the radiating surface may be subdivided so that only a small portion is operative at high frequencies; even so, the directional pattern at the upper end of the audio-frequency range may be narrower, at least in one plane, than that of some conventional loudspeakers.

Probably the most striking feature of the full-range electrostatic loudspeaker is that the usual enclosure may be dispensed with and sound from both surfaces of the diaphragm allowed to radiate into the room; the resulting loss in output at low frequencies through back-to-front interference can be corrected by an internal network. At low frequencies, where the wavelength is large compared with the dimensions of the diaphragm, the unit may be regarded as a doublet source. The directional characteristic is then of figure-of-eight form, and the proportion of reverberant to direct sound received by the listener will therefore be less than with a conventional loudspeaker; there is, however, insufficient evidence to show whether this characteristic of the system is conducive to realism in reproduction.

Fig. 16 shows an external view of a commercial full-range

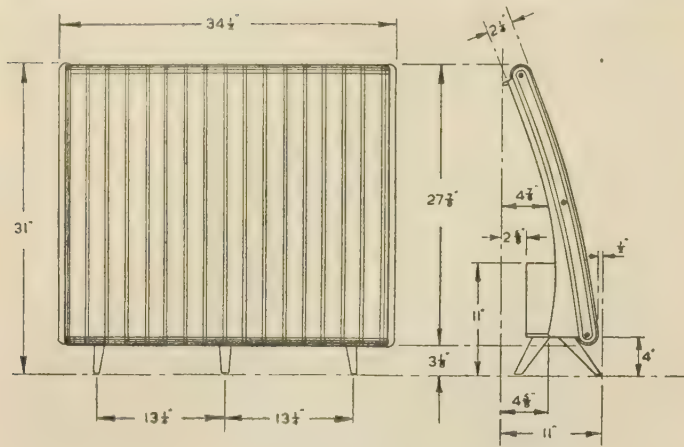


Fig. 16.—Full-range electrostatic loudspeaker.

electrostatic loudspeaker; the unit incorporates a rectifier for providing the polarizing voltage and a matching transformer to enable the loudspeaker to operate from a low-impedance circuit. Whatever the merits or shortcomings of these loudspeakers as a class, it seems likely that their cost may eventually be below that of a moving-coil loudspeaker system of comparable performance.

(6) CONCLUSIONS

In the paper an attempt has been made to bring together, on the one hand, the essentials of the art as they appear in the literature on design and measured performance, and on the other, the accumulated experience, mostly unpublished, of those users of loudspeakers who are in a position to compare the original and reproduced sound.

It will be seen that one of the greatest single obstacles to further progress is the difficulty of formulating in sufficient detail the requirements to be met. The characteristics of the ideal loudspeaker, often regarded as self-evident, are found on closer examination to be indefinable in objective terms. However, as long as the user remains consistent in his demands, there seems no reason why subjective studies should not ultimately yield a set of workable criteria for the guidance of designers.

(7) ACKNOWLEDGMENTS

The author wishes to acknowledge the contributions made to the material of the paper by other members of the B.B.C. Research Department and, in particular, the work of Mr. T. Somerville on subjective assessment of quality, together with that of Messrs. H. D. Harwood and J. R. Chew on the design of loudspeakers and measuring equipment. His thanks are also due to the Acoustical Manufacturing Co. Ltd., the General Electric Co. Ltd., the Institut für Rundfunktechnik G.m.b.H., Hamburg, and the Plessey Company Limited, for supplying technical information and illustrations.

The paper is published by kind permission of the Chief Engineer, British Broadcasting Corporation.

(8) REFERENCES

- (1) 'Recommendations for Ascertaining and Expressing the Performance of Loudspeakers by Objective Measurements', British Standard 2498: 1954.
- (2) McMILLAN, D., and WEST, W.: 'The Design of a Loudspeaker', *Journal I.E.E.*, 1940, 86, p. 432.
- (3) GEE, A., and SHORTER, D. E. L.: 'An Automatic Integrator for Determining the Mean Spherical Response of Loudspeakers and Microphones', B.B.C. Engineering Division Monograph No. 8.
- (4) KAUFMANN, G.: 'Beitrag zur subjektiven Beurteilung von Musikwiedergaben mittels Lautsprecherkombinationen', *Technische Hausmitteilungen des N.W.D.R.*, 1956, 8, No. 5/6, p. 93.
- (5) HELMBOLD, J. G.: 'Oszillographische Untersuchungen von Einschwingvorgängen bei Lautsprechern', *Akustische Zeitschrift*, 1937, 2, p. 256.
- (6) SHORTER, D. E. L.: 'Loudspeaker Transient Response: Its Measurement and Graphical Representation', *B.B.C. Quarterly*, 1946, 1, p. 121.
- (7) CORRINGTON, M. S.: 'Transient Testing of Loudspeakers', *Audio Engineering*, 1950, 34, p. 9.
- (8) KIDD, MARSHAL C.: 'Tone Burst Generator Checks A-F Transients', *Electronics*, 1952, 25, No. 7, p. 132.
- (9) CORRINGTON, M. S.: 'Correlation of Transient Measurements on Loudspeakers with Listening Tests'. Paper presented at the Annual Convention of the Audio Engineering Society, October 16, 1954.
- (10) HENTSCH, J.-C.: 'La fidélité des haut-parleurs dans la reproduction des phénomènes transitoires', *Technische Mitteilungen PTT*, 1951, No. 6, p. 201.
- (11) SEEMANN, E.: 'Beurteilung der Einschwingverzerrungen von Lautsprechern an Hand der Frequenzgänge', *ibid.*, 1952, No. 4, p. 121.
- (12) EWASKIO, C. A., and MAWARDI, O. K.: 'Electroacoustic Phase Shift in Loudspeakers', *Journal of the Acoustical Society of America*, 1950, 22, p. 444.
- (13) NICHOLS, R. H.: 'Effects of Finite Baffles on Response of Source with Back Enclosed', *ibid.*, 1946, 18, p. 151.
- (14) OLSON, H. F.: 'Direct Radiator Loudspeaker Enclosures', *Audio Engineering*, November, 1951, 35, p. 34.
- (15) BRITTAIN, F. H.: 'The Appraisal of Loudspeakers', *G.E.C. Journal*, 1936, 7, p. 266.
- (16) SHORTER, D. E. L.: 'The Influence of High Order Products in Non-Linear Distortion', *Electronic Engineering*, 1950, 22, p. 152.
- (17) SIVIAN, L. J., DUNN, H. K., and WHITE, S. D.: 'Absolute Amplitudes and Spectra of Certain Musical Instruments and Orchestras', *Journal of the Acoustical Society of America*, 1931, 2, p. 330.
- (18) BELGER, D.: 'Untersuchungen über den maximalen Amplitudengehalt der Modulation bei hohen Frequenzen', *Technische Hausmitteilungen des N.W.D.R.*, 1955, 7, No. 7/8, p. 151.
- (19) INGERSLEV, F.: 'Measurement of Non-Linear Distortions in Loudspeakers', *Proceedings of the First I.C.A. Congress on Electro-Acoustics*, 1953, p. 74.
- (20) SOMERVILLE, T.: 'Monitoring Sound Broadcasting Programmes', *Wireless World*, 1956, 62, p. 228.
- (21) HARZ, H., and KÖSTERS, H.: 'Ein neuer Gesichtspunkt für die Entwicklung von Lautsprechern?' *Technische Hausmitteilungen des N.W.D.R.*, 1951, 3, p. 205.
- (22) KLEIN, S.: 'The Ionophone', *Onde Électrique*, 1952, 32, p. 314.
- (23) ENKEL, F.: 'Neue hochwertige Abhöranlage für Regieräume', *Elektronische Rundschau*, 1957, 11, No. 2, p. 51.
- (24) THURAS, A. L.: British Patent No. 1869178: 1930.
- (25) CHAPMAN, R., and TRIER, R. H.: British Patent No. 659063: 1947.
- (26) SOMERVILLE, T., and BROWNLESS, S. F.: 'Listeners' sound-level Preferences', *B.B.C. Quarterly*, 1949, 3, p. 11.

- (27) KUHL, W., and ZOSEL, J. M.: 'Untersuchungen zur Pseudo-stereophonie und Stereophonie mit Kugellautsprechern und "Raumklang"—Geräten', *Akustische Beihefte*, 1956, No. 2, p. 474.
- (28) BRITTAIN, F. H., and LEAKEY, D. M.: 'Two-Channel Stereophonic Sound Systems', *Wireless World*, 1956, **62**, pp. 206 and 331.
- (29) CLARK, H. A. M., DUTTON, G. F., and VANDERLYN, P. B.: 'The "Stereosonic" Recording and Reproducing System', *Proceedings I.E.E.*, Paper No. 2332 R, February, 1957 (**104 B**, p. 417).
- (30) WALKER, P. J.: 'Wide-range Electrostatic Loudspeakers', *Wireless World*, 1955, **61**, pp. 208, 265 and 381.
- (31) HUNT, F. V.: 'Electroacoustics', Harvard Monographs in Applied Science No. 5 (Harvard University Press), pp. 188 *et seq.*

DISCUSSION BEFORE THE RADIO AND TELECOMMUNICATION SECTION, 23RD APRIL, 1958

Dr. G. F. Dutton: The loudspeaker is the last in a varied collection of components in the chain connecting the original sound with the reproduced sound in the studio or listening room. Consequently it has to bear the blame for most shortcomings of the system. The more one improves the performance of the loudspeaker with regard to the frequency range the more critical will be the conditions for showing up high-frequency buzzes, clicks, etc.; and they are all blamed on to the loudspeaker. It is necessary to convince people that these noises are not in the loudspeaker but are in their various components. The only distortion that I have not heard blamed on the loudspeaker is 'wow' and 'flutter'.

I do not agree entirely with the statement in the Summary that the purpose of the broadcasting or recording engineers is to give an approximate approach to a realistic reproduction. It depends on what the sounds are intended to be and what is meant by 'realistic'. The microphone is often placed very close to the instruments to be recorded, in a position much closer than would be normally assumed by a member of the audience, and perhaps closer than a normal person would tolerate. On the other hand, the broadcasting people might prefer to use microphones further away and even over the top of the orchestra—again these are positions not normally assumed by the audience. Therefore, the interpretation of a realistic sound is somewhat difficult.

In the gramophone recording industry we have had this problem of loudspeaker design for monitors for some time. We have been trying to decide whether the characteristics for the standard monitoring loudspeaker should represent the average commercial loudspeaker or should have some ideal smooth characteristic, such as that indicated by the author. We have come to the conclusion that a smooth characteristic up to 12 or 15 kc/s on the axis of a reasonably good spherical radiation characteristic is the one to aim for. No particular fashion has been set for having a high rise in the region of 3 or 4 kc/s, which is very common to most loudspeakers of the lower price range. This is, perhaps, hard to fight in practice because the brighter loudspeakers with the rise at about 3 or 4 kc/s usually play popular recordings very nicely, while the more extended and flatter frequency characteristic tends to show up any distortion in the brass section, and you have to be very careful to judge whether this is real or originates in the system.

I agree with the author that wide-band noise tests can be very useful in quickly assessing the difference between two loudspeakers, and we use these tests for comparing the test monitoring loudspeaker with the standard that we have set ourselves. Very small differences in characteristic can easily be detected by this test.

In Section 3 there is a reference to equalization. I agree that equalization in the loudspeaker amplifier is essential in order to cover adequately a large frequency range, and I consider that this compensation can only be made if the resonances to be corrected are not too sharp. If they are too sharp, of course, the reliability of the compensation is in doubt,

After a great deal of impartial listening, I have come to the conclusion that direct-radiator cone loudspeakers are preferable to the horn-driven types. The reason for this is not quite clear. It is probably due to a number of small reasons rather than one particular one. For instance, directivity is probably very important.

The author refers to the coloration that can occur owing to the break-up of the cone into radial modes. I think we have overcome that trouble by using elliptically-shaped cones.

The monitoring loudspeaker that we have designed and are using in our studios has a cabinet 4 ft high, and the rear baffle for the low-frequency unit is totally enclosed with a volume of $3\frac{1}{2}$ ft³. The high-frequency unit is exactly similar to the one described by the author. It is fitted directly above the cone loudspeaker, and is completely enclosed so that no inter-modulation can exist between the low- and high-frequency units. The power amplifier is placed in the lower compartment. There are three correcting networks applied to the unit. The bass correction starts at about 800 c/s and rises to 40 c/s and is of the order of 6 dB at 40 c/s. The high-frequency correction occurs at about 7 kc/s, and there is a rise at about 11 kc/s.

The elliptical unit is placed with the long axis vertical in order to improve the radiation pattern in the horizontal plane. That unit, with its corrective network, can be within $\pm 1\frac{1}{2}$ dB from 40 c/s to 12 kc/s.

An important point that should be discussed in relation to monitoring loudspeakers is the replay level. Most engineers and 'hi-fi' enthusiasts seem to play loudspeakers at a level much higher than they should be played, or at least higher than the average person for whom the records are made or for whom broadcasts are intended would play them. But the whole balance can be misjudged by playing at too high a level. Whether or not the level should be as high as the original sound is questionable, but the full effect of an orchestra on the *fortes* cannot be obtained unless the level is up to its full original value.

Mr. G. A. Briggs: I agree with the author about the doublet effect with the full-range electrostatic loudspeaker. We have had some experience with a moving-coil doublet system. It is perfectly true that a doublet excites less room resonance than a direct radiator, but this makes it more selective, and the performance is therefore very much affected by its position in the room. The doublet effect can be reduced by placing one edge of the loudspeaker against a wall, or by putting the loudspeaker itself near a corner. It is essential to try various locations in any room, and this latitude seems to make the doublet a popular proposition, whether with a moving-coil or an electrostatic loudspeaker.

With regard to magnets and damping factors, the author very wisely draws attention to the loss of bass response with high-flux-density magnet systems driven by amplifiers with very low output resistance, and suggests as a possible solution the use of smaller magnets and larger amplifiers. I do not agree with this idea for domestic use. A high-flux-density loudspeaker sounds brighter and cleaner than a low-flux-density model.

I submit that the root of the trouble lies in our absurd obsession with high damping factors and constant voltages. Tests show that a damping factor of 15 produces a drop in output of about 3 dB at 40 c/s in a 10 in loudspeaker with a 10-kilogauss magnet; but the drop is 10 dB with a 14-kilogauss magnet. Why should a resistance of 1 ohm be connected in parallel with a high-quality 15-ohm loudspeaker? Why do we not have amplifiers with variable damping factor, using a mixture of voltage and current feedback as produced in America? A preset control could be adjusted to suit the loudspeaker and the room.

Mr. P. J. Walker: A number of attempts have been made in the past to lay down a series of objective tests for loudspeakers which will be meaningful in comparing performance. Their interpretation is based solely on past experience of comparing objective tests with subjective assessment.

It seems relevant to point out that interpretation experience gained on one type of transducer may give misleading results when applied to an entirely different type of transducer.

It is now possible to make electrostatic loudspeakers with low mechanical impedance as opposed to the high mechanical impedance of the moving coil. The change from free field conditions to room conditions will differ in the two cases.

The importance of local response irregularities is dependent upon whether these are due to interference or resonance effects. Here again, a change of transducer type profoundly alters the relationship between the two causes. Similar remarks apply to the shape of distortion curves and some other physical properties.

The confidence with which we can compare overall performance from objective tests varies directly with the physical similarity of the loudspeakers to be compared.

Mr. F. H. Brittain: I entirely agree with Dr. Dutton that the axial response curve should be as flat as possible, and certainly not worse than 5 dB down at a frequency of 10 kc/s and 30° off axis. In my opinion it is never permissible to maintain a good mean spherical response by having a rising response on the listening axis. It does not occur in nature and will not be tolerated.

When examining a frequency-response curve, it must be remembered that shape plays a great part in the appeal to the eye. Shape is best obliterated by taking the mean output over a number of bands of frequencies.

The author suggests that male speech is useful for listening tests, but female speech should also be included because it utilizes different frequencies. In both cases it must be ensured

that pressure-gradient microphones are not used nearer than 6 ft to the person speaking.

With regard to Section 3, it often happens that a high frequency unit is used in conjunction with a 'cross-over' network which effectively disconnects it from the amplifier. In these circumstances, the diaphragm of the h.f. unit is probably undamped at its main resonance and may develop excessive movement from the local sound pressure falling on it, or because it is partially driven electrically. It is then desirable to provide some damping in the form of a series-tuned circuit connected across the h.f. unit.

Mr. J. K. Webb: The author mentions the full-range electrostatic loudspeaker, a commercial model of which has recently become available. I heard this demonstrated recently in direct comparison with a well-known make of large corner horn assembly and did not find that it bore much relation to what I had come to regard as 'hi-fi', whereas the corner horn did. One of my acquaintances, shocked at my verdict, has since persuaded me to read the maker's accompanying pamphlet from which it appears that my judgment is coloured by the fact that I am not musical! While this is reminiscent of the fairy story about the emperor's clothes, it does illustrate the difficulty in assessing performance criteria which are found, as the author says, to be indefinable in objective terms. It would seem, however, that users are now to be persuaded to change their demands and adopt different criteria than heretofore. How, then, does the author suggest that designers should seek guidance?

Mr. P. P. Eckersley: In connection with the demonstration did the author assume a 'perfect' microphone? It is often the case that, when designing a microphone, the designer judges it by a 'perfect' loudspeaker, and when another is designing a loudspeaker he judges it by a 'perfect' microphone. In the case of the demonstration, what was the 'perfect' microphone, what was the 'perfect' recording system and what was the 'perfect' amplifier? I have been told that to do real justice to 'hi-fi' loudspeakers the amplifier ought to have a flat response up to about 100 kc/s, otherwise there will be transient distortion. Is this idea viable? Was such an amplifier used in connection with the demonstration?

On the question of measurement, is the microphone assumed to be 'perfect'? Since the microphone must have a finite size will it not set up standing waves between the loudspeaker and itself, thus vitiating the results, or is some method used to vary the distance while integrating the energy?

THE AUTHOR'S REPLY TO THE ABOVE DISCUSSION

Mr. D. E. L. Shorter (in reply): Dr. Dutton's difficulty in accepting 'realism' as an ideal is understandable in view of the varying interpretations placed on that much overworked word. Realism, as an attribute of a sound-reproducing system, has too often come to be associated with the unpleasant sounds which result when the design of the loudspeaker is based on oversimplified ideas of technical correctness; as used in the paper, however, the term refers solely to the extent to which a listener could imagine himself to be in the presence of the performer, irrespective of the means by which the illusion is produced. It is true that microphones are often located in positions which would not be acceptable for direct listening. This placing does not necessarily represent a departure from realism; it is an artifice employed, in the interests of realism, to compensate for unavoidable shortcomings of the system—in particular for the deficiencies inherent in a monaural transmission. There are certainly cases in which the compensation process has been carried further in an attempt to improve on nature; however, I do not think that

arbitrary factors introduced in this way ought to be regarded as permanent features of the transmission system.

In reply to Mr. Webb, it seems reasonable that the designer of monitoring loudspeakers should be guided by the judgment of those individuals who are best qualified by experience to assess the degree of realism achieved. It so happens that most of these individuals belong to the category which could be described as musical; I would not, however, suggest that musical knowledge is in itself necessary to enable an observer to judge the degree to which a reproduced sound resembles the original.

Mr. Briggs's proposed method of electrical equalization by varying the output impedance of the loudspeaker amplifier is less flexible in its application than the use of corrective network earlier in the chain, and does not overcome the difficulty of transferring power at low frequencies to a load impedance far in excess of the optimum value. Whichever procedure is adopted, however, there is a strong case for treating the amplifier for design purposes as part of the loudspeaker.

I agree with Mr. Brittain on the need for caution in the use of pressure-gradient microphones for speech at close range, although I should have thought that his minimum distance of 6 ft.—for which the ratio of pressure gradient to pressure at 100 c/s is only 4% above the plane-wave value—a little conservative.

In reply to Mr. Eckersley, while the use of negative feedback in amplifiers intended for the audio-frequency band usually results in the response of the stages concerned being maintained up to 100 kc/s or higher, I know of no evidence that such a wide frequency band is necessary for good reproduction. In the equipment demonstrated the upper frequency range was, in any case, restricted to some 20 kc/s by the characteristics of the input and output transformers of the various amplifiers in the chain. The effect of standing waves between microphone and loudspeaker is one which has to be taken into account in carrying out

accurate microphone calibrations, but with modern microphones it is usually small enough to be negligible in loudspeaker measurements. The microphones used in obtaining the demonstration material were of the high-grade studio type, to which the remarks in Section 2.7.4 apply.

I agree with Mr. Walker that much of our past practice in the interpretation of objective tests is based on the general similarity of structure which characterizes the simpler forms of loudspeaker. Successive developments in design, involving increases in the number and spacing of the radiating elements, have made it more and more difficult to produce meaningful objective data. An extreme example of this trend is to be seen in the large-area electrostatic loudspeaker, for which it is impossible, at normal measuring distances, to obtain a frequency-response characteristic free from ambiguities introduced by interference. The situation calls for a careful re-appraisal of all our performance criteria.

DISCUSSION ON

'THE B.B.C. SOUND BROADCASTING SERVICE ON VERY HIGH FREQUENCIES'*

Before the SOUTH-WESTERN SUB-CENTRE at PLYMOUTH 5th December, 1957, the WESTERN CENTRE at BRISTOL 13th January, the SOUTHERN CENTRE at BRIGHTON 15th January, and the SOUTH-EAST SCOTLAND SUB-CENTRE at EDINBURGH 18th March, 1958.

Mr. H. C. O. Stanbury (at Plymouth): I cannot follow the statement that failure of half of the transmitting equipment would produce a drop of 6 dB in radiated power. Surely the drop is only 3 dB?

I question the B.B.C. policy of priorities for v.h.f. stations. The authors stress that the v.h.f. concept is not to replace long- and medium-wave broadcasting but to supplement it; yet the first stations have been sited in populated areas such as the Midlands, where very good reception is possible even on a t.r.f. receiver. It seems possible that the association of v.h.f. transmitters with television transmitters is the reason, but this is poor solace to those living in the more rural and distant areas, such as the toe of Cornwall. Here they enjoy neither good sound nor television reception, and since the v.h.f. service is admitted to be supplementary, it surely ought first to have been provided in such areas where reception conditions with the existing transmitter are admittedly unsatisfactory.

Mr. J. E. Flower (at Plymouth): Although the Post Office receives complaints of interference with television reception, it is the South Western Electricity Board to whom these complaints are frequently referred and who are asked to replace many insulators on their 11 kV system in order to cure the interference. If the output of North Hessary Tor were increased to the standard rating of 20 kW, the interference would automatically be eliminated and the Electricity Board would be saved very considerable expense in renewing insulators on lines which are in perfect condition for the purpose of transmitting power.

Mr. H. Sutcliffe (at Bristol): One reason for the introduction of v.h.f. broadcasting is that the limited area of reception provides protection from interference from transmitters more than about 100 miles away from the receiver. This technical virtue has obvious social and political implications.

On the subject of receiving aerials, both for v.h.f. sound and for television, have the authors any views on size reduction?

A dipole, for instance, has almost the same polar diagram, power gain, and effective absorbing area,† whether it is $\frac{1}{2}\lambda$ long or comparatively short. It is true that short dipoles are highly reactive, and matching to a feeder becomes difficult over a broad band of frequency, but I feel that a compromise is worth while here.

A question of terminology arises in Section 3.1.5, where an aerial aperture is said to be 80 ft. Other authors use the term aperture to describe an area.‡ Is 80 ft the length of the aerial structure or something more subtle?

Mr. N. C. Duret (at Bristol): Many listeners to v.h.f. transmissions from a given station are puzzled because they experience comparative variations in signal strength and quality on Home, Light and Third programmes, although the three transmitters concerned are radiating identical power. Can the authors account for this?

Mr. L. W. Turner (at Brighton): In the Introduction the authors outline the reasons which led to the development of the B.B.C.'s v.h.f. sound broadcasting service. Although it is sometimes asked whether, in the light of the growing number of television viewers, the engineering effort on and cost of the v.h.f. sound service is justified, I feel the answer to be an emphatic affirmative. Although television coverage of this country is now virtually complete, there remain some seven million sound-only licence holders. The fall in this number can, of course, be expected to continue as more television receivers are sold, but there is little doubt that a substantial section of this country's population will remain 'sound only'. Moreover, a good deal of listening to sound broadcasts is done by the 7 500 000 people holding combined sound and television licences, and there is evidence of increased listening now that the v.h.f. service enables better reception to be obtained. These points are underlined by the latest figures of sound-receiver sales. In 1957 there were 1 250 000 new sound receivers sold—slightly more than the

† SMITH, R. A.: 'Aerials for Metre and Decimetre Wavelengths' (Cambridge University Press), p. 29.

‡ SCHELKUNOFF, S. A.: 'Electromagnetic Waves' (Van Nostrand), Chapter IX.

number of new television receivers sold in the same period. Of these some 50% were v.h.f. receivers, and this percentage is rising: the total number of v.h.f. sound receivers now in use is 1 400 000, this figure having doubled during 1957.

Have the authors found it necessary to take any special precautions in the matter of phasing the 8-tier aerial to fill in the gaps in the vertical radiation pattern which occur at steep angles with respect to the horizontal, and thus give rise to relatively low fields near to the transmitting station? If these gaps are not filled, one would expect critical and undesirable reception conditions, with the possibility of multi-path distortion effects. Difficulties arising from this condition have been experienced in television reception, and are overcome by applying the necessary amount of gap-filling to the vertical radiation pattern of the transmitting aerial. I am not aware of any difficulties of this nature having been experienced in v.h.f. sound reception, but this may be due to the fact that the sites of most of the B.B.C.'s v.h.f. sound-broadcasting stations are not near heavily populated areas, and hence there are few listeners in the areas likely to be affected to notice any undesirable effects.

Mr. W. Wilkes (at Edinburgh): I am one of the authors' dissatisfied customers, for I live in the Border country, where reception on medium waves is usually bad. With a little practice it is possible to listen to the news and other speech programmes to the accompaniment of 'Indian summer' music and various other noises from other stations, but to listen to musical programmes, especially symphony concerts and similar programmes, under these conditions is quite impossible. We have therefore been looking forward to the v.h.f. service for quite a long time but we have not got it yet, although I am very pleased to learn that the B.B.C. propose to open a station at Galashiels at some future date.

I do not know whether the authors have any detailed information about medium-wave reception in Central Scotland, but, having lived in that area for many years, I suggest that reception there is at least reasonable. The B.B.C. will probably say that the reason for introducing the service as they have done is that by doing it this way they serve a greater number of listeners from one transmitter. Where there is no existing service I would agree with this policy, but I feel that where there is an existing service the listeners suffering from the poorest reception might have been catered for first. Accordingly, I am not particularly impressed by the B.B.C.'s figure of 96% as being the proportion of the population to whom the v.h.f. service is now available.

Is there any possibility of the number of Home Services from each transmitter being increased? Frequently I find that there are no programmes on Scottish, Light or Third wavelengths in which I am interested, but that there is a programme from another Home Service which I should like to hear, and if I describe reception of the Scottish Home Service in my part of the country as bad, I do not think I can describe at all the reception from other Home Service stations on medium wavelengths.

Mr. C. M. Beckett (at Edinburgh): I am interested to learn of the use of v.h.f. broadcasting in Norway. Surely this long, deeply-indented coastline, with so many of its towns and villages situated on its fiords, would be rather unsuited to a semi-optical method of transmission.

Mr. F. P. Phillips also contributed to the discussion at Bristol.

Messrs. E. W. Hayes and H. Page (in reply): In reply to Mr. Stanbury, in the event of a fault on one half of the transmitting

system the transmitter power is reduced by 3 dB and the aerial gain by 3 dB; the reduction in the effective radiated power is therefore 6 dB.

The B.B.C.'s decision to build the high-power f.m. stations first was determined partly by the poor medium-wave reception conditions in many highly-populated areas, and also because experience of the performance of the high-power f.m. stations was necessary to determine the best sites for the low-power stations. As stated in the paper, there are tentative plans to build a station to serve the toe of Cornwall, and also one to serve the Border country mentioned by Mr. Wilkes. Although medium-wave coverage of the Home Service in Central Scotland is reasonably satisfactory, that of the Third and Light programmes is restricted to a few relatively small areas near the major cities. The long-wave service in Scotland is marred by fading.

Mr. Wilkes is, in effect, asking for a choice of more than three programmes from each station. Two Home Services are radiated from Wenvoe and Sandale to cater for the regional requirements, but there is little prospect of this facility being extended. In any case, no channels are available at present, or likely to be in the near future, for such an extension of the service.

The effective radiated power of the North Hessary Tor station is 60 kW, and we are surprised that Mr. Flower thinks that the relatively modest increase of 3 dB would eliminate interference troubles. It does not seem unreasonable to ask the Electricity Board to minimize interference with other services, in the same way that motor cars, in addition to being suitable for carrying passengers, are also required not to create an undue amount of noise.

We agree with Mr. Sutcliffe that the advantage of the half-wave dipole lies in its convenient impedance and wide bandwidth. One compromise in practical use for indoor installations is a quarter-wave unipole. Shorter elements either involve undue matching difficulties and have a very poor bandwidth, or have a poor pick-up. The length of the radiating portion of the transmitting aerial is 80 ft; we agree with Mr. Sutcliffe's stricture on our use of the term 'aperture'.

The differences in the field strengths of the transmissions radiated from the same site, mentioned by Mr. Duret, are generally due to local reflections which give rise to standing-wave field patterns. In areas unfavourably situated for v.h.f. reception there may be associated differences in quality, for the reasons stated in Section 3.4.2 of the paper, unless an efficient receiving aerial is used.

In reply to Mr. Turner, gap-filling of the radiation pattern of the f.m. aerial is not necessary. There are, of course, field-strength minima, but over the narrow channels considered they do not cause distortion. Moreover, multi-path propagation effects in f.m. transmission are generally important only when the path difference between the direct and the delayed signals is at least 5 miles; for a well-sited station the amplitude of such delayed signals will be negligible compared with the direct signal, even in the regions of minimum field strength, which are less than 1 mile from the transmitting aerial. On the other hand, for a television service, delayed signals of short path difference are important; the field strength of these signals can be more nearly comparable with that of the direct signal in the regions of minimum field strength.

INDEX TO VOLUME 105, PART B

1958

ABBREVIATIONS

- (p)—Address, lecture or paper.
- (p)—Subject dealt with in a paper or address.
- (d)—Discussion on a paper.
- (A)—Abstract of paper or address.

A

- Absorption, effect of earth's magnetic field on, for single-hop ionospheric path. R. W. MEADOWS and A. J. G. MOORAT, (p), 33.
- , ionospheric, effect of fading on accuracy of measurement of. R. W. MEADOWS and A. J. G. MOORAT, (p), 27.
- ABSON, W., SALMON, P. G., and PYRAH, S.
- Boron-trifluoride proportional counters. (p), 357; (d), 369.
- Design, performance and use of fission counters. (p), 349; (d), 369.
- Addition table, stored, decimal adder using. M. A. MACLEAN and D. ASPINALL, (p), 129; (d), 144.
- ADDRESSES.
- BUTLER, K. J., as chairman of North-Western Radio and Telecommunication Group. 118.
- COPE, H. G., as chairman of North Lancashire Sub-Centre. 229.
- FOULKES, C. H., as chairman of South-Western Sub-Centre. 230.
- GOLDUP, T. E., as President. 1.
- McPETRIE, J. S., as chairman of Radio and Telecommunication Section. 11.
- MIDDLETON, G. E., as chairman of East Anglian Sub-Centre. 21.
- ROSCOE, E., as chairman of North-Western Measurement and Control Group. 118.
- SIMS, L. G. A., as chairman of Southern Centre. 19.
- TAYLOR, E. O., as chairman of Scottish Centre. 14.
- TOLEY, L. L., as chairman of South Midland Centre. 17.
- Aerials, Yagi, periodic rod structures for. J. O. SPECTOR, (p), 38.
- Aircraft, high-speed, radio aids for. J. S. McPETRIE, (A), 11.
- ALDOUS, W. H. Thermionic and cold-cathode valves. (p), 273.
- ALLAN, A. H., NEWMAN, M., and CROMBIE, D. D. (See CROMBIE.)
- ALLISON, J., and BENSON, F. A. Measurement of impedance and attenuation of a cable through an arbitrary loss-free junction. (p), 487.
- Amplifier, d.c., transistor high-gain chopper type. G. B. B. CHAPLIN and A. R. OWENS, (p), 258; (d), 270, 559.
- Amplifiers, d.c., transistor input stages for. G. B. B. CHAPLIN and A. R. OWENS, (p), 249; (d), 266.
- , magnetic. G. M. ETTINGER, (p), 237; (d), 266.
- Amplitude and phase of Gaussian noise, simultaneous variation of. T. HAGFORS and B. LANDMARK, (p), 555.
- equalizer networks, constant-resistance. J. S. BELL, (p), 185.
- modulated transmitter class-C output stage. C. G. MAYO and H. PAGE, (p), 523.
- Analogue computing, magnetic-drum store for. J. L. DOUCE and J. C. WEST, (p), 577.

ASPINALL, D., and MACLEAN, M. A. (See MACLEAN.)

Atmospheric radio noise. (See Radio.)

Attenuation of radio waves. (See Radio.)

Audio frequencies, precision thermo-electric wattmeter for. J. J. HILL, (p), 61.

Automatic binary digital computers. (See Digital.)

— working in telephone trunk network. L. L. TOLLEY, (A), 17.

Automation. T. E. GOLDUP, (p), 7.

AWORTHY, F. R. Industrial electrical measuring instruments. (p), 404.

B

Back-scatter of radio waves. (See Radio.)

- BAIN, W. C., and MEADOWS, R. W. Radio observations on Russian satellites. (d), 91.
- BALDWIN, M. W. Relation between picture size, viewing distance and picture quality [television]. (d), 438.
- BARLOW, H. E. M., and KATAOKA, S. Hall effect and its application to power measurement at 10 Gc/s. (p), 53.
- BARRINGTON, A. E., and REES, J. R. Simple 3 cm Q-meter. (p), 511.
- B.B.C. sound broadcasting service. (See Sound.)
- BECK, A. C., NORBURY, F. T., and STORR-BEST, J. L. Frequency-modulated v.h.f. transmitter technique. (d), 305.
- BECKETT, C. M. B.B.C. sound broadcasting service at very high frequencies. (d), 624.
- BELL, J. S. Design of constant-resistance amplitude equalizer networks. (p), 185.
- BELSEY, F. H. Transistor devices and magnetic amplifiers. (d), 270.
- BENSON, F. A., and ALLISON, J. (See ALLISON.)
- BERESFORD, A. N. Radio observations on Russian satellites. (d), 85.
- BEUKERS, J. M., KITCHEN, F. A., BILLAM, E. R., JOY, W. R. R., CLEAVER, R. F., and COOPER-JONES, D. L. (See KITCHEN.)
- BILLAM, E. R., JOY, W. R. R., CLEAVER, R. F., COOPER-JONES, D. L., and KITCHEN, F. A. (See KITCHEN.)
- BILLINGS, A. R. Coder for halving bandwidth of signals. (p), 182.
- BIRKINSHAW, D. C. Relation between picture size, viewing, distance and picture quality [television]. (d), 437.
- BLACKBAND, W. T. Radio observations on Russian satellites. (d), 108, 113.
- Boron-trifluoride proportional counters. W. ABSON, P. G. SALMON and S. PYRAH, (p), 357; (d), 365.
- BORTHWICK, J. B. Servo-operated recording instruments. (d), 482.
- BOWEN, J. H., and MASTERS, E. F. O. Temperature transients in gas-cooled thermal nuclear reactors. (p), 337; (d), 368.
- BOWERS, D. F., and MORCOM, W. J. (See MORCOM.)
- BOYD, R. L. F. Radio observations on Russian satellites. (d), 81.
- BRADSHAW, E., WAGSTAFF, M., and COOKE, F. Train performance computer. (p), 560; (d), 568.
- BRAY, W. J. Printed microwave circuits. (d), 180.
- BRICE, P. J., and PARKER, P. N. Radio observations on Russian satellites. (d), 101.
- BRIGGS, G. A. Monitoring loudspeakers. (d), 621.
- BRITAIN, F. H. Monitoring loudspeakers. (d), 622.
- Broadcasting transmitters, semi-attended. (d), 272.
- BROUGHALL, J. A. Train performance computer. (d), 567.
- BULL, C. S. Space charge as source of flicker effect. (p), 190.
- BURGESS, B. Radio observations on Russian satellites. (d), 112.
- BURNETT, L. C. Transistor devices and magnetic amplifiers. (d), 267.
- BURT, E. G. C. Radio observations on Russian satellites. (d), 95.
- BUTLER, K. J. Address as chairman of North-Western Radio and Telecommunication Group. 118.

C

- Cable, measurement of impedance and attenuation of, through an arbitrary loss-free junction. J. ALLISON and F. A. BENSON, (p), 487.
- CANDY, C. J. N. Transistor devices and magnetic amplifiers. (d), 268.
- CARNT, P. S. New cathode-ray tube for monochrome and colour television. (d), 605.
- Carrier, interfering, distortion in frequency-division-multiplex f.m. systems due to. R. G. MEDHURST, E. M. HICKS and W. GROSSETT, (p), 282.
- Cathode-ray tube for monochrome and colour television. D. GABOR, P. R. STUART and P. G. KALMAN, (p), 581; (d), 604.
- tubes, high-speed-oscillograph, screen efficiency of. R. FEINBERG, (p), 370.

- CATTERMOLE, K. W.
Efficiency and reciprocity in pulse-amplitude modulation: principles. (p), 449; (d), 481.
Transistor pulse generators for time-division multiplex. (p), 471; (d), 481.
- Centre and Sub-Centre Chairmen's Addresses. 14.
- CHAPLIN, G. B. B., and OWENS, A. R.
Transistor high-gain chopper-type d.c. amplifier. (p), 258; (d), 270, 559.
Transistor input stages for high-gain d.c. amplifiers. (p), 249; (d), 270.
- CHAPLIN, G. B. B., and WILLIAMSON, R. Dekatrons and electro-mechanical registers operated by transistors. (p), 231; (d), 270.
- CHARMAN, F. J. H. Printed microwave circuits. (d), 181.
- Chemical structure of high polymers. (See Polymers.)
- CLEAVER, R. F., COOPER-JONES, D. L., BEUKERS, J. M., KITCHEN, F. A., BILLAM, E. R., and JOY, W. R. R. (See KITCHEN.)
- CLOOT, P. L. Basic transistor circuit for construction of digital-computing systems. (p), 213.
- Coder for halving bandwidth of signals. A. R. BILLINGS, (p), 182.
- Colour television. (See Television.)
- Computer, train performance. E. BRADSHAW, M. WAGSTAFF and F. COOKE, (p), 560; (d), 567.
- Control unit of electronic digital computer, design of. M. V. WILKES, W. RENWICK and D. J. WHEELER, (p), 121.
- COOKE, F., BRADSHAW, E., and WAGSTAFF, M. (See BRADSHAW).
- COOKE-YARBOROUGH, E. H. Pulse-amplitude modulation. (d), 481
- COOPER-JONES, D. L., BEUKERS, J. M., KITCHEN, F. A., BILLAM, E. R., JOY, W. R. R., and CLEAVER, R. F. (See KITCHEN.)
- COPE, H. G. Address as chairman of North Lancashire Sub-Centre. 229.
- COUPLINGS, quarter-wave, microwave filters with. (d), 395.
- COX, R. J., and WALKER, J. Control of nuclear reactors. (d), 120.
- CRAVEN, G. Wide-band waveguide filters with short linear tapers. (p), 210.
- CRAVEN, G., and LEWIN, L. Microwave filters with quarter-wave couplings. (d), 396.
- CROMBIE, D. D., ALLAN, A. H., and NEWMAN, M. Phase variations of 16 kc/s transmissions from Rugby as received in New Zealand. (p), 301.
- Current gain of transistors at frequencies up to 105 Mc/s. F. J. HYDE and R. W. SMITH, (p), 221.
- D**
- DAIN, J. Ultra-high-frequency power amplifiers. (p), 513.
- Data recording, magnetic tape for. C. D. MEE, (p), 373; (d), 380.
- DAVIS, J., EVANS, J. V., EVANS, S., GREENHOW, J. S., and HALL, J. E.
Radio observations on Russian satellites. (d), 105.
- DAWSON, R. E. B. Control of nuclear reactors. (d), 119.
- D.C. amplifier. (See Amplifier.)
- Decimal adder using a stored addition table. M. A. MACLEAN and D. ASPINALL, (p), 129; (d), 144.
- Dekatrons and electro-mechanical registers operated by transistors. G. B. B. CHAPLIN and R. WILLIAMSON, (p), 231; (d), 266.
- Dielectric materials, use of, to enhance reflectivity of a surface at microwave frequencies. G. B. WALKER and J. T. HYMAN, (p), 73.
- Digital computer, electroluminescent graphical-output unit for. T. KILBURN, G. R. HOFFMAN and R. E. HAYES, (p), 136; (d), 144.
- computer, electronic, design of control unit of. M. V. WILKES, W. RENWICK and D. J. WHEELER, (p), 121.
- computers, application of, to nuclear-reactor design. J. HOWLETT, (p), 331; (d), 365.
- computers, automatic binary, short-cut multiplication and division in. M. LEHMAN, (p), 496.
- computing systems, basic transistor circuit for construction of. P. L. CLOOT, (p), 213.
- Dipole arrays, methods of calculating the horizontal radiation patterns of, around a support mast. P. KNIGHT, (p), 548.
- Directional couplers, microstrip. J. M. C. DUKES, (p), 147; (d), 180.
- Dispersion curves for circular iris-loaded waveguides, Fourier series representation of. P. N. ROBSON, (p), 69.
- Distortion in frequency-division-multiplex f.m. systems. R. G. MEDHURST, E. M. HICKS and W. GROSSETT, (p), 282.
- Distributed-parameter systems, simulation of. J. F. MEREDITH and E. A. FREEMAN, (p), 569.
- Division and multiplication, short-cut, in automatic binary digital computers. M. LEHMAN, (p), 496.
- DOUCE, J. L., and WEST, J. C. Magnetic-drum store for analogue computing. (p), 577; (d), 580.
- DUKES, J. M. C.
Application of printed-circuit techniques to design of microwave components. (p), 155; (d), 181, 504.
Broad-band slot-coupled microstrip directional couplers. (p), 147; (d), 181.
Re-entrant transmission-line filter using printed conductors. (p), 173; (d), 181.
- DUNSTAN, E. M., and SOMERVILLE, M. J. Reduction of low-frequency noise in feedback integrators. (p), 532.
- DURET, N. C. B.B.C. sound broadcasting service on very high frequencies. (d), 623.
- DUTTON, G. F. Monitoring loudspeakers. (d), 621.
- E**
- E-region of ionosphere, attenuation of radio waves reflected from. R. W. MEADOWS, (p), 22.
- Earth's magnetic field, effect of, on absorption for single-hop ionospheric path. R. W. MEADOWS and A. J. G. MOORAT, (p), 33.
- ECKERSLEY, P. P.
Monitoring loudspeakers. (d), 622.
Printed microwave circuits. (d), 181.
Relation between picture size, viewing distance and picture quality [television]. (d), 437.
- Education and industry, specialization in. E. ROSCOE, (A), 118.
- and training. T. E. GOLDUP, (p), 8.
- for engineers. G. E. MIDDLETON, (A), 21.
- Electrical measuring instruments. (See Measuring.)
- training. (See Training.)
- Electroluminescent graphical-output unit. (See Graphical.)
- Electro-mechanical registers and dekatrons. (See Dekatrons.)
- Electronic digital computer. (See Digital.)
- techniques, application of, to textiles. K. J. BUTLER, (A), 118.
- ELLIOTT, W. S. Digital-computer techniques. (d), 144.
- Engineers, education for. G. E. MIDDLETON, 21.
- , Scottish, and electrical training scheme. E. O. TAYLOR, (A), 14.
- ETTINGER, G. M. Half-wave magnetic amplifiers. (p), 237; (d), 270.
- EVANS, D. J. E. Boron-trifluoride proportional counters. (d), 367.
- EVANS, J. F. Transistor circuits and applications. (d), 316.
- EVANS, J. V., EVANS, S., GREENHOW, J. S., HALL, J. E., and DAVIS, J. (See DAVIS.)
- EVANS, S., GREENHOW, J. S., HALL, J. E., DAVIS, J., and EVANS, J. S. (See DAVIS.)
- F**
- Fading, effect of, on accuracy of measurement of ionospheric absorption. R. W. MEADOWS and A. J. G. MOORAT, (p), 27.
- FARMER, F. R. Boron-trifluoride proportional counters. (d), 365.
- FARREN, L. I. Pulse-amplitude modulation. (d), 480.
- Feedback integrators, reduction of low-frequency noise in. E. M. DUNSTAN and M. J. SOMERVILLE, (p), 532.
- FEINBERG, R. Screen efficiency of sealed-off high-speed-oscilloscope cathode-ray tubes. (p), 370.
- Ferrite loss-factors, measurement of, at 10 Gc/s. C. M. SRIVASTAVA and J. ROBERTS, (p), 204.
- Film bolometers for measurement of power in rectangular waveguides. J. A. LANE, (p), 77; (d), 395.
- scanner, flying-spot, for colour television. H. E. HOLMAN and G. C. NEWTON and S. F. QUINN, (p), 317; (d), 329.
- Filter, transmission-line, using printed conductors. J. M. C. DUKES, (p), 173; (d), 180.
- Fission counters, design, performance and use of. W. ABSON, P. G. SALMON and S. PYRAH, (p), 349; (d), 365.

- FLETCHER, J. N. Transistor devices and magnetic amplifiers. (D), 269.
- Flicker effect, space charge as source of. C. S. BULL, (P), 190.
- FLOOD, J. E. Transistor devices and magnetic amplifiers. (D), 268.
- FLOWER, J. E. B.B.C. sound broadcasting service on very high frequencies. (D), 623.
- FLOWERS, T. H. Pulse-amplitude modulation. (D), 479.
- Flying-spot film scanner. (See Film.)
- FOSTER, K. Printed microwave circuits. (D), 181.
- FOULKES, C. H. Address as chairman of South-Western Sub-Centre. 230.
- Fourier series representation of dispersion curves for circular iris-loaded waveguides. P. N. ROBSON, (P), 69.
- FREEMAN, E. A., and MEREDITH, J. F. (See MEREDITH.)
- Frequencies between 10 kc/s and 30 kc/s, atmospheric radio noise at. J. HARWOOD, (P), 293.
- Frequency-division-multiplex f.m. systems, distortion in, due to an interfering carrier. R. G. MEDHURST, E. M. HICKS and W. GROSSETT, (P), 282.
- Frequency-modulated v.h.f. transmitter technique. (D), 305.
- FROST-SMITH, E. H. Transistor devices and magnetic amplifiers. (D), 267.

G

- GABOR, D., STUART, P. R., and KALMAN, P. G. Cathode-ray tube for monochrome and colour television. (P), 581; (D), 606.
- Gas-cooled nuclear reactors. (See Nuclear.)
- discharge noise sources. (See Noise.)
- Gaussian noise. (See Noise.)
- Generator, pulse-and-bar waveform, for testing television links. I. F. MACDIARMID and B. PHILLIPS, (P), 440.
- Generators, transistor pulse, for time-division multiplex. K. W. CATTERMOLLE, (P), 471; (D), 479.
- GENT, H. Radio observations on Russian satellites. (D), 112.
- GILMOUR, A. Boron-trifluoride proportional counters. (D), 365.
- GOLDER, J. A. Control of nuclear reactors. (D), 119.
- GOLDUP, T. E. Address as President. 1.
- GORDON-SMITH, A. C., and LANE, J. A. Measurements on gas-discharge noise sources at centimetre wavelengths. (P), 545.
- GOURIET, G. G.
- Cathode-ray tube for monochrome and colour television. (D), 605.
- Flying-spot film scanner for colour television. (D), 329.
- Relation between picture size, viewing distance and picture quality [television]. (D), 435.
- Graphical-output unit for a digital computer. T. KILBURN, G. R. HOFFMAN and R. E. HAYES, (P), 136; (D), 144.
- GRATTON, C. P. Boron-trifluoride proportional counters. (D), 367.
- GRAY, A. L. Boron-trifluoride proportional counters. (D), 367.
- GREENHOW, J. S., HALL, J. E., DAVIS, J., EVANS, J. V., and EVANS, S. (See DAVIS.)
- GRIFFITHS, H. V. Radio observations on Russian satellites. (D), 110.
- GROSSETT, W., MEDHURST, R. G., and HICKS, E. M. (See MEDHURST.)
- Group Chairmen's Addresses. 118.

H

- HAGFORS, T., and LANDMARK, B. Simultaneous variation of amplitude and phase of Gaussian noise with applications to ionospheric forward scatter signals. (P), 555.
- HAINES, M. E. Cathode-ray tube for monochrome and colour television. (D), 605.
- Hall effect and its application to power measurement at 10 Gc/s. H. E. M. BARLOW and S. KATAOKA, (P), 53.
- HALL, J. E., DAVIS, J., EVANS, J. V., EVANS, S., and GREENHOW, J. S. (See DAVIS.)
- HAMPTON, D. E. Radio observations on Russian satellites. (D), 95, 99.
- HARWOOD, J. Atmospheric radio noise at frequencies between 10 kc/s and 30 kc/s. (P), 293.
- HAYES, E. W., and PAGE, H. B.B.C. sound broadcasting service at very high frequencies. (D), 624.
- HAYES, R. E., KILBURN, T., and HOFFMAN, G. R. (See KILBURN.)

- HERMAN, R. B. Pulse-amplitude modulation. (D), 480.
- HEWITT, P. J. Relation between picture size, viewing distance and picture quality [television]. (D), 438.
- HEY, J. S. Radio observations on Russian satellites. (D), 107.
- HICKS, E. M., GROSSETT, W., and MEDHURST, R. G. (See MEDHURST.)
- HIGGS, G. R. Train performance computer. (D), 567.
- High-accuracy circuit for measurement of impedance. D. KARO, (P), 505.
- polymers. (See Polymers.)
- HILL, J. J. Precision thermo-electric wattmeter for power and audio frequencies. (P), 61.
- HINTON, L. J. T. Transverse film bolometer for measurement of power in rectangular waveguides. (D), 395.
- HIRSHMAN, C. L. Cathode-ray tube for monochrome and colour television. (D), 605.
- HOFFMAN, G. R., HAYES, R. E., and KILBURN, T. (See KILBURN.)
- HOLMAN, H. E., NEWTON, G. C., and QUINN, S. F. Flying-spot film scanner for colour television. (P), 317; (D), 330.
- HOLMES, F. Transistor devices and magnetic amplifiers. (D), 267.
- HOOKE, E. J. Pneumatic methods for location of sheath faults in pressurized telephone cables. (P), 483.
- HOOPER, J. Printed microwave circuits. (D), 180.
- HOWLETT, J. Application of digital computers to nuclear-reactor design. (P), 331; (D), 368.
- HUGHES, V. A. Radio observations on Russian satellites. (D), 108.
- HUTCHEON, I. C. Transistor devices and magnetic amplifiers. (D), 268.
- HYDE, F. J. Measurements on commercial transistors and their relation to theory. (P), 45.
- HYDE, F. J., and SMITH, R. W. Current gain of transistors at frequencies up to 105 Mc/s. (P), 221.
- HYMAN, J. T., and WALKER, G. B. (See WALKER.)

I

- Impedance and attenuation of a cable, measurement of. (See Cable.)
- , measurement of, in a.f., r.f. and v.h.f. ranges. D. F. KARO, (P), 505.
- Industrial measuring instruments. (See Measuring.)
- Industry, specialization in. E. ROSCOE, (A), 118.
- Infra-red radiation. G. B. B. M. SUTHERLAND, (P), 306.
- Instrument for measurement of surface impedance at microwave frequencies. A. E. KARBOWIAK, (P), 195.
- Ionosphere, attenuation of radio waves reflected from E-region of. R. W. MEADOWS, (P), 22.
- Ionospheric absorption, effect of fading on accuracy of measurement of. R. W. MEADOWS and A. J. G. MOORAT, (P), 27.
- forward scatter signals, noise in. T. HAGFORS and B. LANDMARK, (P), 555.
- path, single-hop, effect of earth's magnetic field on absorption for. R. W. MEADOWS and A. J. G. MOORAT, (P), 33.

J

- Jackson (Willis) Report. 116.
- JACOBS, T. Flying-spot film scanner for colour television. (D), 330.
- JAMES, I. J. P. Relation between picture size, viewing distance and picture quality [television]. (D), 435.
- JAMIESON, E. Application of printed-circuit techniques to design of microwave components. (D), 504.
- JERVIS, M. W. Control of nuclear reactors. (D), 119.
- JESTY, L. C.
- Flying-shot film scanner for colour television. (D), 329.
- Relation between picture size, viewing distance and picture quality [television]. (P), 425; 438.
- JOY, W. R. R., CLEAVER, R. F., COOPER-JONES, D. L., BEUKERS, J. M., KITCHEN, F. A., and BILLIAM, E. R. (See KITCHEN.)

K

- KALMAN, P. G., GABOR, D., and STUART, P. R. (See GABOR.)
- KARBOWIAK, A. E. Instrument for measurement of surface impedance at microwave frequencies. (P), 195.

KARO, D.

High-accuracy circuit for measurement of impedance in a.f., r.f. and v.h.f. ranges. (P), 505.

Servo-operated recording instruments. (D), 482.

KATAOKA, S., and BARLOW, H. E. M. (See BARLOW.)

Kelvin lecture (forty-eighth). G. B. B. M. SUTHERLAND, (P), 306.

— lecture (forty-ninth). H. W. MELVILLE, (P), 397.

KILBURN, T., HOFFMAN, G. R., and HAYES, R. E. Accurate electro-luminescent graphical-output unit for a digital computer. (P), 136; (D), 146.

KILVINGTON, T.

Cathode-ray tube for monochrome and colour television. (D), 605.

Relation between picture size, viewing distance and picture quality [television]. (D), 436.

KITCHEN, F. A. Radio observations on Russian satellites. (D), 96.

KITCHEN, F. A., BILLAM, E. R., JOY, W. R. R., CLEAVER, R. F., COOPER-JONES, D. L., and BEUKERS, J. M. Radio observations on Russian satellites. (D), 89.

KNIGHT, P. Methods of calculating horizontal radiation patterns of dipole arrays around a support mast. (P), 548.

KNOCH, L. K. Microwave filters with quarter-wave couplings. (D), 395.

L

LANDMARK, B., and HAGFORS, T. (See HAGFORS.)

LANE, J. A. Transverse film bolometers for measurement of power in rectangular waveguides. (P), 77; (D), 395.

LANE, J. A., and GORDON-SMITH, A. C. (See GORDON-SMITH.)

LANGDALE, R. M. Transistor devices and magnetic amplifiers. (D), 268.

LAVER, F. J. M. Magnetic tape for data recording. (D), 381.

LAVERICK, E. Printed microwave circuits. (D), 180.

LEA, N. Radio observations on Russian satellites. (D), 108.

LEHMAN, M. Short-cut multiplication and division in automatic binary digital computers. (P), 496.

LESLIE, D. C. Radio observations on Russian satellites. (D), 112.

LEWIN, L. Printed microwave circuits. (D), 180.

LEWIN, L., and CRAVEN, G. (See CRAVEN.)

Linear tapers, waveguide filters with. G. CRAVEN, (P), 210.

LONGDEN, G. B. Radio observations on Russian satellites. (D), 93.

Loss-factors of ferrites. (See Ferrites.)

— free junction, measurement of impedance and attenuation of a cable through. J. ALLISON and F. A. BENSON, (P), 487.

Loudspeakers, monitoring, performance criteria and design considerations for. D. E. L. SHORTER, (P), 607; (D), 621.

M

MACDIARMID, I. F., and PHILLIPS, B. Pulse-and-bar waveform generator for testing television links. (P), 440.

MACLEAN, M. A., and ASPINALL, D. Decimal adder using a stored addition table. (P), 129; (D), 146.

MCPETRIE, J. S. Address as chairman of Radio and Telecommunication Section. 11.

MADDOCK, A. J. Servo-operated recording instruments. (D), 482.

Magnetic amplifiers. (See Amplifiers.)

— drum store for analogue computing. J. L. DOUCE and J. C. WEST, (P), 577.

— field, earth's. (See Earth's.)

— tape for data recording. C. D. MEE, (P), 373; (D), 380.

MASTERS, E. F. O., and BOWEN, J. H. (See BOWEN.)

MAURICE, D. A. Relation between picture size, viewing distance and picture quality [television]. (D), 436.

MAYO, C. G., and PAGE, H. Amplitude-modulated transmitter class-C output stage. (P), 523.

MEADOWS, R. W. Attenuation of radio waves reflected from E-region of ionosphere. (P), 22.

MEADOWS, R. W., and BAIN, W. C. (See BAIN.)

MEADOWS, R. W., and MOORAT, A. J. G.

Effect of earth's magnetic field on absorption for single-hop ionospheric path. (P), 33.

MEADOWS, R. W., and MOORAT, A. J. G.

Effect of fading on accuracy of measurement of ionospheric absorption. (P), 27.

Measurement of ferrite loss-factors. (See Ferrite.)

— of impedance. (See Impedance.)

— of ionospheric absorption. (See Absorption.)

— of power. (See Power.)

— of surface impedance. A. E. KARBOWIAK, (P), 195.

Measurements on commercial transistors. (See Transistors.)

— on gas-discharge noise sources. (See Noise.)

Measuring instruments, industrial electrical. F. R. AXWORTHY, (P), 404.

— instruments, scientific electrical. F. C. WIDDIS, (P), 415.

MEDHURST, R. G., HICKS, E. M., and GROSSETT, W. Distortion in frequency-division-multiplex f.m. systems due to an interfering carrier. (P), 282.

MEE, C. D. Magnetic tape for data recording. (P), 373; (D), 382.

MELVILLE, H. W. Chemical structure of high polymers and their physical behaviour. H. W. MELVILLE, (P), 397.

MEREDITH, J. F., and FREEMAN, E. A. Simulation of distributed-parameter systems, with particular reference to process control problems. (P), 569.

Microstrip directional couplers. J. M. C. DUKES, (P), 147; (D), 180.

Microwave components, application of printed-circuit techniques to design of. J. M. C. DUKES, (P), 155; (D), 180, 504.

— filters with quarter-wave couplings, design of. (D), 395.

— frequencies, instrument for measurement of surface impedance at. A. E. KARBOWIAK, (P), 195.

— frequencies, reflectivity of a surface at. G. B. WALKER and J. T. HYMAN, (P), 73.

MIDDLETON, G. E. Address as chairman of East Anglian Sub-Centre. 21.

MILLINGTON, G. Radio observations on Russian satellites. (D), 95.

MILNES, A. G. Transistor circuits and applications. (D), 316.

Monitoring loudspeakers. (See Loudspeakers.)

Monochrome and colour television. (See Television.)

MONTGOMERIE, G. A. Servo-operated recording instruments. (D), 482.

MOORAT, A. J. G., and MEADOWS, R. W. (See MEADOWS.)

MOPPETT, E. J. H. Printed microwave circuits. (D), 181.

MORCOM, W. J., and BOWERS, D. F. Broadcasting transmitters for automatic and semi-attended operation. (D), 272.

Multiplication and division, short-cut, in automatic binary digital computers. M. LEHMAN, (P), 496.

N

Networks, amplitude equalizer, design of. J. S. BELL, (P), 185.

New Zealand, phase variations in, of 16 kc/s transmissions from Rugby. D. D. CROMBIE, A. H. ALLAN and M. NEWMAN. (P), 301.

NEWMAN, M., CROMBIE, D. D., and ALLAN, A. H. (See CROMBIE.)

NEWTON, G. C., QUINN, S. F., and HOLMAN, H. E. (See HOLMAN.)

Noise, atmospheric radio, at frequencies between 10 kc/s and 30 kc/s. J. HARWOOD, (P), 293.

—, Gaussian, simultaneous variation of amplitude and phase of. T. HAGFORS and B. LANDMARK, (P), 555.

—, low-frequency, in feedback integrators, reduction of. E. M. DUNSTAN and M. J. SOMERVILLE, (P), 532.

—, sources, gas-discharge, measurements on, at centimetre wavelengths. A. C. GORDON-SMITH and J. A. LANE, (P), 545.

NORBURY, F. T., STORR-BEST, J. L., and BECK, A. C. (See BECK.)

NOURSE, O. Control of nuclear reactors. (D), 120.

Nuclear-reactor design, application of digital computers to. J. HOWLETT, (P), 331; (D), 365.

— reactors, control of. (D), 119.

— reactors, gas-cooled, temperature transients in. J. H. BOWEN and E. F. O. MASTERS, (P), 337; (D), 365.

O

OAKES, F. Transistor devices and magnetic amplifiers. (D), 267.

O'NEILL, T. J. Boron-trifluoride proportional counters. (D), 367.

- Output stage, class-C, of amplitude-modulated transmitter. C. G. MAYO and H. PAGE, (p), 523.
— unit, graphical, for digital computer. T. KILBURN, G. F. HOFFMAN and R. E. HAYES, (p), 136; (d), 144.
OWENS, A. R., and CHAPLIN, G. B. B. (See CHAPLIN.)

P

- PAGE, H., and MAYO, C. G. (See MAYO.)
PARKER, P. N., and BRICE, P. J. (See BRICE.)
PARKS, G. H. Pulse-amplitude modulation. (d), 480.
PEACHEY, F. A., and WYNN, R. T. B. (See WYNN.)
Phase variations of 16 kc/s transmissions from Rugby as received in New Zealand. D. D. CROMBIE, A. H. ALLAN and M. NEWMAN, (p), 301.
PHILLIPS, B., and MACDIARMID, I. F. (See MACDIARMID.)
PHILLIPS, G. J. Radio observations on Russian satellites. (d), 111.
Picture size, viewing distance and picture quality [television]. L. C. JESTY, (p), 425; (d), 435.
Plant and production. T. E. GOLDUP, (p), 2.
Pneumatic methods for location of sheath faults in pressurized telephone cables. E. J. HOOKER, (p), 483.
Polymers, high, chemical structure of, and their physical behaviour. H. W. MELVILLE, (p), 397.
PORTER, A. Boron-trifluoride proportional counters. (d), 366.
Power amplifiers, u.h.f. J. DAIN, (p), 513.
— and audio frequencies, precision thermo-electric wattmeter for. J. J. HILL, (p), 61.
— measurement at 10 Gc/s, application of Hall effect to. H. E. M. BARLOW and S. KATAOKA, (p), 53.
— measurement in rectangular waveguides, transverse film bolometers for. J. A. LANE, (p), 77; (d), 395.
PRESSEY, D. C. Transistor devices and magnetic amplifiers. (d), 268.
Preston telephone area. (See Telephone.)
PRICE, J. C. Efficiency and reciprocity in pulse-amplitude modulation: testing and applications. (p), 463; (d), 481.
PRICE, P. J. Transistor high-gain chopper-type d.c. amplifier. (d), 559.
Printed-circuit techniques, application of, to design of microwave components. J. M. C. DUKES, (p), 155; (d), 180, 504.
— conductors, re-entrant transmission-line filter using. J. M. C. DUKES, (p), 173; (d), 180.
Process control problems. J. F. MEREDITH and E. A. FREEMAN, (p), 569.
PROCTOR, W. G. Control of nuclear reactors. (d), 119.
PROGRESS REVIEWS
Industrial electrical measuring instruments. F. R. AXWORTHY, (p), 404.
Scientific electrical measuring instruments. F. C. WIDDIS, (p), 415.
Thermionic and cold-cathode valves. W. H. ALDOUS, (p), 273.
Pulse-amplitude modulation, efficiency and reciprocity in. K. W. CATERMOLE, (p), 449; J. C. PRICE, (p), 463; (d), 479.
Pulse-and-bar waveform generator. (See Generator.)
PYRAH, S., ABSON, W., and SALMON, P. G. (See ABSON.)

Q

- Q-meter, 3 cm. A. E. BARRINGTON and J. R. REES, (p), 511.
QUINN, S. F., HOLMAN, H. E., and NEWTON, G. C. (See HOLMAN.)

R

- Radiation, infra-red. G. B. B. M. SUTHERLAND, (p), 306.
— patterns, horizontal, of dipole arrays around a support mast, methods of calculating. P. KNIGHT, (p), 548.
Radio aids for high-speed aircraft. J. S. MCPETRIE, (a), 11.
— and Telecommunication Section: chairman's address. 11.
— and television. T. E. GOLDUP, (p), 7.
— noise, atmospheric, at frequencies between 10 kc/s and 30 kc/s. J. HARWOOD, (p), 293.
— observations on Russian satellites. (d), 81.
— valve industry in prospect and retrospect. T. E. GOLDUP, (p), 1.
— waves, phase-coherent back-scatter of, at surface of sea. E. SOFAER, (p), 383.

- Radio waves reflected from E-region of ionosphere, attenuation of. R. W. MEADOWS, (p), 22.
RAO, K. L. Semi-attended broadcasting transmitters. (d), 272.
Recording instruments, servo-operated. (d), 482.
REES, J. R., and BARRINGTON, A. E. (See BARRINGTON.)
Reflectivity of a surface at microwave frequencies, use of dielectric materials to enhance. G. B. WALKER and J. T. HYMAN, (p), 73.
RENDALL, A. R. A. Flying-spot film scanner for colour television. (d), 329.
RENWICK, W., WHEELER, D. J., and WILKES, M. V. (See WILKES.)
RIBCHESTER, E. Relation between picture size, viewing distance and picture quality [television]. (d), 437.
ROBERTS, J., and SRIVASTAVA, C. M. (See SRIVASTAVA.)
ROBERTS, M. H. Transistor circuits and applications. (d), 316.
ROBSON, P. N. Fourier series representation of dispersion curves for circular iris-loaded waveguides. (p), 69.
Rod structures, periodic, for Yagi aeriels. J. O. SPECTOR, (p), 38.
ROEBUCK, J. S.
— Servo-operated recording instruments. (d), 482.
— Transistor circuits and applications. (d), 316.
ROSCOE, E. Address as chairman of North-Western Measurement and Control Group. 118.
ROSS, H. MCGREGOR. Boron-trifluoride proportional counters. (d), 367.
Rugby, 16 kc/s transmissions from, as received in New Zealand. (p), 301.
Russian satellites. (See Satellites.)

S

- SALMON, P. G., PYRAH, S., and ABSON, W. (See ABSON.)
Satellites, Russian, radio observations on. (d), 81.
Scientific measuring instruments. (See Measuring.)
Scottish engineers and electrical training scheme. E. O. TAYLOR, (a), 14.
Screen efficiency of sealed-off high-speed-oscillograph cathode-ray tubes. R. FEINBERG, (p), 370.
Sea, phase-coherent back-scatter of radio waves at surface of. E. SOFAER, (p), 383.
SHAKESHAFT, J. R. Radio observations on Russian satellites. (d), 83.
SHEARING, G. Frequency-modulated v.h.f. transmitter technique. (d), 305.
SHEARMAN, E. D. R. Radio observations on Russian satellites. (d), 113.
Sheath faults in telephone cables. (See Telephone.)
SHINN, D. H. Radio observations on Russian satellites. (d), 113.
SHORTER, D. E. L. Performance criteria and design considerations for high-quality monitoring loudspeakers. (p), 607; (d), 622.
Signals, coder for halving bandwidth of. A. R. BILLINGS, (p), 182.
SIMS, L. G. A. Address as chairman of Southern Centre. 19.
SMITH, K. L. Digital-computer techniques. (d), 145.
SMITH, R. W., and HYDE, F. J. (See HYDE.)
SMITH-ROSE, R. L. Radio observations on Russian satellites. (d), 114.
SOFAR, E. Phase-coherent back-scatter of radio waves at surface of sea. (p), 383.
SOMERVILLE, M. J., and DUNSTAN, E. M. (See SOMERVILLE.)
Sound broadcasting service, B.B.C., on very high frequencies. (d), 623.
Space charge as source of flicker effect. C. S. BULL, (p), 190.
SPECTOR, J. O. Investigation of periodic rod structures for Yagi aeriels. (p), 38.
Spot-wobble, use of, on television picture. L. C. JESTY, (p), 425; (d), 435.
SPROSON, W. N. Relation between picture size, viewing distance and picture quality [television]. (d), 437.
SRIVASTAVA, C. M., and ROBERTS, J. Measurement of ferrite loss-factors at 10 Gc/s. (p), 204.
STANBURY, H. C. O. B.B.C. sound broadcasting service on very high frequencies. (d), 623.
STANESBY, H. Radio observations on Russian satellites. (d), 96, 110.
STEPHENSON, J. D. Cathode-ray tube for monochrome and colour television. (d), 604.
STORR-BEST, J. L., BECK, A. C., and NORBURY, F. T. (See BECK.)
STUART, P. R., KALMAN, P. G., and GABOR, D. (See GABOR.)

- Surface impedance, measurement of, at microwave frequencies. A. E. KARBOWIAK, (p), 195.
 SUTCLIFFE, H. B.B.C. sound broadcasting on very high frequencies. (D), 623.
 SUTHERLAND, G. B. B. M. Infra-red radiation. (p), 306.
 SUTTON, R. W. Boron-trifluoride proportional counters. (D), 366.

T

- TAUB, D. M. Digital-computer techniques. (D), 145.
 TAYLOR, D. Boron-trifluoride proportional counters. (D), 365.
 TAYLOR, E. O. Address as chairman of Scottish Centre. 14.
 Teachers for technical colleges, supply and training of (Willis Jackson Report). 116.
 Telephone area, Preston, some aspects of. H. G. COPE, (A), 229.
 — cables, pressurized, location of sheath faults in. E. J. HOOKER, (p), 483.
 — trunk network, automatic working in. L. L. TOLLEY, (A), 17.
 Television. T. E. GOLDDUP, (p), 7.
 —, colour. L. C. JESTY, (p), 425; (D), 435.
 —, colour and monochrome. D. GABOR, P. R. STUART and P. G. KALMAN, (p), 581; (D), 606.
 —, colour, flying-spot film scanner for. H. E. HOLMAN, G. C. NEWTON and S. F. QUINN, (p), 317; (D), 329.
 — links, testing of, by pulse-and-bar waveform generator. I. F. MACDIARMID and B. PHILLIPS, (p), 440.
 Temperature transients in gas-cooled thermal nuclear reactors. J. H. BOWEN and E. F. O. MASTERS, (p), 337; (D), 365.
 Textiles, application of electronic techniques to. K. J. BUTLER, (A), 118.
 Thermionic and cold-cathode valves. W. H. ALDOUS, (p), 273.
 Thermo-electric wattmeter. (See Wattmeter.)
 THOMSON, W. E. Pulse-amplitude modulation. (D), 481.
 Time-division multiplex, transistor pulse generators for. K. W. CATTERMOLE, (p), 471; (D), 479.
 TOLLEY, L. L. Address as chairman of South Midland Centre. 17.
 TOMLINSON, T. B. Digital-computer techniques. (D), 145.
 Train performance computer. E. BRADSHAW, M. WAGSTAFF, and F. COOKE, (p), 560; (D), 567.
 Training scheme, electrical. E. O. TAYLOR, (A), 14.
 Transistor circuit for construction of digital-computing systems. P. L. CLOOT, (p), 213.
 — circuits and applications. (D), 316.
 — high-gain chopper-type d.c. amplifier. G. B. B. CHAPLIN and A. R. OWENS, (p), 258; (D), 266, 559.
 — input stages for high-gain d.c. amplifiers. G. B. B. CHAPLIN and A. R. OWENS, (p), 249; (D), 266.
 — pulse generators for time-division multiplex. K. W. CATTERMOLE, (p), 471; (D), 479.
 Transistors, commercial, measurements on, and their relation to theory. F. J. HYDE, (p), 45.
 —, current gain of, at frequencies up to 105 Mc/s. F. J. HYDE and R. W. SMITH, (p), 221.
 —, dekatrons and electro-mechanical registers operated by. G. B. B. CHAPLIN and R. WILLIAMSON, (p), 231; (D), 266.
 Transmission-line filter. (See Filter.)
 Transmissions, 16 kc/s, from Rugby as received in New Zealand, phase variations of. D. D. CROMBIE, A. H. ALLAN and M. NEWMAN, (p), 301.
 Transmitter, amplitude-modulated, Class-C output stage. C. G. MAYO and H. PAGE, (p), 523.
 — technique, frequency-modulated v.h.f. (D), 305.
 TRUSLOVE, D. J. Digital-computer techniques. (D), 144.
 TURNER, L. W. B.B.C. sound broadcasting service on very high frequencies. (D), 623.

U

- Ultra-high-frequency power amplifiers. (See Power.)

- University, College of Technology and Student Members, contemplation of. L. G. A. SIMS, (A), 26.

V

- Valve development, twenty years of. C. H. FOULKES, (A), 230.
 Valves, thermionic and cold-cathode. W. H. ALDOUS, (p), 273.
 VAN DORP, S. D. Train performance computer. (D), 567.
 Very high frequencies, B.B.C. sound broadcasting service on. (D), 623.
 Viewing distance, picture size and picture quality [television]. L. C. JESTY, (p), 425; (D), 435.
 VINTEN, W. P. Flying-spot film scanner for colour television. (D), 330.

W

- WAGSTAFF, M., COOKE, F., and BRADSHAW, E. (See BRADSHAW.)
 WALKER, G. B., and HYMAN, J. T. Use of dielectric materials to enhance reflectivity of a surface at microwave frequencies. (p), 73.
 WALKER, J., and COX, R. J. (See COX.)
 WALKER, J. S. Transistor devices and magnetic amplifiers. (D), 268.
 WALKER, P. J. Monitoring loudspeakers. (D), 622.
 WATSON, S. N. Relation between picture size, viewing distance and picture quality [television]. (D), 436.
 Wattmeter, thermo-electric, for power and audio frequencies. J. J. HILL, (p), 61.
 Waveguide filters, wide-band, with short linear tapers. G. CRAVEN, (p), 210.
 Waveguides, circular iris-loaded, dispersion curves for. P. N. ROBSON, (p), 69.
 — rectangular, transverse film bolometers for measurement of power in. J. A. LANE, (p), 77; (D), 395.
 WEBB, J. K.
 — Magnetic-drum store for analogue computing. (D), 580.
 — Monitoring loudspeakers. (D), 622.
 WEST, J. C., and DOUCE, J. L. (See DOUCE.)
 WESTCOTT, J. H. Train performance computer. (D), 568.
 WHEELER, D. J., WILKES, M. V., and RENWICK, W. (See WILKES.)
 WHITEHEAD, M. Train performance computer. (D), 567.
 WIDDIS, F. C. Scientific electrical measuring instruments. (p), 415.
 WILKES, M. V., RENWICK, W., and WHEELER, D. J. Design of control unit of electronic digital computer. (p), 121.
 WILKES, W. B.B.C. sound broadcasting service at very high frequencies. (D), 624.
 WILLINSON, T. J. Control of nuclear reactors. (D), 120.
 WILLIAMS, G. M. E. Magnetic tape for data recording. (D), 381.
 WILLIAMSON, R., and CHAPLIN, G. B. B. (See CHAPLIN.)
 WILLIS, D. W.
 — Digital-computer techniques. (D), 145.
 — Magnetic tape for data recording. (D), 380.
 Willis Jackson Report. 116.
 WILLS, W. J. A. Control of nuclear reactors. (D), 120.
 WILSON, I. Transistor devices and magnetic amplifiers. (D), 266.
 WINTON, R. C. Relation between picture size, viewing distance and picture quality [television]. (D), 436.
 WILLIAMS, B. C. F. Relation between picture size, viewing distance and picture quality [television]. (D), 436.
 WOLFENDALE, E. Frequency-modulated v.h.f. transmitter technique. (D), 305.
 WOODHEAD, H. C. Radio observations on Russian satellites. (D), 110.
 WORDSWORTH, D. V. Boron-trifluoride proportional counters. (D), 366.
 WYNN, R. T. B., and PEACHEY, F. A. Automatic control of semi-attended broadcasting transmitters. (D), 272.

Y

- Yagi aerials. (See Aerials.)
 YOUNG, J. E. R. Magnetic tape for data recording. (D), 381.

PROCEEDINGS OF THE INSTITUTION OF ELECTRICAL ENGINEERS

Part B. RADIO AND ELECTRONIC ENGINEERING (INCLUDING COMMUNICATION ENGINEERING), NOVEMBER 1958

CONTENTS

	PAGE
A Novel, High-Accuracy Circuit for the Measurement of Impedance in the A.F., R.F. and V.H.F. Ranges. D. KARO, Dr.Eng., Ph.D., Dipl.Eng.	505
A Simple 3 cm Q-Meter.....A. E. BARRINGTON, Ph.D., B.Sc.(Eng.), and J. R. REES, Ph.D.	511
Ultra-High-Frequency Power Amplifiers.....J. DAIN, M.A.	513
Amplitude-Modulated Transmitter Class-C Output Stage.....C. G. MAYO, M.A., B.Sc., and H. PAGE, M.Sc.	523
The Reduction of Low-Frequency Noise in Feedback Integrators.....E. M. DUNSTAN, M.Sc., and M. J. SOMERVILLE, B.Sc.	532
Measurements on Gas-Discharge Noise Sources at Centimetre Wavelengths.....A. C. GORDON-SMITH and J. A. LANE, M.Sc.	545
Methods of Calculating the Horizontal Radiation Patterns of Dipole Arrays around a Support Mast.....P. KNIGHT, B.A.	548
Simultaneous Variation of Amplitude and Phase of Gaussian Noise, with applications to Ionospheric Forward Scatter Signals. T. HAGFORS, Siv. Ing., and B. LANDMARK, Dr. Phil.	555
Discussion on 'A Transistor High-Gain Chopper-Type D.C. Amplifier'.....	559
A Train Performance Computer.....Prof. E. BRADSHAW, M.B.E., Ph.D., M.Sc.Tech., M. WAGSTAFF, M.Sc.Tech., and F. COOKE	560
The Simulation of Distributed-Parameter Systems, with particular reference to Process Control Problems. J. F. MEREDITH, B.Sc., Ph.D., and E. A. FREEMAN, B.Sc.	569
A Magnetic-Drum Store for Analogue Computing.....J. L. DOUCE, M.Sc., Ph.D., and J. C. WEST, Ph.D., D.Sc.	577
A New Cathode-Ray Tube for Monochrome and Colour Television. Prof. D. GABOR, Dr. Ing., F.R.S., P. R. STUART, Ph.D., and P. G. KALMAN, Ph.D.	581
A Survey of Performance Criteria and Design Considerations for High-Quality Monitoring Loudspeakers...D. E. L. SHORTER, B.Sc.(Eng.)	607
Discussion on 'The B.B.C. Sound Broadcasting Service on Very High Frequencies'.....	623

Declaration on Fair Copying.—Within the terms of the Royal Society's Declaration on Fair Copying, to which The Institution subscribes, material may be copied from issues of the *Proceedings* (prior to 1949, the *Journal*) which are out of print and from which reprints are not available. The terms of the Declaration and particulars of a Photoprint Service afforded by the Science Museum Library, London, are published in the *Journal* from time to time.

Bibliographical References.—It is requested that bibliographical reference to an Institution paper should always include the serial number of the paper and the month and year of publication, which will be found at the top right-hand corner of the first page of the paper. This information should precede the reference to the Volume and Part.

Example.—SMITH, J.: 'Reflections from the Ionosphere', *Proceedings I.E.E.*, Paper No. 3001 R, December, 1954 (102 B, p. 1234).

THE BENEVOLENT FUND

During the last few years the amount received from subscriptions and donations has been insufficient to meet the cost of grants and management charges. The deficiency is met by making encroachments on capital funds. This may one day prove to be disastrous unless it is checked. Will you help to ensure that the income from subscriptions exceeds outgoings?

Subscriptions, preferably under Deed of Covenant, and Donations may be sent by post to

THE HONORARY SECRETARY

THE INCORPORATED BENEVOLENT FUND OF THE INSTITUTION OF
ELECTRICAL ENGINEERS, SAVOY PLACE, W.C.2

or may be handed to one of the Local Honorary Treasurers of the Fund.

Though your gift may be small, please do not hesitate to send it



LOCAL HON. TREASURERS OF THE FUND:

EAST MIDLAND CENTRE R. C. Woods	SCOTTISH CENTRE R. H. Dean, B.Sc.Tech.
IRISH BRANCH A. Harkin, M.E.	NORTH SCOTLAND SUB-CENTRE P. Philip
MERSEY AND NORTH WALES CENTRE D. A. Picken	SOUTH MIDLAND CENTRE Capt. J. H. Patterson, R.A.
NORTH-EASTERN CENTRE J. F. Skipsey, B.Sc.	RUGBY SUB-CENTRE P. G. Ross, B.Sc.
NORTH MIDLAND CENTRE E. C. Walton, Ph.D., B.Eng.	SOUTHERN CENTRE G. D. Arden
SHEFFIELD SUB-CENTRE F. Seddon	WESTERN CENTRE (BRISTOL) A. H. McQueen
NORTH-WESTERN CENTRE E. G. Taylor, B.Sc.(Eng.)	WESTERN CENTRE (CARDIFF) E. W. S. Watt
NORTH LANCASHIRE SUB-CENTRE G. K. Alston, B.Sc.(Eng.)	WEST WALES (SWANSEA) SUB-CENTRE O. J. Mayo
NORTHERN IRELAND CENTRE G. H. Moir, J.P.	SOUTH-WESTERN SUB-CENTRE W. E. Johnson